TSINGHUA-PRINCETON-COMBUSTION INSTITUTE

2025 SUMMER SCHOOL ON COMBUSTION

Turbulent Combustion

Hong G. Im

King Abdullah University of Science and Technology (KAUST), Saudi Arabia

July 06-12, 2025

TSINGHUA-PRINCETON-COMBUSTION INSTITUTE

2025 SUMMER SCHOOL ON COMBUSTION

<table>
<tr><th colspan="6">Key Activities / 重要活动</th></tr>
<tr><td rowspan="2">July 6
(Sunday)
/7月6日
(周日)</td><td>10:00-17:30</td><td>Registration
注册</td><td colspan="3">Northeast Gate, Lee Shau Kee Sci. and Tech. Building
李兆基科技大楼东北门</td></tr>
<tr><td>18:00</td><td>Welcome Reception
开班仪式</td><td colspan="3">A-278, Multifunction Room, Lee Shau Kee Sci. and Tech. Building
李兆基科技大楼多功能厅</td></tr>
<tr><th colspan="6">Class Schedule / 课程安排</th></tr>
<tr><td rowspan="6">July 7-11
(Monday-Friday)
/7月7-11日
(周一至周五)</td><td rowspan="3">Morning
上午</td><td>9:00-9:50</td><td rowspan="3">Combustion Chemistry
Lecturer: Philippe Dagaut
Jianhua Building
建华楼A109</td><td colspan="2" rowspan="3">Turbulent Combustion
Lecturer: Hong G. Im
Jianhua Building
建华楼LG1-21</td></tr>
<tr><td>10:00-10:50</td></tr>
<tr><td>11:00-11:50</td></tr>
<tr><td rowspan="3">Afternoon
下午</td><td>14:00-14:50</td><td rowspan="3">Dynamics of Flames and Detonations in Premixed Gas
Lecturer: Paul Clavin
Jianhua Building
建华楼A109</td><td rowspan="3">Advanced Laser Diagnostics for Chemically Reacting Flows
Lecturer: Mark Linne
Jianhua Building
建华楼A404</td><td rowspan="3">Applications of Combustion Science to Fire Safety
Lecturer: José L. Torero
Jianhua Building
建华楼LG1-11</td></tr>
<tr><td>15:00-15:50</td></tr>
<tr><td>16:00-16:50</td></tr>
<tr><th colspan="6">Special Activities / 特殊活动</th></tr>
<tr><td>July 6
(Sunday)
/7月6日
(周日)</td><td>13:30-17:30</td><td colspan="2">Art Museum Visit / 艺术博物馆参观</td><td colspan="2">Tsinghua University Art Museum
清华大学艺术博物馆</td></tr>
<tr><td>July 7
(Monday)
/7月7日
(周一)</td><td>17:00-17:30</td><td colspan="2">Group Picture Taking / 暑期学校合影</td><td colspan="2">The open-air plaza next to the New Tsinghua Auditorium
天大广场(新清华学堂露天广场)</td></tr>
<tr><td>July 8
(Tuesday)
/7月8日
(周二)</td><td>17:00-18:00</td><td colspan="2">Campus Tour / 校园游览</td><td colspan="2">Tsinghua University
清华大学</td></tr>
<tr><td>July 9
(Wednesday)
/7月9日
(周三)</td><td>18:30-19:30
19:30-21:00</td><td colspan="2">Poster Presentation / 海报展示
Career Panel / 职业发展论坛</td><td colspan="2">B-518, Lee Shau Kee Sci. and Tech. Building
李兆基科技大楼B-518会议室</td></tr>
<tr><td>July 10
(Thursday)
/7月10日
(周四)</td><td>18:00</td><td colspan="2">Farewell Reception / 欢送会</td><td colspan="2">Guan Chou Yuan Restaurant
观畴园餐厅</td></tr>
<tr><td>July 11
(Friday)
/7月11日
(周五)</td><td>8:00-18:00</td><td colspan="2">Program Certificate Distribution / 学习证书发放</td><td colspan="2">Jianhua Building
建华楼</td></tr>
<tr><td>July 12
(Saturday)
/7月12日
(周六)</td><td>9:30-11:30</td><td colspan="2">CCE Laboratory Tour / 燃烧能源中心实验室参观</td><td colspan="2">Northeast Gate, Lee Shau Kee Sci. and Tech. Building
李兆基科技大楼东北门</td></tr>
</table>

جامعة الملك عبدالله للعلوم والتقنية
King Abdullah University of Science and Technology

Clean Energy Research Platform

Tsinghua-Princeton-Combustion Institute
2025 Summer School on Combustion
Tsinghua University, July 7-11, 2025

Philippe Dagaut, CNRS, Orléans, France

Turbulent Combustion

Introduction

Hong G. Im
Clean Energy Research Platform (CERP)
King Abdullah University of Science and Technology (KAUST)

Established in 2009 as a graduate-level STEM research university located on the shores of the Red Sea, north of Jeddah.

At KAUST scientists and engineers aim to address global challenges by conducting research in the broad strategic themes of water, food, energy and the environment. We do that by offering expertise in 19 research areas and through creating a collaborative and interdisciplinary problem-solving environment.

Our campus community is comprised of distinct residential, academic and commercial districts seamlessly integrating all facets of community and work life. **KAUST welcomes an international community of more than 7,400 residents from over 115 countries.**

KAUST **Quick Facts**

*Academic year 2021-2022

Total campus size

39

square kilometers

Our Community Stats

8000+
Community Members

100+
Nationalities

Our Academic Stats

1530
Students

77%
of Students are Ph.D.

7:1
Student to Faculty Ratio

191
Faculty

2000 +
Alumni

65%
of Students are International

370
Research Scientists & Staff

500
Post Docs

KAUST **Students**

As of 2020-2021

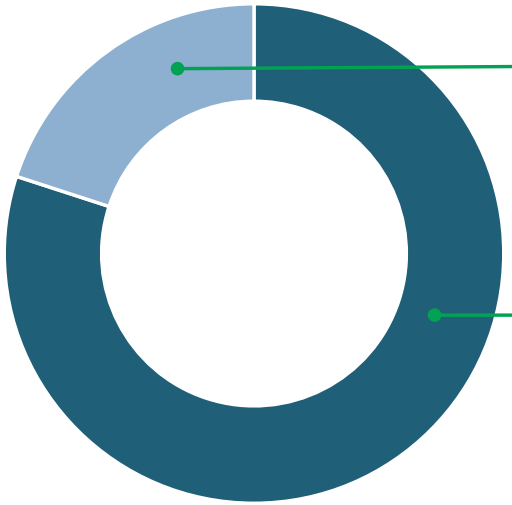

23%

M.S. Students

77%

Ph.D. Students

64%

Men

36%

Women

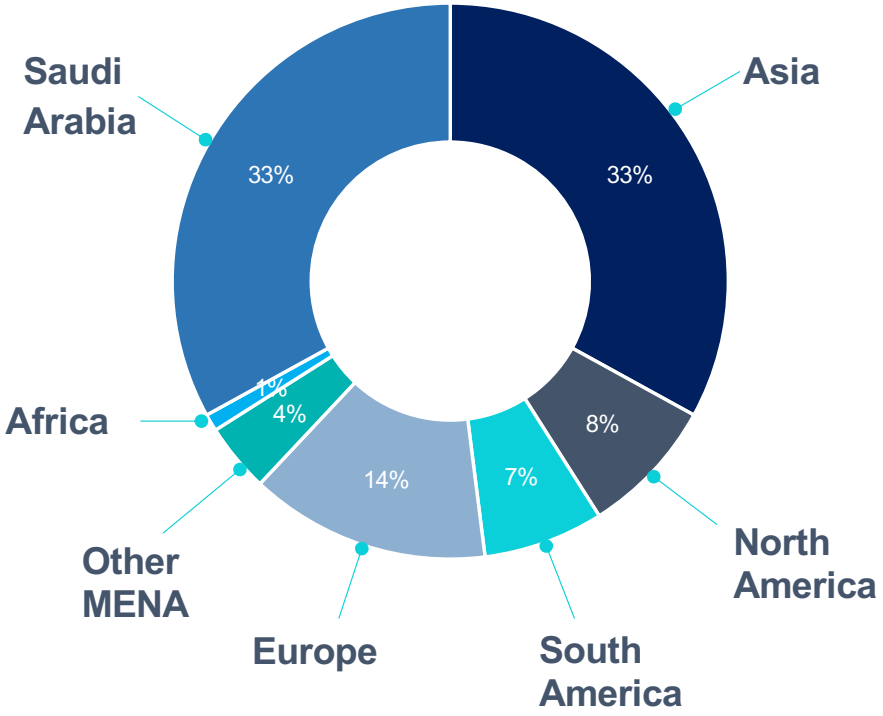

Registered Students by Nationality*

*As of 20th day of Fall 2020. There is one student from Oceania which is not included in the percentage total. Due to rounding, combined regional percentages will sum to more than 100%

The KAUST **Fellowship**

- All admitted students receive the KAUST Fellowship,
- which supports the student for the duration of their graduate studies.

The KAUST Fellowship includes:

- Full Free Tuition Support
- Monthly Living Allowance
  (From $20,000 to $30,000 annually, depending on qualifications and degree progress)
- On-Campus Housing
- Medical and dental coverage
- Relocation Support

Visiting Student Research Program (VSRP)

https://vsrp.kaust.edu.sa

Eligibility

- **3rd year B.S. and M.S. students**
- **3.50/4.00 GPA** or 14/20 Equivalent to ECTS B
- Strong verbal and written English Skills
- 3 to 6 Month Internship
- **250+ projects available now**

Applications accepted year-round!

Benefits

- US $1,000 Monthly Living Allowance
- Access to Core laboratories and major research and community facilities
- Recreation & Sports Facilities
- Free Housing
- Full Airfare & Visa Fees
- Medical Insurance

VSRP Quick Facts:

888 VSRP Interns*
since 2014

63% Male

37% Female

74 Nationalities*

*Individual and Workshops

Top Countries

- United Kingdom
- Italy
- United States
- Germany
- Mexico
- France

Clean Energy Research Platform (CERP): Faculty

Leadership Committee

Mani Sarathy
Chair, Professor
Chemical Engineering

Hong G. Im
Deputy Chair, Professor
Mechanical Engineering

Member Faculty

William Roberts
Director CCRC (2014-2024)
Mechanical Engineering

Bassam Dally
Professor
Mechanical Engineering

James Turner
Professor
Mechanical Engineering

Yun Hau Ng
Professor
Chemical Engineering

Aamir Farooq
Professor
Mechanical Engineering

Thibault Guiberti
Assistant Research Professor
Mechanical Engineering

Deanna Lacoste
Associate Professor
Mechanical Engineering

Xu Lu
Assistant Professor
Mechanical Engineering

Anqi Wang
Assistant Professor
Chemistry

CERP builds on the culture and reputation of the Clean Combustion Research Center (CCRC)

- Targeting collective success
- Striving for excellence in academic and research performance
- Proactively securing external funding
- Leadership in KAUST, KSA, and global energy community

Linking fundamental knowledge to real world systems

A suite of experiments to study basic interactions

- Ignition and fuel characterization in CFR engine
- Fuel/engine design in single cylinder research engines
- Optical access to reactors with laser diagnostic measurements
- Special engines for pre-ignition and superknock studies

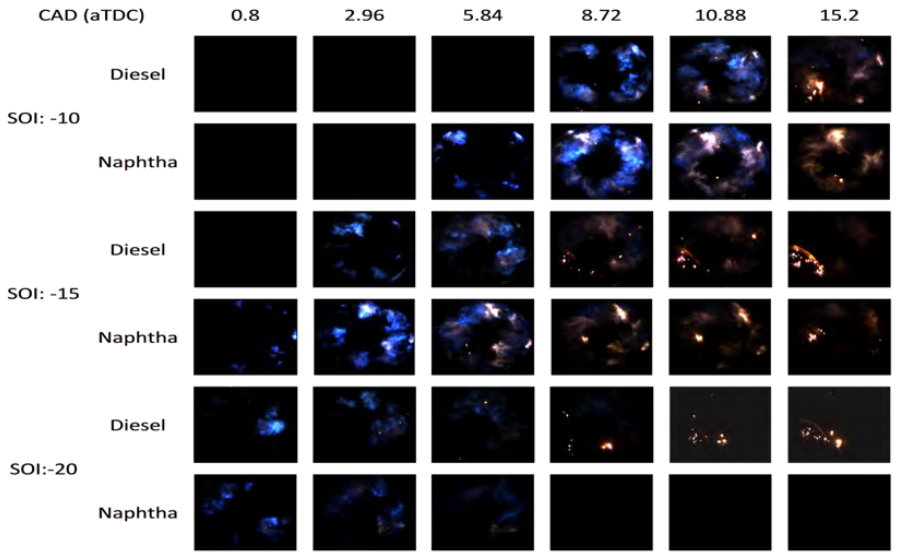

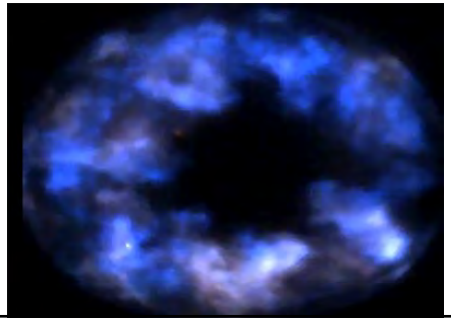

High Pressure Combustion Duct

- A reduced-scale and optically-accessible burner can be installed in KAUST's HPCD
- A comprehensive suite of advanced optical diagnostics is available

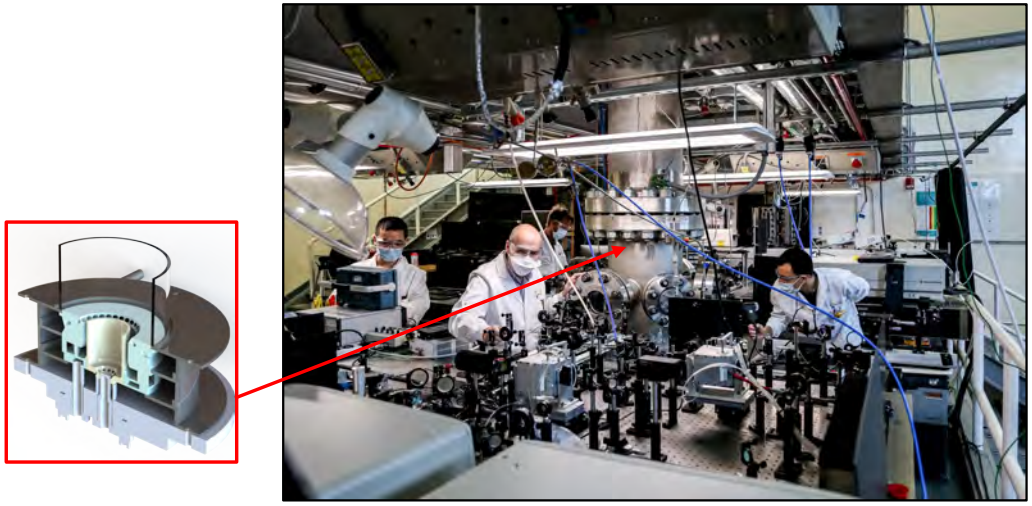

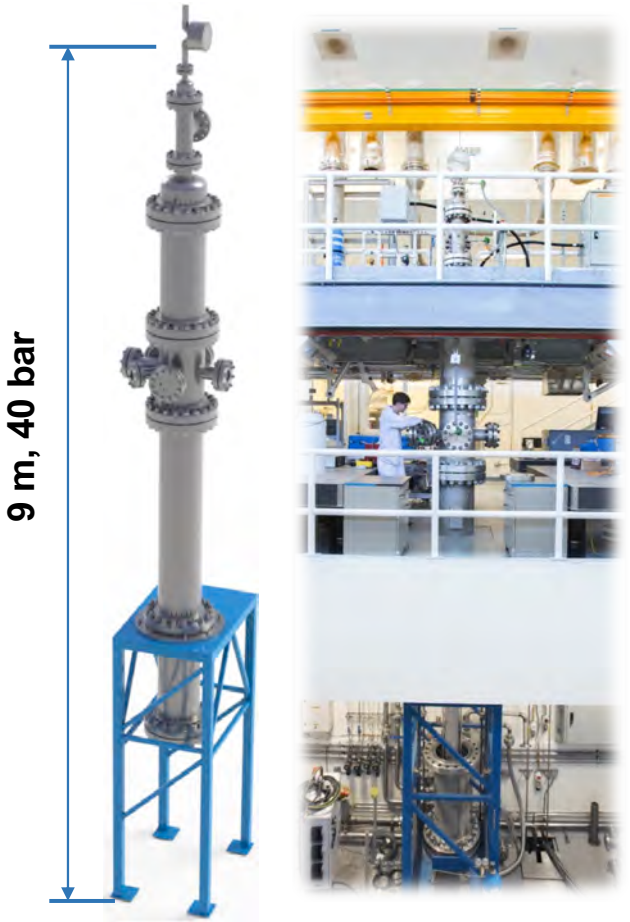

CERP's Synergistic and Multi-scale Rearch

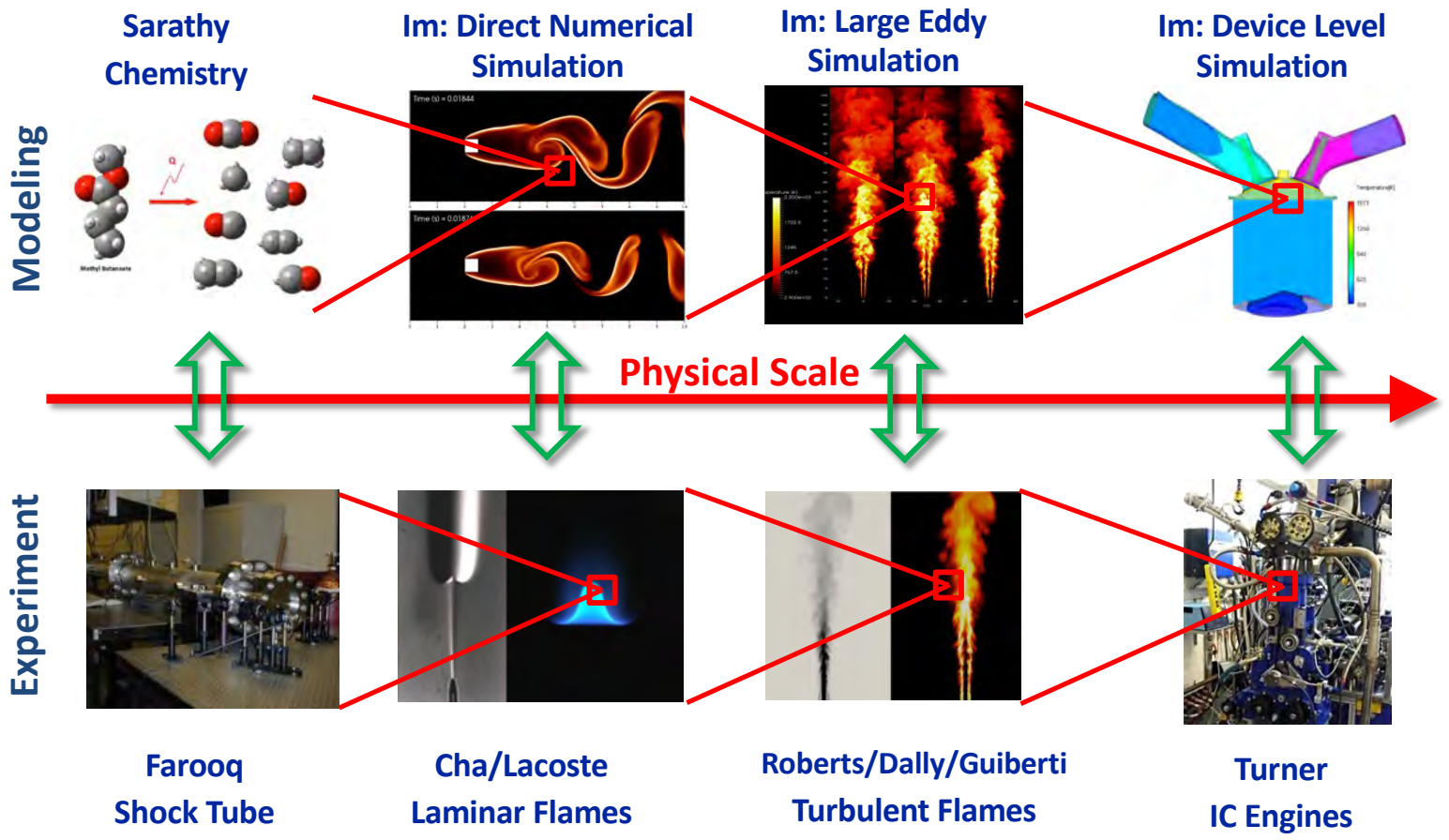

Computational Reacting Flows Laboratory (CRFL)
Personnel (18 members, 12 countries)

Hong G. Im
Principal Investigator

Francisco
Hernández Pérez
Research Scientist

Junjun Guo
Research Scientist

Xinlei Liu
Research Scientist

Postdocs

Mohammad
Rafi Malik

Erica
Quadarella

Raghib
Shakeel

M.S. Students

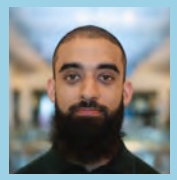

Omar
Shafiq

Abdulmohsen
Alsubaie

Ali
Marzooq

Ph.D. Students

Suliman
Abdelwahid

Vijay
Vijayarangan

Xiao
Shao

Abdullah
Zaihi

Po-Han
Chen

Urbano
Medina Martinez

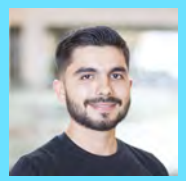

Rafael
Menaca Cabrera

Alessandro
Carinci

Predictive Simulations of Multi-scale Combustion

Direct numerical simulations (DNS) of turbulent flame propagation

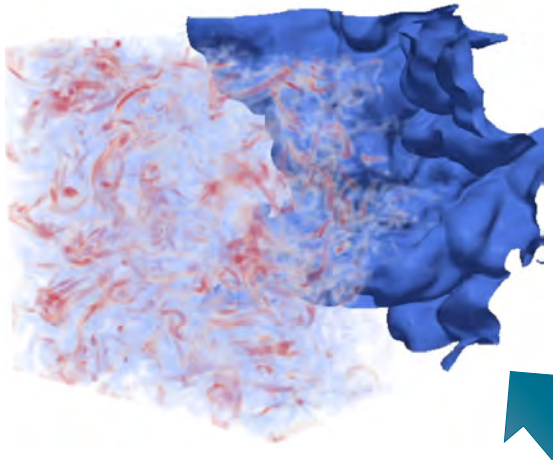

Full-cycle simulations of combustion engines

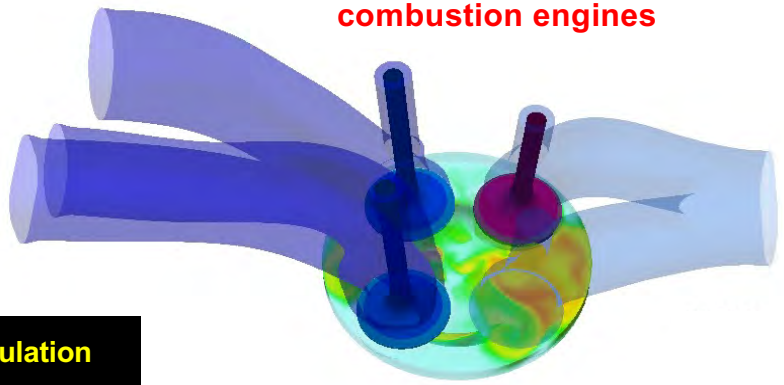

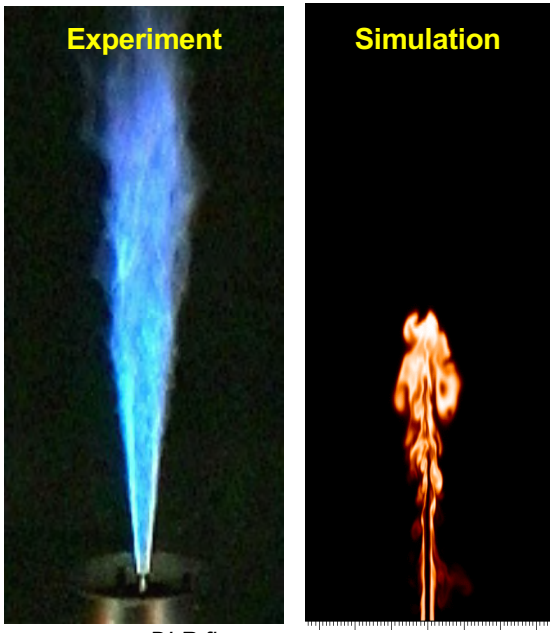

DLR flame

High performance computing enables predictive analysis of combustion and pollutant formation, allowing intelligent design of advanced engines at lower development costs.

Large eddy simulations (LES) of laboratory-scale flames

High Fidelity Direct Numerical Simulations

in collaboration with KSL (Jysoo Lee), ECRC (David Keyes)

KAUST Adaptive Reacting Flow Solver (KARFS)

Scalable, performance portable solver for current and future high performance computing architectures

- **Scalability:** Needs to scale to the full capability of current and future systems such as Shaheen-II (KAUST) and Summit (ORNL)
- **Performance Portable** on multiple architectures such as multi-core, many-core (Xeon Phi) and accelerators (GPU)
- **Extensibility** to multiple applications including fully compressible finite difference DNS, low Mach AMR, etc.
- **Leverage** open source libraries for combustion models and programming abstractions

Number of species/reactions	1 CPU (1 core)	1 GPU + 1 CPU (1 core)	Acceleration (1 GPU versus 1 CPU – 1 core)
55/290	0.002	0.055	0.04
171/861	0.010	0.030	0.03
654/5258	0.351	0.109	3.22
1271/9785	1.807	0.275	6.57
2115/15787	11.269	0.789	14.28
2855/18049	35.803	1.408	25.43
7171/47793	334.164	6.961	48.01

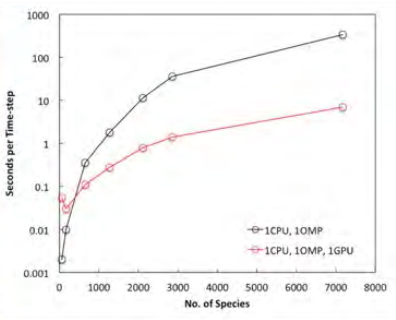

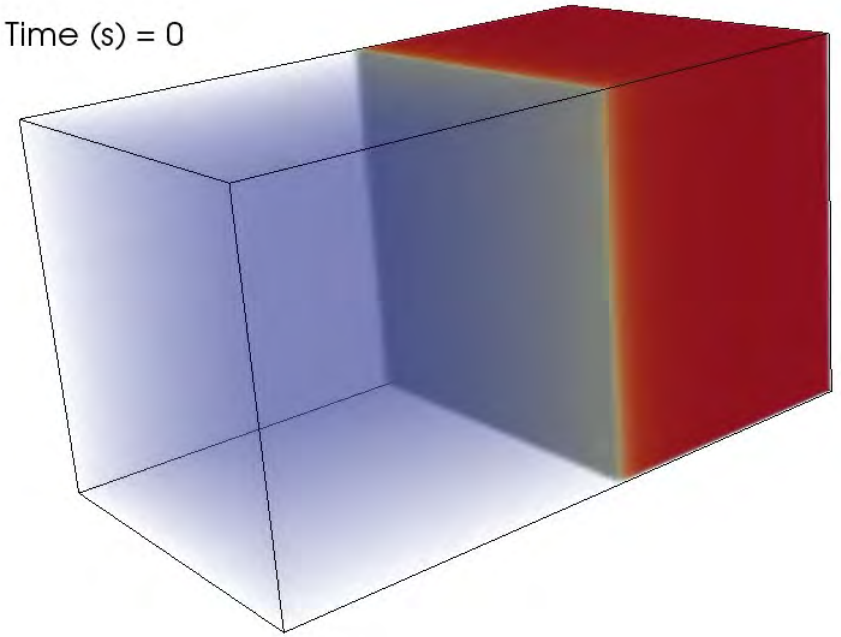

DNS of highly turbulent premixed flame propagation. 3D domain size of approximately a few cm^3 requires billions of grid points and ~10M CPU hours. Temperature isosurface (1200 K) and H_2O_2 contours are shown.

LES of Turbulent Nonpremixed Flames at High Pressures

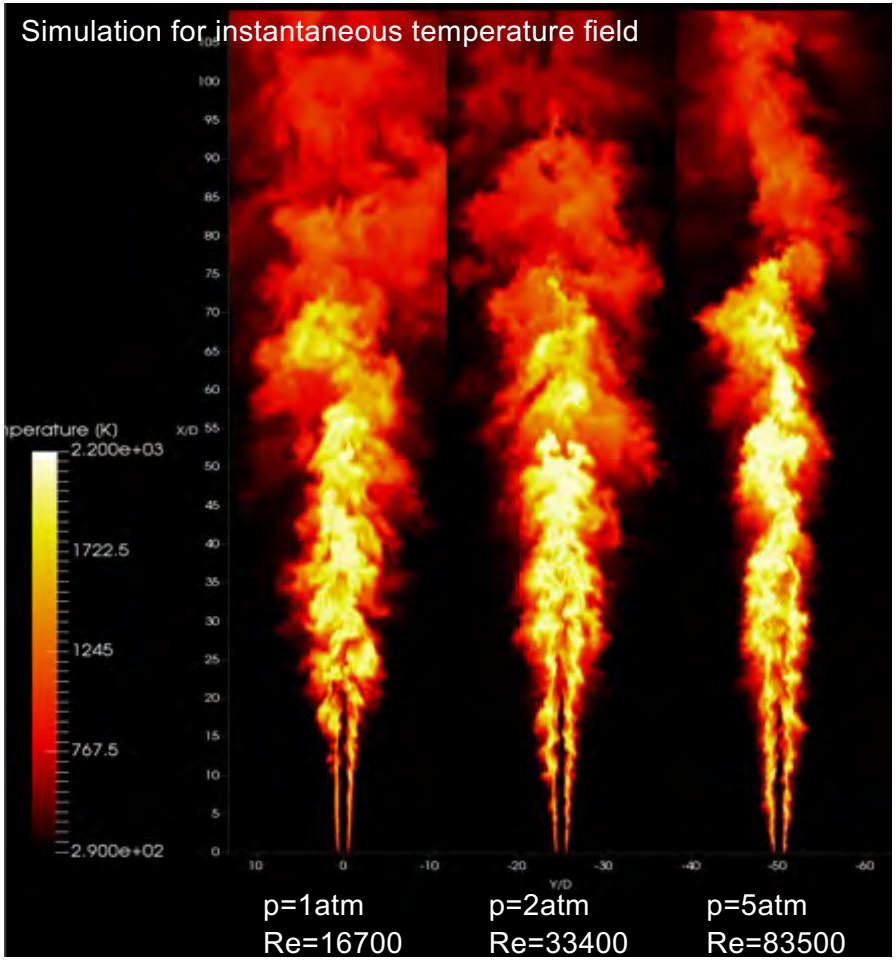

- Three-dimensional large eddy simulations of turbulent syngas/air flames using a flamelet approach
- The study investigates the effect of pressure on turbulent nonpremixed flames. The findings will guide the experiments to be conducted in high pressure combustion test facility at CCRC.

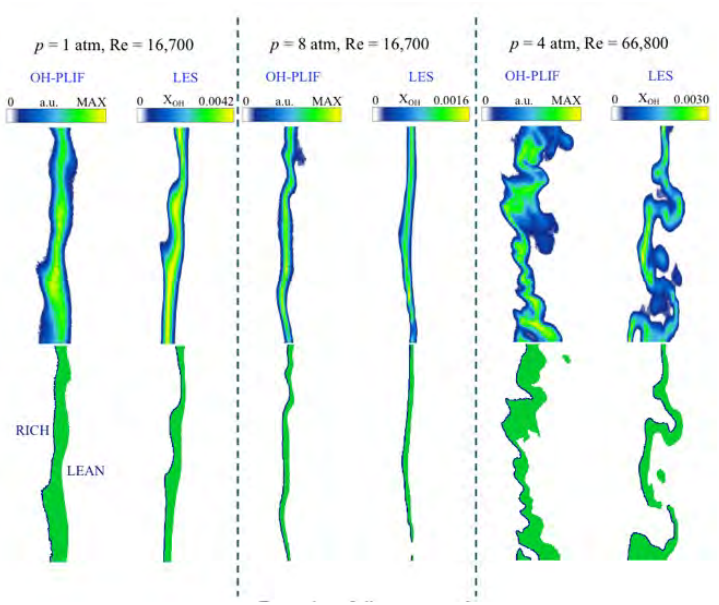

OH profiles from experiment (left) and simulation (right)

High Fidelity Simulations of Advanced Engines

In- and near-nozzle flow simulation

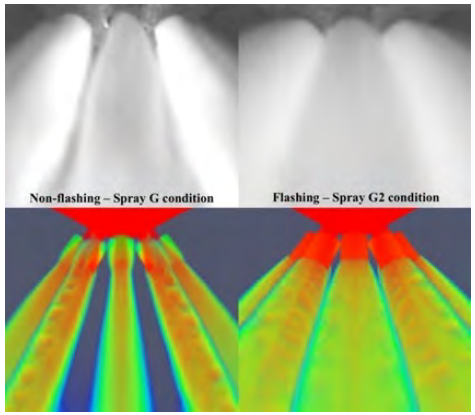

Spray simulation and experiment

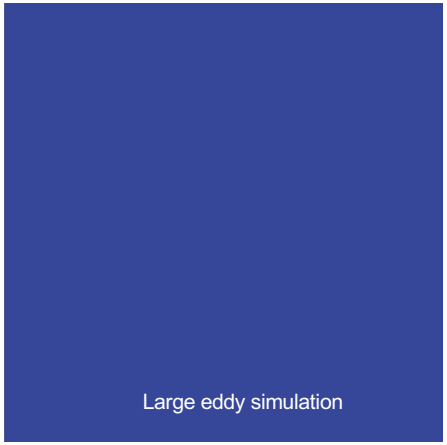

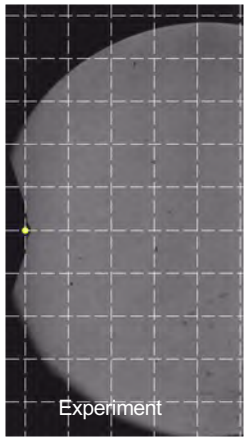

Saudi Aramco's FUELCOM project aims to develop high fidelity modeling capabilities for high efficiency engines with future fuels.

- Eulerian simulation of liquid spray inside the nozzle to provide accurate boundary conditions for spray dynamics
- Lagrangian spray models to predict accurate spray break-up and evaporation
- Full cycle engine simulations with high-fidelity combustion submodels to represent mixed-mode combustion.

Engine simulation

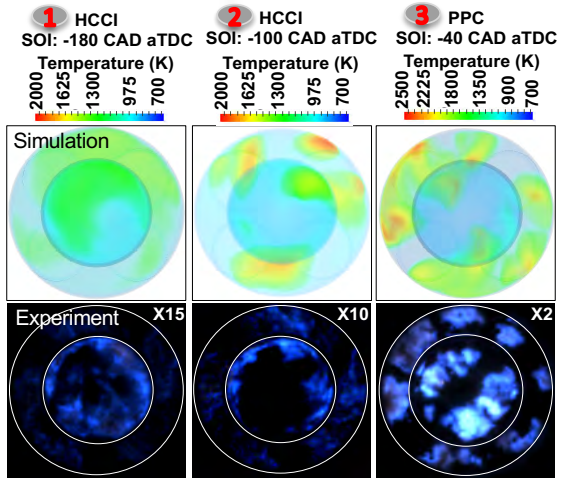

Level of stratification

Simulation of pre-ignition/super-knock

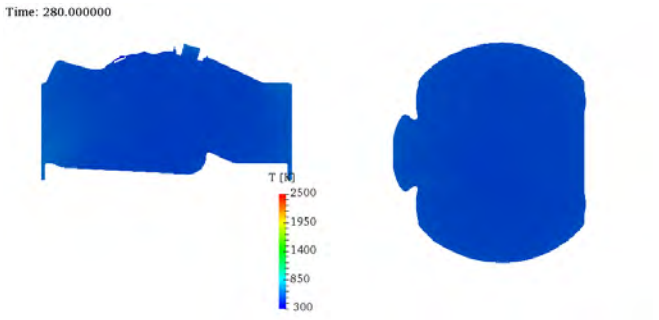

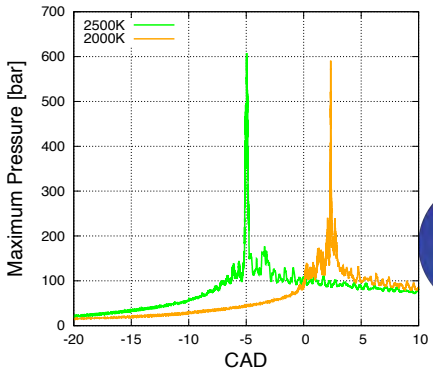

What's at Stake?

Future of Combustion Research

We Want to Decarbonize the Energy…

Figure 3.1 ▷ Global total energy supply by source and fossil fuel share by scenario, 2000-2050

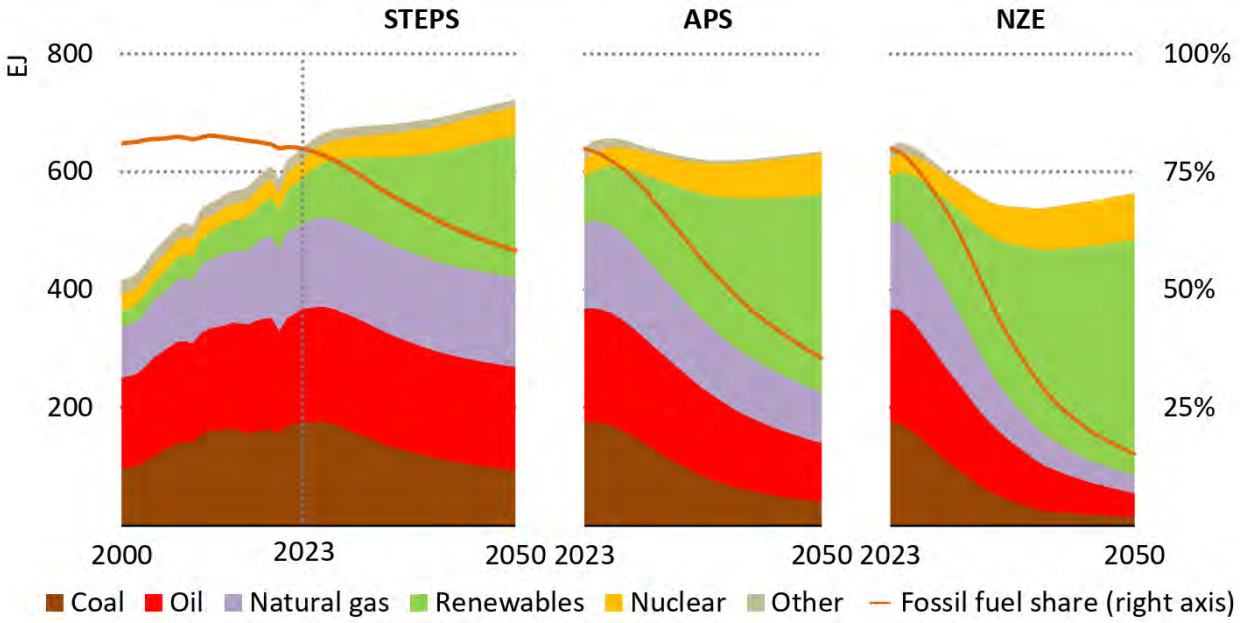

IEA. CC BY 4.0.

Each fossil fuel peaks by 2030 in all scenarios and then declines over time as renewables and other low-emissions sources of energy increase strongly

Notes: EJ = exajoules; STEPS = Stated Policies Scenario; APS = Announced Pledges Scenario; NZE = Net Zero Emissions by 2050 Scenario. Renewables includes modern bioenergy. Other includes the traditional use of biomass and non-renewable waste.

The last decade has seen the share of fossil fuels in the global energy mix gradually come down from 82% in 2013 to 80% in 2023. Demand for energy has increased by 15% over this period and 40% of this growth has been met by clean energy, i.e. renewables in the power and end-use sectors, nuclear, and low-emissions fuels, including carbon capture, utilisation and storage (CCUS).

World Energy Outlook, 2024

US: Renewable Will Supply 44% of Electricity by 2050

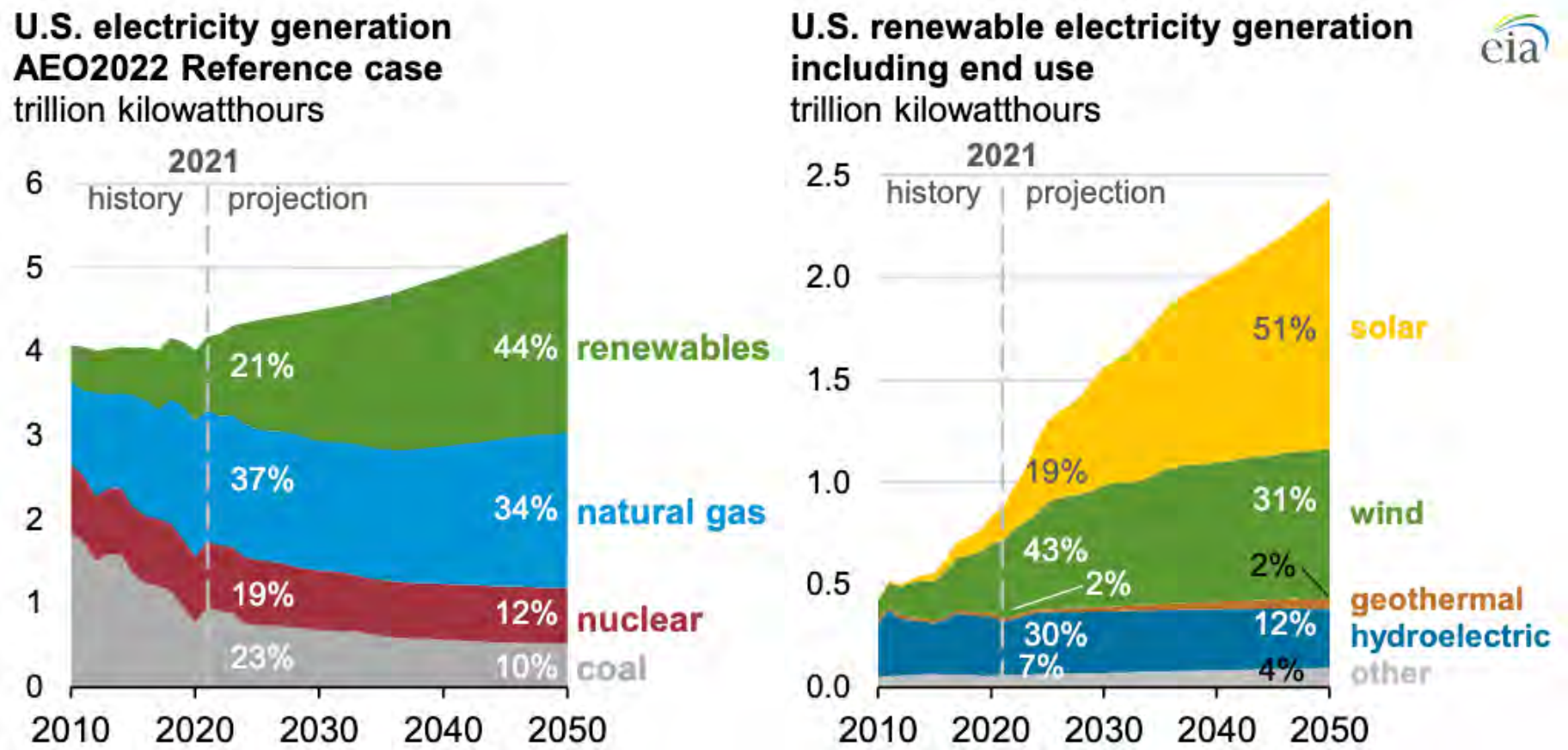

Source: U.S. Energy Information Administration, *Annual Energy Outlook 2022* (AEO2022)
Note: Biofuels are both shown separately and are included in petroleum and other liquids.

Electrification!
There is no silver bullet for all.

MORE THAN 300 NEW MINES REQUIRED TO MEET BATTERY DEMAND BY 2035

6th September 2022 | Battery raw materials

More than 300 new mines could need to be built over the next decade to meet the demand for electric vehicle and energy storage batteries, according to a Benchmark forecast.

At least 384 new mines for graphite, lithium, nickel and cobalt are required to meet demand by 2035, based on average mine sizes in each industry, according to Benchmark. Taking into account recycling of raw materials, the number is around 336 mines.

The data highlights the height of the raw material challenge facing global automakers as they look to scale up production of electric vehicles this decade. Demand for lithium ion batteries is set to grow six-fold by 2032, according to Benchmark.

Yet supplies of lithium, graphite, nickel and cobalt will need to keep pace with demand, especially post 2030.

While recycling of raw materials will have the most impact on future cobalt supply, it's not yet set to have much impact on materials such as graphite, according to Benchmark.

Though given the shorter lead time to build recycling facilities, new recycling technologies could displace some of the new mine requirements.

https://www.benchmarkminerals.com/membership/more-than-300-new-mines-required-to-meet-battery-demand-by-2035/

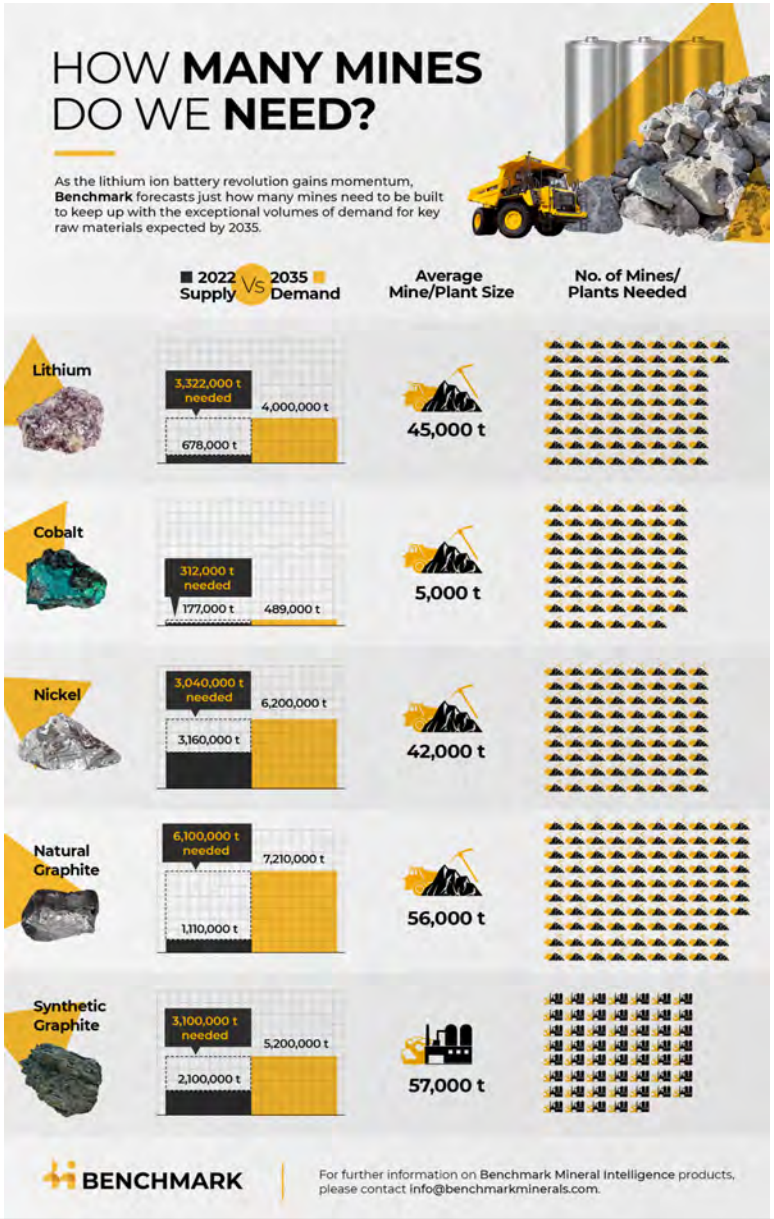

Power-to-X: E-Fuels for Storage at Scale

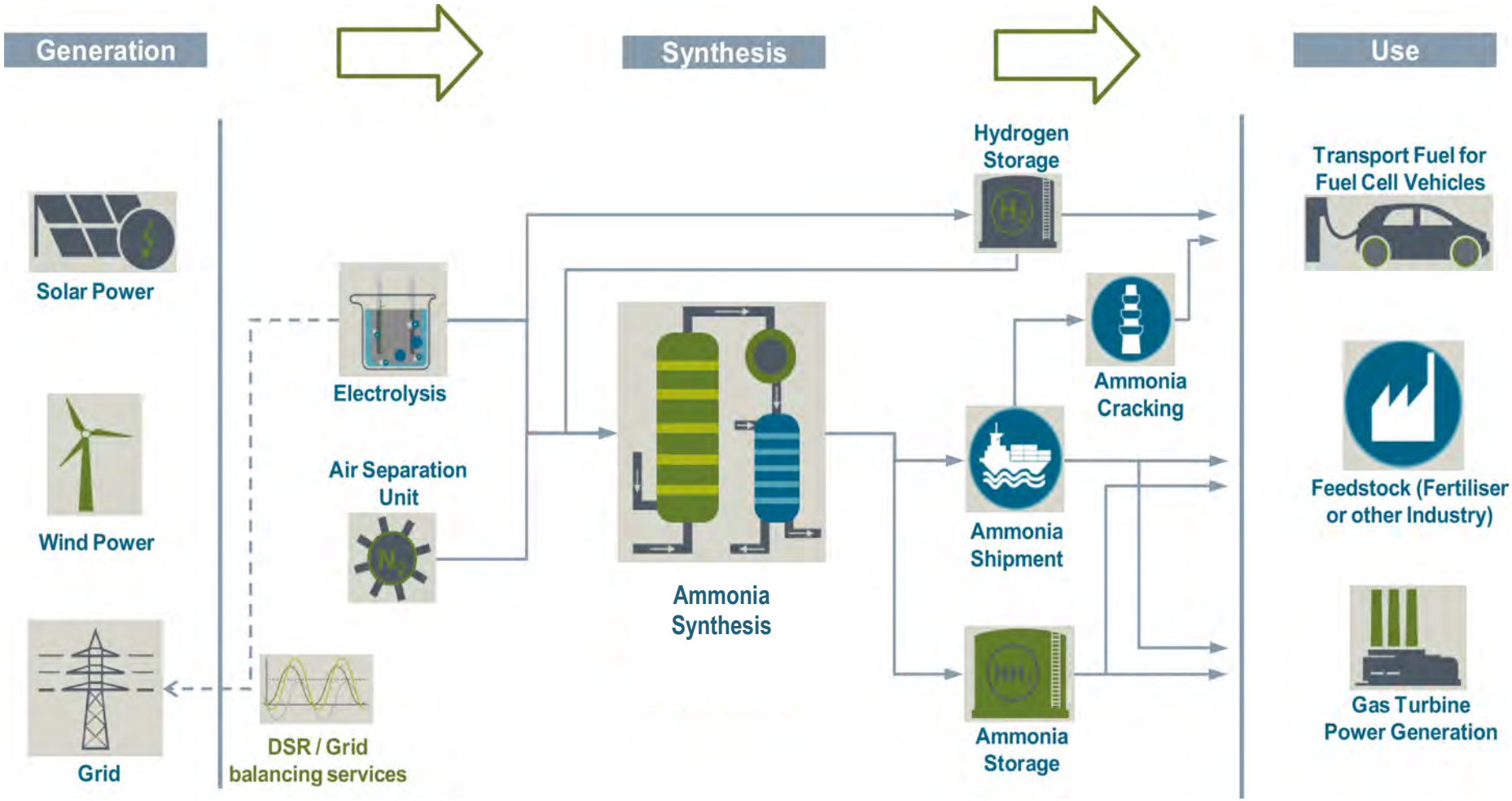

Valera-Medina et al., PECS, 69:63-102 (2018)

Combustion for Power and Transportation Is Here to Stay !!!

Home / 2024 / March / 10 / Sobering Up? EU May Scrap Its Plans To Ban Internal Combustion Engines By 2035

NEWS

06 Jun 2025, 13:04 Sören Amelang | EU

German car industry calls for reversal of EU 2035 combustion engine ban

#Cars #Industry #Policy #EU

CLIMATE POLITICS EVS

Sobering Up? EU May Scrap Its Plans To Ban Internal Combustion Engines By 2035

2 months ago Guest Blogger

From the NoTricksZone

By P Gosselin

After vote in Brussels last Monday evening, a majority of the European Parliament favored a Commission proposal that would no longer automatically classify electric cars as climate-neutral vehicles.

CERP Research Areas

Research Environment Forecast

- Hydrocarbon will be important fuels due to high energy density and ability to make use of existing infrastructure
- Hydrogen and its carriers will accelerate in importance as production cost continues to decrease
- Petroleum will be utilized in difficult-to-decarbonize sectors like aviation and marine propulsion
- CO_2 reduction will drive combustion to extreme conditions
- To achieve a circular carbon economy, cost effective, scalable carbon capture and utilization is essential

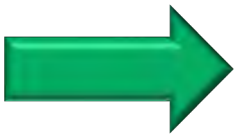

Research Directions

- Efficiency gains and emissions reductions
- Fuel formulation and diversity, sustainable aviation fuels (SAF)
- Valorization of fossil fuel resources
- Innovative combustion concepts and thermodynamic cycles
- Production of hydrogen and renewable fuels, electrolysis and photocatalysis
- Organic materials for energy storage
- Carbon capture, utilization, and storage (CCUS) processes
- Computational predictive tool development
- AI and ML tools

Ammonia/Hydrogen Research in CERP

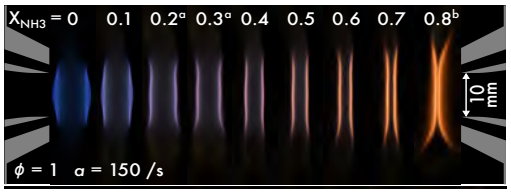

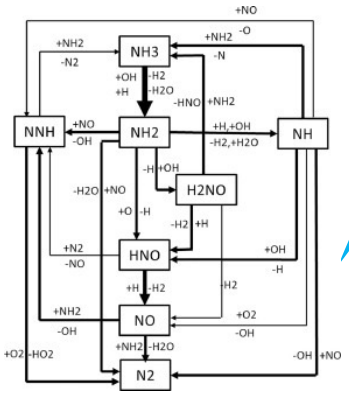

Chemical Kinetics

Flame Speed

Laminar Flames

Turbulent Flames

Industrial applications

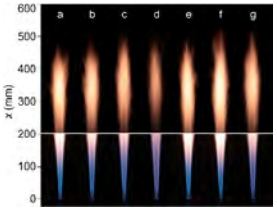

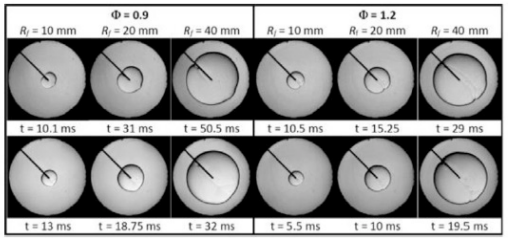

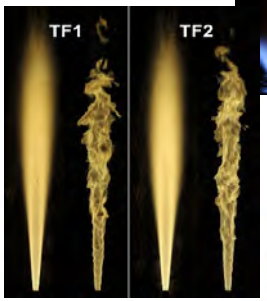

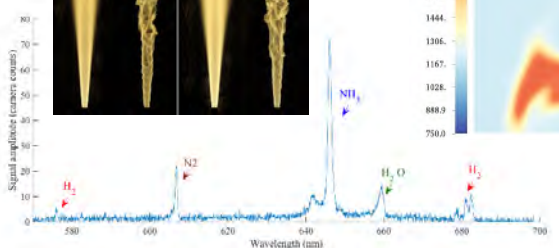

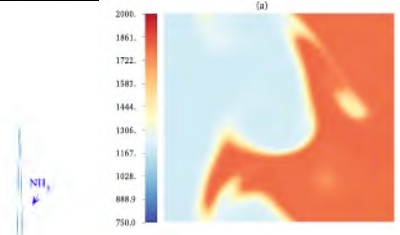

Towards Efficient and Clean Combustion

- High pressure
- Lean burn
- Preheated (MILD)
- Mixed-mode
- Fuel flexible
- CO2

Highly complex!!

Echogen

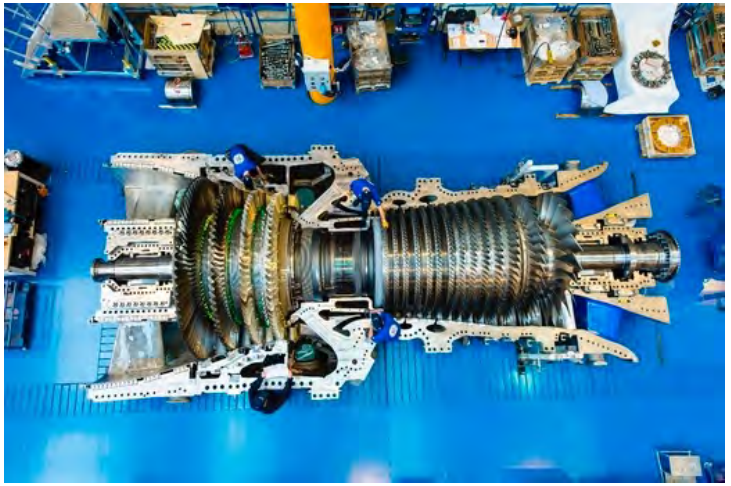

GE 9HA gas turbine

Mazda Skyactive X

Turbulent Combustion

Why is it so difficult?

Challenges in Turbulent Combustion Research

Large dimensionality

- Number of unknown variables ~ 10-1000s

Large scale disparity

- Spectrum of length scales increases with Re, Da
- Spectrum of chemical time scales varies widely for many reactions

Nonlinearity

- Chemical reactions with large activation energy

Randomness

- Many critical events (flashback, knock, blow-off) are rare and difficult to predict.

Multi-phase

- Liquid spray evaporation
- Soot formation

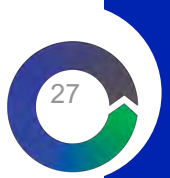

Role of Research in Design, Development & Control

Provide insights into fundamental characteristics

- e.g., effects of pressure on flame speed, soot production

Data analysis to find the scaling laws

- e.g. flame speed behavior, extinction limits, POD analysis for dominant modes

Prediction of quantitative outcome

- e.g. high fidelity simulation, non-intrusive diagnostics

Reduced order models for rapid design

- e.g. engineering correlations, digital twins

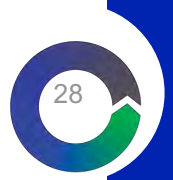

Use minimal complexity to answer questions

Beware of overkill!

Laminar vs. turbulent

- Does your question require full 3D turbulent flames?

Chemical complexity

- A few species may be ok to predict flame speed, but a bigger mechanism is needed to predict pollutant formation.

RANS vs. LES

- Steady operation vs. random anomaly (e.g. extinction, knock)

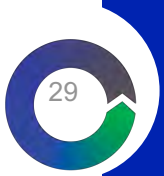

Outline of Course

Day 1: Laminar flame theory (69 slides)

- Basic equations
- The S-curve, asymptotic analysis and scaling
- Modeling of canonical flames

Day 2: Turbulent flow and flame physics (85 slides)

- Statistical theory of turbulence
- Turbulent combustion regimes
- Turbulent burning velocities and revised regime diagram

Day 3: Turbulent combustion modeling (97 slides)

- Modeling of premixed combustion
- Modeling of nonpremixed combustion
- Modeling of mixed-mode combustion

Day 4: Accelerated high fidelity simulation (43 slides)

- Reduced chemistry and GPU acceleration
- ROM for dimensional and time scale reduction

Day 5: AI for fluid dynamics and combustion (76 slides)

- Machine learning basics
- ML for closure models and feature extraction
- Data-based ROM for dynamics
- Generative algorithms, LLM

References

Physical Concepts:

Liñán, A., Williams, F.A., Fundamental Aspects of Combustion, Oxford University Press, 1993 (Out of print).

Law, C. K., Combustion Physics, Cambridge University Press, 2006.

Peters, N., Turbulent Combustion, Cambridge University Press, 2000.

Pope, S. B., Turbulent Flows, Cambridge University Press, 2000.

Advanced Modeling:

De, S., Agarwal, A.K., Chaudhuri, S., Sen, S., ed., Modeling and Simulation of Turbulent Combustion, Springer, 2018.

Echekki, T., Mastorakos, E., Turbulent Combustion Modeling: Advances, New Trends and Perspectives, Springer, 2011.

Poinsot, T., Veynante, D., Theoretical and Numerical Combustion, 2nd ed., Edwards, 2005.

Swaminathan, N., Bray, K.N.C. (Ed), Turbulent Premixed Flames, Cambridge University Press, 2011.

Fox, R.O., Computational Models for Turbulent Reactive Flows, Cambridge University Press, 2003.

جامعة الملك عبدالله للعلوم والتقنية
King Abdullah University of Science and Technology

Clean Energy Research Platform

Tsinghua-Princeton-Combustion Institute
2025 Summer School on Combustion
Tsinghua University, July 7-11, 2025

Turbulent Combustion

Day 1: Laminar Flame Theory

Hong G. Im
Clean Energy Research Platform (CERP)
King Abdullah University of Science and Technology (KAUST)

Combustion Basics

Classification and Formulation

Classification of Combustion Modes

Premixed	Nonpremixed	Partially Premixed
Bunsen burner	Match light	Lifted jet flame (?)
SI engine	Natural fire	Turbulent combustion with extinction/reignition
Solid propellant rocket	Droplet/spray	Two-stage combustion
Low-NOx gas turbine	Diesel engine	Mixed mode IC engine combustion
	Coal combustion	
	Aircraft turbine	

Combustion = Mixing (transport) + Reaction

Premixed: Reactants are mixed at molecular level prior to combustion

Nonpremixed: Reactants are mixed as they burn.

Partially premixed: Featuring both modes simultaneously

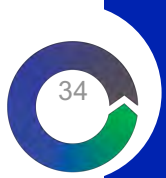

Premixed vs. Nonpremixed Flames

Premixed	Nonpremixed
Reaction-controlled	**Transport-controlled**
$S_L \sim [\alpha RR]^{1/2}$	**$S_L = 0$**
$T_f = f(\phi)$	**$T_f \simeq T_{ad}$**
Burning rate ~ S_L	**Burning rate ~ transport**
Infinite chemistry impossible	**Burning rate is finite even for infinite chemistry**

Combustion = Mixing (transport) + Reaction

Premixed: Kinetically controlled (reactant mixing not necessary)

Burning rate ~ flame propagation speed

Nonpremixed: Mixing controlled (fast reaction)

Burning rate ~ reactant transport rate (up to a certain limit)

Other Classifications

Based on flow conditions

- **Laminar flames:**
  - Low Reynolds number flows, well-defined structures
  - One-dimensional, deterministic analysis
- **Turbulent flames:**
  - High Reynolds number flows, random nature
  - Various regimes (flamelet, distributed, etc.)
  - Transient, 3-D, statistic analysis

Based on phases involved

- **Homogeneous: single phase**
  - Gaseous or aqueous
- **Heterogeneous: multi-phase**
  - Droplet, coal, metal combustion
  - May or may not involve surface reactions

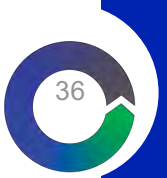

Basic Structure of a Premixed Flame

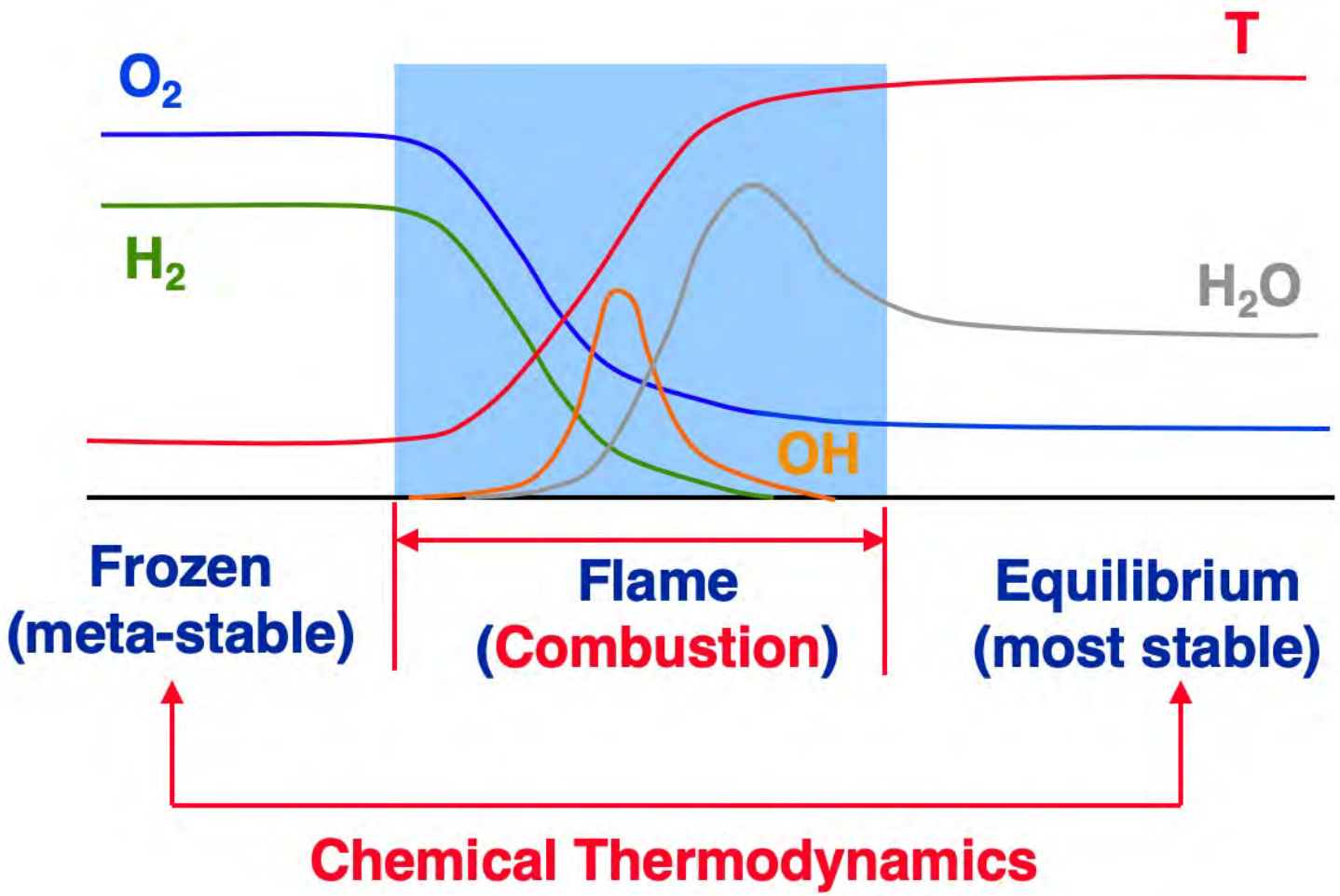

Review of Asymptotic Theory

Scaling is everything!

Key Nondimensional Parameters in Combustion

Damköhler Number:

$$\mathrm{Da} = \frac{B}{\kappa} = \frac{\text{Characteristic Reaction Rate}}{\text{Characteristic Flow Rate}} \sim \frac{1}{\chi}$$

Zeldovich Number:

$$\mathrm{Ze} = \frac{E_a}{RT_c} = \text{Nondimensional Activation Energy}$$

For typical combustion systems, Da and Ze are large.

- Turbulence may reduce Da, but not Ze
- For actual systems, there exist a number of chemical time scales, making a definite characterization difficult.

Effects of Da and Ze: Laminar Nonpremixed Flames

Effect of Da

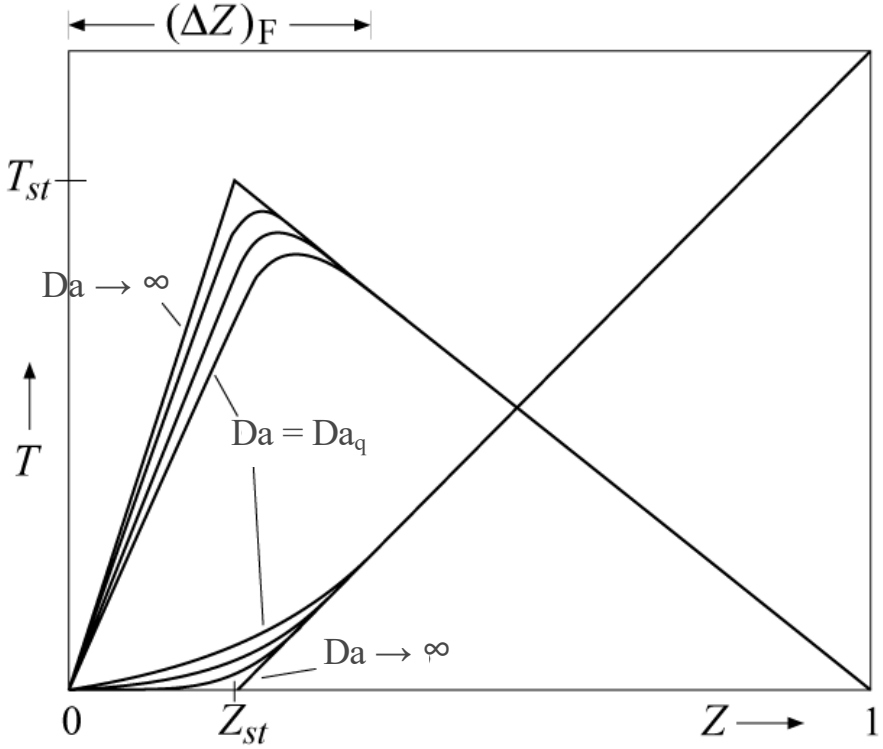

Effect of Ze

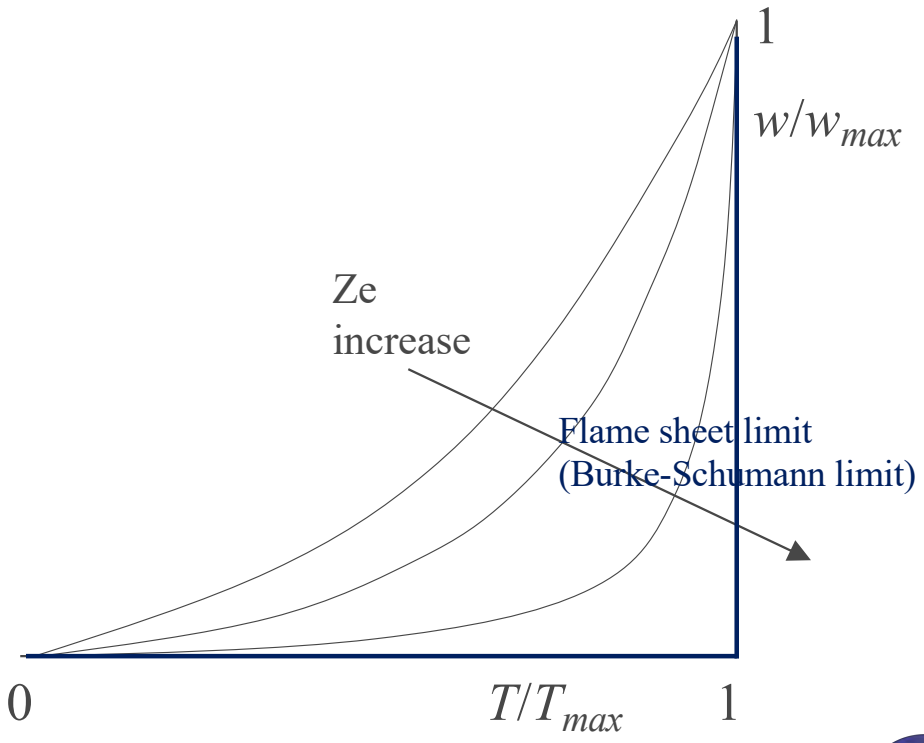

Physical flame thickness $\sim \frac{1}{|\nabla Z|} \sim \frac{1}{\sqrt{\chi}}$

For nonpremixed flames, Ze → ∞ is a valid asymptotic limit.

Effects of Da and Ze: Laminar Premixed Flames

Effect of Da

Not so simple; e.g. for equi-diffusive flames (Le = 1),

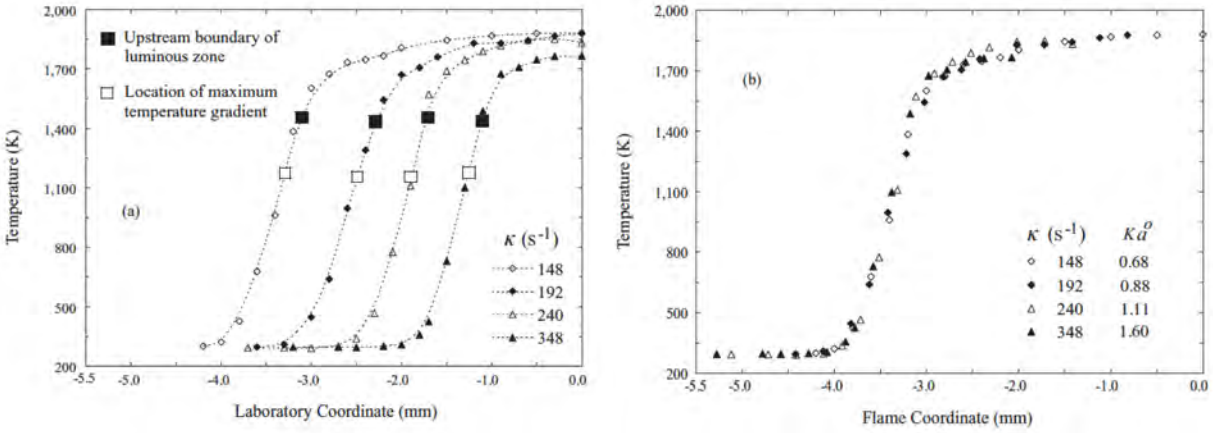

Law, C. K., Combustion Physics (2006).

Effect of Ze

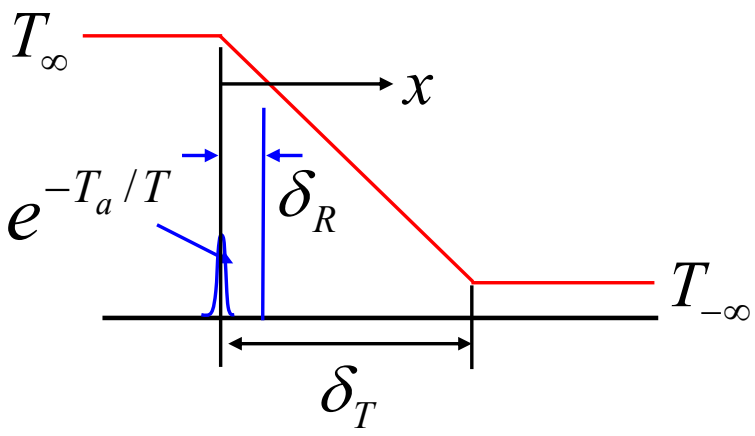

$$e^{-\frac{T_a}{T}} = \exp\left(-\frac{T_a}{T_\infty}\right)\exp(-\mathrm{Ze}\frac{x}{\delta_T})$$

$$\mathrm{Ze} = \frac{T_a(T_\infty - T_{-\infty})}{T_\infty^2} \sim \frac{\delta_T}{\delta_R}$$

Effects of strain rates are not directly translated to the flame thickness.

For premixed flames, Ze → ∞ is NOT a valid asymptotic limit.

The S-Curve: Steady Combustion Response

The S-Curve Behavior:
Characteristic of Reaction Nonlinearity with Large Activation Energy

- Ignition: as Da is increased from the frozen limit, the mixture becomes increasingly reactive, and reaches a point at which loss cannot balance generation.
- Extinction: as Da is decreased from the equilibrium limit, the flame becomes weaker, and reaches a point at which the reaction cannot be sustained.
- Note that the S-curve shows the STEADY response, and does not tell us about how long it takes to ignite or extinguish.

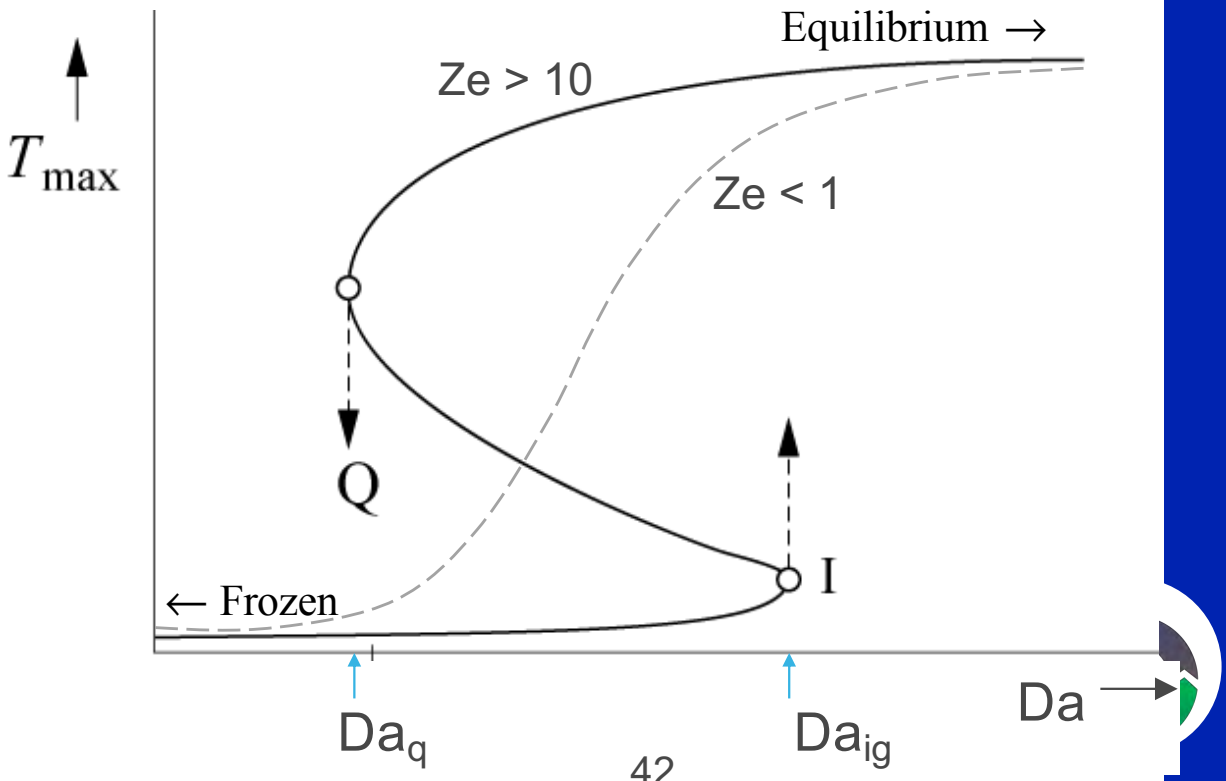

Steady/Unsteady Combustion Characteristics

Unsteady dynamics overlaid on the steady S-curve

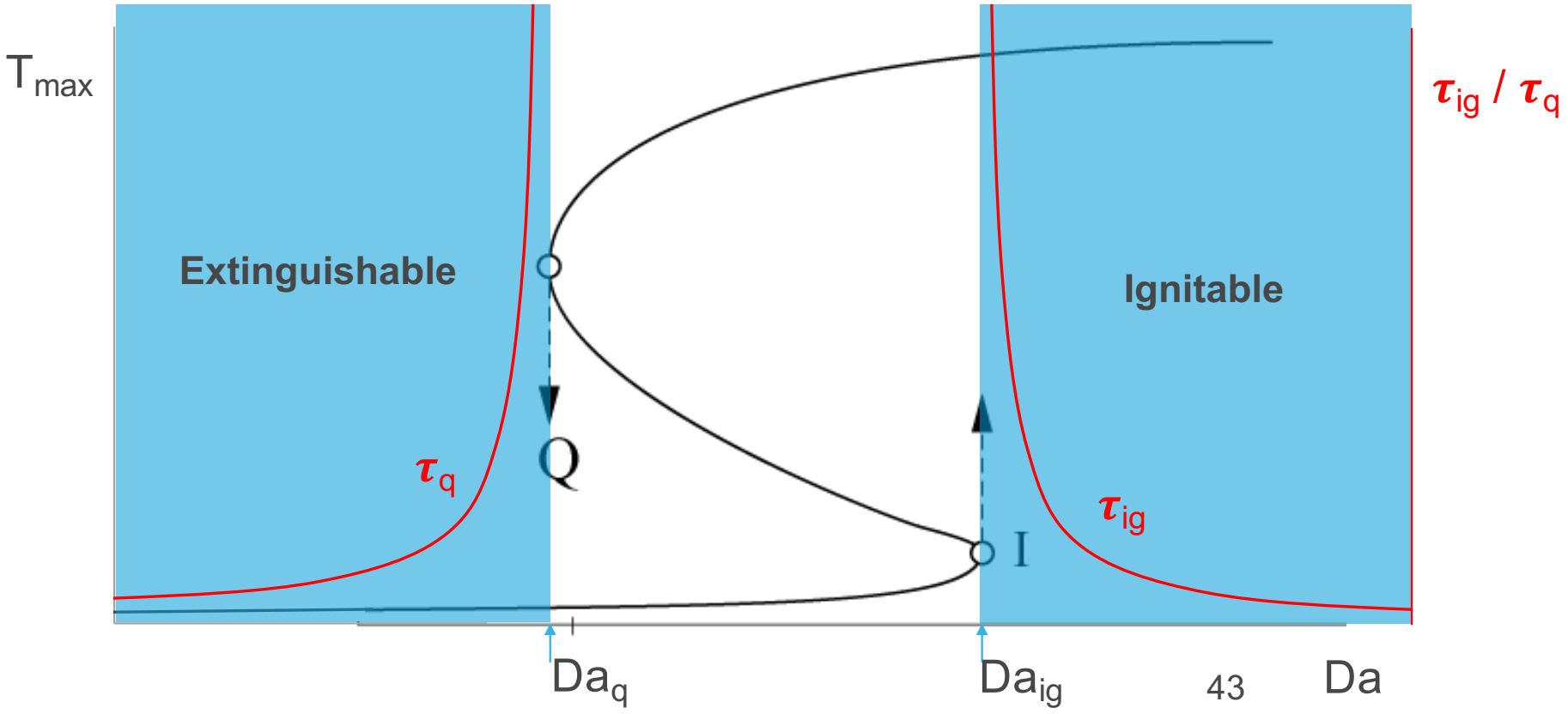

Basic Nonpremixed Flame Analysis

One-step irreversible reaction: $\nu_F[F]+\nu_O[O]\rightarrow[P]$

and assume no convective velocity:

$$\frac{d}{dx}\left[\frac{\lambda}{c_p}\frac{d(c_pT)}{dx}\right]=-Qw_F \qquad Q=\frac{\sum h_{f,i}^0 W_i(\nu_i''-\nu_i')}{-W_F\nu_F}$$

$$\frac{d}{dx}\left[\rho D_F\frac{dY_F}{dx}\right]=w_F=-W_F\nu_F AT^{\beta}c_Fc_O\exp(-E/RT)$$

$$\frac{d}{dx}\left[\rho D_O\frac{dY_O}{dx}\right]=\gamma w_F \qquad \gamma=W_O\nu_O/W_F\nu_F$$

Boundary conditions:

$$x=0:\ T=T_0,\ Y_F=Y_{F,0},\ Y_O=0$$

$$x=L:\ T=T_L,\ Y_F=0,\ Y_O=Y_{O,L}$$

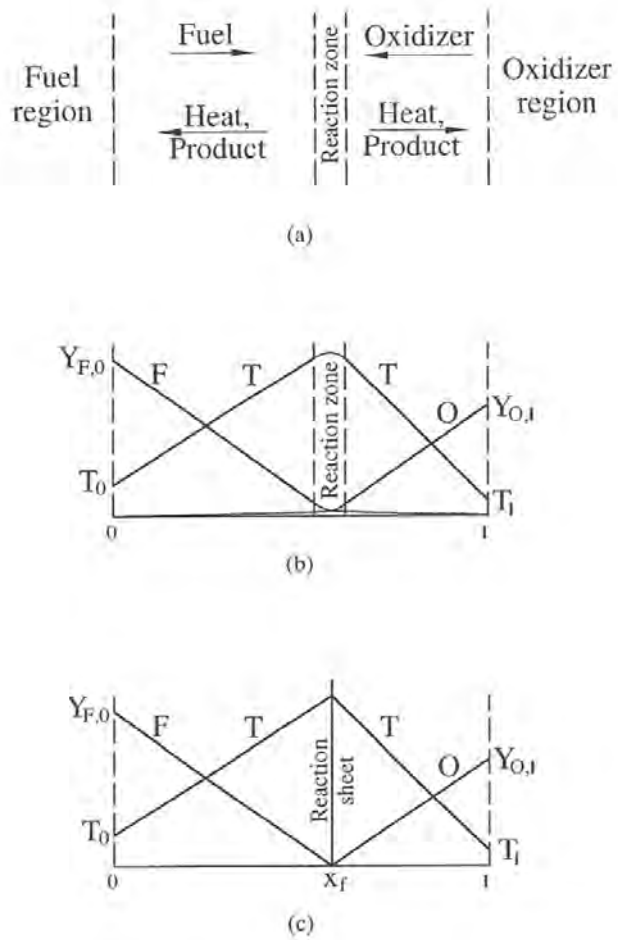

 From Law (2006)

Shvab-Zeldovich Coupling Function

Assume unity Lewis numbers,

$$Le_F = \lambda / \rho c_p D_F;\ Le_O = \lambda / \rho c_p D_O = 1 \qquad \text{and assuming} \quad \lambda / c_p = \text{constant}$$

Defining nondimensional variables $\theta = c_p T / Q Y_{F,0},\ \psi_F = Y_F / Y_{F,0},\ \psi_O = Y_O / \gamma Y_{F,0}$

$$-\frac{d^2\theta}{dx^2} = \frac{d^2\psi_F}{dx^2} = \frac{d^2\psi_O}{dx^2} = \frac{c_p}{\lambda Y_{F,0}} w_F$$

$$x = 0:\ \theta = \theta_0,\ \psi_F = 1,\ \psi_O = 0$$

$$x = L:\ \theta = \theta_L,\ \psi_F = 0,\ \psi_O = \psi_{O,L}\ \left(= 1 \text{ if stoichiometric}\right)$$

Defining coupling functions (2 independent ones): $\beta_F = \theta + \psi_F,\ \beta_O = \theta + \psi_O$

$$\frac{d^2\beta_F}{dx^2} = 0, \quad \frac{d^2\beta_O}{dx^2} = 0$$

The solutions:

$$\beta_F = \theta + \psi_F = (\theta_0 + 1) + (\theta_L - \theta_0 - 1)(x / L)$$

$$\beta_O = \theta + \psi_O = \theta_0 + (\theta_L + \psi_{O,L} - \theta_0)(x / L)$$

Note that these coupling functions are valid throughout the entire domain $0 \le x \le L$ regardless of reaction.

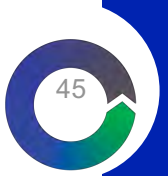

Flame-Sheet Limit and Jump Conditions

The flame sheet limit: $E \to \infty$

$\Rightarrow$ Reaction is confined within an infinitesimally thin layer.

Recognizing $\psi_F = 0$ for $x_f < x < L$ $\psi_O = 0$ for $0 < x < x_f$

The solutions for temperature & species concentration:

$$\left.\begin{aligned} \theta &= \theta_0 + \left(\theta_L + \psi_{O,L} - \theta_0\right)(x/L) \\ \psi_F &= 1 - x/x_f \\ \psi_O &= 0 \end{aligned}\right\} \text{ for } 0 < x < x_f \qquad \left.\begin{aligned} \theta &= (\theta_0 + 1) + (\theta_L - \theta_0 - 1)(x/L) \\ \psi_F &= 0 \\ \psi_O &= (x - x_f)/(L - x_f) \end{aligned}\right\} \text{ for } x_f < x < L$$

To determine the flame temperature and location, jump conditions are obtained by integrating the equation across the flame sheet:

$$\int_{x_f^-}^{x_f^+} \frac{d^2}{dx^2}(\theta + \psi_i)\,dx = 0 \quad \Rightarrow \quad \left[\frac{d\theta}{dx}\right]_{x_f^-}^{x_f^-} = -\left[\frac{d\psi_F}{dx}\right]_{x_f^-}^{x_f^-} \qquad \left[\frac{d\theta}{dx}\right]_{x_f^-}^{x_f^-} = \left[\frac{d\psi_O}{dx}\right]_{x_f^-}^{x_f^-}$$

Final Flame-Sheet Solution

The solutions:

$$x_f = \frac{L}{1+\psi_{O,L}}, \quad \theta_f = \frac{\theta_L + (\theta_0 + 1)\psi_{O,L}}{1+\psi_{O,L}}$$

In dimensional form:

$$x_f = \frac{L}{1 + Y_{O,L}/\gamma Y_{F,0}}$$

$$T_f = \left(\frac{T_L}{Y_{O,L}/\gamma} + \frac{T_0 + QY_{F,0}/c_p}{Y_{F,0}} \right) \left(\frac{1}{Y_{O,L}/\gamma} + \frac{1}{Y_{F,O}} \right)^{-1} \quad \Rightarrow \quad \frac{T_f - T_0}{Y_{F,0}} + \frac{T_f - T_L}{Y_{O,L}/\gamma} = \frac{Q}{c_p}$$

or

$$(T_f - T_0)\left(1 + \frac{1 - Y_{F,0}}{Y_{F,0}}\right) + \gamma (T_f - T_L)\left(1 + \frac{1 - Y_{O,L}}{Y_{O,L}}\right) = \frac{Q}{c_p}$$

fuel inert in fuel side — oxid. inert in oxid. side

Adiabatic flame temperature

Summary of Nonpremixed Flame Solutions

Schematic of solution variables for $\psi_{O,L} = 1$ (stoichiometric)

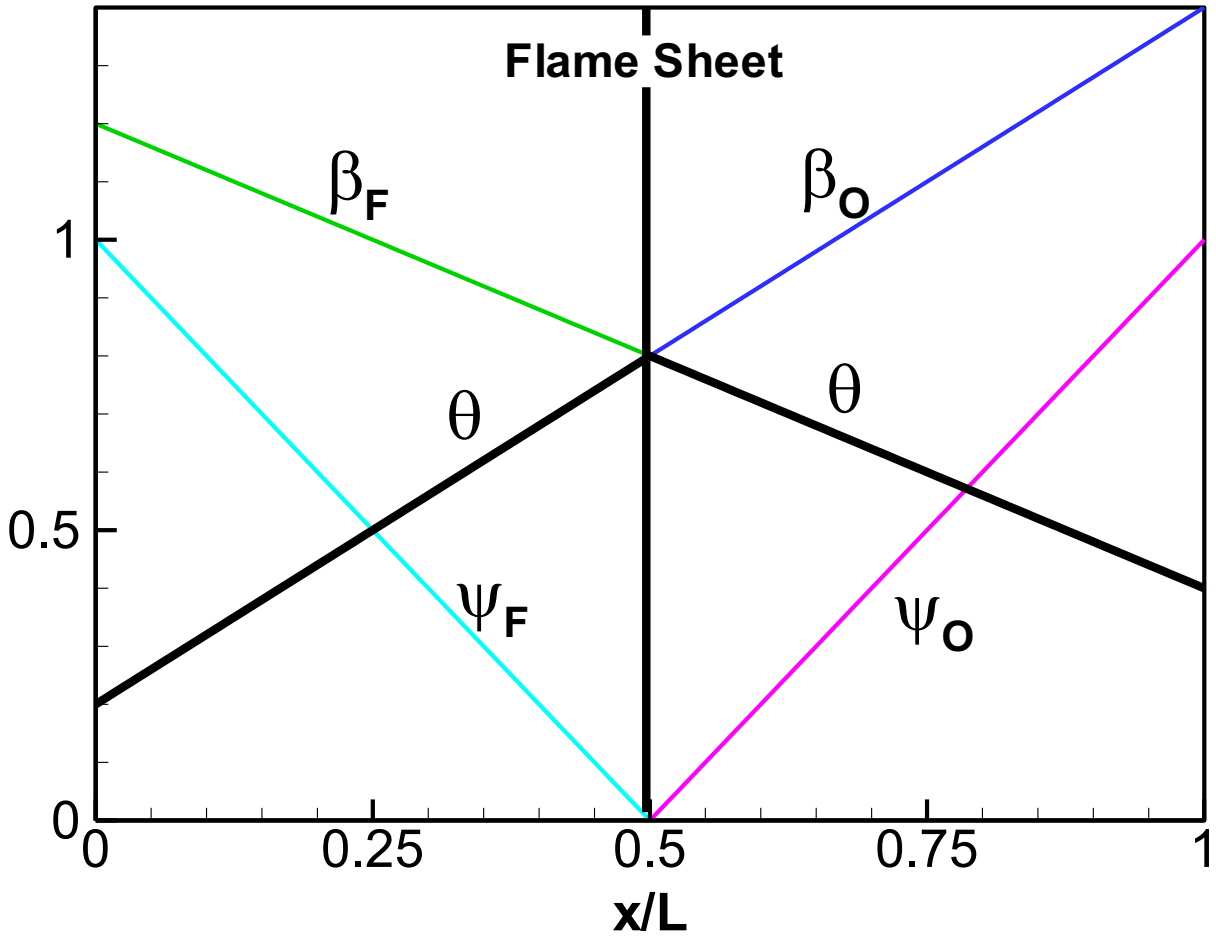

Counterflow Nonpremixed Flames

One of the most commonly adopted configuration to study laminar nonpremixed flames.

- 1-D similarity solution for simple mathematical analysis (potential flow or opposed-jet flow)
- Easy experimental set-up (opposed-jet only)
- Parametric study on the aerodynamic effects on flames by allowing an ***independent*** control of the flow time scale (strain rate).

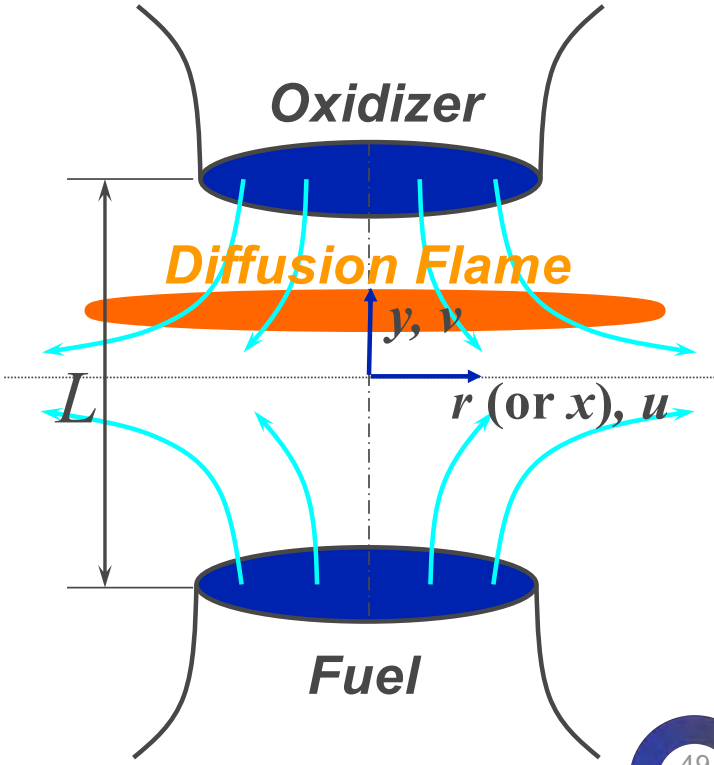

Acta Astronautica. Vol. 1, pp. 1007–1039. Pergamon Press 1974. Printed in the U.S.A.

The asymptotic structure of counterflow diffusion flames for large activation energies

AMABLE LIÑÁN

Instituto Nacional de Técnica Aeroespacial and Escuela Técnica Superior de Ingenieros Aeronáuticos, Madrid, Spain

(*Received* 7 *September* 1973)

Abstract—The structure of steady state diffusion flames is investigated by analyzing the mixing and chemical reaction of two opposed jets of fuel and oxidizer as a particular example. An Arrhenius one-step irreversible reaction has been considered in the realistic limit of large activation energies. The entire range of Damköhler numbers, or ratio of characteristic diffusion and chemical times, has been covered. When the resulting maximum temperature is plotted in terms of the Damköhler number (which is inversely proportional to the flow velocity) the characteristic S curve emerges from the analysis, with segments from the curve resulting from:

(a) A nearly frozen ignition regime where the temperature and concentrations deviations from its frozen flow values are small. The lower branch and bend of the S curve is covered by this regime.

(b) A partial burning regime, where both reactants cross the reaction zone toward regions of frozen flow. This regime is unstable.

(c) A premixed flame regime where only one of the reactants leaks through the reaction zone, which then separates a region of frozen flow from a region of near-equilibrium.

(d) A near-equilibrium diffusion controlled regime, covering the upper branch of the S curve, with a thin reaction zone separating two regions of equilibrium flow.

Analytical expressions are obtained, in particular, for the ignition and extinction conditions.

1D Potential Flow Formulation

Axisymmetric Geometry (r,z)

$$u_r = \frac{a}{2} r, \quad u_z = -az$$

satisfies the continuity equation.

Energy & Species Equations $\left(\frac{\lambda}{\rho c_p} = D_F = D_O \right)$

$$u\frac{\partial \tilde{T}}{\partial \tilde{r}} + w\frac{\partial \tilde{T}}{\partial \tilde{z}} = D_F\left[\frac{\partial^2 \tilde{T}}{\partial \tilde{z}^2} + \frac{1}{\tilde{r}}\frac{\partial}{\partial \tilde{r}}\left(\tilde{r}\frac{\partial \tilde{T}}{\partial \tilde{r}}\right)\right] + \frac{Q}{c_p} w_F$$

$$u\frac{\partial Y_F}{\partial \tilde{r}} + w\frac{\partial Y_F}{\partial \tilde{z}} = D_F\left[\frac{\partial^2 Y_F}{\partial \tilde{z}^2} + \frac{1}{\tilde{r}}\frac{\partial}{\partial \tilde{r}}\left(\tilde{r}\frac{\partial Y_F}{\partial \tilde{r}}\right)\right] + w_F$$

$$u\frac{\partial Y_O}{\partial \tilde{r}} + w\frac{\partial Y_O}{\partial \tilde{z}} = D_F\left[\frac{\partial^2 Y_O}{\partial \tilde{z}^2} + \frac{1}{\tilde{r}}\frac{\partial}{\partial \tilde{r}}\left(\tilde{r}\frac{\partial Y_O}{\partial \tilde{r}}\right)\right] + \nu w_F$$

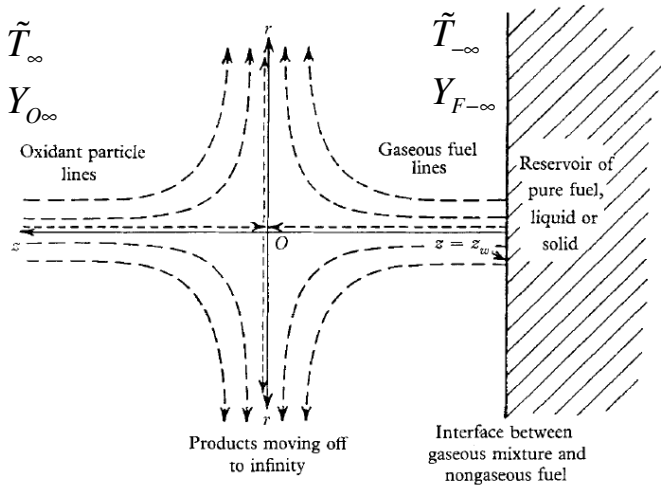

Fendell, F.E., J. Fluid Mech. 21: 281-303 (1965)

$$[F] + \nu_O [O] \rightarrow [P]$$

$$w_F = Z Y_O Y_F \exp\left(-E / R\tilde{T}\right)$$

$$\nu = \frac{\nu_O W_O}{W_F}$$

Mathematical Reduction: Similarity Transformation

Nondimensional Variables

$$T = \frac{c_P \tilde{T}}{Q Y_{F-\infty}}, \quad y_F = \frac{Y_F}{Y_{F-\infty}}, \quad y_O = \frac{Y_O}{\nu Y_{F-\infty}}$$

$$r = \left(a / D_F\right)^{1/2} \tilde{r}, \quad z = \left(2a / D_F\right)^{1/2} \tilde{z}$$

Similarity approximation (Fendell, 1965)

$$T = T(z), \; y_i = y_i(z) \; (i = F, O)$$

Coordinate transformation

$$x = \frac{1}{2}\operatorname{erfc}\left(\frac{z}{\sqrt{2}}\right) = \frac{1}{\sqrt{\pi}} \int_{z/\sqrt{2}}^{\infty} e^{-y^2} \, dy$$

so that $x = 0, \; z \to \infty; \quad x = 1, \; z \to -\infty$

Transformed Governing Equations

$$\frac{d^2 T}{dx^2} = -2\pi \exp\left(z^2\right) D y_O y_F \exp\left(-T_a / T\right)$$

$$\frac{d^2}{dx^2}\left(T + y_F\right) = 0$$

$$\frac{d^2}{dx^2}\left(T + y_O\right) = 0$$

Boundary conditions:

$x = 1$:

$$T = T_\infty - \beta, \; y_F = 1, \; y_O = 0$$

$x = 0$:

$$T = T_\infty, \quad y_F = 0, \; y_O = \alpha$$

$$\alpha = \frac{Y_{O\infty}}{\nu Y_{F-\infty}}, \; \beta = T_\infty - T_{-\infty}$$

Mathematical Reduction: Coupling Function

Coupling Function Solutions

$$\frac{d^2}{dx^2}\left(T + y_F\right) = 0 \qquad \frac{d^2}{dx^2}\left(T + y_O\right) = 0$$

$$y_F = x + T_f - T$$

$$y_O = \alpha\left(1 - x\right) + T_f - T$$

$$T_f = T_\infty - \beta x \quad \text{(frozen solution)}$$

$$x = \frac{1}{2}\operatorname{erfc}\left(\frac{z}{\sqrt{2}}\right)$$

Boundary conditions:

$x = 1$:

$$T = T_\infty - \beta,\ y_F = 1,\ y_O = 0$$

$x = 0$:

$$T = T_\infty,\ \ y_F = 0,\ y_O = \alpha$$

$$\alpha = \frac{Y_{O\infty}}{\nu Y_{F-\infty}},\ \beta = T_\infty - T_{-\infty}$$

The problem boils down to:

$$\frac{d^2T}{dx^2} = -2\pi \exp\left(z^2\right) D y_O(T) y_F(T) \exp\left(-T_a / T\right)$$

$$x = 0 : T = T_\infty; \qquad x = 1 : T = T_\infty - \beta,$$

Base Solutions

Base solutions: $$\frac{d^2T}{dx^2} = -2\pi \exp\left(z^2\right) D y_O y_F \exp\left(-T_a / T\right)$$

$$x = 0 : T = T_\infty; \qquad x = 1 : T = T_\infty - \beta,$$

$$\alpha = \frac{Y_{O\infty}}{\nu Y_{F-\infty}}, \quad \beta = T_\infty - T_{-\infty}$$

Frozen flow:

$$\frac{d^2T}{dx^2} = 0 \;\Rightarrow\; T_f = T_\infty - \beta x$$

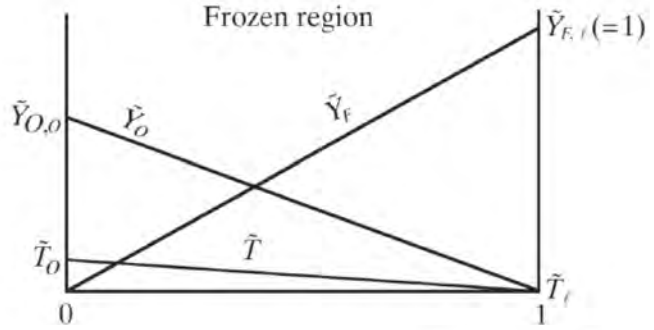

Equilibrium flow:

$$0 < x < x_e \text{ (Oxidizer side):} \qquad T = x + T_\infty - \beta x$$

$$x_e < x < 1 \text{ (Fuel side):} \qquad T = \alpha(1 - x) + T_\infty - \beta x$$

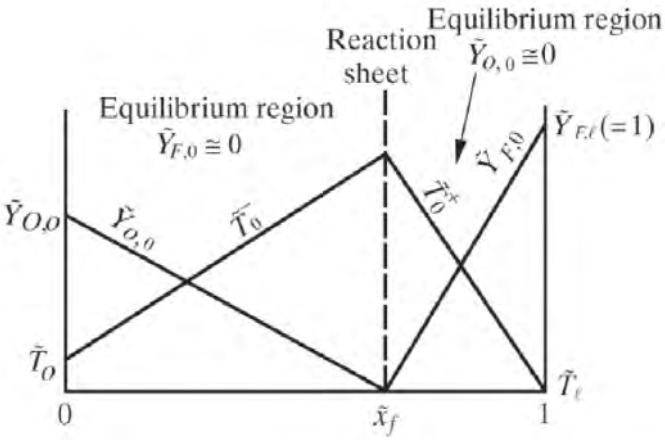

Liñán's Regimes

D.F.: Diffusion Flame, P.F.: Premixed Flame, F.F.: Frozen Flow, P.B.: Partial Burning

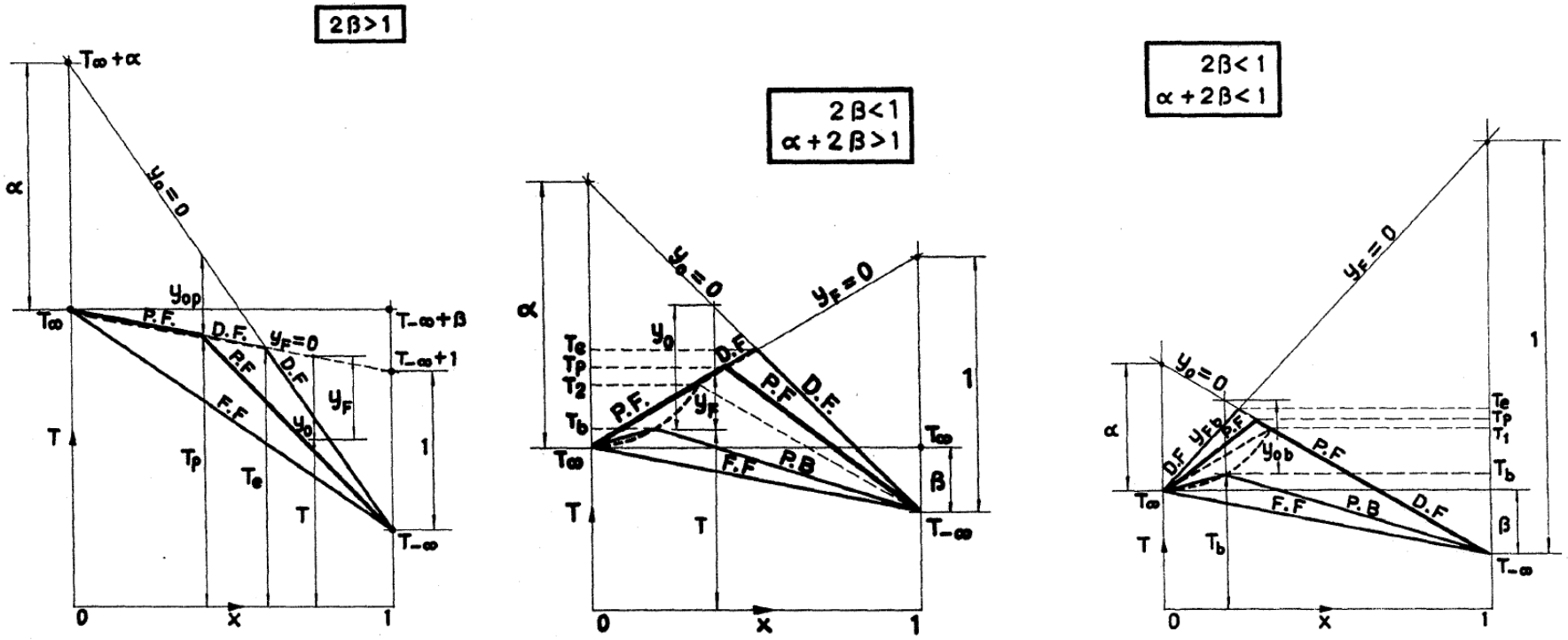

Generalized theory allows the analysis of premixed flames (in the P.F. regime)

Extinction Analysis in Near-Equilibrium Regime

The inner reactive-diffusive zone equation:

$$\frac{d^2\beta_1}{d\xi^2} = (\beta_1 - \xi)(\beta_1 + \xi)\exp\left\{-\delta_0^{-1/3}(\beta_1 + \gamma\xi)\right\}$$

with boundary conditions:

$$\frac{d\beta_1}{d\xi} = 1, \quad \xi \to \infty; \quad \frac{d\beta_1}{d\xi} = -1, \quad \xi \to -\infty$$

Reduced Damköhler number at extinction:

$$\delta_{0E} = e\left\{(1-\gamma) - (1-\gamma)^2 + 0.26(1-\gamma)^3 + 0.055(1-\gamma)^4\right\}$$

For small values of $(1-\gamma)$

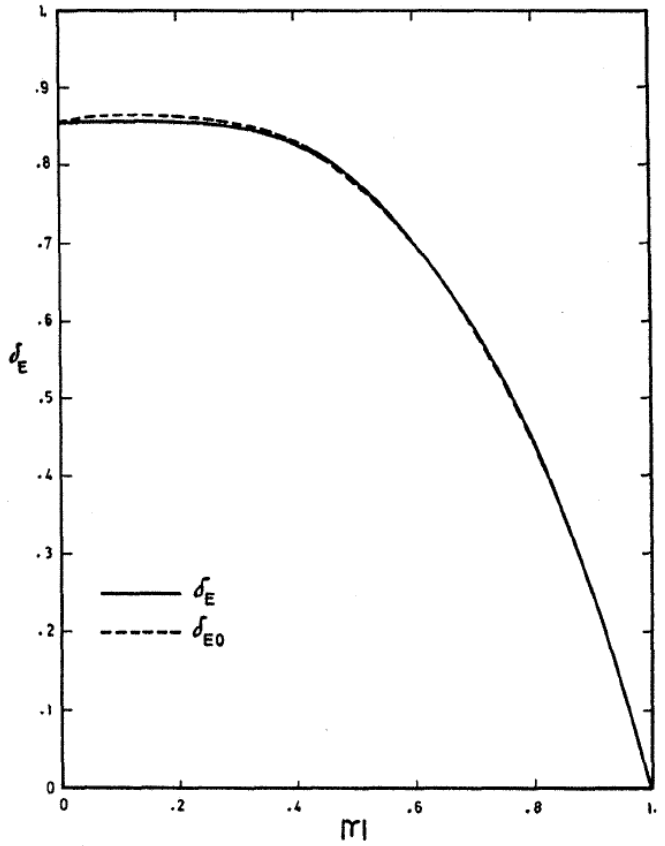

Fig. 12. The first approximation for the Damköhler number of extinction δ_E is shown as a function of $|\gamma|$, as obtained from the numerical solutions (solid line) and as given by Eq. (82) (dashed line).

Ignition Analysis in Nearly Frozen Regime

For hot boundary ignition $\beta = T_\infty - T_{-\infty} = O(1)$

The inner structure equation:

$$\chi^2 \frac{d^2\theta_1}{d\chi^2} = -\Delta\left(\chi - \beta\theta_1\right)\exp\left(\theta_1 - \chi\right)$$

$$\theta_1(0) = 0, \quad \frac{d\theta_1}{d\chi}(\infty) = 0$$

with the reduced Damköhler number:

$$\Delta = \beta^{-1} z_\varepsilon^{-2} \alpha D \exp\left(-T_a / T_\infty\right)$$

Correlations for the ignition criterion: $\beta = O(1)$

$$D_I \alpha \exp\left(-T_a / T_\infty\right) z_\varepsilon^{-2} \simeq 2e^{-2}\left(1-\beta\right)^{-2}\left(2\beta - \beta^2\right)$$

$$z_\varepsilon^2 = -\ln\left[8\pi\varepsilon^2 z_\varepsilon^2 / \beta^2\left(1-\beta\right)^2\right]$$

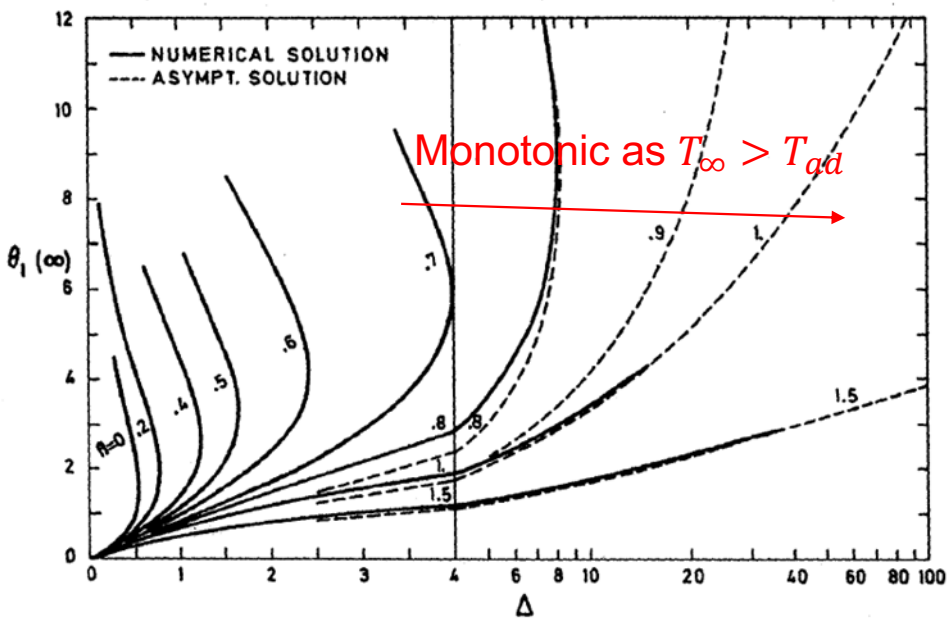

Go/No-go Criterion
(Ignition turning point)

Unsteady Ignition Analysis

Adiabatic system with a homogeneous reactant mixture.

$$\rho_0 c_v \frac{dT}{dt} = -Q_c \frac{dc_F}{dt} = BQ_c c_F \exp\left(-T_a / T\right) \qquad \text{I.C.:}\ \ T = T_0,\ c_F = c_{F,0};\ \ t = 0$$

Nondimensionalization:

$$\tilde{T} = \frac{c_v \rho_0 T}{Q_c c_{F,0}} = \frac{c_v T}{q_c Y_{F,0}};\ \ \tilde{c}_F = \frac{c_F}{c_{F,0}}$$

Coupling function: $\dfrac{d}{dt}\left(\tilde{T} + \tilde{c}_F\right) = 0;\ \ \tilde{T} - \tilde{T}_0 = 1 - \tilde{c}_F$

$$\frac{d\tilde{T}}{dt} = B\left(1 + \tilde{T}_0 - \tilde{T}\right)\exp\left(-\tilde{T}_a / \tilde{T}\right) \qquad \text{I.C.:}\ \ \tilde{T} = \tilde{T}_0;\ \ t = 0$$

Asymptotic expansion: $\tilde{T} = \tilde{T}_0 + \varepsilon\theta\left(t\right) + O\left(\varepsilon^2\right) \qquad \varepsilon = \tilde{T}_0^2 / \tilde{T}_0$

$$\tilde{c}_F = 1 + \tilde{T}_0 - \tilde{T} = 1 - \varepsilon\theta\left(t\right) \simeq 1 + O\left(\varepsilon\right)$$

Unsteady Ignition Analysis

The solution:

$$\frac{d\theta}{d\tau} = \exp(\theta)$$

I.C.: $\theta(\tau = 0) = 0$

$$\theta(\tau) = -\ln(1-\tau)$$

Ignition at $\tau = 1$

or

$$t_{ig} = t_c = \frac{\varepsilon}{B}\exp\left[\frac{\tilde{T}_a}{\tilde{T}_0}\right]$$

$$t_{ig} = \frac{c_v\left(\tilde{T}_0^2 / \tilde{T}_a\right)}{q_c Y_{F,0} B \exp\left(-\tilde{T}_a / \tilde{T}_0\right)}$$

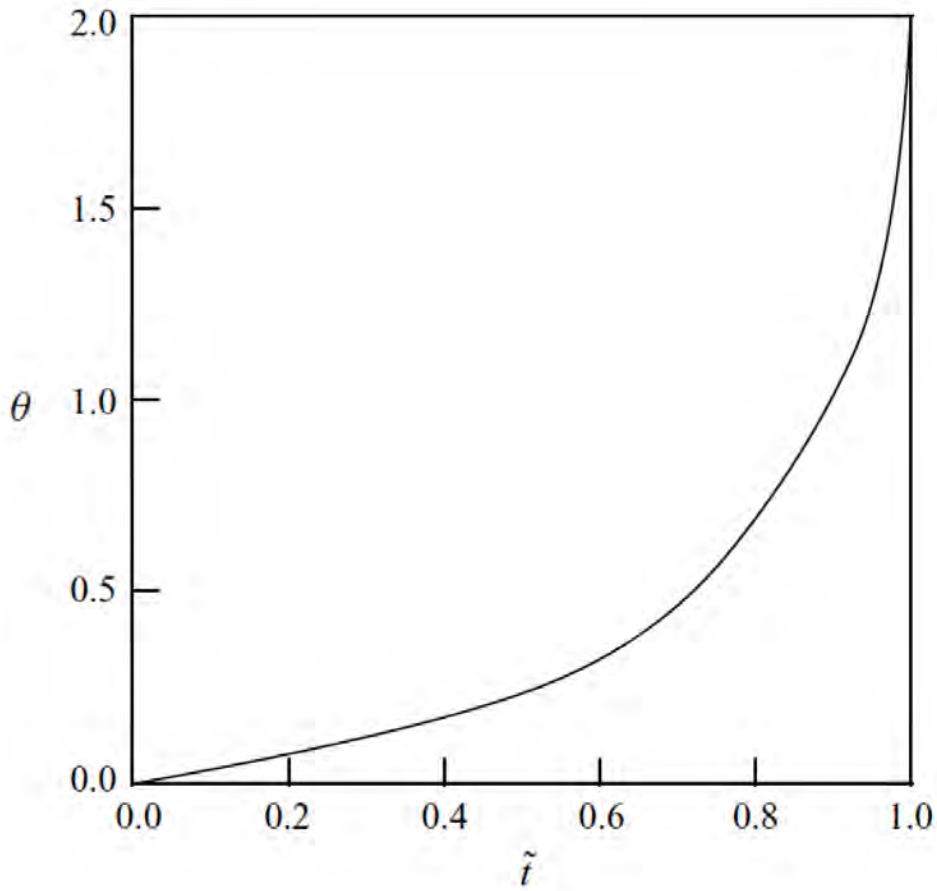

Law, Combustion Physics (2016)

Intrinsic Flame Instabilities

- Practical Relevance to Turbulent Combustion
  - Self-turbulization + Baroclinic Torque
    ⇒ Enhanced burning (turbulence-flame interaction)

- Primary Modes of Intrinsic Flame Instabilities
  - Hydrodynamic (Darrieus 1938, Landau 1944)
    - Streamline deformation due to thermal expansion
  - Diffusive-Thermal (Turing 1952, Sivashinsky 1977)
    - Thermal vs. mass diffusion imbalance
  - Buoyancy-Induced (Rayleigh 1883, Taylor 1950)
    - Gravitational acceleration of product gases
  - Viscosity-Induced (Saffman and Taylor 1958)
    - Combustion in a narrow channel

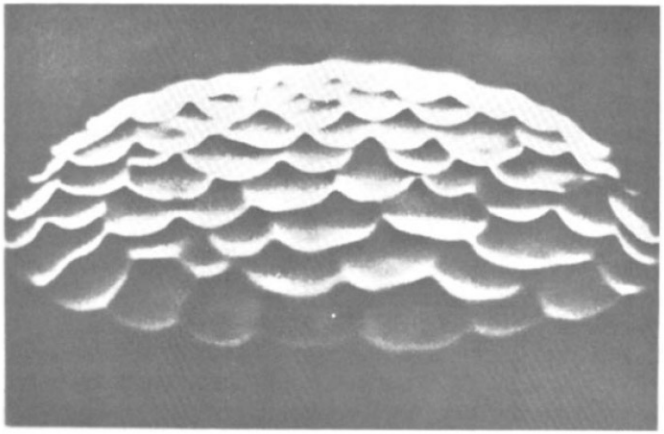

Rich propane-air cellular flame in state of chaotic self-motion (Sabathier et al., 1981)

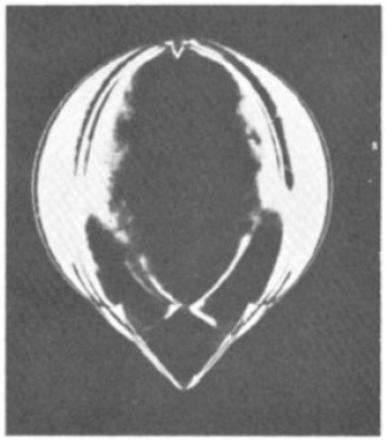

Lean butane-air (stable)

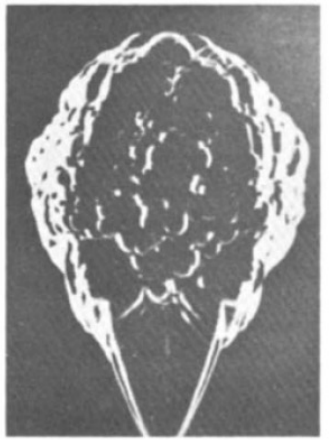

Lean hydrogen-air (unstable)

(Strehlow, 1968)

Darrieus-Landau Model (1945)

- Basic Assumptions
  - Constant flame speed, normal to the front
  - Flame is a discontinuous surface

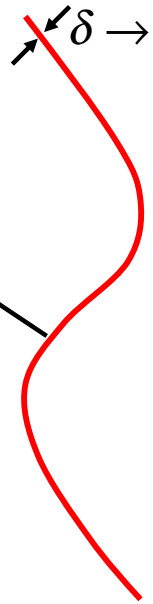

$$\delta = \ell_D / L \to 0$$

Unburned

$$\rho = 1$$
$$T = 1$$
$$Y = 1$$

$$\mathbf{n} = \frac{\nabla F}{|\nabla F|}$$

Burned

$$\rho = 1/(1+q)$$
$$T = 1+q$$
$$Y = 0$$

$$F(\mathbf{x},t) = x - f(y,z,t) = 0$$

Method of normal modes

$$\mathbf{v}' = \exp(\omega t + ik_1 y + ik_2 z)\bar{\mathbf{v}}$$
$$p' = \exp(\omega t + ik_1 y + ik_2 z)\bar{p}$$
$$f = \exp(\omega t + ik_1 y + ik_2 z)A$$

& Seek dispersion relation

$$\omega = \Im(k)$$

D-L Instability: Physical Mechanism

Dispersion relation: $(2+q)\omega^2 + 2(1+q)k\omega + qk\left[g-(1+q)k\right]=0$

Streamline deflection due to heat release

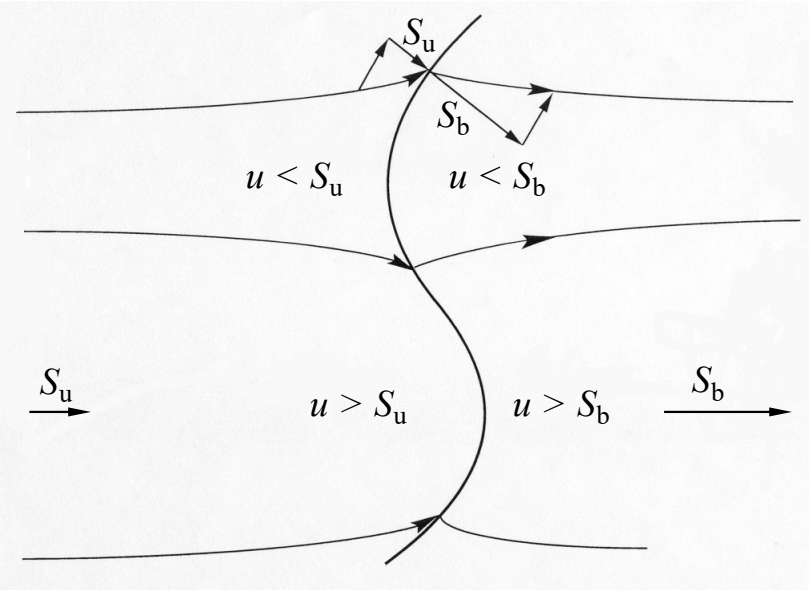

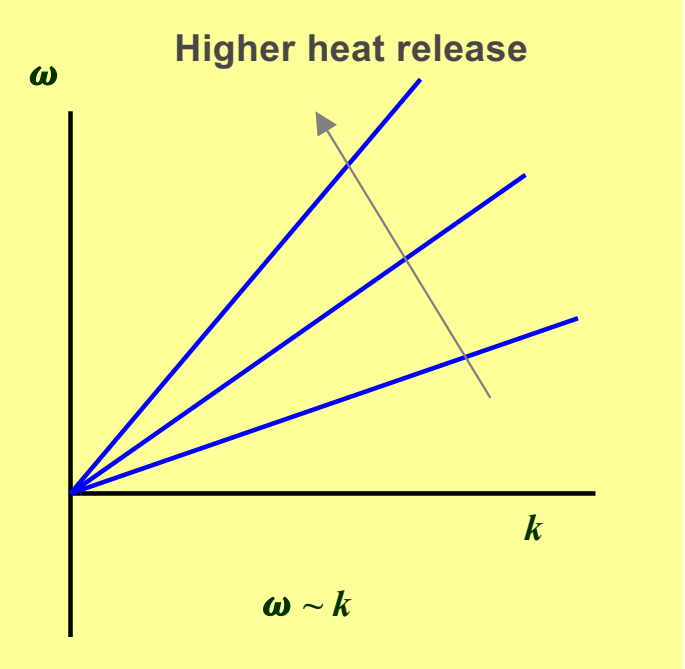

Paradox can be resolved by allowing variable S_L

$$S_L = 1-\mu\nabla^2 f = 1-\mu/R$$ Markstein (1950)

Unconditionally unstable!

Large Activation Energy Asymptotics

- Asymptotic Structure of a Premixed Flame
  Diffusive-Thermal Model: Sivashinsky (1979)

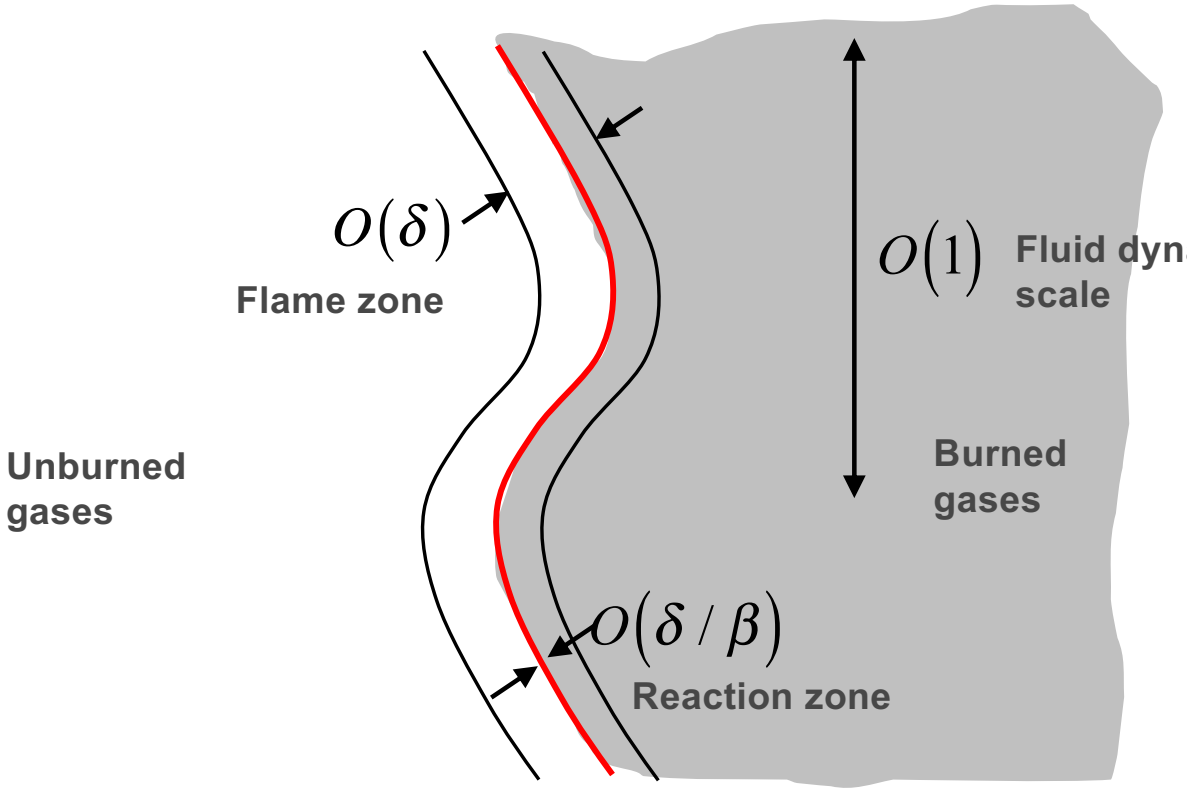

$$\frac{\ell_D}{L} = O(\delta)$$

$$\frac{\ell_R}{\ell_D} = O\left(\frac{1}{\beta}\right) = O(\varepsilon)$$

D-T Instability: Physical Mechanism

Dispersion Relation

$$64\omega^3+\left(192k^2+32+8l-l^2\right)\omega^2$$
$$+2\left(2+8k^2+l\right)\left(1+12k^2\right)\omega+\left(2+8k^2+l\right)^2k^2=0$$

$$l=(\mathrm{Le}-1)/\varepsilon$$

$$\mathrm{Le}=\frac{\alpha}{D}$$ **Lewis Number**

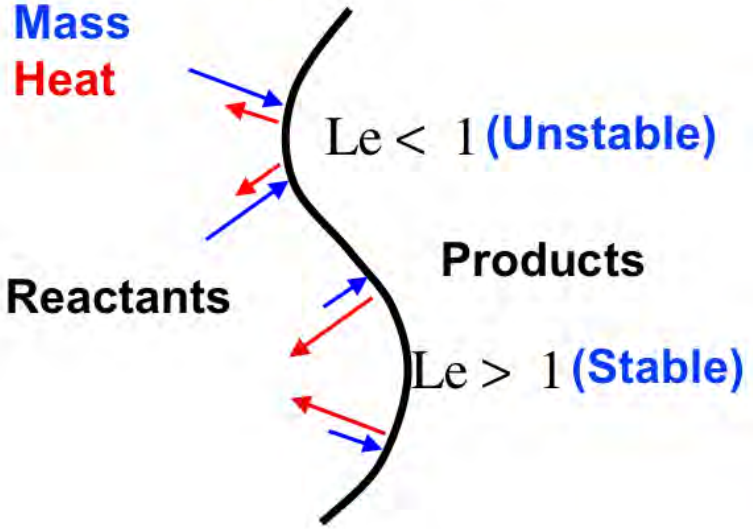

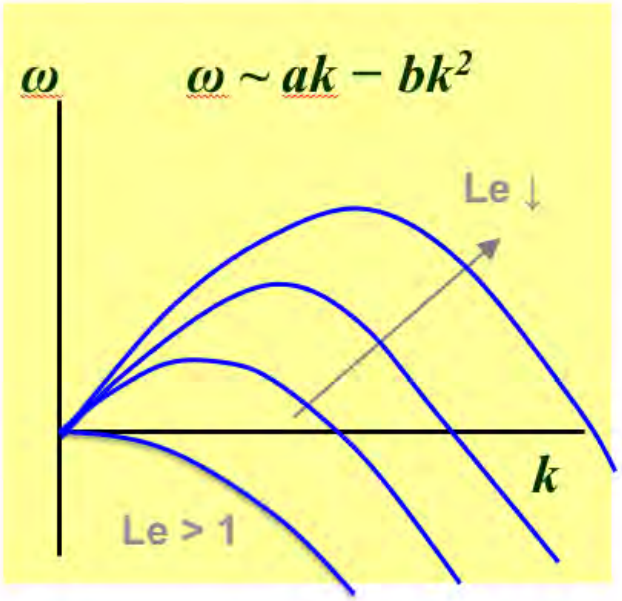

Short wave stabilizing

D-T Instability: Experimental Observation

Le < 1 (Unstable):
- Cellular instability

- **Lean H_2-air**
- **Rich C_3H_8-air**

Le > 1 (Stable):
- Hydrodynamic instability

- **Rich H2-air**
- **Lean C3H8-air**

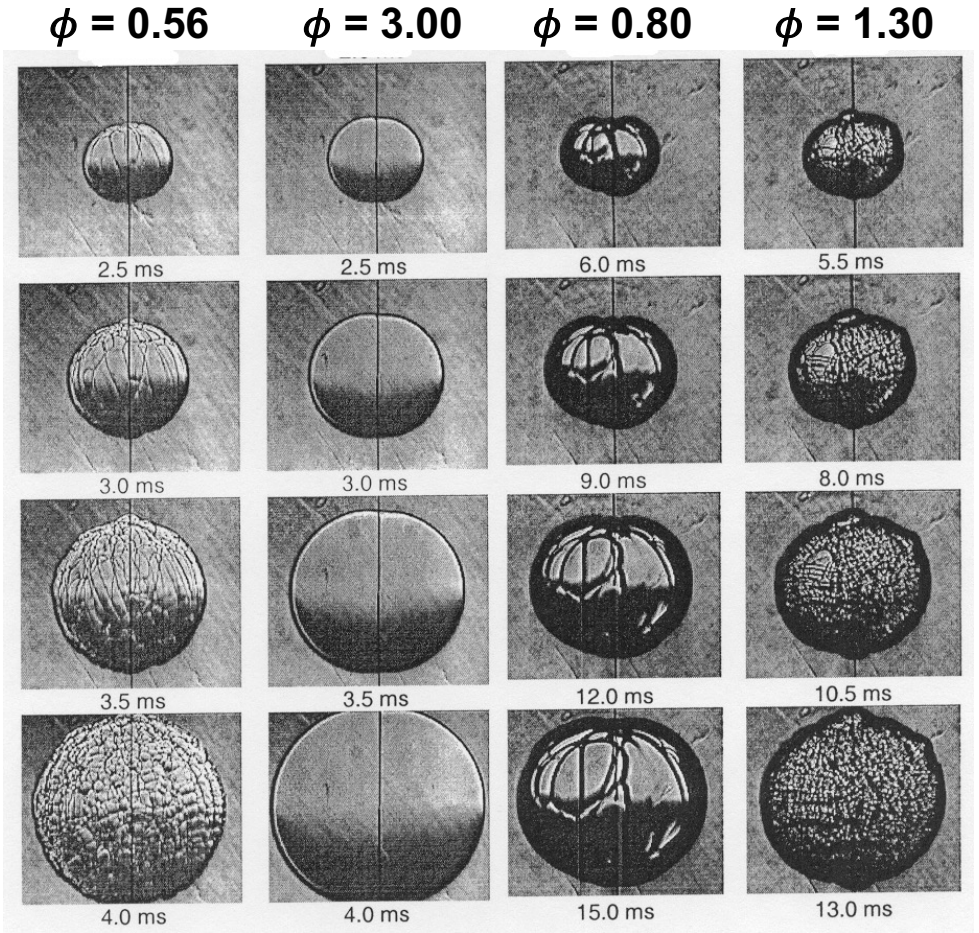

Hydrogen-air flames (2atm) **Propane-air flames (10atm)**

Experiment by C. K. Law *et al.*

Nonlinear Stability Analysis

- The linear analysis only predicts the onset of instability
  - How does flame evolve when the neutral boundary is crossed? ⇒ Nonlinear stability analysis is needed.
- Heuristic Derivation
  - The dispersion relation from the D-T theory in the long wave limit $(k \to 0)$

$$\omega \sim -\frac{1}{2}(l+2)k^2 + \frac{1}{8}l^2(l-6)k^4 + \cdots$$

  - In a small neighborhood about $l_c = -2$

$$\omega \sim -\frac{1}{2}(l-l_c)k^2 - 4k^4 + \cdots$$

Nonlinear Stability Analysis (II)

- Heuristic Derivation (continued)

$$\omega \sim -\frac{1}{2}\left(l - l_c\right)k^2 - 4k^4 + \cdots$$

- Recall $F = A\exp\left(\omega t + iky\right)$

  we can retrieve an equation for the flame front

$$F_t - \frac{1}{2}\left(l - l_c\right)F_{yy} + 4F_{yyyy} = 0$$

The missing nonlinear term in the above can be derived by using the flame speed equation (Sivashinsky)

$$F_t - 1 = -\sqrt{1 + F_y^2}$$

near boundary $k \to 0,\ F_y^2 << 1$

$$\Rightarrow F_t + \frac{1}{2}F_y^2 \approx 0$$

Nonlinear Stability Analysis (III)

- Heuristic Derivation (continued)

$$\omega \sim -\frac{1}{2}\left(l - l_c\right)k^2 - 4k^4 + \cdots$$

- Recall $F = A\exp\left(\omega t + iky\right)$

  we can retrieve an equation for the flame front

$$F_t - \frac{1}{2}\left(l - l_c\right)F_{yy} + 4F_{yyyy} = 0$$

The missing nonlinear term in the above can be derived by using the flame speed equation (Sivashinsky)

$$F_t - 1 = -\sqrt{1 + F_y^2}$$

near boundary $k \to 0,\ F_y^2 << 1$

$$\Rightarrow F_t + \frac{1}{2}F_y^2 \approx 0$$

68

Nonlinear Stability Analysis (IV)

- Combining the two equations, we obtain

$$F_t - \frac{1}{2}(l - l_c)F_{yy} + 4F_{yyyy} + \frac{1}{2}F_y^2 = 0$$

The Kuramoto-Sivashinsky Equation

The equation can also be derived by a formal asymptotic analysis, in a generalized parameter-free form as

$$F_t + \nabla^2 F + 4\nabla^4 F + \frac{1}{2}(\nabla F)^2 = 0$$

which can be solved numerically (Michelson & Sivashinsky, 1982)

Numerical Solutions of K-S Equation

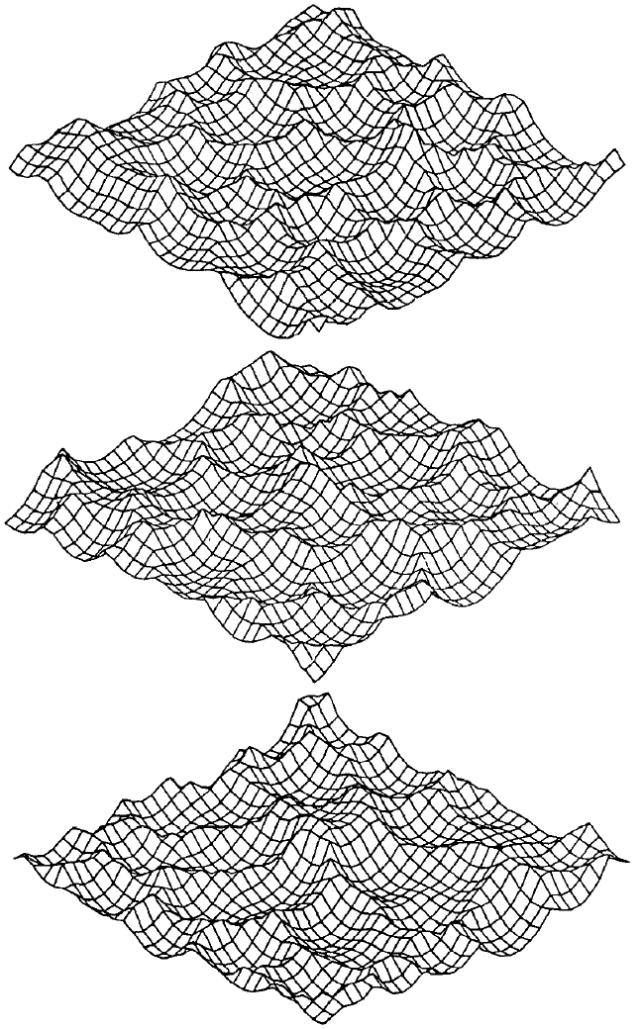

The numerical solutions to the Kuramoto-Sivashinsky equation reveals cellular flame structure that continually divides and recombines in a chaotic manner.
Each surface represents the configuration of the flame front at three consecutive instants of time.

⇒ **Self-turbulization**
(Sivashinsky, 1983)

Numerical Solutions of K-S Equation

$$F_t + 4(1+\epsilon)^2 F_{xxxx} + \epsilon F_{xx} + \frac{1}{2}F_x^2 = (1-\sigma)I(F)$$

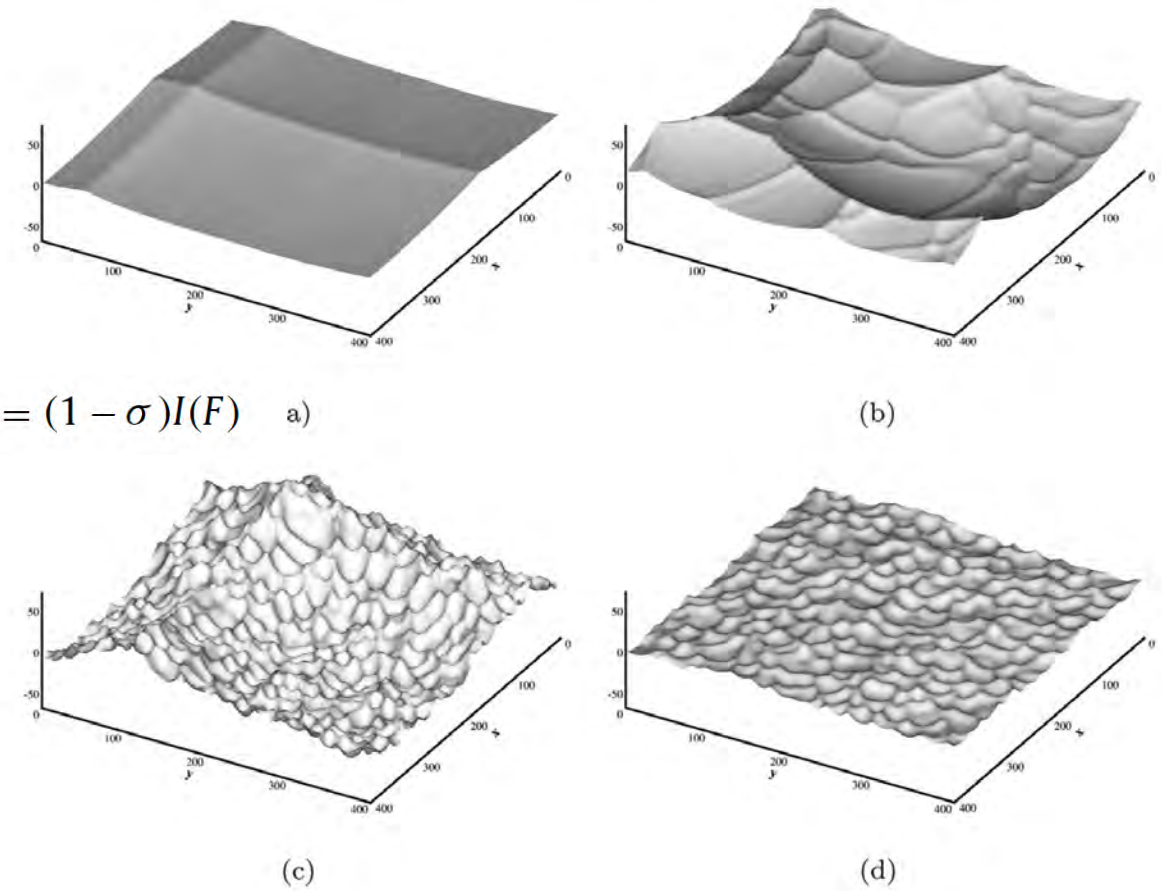

Fig. 5. Solutions $F(x, y, t)$ of the two-dimensional form of Eq. (1) in a square domain of size $L = 400$ and for the following parameters (a) $\epsilon = -0.3$, $\sigma = 0.9$ ($\beta \approx -1.1$) (b) $\epsilon = -0.3$, $\sigma = 0.7$ ($\beta \approx -0.53$) (c) $\epsilon = 0.5$, $\sigma = 0.5$ ($\beta \approx 0.53$) (d) $\epsilon = 0.5$, $\sigma = 0.9$ ($\beta \approx 1.1$)

Aerodynamics of Flame: The Flame Stretch

Karlovitz (1953): $\kappa = \dfrac{dU}{dy}$

Williams (1975): $\kappa = \dfrac{1}{A}\dfrac{dA}{dt}, \quad \mathrm{Ka} = \dfrac{\delta_T \kappa}{S_L}$ (Karlovitz Number)

Kinematic consideration

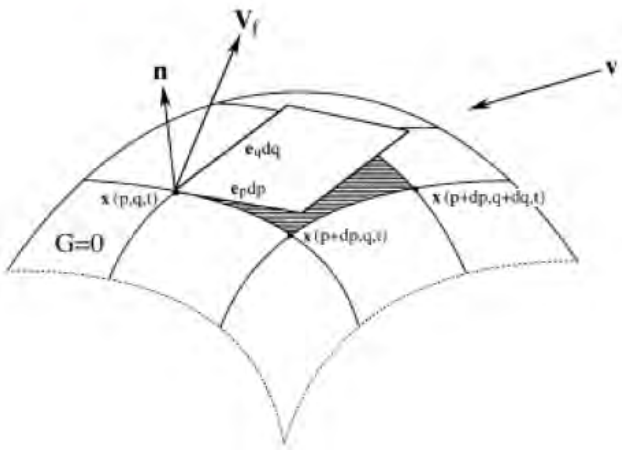

n: unit normal vector

$\mathbf{V}_f$: surface velocity (lab frame)

v: flow velocity (lab frame)

$\mathbf{e}_p, \mathbf{e}_q$: tangent vectors on surface

$$S_L = \left[\mathbf{V}_f \cdot \mathbf{n} - \mathbf{v} \cdot \mathbf{n}\right]_{G=0}$$

Examples of stretched flames

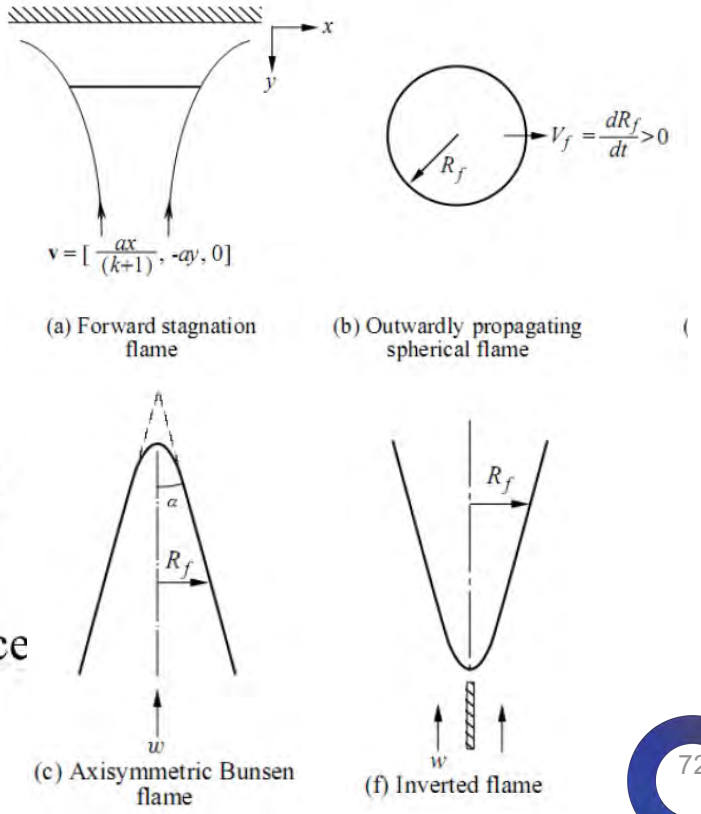

Law, C. K., Combustion Physics (2006).

The Markstein Number

Markstein (1950)

$$\frac{S_L}{S_{L,\kappa=0}} = 1 - \mu \nabla f \quad \text{(heuristic curvature effect)}$$

Asymptotic Analysis for Low Stretch Flames

$$\frac{S_L}{S_{L,\kappa=0}} = 1 - L\kappa + \cdots \quad = 1 - \mathrm{MaKa}$$

$$\mathrm{Ma} = \frac{L}{\delta} \quad \text{Markstein number;} \quad \mathrm{Ka} = \frac{\delta \kappa}{S_L} \quad \text{Karlovitz number}$$

Clavin & Williams (1982), Clavin & Garcia (1983)

$$\mathrm{Ma} = \frac{1}{\gamma} J + \frac{\beta(\mathrm{Le}-1)}{2}\left(\frac{1-\gamma}{\gamma}\right) D$$

$$\gamma = \frac{T_b - T_u}{T_b}; \quad J = \int_{T_u}^{T_b} \frac{\lambda}{\lambda(T_u)} \frac{dT}{T}$$

$$D = \left(\frac{T_u}{T_b - T_u}\right) \int_{T_u}^{T_b} \frac{\lambda}{\lambda(T_u)} \ln\left(\frac{T_b - T_u}{T - T_u}\right) \frac{dT}{T}$$

Intrinsic Flame Instabilities – How Does It Matter?

Diffusive-Thermal Instability

- Self-turbulization ⇒ turbulent kinetic energy backscatter

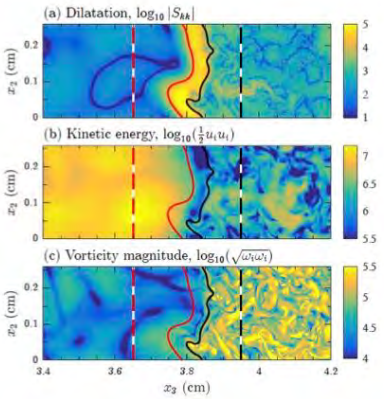

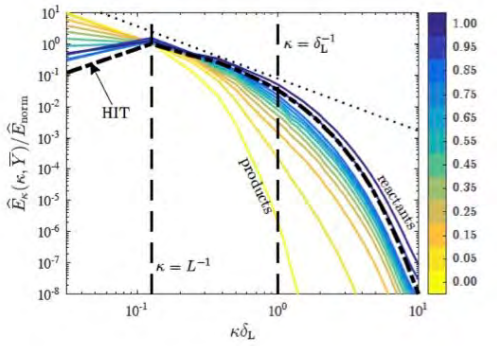

Towery, Poludnenko, et al., Phys. Fluids (2016)

Creta et al., Phys. Review E (2016)

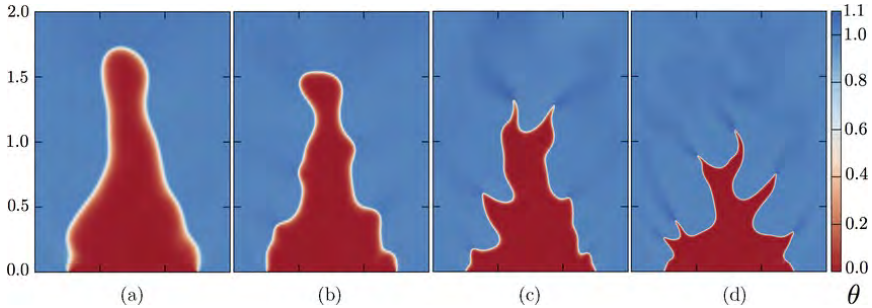

Darrieus-Landau Instability

- Increases with the system size
- Likely a significant (dominant?) factor in S_T enhancement
  - Creta et al. (2016)
  - The “Lambda” Flame, Aspden (2016)

Unsteady Flames – Markstein Transfer Function

Unsteady Effects (Im & Chen, 2000)

- Flame response to harmonic oscillation in strain rate

$$a = a_0\left(1 + A\sin\omega t\right)$$

$$M = \left|\frac{S_{L,\max} - S_{L,\min}}{\mathrm{Ka}_{\max} - \mathrm{Ka}_{\min}}\right| = F\left(\omega\right) \quad \text{Markstein transfer function}$$

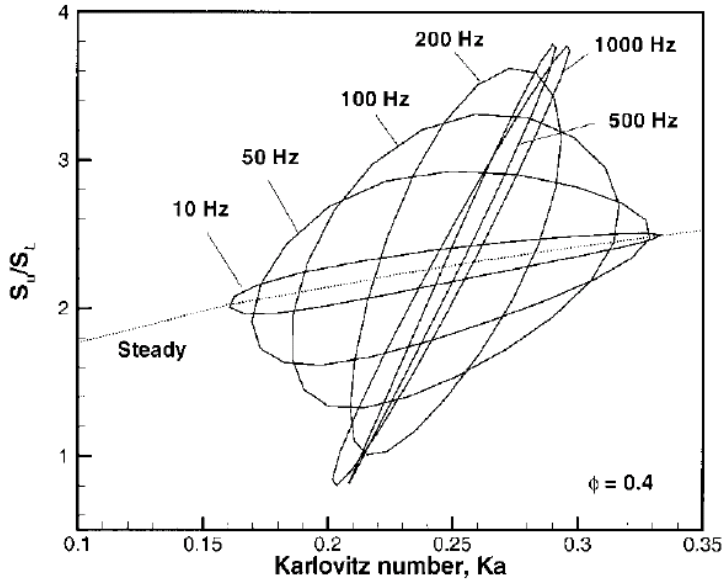

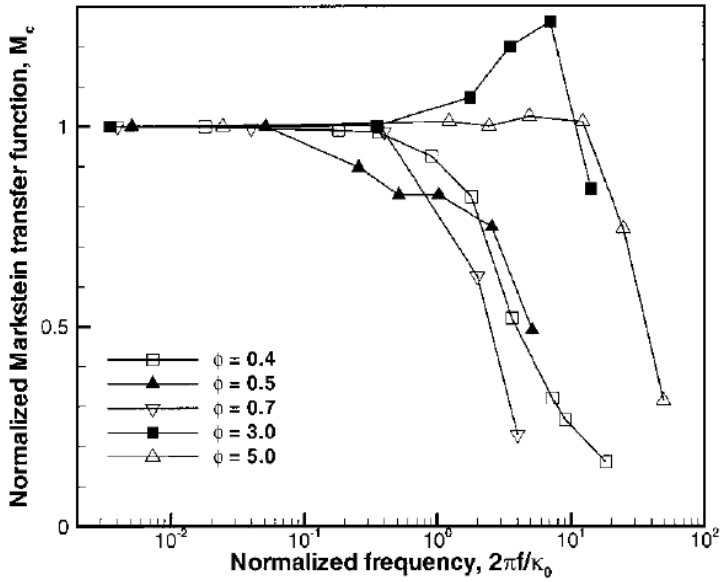

Summary

- Combustion dynamics is highly nonlinear due to large activation energy.
- Damköhler number serves as a determining parameter for combustion state.
- Steady vs. unsteady representations of combustion phenomena
  - Go/no-go is often sufficient for practical criteria
  - Transient dynamics is needed to design combustion systems (ignition in engines)
- Theoretical models need not be physically realistic to be good.
  - Large activation energy, flame sheet limit
  - Darrieus-Landau model with infinitely thin flame front
  - Constant density diffusive thermal model

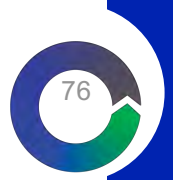

References

Law, C. K., *Combustion Physics,* Cambridge University Press (2006).

Law, C. K. and Sung, C. J., *Prog. Energy Combust. Sci.*, v. 26, p. 459 (2000).

Liñán, A., *Acta Astronautica*, v. 1, p. 1007 (1974).

Liñán, A. and Williams, F. A., *Fundamental Aspects of Combustion*, Oxford University Press (1993).

Poinsot, T. and Veynante, D., *Theoretical and Numerical Combustion*, 2nd ed., Edwards (2005).

Sivashinsky, G. I., *Ann. Rev. Fluid Mech.*, v.15, p.179 (1983).

Williams, F. A., *Combustion Theory*, 2nd ed., Addison-Wesley (1985).

Numerical Modeling of Thermochemistry

Building blocks for detailed flame simulations

Conservation Equations for Multicomponent Reacting Flows

Convective (Nonconservative) Form

$$\frac{D\rho}{Dt} + \rho\nabla\cdot\mathbf{v} = 0$$

$$\rho\frac{D\mathbf{v}}{Dt} = -\nabla\cdot\mathbf{P} + \rho\sum Y_i\mathbf{f}_i$$

$$\rho\frac{DY_i}{Dt} = -\nabla\cdot\left(\rho\mathbf{V}_i Y_i\right) + w_i,$$

$$\rho\frac{De}{Dt} = -\nabla\cdot\mathbf{q} - \mathbf{P}:\nabla\mathbf{v} + \rho\sum Y_i\mathbf{f}_i\cdot\mathbf{V}_i$$

Conservative Form

$$\frac{\partial\rho}{\partial t} = -\nabla\cdot(\rho\mathbf{u})$$

$$\frac{\partial\rho\mathbf{v}}{\partial t} = -\nabla\cdot(\mathbf{P} + \rho\mathbf{v}\mathbf{v}) + \rho\sum Y_i\mathbf{f}_i$$

$$\frac{\partial\rho Y_i}{\partial t} = -\nabla\cdot\left(\rho\mathbf{v}Y_i\right) - \nabla\cdot\left(\rho\mathbf{V}_i Y_i\right) + w_i, \quad i = 1,\cdots,N$$

$$\frac{\partial}{\partial t}(\rho E) = -\nabla\cdot\left[\rho\mathbf{v}E + \mathbf{v}\cdot\mathbf{P} + \mathbf{q}\right] + \rho\sum\left(\mathbf{v} + \mathbf{V}_i\right)\cdot Y_i\mathbf{f}_i$$

$$\left(E = e + \frac{1}{2}\mathbf{v}\cdot\mathbf{v}\right)$$

Constitutive Relations – Nonreacting Flows

Stress Tensor: $\mathbf{P} = [p + (\frac{2}{3}\mu - \kappa)\nabla \cdot \mathbf{v}]\mathbf{U} - \mu\left[(\nabla \mathbf{v}) + (\nabla \mathbf{v})^T\right]$

Unit tensor

Bulk viscosity = 0 (Stokes assumption)

Heat Flux Vector: $\mathbf{q} = -\lambda \nabla T + \rho \sum_{i=1}^{N} h_i Y_i \mathbf{V}_i + \sum_{i=1}^{N}\sum_{j=1}^{N}\left(\frac{X_j D_i^T}{W_i D_{ij}}\right)\left(\mathbf{V}_i - \mathbf{V}_j\right) + \mathbf{q}_{\text{rad}}$

Fourier conduction

enthalpy transport by diffusion

Dufour effect

radiation

Equation of State: $p = p(e, \rho)$ for ideal gas: $p = \rho R^0 T / \bar{W} = \rho R^0 T \sum_{i=1}^{N}\left(Y_i / W_i\right)$

Enthalpy & Internal Energy: $h = \sum Y_i h_i = e + p / \rho$

$$h_i = h_{f,i}^0\left(T^0\right) + \int_{T_0}^{T} c_{p,i} dT,\ c_{p,i}(T) = \sum_{m=0}^{6} a_{m,i} T^m \left(\text{NASA polynomial}\right)$$

$X_i - Y_i$ Conversion: $X_i = \dfrac{Y_i / W_i}{\sum_{j=1}^{N}\left(Y_j / W_j\right)}$; $Y_i = \dfrac{X_i W_i}{\sum_{j=1}^{N}\left(X_j W_j\right)}$

Constitutive Relations – Reaction Source Terms

For a system of K reversible reactions:

$$\sum_{i=1}^{N} \nu'_{i,k} \mathrm{M}_i \leftrightarrow \sum_{i=1}^{N} \nu''_{i,k} \mathrm{M}_i \quad k = 1, \cdots, K$$

Reaction Rate for Species i:

$$w_i = W_i \hat{\omega}_i = W_i \sum_{k=1}^{K} \left(\nu''_{i,k} - \nu'_{i,k} \right) \left[k_{f,k} \prod_{j=1}^{N} \left(\frac{X_j p}{R^0 T} \right)^{\nu'_{j,k}} - k_{b,k} \prod_{j=1}^{N} \left(\frac{X_j p}{R^0 T} \right)^{\nu''_{j,k}} \right]$$

$$k_{f,k} = A_k T^{\beta_k} \exp\left(-\frac{E_k}{RT} \right), \qquad k_{b,k} = \frac{k_{f,k}}{K_{C,k}}$$

```
! GRI-Mech Version 3.0 7/30/99  CHEMKIN-II format
! See README30 file at anonymous FTP site unix.sri.com, directory gri;
! WorldWideWeb home page http://www.me.berkeley.edu/gri_mech/ or
! through http://www.gri.org , under 'Basic  Research',
! for additional information, contacts, and disclaimer
ELEMENTS
O  H  C  N  AR
END
SPECIES
H2        H         O         O2        OH        H2O       HO2       H2O2
C         CH        CH2       CH2(S)    CH3       CH4       CO        CO2
HCO       CH2O      CH2OH     CH3O      CH3OH     C2H       C2H2      C2H3
C2H4      C2H5      C2H6      HCCO      CH2CO     HCCOH     N         NH
NH2       NH3       NNH       NO        NO2       N2O       HNO       CN
HCN       H2CN      HCNN      HCNO      HOCN      HNCO      NCO       N2
AR        C3H7      C3H8      CH2CHO    CH3CHO
END
!THERMO
! Insert GRI-Mech thermodynamics here or use in default file
!END
REACTIONS                                      A_k       β_k       E_k
2O+M<=>O2+M                                 1.200E+17   -1.000      .00
H2/ 2.40/ H2O/15.40/ CH4/ 2.00/ CO/ 1.75/ CO2/ 3.60/ C2H6/ 3.00/ AR/  .83/
O+H+M<=>OH+M                                5.000E+17   -1.000      .00
H2/2.00/ H2O/6.00/ CH4/2.00/ CO/1.50/ CO2/2.00/ C2H6/3.00/ AR/ .70/
O+H2<=>H+OH                                 3.870E+04    2.700     6260.00
O+HO2<=>OH+O2                               2.000E+13     .000       .00
O+H2O2<=>OH+HO2                             9.630E+06    2.000     4000.00
O+CH<=>H+CO                                 5.700E+13     .000       .00
O+CH2<=>H+HCO                               8.000E+13     .000       .00
O+CH2(S)<=>H2+CO                            1.500E+13     .000       .00
O+CH2(S)<=>H+HCO                            1.500E+13     .000       .00
O+CH3<=>H+CH2O                              5.060E+13     .000       .00
O+CH4<=>OH+CH3                              1.020E+09    1.500     8600.00
O+CO(+M)<=>CO2(+M)                          1.800E+10     .000     2385.00
   LOW/ 6.020E+14    .000    3000.00/
H2/2.00/ O2/6.00/ H2O/6.00/ CH4/2.00/ CO/1.50/ CO2/3.50/ C2H6/3.00/ AR/ .50/
O+HCO<=>OH+CO                               3.000E+13     .000       .00
O+HCO<=>H+CO2                               3.000E+13     .000       .00
O+CH2O<=>OH+HCO                             3.900E+13     .000     3540.00
```

N

K

Note:

- For a given species, the number of exponential function evaluations ~ K
- Inside the reaction routine, there are numerous operations to convert mole to mass fractions.

Constitutive Relations – Transport

Diffusion Velocity:

$$\nabla X_i = \sum_{j=1}^{N}\left(\frac{X_i X_j}{D_{ij}}\right)\left(\mathbf{V}_j - \mathbf{V}_i\right) + \left(Y_i - X_i\right)\left(\frac{\nabla p}{p}\right) + \left(\frac{\rho}{p}\right)\sum_{j=1}^{N} Y_i Y_j\left(\mathbf{f}_i - \mathbf{f}_j\right)$$

binary diffusion

diffusion by pressure gradient

diffusion by body force

$$+\sum_{j=1}^{N}\left[\left(\frac{X_i X_j}{\rho D_{ij}}\right)\left(\frac{D_j^T}{Y_j} - \frac{D_i^T}{Y_i}\right)\right]\left(\frac{\nabla T}{T}\right),\ i = 1,\cdots,N$$

Soret effect.

which is an implicit relation (expensive).

Transport properties of each species is determined by the molecular kinetic parameters (tran.dat). At the beginning of the problems, polynomial fits are computed for pure species:

$$\ln\mu_i = \sum_{n=1}^{N} a_{n,i}\left(\ln T\right)^{n-1} \qquad \ln\lambda_i = \sum_{n=1}^{N} b_{n,i}\left(\ln T\right)^{n-1} \qquad \ln D_{ji} = \sum_{n=1}^{N} d_{n,ji}\left(\ln T\right)^{n-1}\left[\frac{p_0}{p}\right]$$

Multicomponent Properties (EGLib)

Ern & Giovangigli, http://www.cmap.polytechnique.fr/www.eglib/

The *L* Matrix:

block submatrices

$$\begin{pmatrix} L^{00,00} & L^{00,10} & 0 \\ L^{10,00} & L^{10,10} & L^{10,01} \\ 0 & L^{01,10} & L^{01,01} \end{pmatrix} \begin{pmatrix} a^1_{00} \\ a^1_{10} \\ a^1_{01} \end{pmatrix} = \begin{pmatrix} 0 \\ X \\ X \end{pmatrix}$$

mole fraction vector

Computational cost ~ N^2

With the solutions for $a^1_{00}, a^1_{10}, a^1_{01}$

$$\lambda = \lambda_{\text{tr}} + \lambda_{\text{int}} \qquad \lambda_{\text{tr}} = -\sum_{j=1}^{N} X_j a^1_{j,10}, \quad \lambda_{\text{int}} = -\sum_{j=1}^{N} X_j a^1_{j,01} \qquad \underset{\text{Soret}}{D_i^T} = \frac{8 m_i X_i}{5 R^0} a^1_{i,00}$$

$$\mathbf{V}_i = -\frac{1}{X_i \bar{W}} \sum_{j \neq 1}^{N} W_j \hat{D}_{ij} \mathbf{d}_j - \frac{D_i^T}{\rho Y_i} \frac{\nabla T}{T}$$

multicomponent diffusion coeff.

where $\hat{D}_{ij} = X_i \frac{16T}{25p} \frac{\bar{W}}{W_j} \left(P_{ij} - P_{ii} \right), \qquad P = \left(L^{00,00} \right)^{-1}$

Mixture-Averaged Formula

Transport properties are approximated as a weighted average:

$$\mu = \sum_{i=1}^{N} \frac{X_i \mu_i}{\sum_{j=1}^{N} X_j \Phi_{ij}} \qquad \Phi_{ij} = \frac{1}{\sqrt{8}} \left(1 + \frac{W_i}{W_j}\right)^{-1/2} \left(1 + \left(\frac{\mu_i}{\mu_j}\right)^{1/2} \left(\frac{W_j}{W_i}\right)^{1/4}\right)^2$$ (Wilke, 1950)

$$\lambda = \frac{1}{2}\left(\sum_{i=1}^{N} X_i \lambda_i + \frac{1}{\sum_{i=1}^{N} X_i / \lambda_i}\right)$$ (Mathur, 1967)

$$\mathbf{V}_i = -\frac{1}{X_i} \hat{D}_{im} \mathbf{d}_i - \frac{D_i^T}{\rho Y_i} \frac{\nabla T}{T}$$

mixture-averaged diffusion coeff.

where $\mathbf{d}_i = \nabla X_i + \left(X_i - X_j\right) \frac{\nabla p}{p}$ $\qquad \hat{D}_{im} = \frac{1 - Y_i}{\sum_{j \neq 1}^{N} X_j / D_{ji}}$

Modeling of Canonical Laminar Flames

Homogeneous reactor
Continuous stirred tank reactor (CSTR)
Premixed flame
Opposed jet diffusion flame

Homogeneous Reactor

Constant Pressure:

$$c_p \frac{dT}{dt} = -\frac{1}{\rho}\sum_{i=1}^{N} h_i W_i \hat{\omega}_i, \quad \frac{dY_i}{dt} = \frac{W_i}{\rho}\hat{\omega}_i$$

Constant Volume:

$$c_v \frac{dT}{dt} = -\frac{1}{\rho}\sum_{i=1}^{N} e_i W_i \hat{\omega}_i, \quad \frac{dY_i}{dt} = \frac{W_i}{\rho}\hat{\omega}_i$$

0D IC Engine:

$$c_v \frac{dT}{dt} = -\frac{1}{\rho}\sum_{i=1}^{N} e_i W_i \hat{\omega}_i + \frac{p}{m}\frac{dV(t)}{dt}$$

$$\frac{dY_i}{dt} = \frac{W_i}{\rho}\hat{\omega}_i$$

Associated Numerics:

- Stiff time integrator
  - One-step Runge-Kutta
  - Multistep (backward differentiation – CVODE)

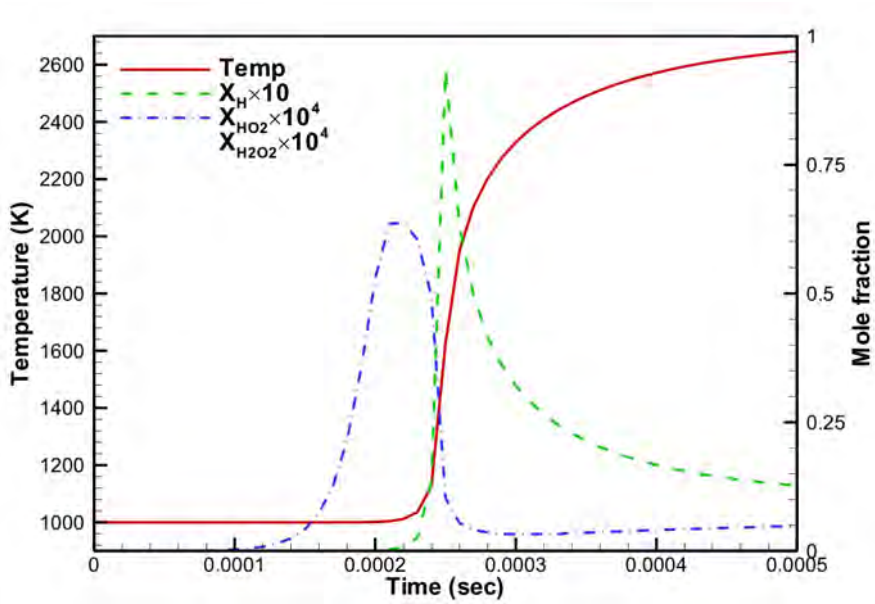

Continuous Stirred Tank Reactor

$$\frac{dY_i}{dt} = \frac{W_i}{\rho}\hat{\omega}_i + \frac{\left(Y_{i,in} - Y_i\right)}{\tau_{cstr}}$$

$$c_p \frac{dT}{dt} = -\frac{1}{\rho}\sum_{i=1}^{N} h_i W_i \hat{\omega}_i + \frac{\left(h_{in} - h\right)}{\tau_{cstr}}$$

$\tau_{cstr} = V_{cstr} / Q$ residence time

Associated Numerics:

- Stiff time integrator
  - One-step Runge-Kutta
  - Multistep (backward differentiation – CVODE)

Extended to zone models

- Reactor volume broken into M well-mixed zones

$$\frac{dY_i^{(m)}}{dt} = \frac{W_i}{\rho}\hat{\omega}_i + \sum_{k=0}^{M+1}\left(f_{km}Y_i^{(k)} - f_{mk}Y_i^{(m)}\right), \quad k = 1,\ldots,M$$

- Commonly used as turbulent combustion closure (PaSR: partially stirred reactor model)

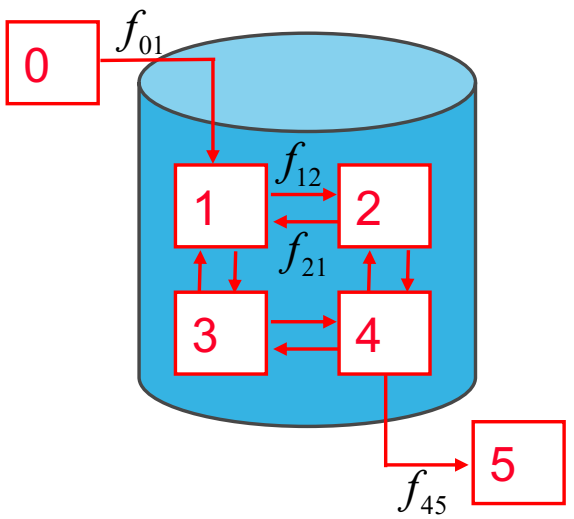

1D Steady Premixed Flames (PREMIX)

$$\dot{M} = \rho u A$$

$$\dot{M}\frac{dT}{dx} - \frac{1}{c_p}\frac{d}{dx}\left(\lambda A \frac{dT}{dx}\right) + \frac{A}{c_p}\sum_{i=1}^{N}\rho Y_i V_i c_{p,i}\frac{dT}{dx} = -\frac{A}{c_p}\sum_{i=1}^{N} h_i W_i \hat{\omega}_i$$

$$\dot{M}\frac{dY_i}{dx} + \frac{d}{dx}\left(\rho A Y_i V_i\right) = A W_i \hat{\omega}_i,\ i = 1,\ldots,N$$

$$\rho = \frac{p\bar{W}}{RT}$$

$$\dot{m} = \frac{\dot{M}}{A} = \rho u \quad \text{mass flux}$$

- Eigenvalue ρS_L (for freely propagating flame)
- Prescribed input constant (for burner-stabilized flame)

Associated Numerics:

- Nonlinear Newton-Raphson solver (Twopnt).
- Adaptive grid refinement
- Pseudo time-stepping

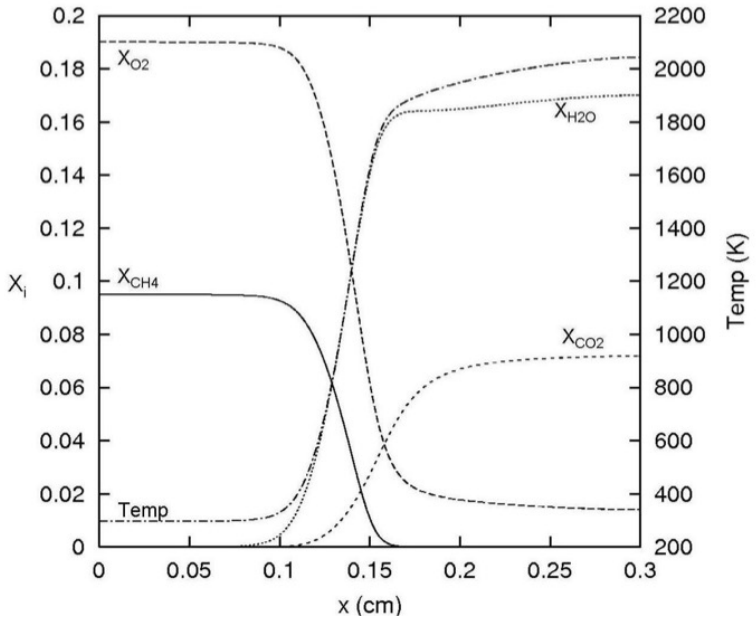

Counterflow Nonpremixed Flames – Potential Flow

$$u_\infty = ar, \quad v_\infty = -2az; \qquad a = -\frac{1}{2}\frac{\partial v_\infty}{\partial z} \text{ (given or eigenvalue)}$$

$$f' = \frac{u}{u_\infty}$$

$$V = \rho v$$

$$\frac{dV}{dz} + 2a\rho f' = 0$$

$$\frac{d}{dz}\left(\mu\frac{df'}{dz}\right) - V\frac{df'}{dz} + a\left[\rho_\infty - \rho\left(f'\right)^2\right] = 0$$

$$-\frac{d}{dz}\left(\rho Y_i V_i\right) - V\frac{dY_k}{dz} + W\hat{\omega}_i = 0, \; i = 1,\ldots,N$$

$$\frac{d}{dz}\left(\lambda\frac{dT}{dz}\right) - c_p V\frac{dT}{dz} - \sum_{i=1}^{N}\rho Y_i V_i c_{p,i}\frac{dT}{dz} - \sum_{i=1}^{N} h_i W_i \hat{\omega}_i = 0$$

Puri, Seshadri, Smooke, Keyes, CST 56 (1987)

Associated Numerics:

- Nonlinear Newton-Raphson solver (Twopnt).
- Adaptive grid refinement

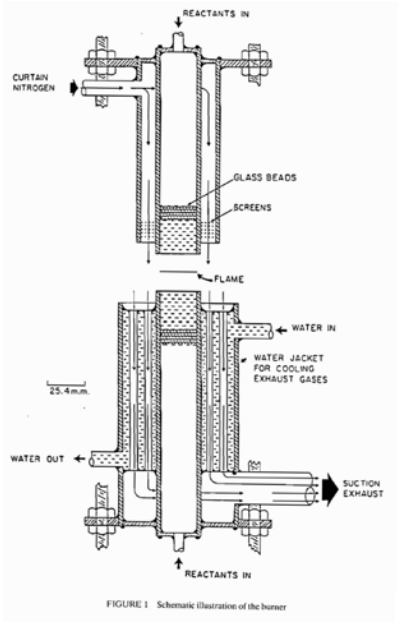

FIGURE 1 Schematic illustration of the burner

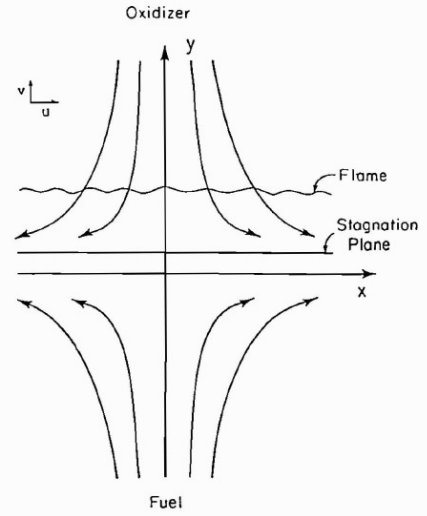

FIGURE 2 Schematic illustration of a counterflow flame.

Counterflow Nonpremixed Flames – Oppdif

Continuity: $\frac{\partial}{\partial x}(\rho u)+\frac{1}{r}\frac{\partial}{\partial r}(\rho v r)=0$

Key similarity assumption (von Karman)

$$G(x)=-\frac{\rho v}{r},\ F(x)=\frac{\rho u}{2}$$

Continuity: $G(x)=\frac{dF(x)}{dx}$

Eigenvalue: $H=\frac{1}{r}\frac{\partial p}{\partial r}=\text{constant}\quad\left(\frac{dH}{dx}=0\right)$

Radial momentum:

$$H-2\frac{d}{dx}\left(\frac{FG}{\rho}\right)+\frac{3G^2}{\rho}+\frac{d}{dx}\left[\mu\frac{d}{dx}\left(\frac{G}{\rho}\right)\right]=0$$

Lutz, Kee, Grcar, Rupley SAND96-8243 (1997)

Associated Numerics:

- Nonlinear Newton-Raphson solver (Twopnt).
- Adaptive grid refinement

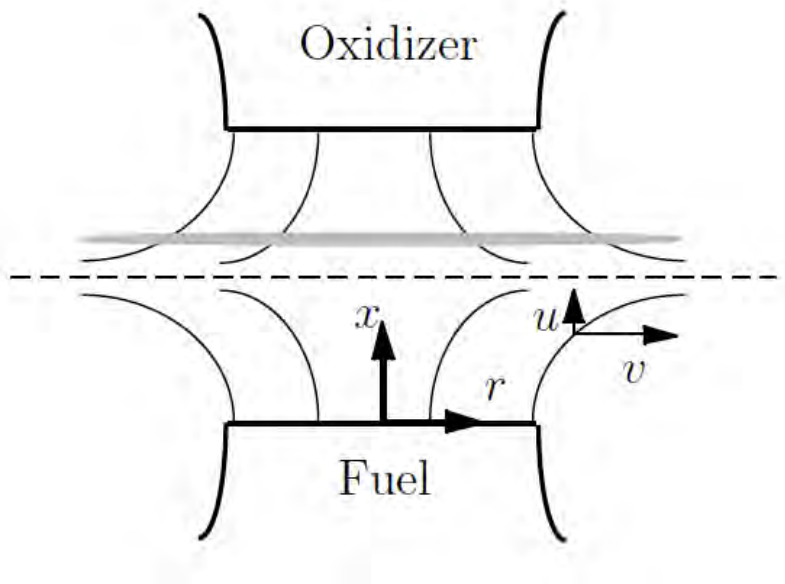

Unsteady Opposed Flow Flames – OPUS/Ember

Im, Raja, Kee, Petzold, CST (2000)

Compressible treatment

$$P = p_0(t) + p(t,r) + \frac{1}{2}H(t)r^2 + O(\mathrm{Ma}^4)$$

$$\frac{\rho}{p_{tot}}\frac{\partial p}{\partial t} - \frac{\rho}{T}\frac{\partial T}{\partial t} - \rho\bar{W}\sum_{i=1}^{N}\frac{1}{W_i}\frac{\partial Y_i}{\partial t} + \frac{\partial}{\partial x}\left(\rho u\right) + 2\rho V = 0$$

$$\rho\frac{\partial u}{\partial t} + \rho u\frac{\partial u}{\partial x} + \frac{\partial p}{\partial x} - 2\mu\frac{\partial V}{\partial x} - \frac{4}{3}\frac{\partial}{\partial x}\left(\mu\left[\frac{\partial u}{\partial x} - V\right]\right) = 0$$

$$\rho\frac{\partial V}{\partial t} + \rho u\frac{\partial V}{\partial x} + \rho V^2 - \frac{\partial}{\partial x}\left(\mu\frac{\partial V}{\partial x}\right) + H = 0$$

$$\rho c_p\frac{\partial T}{\partial t} + \rho c_p u\frac{\partial T}{\partial x} - \frac{\partial}{\partial x}\left(\lambda\frac{\partial T}{\partial x}\right) - \frac{\partial p_0}{\partial t} - u\frac{\partial p}{\partial x} + \sum_{i=1}^{N}\rho Y_i V_i c_{p,i}\frac{\partial T}{\partial x} + \sum_{i=1}^{N}h_i W_i\hat{\omega}_i = 0$$

$$\rho\frac{\partial Y_i}{\partial t} + \rho u\frac{\partial Y_i}{\partial x} + \frac{\partial}{\partial x}\left(\rho Y_i V_i\right) - W_i\hat{\omega}_i = 0$$

Eigenvalue: $H(t) = \frac{1}{r}\frac{\partial p}{\partial r}$ $\left(\frac{dH}{dx} = 0\right)$

Associated Numerics:

- Differential-algebraic equations (DAE) solver (DASPK)
- Compressible flow formulation with index reduction

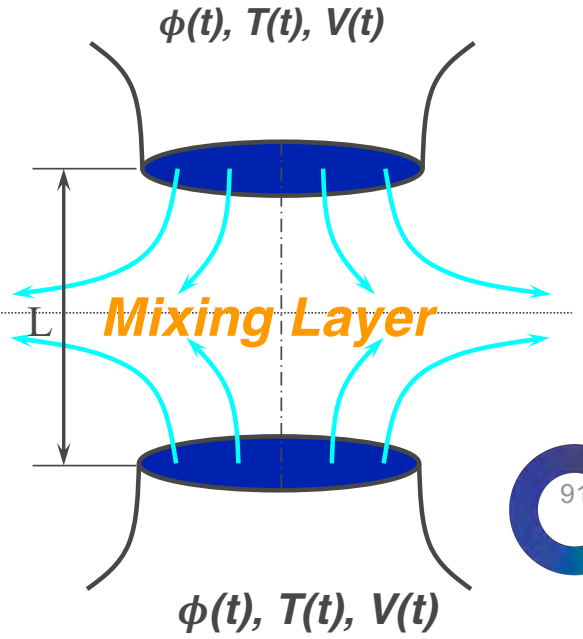

The Strain Rate – Various Definitions

The Strain Rate

- For potential (Hiemenz) flow

$$u_\infty = \begin{cases} ax & \text{2-D slot jet} \\ ar & \text{round jet} \end{cases},$$

$$v_\infty = -2az \Rightarrow a = -\frac{1}{2}\frac{\partial v_\infty}{\partial z}$$

- For opposed-jet (plug) flow

$$a = \frac{1}{r}\frac{\partial}{\partial r}(ru) \text{ at flame}$$

- Approximate formula

$$a = \frac{V_O + V_F}{L}$$

$$a = \frac{2V_O}{D}\left(1 + \frac{V_F\sqrt{\rho_F}}{V_O\sqrt{\rho_O}}\right) \text{ (Seshadri \&Williams)}$$

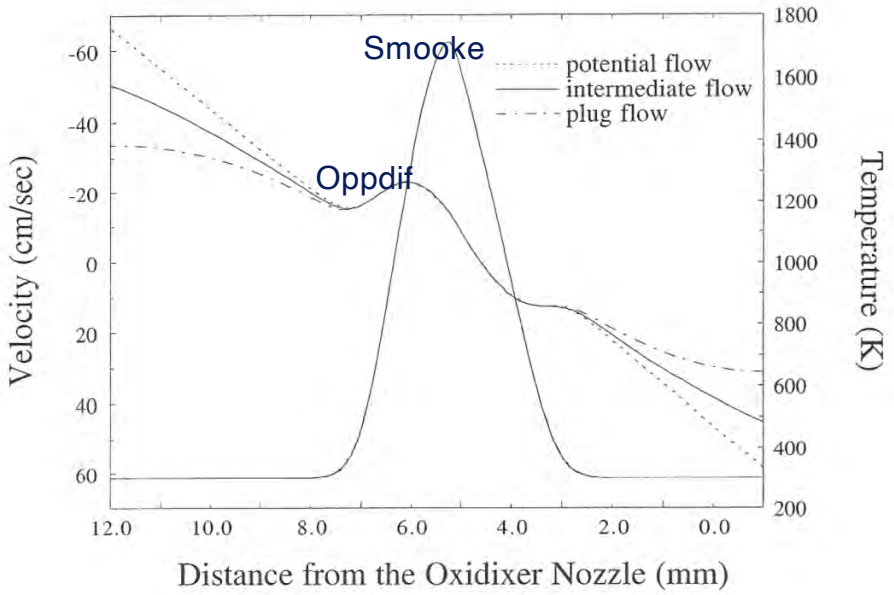

C.K. Law, Combustion Physics (2006)

$$a \sim \frac{1}{\text{Da}} \text{ (Damkohler number)}$$

$$a \uparrow \Rightarrow \text{Da} = \frac{\text{residence time}}{\text{chemical time}} \downarrow \Rightarrow \text{Extinction}$$

a is uniquely related to χ

The Scalar Dissipation Rate

Alternatively, the flow time scale can be characterized by the scalar dissipation rate:

Elemental mass fraction

$$Z_j = \frac{m_j}{m} = \sum_{i=1}^{N} \frac{a_{ij} W_j}{W_i} Y_i$$

i : species index ($i = 1, \ldots, N$)

j : element index (C, H, O)

Bilger's mixture fraction

$$Z = \frac{2Z_C / W_C + 0.5 Z_H / W_H + \left(Z_{O,O} - Z_O\right) / W_O}{2Z_{C,F} / W_C + 0.5 Z_{H,F} / W_H + Z_{O,O} / W_O}$$

The scalar dissipation rate

$$\chi = 2D\left|\nabla Z\right|^2 \quad [\mathrm{s}^{-1}]$$

At the stoichiometric mixture fraction

$$\chi_{st} = 2D\left|\nabla Z_{st}\right|^2 \quad [\mathrm{s}^{-1}]$$

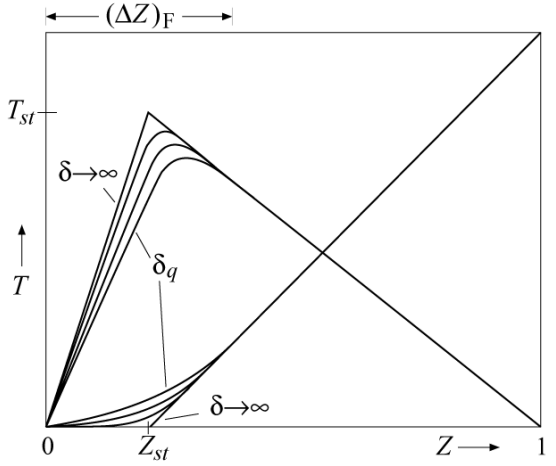

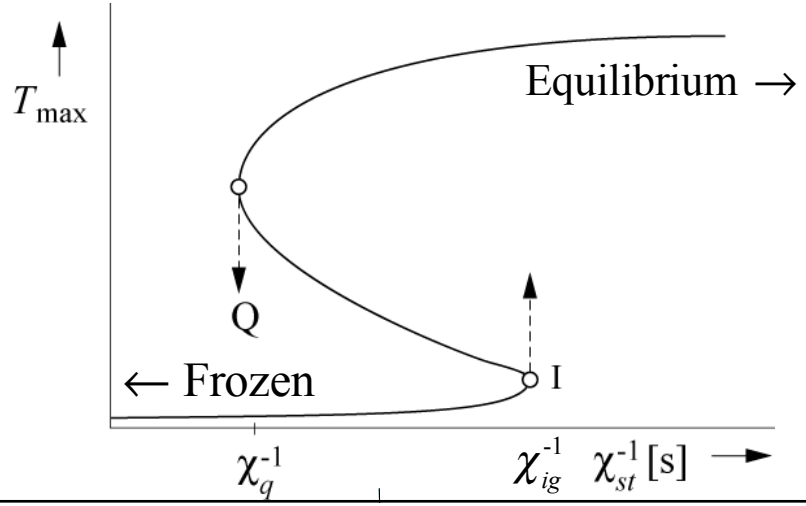

The Conserved Scalar Variable and Flamelet Model

Mixture Fraction Variable for a Multicomponent System (Warnatz et al.) for C/H/O system

Define the elemental mass fraction

$$Z_j = \frac{m_j}{m} = \sum_{i=1}^{N} \frac{a_{ij} W_j}{W_i} Y_i$$

i : species index ($i = 1, \ldots, N$)

j : element index (C, H, O)

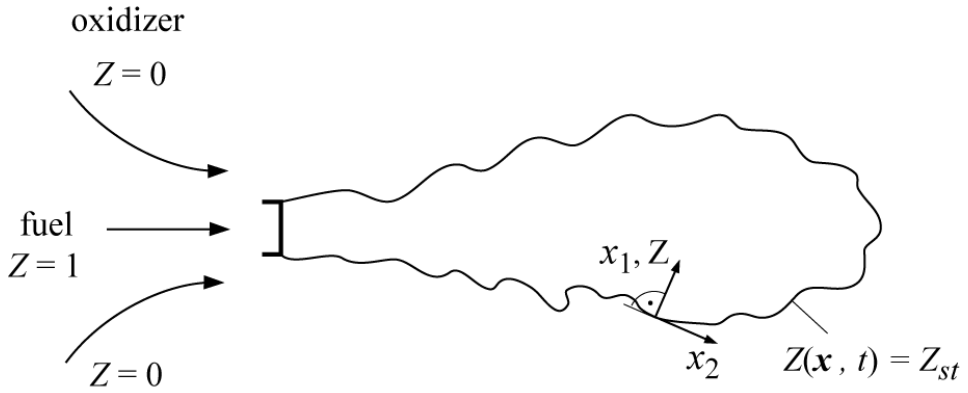

$$\rho \frac{\partial Z}{\partial t} + \rho u_j \frac{\partial Z}{\partial x_j} - \frac{\partial}{\partial x_j}\left(\rho D \frac{\partial Z}{\partial x_j} \right) = 0$$

$$\rho \frac{\partial Y_i}{\partial \tau} = \rho \frac{\chi}{2} \frac{\partial^2 Y_i}{\partial Z^2} + w_i \quad \text{if } \left(\rho D \neq f(Z) \right)$$

$$Y_i(Z, \chi) \qquad \chi = 2D|\nabla Z|^2$$

Flame Ignition/Extinction Study

Arc-length continuation
(Giovangigli and Smooke, CST 1987)

Repeated restart of calculations with incremental change in strain rates.

A flame-controlling continuation
(Nishioka et al., C&F 1996)

Scalar variables (T or Y_i) used as a controlling parameter.

Quantitative predictions of ignition/extinction limits.

Applicable to premixed flames

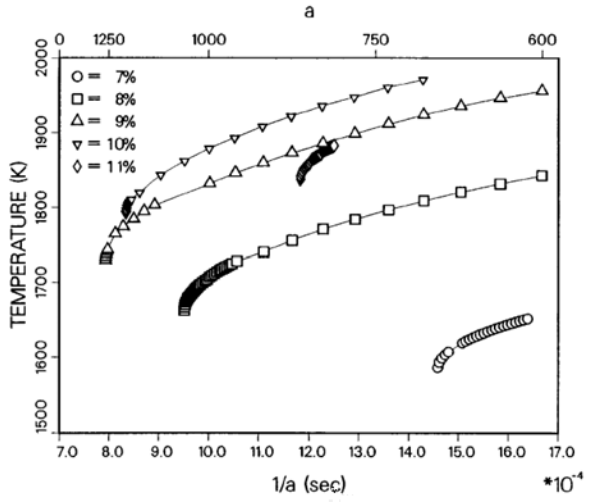

Kee, Miller, Evans, Dixon-Lewis, 22nd Symp. (1988)

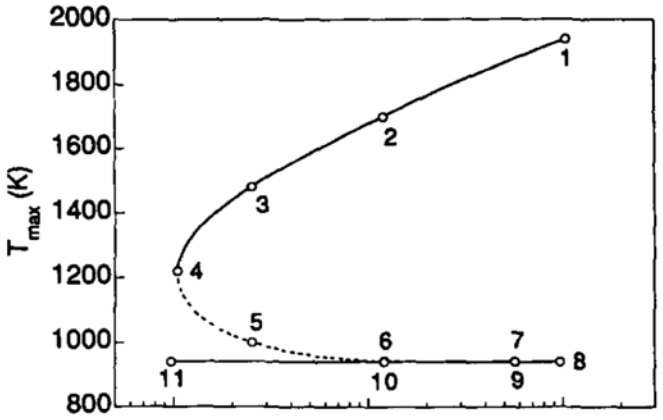

Nishioka, Law, Takeno, C&F (1996)

NTC Behavior & Complex S-Curves

Complex bifurcation behavior is manifested as multiple turning points in the steady phase diagram.

Each turning point involves specific chemical (exponential) nonlinearity.

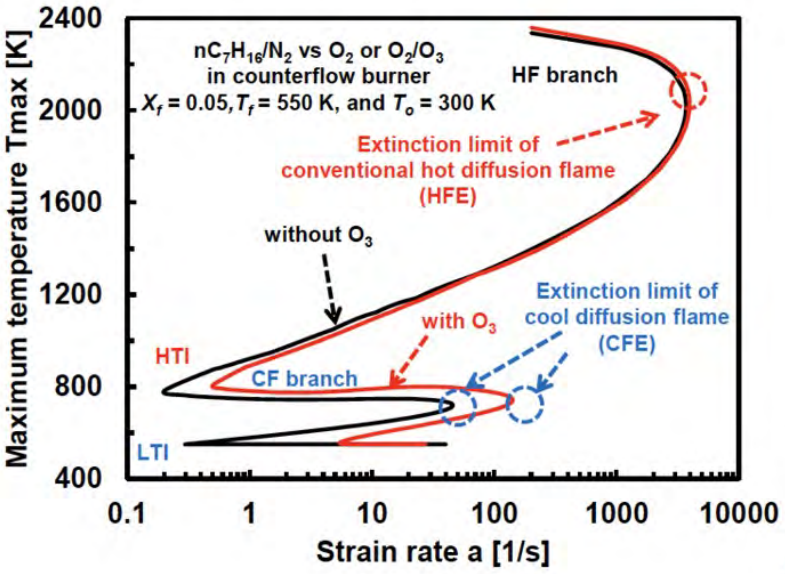

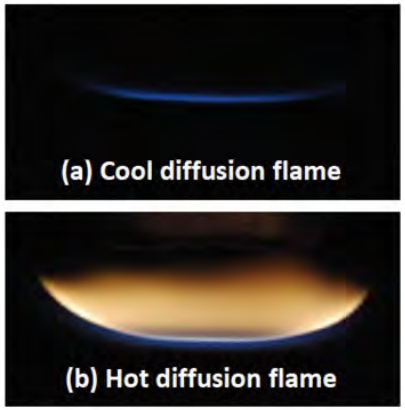

Won, S.H., et al., 2015, *Proceedings of the Combustion Institute, 35*.

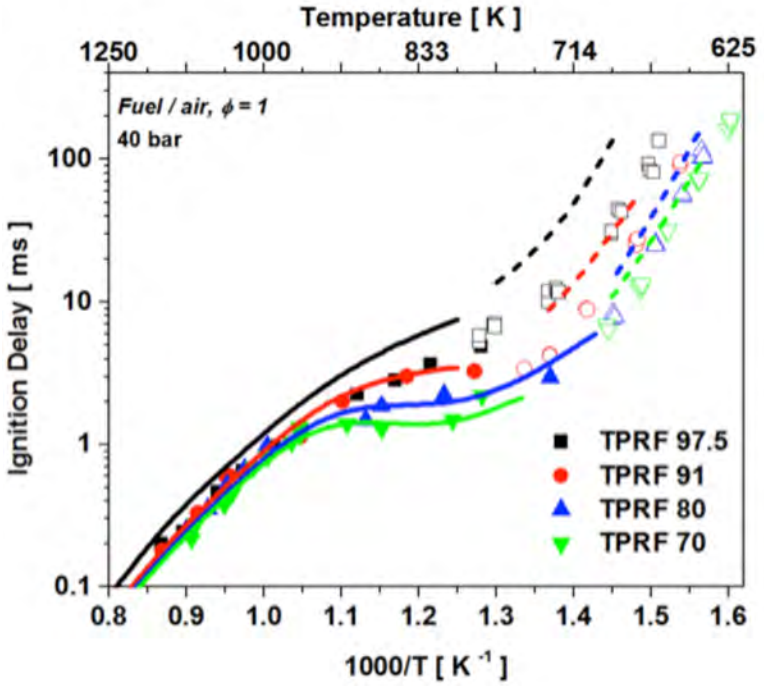

Farooq et al., https://ccrc.kaust.edu.sa/aramco/Pages/isn.aspx

Unsteady Ignition Studies

Bansal, Im, Lee, PROCI 28 (2009)

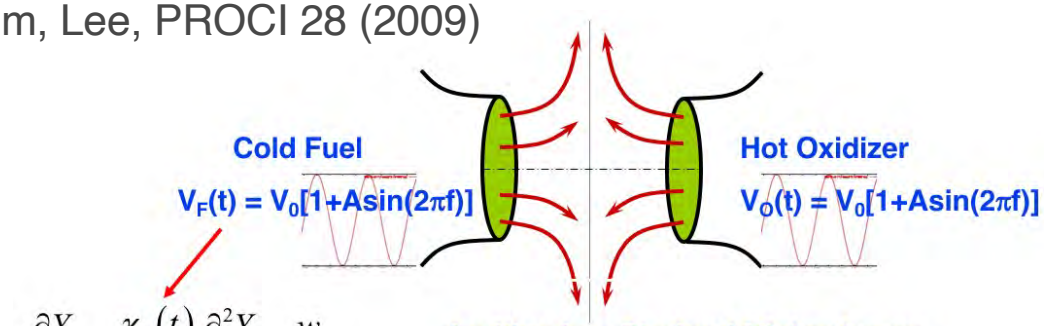

$$\frac{\partial Y_i}{\partial t} = \frac{\chi_z(t)}{2}\frac{\partial^2 Y_i}{\partial Z^2} + \frac{w_i}{\rho}$$

Ignition in a Strained Mixing Layer with Harmonic Velocity Fluctuations

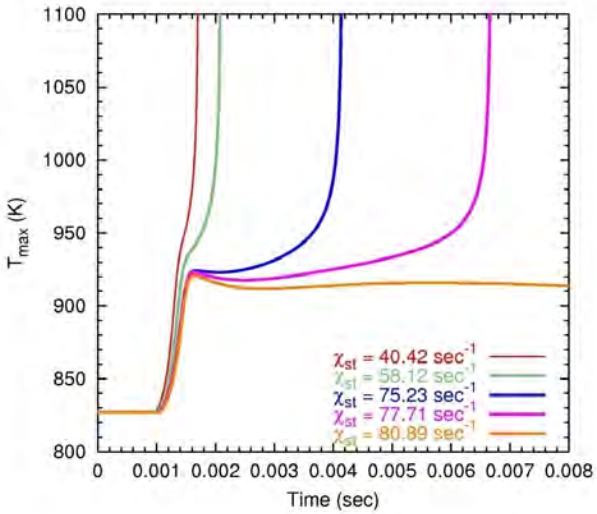

1st stage ignition kernel sits very close to oxidizer side (high temp.) – very low χ

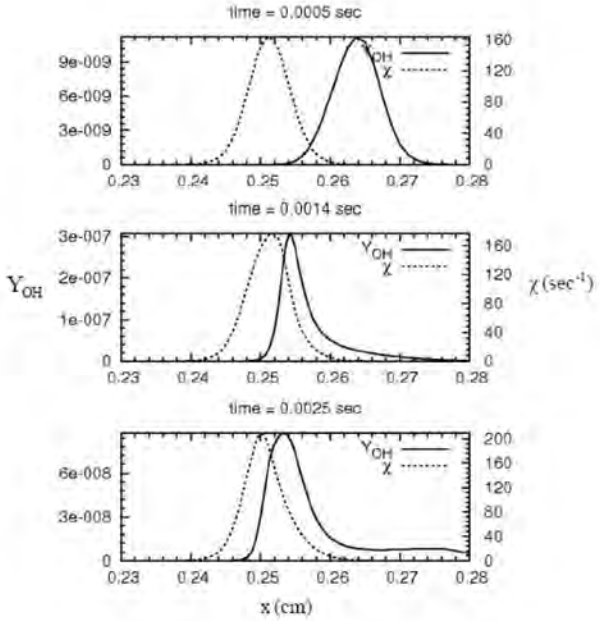

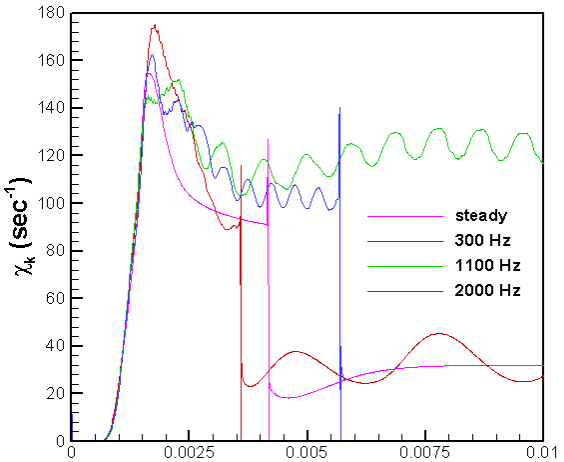

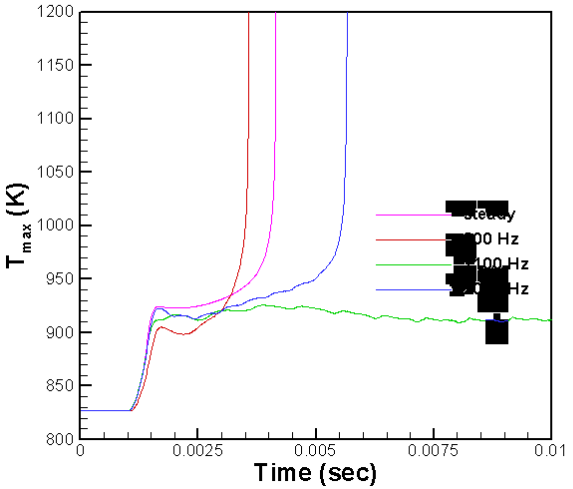

Nonmonotonic ignition response to frequency of imposed χ oscillation

Summary

- For simple flames, first principle continuum simulations can incorporate all detailed physical/chemical parameters
  - Fidelity is subjected to the accuracy of thermo-chemistry and chemical kinetic, transport models
- Canonical flame studies are valuable for cross-validation of quantitative prediction. This is an essential step before moving into complex turbulent combustion systems.

References

Kee, R. J., Coltrin, M. E., Glarborg, P., *Chemically Reacting Flow: Theory and Practice*, Wiley, 2003.

Law, C. K., *Combustion Physics,* Cambridge University Press (2006).

Poinsot, T. and Veynante, D., *Theoretical and Numerical Combustion*, 2nd ed., Edwards (2005).

Williams, F. A., *Combustion Theory*, 2nd ed., Addison-Wesley (1985).

جامعة الملك عبدالله للعلوم والتقنية
King Abdullah University of Science and Technology

Clean Energy Research Platform

Tsinghua-Princeton-Combustion Institute
2025 Summer School on Combustion
Tsinghua University, July 7-11, 2025

Turbulent Combustion

Day 2: Turbulent Flow and Flame Physics

Hong G. Im
Clean Energy Research Platform (CERP)
King Abdullah University of Science and Technology (KAUST)

Outline

- Statistical description of turbulence
- Turbulence scaling
- Turbulent flow/combustion simulations:
  - RANS vs. LES formulation and closure
  - Some computational implications
- Turbulent combustion scaling and regimes

Statistical Description of Turbulence

Time vs. Ensemble Average

Time Average

$$U_{avg}(\mathbf{x},t_0)=\lim_{t\to\infty}\frac{1}{t-t_0}\int_{t_0}^{t}u(\mathbf{x},t)dt$$

$$u(\mathbf{x},t)=U_{avg}(\mathbf{x},t_0)+u'(\mathbf{x},t)$$

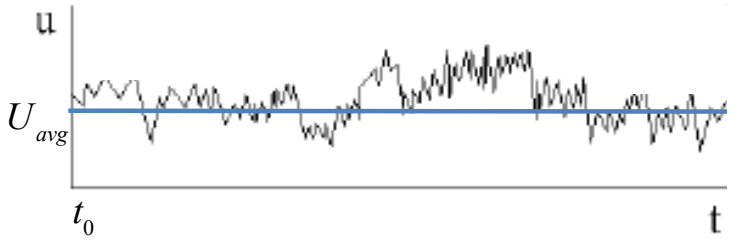

Ensemble Average

$$U(\mathbf{x},t)=\lim_{N\to\infty}\frac{1}{N}\sum_{n=1}^{N}u^{(n)}(\mathbf{x},t)$$

$$u(\mathbf{x},t)=U(\mathbf{x},t)+u'(\mathbf{x},t)$$

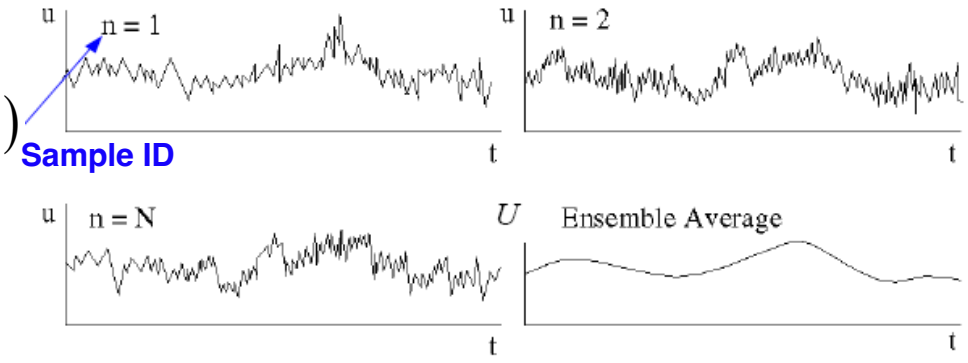

Reynolds averaging is an ensemble averaging!

For stationary turbulence, the two are identical.

Favre (density-weighted) Average

Useful for flows with large density variations (combustion)

$$\tilde{u}(\mathbf{x},t) = \overline{\rho u}(\mathbf{x},t) / \bar{\rho}$$

such that

$$u(\mathbf{x},t) = \tilde{u}(\mathbf{x},t) + u''(\mathbf{x},t)$$

and by definition:

$$\widetilde{u''} = 0 \quad \text{or} \quad \overline{\rho u''} = 0$$

and it follows that:

$$\overline{\rho u} = \overline{\rho(\tilde{u} + u'')} = \overline{\rho\tilde{u}} + \overline{\rho u''} = \bar{\rho}\tilde{u}$$

Characterizing Turbulence Scales

Turbulent scales: two-point velocity correlations

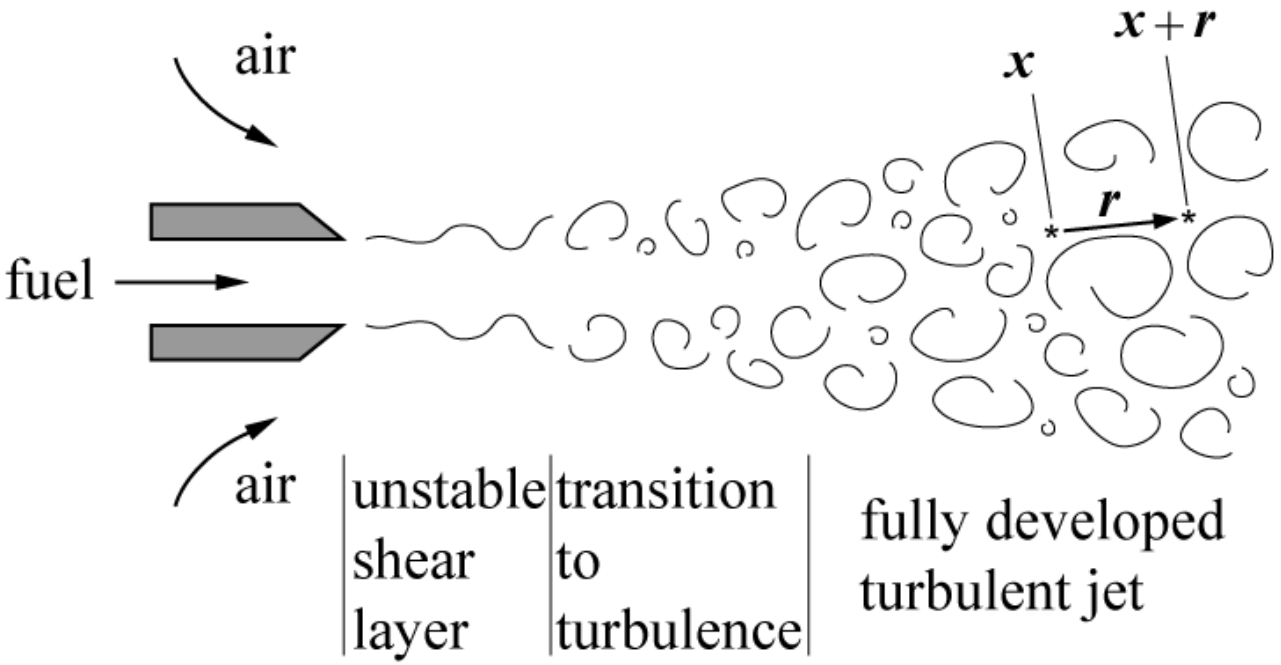

- Turbulence is commonly generated by a strong shear flow.
- Fully developed turbulent flow is characterized by the velocity and length scale of turbulent “eddies” at various sizes.

Length and Time Scales of Turbulence

Length:

$$R(\mathbf{x},\mathbf{r},t) = \overline{u'(\mathbf{x},t)u'(\mathbf{x}+\mathbf{r},t)}: \text{ two-point velocity correlation}$$

$$= R(r,t) \text{ for homogeneous turbulence } (r = |\mathbf{r}|)$$

$$f(r,t) = \frac{R(r,t)}{\overline{u'^2(t)}} : \text{normalized correlation}$$

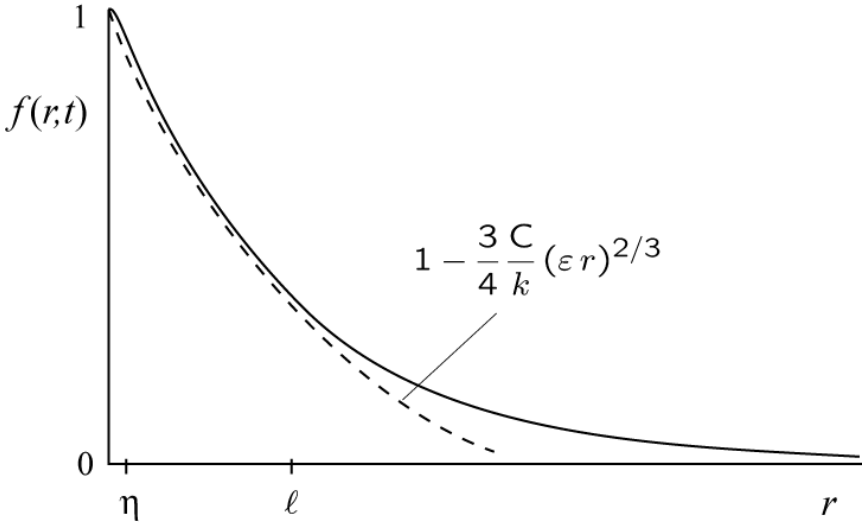

$$\ell(t) = \frac{\int_0^\infty R(r,t)\,dr}{\overline{u'^2(t)}} : \text{ Integral scale}$$

(typically a fraction of the system dimension)

$$\mathrm{Re}_\ell = \frac{u'\ell}{\nu} : \text{ turbulent Reynolds number}$$

Length and Time Scales of Turbulence

Summary: Turbulence Scales

Length: $\ell(t) = \dfrac{\int_0^\infty R(r,t)\,dr}{\overline{u'^2(t)}}$: the integral length scale

Velocity: $u' = u - \bar{u} = \begin{cases} \sqrt{2k/3} \\ \text{or } \sqrt{2k} \end{cases}$: RMS velocity fluctuation

Time: $\tau = \ell / u'$: eddy turnover time $(= k/\varepsilon)$

Key dimensionless parameter:

$$\mathrm{Re}_\ell = \frac{u'\ell}{\nu}: \text{ turbulent Reynolds number}$$

Length and Time Scales of Turbulence

Summary: Turbulence Scales

Length: $\ell(t) = \dfrac{\int_0^\infty R(r,t)\,dr}{\overline{u'^2(t)}}$: the integral length scale

Velocity: $u' = u - \bar{u} = \begin{cases} \sqrt{2k/3} \\ \text{or } \sqrt{2k} \end{cases}$: RMS velocity fluctuation

Time: $\tau = \ell / u'$: eddy turnover time $(= k/\varepsilon)$

Key dimensionless parameter:

$$\mathrm{Re}_\ell = \frac{u'\ell}{\nu}: \text{ turbulent Reynolds number}$$

Turbulent Energy Cascade

$$\varepsilon \sim \nu \overline{\left(\frac{\partial u'}{\partial x}\right)^2}\ ;\ \varepsilon \sim \frac{\nu u'^2}{\lambda^2}$$

Kolmogorov Theory (for homogeneous isotropic turbulence)

$$\Rightarrow \lambda \sim \left(\frac{\nu}{\varepsilon}\right)^{1/2} \qquad u' = u'\tau_\eta$$

Net energy flows from large to small scales at a steady rate

ε : energy dissipation rate

$$\varepsilon = \frac{\text{energy}}{\text{time}} = \frac{u'^2}{\ell / u'} = \frac{u'^3}{\ell}$$

eddy turnover time

$$\frac{u'^3}{\ell} = \frac{u_\lambda'^3}{\lambda} = \frac{u_\eta'^3}{\eta}$$

Scale invariance
Universality hypothesis

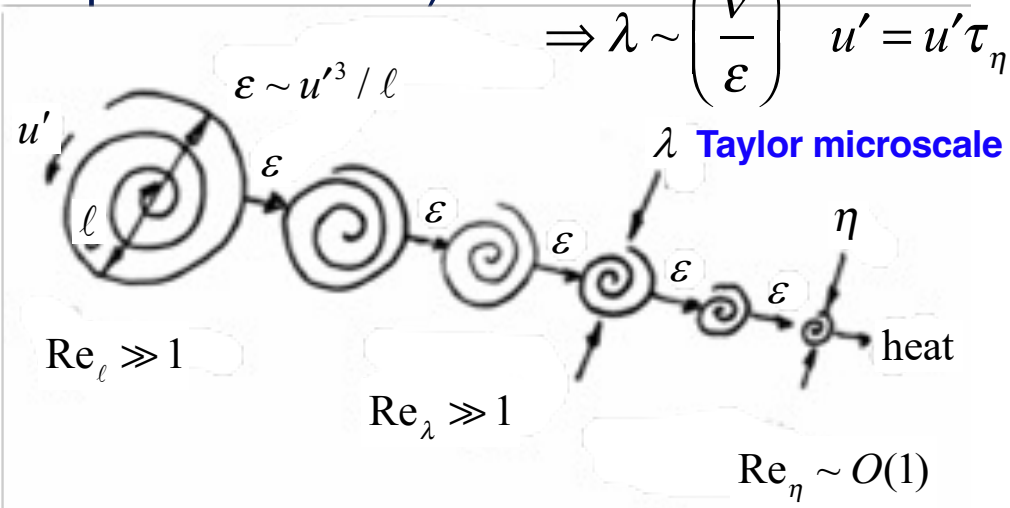

Where does it end?
- Energy dissipation (ε) by viscosity (ν)

Dimensional analysis yields:

$$\eta = \left(\frac{\nu^3}{\varepsilon}\right)^{1/4}\ ;\ \tau_\eta = \left(\frac{\nu}{\varepsilon}\right)^{1/2}\ ;\ u_\eta = (\nu\varepsilon)^{1/4}$$

Kolmogorov scale $\qquad \mathrm{Re}_\eta = \frac{u_\eta' \eta}{\nu} = 1$

Turbulence Scales and Relations

	Integral	Taylor	Kolmogorov
L	$\ell = \int_0^\infty f\, dr$	$\lambda = u'\tau_\eta = \left(\frac{2k\nu}{\varepsilon}\right)^{1/2}$	$\eta = \left(\frac{\nu^3}{\varepsilon}\right)^{1/4}$
U	$u' = \sqrt{2k}$	$u'_\lambda = \left(\lambda\varepsilon\right)^{1/3}$	$u'_\eta = \left(\nu\varepsilon\right)^{1/4}$
T	$\tau = \frac{\ell}{u'} = \frac{k}{\varepsilon}$	$\tau_\lambda = \frac{\lambda}{u'_\lambda}$	$\tau_\eta = \left(\frac{\nu}{\varepsilon}\right)^{1/2}$

Important Scaling Relations:

$$\frac{\lambda}{\ell} = \frac{\nu^{1/2}u'}{\varepsilon^{1/2}\ell} = \frac{\nu^{1/2}u'}{u'^{3/2}\ell^{1/2}} = \mathrm{Re}_\ell^{-1/2} \qquad \frac{\eta}{\ell} = \frac{\nu^{3/4}}{\varepsilon^{1/4}\ell} = \frac{\nu^{3/4}}{u'^{3/4}\ell^{3/4}} = \mathrm{Re}_\ell^{-3/4}$$

The Kolmogorov Hypothesis

Steady, homogeneous, isotropic turbulence

In the inertial subrange, $E = dk/dK$ is independent of ν, and is a function of wave number (K) and ε.

$$[K] = \frac{1}{L}, \quad [\varepsilon] = \frac{L^2}{T^3}$$

Dimensional analysis yields:

$$[E] = \frac{\text{energy/mass}}{\text{wave no.}} = \frac{L^2/T^2}{1/L} = \frac{L^3}{T^2}$$

$$\Rightarrow E(K) = \frac{dk}{dK} = C\varepsilon^{2/3}K^{-5/3}$$

The -5/3 Law

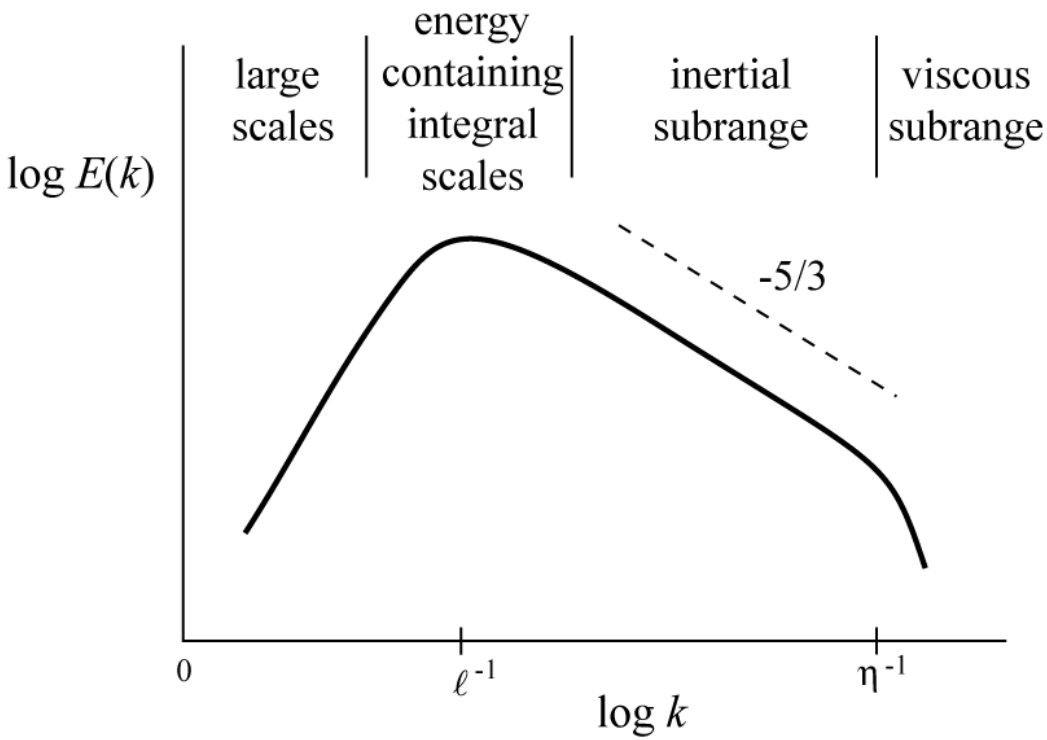

Turbulent Flow/Combustion Simulations

How much do we need to resolve?

Predictive Simulations of Multi-scale Combustion

Direct numerical simulations (DNS) of turbulent flame propagation

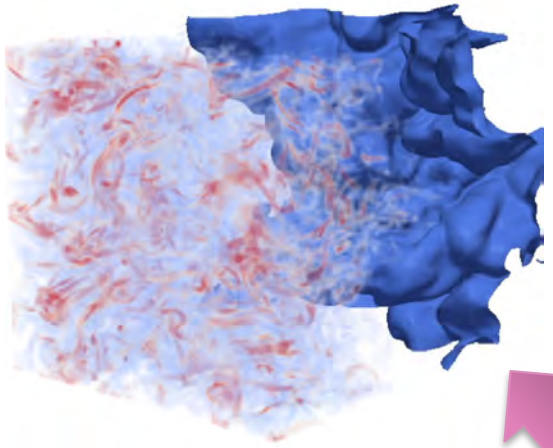

Full-cycle simulations of combustion engines

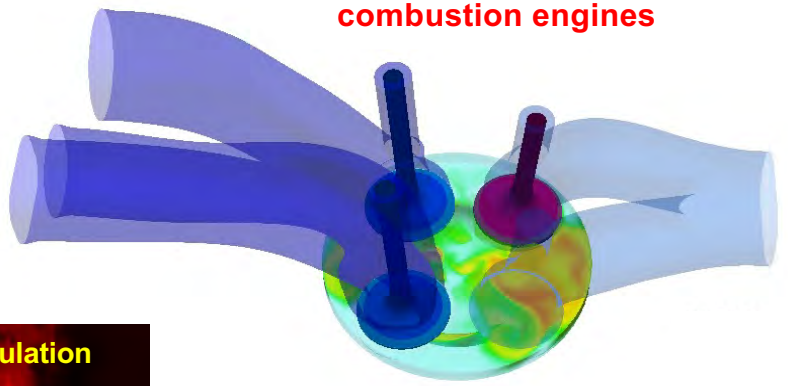

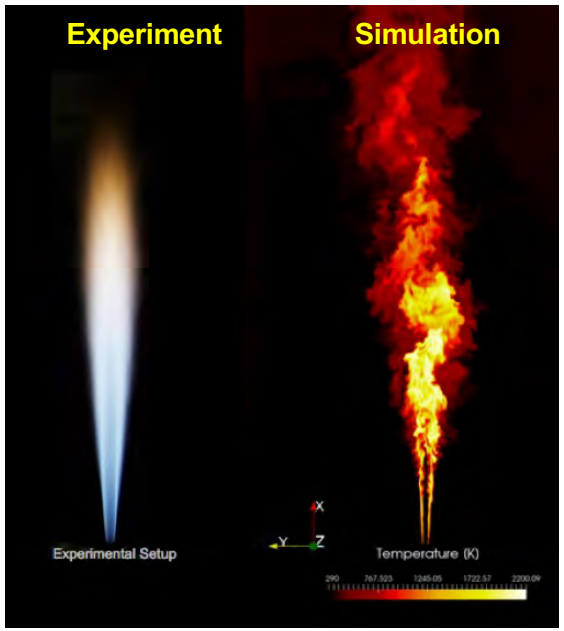

High performance computing enables predictive analysis of combustion and pollutant formation, allowing intelligent design of advanced engines at lower development costs.

Large eddy simulations (LES) of laboratory-scale flames

Hierarchy of Turbulent Combustion Modeling

Direct Numerical Simulation (DNS)

- Resolves all relevant physical scales
- Key issues: accuracy, stability, efficiency

Large Eddy Simulation (LES)

- Resolves large-scale eddies, model subgrid scales
- Key issues: accuracy, numerical dissipation, subgrid modeling

Reynolds-Averaged Navier Stokes (RANS)

- Statistical average
- Key issues: closure of higher-order moments
  - Zero-equation models
  - One-equation models
  - Two-equation models
  - Reynolds-stress model

  Lots of empirical, case-by-case tuning…

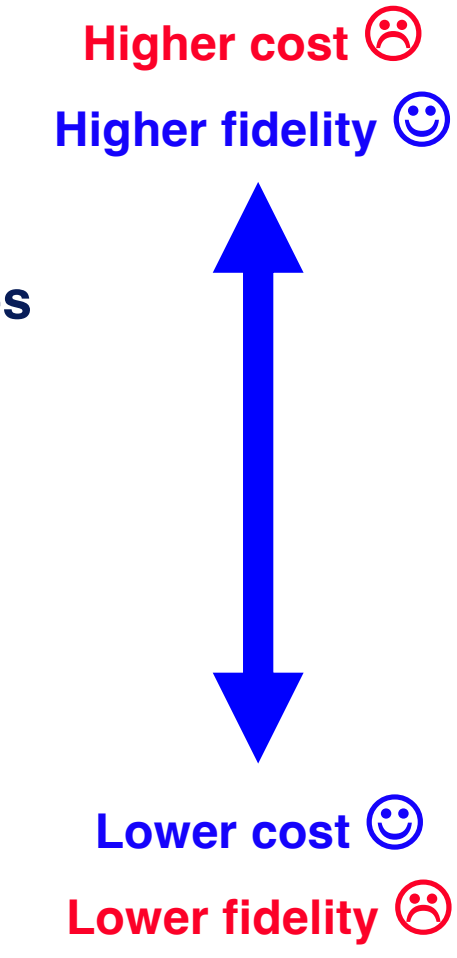

RANS: Special Cases

Reynolds average = Time average when

- The statistical average does not change over time (statistical stationary)
  - Turbulent jet flames
  - Most combustors at steady operation
- Turbulence is homogeneous in one direction
  - Turbulent channel flows

For unsteady problems, simple time-averaging may yield completely wrong results

- IC engines
- von Karman vortex shedding

RANS vs. LES

Modeling turbulence involves averaging of small fluctuations

Reynolds-averaged Navier-Stokes (RANS): the (ensemble) averaging represents averages over regions in physical space that are of the order of the integral scale.

Large eddy simulation (LES): the "filtering" operation is done at scales smaller than the integral scale, thus smearing out the smaller ("sub-grid") scale features.

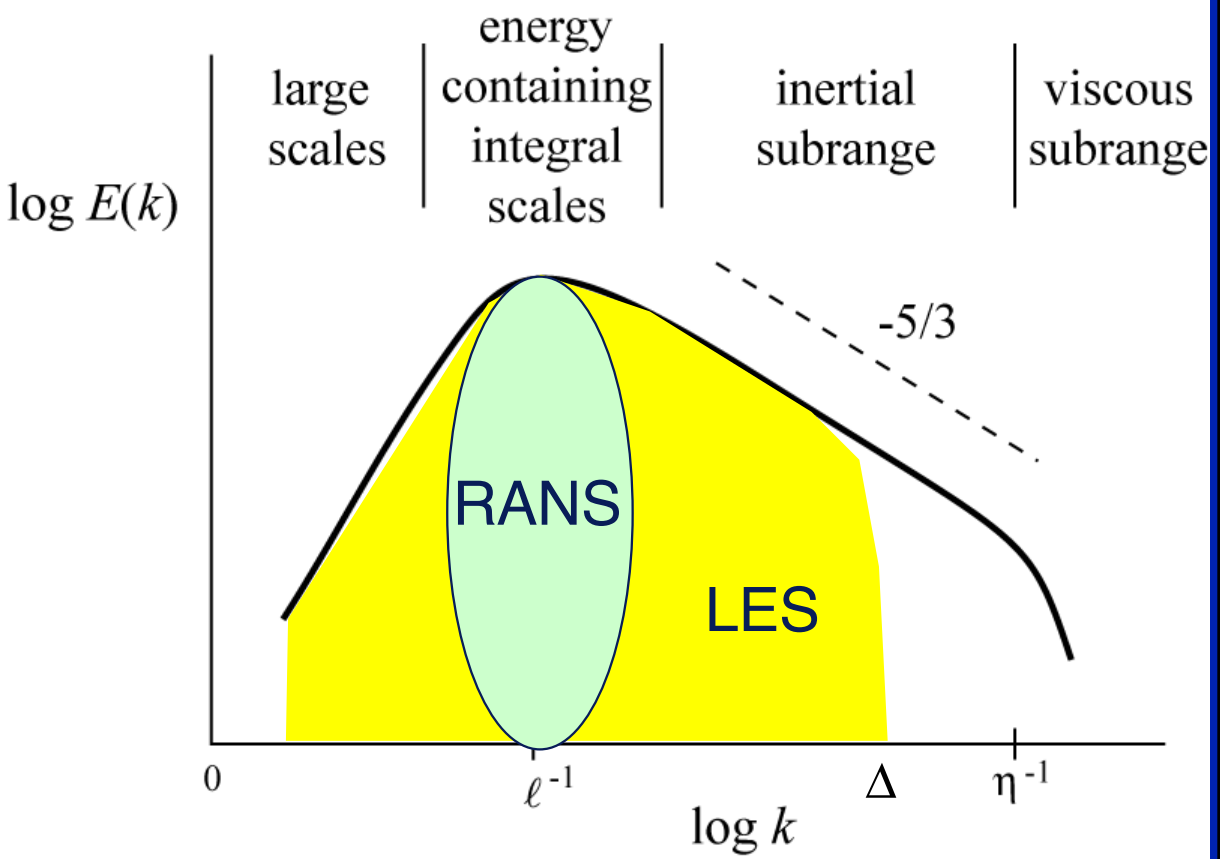

RANS Formulation

$u(\mathbf{x},t) = U(\mathbf{x},t) + u'(\mathbf{x},t)$ and taking the ensemble average,

$$\overline{\frac{\partial(U_i + u_i')}{\partial t}} + \overline{(U_k + u_k')\frac{\partial(U_i + u_i')}{\partial x_k}} = -\frac{1}{\rho}\overline{\frac{\partial(p + p')}{\partial x_i}} + \overline{\frac{\partial}{\partial x_j}\left(\nu \frac{\partial(U_i + u_i')}{\partial x_j}\right)}$$

$$\Rightarrow \frac{\partial U_i}{\partial t} + U_k \frac{\partial U_i}{\partial x_k} = -\frac{1}{\rho}\frac{\partial \overline{p}}{\partial x_i} + \frac{\partial}{\partial x_j}\left(\nu \frac{\partial U_i}{\partial x_j}\right) + \frac{\partial R_{ij}}{\partial x_j}$$

where $R_{ij} = -\overline{u_i' u_j'}$ (Reynolds stress tensor)

$$\overline{u_i' u_j'} = \begin{bmatrix} \overline{u'u'} & \overline{u'v'} & \overline{u'w'} \\ \overline{v'u'} & \overline{v'v'} & \overline{v'w'} \\ \overline{w'u'} & \overline{w'v'} & \overline{w'w'} \end{bmatrix}$$

The “Closure” Problem

One can derive higher order equations, which will only lead to additional higher order terms to be closed.

Gradient Transport Model (Boussinesq)

$$R_{ij} = -\overline{u_i' u_j'} = 2\nu_t S_{ij} - \frac{2}{3}\nu_t \frac{\partial U_k}{\partial x_k}\delta_{ij} - \frac{2}{3}\frac{\kappa_{bulk}}{\rho}\delta_{ij}$$

$$S_{ij} = \frac{1}{2}\left(\frac{\partial U_i}{\partial x_j} + \frac{\partial U_j}{\partial x_i}\right): \text{ strain rate tensor}$$

$$\nu_t : \text{ turbulent viscosity}$$

Determining turbulent viscosity

- Zero equation: Prandtl mixing length, Smagorinsky
- One equation: transport equation for k, model t_c
- Two equation: transport equations for k and ε.

Large Eddy Simulation: Concept

Spatial filtering of small scale details

- Large eddies
  - Determines the overall transport process
  - Anisotropic, transient, sensitive to IC/BC
- Small eddies
  - Mainly responsible for dissipation of kinetic energy
  - More isotropic, less dependent on IC/BC
- Compromise
  - Simulate large scales as in DNS
  - Model small (subgrid) scales (as in RANS)

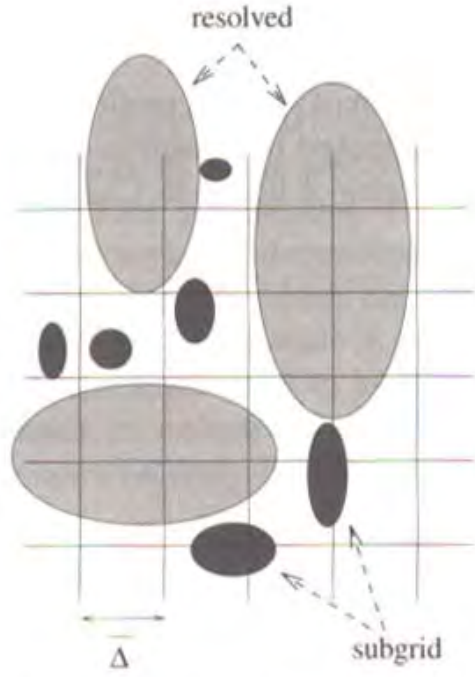

PHYSICAL SPACE

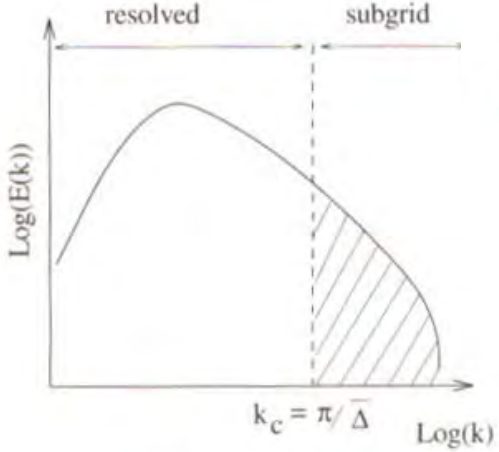

FOURIER SPACE

LES Filtering

$$\bar{u}_i(x,t) = \int G(x-\xi;\bar{\Delta})u(\xi,t)d\xi$$

$G(x-\xi)$: filter kernel $\bar{\Delta}$: filter size

$$G(x-\xi) = \begin{cases} \dfrac{1}{\bar{\Delta}} \text{ if } |x-\xi| \le \dfrac{\bar{\Delta}}{2} \\ 0 \quad \text{otherwise} \end{cases}$$

Box (top-hat) filter

$$G(x-\xi) = \left(\frac{\gamma}{\pi\bar{\Delta}^2}\right)^{1/2} \exp\left(\frac{-\gamma|x-\xi|^2}{\bar{\Delta}^2}\right)$$

Gaussian filter

$$G(x-\xi) = \frac{\sin\left(\pi(x-\xi)/\bar{\Delta}\right)}{\pi(x-\xi)/\bar{\Delta}}$$

Sharp cutoff filter

LES Equations

Navier-Stokes Equations

$$\frac{\partial u_i}{\partial t}+\frac{\partial}{\partial x_j}\left(u_i u_j\right)=-\frac{1}{\rho}\frac{\partial p}{\partial x_i}+\nu\frac{\partial}{\partial x_j}\left(\frac{\partial u_i}{\partial x_j}+\frac{\partial u_j}{\partial x_i}\right)$$

Filtered equations

$$\frac{\partial \overline{u}_i}{\partial t}+\frac{\partial}{\partial x_j}\left(\overline{u_i u_j}\right)=-\frac{1}{\rho}\frac{\partial \overline{p}}{\partial x_i}+\nu\frac{\partial}{\partial x_j}\left(\frac{\partial \overline{u}_i}{\partial x_j}+\frac{\partial \overline{u}_j}{\partial x_i}\right)$$

unknown

Rewriting

$$\frac{\partial \overline{u}_i}{\partial t}+\frac{\partial}{\partial x_j}\left(\overline{u}_i \overline{u}_j\right)=-\frac{1}{\rho}\frac{\partial \overline{p}}{\partial x_i}-\frac{\partial}{\partial x_j}\left(\overline{u_i u_j}-\overline{u}_i \overline{u}_j\right)+\nu\frac{\partial}{\partial x_j}\left(\frac{\partial \overline{u}_i}{\partial x_j}+\frac{\partial \overline{u}_j}{\partial x_i}\right)$$

subgrid stress tensor

Subgrid Model

Modeling subgrid stress tensor $\tau_{ij} = \overline{u_i u_j} - \overline{u}_i \overline{u}_j$

Zero equation: Smagorinsky model (gradient transport)

$$\tau_{ij} - \frac{1}{3}\delta_{ij}\tau_{kk} = -2\nu_t \overline{S}_{ij}, \quad \nu_t = C_S \overline{\Delta}^2 \left|\overline{S}\right| \quad \textbf{eddy viscosity}$$

$$\overline{S}_{ij} = \frac{1}{2}\left(\frac{\partial \overline{u}_i}{\partial x_j} + \frac{\partial \overline{u}_j}{\partial x_i}\right), \qquad \left|\overline{S}\right| = \left|2\overline{S}_{ij}\overline{S}_{ij}\right|^{1/2}$$

One equation viscosity model (solve transport equation for k_{sgs})

$$\nu_t = C_s \Delta \sqrt{k_{sgs}}$$

One equation dynamic structure (non-viscosity) model (Rutland et al.)

$$\tau_{ij} = - C_{ij} k_{sgs}$$

DNS vs. LES vs. RANS

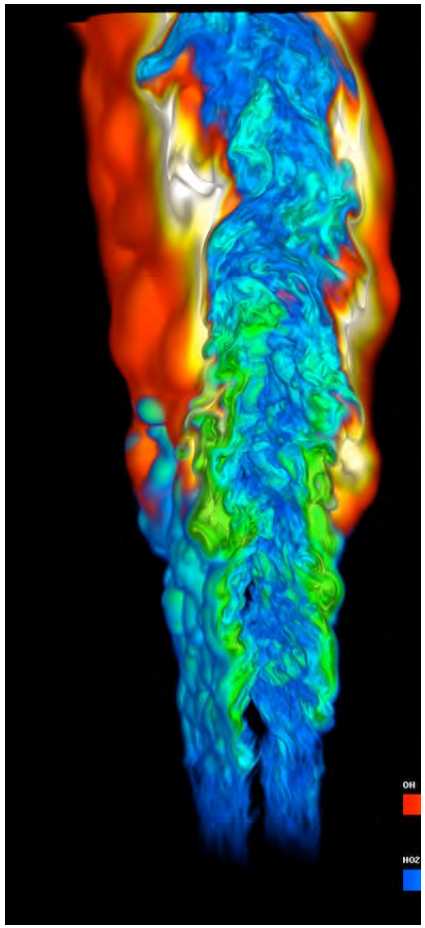

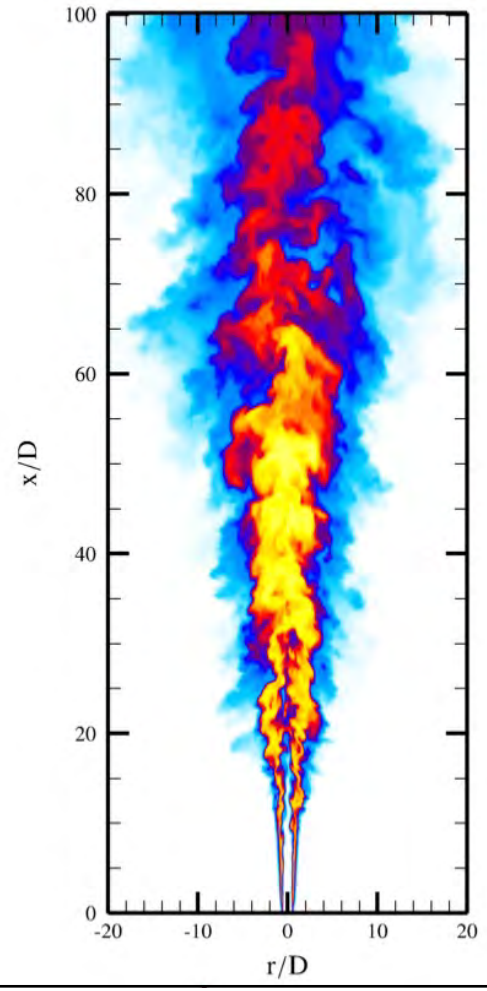

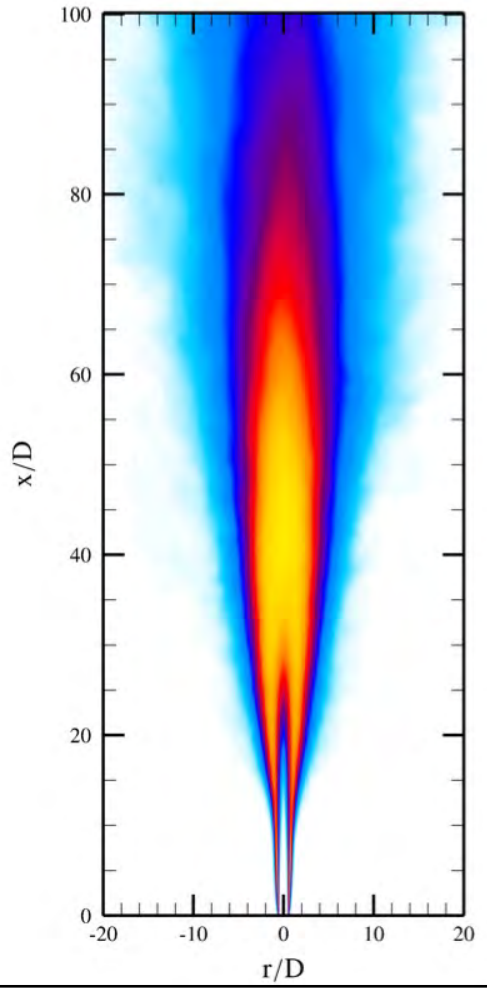

RANS vs. LES

Reynolds-averaged

$$u(x,t) = \bar{u}(x,t) + u'(x,t)$$

LES-filtered

$$\bar{u}_i(x,t) = \int_\Delta G(x-\xi)u(\xi,t)\,d\xi$$

$$\frac{\partial \bar{u}_i}{\partial t} + \frac{\partial}{\partial x_j}\left(\bar{u}_i\bar{u}_j\right) = -\frac{1}{\rho}\frac{\partial \bar{p}}{\partial x_i} - \frac{\partial \tau_{ij}}{\partial x_j} + \nu\frac{\partial}{\partial x_j}\left(\frac{\partial \bar{u}_i}{\partial x_j} + \frac{\partial \bar{u}_j}{\partial x_i}\right)$$

$$\tau_{ij} = \overline{u_i'u_j'} = -\nu_t\left(\frac{\partial \bar{u}_i}{\partial x_j} + \frac{\partial \bar{u}_j}{\partial x_i}\right) + \frac{2}{3}\nu_t\frac{\partial \bar{u}_k}{\partial x_k}\delta_{ij}$$

$$\nu_t = C_\mu\frac{k^2}{\varepsilon}$$

Reynolds stress

$$\tau_{ij} = \frac{1}{3}\delta_{ij}\tau_{kk} - \nu_t\left(\frac{\partial \bar{u}_i}{\partial x_j} + \frac{\partial \bar{u}_j}{\partial x_i}\right)$$

$$\nu_t = C_S\bar{\Delta}^2\left|2\bar{S}_{ij}\bar{S}_{ij}\right|^{1/2}$$

Leonard subgrid stress

Just change a few lines in the code!!

RANS vs. LES Codes

So why not modify RANS code to do LES simulations?

$$\mathrm{Re}_{num} = \frac{UL}{\nu_{lam} + \nu_{turb} + \nu_{num}}$$

T. Poinsot, Princeton CEFRC Summer School 2013, 2015

- RANS simulations involve a large level of turbulent viscosity, and the results are more forgiving on numerical viscosity (upwind schemes, lower order schemes) - ν_{turb} dominates.
- LES simulations have a much lower level of turbulent (subgrid) viscosity, and thus need lower numerical viscosity (higher order schemes, finer grid resolution) - ν_{turb} much smaller, competing with ν_{num}.

⇒ A good LES code needs:

- High order spatial discretization schemes
- High order time integration schemes with smaller time steps

so as to capture the large eddy behavior correctly.

Turbulent Combustion Regimes

Turbulence-flame interaction manifests differently

Why do we care about combustion regimes?

Key design target quantities (burning rate, emissions, etc.) depend strongly on the effects of turbulent fluctuations on nonlinear reaction terms.

Unlike turbulent kinetic/scalar energy transport which can be estimated/extrapolated, the higher order/subgrid reaction terms must be modeled **entirely**.

No universal combustion submodels exist. A better strategy is to model combustion processes in different "regimes".

Note that many combustion submodels are equally applicable to both RANS and LES approaches.

$$w = B\psi \exp\left(-\frac{E}{RT}\right)$$

$$\text{with } \psi = \bar{\psi} + \psi', T = \bar{T} + T' \quad (T' \ll \bar{T}),$$

$$\bar{w} = \overline{B\left(\bar{\psi} + \psi'\right)\exp\left(-\frac{E}{R\left(\bar{T} + T'\right)}\right)}$$

$$= B\bar{\psi}\exp\left(-\frac{E}{R\bar{T}}\right)\overline{\left[1 + \frac{E}{R\bar{T}^2}T' + \frac{1}{2}\left(\frac{E}{R\bar{T}}\right)^2\left(\frac{T'}{\bar{T}}\right)^2 + \cdots\right]}$$

$$= B\bar{\psi}\exp\left(-\frac{E}{R\bar{T}}\right)\overline{\left[1 + \frac{1}{2}\left(\frac{E}{R\bar{T}}\right)^2\left(\frac{T'}{\bar{T}}\right)^2 + \cdots\right]}$$

Not small for $\frac{E}{R} \gg \bar{T}$

(large activation energy)

Physical Scales of Turbulent Combustion

For scaling purposes, we assume

$$\mathrm{Pr} = \frac{\nu}{\alpha} = 1, \quad \mathrm{Sc} = \frac{\nu}{D} = 1$$

Characteristic velocity

S_L : laminar flame speed (for premixed combustion)

Characteristic length

$l_f = \dfrac{\nu}{S_L}$: (nominal) laminar flame thickness

Characteristic time

$\tau_c = \tau_f = \dfrac{\nu}{S_L^2} = \dfrac{l_f}{S_L}$: chemical time $\left(l_f = \sqrt{\nu \tau_c} \right)$

$\tau = \dfrac{\ell}{u'} = \dfrac{\ell}{\sqrt{2k}}$: turbulent flow (eddy turnover) time

Damköhler and Karlovitz Numbers

Damköhler

$$\mathrm{Da}_\ell = \frac{\tau}{\tau_c} = \frac{\ell / u'}{\tau_c} = \frac{\ell / u'}{l_f / S_L} = \frac{\ell / u'}{\nu / S_L^2} = \frac{\text{eddy turnover time}}{\text{flame time}}$$

Karlovitz

$$\mathrm{Ka} = \frac{\tau_c}{\tau_K} : \text{Karlovitz number} \left(= 1 / \mathrm{Da}_K \text{ per Linan \&Williams} \right)$$

$$= \frac{l_f / S_L}{\left(\nu / \varepsilon\right)^{1/2}} = \frac{l_f / S_L}{\left(\nu \ell\right)^{1/2} / u'^{3/2}} = \left(\frac{u' \ell}{\nu} \right)^{1/2} \frac{l_f / S_L}{\ell / u'} = \mathrm{Re}_\ell^{1/2} / \mathrm{Da}_\ell$$

Recall turbulent Reynolds number

$$\mathrm{Re}_\ell = \frac{u' \ell}{\nu} = \frac{u' \ell}{S_L l_f}$$

Relations among Nondimensional Numbers

$$\mathrm{Ka} = \mathrm{Re}_\ell^{1/2} / \mathrm{Da}_\ell \quad \text{or} \quad \mathrm{Re}_\ell = \left(\mathrm{KaDa}_\ell\right)^2$$

It follows that

$$\mathrm{Ka} = \frac{\tau_c}{\tau_K} = \frac{l_f / S_L}{\eta / u'_\eta} = \frac{\nu / S_L^2}{\nu / u'^2_\eta} = \left(\frac{u'_\eta}{S_L}\right)^2 = \left(\frac{l_f}{\eta}\right)^2$$

$$\mathrm{Re}_\ell / \mathrm{Da}_\ell = \left(\frac{u'}{S_L}\right)^2 \qquad \mathrm{Re}_\ell \, \mathrm{Da}_\ell = \left(\frac{\ell}{l_f}\right)^2$$

Flow turbulence

$$\eta = \left(\frac{\nu^3}{\varepsilon}\right)^{1/4}$$ Kolmogorov scale

Scalar turbulence

$$\ell_C = \left(\frac{D^3}{\varepsilon}\right)^{1/4}$$ Obukhov-Corrsin scale

Since we assumed $\nu = D$, $\ell_C = \eta$

Two Important Non-D Numbers:

Re_ℓ: a measure of turbulence intensity

Da_ℓ: a measure of chemical intensity (relative to integral scale flow)

$$\mathrm{Da}_\ell = \left(\frac{u'}{S_L}\right)^{-2} \mathrm{Re}_\ell; \qquad \mathrm{Da}_\ell = \mathrm{Ka}^{-1} \mathrm{Re}_\ell^{1/2}; \qquad \mathrm{Da}_\ell = \left(\frac{\ell}{l_f}\right)^2 \mathrm{Re}_\ell^{-1}$$

Characteristic Scales: Turbulent Premixed Combustion

	Turbulence (Integral)	Turbulence (Kolmogorov)	Combustion (Premixed flames)	
Length	$\ell = \int_0^\infty f\, dr$	$\eta = \left(\frac{\nu^3}{\varepsilon}\right)^{1/4}$	$\ell_f = \nu / S_L$	
Velocity	$u' = \sqrt{2k}$	$u'_K = (\nu\varepsilon)^{1/4}$	S_L	
Time	$\tau_\ell = \frac{\ell}{u'}$	$\tau_K = \left(\frac{\nu}{\varepsilon}\right)^{1/2}$	$\tau_f = \ell_f / S_L$	
Non-D Parameter	$\mathrm{Re}_\ell = \frac{u'\ell}{\nu}$	$\mathrm{Re}_K = \frac{u'_\eta \eta}{\nu} = 1$	$\mathrm{Da}_\ell = \frac{\tau_\ell}{\tau_f}$	$\mathrm{Da}_K = \frac{\tau_K}{\tau_f} = \frac{1}{\mathrm{Ka}}$

$$\frac{\tau_\ell}{\tau_K} = \mathrm{Re}_\ell^{1/2} = \mathrm{DaKa} \qquad \mathrm{Ka} = \left(\frac{\ell_f}{\eta}\right)^2 \qquad \mathrm{Re}_\ell/\mathrm{Da}_\ell = \left(\frac{u'}{S_L}\right)^2 \qquad \mathrm{Re}_\ell\,\mathrm{Da}_\ell = \left(\frac{\ell}{l_f}\right)^2$$

Relations for Regime (Borghi) Diagram

Using

$$\mathrm{Ka} = \left(\frac{l_f}{\eta}\right)^2 \quad \text{and} \quad \mathrm{Re}_\ell = \frac{u'\ell}{S_L l_f}$$

$$\text{Since } \eta = \left(\frac{\nu^3}{\varepsilon}\right)^{1/4}, \quad \eta^2 = \left(S_L^3 l_f^3 \frac{\ell}{u'^3}\right)^{1/2}$$

$$\frac{u'}{S_L} = \mathrm{Re}_\ell \left(\frac{\ell}{l_f}\right)^{-1} = \mathrm{Ka}^{2/3}\left(\frac{\ell}{l_f}\right)^{1/3} \qquad \log\left(\frac{u'}{S_L}\right) = \frac{2}{3}\log \mathrm{Ka} + \frac{1}{3}\log\left(\frac{\ell}{l_f}\right)$$

Laminar Flamelet / Thin Reaction Sheet Regimes

The Klimov-Williams criterion:

$$\mathrm{Ka} = \left(\frac{\ell_f}{\eta}\right)^2 < 1$$

determines the conditions where the laminar flame structure is intact.

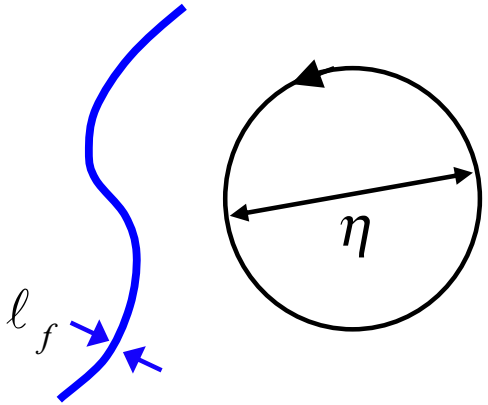

Peters's extension:

$$\mathrm{Ka}_R = \frac{\tau_R}{\tau_K} = \left(\frac{\ell_R}{\eta}\right)^2 = \left(\frac{\ell_R}{\ell_f}\right)^2 \left(\frac{\ell_f}{\eta}\right)^2 = \mathrm{Ze}^{-2}\mathrm{Ka}$$

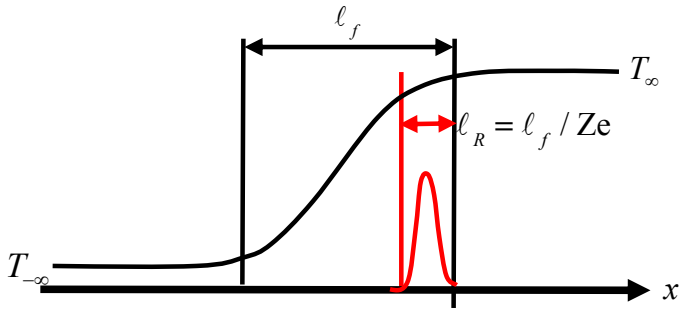

Asymptotic structure of flame

If $\mathrm{Ze} = 10$ (realistic), $\mathrm{Ka}_R = \mathrm{Ka}/100$

$\Rightarrow\ \mathrm{Ka}_R < 1$ even for $1 < \mathrm{Ka} < 100$, thus the reaction zone regime is extended.

The Borghi-Peters Diagram (Premixed)

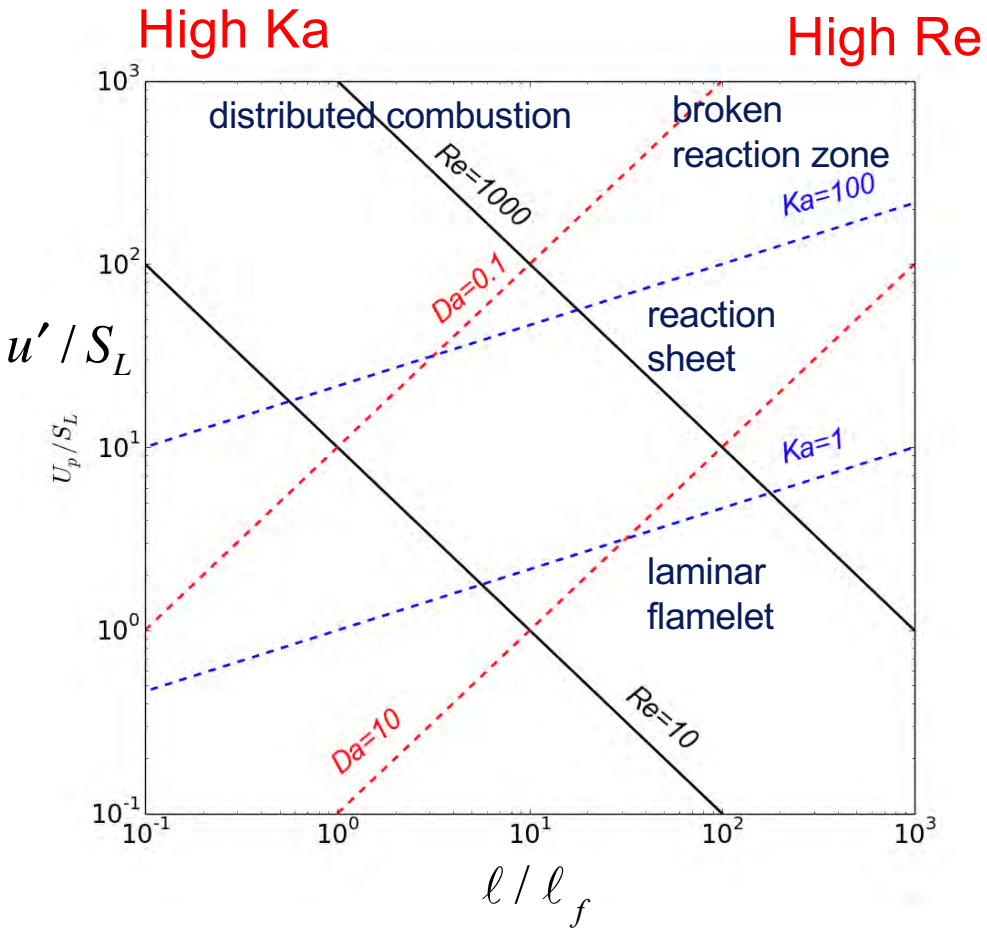

Criticisms:

- ✓ Both ℓ and u' are system-dependent parameters, lacking in generality in describing universal turbulent combustion characteristics.
- ✓ ℓ_f and S_L are properties of premixed flames, so the diagram cannot be extended to nonpremixed combustion.
- ✓ High Ka and high Re appear on two different corners, giving a misleading impression that the two conditions are reached distinctively.

The Williams Diagram (Premixed)

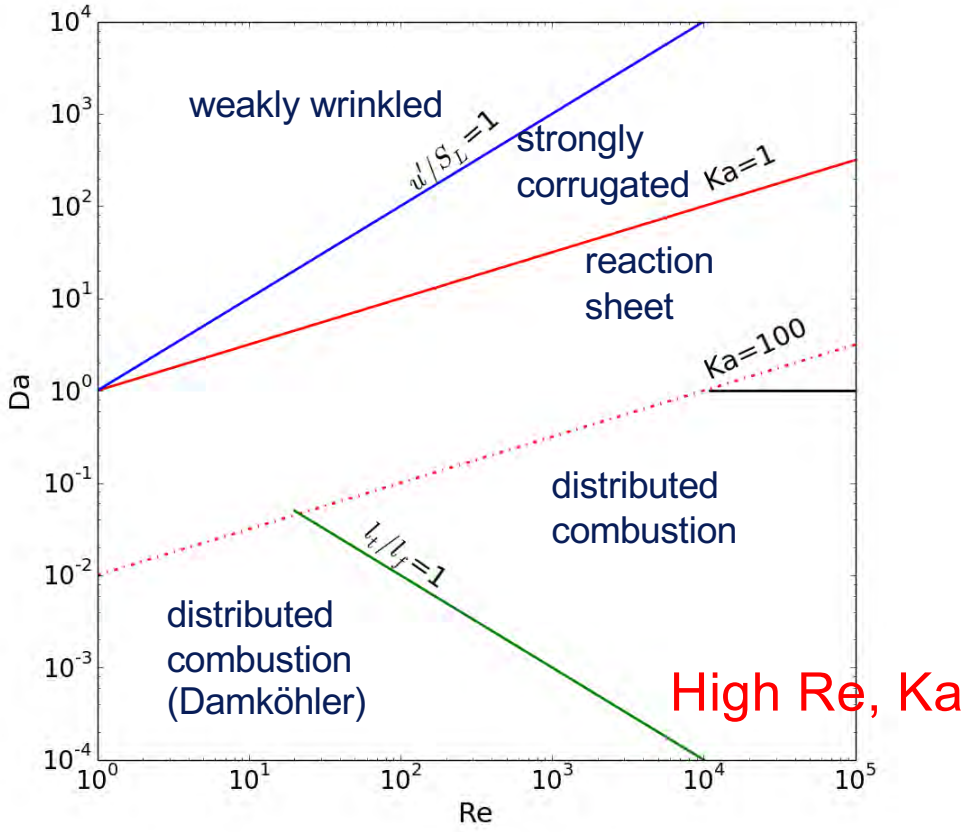

- ✓ Re and Da, respectively, represent intensities of turbulence and chemical reactivity.
- ✓ Directions of high Re and Ka are aligned (lower right corner).
- ✓ The diagram can be extended to turbulent nonpremixed combustion in a consistent manner.

Effects of Ka on Flame Topology

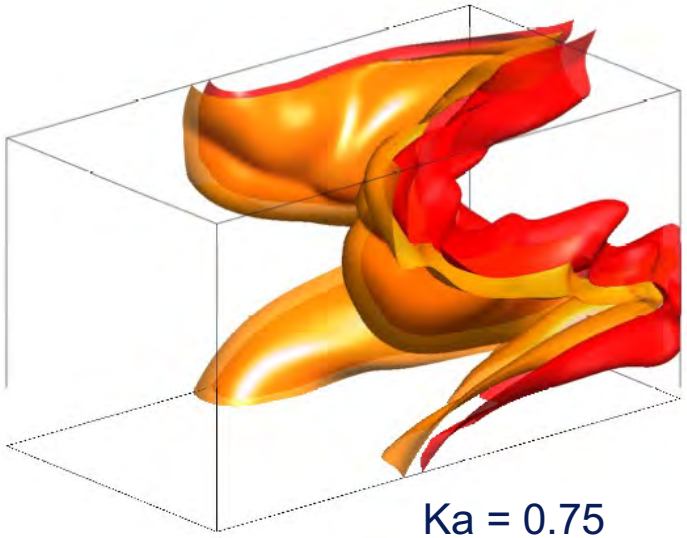

Ka = 0.75

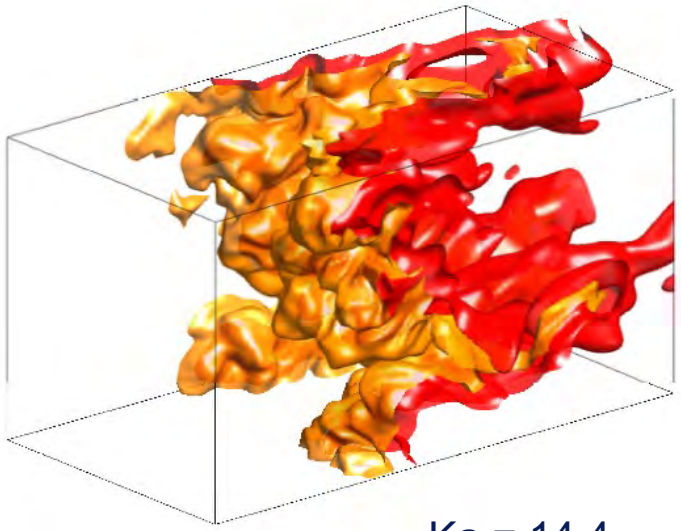

Ka = 14.4

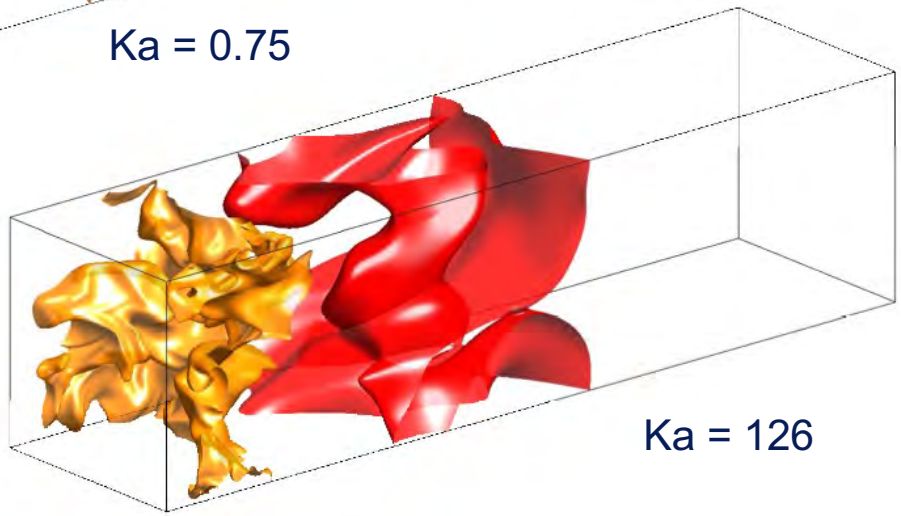

Ka = 126

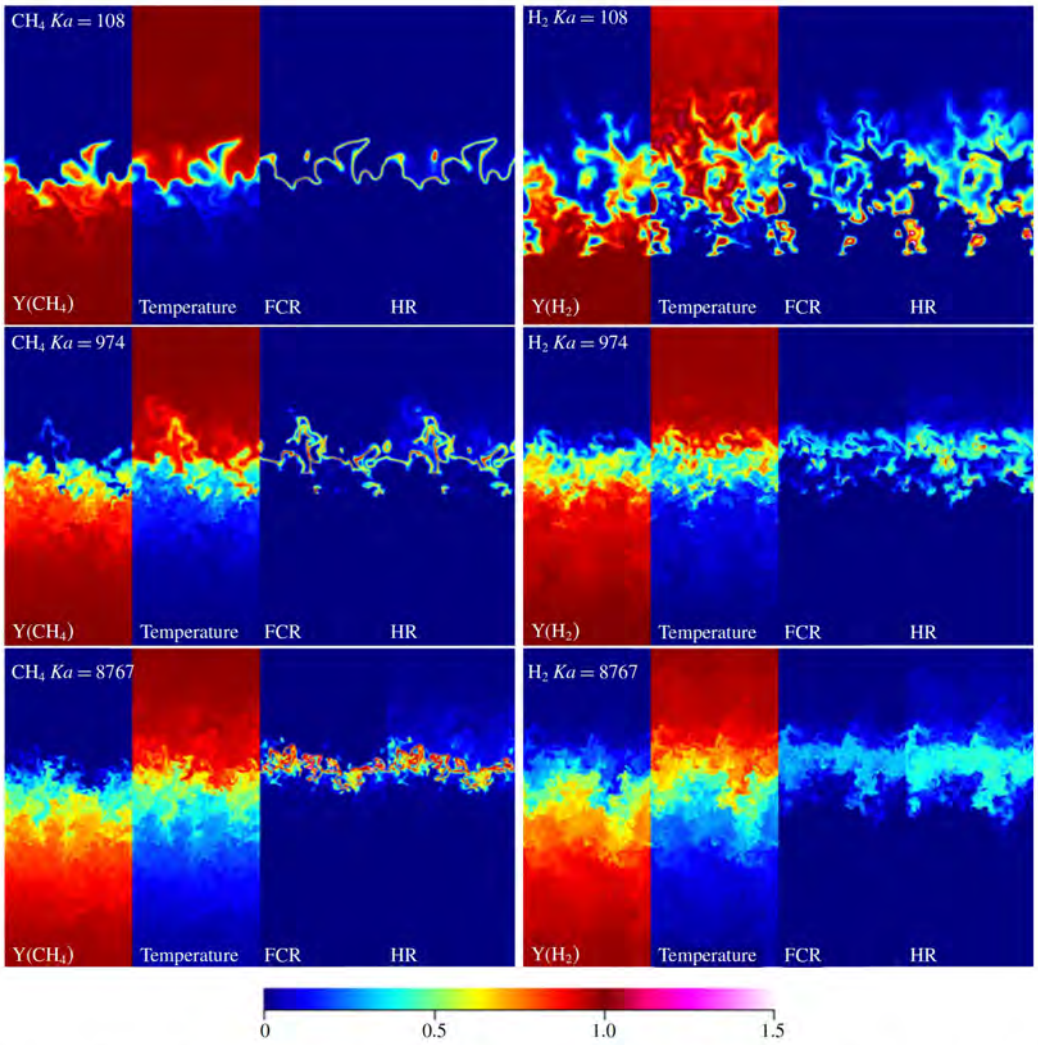

FIGURE 2. (Colour online) Slices of fuel mass fraction, temperature, fuel consumption rate and heat release for CH_4 and H_2 flames at $Ka = 108$, 974 and 8767, respectively. Each part of each panel shows $20l_F \times 50l_F$ (note that periodicity has been exploited to stitch together x–z and y–z planes to show more flame surface).

Aspden, Day, Bell, JFM (2019)

Characteristic Scales: Turbulent Nonpremixed Combustion

Main differences from the premixed flame case:

1. No S_L : how to determine τ_c ?

2.Outer transport zone thickness is little affected by chemical reaction.

Transport zone thickness

$$\ell_L = \frac{1}{|\nabla Z|_{st}} = \sqrt{\frac{\nu}{\chi_{st}}}; \quad \tau_L = \frac{\ell_L^2}{\nu} = \frac{1}{\chi_{st}} \quad \left(\text{Note that } \tau_L \neq \tau_c \text{ unlike premixed flames}\right)$$

where Z : mixture fraction, $\chi_{st} = 2\nu|\nabla Z|_{st}^2$

In turbulent flows, the Kolmogorov eddies have the shortest turnover time and are most effective in transport: $\Rightarrow \ell_L \simeq \ell_K; \quad \tau_L \simeq \tau_K$

$$\mathrm{Da}_0 = \frac{\tau_0}{\tau_c} = \left(\frac{\tau_0}{\tau_K}\right)\left(\frac{\tau_K}{\tau_c}\right) \simeq \left(\frac{\tau_0}{\tau_K}\right)\left(\frac{\tau_L}{\tau_c}\right) = \mathrm{Re}_0^{1/2}\,\mathrm{Da}_L; \quad \mathrm{Da}_L = \mathrm{Da}_0\,\mathrm{Re}_0^{-1/2}$$

The Williams Diagram for Turbulent Nonpremixed Combustion

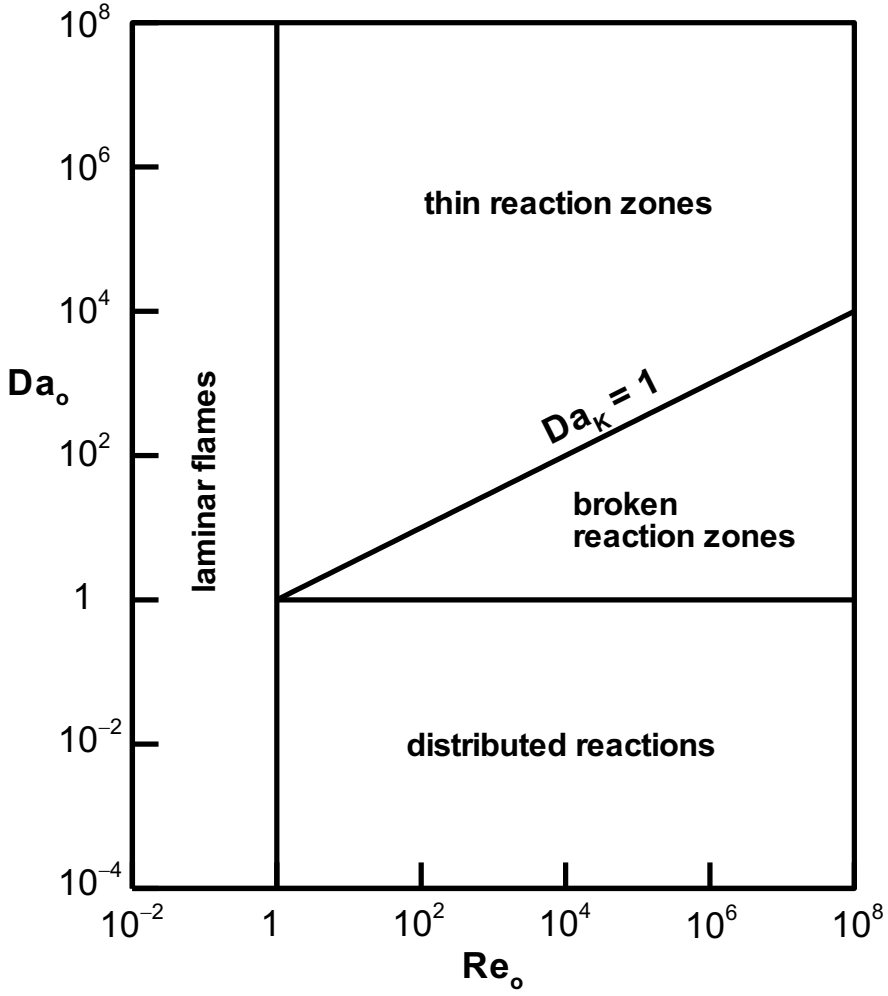

Combustion Regimes

1. $\mathrm{Re}_0 < 1$: laminar flames
2. $\mathrm{Da}_0 < 1$: distributed combustion
   - eddies at all scales can quench the flame
3. $\mathrm{Da}_L \left(= \mathrm{Da}_K\right) < 1, \mathrm{Da}_0 > 1$:
   broken reaction zones
   - some eddies can quench the flame
4. $\mathrm{Da}_L > 1$: thin reaction zones
   - flamelet regime

The Cuenot-Poinsot Diagram for Turbulent Nonpremixed Combustion

Cuenot & Poinsot, Proc. Comb. Inst. 25 (1994)

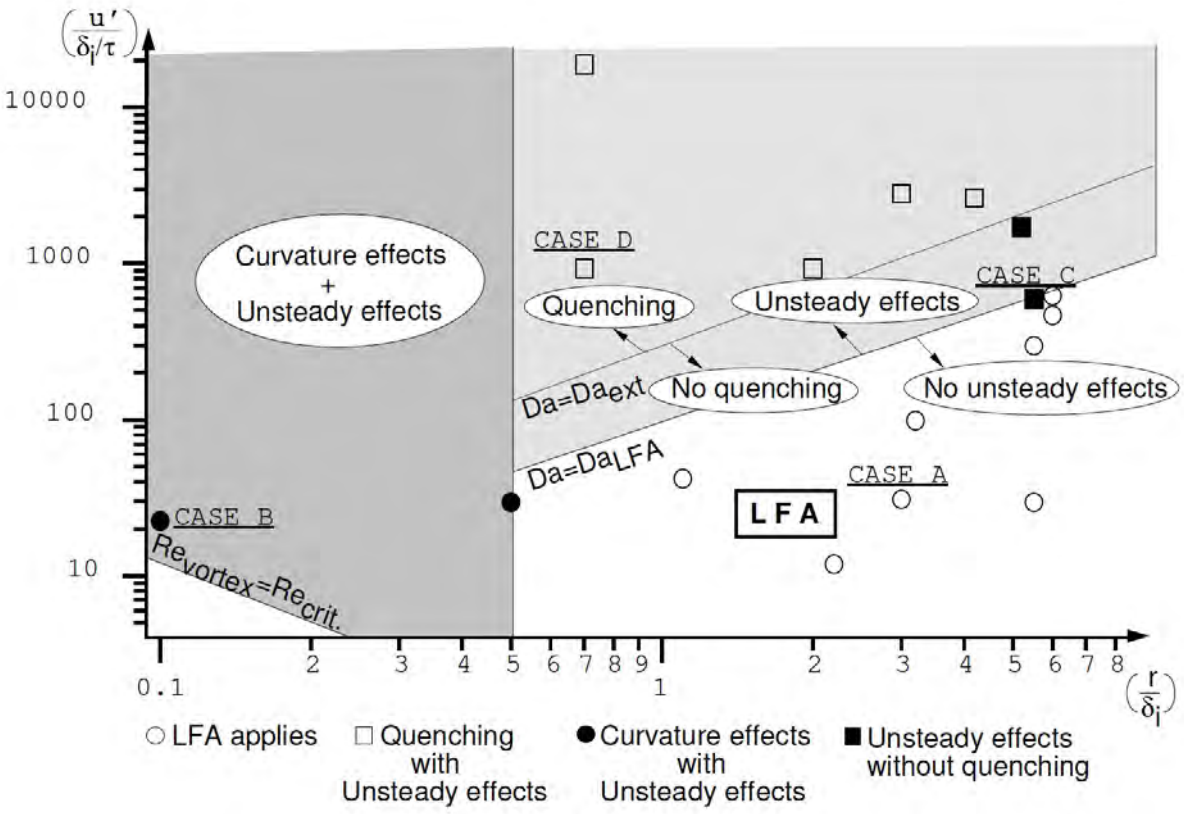

	Length scale	Velocity scale
Flame	$\delta_i = (1/\lvert\nabla z\rvert)_{z=z_{st}} = \sqrt{2\mathcal{D}_{st}/\chi_{st}}$	δ_i/τ_c
Vortex	r	u'
Ratio	r/δ_i	$u'\tau_c/\delta_i$

$$D_a = \frac{r/u'}{\tau_c} = \frac{r}{\delta_i}\left(\frac{u'}{\delta_i/\tau_c}\right)^{-1}$$

$$Re_{vortex} = \frac{u'r}{\nu} = \frac{\tau_d}{\tau_c}\left(\frac{u'}{\delta_i/\tau_c}\right)\left(\frac{r}{\delta_i}\right)$$

Summary

- High Re flows increase scale disparity – small scale fluctuations need to be modeled.
- RANS vs. LES: ensemble averaging vs. spatial filtering
- Computational implications on RANS vs. LES
- Turbulent combustion scales and regimes help fundamental understanding and proper strategies in developing combustion closure models.

References

Sagaut, P., Large Eddy Simulation for Incompressible Flows, 2nd Ed., Springer (2001).

Smagorinsky, J., General circulation experiments with the primitive equations. I. the basic experiment, *Month. Weath. Rev.,* 91 (3), 99-165 (1963).

Germano, M., Turbulence: the filtering approach., *J. Fluid Mech.,*238: 325-336 (1992).

Germano, M., Fundamentals of large-eddy simulation, in *Advanced Turbulent Flows Computations*, Peyret and Krause, eds., CISM Courses and Lectures 395, Springer, 81-130 (1998).

Lilly, D. K., A proposed modification of the Germano subgrid-scale closure method, *Phys. Fluids A*, 4 (3), 633-635 (1992).

Lesieur, M. and Metais, O., New trends in large-eddy simulations of turbulence, *Ann. Rev. Fluid Mech.*, 28, 45-82 (1996).

Pomraning, E. and Rutland, C. J., A dynamic one-equation non-viscosity LES model, *AIAA J.,* 40 (4), 689-701 (2002).

Peters, N., Turbulent Combustion, Cambridge University Press (2000).

Libby, P. A. and Williams, F. A., eds., Turbulent Reacting Flows, Academic Press (1994).

Liñán, A. and Williams, F. A., Fundamental Aspects of Combustion, Oxford University Press (1993).

Poinsot, T. and Veynante, D., Theoretical and Numerical Combustion, 2nd ed., Edwards (2005).

De, S., Agarwal, A.K., Chaudhuri, S., Sen, S., eds. Modeling and Simulation of Turbulent Combustion, Springer (2018).

جامعة الملك عبدالله للعلوم والتقنية
King Abdullah University of Science and Technology

Clean Energy Research Platform

Tsinghua-Princeton-Combustion Institute
2025 Summer School on Combustion
Tsinghua University, July 7-11, 2025

Turbulent Combustion

Day 3a: Turbulent Burning Velocities

Hong G. Im
Clean Energy Research Platform (CERP)
King Abdullah University of Science and Technology (KAUST)

Outline

- Experimental measurements and correlations
- Borghi-Peters diagram and regime consideration
- Theoretical predictions: Damköhler, Peters, etc.
- Regime diagram revisited: modified Ka
- DL and DT instabilities: effects on turbulent flames

Turbulent Burning Velocities: Experiment and Theory

Twenty-Fourth Symposium (International) on Combustion/The Combustion Institute, 1992/pp. 247–262

INVITED LECTURE

HOW FAST CAN WE BURN?

DEREK BRADLEY
Department of Mechanical Engineering
University of Leeds
Leeds LS2 9JT, United Kingdom

The roots of our present understanding of turbulence, flame chemistry and their interaction are traced. Attention is then focused on premixed turbulent combustion and the different analyses of stretch—free theories of turbulent burning velocity, u_t, are reviewed and new work presented. The various expressions for u_t are very different and this becomes more important when allowance must be made for flame stretch. On the basis of previous asymptotic analyses the appropriate dimensionless groups emerge for the correlation of experimental values of u_t and a correlation based on these is presented save that, 'pro tem', the Lewis rather than the Markstein number is employed.

The presented correlations are used as a test bed for a stretched flame, Reynolds stress, laminar flamelet model of turbulent combustion. Computed laminar flame data on flame quenching by stretch are generalised and used in the model. The problems of appropriate probability density functions of both stretch and temperature are discussed. There is good agreement between model predictions and experiment over a wider range than would be expected from the Williams criterion for flamelet modelling: namely, that the Kolmogorov distance scale should be greater than the laminar flame thickness. The reasons for this wider applicability are discussed, particularly in relation to recent direct numerical simulations.

Some of the concepts discussed are applied to spherical explosions and continuous swirling combustion. There is wide diversity in burning rates because of widely different circumstances, but our knowledge is becoming adequate enough to develop reasonably accurate mathematical models for the wide range of engineering applications.

Can we define turbulent flame speed?

Laminar flames:

- “Reference flame”: unstrained, freely propagating, adiabatic
- Flame speed is a unique function of thermochemical properties of the mixture.

Turbulent flames:

- May be defined as the mean propagation speed in a statistically steady state of a turbulent flow.
- Wide scatters in the experimental data cast doubt on unambiguous definition of turbulent flame speed.
- Even if we can define it, turbulent flame speed is expected to depend on the flow conditions and configuration.
- Nevertheless, the practical importance led to extensive studies.

Experimental Setup

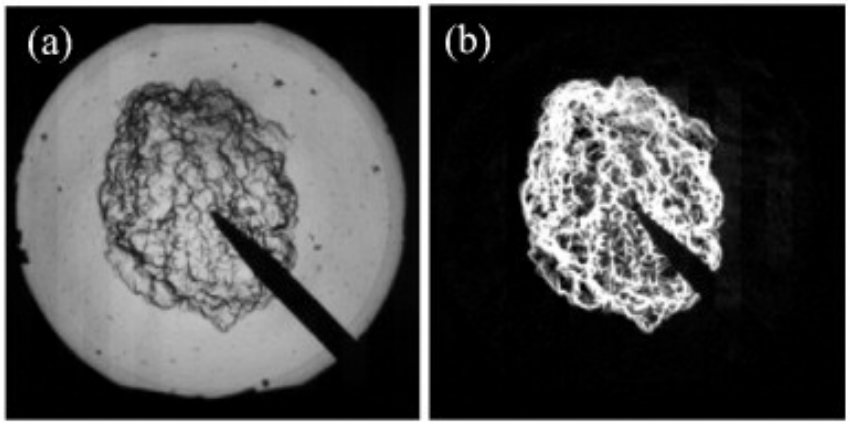

Spherical expanding flame
Bradley, U. Leeds

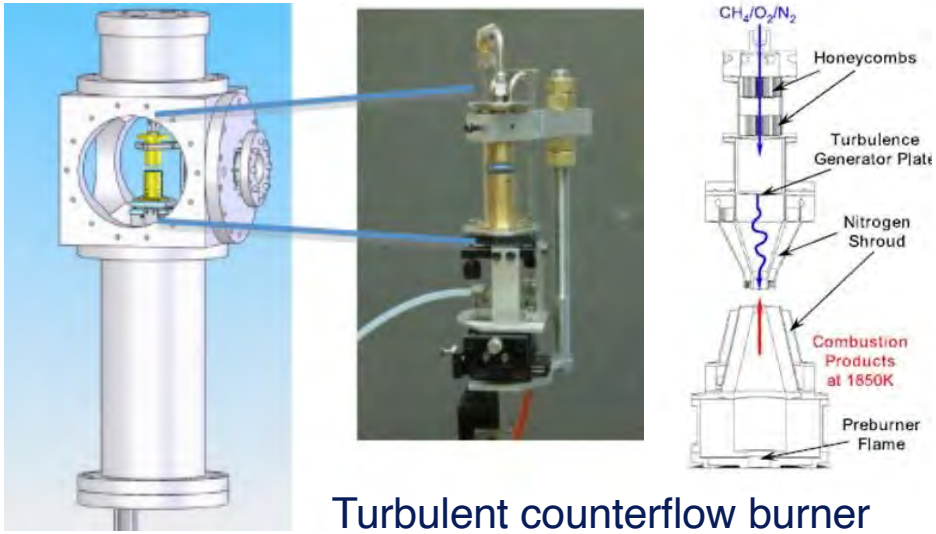

Turbulent counterflow burner
Gomez, Yale U.

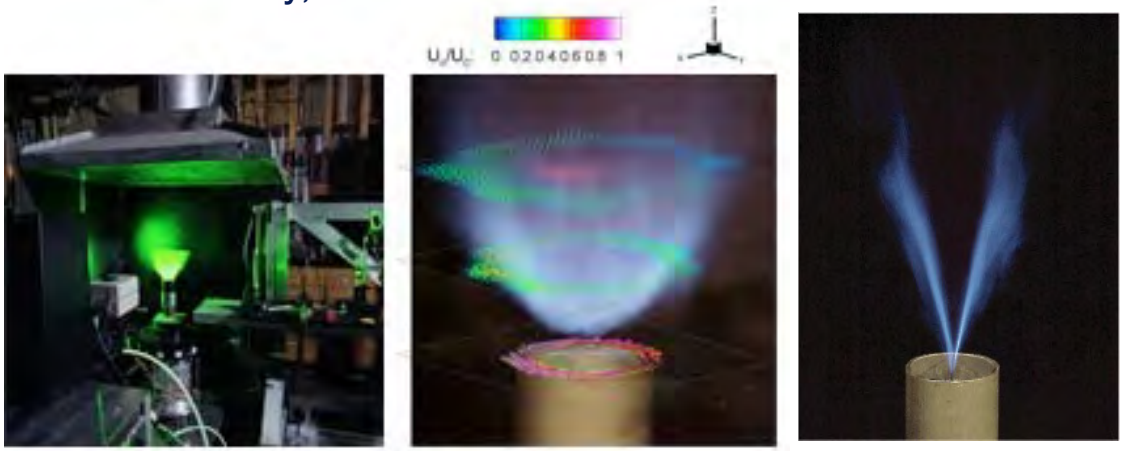

Turbulent rod-stabilized flame, Cheng, LBNL

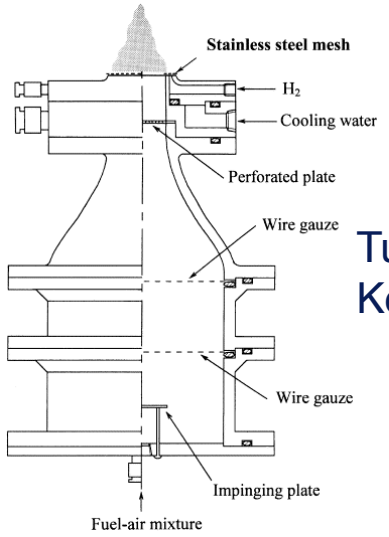

Turbulent Bunsen burner
Kobayashi, Tohoku U.

Turbulent Flame Speed

Bradley and coworkers (1992)

Compiled data for $S_T / S_L = f\left(u' / S_L\right)$

$$K = 0.157\left(\frac{u'}{S_L}\right)^2 R_L^{-0.5}$$

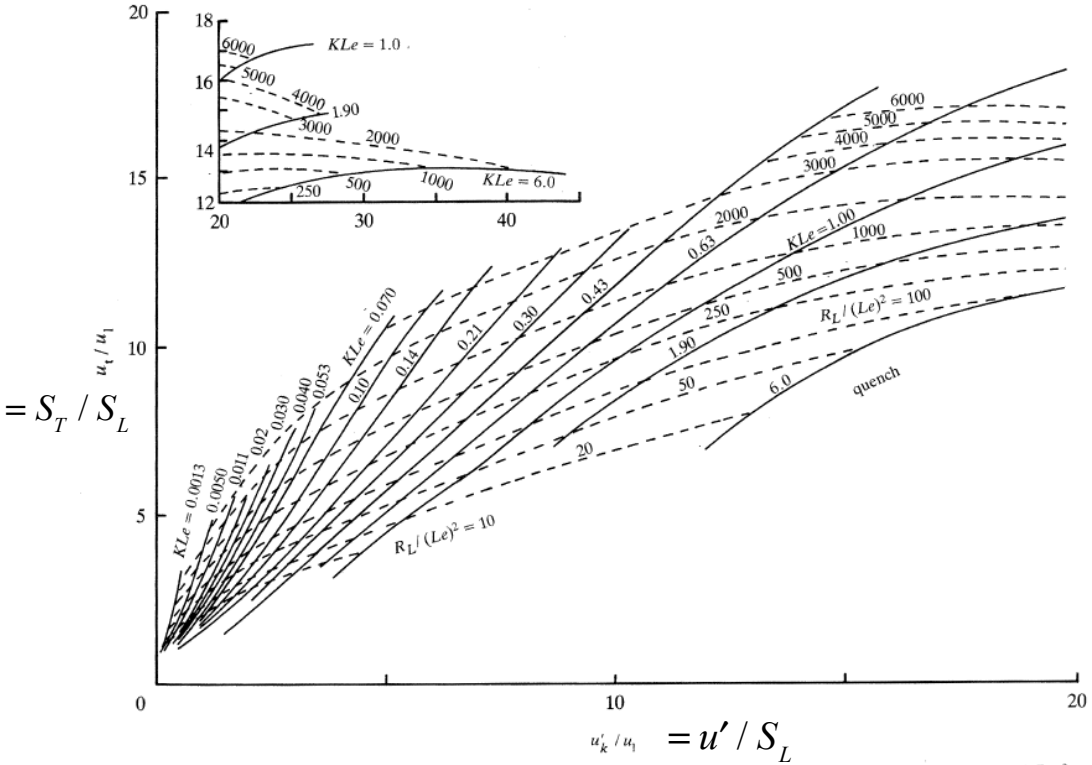

Figure 4. Smoothed data for u_t/u_1 against u'_k/u_1 at different stretch rates; dashed curves show $R_L/(Le)^2$.

The Bending Effect

Kobayashi and coworkers (1996)

- Demonstrated a statistically stationary turbulent flames with a measurable average flame shape.
- But is the observation valid for all regimes of turbulent combustion?
- Observed a bending shape of the turbulent flame speed increase with the turbulence intensity.

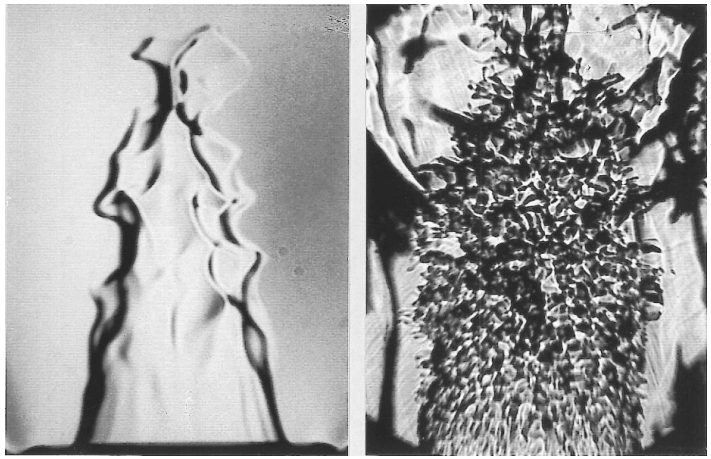

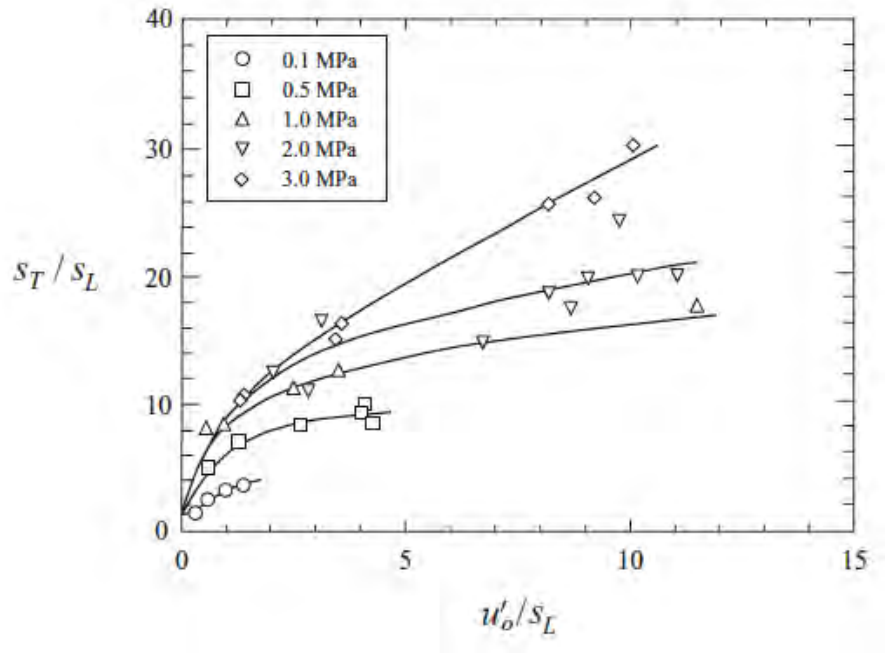

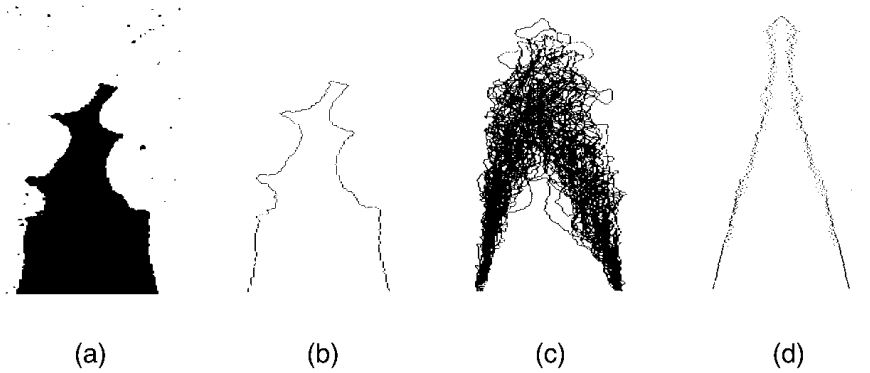

Damköhler's Theory (1940)

Two Different Regimes

- Large scale turbulence: (corrugated) flamelet regime
- Small scale turbulence: distributed combustion/reaction sheet regimes

A. Large scale turbulence

: primarily the area increase effect

$$\dot{m} = \rho_u S_L A_T = \bar{\rho}_u S_T A$$

Assuming the upstream density is constant,

$$\frac{S_T}{S_L} = \frac{A_T}{A}$$

A_T / A is purely kinematic,

$$\tan\theta = \frac{u'}{S_L}; \qquad \frac{S_T}{S_L} = \sqrt{1 + \left(\frac{u'}{S_L}\right)^2}$$

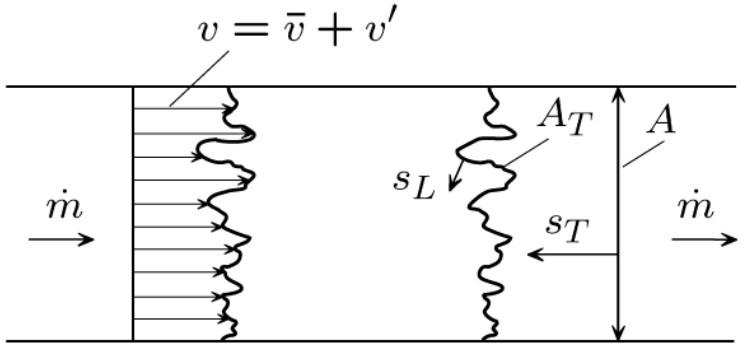

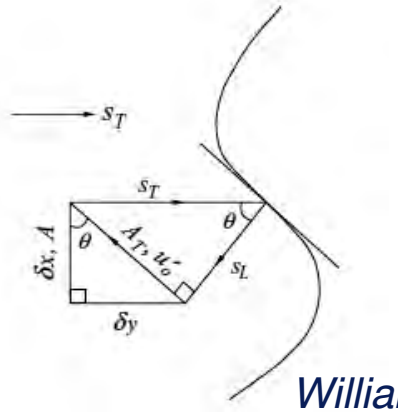

Williams (1985)

Damköhler's Theory (1940)

A. Large scale turbulence (continued)

- Weak turbulence

$$\frac{S_T}{S_L} = \sqrt{1+\left(\frac{u'}{S_L}\right)^2} \simeq 1+\frac{1}{2}\left(\frac{u'}{S_L}\right)^2, \quad \frac{u'}{S_L} \ll 1$$

- Strong turbulence

$$\frac{S_T}{S_L} = \sqrt{1+\left(\frac{u'}{S_L}\right)^2} \simeq \frac{u'}{S_L}, \; S_T \approx u', \quad \frac{u'}{S_L} \gg 1$$

implying that the flame surface is passively convected by turbulent eddies, and the turbulent flame speed is determined solely by the turbulent intensity.
⇒ Contradicts experimental observations (bending effects).

Damköhler's Theory (1940)

B. Small scale turbulence: reaction sheet or distributed combustion regimes

- Damköhler postulated that turbulence only modifies the transport properties
- Peters (2000) argued that this assumption is only valid in the reaction sheet limit,

$$Ka_\delta = \left(\frac{\ell_\delta}{\eta}\right)^2 < 1$$

In this case,

$$S_L \sim \left(\frac{D}{t_c}\right)^{1/2}, \quad S_T \sim \left(\frac{D_t}{t_c}\right)^{1/2}$$

$$\frac{S_T}{S_L} \sim \left(\frac{D_T}{D}\right)^{1/2} \quad \text{or} \quad \frac{S_T}{S_L} \sim \left(\frac{u'}{S_L}\frac{\ell}{\ell_f}\right)^{1/2}$$

Other Theoretical Predictions

Schelkin (1947): strongly corrugated flames

$$\frac{S_T}{S_L} = \sqrt{1 + \left(\frac{2u'}{S_L}\right)^2}$$

Clavin and Williams (1979): weakly wrinkled flames

$$\frac{S_T}{S_L} = 1 + \left(\frac{u'}{S_L}\right)^2$$

$$\Rightarrow \quad \frac{S_T}{S_L} = 1 + C\left(\frac{u'}{S_L}\right)^n$$

Semi-empirical

Yakhot (1988): renormalization group theory (RNG)

$$\frac{S_T}{S_L} = \exp\left[\frac{\left(u'/S_L\right)^2}{\left(S_T/S_L\right)^2}\right] \quad \text{for general } u'/S_L$$

$$\Rightarrow \frac{S_T}{S_L} = \frac{u'/S_L}{\left[\ln\left(S_T/S_L\right)\right]^{1/2}}$$

Fits bending effects well.

Fractal Theory

Gouldin et al. (1987)

$$\frac{S_T}{S_L} = \left(\frac{L_{outer}}{L_{inner}} \right)^{D-2}$$

L_{outer} : outer cut-off scale (= integral scale)

L_{inner} : inner cut-off scale

Peters/Kerstein: Gibson scale

Gülder: Kolmogorov scale.

D : Fractal dimension of the flame surface $(2 < D < 3)$

Kerstein: $D = 7/3$

Gülder et al.: $D < 7/3$

Tanahashi et al.: $D = 2.3 - 2.5$

Hawkes et al.: $D = 8/3$

$D = 7/3, L_{inner} = \eta$:

$$\frac{S_T}{S_L} = \left(\frac{\ell_I}{\eta} \right)^{7/3-2} = \left(\mathrm{Re}_\ell^{3/4} \right)^{1/3} = \mathrm{Re}_\ell^{1/4}$$

$D = 7/3, L_{inner} = \ell_G$:

$$\frac{S_T}{S_L} = \left(\frac{\ell_I}{\ell_G} \right)^{7/3-2} = \left(\left(\frac{u'}{S_L} \right)^3 \right)^{1/3} = \frac{u'}{S_L}$$

Comparison of Theory and Experiment

How do the theoretical predictions compare with experimental observations?

⇒ *All over the map!!*

Is the bending effect real or is it just an experimental error?

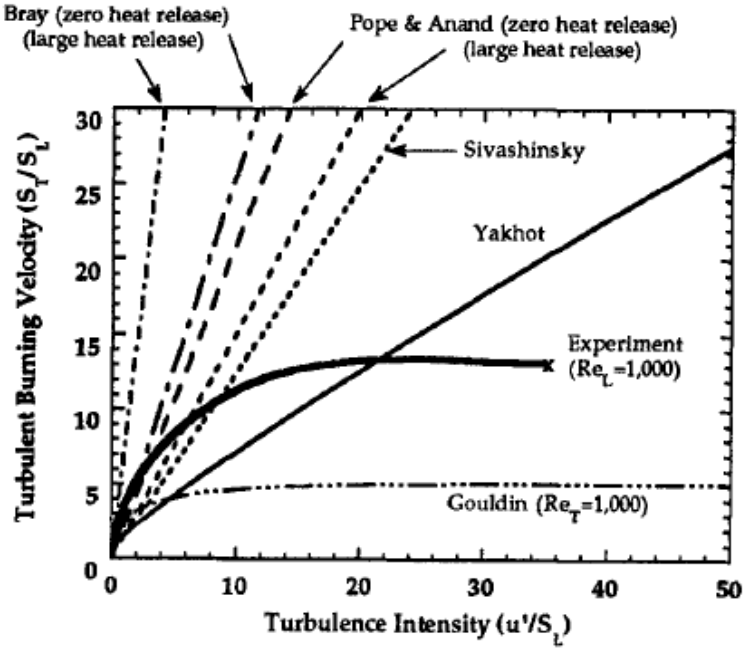

Figure 3. Predicted effect of turbulence intensity (u'/S_L) on turbulent burning velocity (S_T/S_L) from "thin-flame" theories: Bray [15] with zero heat release and large (density ratio = 7) heat release; Anand and Pope [16] with zero and infinite heat release; Yakhot [17]; Sivashinsky [18]; Gouldin [19] with Re_L = 1,000; experimental values from Bradley [1] for Re_L = 1,000. Where Re_L is not specified, predictions are independent of Re_L.

From Ronney (1994)

D-L Instability Affecting the Bending Effect

Thermal Expansion

- Reduces Re: decreases flame speed?
- Source of Darrieus-Landau instability: increases flame speed?

Cambray and Joulin (1992)

$$\frac{S_T}{S_L} = 1 + C\left(\frac{u'}{S_L}\right)^{4/3}$$

in the low turbulence limit.

⇒ A potential explanation for the bending effect?

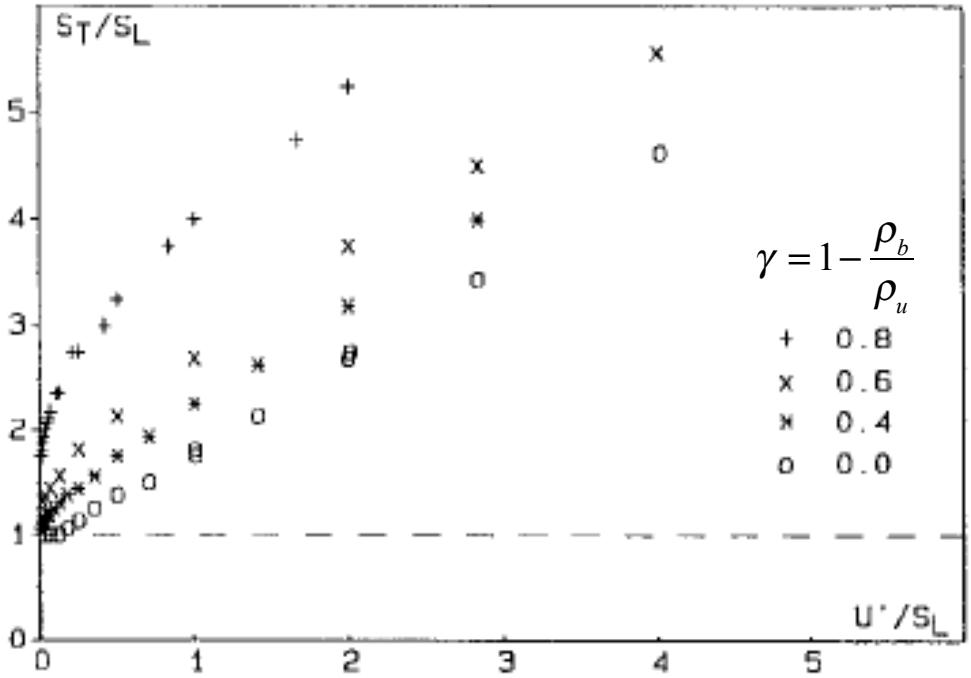

Spherical Flames

Chaudhuri et al. (2012)
Turbulent flame speed measured by the average flame radius

$$\frac{S_T}{S_L} = \frac{d\langle R\rangle}{dt}\frac{1}{S_L}$$

$$\mathrm{Re}_{T,\langle R\rangle} = \frac{u_{\mathrm{rms}}}{S_L}\frac{\langle R\rangle}{\delta_L} = \frac{u_{\mathrm{rms}}\langle R\rangle}{\alpha}$$

Turbulent Reynolds number with <R> being the length scale, and ν replaced by α.

$$\frac{S_T}{S_L} \sim \mathrm{Re}_{T,\langle R\rangle}^{0.5}$$

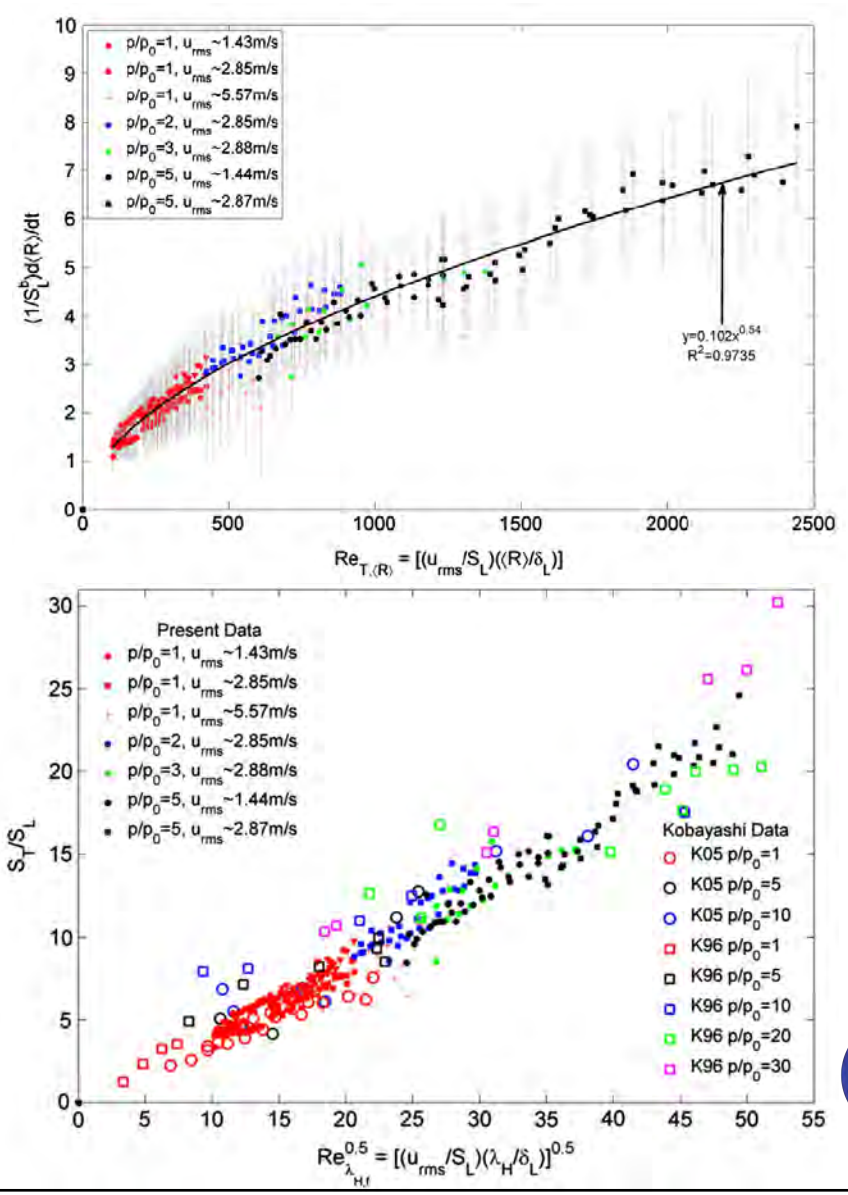

Modified Borghi Regime Diagram

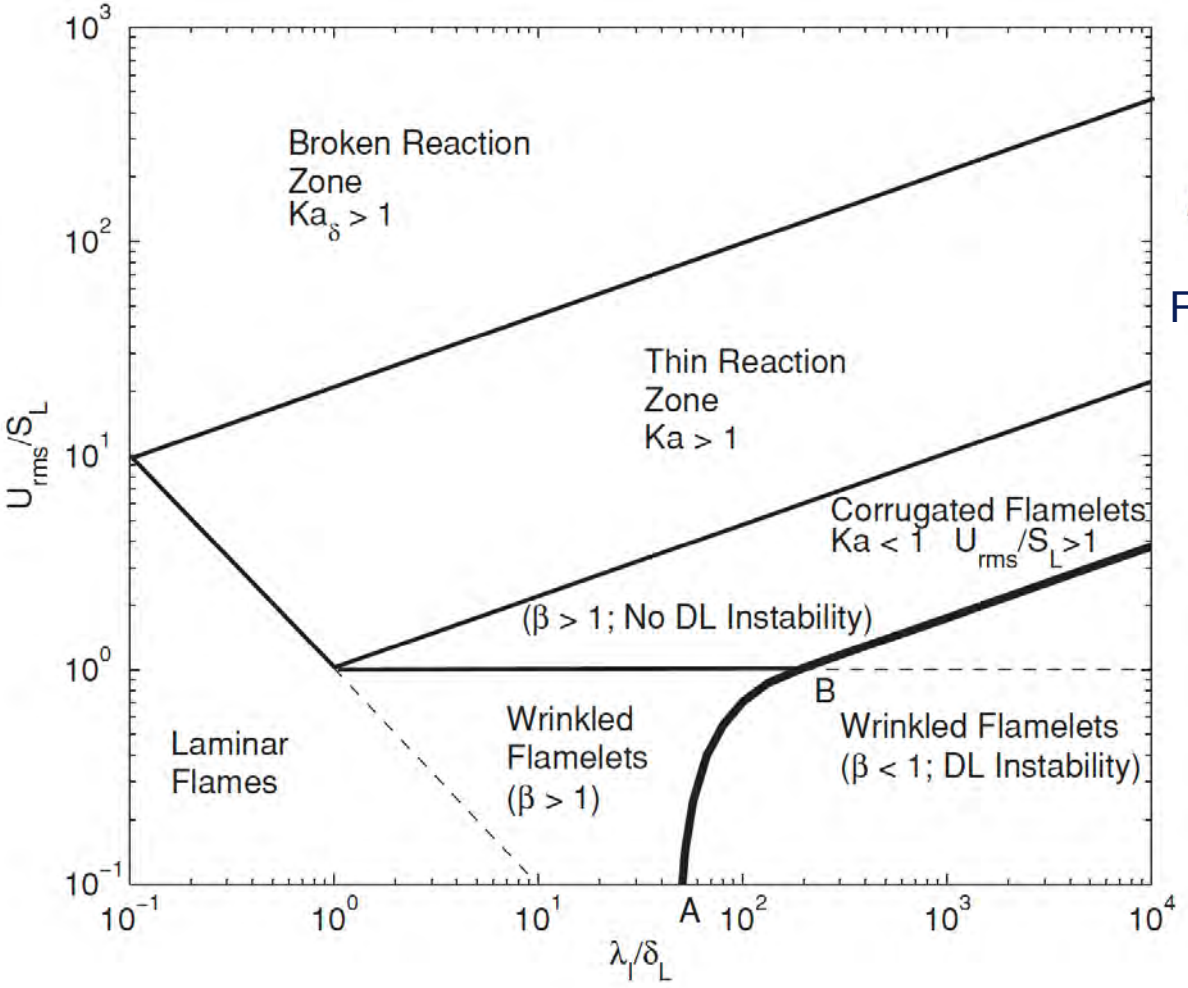

Chaudhuri, Akkerman, Law (2011)

$$\beta = \min_{\forall k > k_I} \left\{ \frac{\omega_{\text{turb}}^{(k)}}{\sigma_{\text{DL}}^{(k)}} \right\} = \min_{k_c > k > k_I} \left\{ \frac{U_{\text{rms}}}{\text{X}\, S_L} \left(\frac{k_I}{k} \right)^{1/3} \left(1 - \frac{k}{k_c} \right)^{-1} \right\}$$

Ratio of DL instability to turbulence time scales

For $\beta < 1$, DL instability contributes to additional flame wrinkling and increased turbulent flame speed.

General Correlations

Nguyen and Shy (2019)

- Spherical flame chamber (“cruciform”)
- Different fuels, high pressure data
- Da scaling works best

Kobayashi

$$S_{T,c=0.5}/S_L = 2.54[(u\prime/S_L)(p/p_0)Le^{-1}]^{0.42};\ R^2 = 0.91.$$

Chaudhuri

$$S_{T,c=0.5}/S_L = 0.26\left(Re_{T,flame}Le^{-1}\right)^{0.5};\ R^2 = 0.87.$$

Nguyen and Shy

$$S_{T,c=0.5}/u\prime = 0.09(DaLe^{-1})^{0.5};\ R^2 = 0.96.$$

$$Da = (L_I/u')(S_L/\delta_L)$$

- Le adjustment improves the agreement (per Kobayashi).

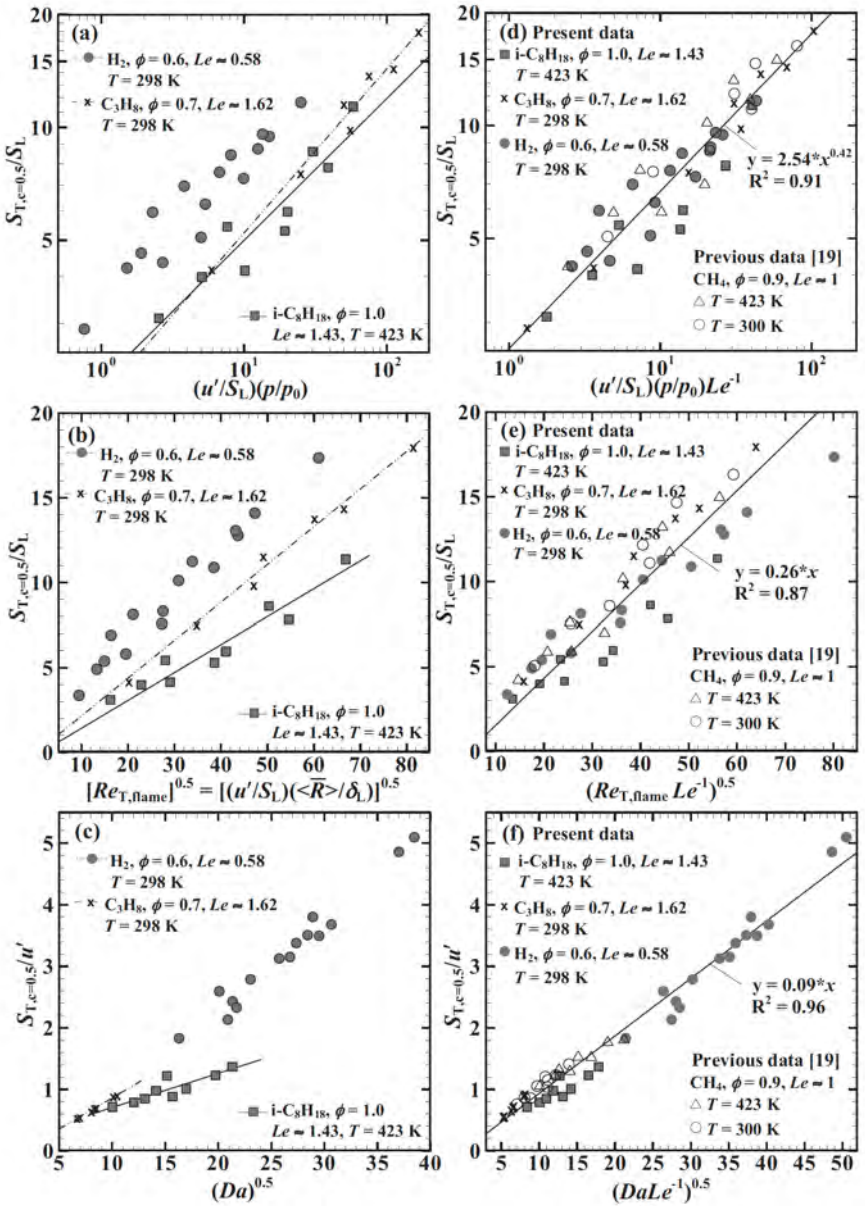

DNS of Turbulent Hydrogen/Air Flames

Song, Hernandez Perez, Tingas, Im, CNF (2021)

- Borghi diagram

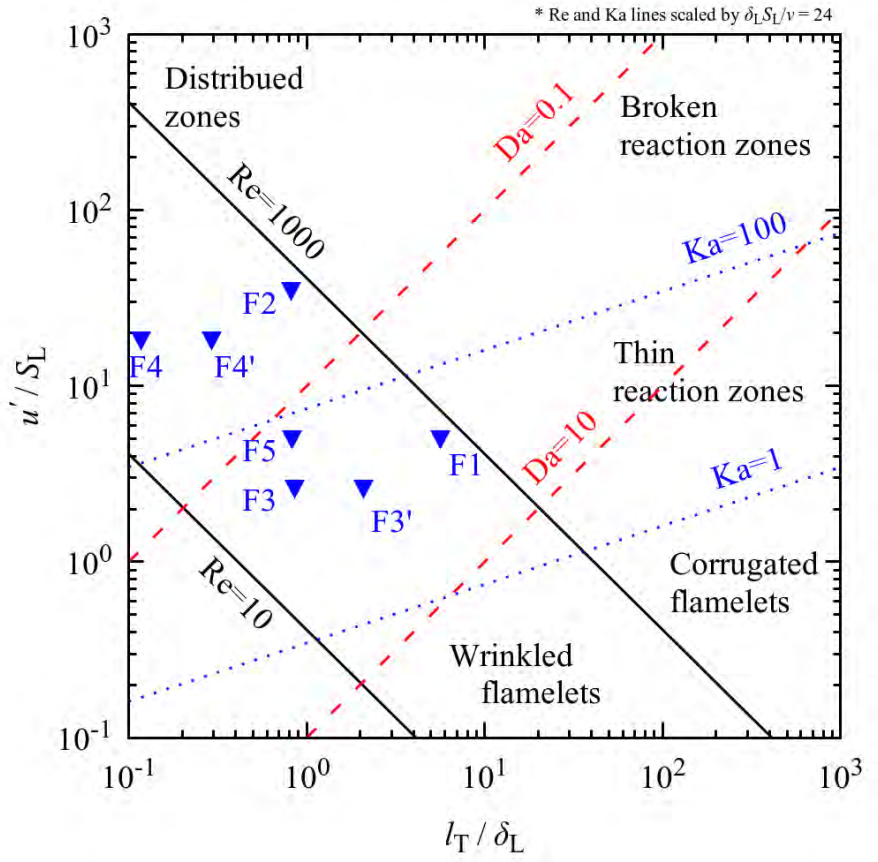

ϕ = 0.7, T_u = 300K, P = 1 atm

Case	l_T/δ_L [-]	u'/S_L [-]	Re [-]	Da [-]	Ka [-]	$\delta_L/\Delta x$ [-]	Grid [M]	Cost [Mh]
F1	5.65	5	686	1.13	23	17.7	250	6.1
F2	0.82	35	700	0.02	1126	136.2	516	6.3
F3	0.86	2.6	55	0.44	22	17.7	1.3	0.03
F4	0.12	18.3	52	0.01	1126	136.2	15.6	0.39
F5	0.83	5	101	0.17	60	30.8	8.2	0.14
F3′	2.08	2.6	132	0.80	14	136.2	52	0.8
F4′	0.29	18.3	131	0.02	722	131	6.3	0.25

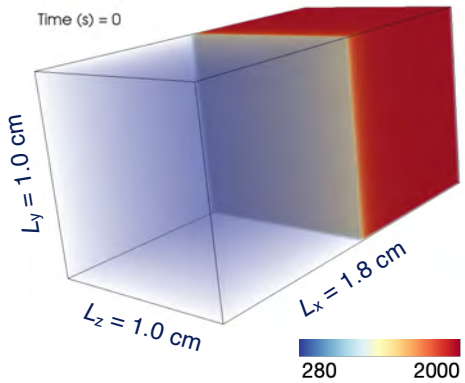

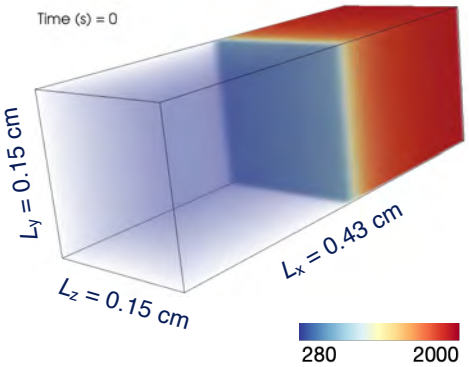

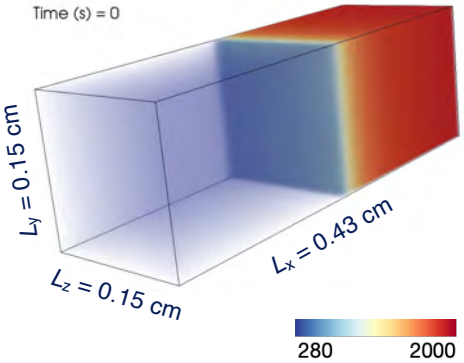

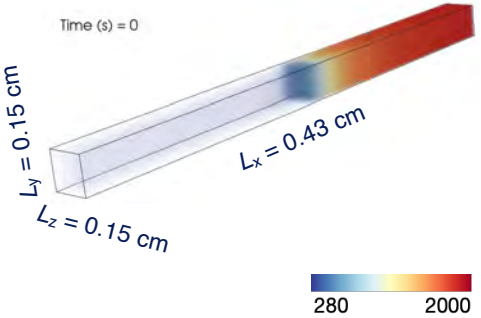

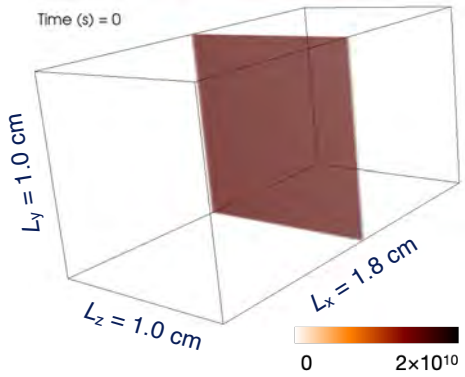

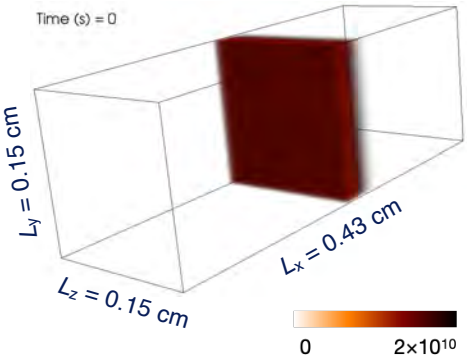

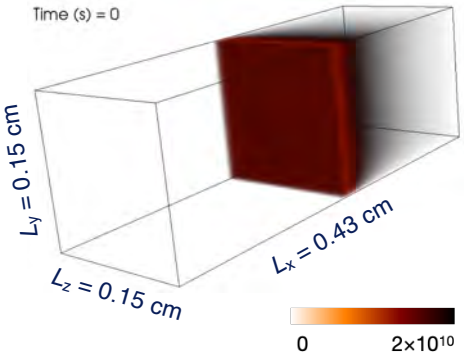

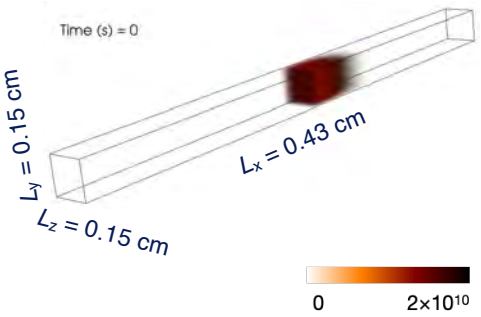

Evolution of temperature and heat release rate (HRR)

Case F1 (thin R. zone)
Ka = 20
Re = 700

Case F2 (distrib. regime)
Ka = 1100
Re = 700

Case F3 (thin R. zone)
Ka = 20
Re = 50

Case F4 (distrib. regime)
Ka = 1100
Re = 50

T [K]

Turbulent flame speed and surface area

- Correlation of S_T/S_L vs. A_T/A_L (stretch factor)

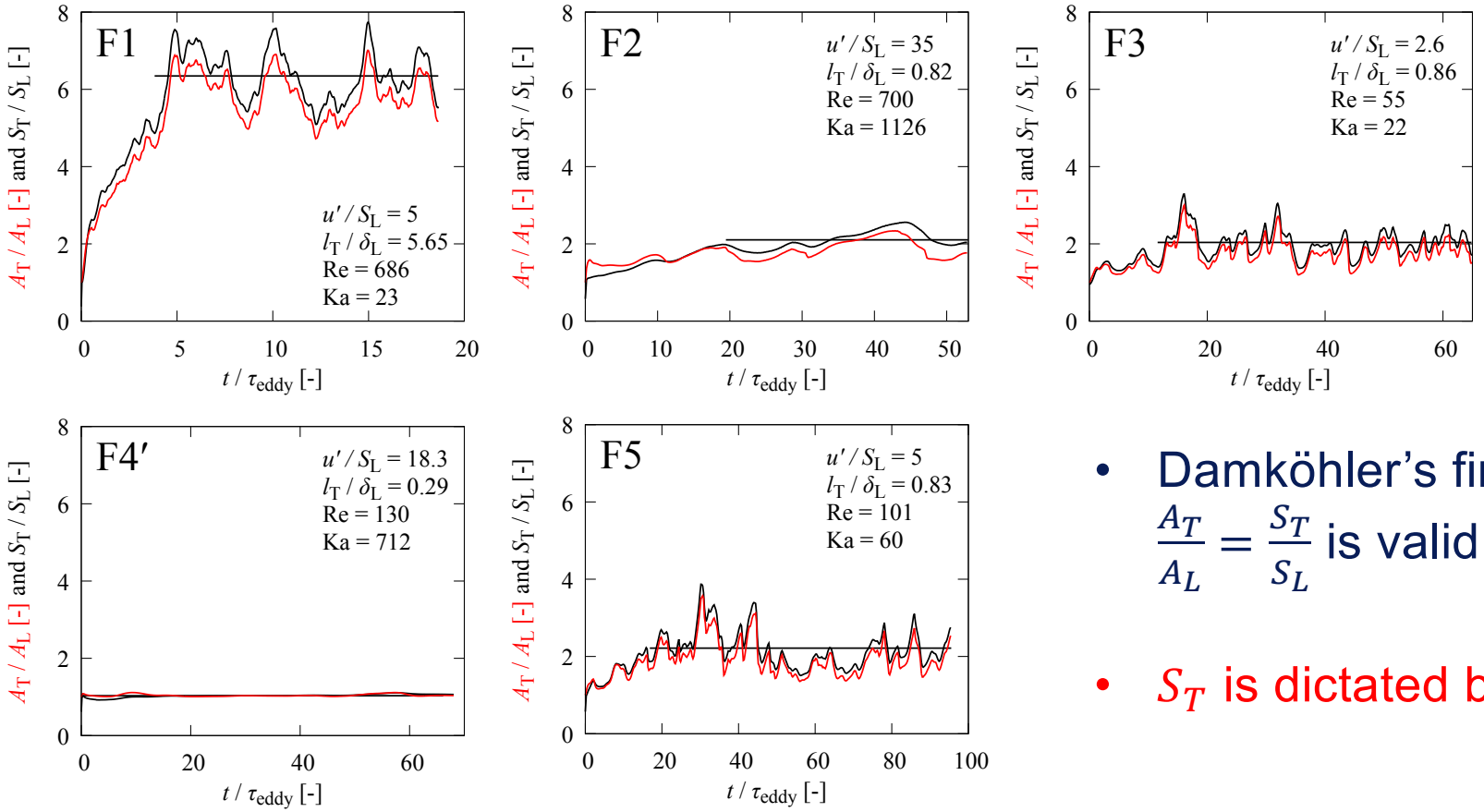

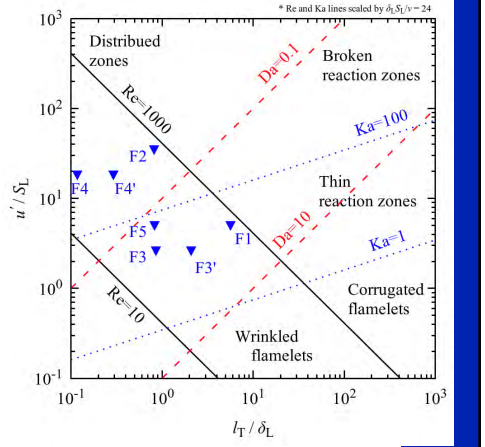

- Damköhler's first hypothesis: $\frac{A_T}{A_L} = \frac{S_T}{S_L}$ is valid at Ka > 1,000
- S_T is dictated by l_T

Integral length scale as key parameter

- Mean stretch factor, mean flame surface area, and mean turbulent flame speed

$$\bar{I}_0 = \frac{\bar{S}_T / S_L}{\bar{A}_T / A_L}$$

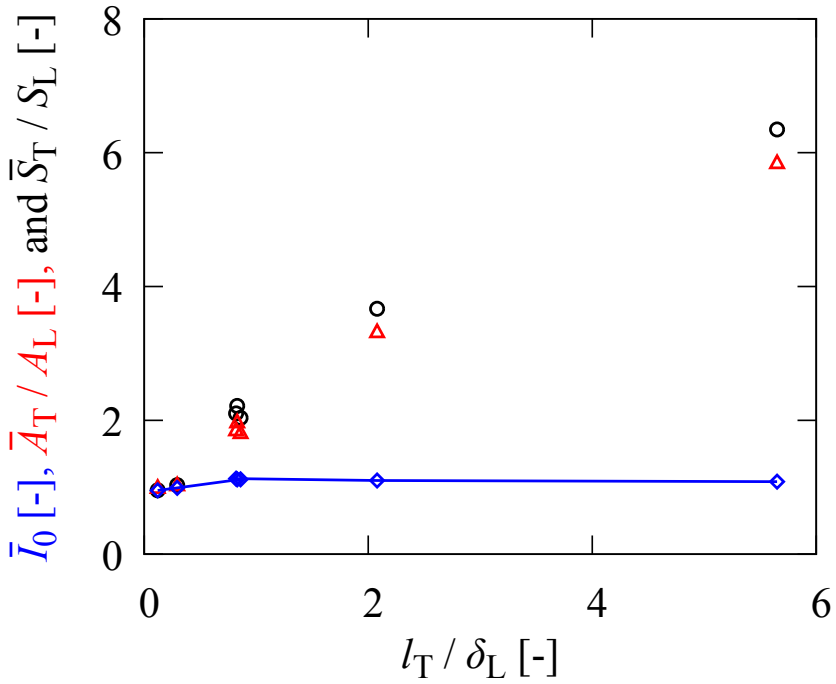

- For a wide range of l_T and u', $\bar{S}_T$ is correlated well with l_T

Turbulent Premixed Combustion Regime Diagram Revisited

per Andy Aspden (Newcastle University)

The Borghi-Peters Diagram

Important nondimensional numbers

(for simplicity, $u' = u$)

$$\mathrm{Re}_\ell = \frac{u\ell}{\nu} = \frac{u}{S_L}\frac{\ell}{\ell_f}$$

$$\mathrm{Da} = \frac{\tau_\ell}{\tau_f} = \frac{\ell/u}{S_L/\ell_f} = \frac{S_L}{u}\frac{\ell}{\ell_f}$$

$$\mathrm{Ka}_\eta = \frac{\tau_{\ell_f}}{\tau_\eta} = \left(\frac{\ell_f}{\eta}\right)^2 = \mathrm{Re}_\ell^{1/2}/\mathrm{Da}$$

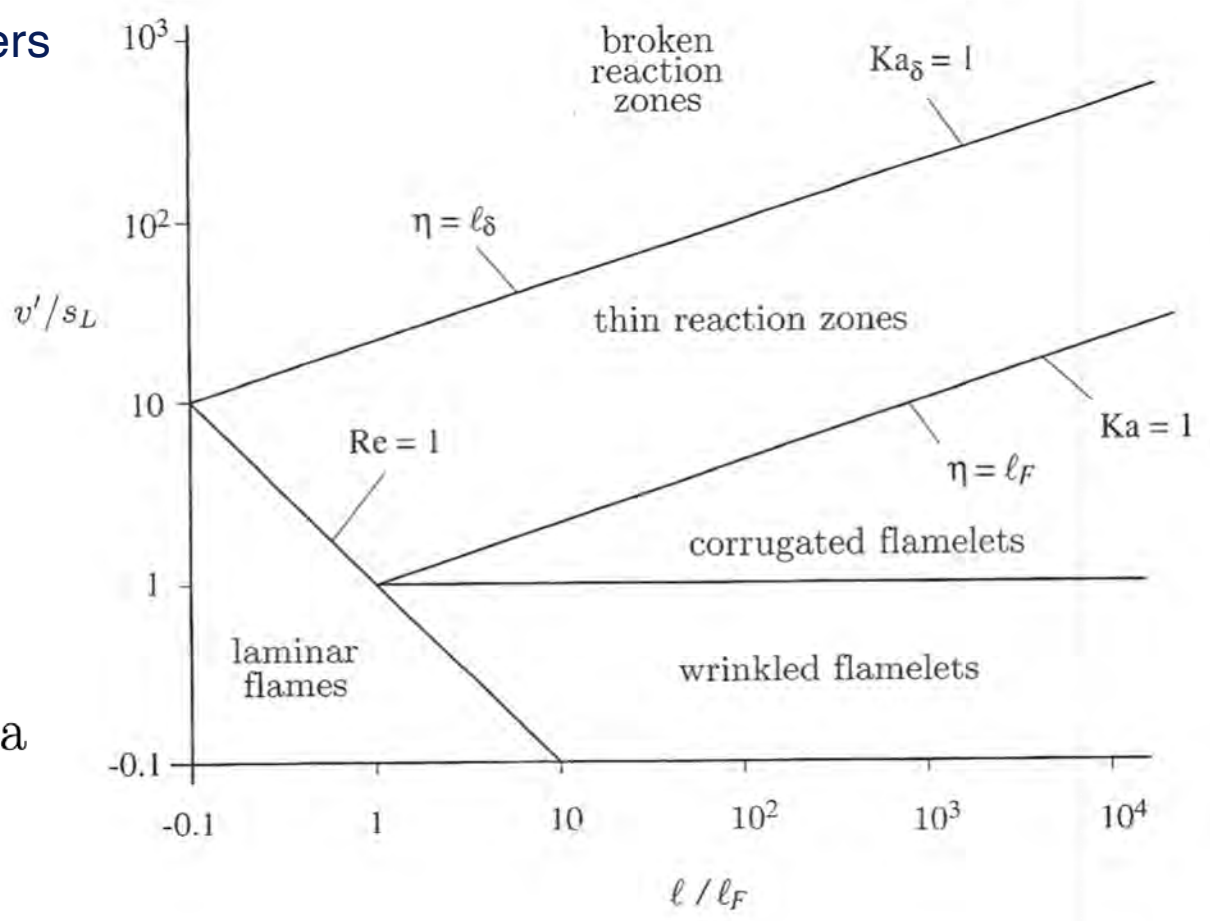

Regime Diagram Revisited

Courtesy of Andy Aspden, Newcastle University

- Usual description of non-reacting turbulence cascade
  - ✓ Inertial subrange depends only on $\epsilon = u^3/\ell$ (for simplicity, $u' = u$)
  - ✓ Dissipation subrange depends on ϵ and ν : $\eta = \left(\frac{\nu^3}{\epsilon}\right)^{1/4}$
  - ✓ With $\mathrm{Ka} > 1, \ell > \ell_f > \eta$ and small eddies less than flame thickness perturbs the flame structure.
- In reacting turbulence, energy cascades down to smaller scales **until dilatation at the flame scale**
  - ✓ Relevant energy cascade stops at l_f, and through the inertial subrange:

$$\epsilon = \frac{u^3}{\ell} = \frac{u_r^3}{\ell_r} = \frac{u_{\ell_f}^3}{\ell_f}$$

Regime Diagram Revisited

Courtesy of Andy Aspden, Newcastle University

- The key is the strength of the turbulence at the flame scale

Considering $$\epsilon = \frac{u^3}{\ell} = \frac{u_r^3}{\ell_r} = \frac{u_{\ell_f}^3}{\ell_f}$$

The turbulence intensity at the flame scale is written as:

$$\frac{u_{\ell_f}}{S_L} = \frac{u}{S_L}\left(\frac{\ell_f}{\ell}\right)^{1/3} = \mathrm{Ka_F}^{2/3}$$

Leading to a new “flame” Karlovitz number:

$$\mathrm{Ka_F} = \sqrt{\frac{u^3}{S_L^3}\frac{\ell_f}{\ell}}$$

$$\mathrm{Ka}_\eta = \mathrm{Re_F}^{1/2}\mathrm{Ka_F}$$

where $$\mathrm{Re_F} = \frac{S_L \ell_f}{\nu}$$

Flame Reynolds number ~ O(10)

Turbulent Flame Speed Generalized

A general form of the algebraic turbulent flame speed correlation:

$$\frac{S_T}{S_L} = 1 + C\Upsilon_F^n \mathrm{Da}^m$$

where

$$\Upsilon_F = \frac{u}{S_L} \qquad \Lambda_F = \frac{\ell}{\ell_f}$$

such that

$$\mathrm{Re_F} = \Upsilon_F \Lambda_F$$

$$\mathrm{Da} = \Lambda_F / \Upsilon_F$$

$$\mathrm{Ka_F}^2 = \Upsilon_F^3 / \Lambda_F$$

Most existing correlations fits into the form.

Hunt, Aspden, CNF (2025)

Peters Correlation

$$\frac{S_T}{S_L} = 1 - \frac{a_4 b_3^2}{2b_1}\frac{\ell}{\ell_f} + \left[\left(\frac{a_4 b_3^2}{2b_1}\frac{\ell}{\ell_f}\right)^2 + a_4 b_3^2 \frac{u}{S_L}\frac{\ell}{\ell_f}\right]$$

Captures the transition from Damköhler's large to small scale turbulence limits.

Defining, $\alpha = b_1, \quad \beta = 4b_1^2/a_4 b_3^2, \quad \xi_F = \mathrm{Da}/\beta$

$$\frac{S_T/S_L - 1}{2\alpha \Upsilon_F} = \sqrt{\xi_F^2 + \xi_F} - \xi_F$$

The flame surface wrinkling scales with Da.

Turbulence-flame interaction is characterized by $\mathrm{Ka_F}$ and Da.

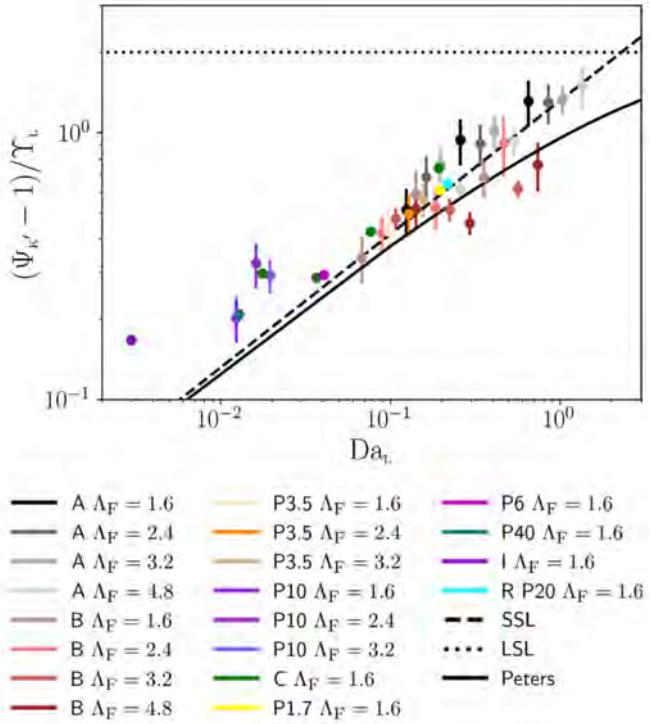

Hunt, Aspden, CNF (2025)

Turbulent spectra on (conventional) regime diagram

- Start with the conventional diagram
- Let's fix Re and pick a low Ka
  - For Ka < 1, then $\eta > \ell_F$
    $\Rightarrow$ no turb-flame interaction (flamelet)
- Increase Ka at the same Re
  - At Ka ~ 1, then $\eta \sim \ell_F$
    $\Rightarrow$ beginnings of turb-flame interaction
- Continue to increase Ka at same Re
  - At Ka > 1, then $\eta < \ell_F$
    $\Rightarrow$ turb-flame interaction (TRZ)
- Eventually becomes distributed (DBR)

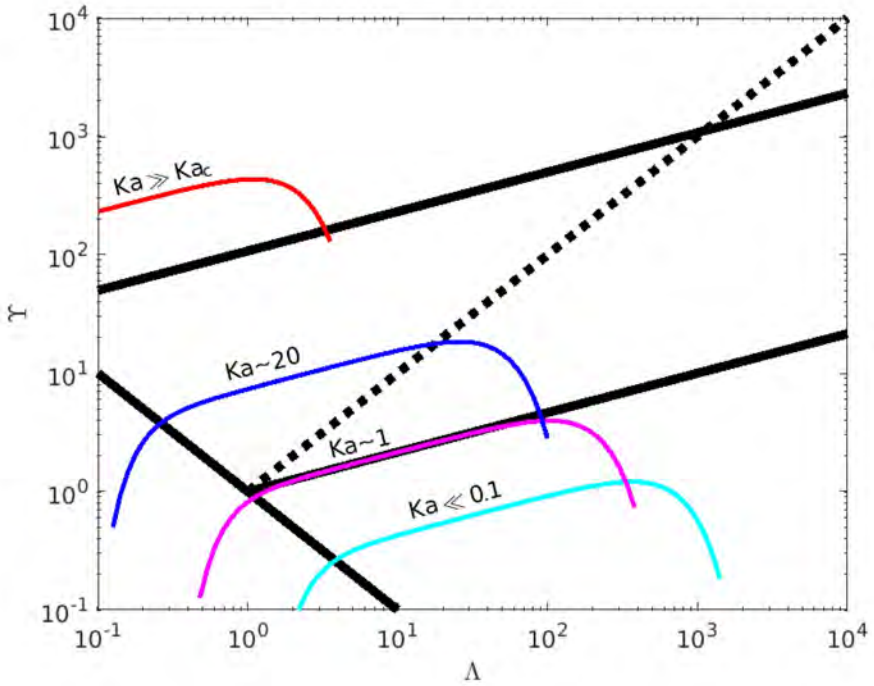

Karlovitz number determines burning regime (i.e. flamelet, TRZ, DBR)

Courtesy of Andy Aspden, Newcastle University

Turbulent spectra on (conventional) regime diagram

- Now let's fix Ka and increase Re
  - Equivalent to increasing Λ or Da
- Pick an arbitrary $\mathrm{Ka} > 1$ (TRZ)
  - Sets flame-scale turb-flame interaction
- Start with low Da (SSL)
  - Integral time scale shorter than flame
- Increase to $\mathrm{Da} \approx 1$ (transition)
  - Integral time scale equal to flame
- Increase to high Da (LSL)
  - Integral time scale longer than flame

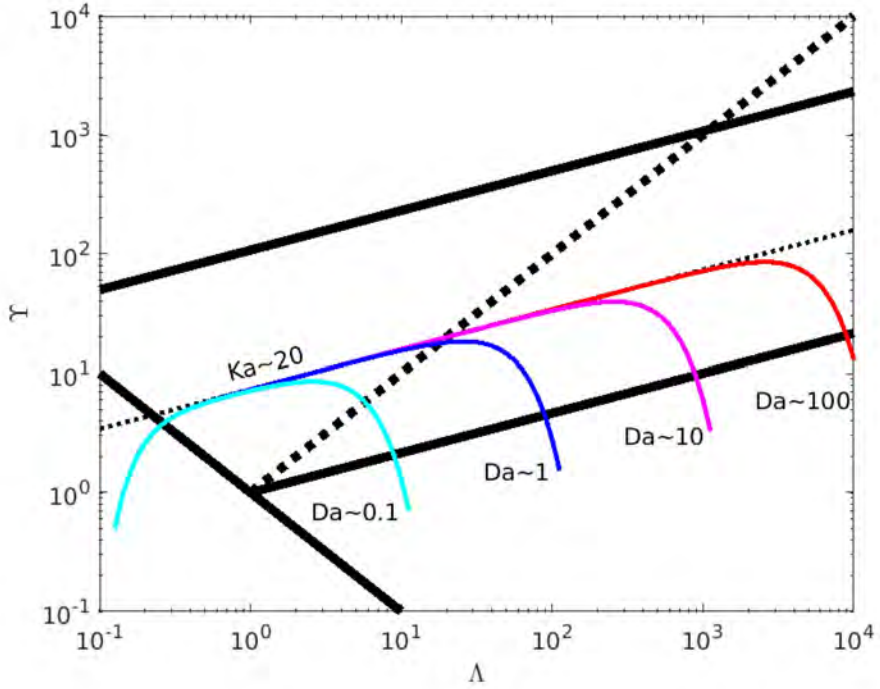

Damköhler number determines small/large-scale turbulent limit

Courtesy of Andy Aspden, Newcastle University

Premixed regime diagram revisited

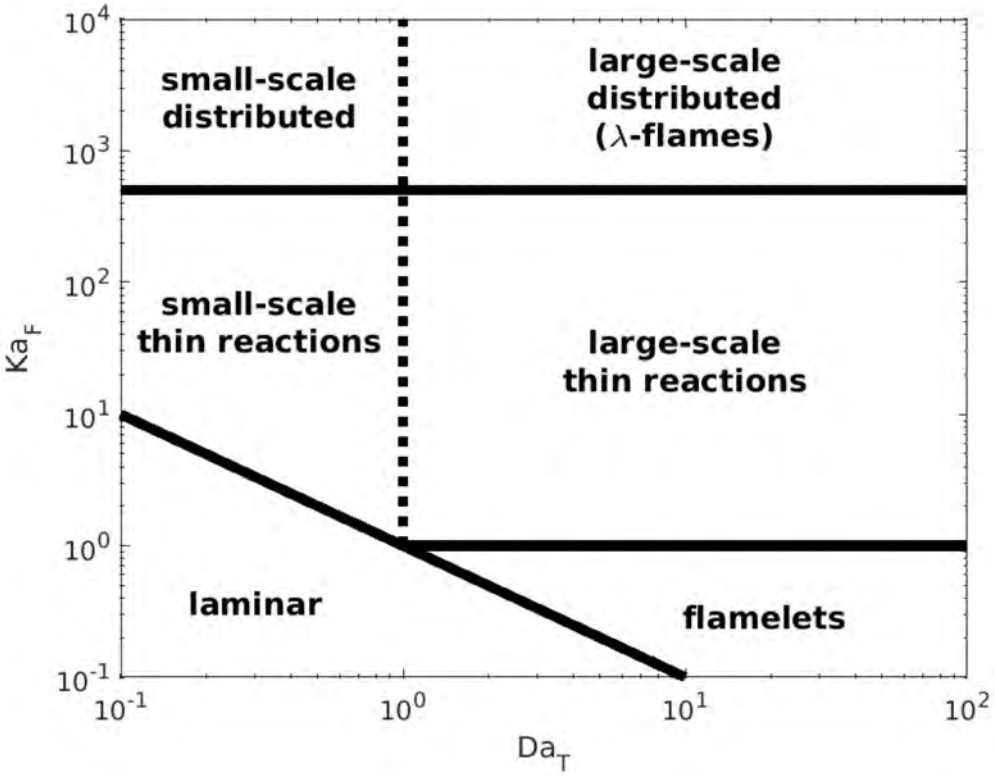

- Karlovitz number determines small-scale interactions
  - Flamelet, thin reaction zone (TRZ), distributed burning (DBR)
  - Use F-based values for H_2
- Damköhler number determines large-scale interactions
  - Large- and small-scale limits
  - Da_T needs turbulent flame time-scale
- A rotation of conventional diagram
- Can normalise Da & Ka independently
- TRZ and DBR have both LSL and SSL
- SSL is embedded within the LSL

Courtesy of Andy Aspden, Newcastle University

Turbulent isosurfaces (flame speed): $Ka_F = 4$ vs. $Ka_L = 4$

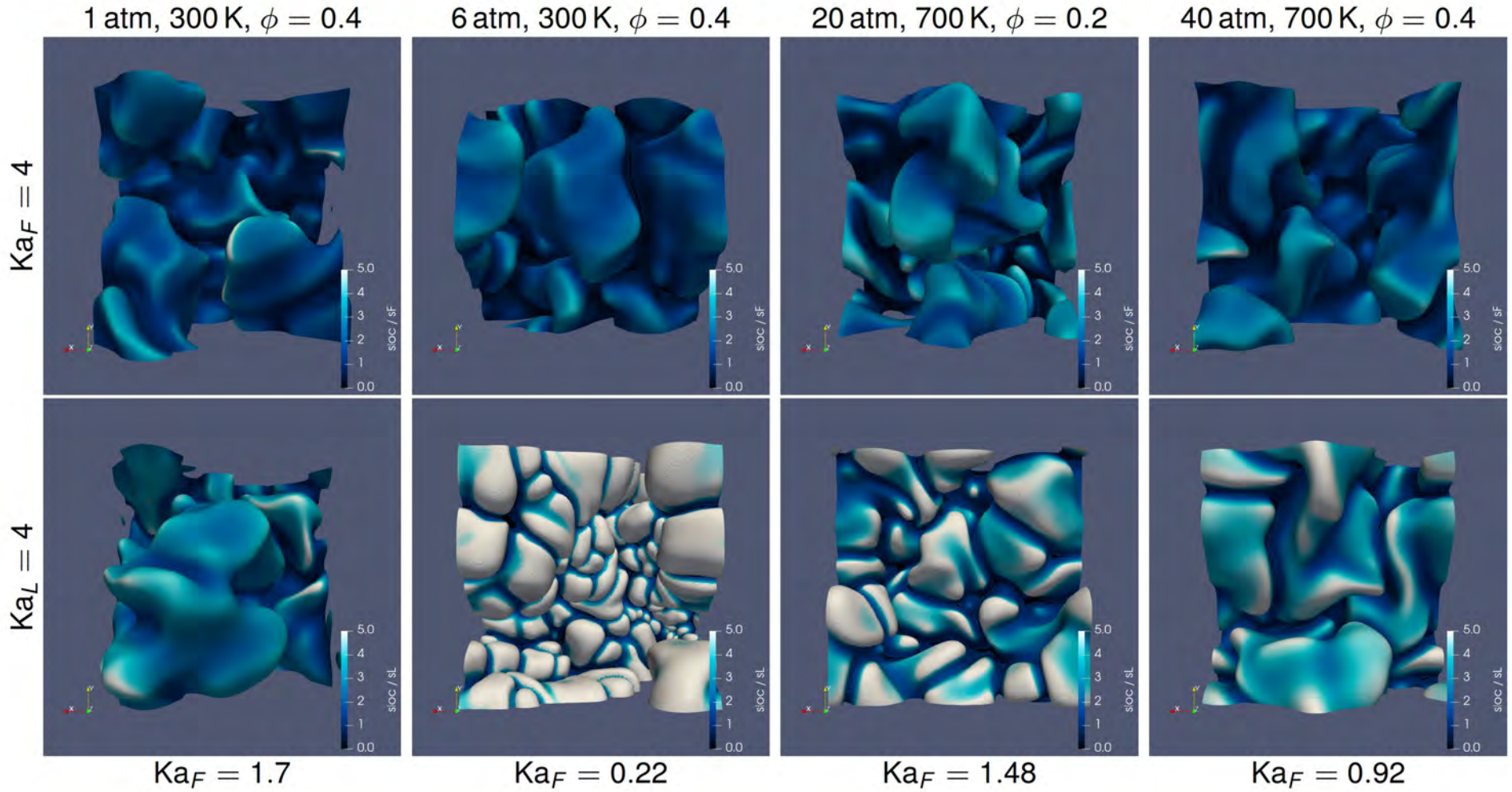

Hunt, Aspden, CNF (2025)

DL Instability and Large Eddies

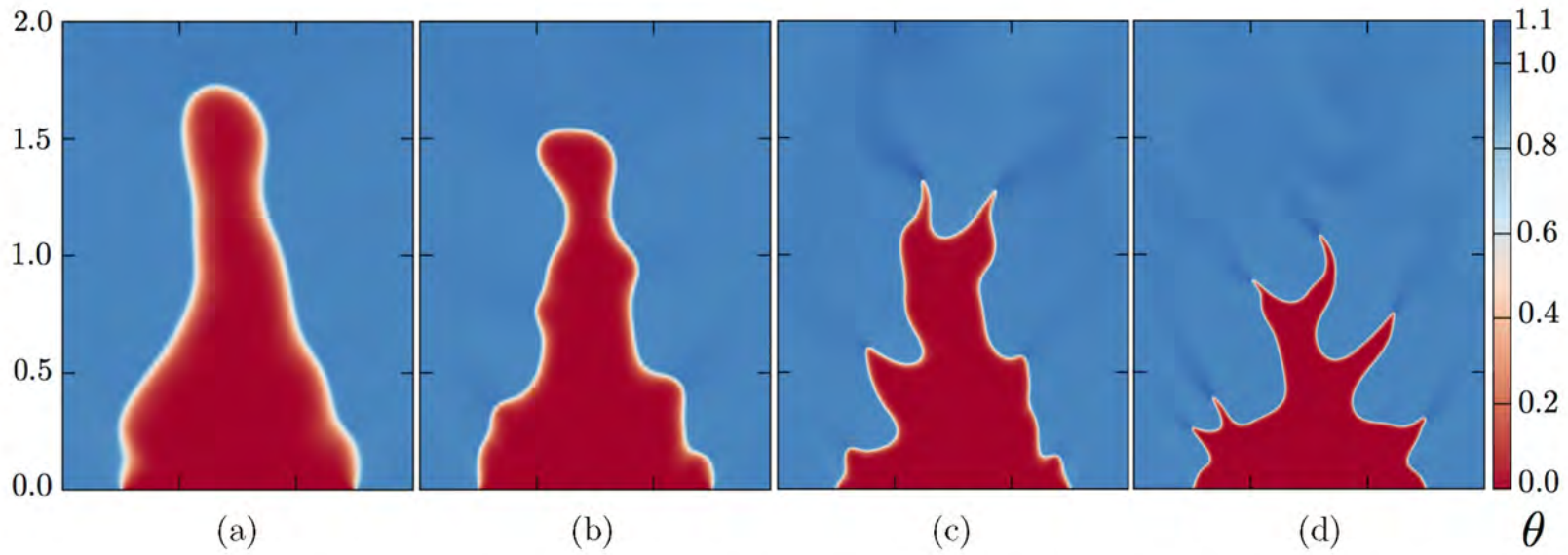

FIG. 3. Two-dimensional simulations of slot burner flames with $\sigma = 8$, $\mathrm{Le} = 1.2$, and of different nondimensional thickness $\delta = \ell_D/L$ with ℓ_D the flame thickness and L the burner diameter. The displayed field is nondimensional temperature θ. Flames with $\delta < \delta_c$ where $\delta_c = 0.015$ is the critical value, exhibit DL instability. (a) $\delta = 0.0275 > \delta_c$, (b) $\delta = 0.015 \sim \delta_c$, (c) $\delta = 0.008 < \delta_c$, (d) $\delta = 0.004 < \delta_c$. Note superadiabatic temperatures ($\theta > 1$) issuing from highly curved flame crests. The domain shown is smaller than the entire actual computational domain.

Large dimension (large integral eddies, ℓ/ℓ_f) enhances DL instability for enhanced burning

Hydrogen Flames & Diffusive-Thermal Instabilities

Practical Issues

Latest kinetic mechanism underpredicts the pressure curve for ultra-lean hydrogen spark-ignition engines.

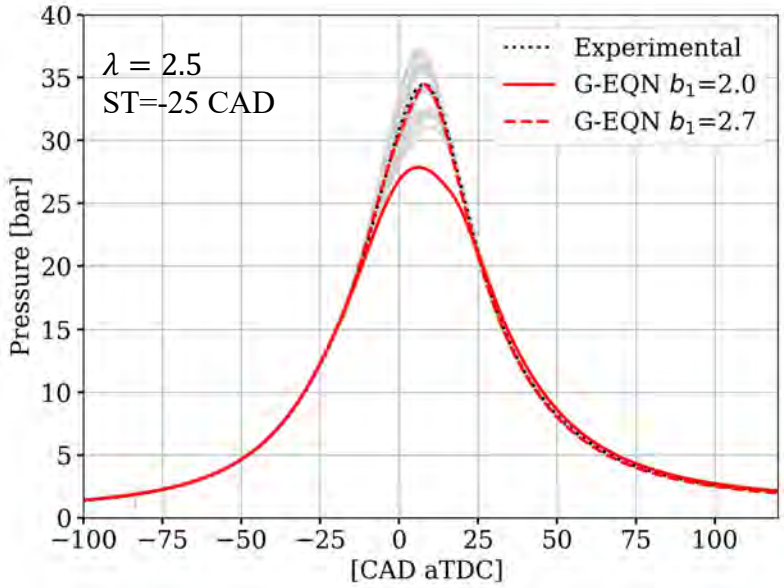

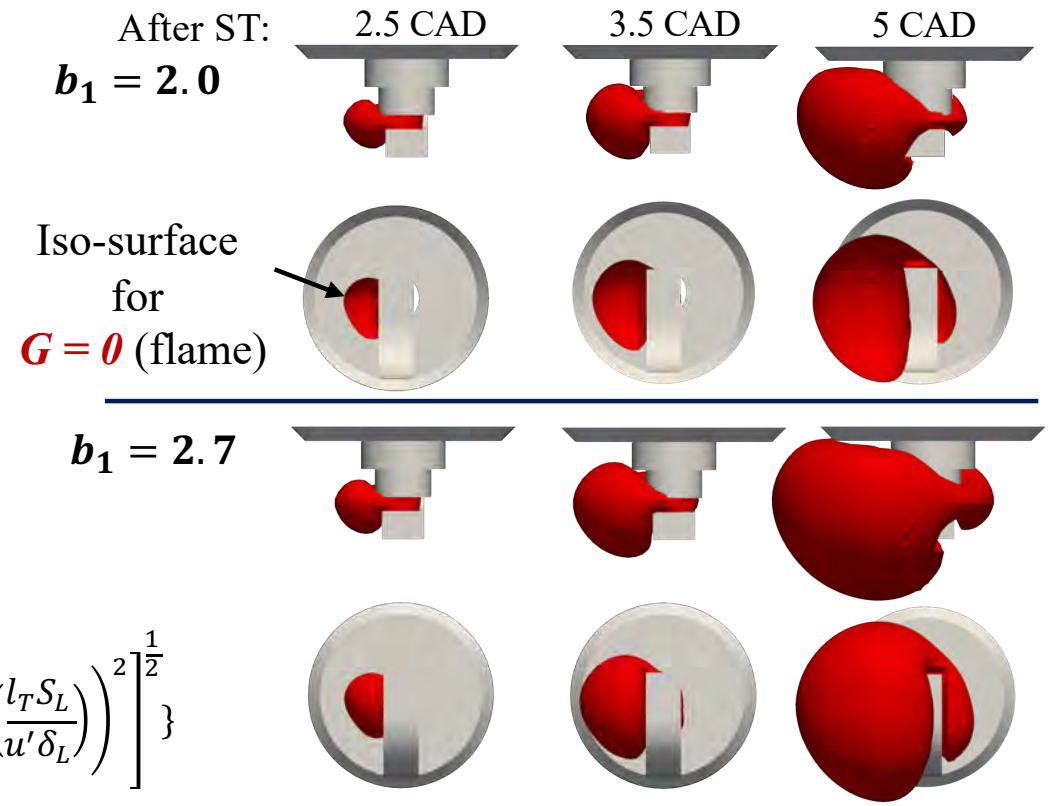

$$S_T = S_L + u'\{-\frac{a_4 b_3^2}{2\boldsymbol{b_1}}\left(\frac{l_T S_L}{u'\delta_L}\right) + \left[\left(\frac{a_4 b_3^2}{2\boldsymbol{b_1}}\left(\frac{l_T S_L}{u'\delta_L}\right) + a_4 b_3^2\left(\frac{l_T S_L}{u'\delta_L}\right)\right)^2\right]^{\frac{1}{2}}\}$$

G-equation model with Peters correlation

DNS for DT Instability Effects

L. Berger, A. Attili and H. Pitsch

Berger, Attili, Pitsch, CNF (2022b)

Combustion and Flame 240 (2022) 111936

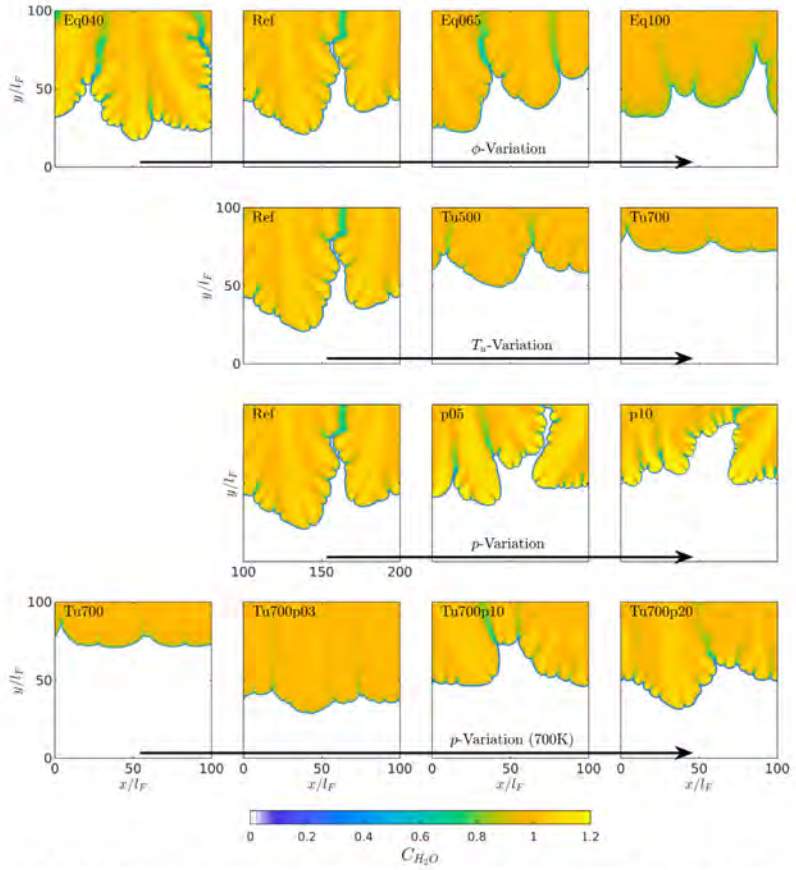

Fig. 3. Snapshots of the spatial distribution of progress variable for all performed simulations. For the sake of comparability, only a part of the simulation domain of $100l_F \times 100l_F$ is shown and movies of the flame evolution in the full computational domain are provided in the supplementary material.

X. Wen et al.

Wen et al., CNF (2024)

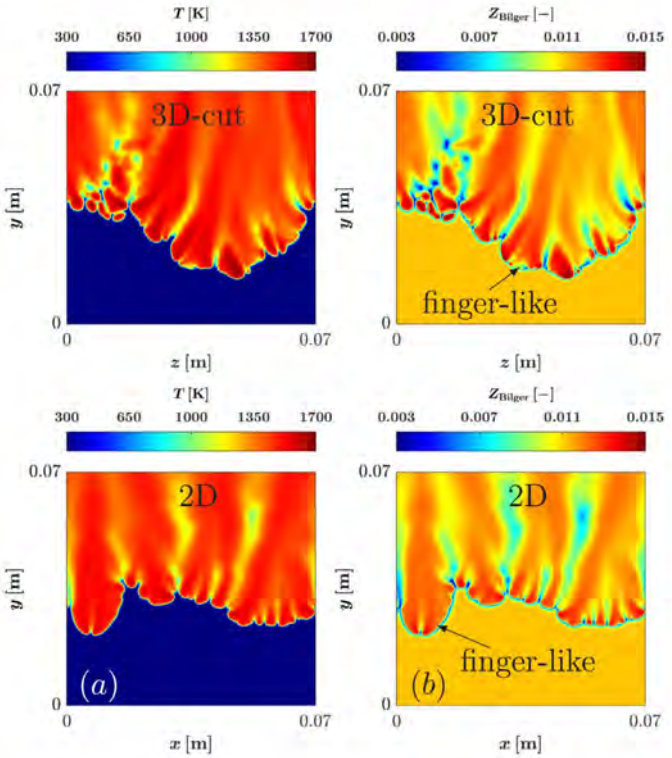

Fig. 2. Instantaneous distributions of the (a) temperature, and (b) Bilger mixture fraction, comparing the y-z plane of the 3D simulation (upper row) with the corresponding 2D simulation (lower row). The y-z plane of the 3D domain is cut in the x direction to keep the domain size the same as that of the 2D simulation. The finger-like structures in 2D and 3D simulations are indicated.

DNS for DT Instability Effects

Berger, Attili, Pitsch, CNF (2022c)

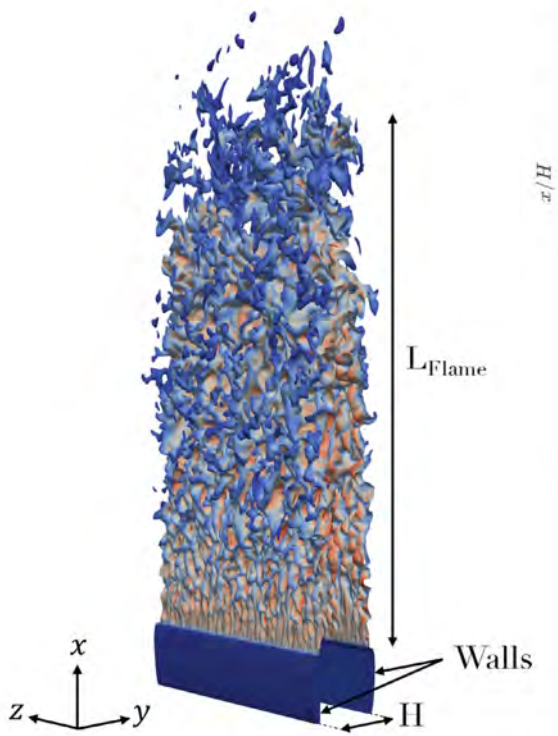

Fig. 1. Visualization of the *TurbUnstable* flame represented by an iso-surface of temperature that is colored by the heat release.

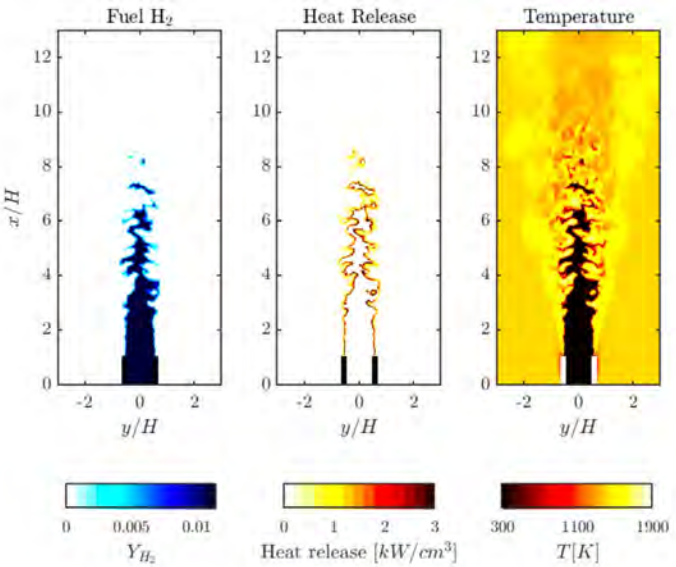

(a) *TurbUnstable* case

Differential diffusion not only creates DL instability for increased flame surface, but it also creates fluctuations in local equivalence ratio and reactivity

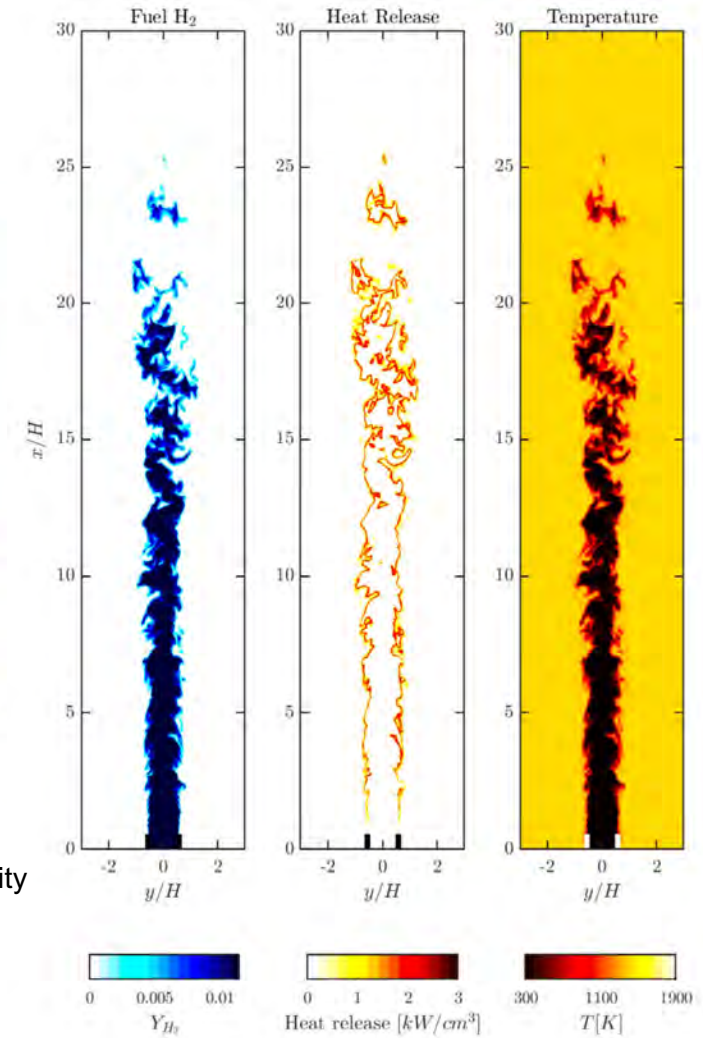

(b) *TurbStable* case

Laminar Flame Speed Adjustment

Matalon, Cui, Bechtold (2003)

$$\omega_2 = -B_1 + \beta\left(Le_{eff} - 1\right)B_2 + \Pr B_3$$

$$Le_{eff} = \begin{cases} \dfrac{Le_o + ALe_f}{1+A}, A = 1+\beta\left(\phi^{-1}-1\right) \text{if } \phi < 1 \\ \dfrac{Le_f + ALe_o}{1+A}, A = 1+\beta\left(\phi - 1\right) \text{if } \phi > 1 \end{cases}$$

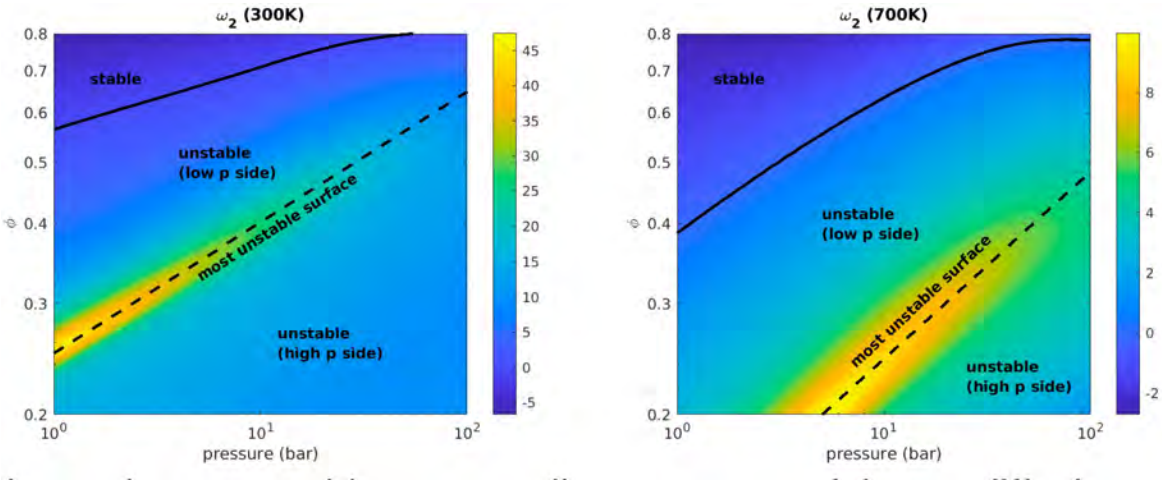

Howarth, Hunt, Aspden (2022)

$$\frac{s_F}{s_L} = \begin{cases} \exp\left(0.08\omega_2\right), \text{if } P < \Pi_c \\ 1 + 0.47\omega_2 \text{ otherwise} \end{cases}$$

$$\frac{l_F}{l_L} = \begin{cases} \exp\left(-0.06\omega_2\right), \text{if } P < \Pi_c \\ \dfrac{1}{1+0.26\omega_2} \text{ otherwise} \end{cases}$$

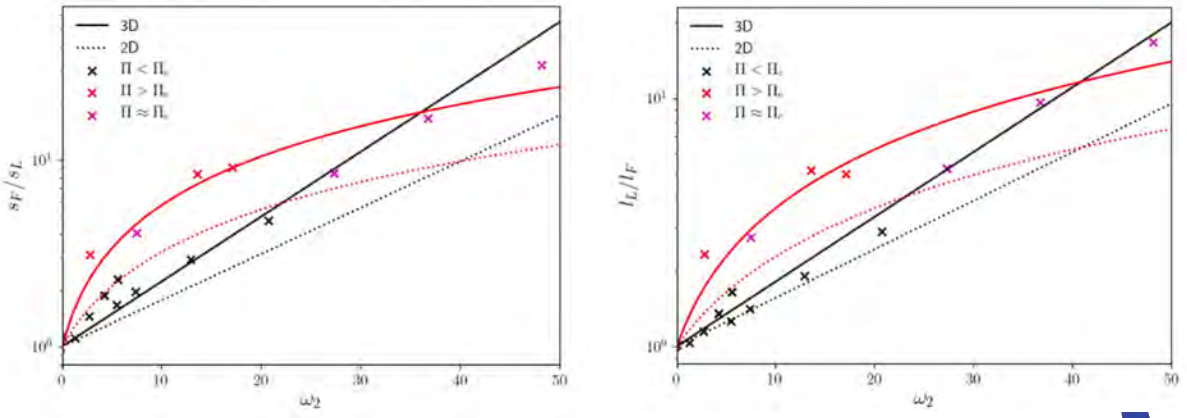

NH_3-H_2-N_2/Air Flame and *Le* Effect

Khamedov, Hernandez Perez, Im, PROCI 40 (2024)

- How does flame speed change with hydrogen addition to the flame? or with changes in the turbulence conditions?
- What is the effect of the Lewis number on the S_T?

➢ Only lean flames with $\boldsymbol{\varphi = 0.81}$ are considered

(by matching flame temperature T_b, $\frac{l_T}{\delta_L} = 3.5$, $\frac{u'}{S_L} = 10$)

Case	Fuel (NH3-H2-N2)	S_L [m/s]	δ_L [mm]	T_r [K]	Re [-]	Da [-]	Ka [-]	Grid [M]	Le_{eff}
A2	**100-0-0**	0.21	1.43	600	197	0.35	40	11.6	0.88
A2-H1	**60-25-15**	0.54	0.67	600	225	0.35	42	15.5	0.85
A2-H2	**40-45-15**	0.93	0.43	520	316	0.35	50	31.7	0.78

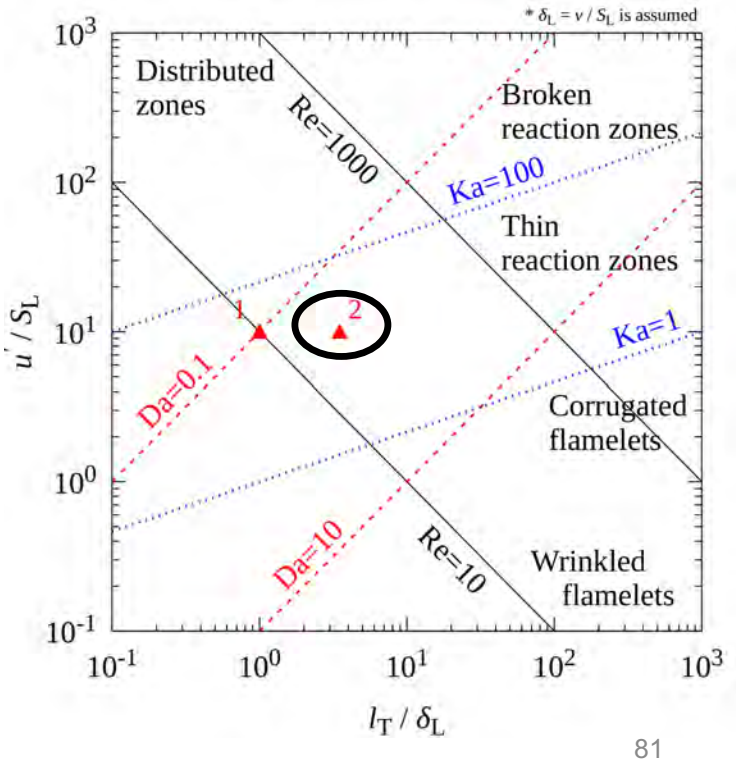

Turbulence-Flame Interaction: S_T

NH_3/air

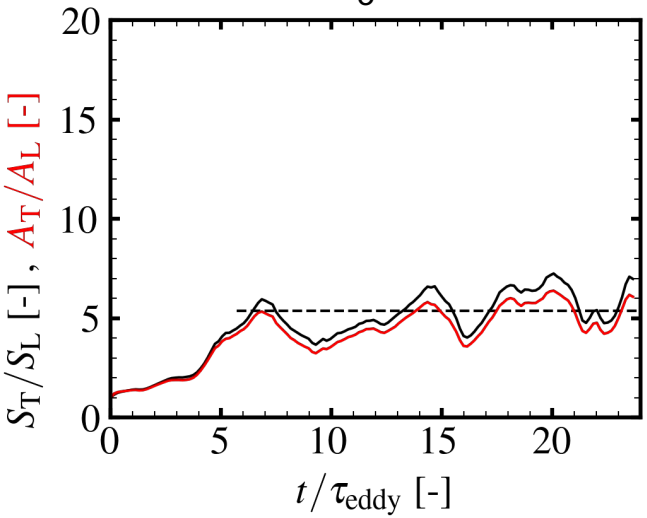

60%NH_3-**25**%H_2-15%N_2/air

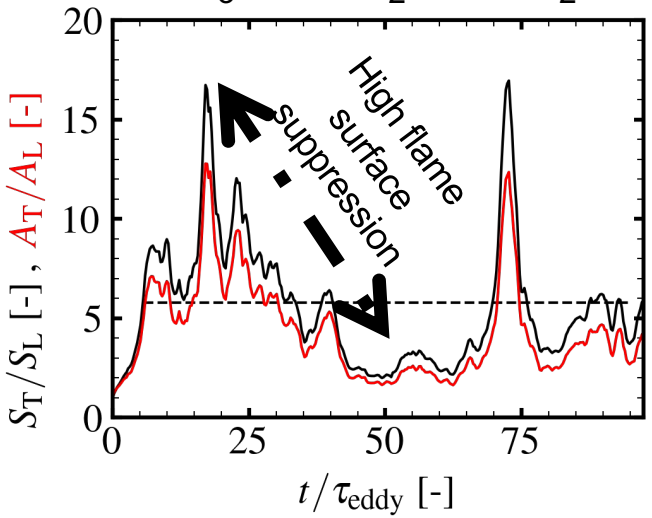

40%NH_3-**45**%H_2-15%N_2/air

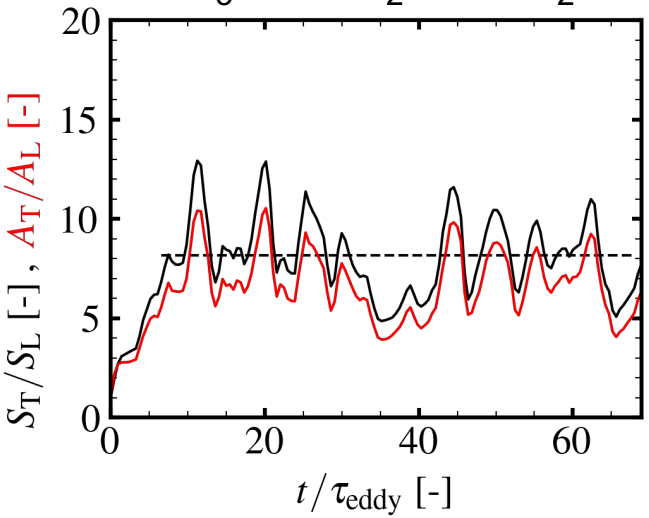

HRR [W/m^3]

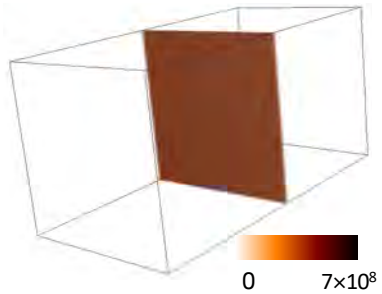

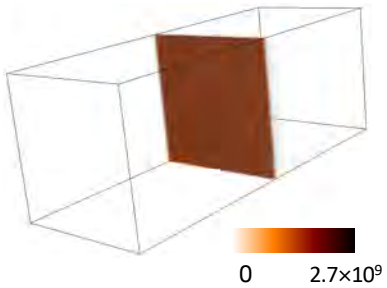

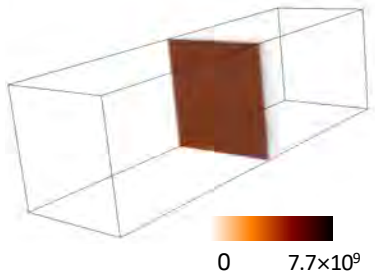

Flame Topology

- Instantaneous snapshot of NH_3 and H_2 mass fraction distribution

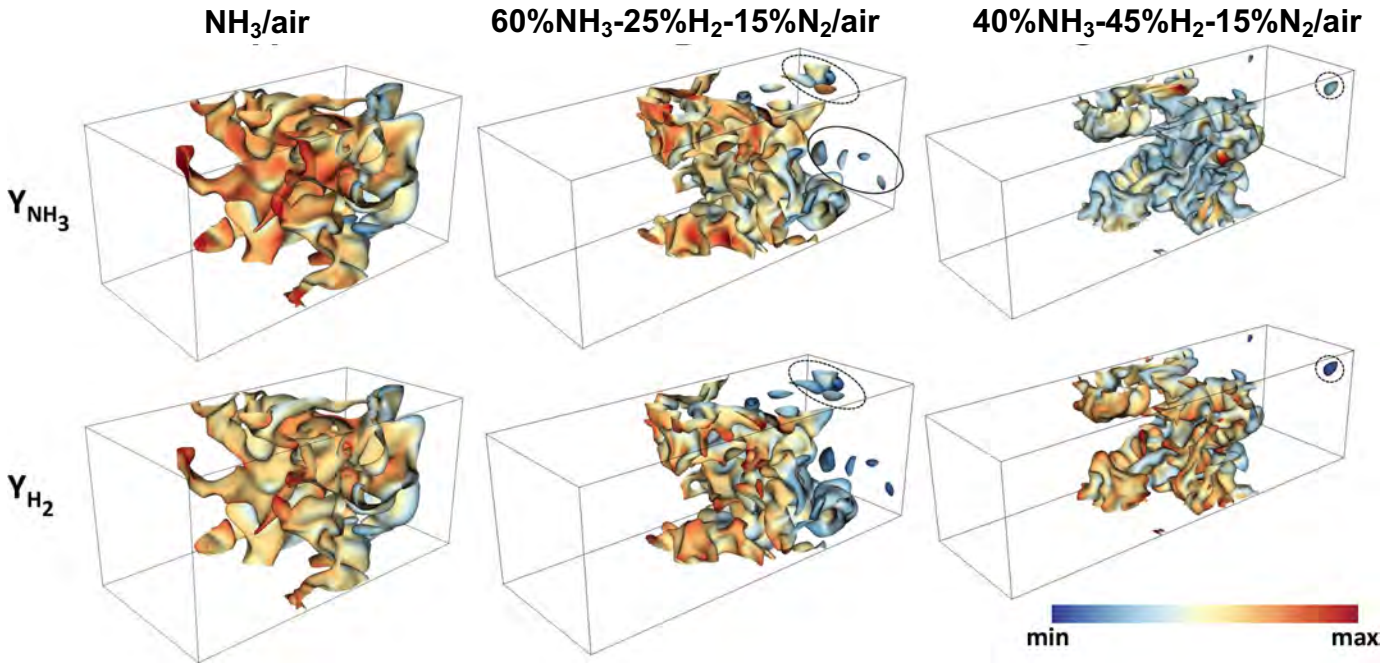

60%NH_3-25%H_2-15%N_2/air flame

- More unburned mixture elements (UME) in product side
- Lower H_2 mass fraction in UME compared to leading flames elements
- Significant NH_3 presence in UME

60%NH_3-25%H_2-15%N_2/Air Flame

Temporal evolution of S_T/S_L (with *Le ǂ 1* and *Le = 1* transport models) and A_T/A_L

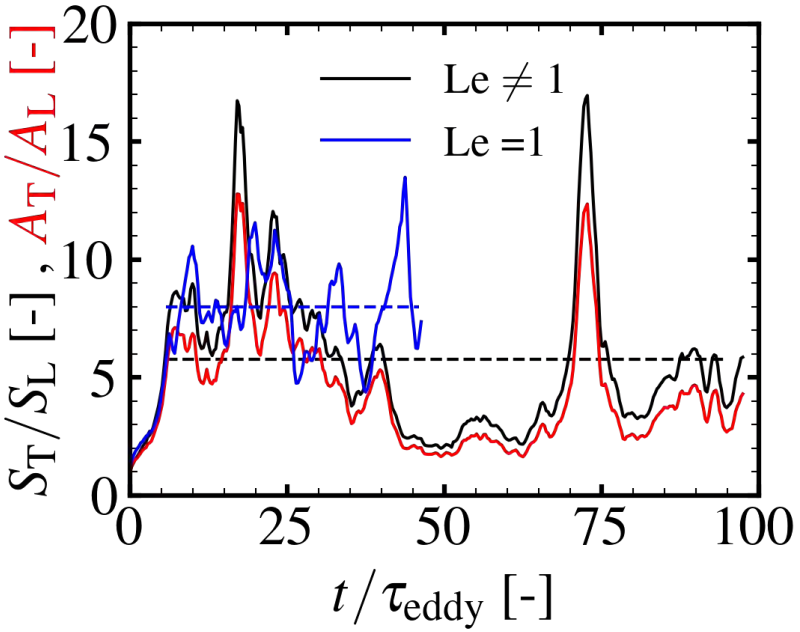

- Thermal diffusive instability plays a role in the high oscillations observed in turbulent flame speed

Summary

- Experimental measurements of turbulent flame speed have been compiled and scaling relations have been tested.
- Damköhler's large and small scale turbulence limit lays out a general categorization.
- It is important to define proper nondimensional numbers to characterize turbulence-flame interactions at different regimes (Re, Da, Ka, etc.)
- Regime diagram revisited.
- Effects of differential diffusion, laminar flame theory of DL and DT instabilities are highly relevant in understanding highly turbulent flame characteristics.

جامعة الملك عبدالله للعلوم والتقنية
King Abdullah University of Science and Technology

Clean Energy Research Platform

Tsinghua-Princeton-Combustion Institute
2025 Summer School on Combustion
Tsinghua University, July 7-11, 2025

Turbulent Combustion

Day 3: Turbulent Combustion Modeling

Hong G. Im
Clean Energy Research Platform (CERP)
King Abdullah University of Science and Technology (KAUST)

Turbulent Combustion Modeling
General Aspects

Hierarchy of Turbulent Combustion Modeling

Direct Numerical Simulation (DNS)

- Resolves all relevant physical scales
- Key issues: accuracy, stability, efficiency

Large Eddy Simulation (LES)

- Resolves large-scale eddies, model subgrid scales
- Key issues: accuracy, numerical dissipation, subgrid modeling

Reynolds-Averaged Navier Stokes (RANS)

- Statistical average
- Key issues: closure of higher-order moments
  - Zero-equation models
  - One-equation models
  - Two-equation models
  - Reynolds-stress model

  Lots of empirical, case-by-case tuning…

Higher cost ☹

Higher fidelity ☺

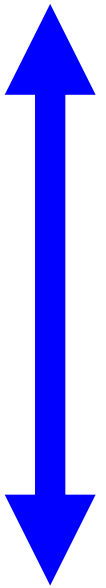

Lower cost ☺

Lower fidelity ☹

DNS vs. LES vs. RANS

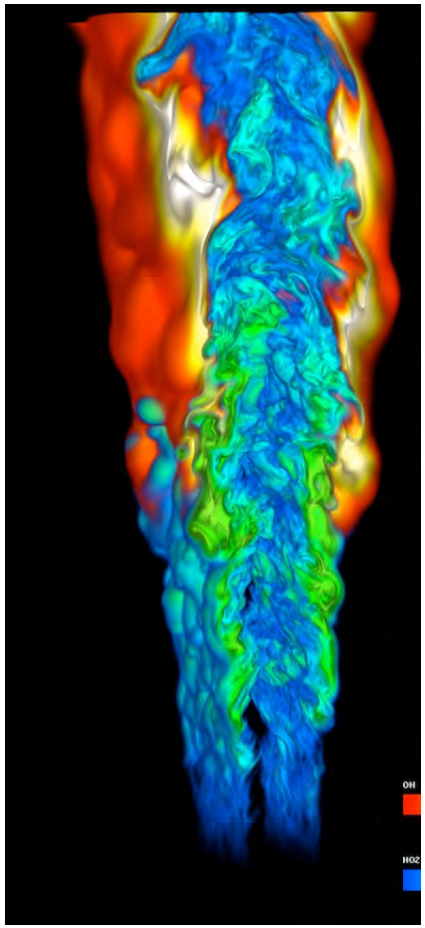

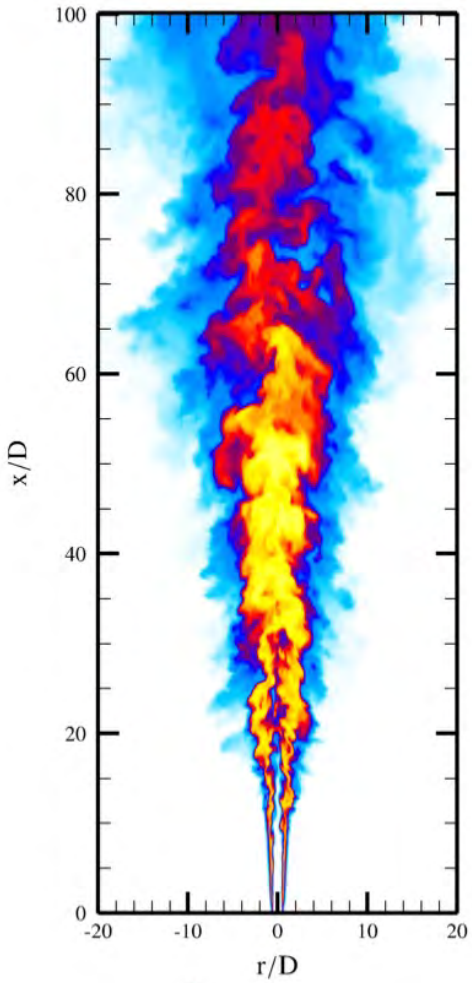

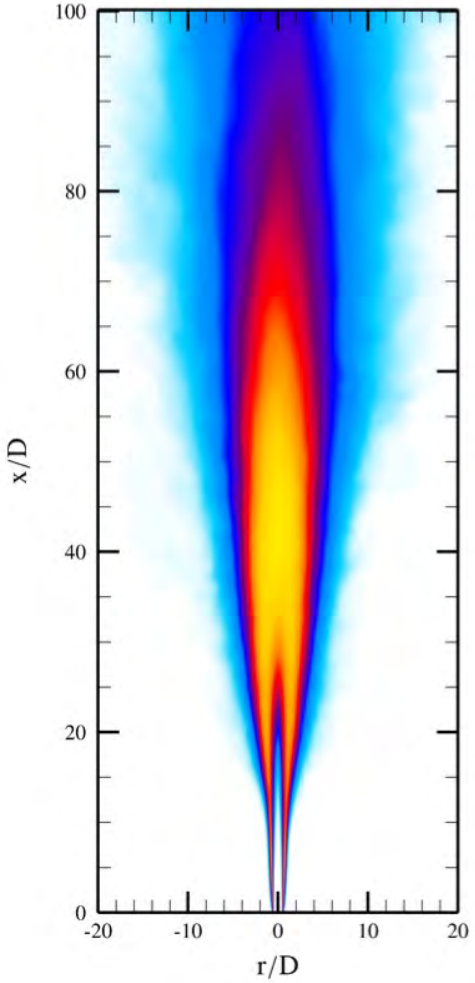

Modeling of Turbulent Premixed Combustion
Regime by Regime

Outline - Premixed Combustion Modeling

Reynolds-Averaged Navier-Stokes (RANS)

- Chemistry-Controlled (Chemical Engineering)
  - Plug-flow reactor (PFR)
  - Continuous-stirred-tank reactor (CSTR)
- Transport-Controlled (Fluid Mechanics)
  - Reaction progress variable and transport equations
  - Bray-Moss-Libby (BML) model
  - Coherent flame model (CFM)
  - Level-set (G-equation) model

Large Eddy Simulation (LES)

Generally follows RANS practice, with additional issues

Perfectly-Stirred Reactor Model (Turbulent Pipe Flow)

Valid for $Da_0 < 1$, large Re_0

Assumptions:

- Plug flow in radial direction
  (mixing at the same axial location is infinitely fast)
- Axial dispersion (mixing) negligible

For species concentration ϕ

$$\frac{d\phi}{d\tilde{z}} = \tau_{pfr} S(\phi)$$

$\tilde{z} = z / L_{pfr}$: normalized reactor length

$\tau_{pfr} = L_{pfr} / \bar{U}_z$: mean residence time

($\bar{U}_z$: mean axial velocity)

Space-to-Time Conversion (Lagrangian)

$\alpha = \tau_{pfr} \tilde{z}$: elapsed time (age) in the reactor

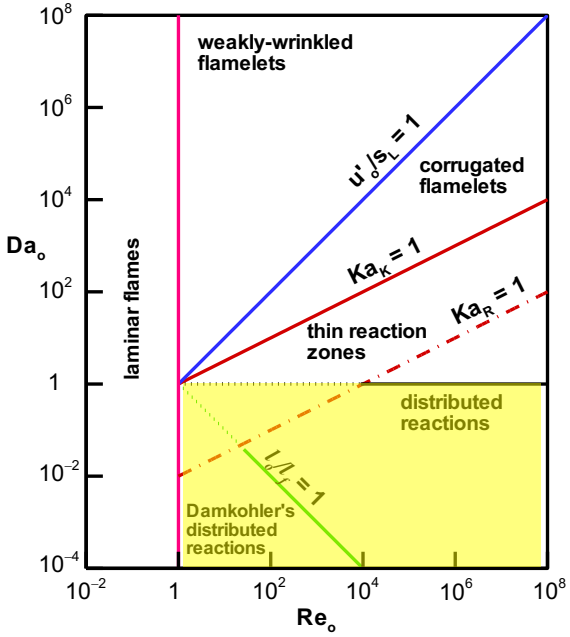

Continuous-Stirred-Tank Reactor

Stirred vessel with continuous inflow and outflow
(uniform concentration inside the vessel)

Valid for $\mathrm{Da}_0 < 1$, large Re_0

For the outlet species concentration ϕ

$$\frac{d\phi}{d\tilde{t}} = \tau_{cstr} S(\phi) + \phi_{in} - \phi$$

$\tilde{t} = t / \tau_{cstr}$: nondimensional time

$\tau_{cstr} = V_{cstr} / q_{in}$: mean residence time

(V_{cstr} : tank volume, q_{in} : inlet flow rate)

Zone Models (for non-ideal reactors)
- Reactor volume broken into N well-mixed zones

$$\frac{d\phi^{(i)}}{d\tilde{t}} = \sum_{j=0}^{N+1} \left(f_{ji}\phi^{(j)} - f_{ij}\phi^{(i)} \right) + S(\phi), \quad i = 1, \ldots, N$$

f_{ij} : transport rate of fluid from zone i to zone j

$i = 0$: inlet zone; $i = N+1$: outlet zone

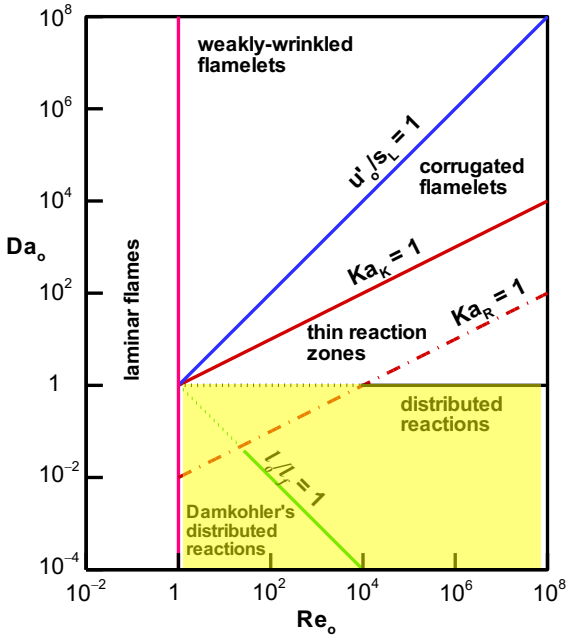

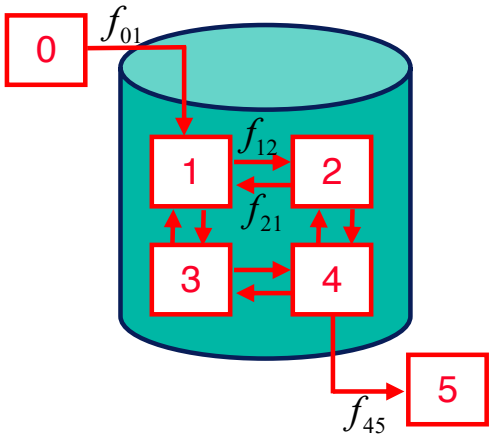

RANS & LES

Can we follow turbulence modeling practice?

RANS: closure of higher order reaction terms
LES: subgrid models for reaction terms

Unlike turbulence where the Reynolds/Leonard stress terms can be estimated/extrapolated, the higher order/subgrid reaction terms must be modeled **entirely**.

No universal combustion submodels exist. A better strategy is to model combustion processes in different “regimes”.

Note that many combustion submodels are equally applicable to both RANS and LES approaches.

Reaction Term Closure

(applicable to both nonpremixed and premixed combustion)

- *The Fundamental Difficulty in Combustion Modeling*

A typical single-species reacting system

$$\rho\frac{\partial \psi}{\partial t}+\rho\mathbf{u}\cdot\nabla\psi=\nabla\cdot\left(\rho D\nabla\psi\right)+w,\ \text{where}\ w=B\psi\exp\left(-\frac{E}{RT}\right)$$

with $\psi=\bar{\psi}+\psi'$, $T=\bar{T}+T'$ $(T'\ll\bar{T})$ and Reynolds averaging,

$$\bar{w}=\overline{B\left(\bar{\psi}+\psi'\right)\exp\left(-\frac{E}{R\left(\bar{T}+T'\right)}\right)}$$

$$=B\bar{\psi}\exp\left(-\frac{E}{R\bar{T}}\right)\overline{\left[1+\frac{E}{R\bar{T}^2}T'+\frac{1}{2}\left(\frac{E}{R\bar{T}}\right)^2\left(\frac{T'}{\bar{T}}\right)^2+\cdots\right]}$$

$$=B\bar{\psi}\exp\left(-\frac{E}{R\bar{T}}\right)\overline{\left[1+\frac{1}{2}\left(\frac{E}{R\bar{T}}\right)^2\left(\frac{T'}{\bar{T}}\right)^2+\cdots\right]}$$

Not small for $\frac{E}{R}\gg\bar{T}$

(large activation energy)

Combustion Closure in RANS

For RANS formulation:

$$\frac{\partial \bar{\rho}\tilde{Y}_i}{\partial t} + \nabla \cdot \left(\bar{\rho}\tilde{\mathbf{v}}\tilde{Y}_i \right) - \nabla \cdot \left(\bar{\rho} D_i \nabla \tilde{Y}_i \right) = -\nabla \cdot \left(\widetilde{\bar{\rho}\mathbf{v}''Y_i''} \right) + \bar{w}_i$$

where

$$\overline{w_i\left(\rho, Y_i, T\right)} \neq w_i\left(\bar{\rho}, \bar{Y}_i, \bar{T}\right)$$

This is called “laminar closure”, i.e. no closure.

Reaction source term closure:

1. Keep the equation form, and approximate the reaction source terms using simplified assumptions.
2. Reformulate the equations with exact closure (PDF model)
3. Reformulate the equations completely (depending on the combustion regimes)

Multi-zone Model (option 1)

Assumes that combustion is primarily controlled by chemical kinetics with little effect of subgrid-scale turbulence and mixing.

Computational cells are mapped into scalar phase space to save computational cost.

Good approximation for nearly homogeneous combustion (HCCI, PPC)

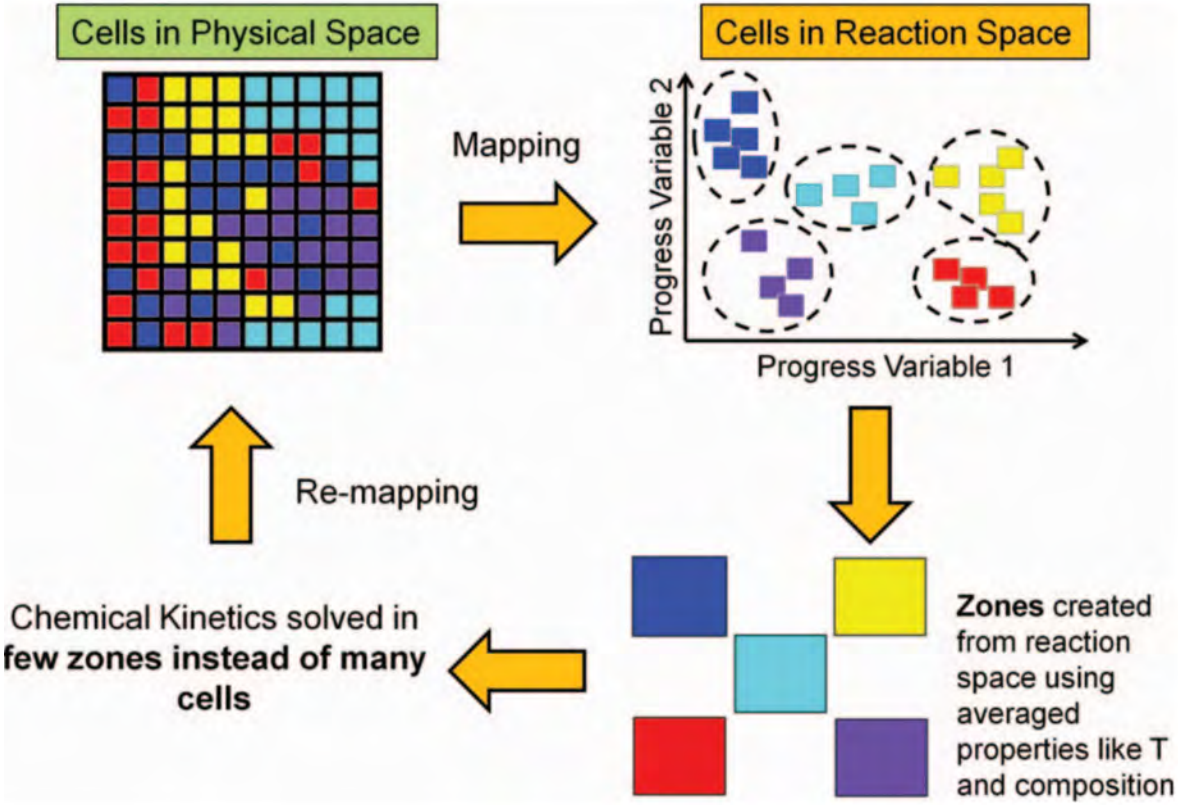

Kodavasal et al. (2011)

EDC/PaSR Models (option 1)

Eddy dissipation concept / Partially stirred reactor

$$\frac{dC_1}{dt} = \frac{C_1 - C_0}{\tau} = w(C_1)\frac{\tau_c}{\tau_c + \tau_{mix}}$$

Mixing time $\tau_{mix} = \frac{k}{\varepsilon}\left(C_\mu / \mathrm{Re}_t\right)^{\frac{1-\alpha}{2}}$

Chemical time τ_c

For detailed reaction mechanisms, one may incorporate identification of representative chemical time based on eigenvalue analysis.

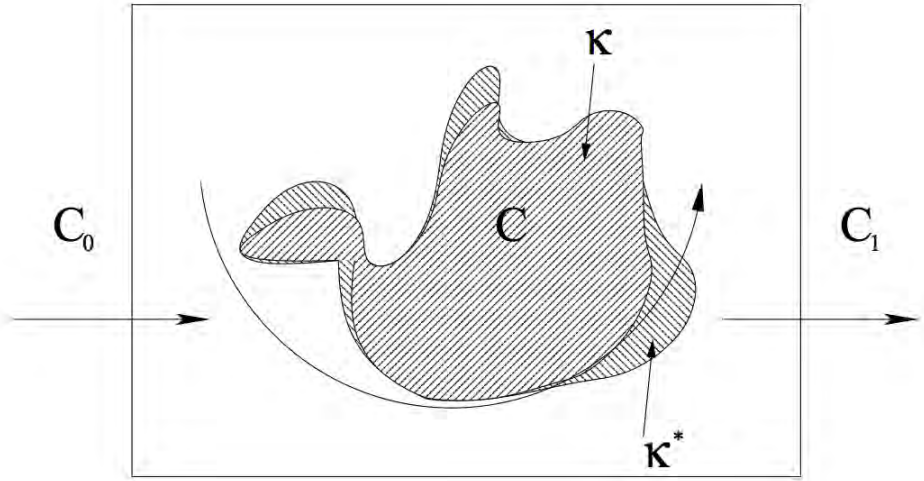

Golovichev, Chalmers University

One of the most commonly adopted models in large scale RANS/LES simulations of practical devices.

Transported Probability Density Function (PDF) (option 2)

- Closures for the (high) moment terms in transport equations

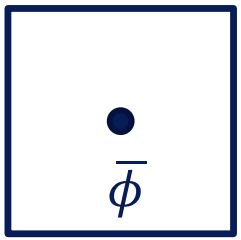

$$\overline{S_k(\boldsymbol{\phi})} \neq S_k(\overline{\boldsymbol{\phi}})$$

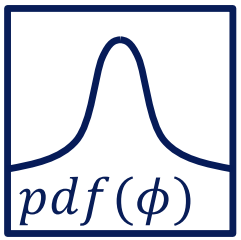

$$\overline{S_k(\boldsymbol{\phi})} = \int S_k(\boldsymbol{\phi}) pdf(\boldsymbol{\phi}) d\boldsymbol{\phi}$$

Any moment of variable ϕ can be accurately computed given its $f_\phi(\psi)$

- Transport equations of the PDF of fluid properties
  - Turbulent reacting flow is represented by the joint probability density function (PDF) of fluid properties ($\boldsymbol{\phi}$, $\boldsymbol{u}$, $\boldsymbol{x}$)
  - Joint composition pdf transport equation **(one-point, one-time)**:

$$\frac{\partial \mathcal{F}_\phi}{\partial t} + \frac{\partial \mathcal{F}_\phi \widetilde{v_i|\psi}}{x_i} = -\frac{\partial}{\partial \psi_\alpha}\left[\frac{\mathcal{F}_\phi}{\bar{\rho}} \overline{\frac{\partial J_{\alpha i}}{\partial x_i}|\psi}\right] - \frac{\partial \mathcal{F}_\phi S_\alpha}{\partial \psi_\alpha}$$

Turbulent Premixed Combustion in Flamelet Regime (option 3)

In the flamelet regime $\mathrm{Ka_K} < 1$ (or $\mathrm{Ka_R} < 1$)
Define the progress variable:

$$c = \frac{T - T_u}{T_b - T_u} = \frac{Y_P}{Y_{P,b}} = \frac{Y_F - Y_{Fu}}{Y_{Fb} - Y_{Fu}} \quad (0 < c < 1)$$

which may be used to uniquely determine all the solution variables (including reactive scalars).

Other variables may be used for the definition of the progress variable, provided that they vary monotonically from the unburned to burned side.

Temperature is a good choice only for an adiabatic system.

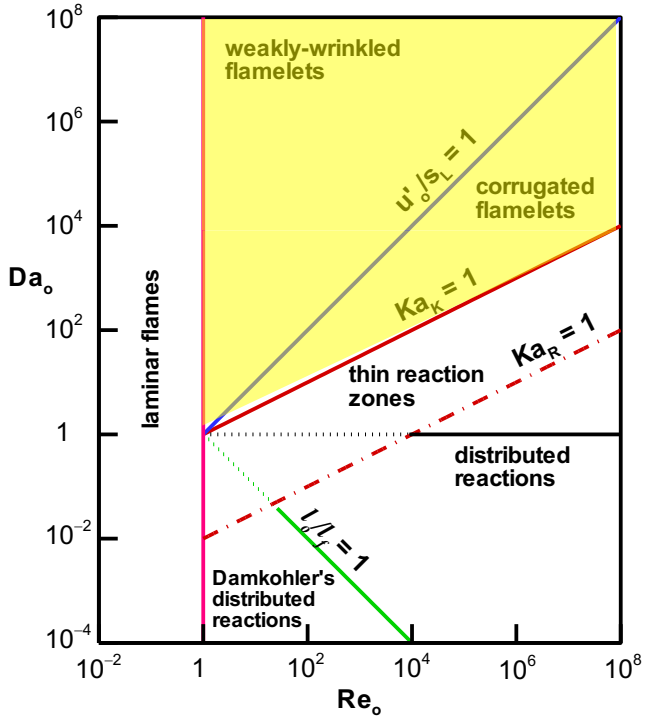

The problem then boils down to a single scalar transport equation (in addition to continuity and momentum conservation).

Transport Equation for Progress Variable

For a suitable definition of the reaction progress variable, a transport equation can be derived from the relevant transport equations for the reactive scalar variables:

$$\rho\frac{\partial c}{\partial t}+\rho u_j\frac{\partial c}{\partial x_j}=\frac{\partial}{\partial x_j}\left(\rho D_c\frac{\partial c}{\partial x_j}\right)+w$$

For RANS, the Favre-averaged reaction progress variable transport equation is written as

$$\bar{\rho}\frac{\partial \tilde{c}}{\partial t}+\bar{\rho}\tilde{u}_j\frac{\partial \tilde{c}}{\partial x_j}=\frac{\partial}{\partial x_j}\left(\overline{\rho D_c\frac{\partial c}{\partial x_j}}\right)-\frac{\partial}{\partial x_j}\left(\bar{\rho}\widetilde{u_j''c''}\right)+\bar{w}$$

Terms to be closed:

$\overline{\rho D_c\dfrac{\partial c}{\partial x_j}}$: Molecular transport term

$\widetilde{u_j''c''}$: Reynolds transport term

$\bar{w}$: Reaction term

Closure of Molecular Transport

$$\bar{\rho}\frac{\partial \tilde{c}}{\partial t}+\bar{\rho}\tilde{u}_j\frac{\partial \tilde{c}}{\partial x_j}=\frac{\partial}{\partial x_j}\left(\overline{\rho D_c\frac{\partial c}{\partial x_j}}\right)-\frac{\partial}{\partial x_j}\left(\bar{\rho}\widetilde{u_j''c''}\right)+\bar{w}$$

For RANS, the molecular diffusion term is negligible.

For LES, the grid-scale Re is not large enough to justify this simplification. The simplest closure is based on the assumption that the mass diffusivity is independent of the progress variable, such that

$$\overline{\rho D_c\frac{\partial c}{\partial x_i}}\simeq\overline{\rho D_c}\frac{\partial \tilde{c}}{\partial x_i}$$

which further requires an assumption that $\overline{\frac{\partial c}{\partial x_i}}\simeq\frac{\partial \tilde{c}}{\partial x_i}$

Although the approximations are crude, additional refinement is hardly justified considering its significance relative to other closure models (turbulent transport, reaction).

Closure of Turbulent (Reynolds) Transport

$$\bar{\rho}\frac{\partial \tilde{c}}{\partial t}+\bar{\rho}\tilde{u}_j\frac{\partial \tilde{c}}{\partial x_j}=\frac{\partial}{\partial x_j}\left(\overline{\rho D_c\frac{\partial c}{\partial x_j}}\right)-\frac{\partial}{\partial x_j}\left(\bar{\rho}\widetilde{u_j''c''}\right)+\bar{w}$$

A standard approach is the gradient transport model:

$$\widetilde{u_j''c''}=-D_T\frac{\partial \tilde{c}}{\partial x_j}$$

where D_T is a turbulent diffusivity to be determined.

Across the flame (R to P), $\tilde{u}_P>\tilde{u}_R$ (thermal expansion), $\tilde{c}_P>\tilde{c}_R$

Therefore, the physically correct situation is $\widetilde{u_j''c''}>0$ near the flame region. This means that the turbulent diffusivity needs to be negative in some regions of the flow field.

⇒ The code blows up! (counter-gradient diffusion)

(More on this discussion later in BML)

Strong turbulence promotes gradient diffusion

Strong heat release promotes counter-gradient diffusion

Closure of Chemical Reaction

Eddy Break-up (EBU) and Eddy Dissipation Concept (EDC) Models

- *Simple algebraic models for reaction term closure*

EBU (Spalding): reaction rate is controlled by the mixing process only

$$\bar{w} = \bar{\rho} C_{EBU} \left(\frac{\tilde{\varepsilon}}{\tilde{k}} \right) \left(\overline{Y_F''^2} \right)^{1/2} \quad \text{(nonpremixed combustion)}$$

inverse of turbulent mixing (eddy turnover) time

$$\bar{w} = \bar{\rho} C_{EBU} \left(\frac{\tilde{\varepsilon}}{\tilde{k}} \right) \widetilde{c'' c''} \quad \text{(premixed combustion)}$$

EDC (Eddy Dissipation Concept) (Magnussen):
adding sensitivity to chemistry (mixture composition)

$$\bar{w}_F = \bar{\rho} A \bar{Y}_F \frac{\tilde{\varepsilon}}{\tilde{k}}$$ Mean fuel mass fraction

$$\bar{w}_O = \bar{\rho} A \frac{\bar{Y}_O}{\left(Y_O / Y_F \right)_{st}} \frac{\tilde{\varepsilon}}{\tilde{k}}$$ Mean oxidizer mass fraction

The Bray-Moss-Libby (BML) Model

Introducing a presumed PDF for the progress variable:

$$P(c;\mathbf{x},t)=\alpha(\mathbf{x},t)\delta(c)+\beta(\mathbf{x},t)\delta(1-c)+\zeta(\mathbf{x},t)f(c;\mathbf{x},t)$$

where $\delta(c)$: Dirac delta function

$f(c;\mathbf{x},t)$: distribution of c in the reacting state.

$$\int_0^1 f(c;\mathbf{x},t)dc=1$$

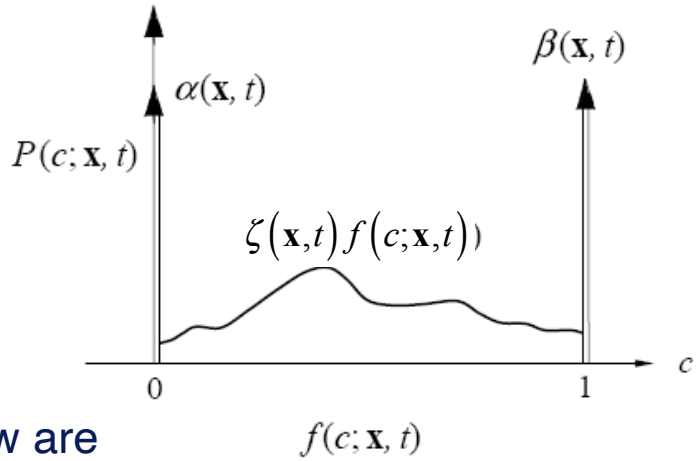

If the flame is very thin,

$$\zeta(\mathbf{x},t)\ll 1; \qquad \alpha(\mathbf{x},t)+\beta(\mathbf{x},t)=1$$

Then we expect that the thermodynamic aspects of the flow are mainly affected by $\alpha(\mathbf{x},t)$ and $\beta(\mathbf{x},t)$ only, while the average reaction rate$(\bar{w})$ is solely controlled by $\zeta(\mathbf{x},t)f(c;\mathbf{x},t)$, because reaction vanishes for $c=0$ and $c=1$

Transport Closure by BML

Define $\gamma = 1 - \frac{\rho_b}{\rho_u}$ $\qquad \frac{\rho}{\rho_u} = \frac{T_u}{T} = \frac{1-\gamma}{1-\gamma(1-c)}$

For a thin flame limit $P(c;\mathbf{x},t) = \alpha(\mathbf{x},t)\delta(c) + \beta(\mathbf{x},t)\delta(1-c);\ \alpha+\beta=1$

$$\frac{\overline{\rho}(\mathbf{x},t)}{\rho_u} = \int_0^1 \rho P(c;\mathbf{x},t)\,dc = \alpha(\mathbf{x},t) + \beta(\mathbf{x},t)(1-\gamma) = 1 - \beta(\mathbf{x},t)\gamma$$

$$\tilde{c}(\mathbf{x},t) = \frac{\overline{\rho c}}{\overline{\rho}} = \frac{\rho_u}{\overline{\rho}} \int_0^1 \frac{(1-\gamma)c}{1-\gamma(1-c)} P(c;\mathbf{x},t)\,dc = \frac{\rho_u}{\overline{\rho}} \beta(\mathbf{x},t)(1-\gamma) = \beta(\mathbf{x},t)$$

Using the joint PDF $P(u,c;\mathbf{x},t)$ it can be shown that

$$\tilde{u}(\mathbf{x},t) = (1-\tilde{c})\overline{u}_u(\mathbf{x},t) + \tilde{c}\overline{u}_b(\mathbf{x},t)$$

$$\widetilde{u''c''} = \frac{\overline{\rho(u-\tilde{u})(c-\tilde{c})}}{\overline{\rho}} = \tilde{c}(1-\tilde{c})(\overline{u}_b - \overline{u}_u)$$

Since $\overline{u}_b > \overline{u}_u$, $\widetilde{u''c''} > 0$ usually. This contradicts the usual gradient transport assumption

$$\widetilde{u''c''} = -D_t \frac{\partial \tilde{c}}{\partial x} > 0$$ Counter-gradient diffusion problem

Verifying Counter-Gradient Diffusion Using DNS

Veynante, Trouve, Bray, Mantel, J. Fluid Mech., 332:263-293 (1997).

Two data considered:

- DNS 1: low turbulence (Rutland et al.): $u' / S_L = 1$
- DNS 2: high turbulence (Trouve et al.): $u' / S_L = 10$

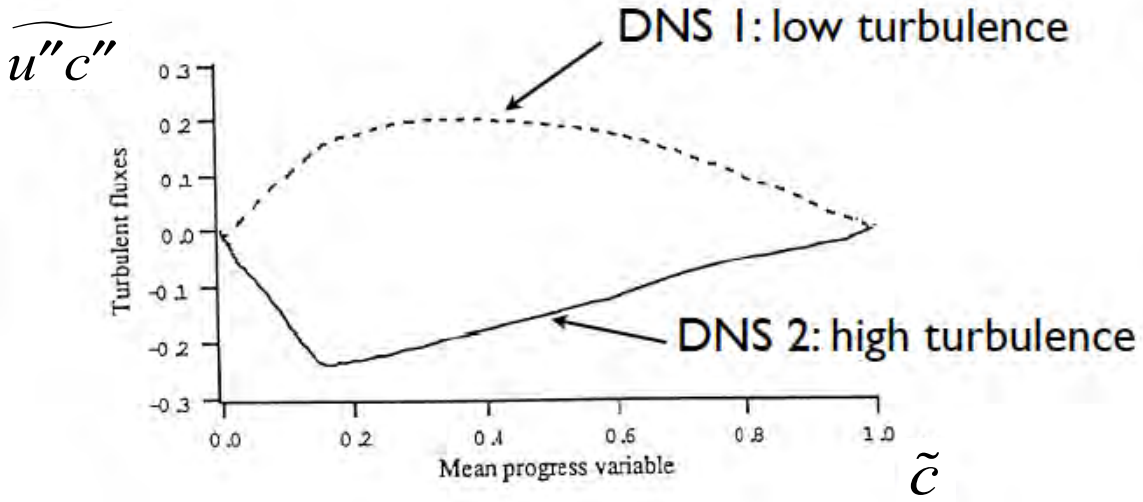

Low turbulence case exhibits counter-gradient diffusion.

Transport Closure by BML

A simple remedy to the counter-gradient diffusion was proposed by Veynante et al. (1997):

$$\widetilde{u''c''} = \tilde{c}\left(1-\tilde{c}\right)\left(\frac{\gamma}{1-\gamma}S_L - 2\alpha u'\right)$$

where $\gamma = 1-\frac{\rho_b}{\rho_u}$ and α is an efficiency function of order unity.

The Bray number:

$$N_B = \frac{\gamma S_L}{2\left(1-\gamma\right)\alpha u'}$$

$N_B > 1$ Counter-gradient diffusion

$N_B < 1$ Gradient diffusion

Reaction Term Closure by BML

Furthermore, the reaction term closure

$$\overline{w}(\mathbf{x},t)=\int_0^1 w(c;\mathbf{x},t)\,P(c;\mathbf{x},t)\,dc=\int_0^1 w(c;\mathbf{x},t)\,\zeta(\mathbf{x},t)\,f(c;\mathbf{x},t)\,dc$$

requires the specification of the distribution function $f(c;\mathbf{x},t)$

Model 1: Mixing-controlled reaction (EBU type)

$$\overline{w}=C\overline{\rho}\left(\frac{\tilde{\varepsilon}}{\tilde{k}}\right)\widetilde{c''c''}=C\overline{\rho}\left(\frac{\tilde{\varepsilon}}{\tilde{k}}\right)\tilde{c}(1-\tilde{c}$$

Model 2: Flame crossing frequencies

$$\overline{w}=w_c f_c$$

w_c : reaction rate per flame crossing

f_c : flame crossing frequency

$$f_c=2\frac{\overline{c}(1-\overline{c})}{\hat{T}}$$

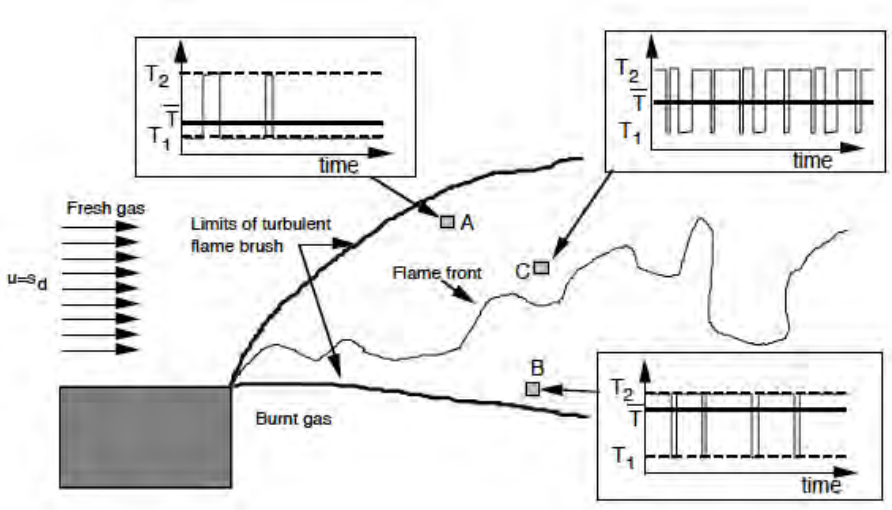

From Veynante & Poinsot (2005)

Reaction Term Closure by BML

The mean period of the signal, $\hat{T}$, is again related to the turbulent time:

$$\hat{T} = \tau_t = \frac{\tilde{\varepsilon}}{\tilde{k}}$$

and the reaction rate per crossing flame:

$$w_c = \frac{\overline{\rho}_u S_L^0}{\delta_L^0 / \tau_f}$$

laminar flame thickness

laminar flame time

leading to:

$$\overline{w} = 2\frac{\overline{\rho}_u S_L^0}{\delta_L^0 / \tau_f}\frac{\tilde{\varepsilon}}{\tilde{k}}\overline{c}\left(1-\overline{c}\right)$$

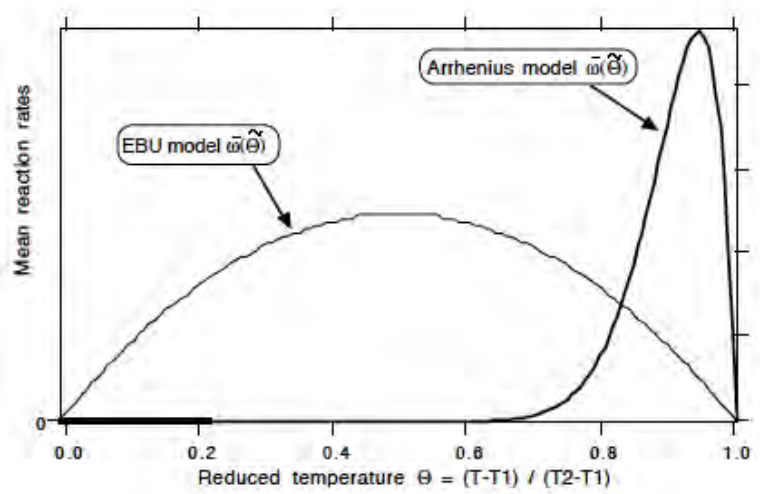

From Veynante & Poinsot (2005)

Note that the EBU expression is recovered if $\tau_f = \delta_L^0 / S_L^0$

Model 3: the flame surface density (FSD) model $\overline{w} = \overline{\rho}_u S_L I_0 \Sigma$

The Flame Surface Density (FSD) Model

Also known as the coherent flamelet model (CFM):

$$\overline{w} = \overline{\rho}_u \left\langle S_c \right\rangle_s \Sigma$$

Σ : Flame surface density (area/volume)

$\left\langle S_c \right\rangle_s$: Average consumption speed per unit flame area

Considering that the flame speed depends on the stretch,

$$\left\langle S_c \right\rangle_s = \int_{-\infty}^{\infty} S_c(\kappa)\, p(\kappa)\, d\kappa$$

The net effect is represented by the “stretch factor”, such that

$$\left\langle S_c \right\rangle_s = S_L^0 I_0$$

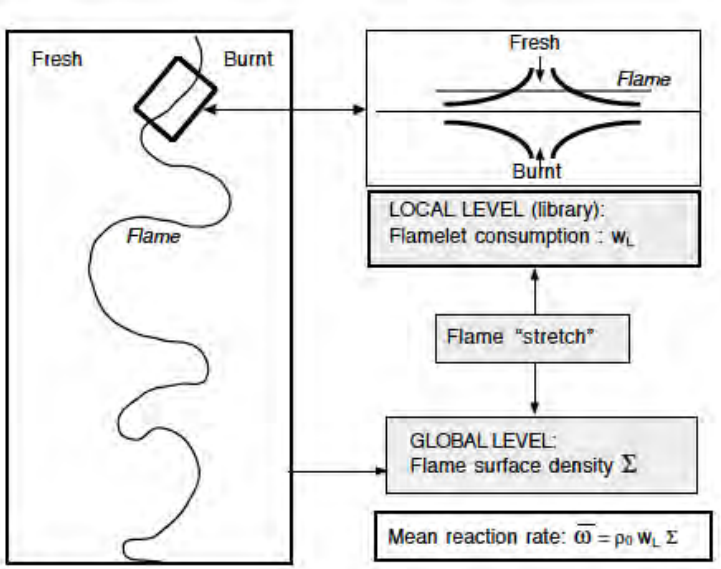

From Veynante & Poinsot (2005)

Algebraic Closure of FSD

Algebraic Closure 1:
Building on the flame crossing idea, the flame surface density can be computed as:

$$\Sigma = \frac{g\overline{c}\left(1-\overline{c}\right)}{L_y\overline{\left|\cos\alpha\right|}}$$

g : Constant

L_y : The flame crossing length scale

α : Crossing angle

$$L_y = C\ell_I\left(\frac{S_L^0}{u'}\right)^n$$

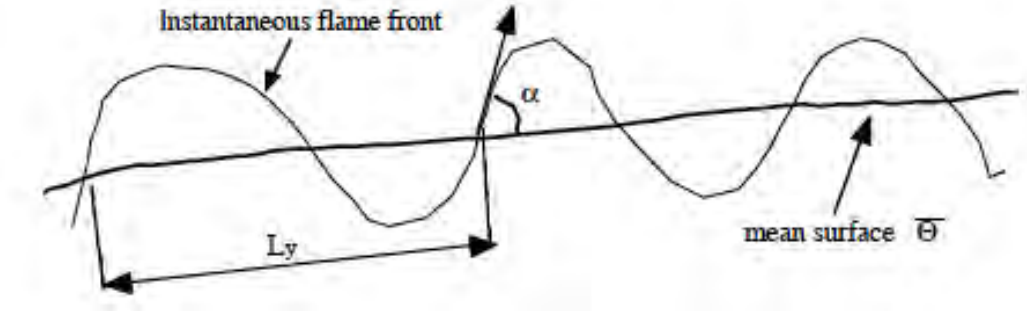

From Veynante & Poinsot (2005)

If assuming $n=1, \left\langle S_c \right\rangle_s = S_L^0$

$$\overline{w} = \overline{\rho}_u \frac{g}{C\overline{\left|\cos\alpha\right|}} \frac{u'}{l_I}\overline{c}\left(1-\overline{c}\right)$$

and a form similar to the BML expressions is recovered.

Algebraic Closure of FSD

Algebraic Closure 2:
Fractal Theory (Gouldin et al., 1987)

$$\Sigma = \frac{1}{L_{outer}} \left(\frac{L_{outer}}{L_{inner}} \right)^{D-2}$$

L_{outer} : outer cut-off scale (= integral scale)

L_{inner} : inner cut-off scale

Peters/Kerstein: Gibson scale

Gülder: Kolmogorov scale.

D : Fractal dimension of the flame surface $(2 < D < 3)$

Kerstein: $D = 7/3$

Gülder et al.: $D < 7/3$

Tanahashi et al.: $D = 2.3 - 2.5$

Hawkes et al.: $D = 8/3$

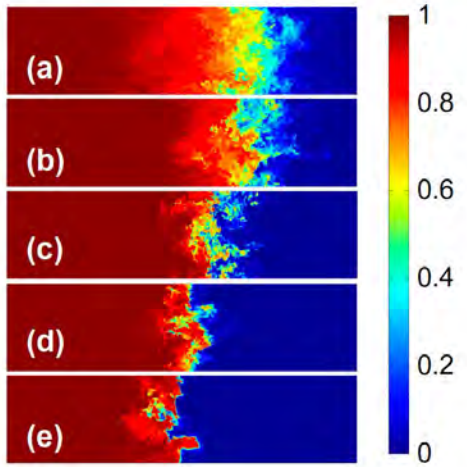

Fig. 10. Contours of mass fraction (12C) for case A (a), case B (b), case C (c), R2 (d) and R3 (e).

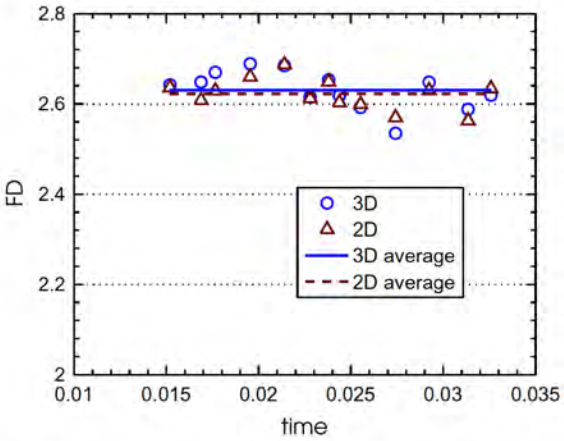

Fig. 12. Comparison of three-dimensional and two-dimensional fractal dimension in the supernovae case C.

Chatakonda, Hawkes et al., CNF (2013)

The FSD Transport Equation

$$\overline{w} = \overline{\rho}_u S_L I_0 \Sigma$$

Σ : Flame surface density (area/volume)

I_0 : Stretch factor (strain, curvature)

After the closure, the FSD transport equation is derived as:

$$\frac{\partial \Sigma}{\partial t} + \frac{\partial (\tilde{u}_j \Sigma)}{\partial x_j} = \frac{\partial}{\partial x_j}\left(D_t \frac{\partial \Sigma}{\partial x_j}\right) + \kappa_m \Sigma + \kappa_t \Sigma - D$$

$\kappa_m \Sigma$: flame generation by mean flow strain

$\kappa_t \Sigma$: flame generation by turbulence

D : flame destruction

Many variants & refinements of the model have been suggested.
(Poinsot & Veynante, *2005*)

Various Closure Models for FSD Transport Equation

MODEL	$\kappa_m\Sigma$	$\kappa_t\Sigma$	D
CPB Cant et al.[85]	$A_{ik}\frac{\partial\widetilde{u}_k}{\partial x_i}\Sigma$	$\alpha_0 C_A\sqrt{\frac{\varepsilon}{\nu}}\Sigma$	$\beta_0\langle s_c\rangle_s\frac{2+e^{-aR}}{3(1-\widetilde{\Theta})}\Sigma^2$ $R=\frac{(1-\widetilde{\Theta})\varepsilon}{\Sigma\langle s_c\rangle_s k}$
CFM1	$A_{ik}\frac{\partial\widetilde{u}_k}{\partial x_i}\Sigma$	$\alpha_0\frac{\varepsilon}{k}\Sigma$	$\beta_0\frac{\langle s_c\rangle_s+C\sqrt{k}}{1-\widetilde{\Theta}}\Sigma^2$
CFM2-a	$A_{ik}\frac{\partial\widetilde{u}_k}{\partial x_i}\Sigma$	$\alpha_0\Gamma_K\frac{\varepsilon}{k}\Sigma$	$\beta_0\frac{\langle s_c\rangle_s+C\sqrt{k}}{1-\widetilde{\Theta}}\Sigma^2$
CFM2-b Duclos et al.[151]	$A_{ik}\frac{\partial\widetilde{u}_k}{\partial x_i}\Sigma$	$\alpha_0\Gamma_K\frac{\varepsilon}{k}\Sigma$	$\beta_0\frac{\langle s_c\rangle_s+C\sqrt{k}}{\widetilde{\Theta}\left(1-\widetilde{\Theta}\right)}\Sigma^2$
CFM3 Veynante et al.[532]	$A_{ik}\frac{\partial\widetilde{u}_k}{\partial x_i}\Sigma$	$\alpha_0\Gamma_K\frac{\varepsilon}{k}\Sigma$	$\beta_0\langle s_c\rangle_s\frac{\Theta^*-\widetilde{\Theta}}{\widetilde{\Theta}\left(1-\widetilde{\Theta}\right)}\Sigma^2$
MB Mantel and Borghi[333]	$E\frac{\widetilde{u_i''u_k''}}{k}\frac{\partial\widetilde{u}_k}{\partial x_i}\Sigma$	$\alpha_0\sqrt{Re_t}\frac{\varepsilon}{k}\Sigma$ $+\frac{F}{\langle s_c\rangle_s}\frac{\varepsilon}{k}\widetilde{u_i''\Theta''}\frac{\partial\widetilde{\Theta}}{\partial x_i}$	$\frac{\beta_0\langle s_c\rangle_s\sqrt{Re_t}\Sigma^2}{\widetilde{\Theta}\left(1-\widetilde{\Theta}\right)\left(1+c\frac{\langle s_c\rangle_s}{\sqrt{k}}\right)^{2\gamma}}$
CD Cheng and Diringer[95]		$\alpha_0\lambda\frac{\varepsilon}{k}\Sigma$ if $\kappa_t\leq\alpha_0 K\frac{\langle s_c\rangle_s}{\delta_L}$	$\beta_0\frac{\langle s_c\rangle_s}{1-\widetilde{\Theta}}\Sigma^2$
CH1		$\alpha_0\sqrt{\frac{\varepsilon}{15\nu}}\Sigma$	$\beta_0\frac{\langle s_c\rangle_s}{\widetilde{\Theta}\left(1-\widetilde{\Theta}\right)}\Sigma^2$
CH2 Choi and Huh[98]		$\alpha_0\frac{u'}{l_{tc}}\Sigma$	$\beta_0\frac{\langle s_c\rangle_s}{\widetilde{\Theta}\left(1-\widetilde{\Theta}\right)}\Sigma^2$

From Veynante & Poinsot (2005)

The Level Set (G-Equation) Model

Flame is represented by an iso-scalar surface

$$G(\mathbf{x},t) = G_0$$

A field equation for *G* can be derived as:

$$\frac{\partial G}{\partial t} + u_j \frac{\partial G}{\partial x_j} = S_L |\nabla G|$$

where the flame speed is a function of strain rate and curvature

$$S_L = S_L^0 - S_L^0 L\kappa - L\sigma$$

κ : curvature

σ : strain rate

L : Markstein length

$$\frac{\partial G}{\partial t} + u_j \frac{\partial G}{\partial x_j} = S_L^0 |\nabla G| - S_L^0 L\kappa |\nabla G| - L\sigma |\nabla G|$$

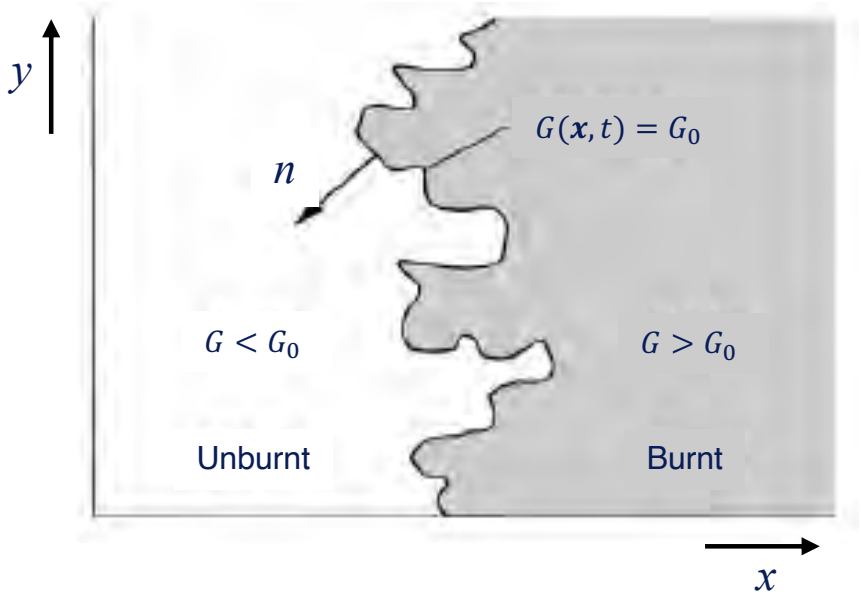

The Level Set in the Thin Reaction Zones Regime

Peters (2001) extended the G-equation model to the thin reaction zone regime.

The location of the inner thin reaction layer is defined by the temperature T^0

and a modified version of the G-equation is derived as:

$$\frac{\partial G}{\partial t} + u_j \frac{\partial G}{\partial x_j} = S_{L,s} \left|\nabla G\right| - D\kappa \left|\nabla G\right|$$

$$S_{L,s} = S_n + S_r = \frac{\mathbf{n} \cdot \nabla\left(\rho D \mathbf{n} \cdot \nabla T\right)}{\rho \left|\nabla T\right|} + \frac{w_T}{\rho \left|\nabla T\right|} \neq S_L^0$$

which implicitly contains the strain effect.

κ : curvature (at the reaction layer)

D : molecular diffusivity (at the reaction layer)

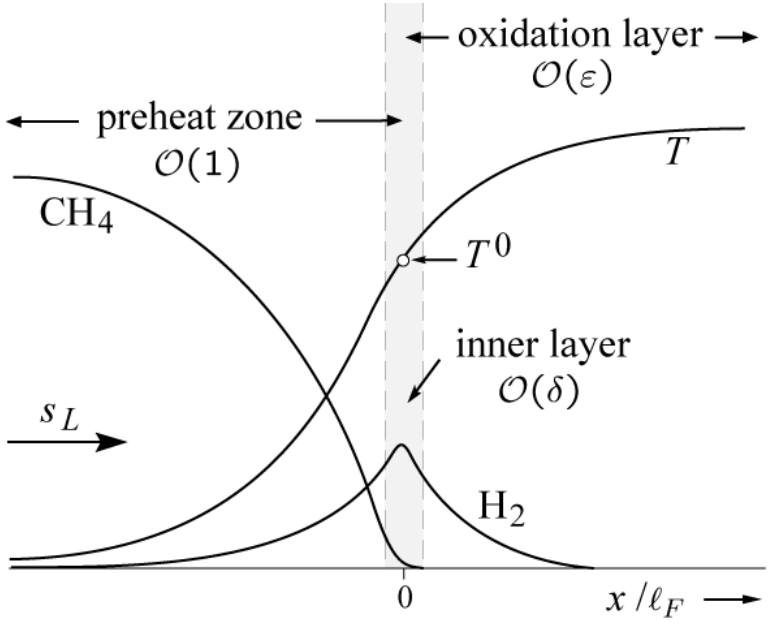

From Peters (2001)

The Level Set Model for Turbulent Combustion

In RANS application, the equations for the Favre mean and variance can be derived as (with some additional assumptions):

$$\bar{\rho}\frac{\partial \tilde{G}}{\partial t}+\bar{\rho}\tilde{u}_j\frac{\partial \tilde{G}}{\partial x_j}+\frac{\partial}{\partial x_j}\left(\bar{\rho}\widetilde{u_j''G''}\right)=\overline{\rho S_d \kappa\left|\nabla G\right|} \qquad \left(S_d=S_L^0-S_L^0 L\kappa-L\sigma\right)$$

Using the gradient transport model

$$\frac{\partial}{\partial x_j}\left(\bar{\rho}\widetilde{u_j''G''}\right)=-\frac{\partial}{\partial x_j}\left(\bar{\rho}D_T\frac{\partial \tilde{G}}{\partial x_j}\right)$$

$$\overline{\rho S_d \kappa\left|\nabla G\right|}=\left(\bar{\rho}S_T\right)\left|\nabla \tilde{G}\right|$$

$$\bar{\rho}\frac{\partial \tilde{G}}{\partial t}+\bar{\rho}\tilde{u}_j\frac{\partial \tilde{G}}{\partial x_j}=\left(\bar{\rho}S_T\right)\left|\nabla \tilde{G}\right|+\frac{\partial}{\partial x_j}\left(\bar{\rho}D_T\frac{\partial \tilde{G}}{\partial x_j}\right)$$

or (depending on the definition of S_T)

$$\bar{\rho}\frac{\partial \tilde{G}}{\partial t}+\bar{\rho}\tilde{u}_j\frac{\partial \tilde{G}}{\partial x_j}=\left(\bar{\rho}S_T\right)\left|\nabla \tilde{G}\right|-\bar{\rho}D_T\bar{\kappa}\left|\nabla \tilde{G}\right|$$

The Level Set Model for Turbulent Combustion

A full closure is obtained if the turbulent burning velocity is determined:

$$\frac{S_T}{S_L^0} = 1 + C\left(\frac{u'}{S_L^0}\right)^n = 1 + C\left(\frac{\sqrt{2k}}{S_L^0}\right)^n$$

Or, a more rigorous determination of the turbulent burning velocity can be made by solving for the higher order variance equation:

$$\bar{\rho}\frac{\partial\widetilde{G''^2}}{\partial t} + \bar{\rho}\tilde{u}_j\frac{\partial\widetilde{G''^2}}{\partial x_j} + \frac{\partial}{\partial x_j}\left(\bar{\rho}\widetilde{u_j''G''^2}\right) = -2\bar{\rho}\widetilde{u_j''G''}\frac{\partial\tilde{G}}{\partial x_j} - \bar{\rho}\tilde{\omega} - \bar{\rho}\tilde{\chi} - \left(\rho D\right)\overline{\kappa\left|\nabla G\right|}$$

with additional closure assumptions such as

$$\tilde{\omega} = -2\left(\rho S_L^0\right)\overline{G''\sigma}/\bar{\rho}, \quad \tilde{\chi} = 2\left(\rho D\right)\left(\widetilde{\nabla G''}\right)^2/\bar{\rho}$$

See Peters (2000) for details.

LES of Premixed Turbulent Combustion

Combustion LES: subgrid models for reaction terms

Unlike turbulence where the subgrid stress terms can be estimated (extrapolated), the subgrid reaction terms must be modeled entirely.

No universal combustion submodels exist. A better strategy is to model combustion processes in different “regimes”.

Note that many combustion submodels are equally applicable to both RANS and LES approaches.

Therefore, many approaches for the RANS combustion closure are applicable to LES.

LES with Filtered G-Equation

For simplicity, consider incompressible G-equation (Im et al., PoF, 1997):

$$\frac{\partial G}{\partial t} + u_j \frac{\partial G}{\partial x_j} = S_L^0 \left|\nabla G\right| + D\nabla^2 G$$

A filtered equation can be derived as:

$$\frac{\partial \bar{G}}{\partial t} + \bar{u}_j \frac{\partial \bar{G}}{\partial x_j} = -\frac{\partial}{\partial x_j}\left(\overline{u_j G} - \bar{u}_j \bar{G}\right) + S_L^0 \overline{\left|\nabla G\right|} + D\nabla^2 \bar{G}$$

where the $\bar{G} = G_0$ front represents the filtered turbulent flame front.

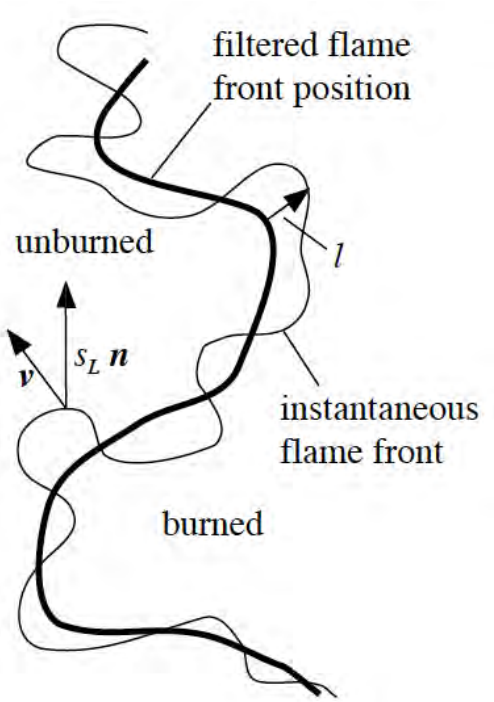

From Pitsch (2002)

Turbulent transport closure: $\overline{u_j G} - \bar{u}_j \bar{G} = -\alpha_t \frac{\partial \bar{G}}{\partial x_i}$

Combustion closure: $S_L^0 \overline{\left|\nabla G\right|} = S_T \left|\nabla \bar{G}\right|$ with $\frac{S_T}{S_L^0} = f\left(\frac{u'}{S_L^0}\right);\ u' = \Delta \left|2\tilde{S}_{ij}\tilde{S}_{ij}\right|^{1/2}$

LES with Flame Surface Density Model

Back to the original transport equation for a progress variable:

$$\frac{\partial \rho c}{\partial t} + \frac{\partial (\rho u_j c)}{\partial x_j} = \frac{\partial}{\partial x_j}(\rho D \frac{\partial c}{\partial x_j}) + w_c = \rho S_d |\nabla c|$$

Applying spatial filters,

$$\frac{\partial \bar{\rho}\bar{c}}{\partial t} + \frac{\partial (\bar{\rho}\tilde{u}_j \tilde{c})}{\partial x_j} = -\frac{\partial}{\partial x_j}\left(\bar{\rho}\widetilde{u_j c} - \bar{\rho}\tilde{u}_j\tilde{c}\right) + \frac{\partial}{\partial x_j}(\overline{\rho D \frac{\partial c}{\partial x_j}}) + \bar{w}_c = \overline{\rho S_d |\nabla c|}$$

Gradient transport model:

$$\widetilde{u_j c} - \tilde{u}_j \tilde{c} = -\frac{\nu_t}{\mathrm{Sc}_k}\frac{\partial \tilde{c}}{\partial x_j}$$

Reaction closure:

$$\overline{\rho S_d |\nabla c|} \simeq \bar{\rho}_u S_L \Sigma = \bar{\rho}_u S_L \Xi |\nabla \bar{c}|$$

Ξ : subgrid scale wrinkling factor $\left(\sim \frac{A_T}{A_L}\right)$

Thickened Flame LES (TFLES)

Considering that the flame speed prediction is the most critical aspects in turbulent combustion, the grid resolution burden can be reduced by artificially thickening the flame at the same speed.

$$\rho\frac{\partial Y_k}{\partial t}+\rho u_j\frac{\partial Y_k}{\partial x_j}=\frac{\partial}{\partial x_j}\left(\rho D_k\frac{\partial Y_k}{\partial x_j}\right)+w_k;\quad \delta_f=\frac{D_k}{S_L}$$

$$\rho\frac{\partial Y_k}{\partial t}+\rho u_j\frac{\partial Y_k}{\partial x_j}=\frac{\partial}{\partial x_j}\left(\rho FD_k\frac{\partial Y_k}{\partial x_j}\right)+\frac{w_k}{F};\quad \delta_f=\frac{FD_k}{S_L}$$

Obviously, the thickened flame does not respond to turbulence exactly like the real think flame. This effect (subgrid scale wrinkling) can be parameterized by the "efficiency function" E

$$\rho\frac{\partial Y_k}{\partial t}+\rho u_j\frac{\partial Y_k}{\partial x_j}=\frac{\partial}{\partial x_j}\left(\rho FD_k\frac{\partial Y_k}{\partial x_j}\right)+\frac{E}{F}w_k\qquad E=\frac{RR_1}{RR_2}=f\left(\frac{u'}{S_L^0},\frac{\delta_{thick}}{\delta_L^0}\right)$$

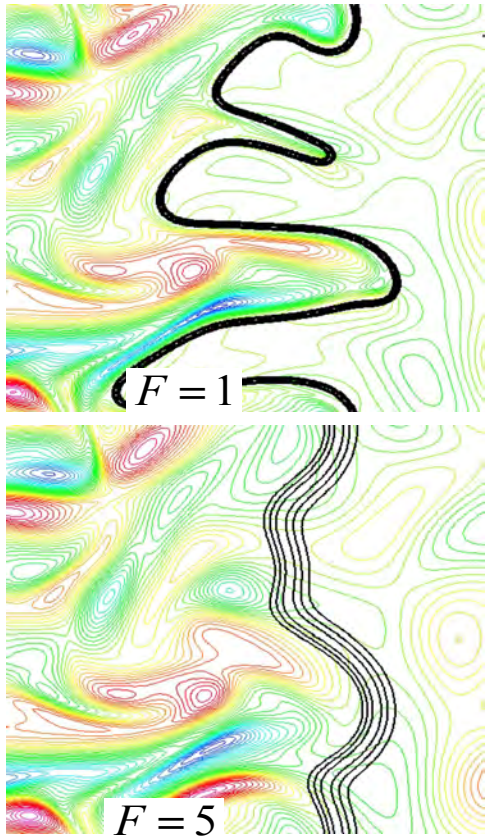

Poinsot & Veynante (2005)

Example: KAUST Natural Gas Pre-Chamber Engine Simulation

- **Research Optical Engine**

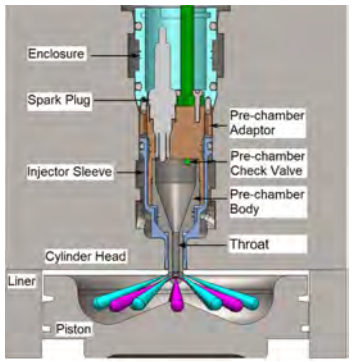

Table. Engine specifications.

Displacement (L)	2.13
CR	11.5:1
Swirl ratio	0
Engine speed (rpm)	1200
IMEP (bar)	~9.0

- **G-Equation and Peters Correlation**

$$S_T = S_L + u'\{-\frac{a_4 {b_3}^2}{2b_1}Da + \left[\left(\frac{a_4 {b_3}^2}{2b_1}Da\right)^2 + a_4 {b_3}^2 Da\right]^{0.5}\}$$

$$Da = \frac{l_T S_L}{u'\delta_L},\ \tau_{flow} = \frac{l_T}{u'},\ \tau_{chem} = \frac{\delta_L}{S_L}$$

- **Real-Fluid EOS and RNG *k*-ε**

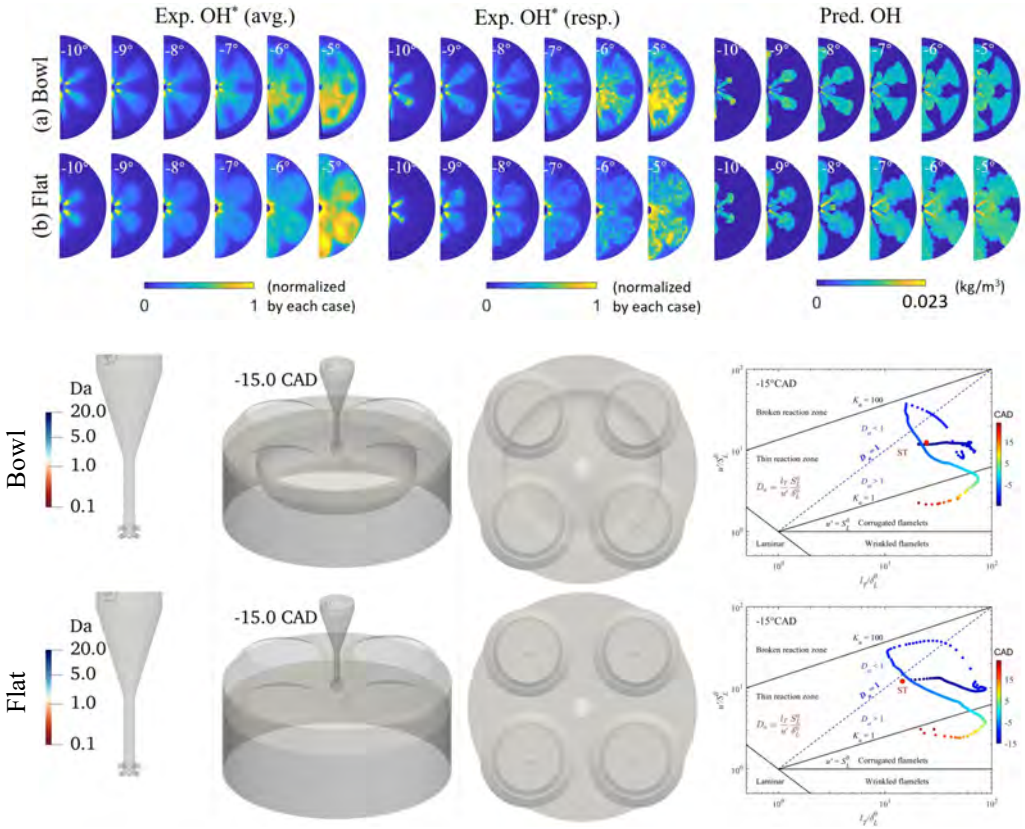

Validations against measurements and predicted flame evoluation characteristics (Liu et al. Fuel 341 (2023) 127659).

Example: KAUST natural gas pre-chamber engine simulation

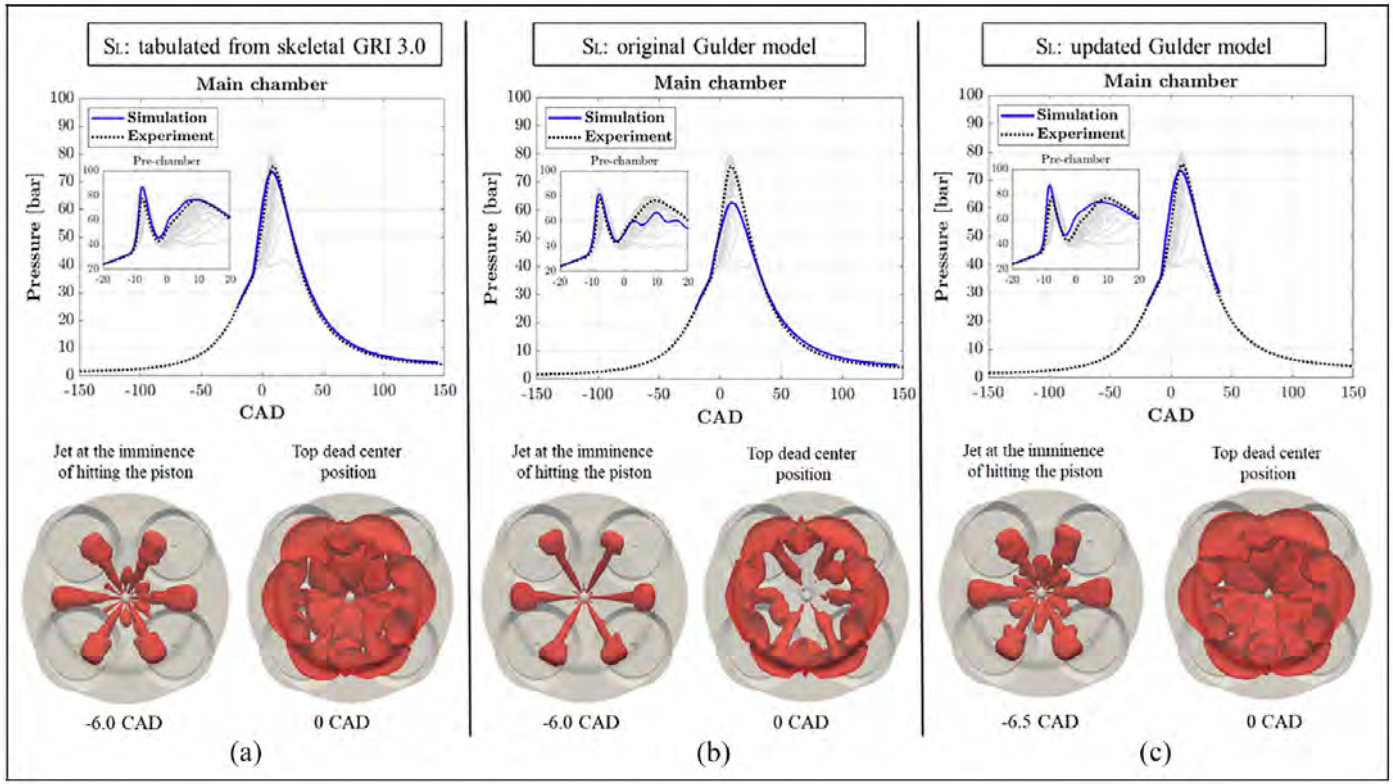

RNG κ-ε model
G-equation model
Turbulent flame speed:

$$S_T = S_L + u' \left\{ -\frac{a_4 {b_3}^2}{2b_1} Da + \left[\left(\frac{a_4 {b_3}^2}{2b_1} Da \right)^2 + a_4 {b_3}^2 Da \right]^{0.5} \right\}$$

A good agreement between the simulation and experiment was obtained by **correcting the prediction of the laminar flame speed**, while maintaining the modeling exponents in Peters's turbulent flame speed correlation representing the turbulence effects.

From Alkhamis et al. (2023)

Laminar Nonpremixed Flames

Conserved Scalar Variable

Outline - Nonpremixed Combustion Modeling

- Mathematical Formulation: Conserved Scalar
- Turbulent Combustion Models
  - Flamelet Model
  - Flamelet-Progress Variable (FPV) Model
  - Conditional Moment Closure
  - Transported PDF Model
  - Filtered Density Function (FDF) Model
  - Partially Stirred Reactor (PaSR) Model

A Conserved Scalar Variable: Concept

- Nonpremixed combustion system can be described by a unique scalar variable (e.g. a S-Z coupling function) that is inert to chemical reactions.

- For example, we can define normalized variables:

$$\zeta_F = \frac{\beta_F - \beta_{F,L}}{\beta_{F,0} - \beta_{F,L}}; \quad \text{or} \quad \zeta_O = \frac{\beta_O - \beta_{O,L}}{\beta_{O,0} - \beta_{O,L}};$$

  such that both vary from 0 (oxidizer side) to 1 (fuel side) monotonically.

- This implies that such a quantity can be used as the independent variable to uniquely describe all thermo-chemical quantities (temperature, species concentrations).

  ⇒ Mixture Fraction Variable

The Mixture Fraction Variable

Definition of the Mixture Fraction Variable: Two-Reactant System

$$\nu'_F[F] + \nu'_O[O_2] \rightarrow [P]$$

$$\nu = \frac{\nu'_O W_{O_2}}{\nu'_F W_F} \quad : \text{stoichiometric ratio}$$

e.g. for $CH_4 + 2O_2 \rightarrow CO_2 + 2H_2O$

$$\nu = \frac{2 \times 32}{16} = 4$$

$$Z = \frac{\nu Y_F - Y_{O_2} + Y_{O_2,2}}{\nu Y_{F,1} + Y_{O_2,2}}$$

At fuel stream, $Y_{O_2} = 0, Y_F = Y_{F,1}; \; Z = 1$

At oxidizer stream, $Y_{O_2} = Y_{O_2,2}, Y_F = 0; \; Z = 0$

At flame, $Y_{O_2} = 0, Y_F = 0;$

$$Z_{st} = \frac{Y_{O_2,2}}{\nu Y_{F,1} + Y_{O_2,2}} = \left[1 + \frac{\nu Y_{F,1}}{Y_{O_2,2}}\right]^{-1}$$

Stoichiometric mixture fraction
(the flame location in the Z space)

Can we extend the concept to a real system with many species/reactions?
What are the quantities that do not change with chemical reaction??

The Bilger Mixture Fraction Variable

Mixture Fraction Variable for a Multicomponent System for C/H/O system (Warnatz, Dibble, Maas, *Combustion*)

Define the elemental mass fraction

$$Z_j = \frac{m_j}{m} = \sum_{i=1}^{N} \frac{a_{ij} W_j}{W_i} Y_i$$

i : species index ($i = 1, \ldots, N$)

j : element index (C, H, O)

e.g. for three species: $CH_4 (i=1), O_2 (i=2), CO_2 (i=3)$ with C($j=1$), H($j=2$), O($j=3$)

$$(a_{ij}) = \begin{pmatrix} 1 & 4 & 0 \\ 0 & 0 & 2 \\ 1 & 0 & 2 \end{pmatrix}$$

Bilger (1988):

Coupling function: $\beta = C_C \frac{Z_C}{W_C} + C_H \frac{Z_H}{W_H} + C_O \frac{Z_O}{W_O}$

$C_C = 2$
$C_H = 1/2$
$C_O = -1$

With normalization: $Z = \frac{\beta - \beta_2}{\beta_1 - \beta_2}$

$$Z = \frac{2Z_C / W_C + 0.5 Z_H / W_H + \left(Z_{O,O} - Z_O\right) / W_O}{2Z_{C,F} / W_C + 0.5 Z_{H,F} / W_H + Z_{O,O} / W_O}$$

The Conserved Scalar Variable – A Unified Coordinate

The Mixture Fraction Variable (Z)

- Conserved through chemical reaction
- Only transported by convection and diffusion
- Monotonically changes through the flame

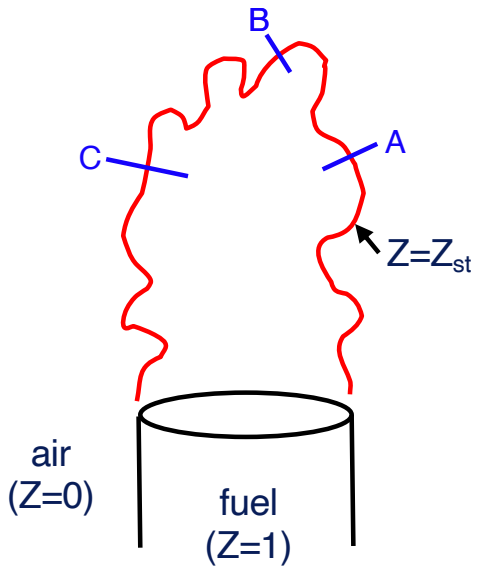

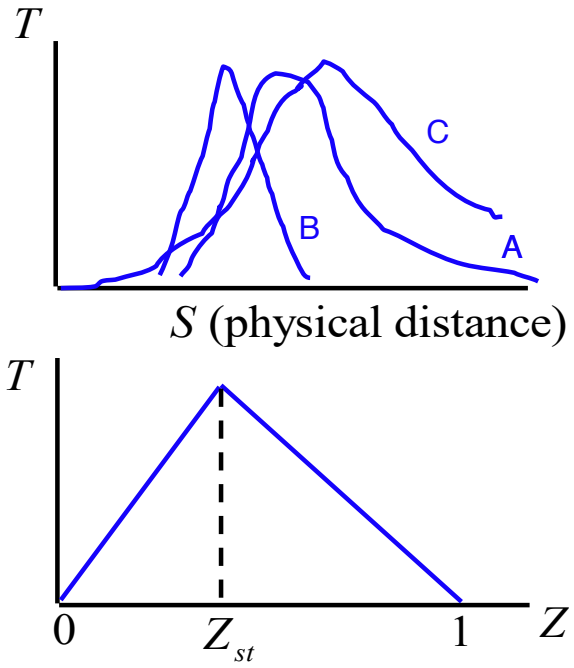

Transport Equation for Mixture Fraction Variable

Now the description of chemical reacting system boils down to determining the mixture fraction variable distribution in space and time.

Derive the transport equations for mixture fraction, temperature and species (Peters, 2000)

$$\rho\frac{\partial Z}{\partial t}+\rho u_j\frac{\partial Z}{\partial x_j}-\frac{\partial}{\partial x_j}\left(\rho D\frac{\partial Z}{\partial x_j}\right)=0$$

$$\rho\frac{\partial T}{\partial t}+\rho u_j\frac{\partial T}{\partial x_j}-\frac{\partial}{\partial x_j}\left(\rho D\frac{\partial T}{\partial x_j}\right)=\sum_{i=1}^{N}w_i\frac{h_i}{c_p}+\frac{\dot{q}}{c_p}+\frac{1}{c_p}\frac{\partial p}{\partial t}$$

$$\rho\frac{\partial Y_i}{\partial t}+\rho u_j\frac{\partial Y_i}{\partial x_j}-\frac{\partial}{\partial x_j}\left(\rho D\frac{\partial Y_i}{\partial x_j}\right)=w_i,\quad i=1,2,\ldots,N$$

With an important assumption:

$$\mathrm{Le}_i=\frac{\lambda}{\rho c_p D_i}=1,\ \text{for all species};\qquad D=\frac{\lambda}{\rho c_p}$$

Transformation of Reactive Scalar Equations

Can we transform the temperature and species equation into the mixture fraction space?

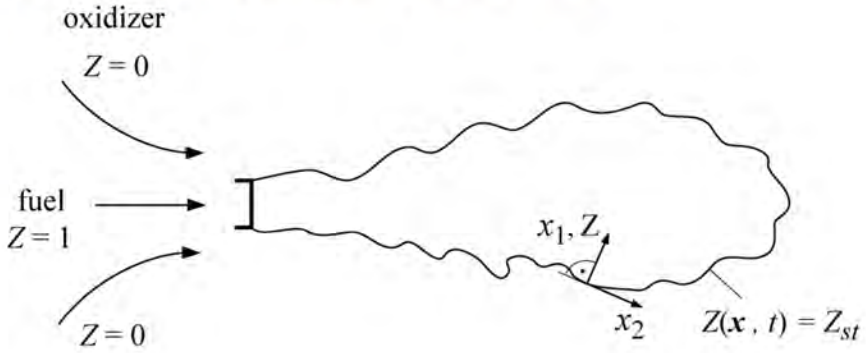

Assume that the flame structure is nearly one-dimensional, i.e. Z is in the direction normal to the flame, and Z_2, Z_3 are the other two normal directions.

Using the chain rule: $(x, y, z, t) \rightarrow (Z, \tau)$, with $\tau = t$

$$\frac{\partial}{\partial t} = \frac{\partial}{\partial \tau}\frac{\partial \tau}{\partial t} + \frac{\partial}{\partial Z}\frac{\partial Z}{\partial t} = \frac{\partial}{\partial \tau} + \frac{\partial Z}{\partial t}\frac{\partial}{\partial Z}$$

$$\frac{\partial}{\partial x} = \frac{\partial}{\partial \tau}\frac{\partial \tau}{\partial x} + \frac{\partial}{\partial Z}\frac{\partial Z}{\partial x} = \frac{\partial Z}{\partial x}\frac{\partial}{\partial Z} \qquad \frac{\partial}{\partial y} = \frac{\partial Z}{\partial y}\frac{\partial}{\partial Z}, \quad \frac{\partial}{\partial z} = \frac{\partial Z}{\partial z}\frac{\partial}{\partial Z}$$

The Flamelet Equation

The transformed species equation becomes (temperature equation can also be derived similarly)

$$\rho\frac{\partial Y_i}{\partial \tau}+\rho u_j\frac{\partial Z}{\partial x_j}\frac{\partial Y_i}{\partial Z}-\left[\left(\frac{\partial Z}{\partial x}\right)^2+\left(\frac{\partial Z}{\partial y}\right)^2+\left(\frac{\partial Z}{\partial y}\right)^2\right]\frac{\partial}{\partial Z}\left(\rho D\frac{\partial Y_i}{\partial Z}\right)$$

$$=\rho\frac{\partial Y_i}{\partial \tau}+\rho u_j\frac{\partial Z}{\partial x_j}\frac{\partial Y_i}{\partial Z}-\left|\nabla Z\right|^2\frac{\partial}{\partial Z}\left(\rho D\frac{\partial Y_i}{\partial Z}\right)=w_i$$

Considering that the steep gradient $\left(\left|\nabla Z\right|^2\right)$ across the flame dominates the flame characteristics, we obtain the "flamelet equation"

$$\rho\frac{\partial Y_i}{\partial \tau}=\left|\nabla Z\right|^2\frac{\partial}{\partial Z}\left(\rho D\frac{\partial Y_i}{\partial Z}\right)+w_i$$

$$\rho\frac{\partial Y_i}{\partial \tau}=\rho\frac{\chi}{2}\frac{\partial^2 Y_i}{\partial Z^2}+w_i \quad \text{if } \left(\rho D\neq f\left(Z\right)\right)$$

$$\chi=2D\left|\nabla Z\right|^2$$ The scalar dissipation rate

The Flamelet Formulation: Summary

In summary, the description of the chemically reacting system can be simplified as:

$$\rho\frac{\partial Z}{\partial t}+\rho u_j\frac{\partial Z}{\partial x_j}-\frac{\partial}{\partial x_j}\left(\rho D\frac{\partial Z}{\partial x_j}\right)=0$$

which is a transport equation for nonreactive scalar in physical space (solved by the CFD code) coupled with the reactive scalar equations in a reduced-dimensional "flamelet" space

$$\rho\frac{\partial Y_i}{\partial \tau}=\rho\frac{\chi}{2}\frac{\partial^2 Y_i}{\partial Z^2}+w_i$$

$$\rho\frac{\partial T}{\partial t}=\rho\frac{\chi}{2}\frac{\partial^2 T}{\partial Z^2}+\sum_{i=1}^{N}w_i\frac{h_i}{c_p}+\frac{\dot{q}}{c_p}+\frac{1}{c_p}\frac{\partial p}{\partial t}$$

where the coupling between the two space is made through the scalar dissipation rate:

$$\chi=2D\left|\nabla Z\right|^2$$

Experimental Results

Does the flamelet approach (reduced-dimensional mapping in the reactive space) work?

Experiment: point measurements of major species concentrations and temperature in a turbulent jet diffusion flame (the Sandia flame)

The data points roughly fall on the curves, but why are the scatters?

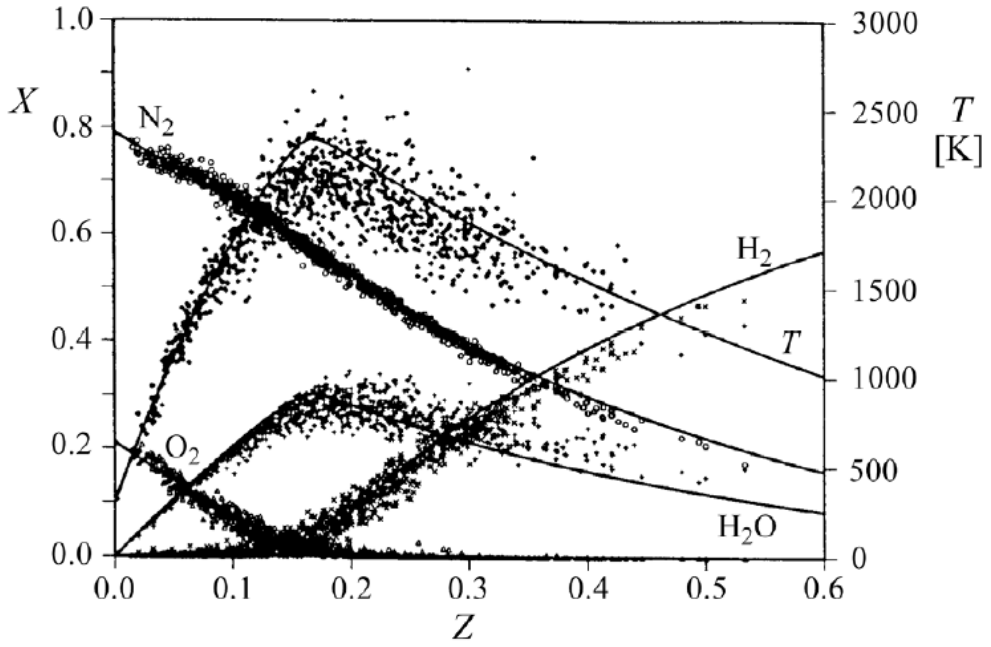

From Barlow et al. (1990)

Strained Laminar Diffusion Flame

Let's examine the flamelet equation in the steady state:

$$\rho\frac{\partial Y_i}{\partial \tau} = 0 = \rho\frac{\chi}{2}\frac{\partial^2 Y_i}{\partial Z^2} + w_i \Rightarrow \frac{\partial^2 Y_i}{\partial Z^2} = -\frac{2}{\rho}\frac{w_i}{\chi}$$

The normalized reaction rate depends on the scalar dissipation rate.

$\chi \to 0$ Infinite chemistry, Burke-Schumann limit, equilibrium

$\chi \to \infty$ No reaction, extinguished (frozen) mixing layer.

$$\chi = 2D\left|\nabla Z\right|^2 \quad [\mathrm{s}^{-1}]$$

Represents the inverse of the mixing/transport (flow residence) time scale.

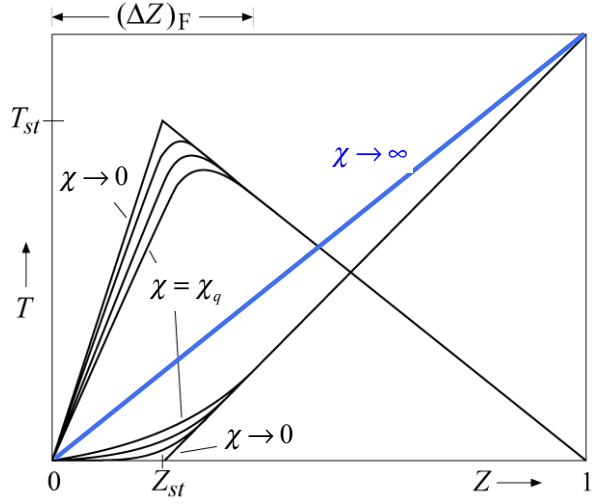

Steady Strained Flamelet Characteristics

The S-Curve Behavior:
Hysteresis between ignition and extinction

- As χ is increased from the frozen limit, the mixture becomes increasingly reactive, and reaches a point at which loss cannot balance generation.
- As χ is decreased from the equilibrium limit, the flame becomes weaker, and reaches a point at which the reaction cannot be sustained.

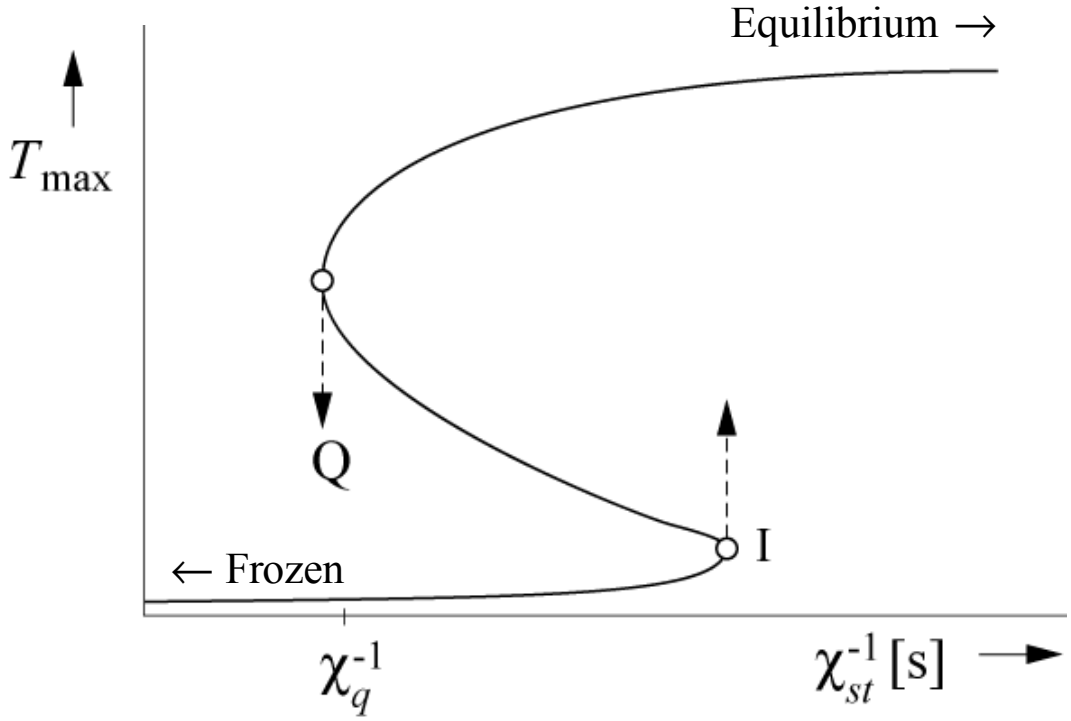

Modeling of Turbulent Nonpremixed Combustion

The Flamelet Approach

The Flamelet Model in Turbulent Combustion

The RANS equation for the mixture fraction becomes

$$\bar{\rho}\frac{\partial \tilde{Z}}{\partial t}+\bar{\rho}\tilde{\mathbf{u}}\cdot\nabla\tilde{Z}=\nabla\cdot\left(\cancel{\overline{\rho D\nabla Z}}-\bar{\rho}\widetilde{u''Z''}\right)$$

negligible

with the gradient transport closure:

$$\widetilde{u''Z''}=-D_t\nabla\tilde{Z}$$

The variance equation is also needed to close the flamelet equation:

$$\bar{\rho}\frac{\partial \widetilde{Z''^2}}{\partial t}+\bar{\rho}\tilde{\mathbf{u}}\cdot\nabla\widetilde{Z''^2}=-\nabla\cdot\left(\bar{\rho}\widetilde{u''Z''^2}\right)+2\bar{\rho}D_t\left(\nabla\tilde{Z}\right)^2-\bar{\rho}\tilde{\chi}$$

with the closure:

$$\widetilde{u''Z''^2}=-D_t\nabla\widetilde{Z''^2}$$

$$\tilde{\chi}=c_\chi\frac{\tilde{\varepsilon}}{\tilde{k}}\widetilde{Z''^2};\quad c_\chi\simeq 2.0$$

The Flamelet Equation in Turbulent Combustion

The DNS flamelet equation

$$\rho \frac{\partial \psi_i}{\partial t} = \frac{\rho \chi}{2} \frac{\partial^2 \psi_i}{\partial Z^2} + w_i$$

is extended to turbulent flow simulations by adopting the concept of "representative flamelets", where a single flamelet equation represents all reactive scalar evolution.

In the statistical average, this is approximated by:

$$\rho \frac{\partial \psi_i}{\partial t} = \frac{\rho \tilde{\chi}_Z}{2} \frac{\partial^2 \psi_i}{\partial Z^2} + w_i$$

where $\tilde{\chi}_Z = \langle \rho \chi \,|\, Z \rangle / \langle \rho \,|\, Z \rangle$ is the conditional Favre-mean over Z, and must be modelled.

The solution to the equation yields

$$\psi_i \left(Z, \tilde{\chi}_Z, t \right)$$

Determining Reactive Scalar Variables

The statistical moments of reactive scalars are computed by

$$\tilde{\psi}_i(\mathbf{x},t) = \int_0^1 \psi_i\left(Z,\tilde{\chi}_Z,t\right)\tilde{P}(Z;\mathbf{x},t)dZ$$

with a number of underlying assumptions (Peters, 2000)

The presumed PDF is defined using the β-function

$$\tilde{P}(Z;\mathbf{x},t) = \frac{Z^{\alpha-1}(1-Z)^{\beta-1}}{\Gamma(\alpha)\Gamma(\beta)}\Gamma(\alpha+\beta)$$

$$\alpha = \tilde{Z}\gamma, \quad \beta = (1-\tilde{Z})\gamma$$

$$\gamma = \frac{\tilde{Z}(1-\tilde{Z})}{\widetilde{Z''^2}} - 1 \geq 0$$

In the limit of $\widetilde{Z''^2} \to 0 \left(\gamma \to \infty\right)$, the PDF approaches a Gaussian distribution.

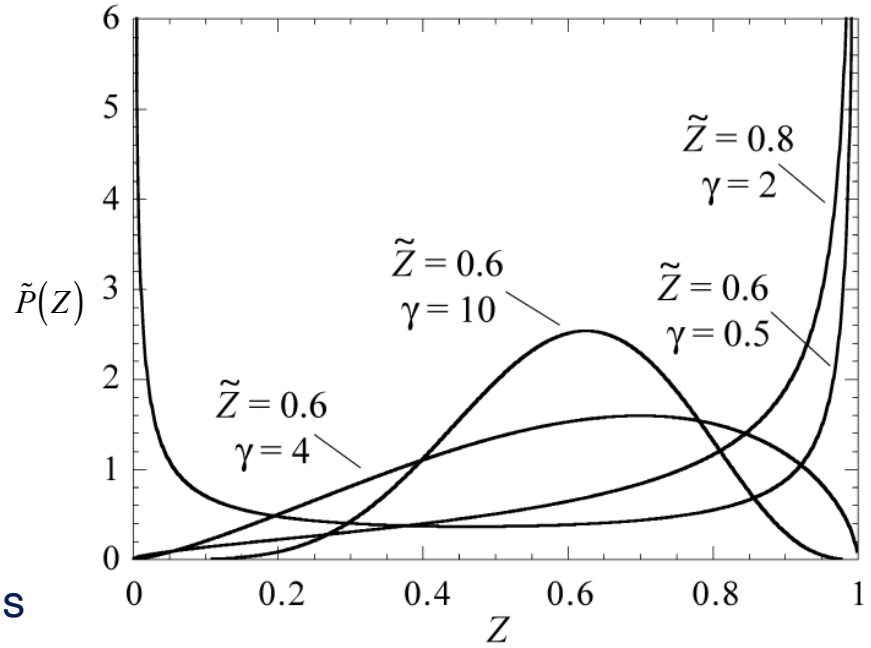

Unsteady Flamelet Model (Representative Interactive Flamelet)

Determining $\psi_i\left(Z,t;\tilde{\chi}_Z\right)$ is done by solving the unsteady flamelet equation:

$$\rho\frac{\partial\psi_i}{\partial t}=\frac{\rho}{\mathrm{Le}_i}\frac{\tilde{\chi}_Z}{2}\frac{\partial^2\psi_i}{\partial Z^2}+w_i$$

$$\tilde{\chi}_Z=\frac{\left\langle\rho\chi\,|\,Z\right\rangle}{\left\langle\rho\,|\,Z\right\rangle}$$ Conditional Favre-mean scalar dissipation rate

Modeling $\tilde{\chi}_Z$

$$\tilde{\chi}_Z=\tilde{\chi}_{st}\frac{f\left(Z\right)}{f\left(Z_{st}\right)}\qquad \text{e.g. } f\left(Z\right)=\exp\left(-2\left[\mathrm{erfc}^{-1}\left(2Z\right)\right]^2\right)$$

$$\Rightarrow\ \tilde{\chi}=\int_0^1\tilde{\chi}_Z\tilde{P}\left(Z\right)dZ=\tilde{\chi}_{st}\int_0^1\frac{f\left(Z\right)}{f\left(Z_{st}\right)}\tilde{P}\left(Z\right)dZ$$

$$\tilde{\chi}_{st}=\frac{\tilde{\chi}f\left(Z_{st}\right)}{\int_0^1 f\left(Z\right)\tilde{P}\left(Z\right)dZ}$$

Steady Flamelet Model

1. Assuming infinite chemistry, $\psi_i\left(Z,t;\tilde{\chi}_Z\right)=\psi_i\left(Z\right)$ only

$$\Rightarrow \tilde{\psi}_i\left(\mathbf{x},t\right)=\int_0^1 \psi_i\left(Z\right)\tilde{P}\left(Z;\mathbf{x},t\right)dZ$$

Problem closed with the prescribed beta-PDF function.

2. To accommodate finite-rate chemistry, $\psi_i\left(Z;\tilde{\chi}_Z\right)=\psi_i\left(Z;\chi_{st}\right)$ are solved by the steady laminar flamelet equation:

$$\frac{\rho}{\mathrm{Le}_i}\frac{\tilde{\chi}_Z}{2}\frac{\partial^2\psi_i}{\partial Z^2}=-w_i$$

$$\tilde{\chi}_Z=\tilde{\chi}_{st}f\left(Z\right)/f\left(Z_{st}\right) \qquad \text{prescribed}$$

The equation can be solved once and for all, and tabulated.
(Flamelet Library)

Flamelet Modeling Procedure

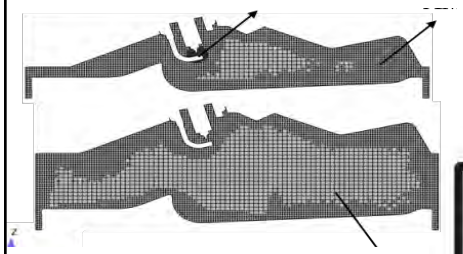

$$\tilde{P}(Z;\mathbf{x},t)=\frac{Z^{\alpha-1}(1-Z)^{\beta-1}}{\Gamma(\alpha)\Gamma(\beta)}\Gamma(\alpha+\beta)\quad \alpha,\beta,\gamma=f\left(\tilde{Z},\widetilde{Z''^2}\right)$$

$$\bar{\rho}\frac{\partial\tilde{Z}}{\partial t}+\bar{\rho}\tilde{\mathbf{u}}\cdot\nabla\tilde{Z}=-\nabla\cdot\left(\bar{\rho}\widetilde{u''Z''}\right)$$

$$\bar{\rho}\frac{\partial\widetilde{Z''^2}}{\partial t}+\bar{\rho}\tilde{\mathbf{u}}\cdot\nabla\widetilde{Z''^2}$$

$$=-\nabla\cdot\left(\bar{\rho}\widetilde{u''Z''^2}\right)+2\bar{\rho}D_t\left(\nabla\tilde{Z}\right)^2-\bar{\rho}\tilde{\chi}$$

$$\tilde{\chi}=2.0\frac{\tilde{\varepsilon}}{\tilde{k}}\widetilde{Z''^2}$$

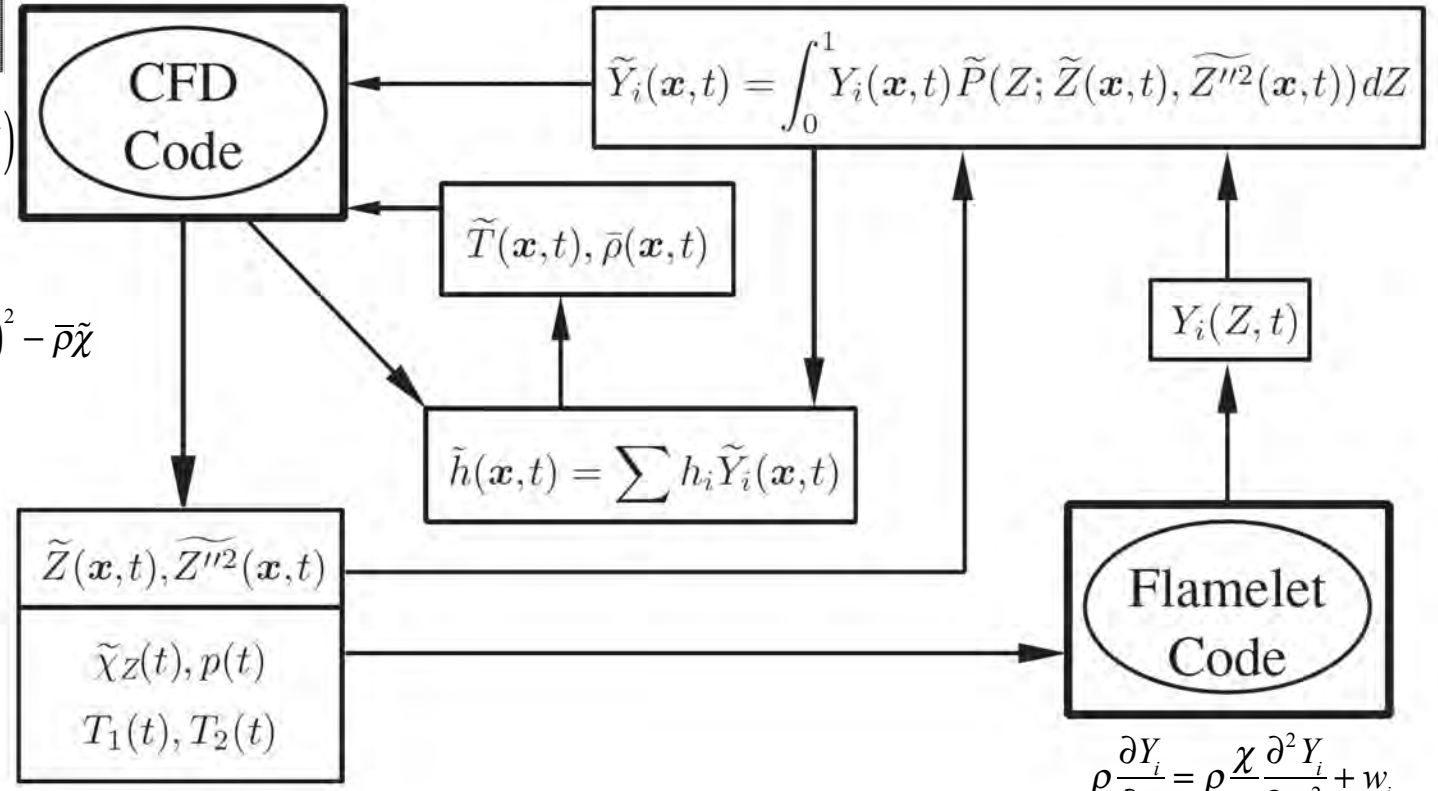

$$\rho\frac{\partial Y_i}{\partial\tau}=\rho\frac{\chi}{2}\frac{\partial^2 Y_i}{\partial Z^2}+w_i$$

Peters (2000)

or tabulate

The Flamelet Model for LES

- Most of the RANS flamelet modeling framework can be adapted to LES.
- The only difference is that the PDF only represents the subgrid fluctuations.
- For example, for infinitely fast chemistry,

$$\tilde{\psi}_i(\mathbf{x},t) = \int_V \int_0^1 \psi_i(\zeta)\delta\left(Z(\mathbf{x})-\zeta\right)F(\mathbf{x}-\mathbf{z})\,d\zeta\,d\mathbf{z}$$

$$= \int_0^1 \psi_i(\zeta)\int_V \delta\left(Z(\mathbf{x})-\zeta\right)F(\mathbf{x}-\mathbf{z})\,d\mathbf{z}\,d\zeta$$

Filtered PDF of Z

- Subgrid mixing model (Pierce & Moin, 2004)

$$\overline{\rho}\widetilde{Z''^2} = C_Z\overline{\rho}\Delta^2\left|\nabla\tilde{Z}\right|^2$$

$$\overline{\rho}\tilde{\chi} = \overline{\rho}\left(D+D_t\right)\left|\nabla\tilde{Z}\right|^2$$

Example: Turbulent Hydrogen-Air Diffusion Flame

Unsteady flamelet approach (solid line) vs. steady flamelet library (dashed line)

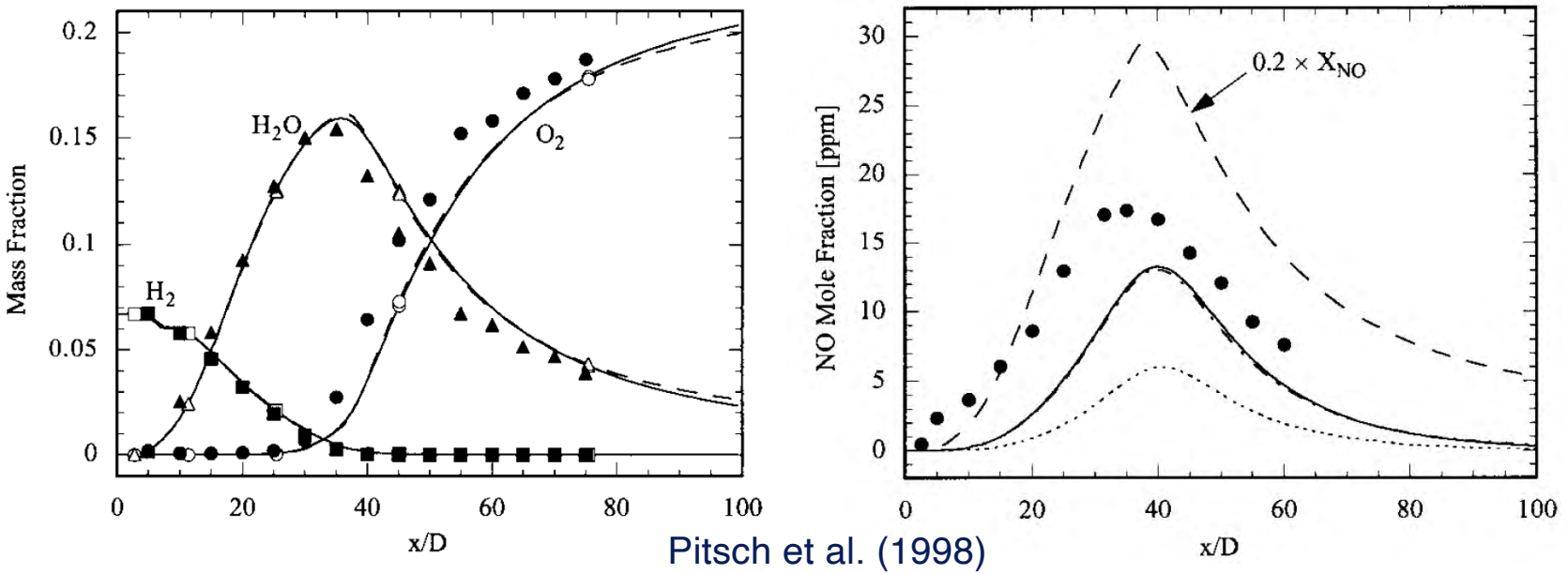

Pitsch et al. (1998)

- Transient effects can be neglected for predictions of heat release, concentrations of major chemical components, and even the OH concentrations.
- Compared to steady flamelet model, unsteady flamelet model better capture the slow formation processes, such as the NO formation.

Flamelet/Progress Variable (FPV) Model

Steady Flamelet Model only considers the solutions of fully burning or fully extinguished.

An alternative approach based on the progress variable, rather than the scalar dissipation rate, allows for consideration of the unstable branch of the S-shaped curve. (Pierce & Moin, 2004).

$$\frac{\partial\left(\bar{\rho}\tilde{c}\right)}{\partial t}+\nabla\cdot\left(\bar{\rho}\tilde{\mathbf{u}}\tilde{c}\right)=\nabla\cdot\left(\bar{\rho}D_t\nabla\tilde{c}\right)+\tilde{w}_c$$

and the mean reactive scalar variables are determined by:

$$\tilde{\psi}_i\left(\mathbf{x},t\right)=\int_0^1\int_0^1\psi_i\left(Z,c\right)\tilde{P}\left(Z,c\right)dZdc$$

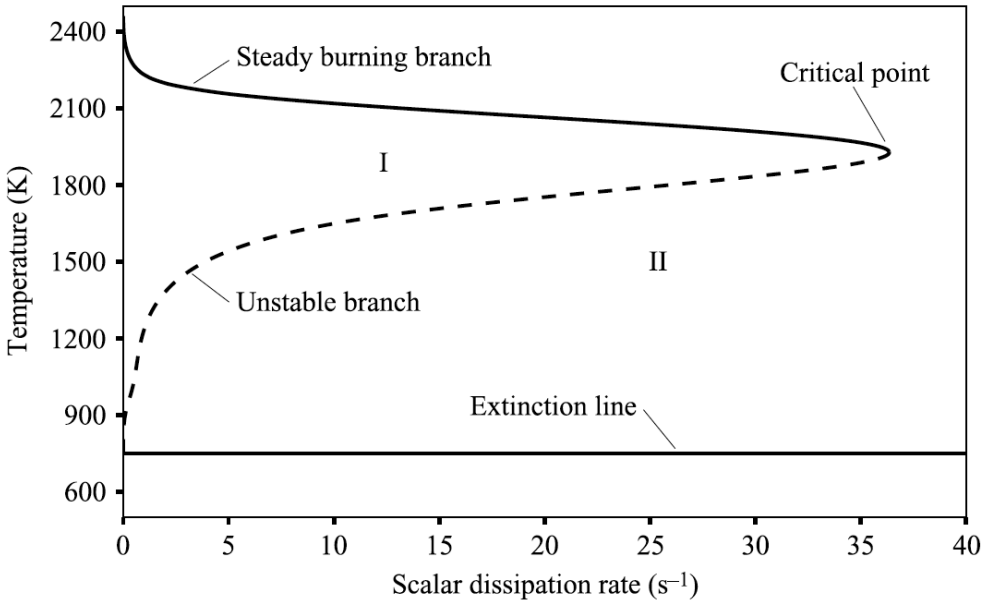

Presumed PDF for FPV Approach

The mean reactive scalar variables are determined by:

$$\tilde{\psi}_i(\mathbf{x},t) = \int_0^1 \int_0^1 \psi_i(Z,c)\,\tilde{P}(Z,c)\,dZdc$$

with the assumption that Z and c are independent in the joint PDF:

$$\tilde{P}(Z,c) = \tilde{P}(c \mid Z)\,\tilde{F}(Z)$$

Z : Beta PDF

c :

- Delta PDF = Simplicity
- Beta PDF: need modeling or transporting c variance
- Statistically most likely distribution (SMLD) (Ihme & Pitsch, CNF, 2008)

Example: Methane Coaxial Jet Combustor

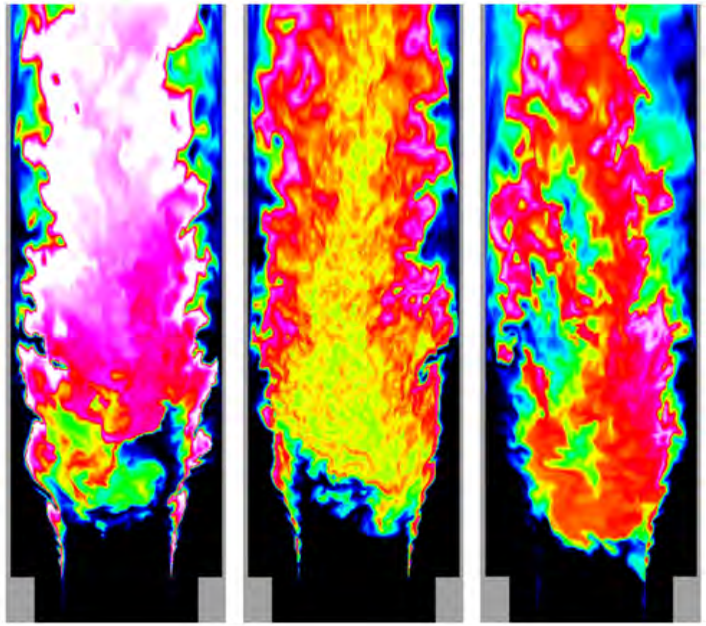

fast-chemistry steady-flamelets FPV

Pierce & Moin, 2004

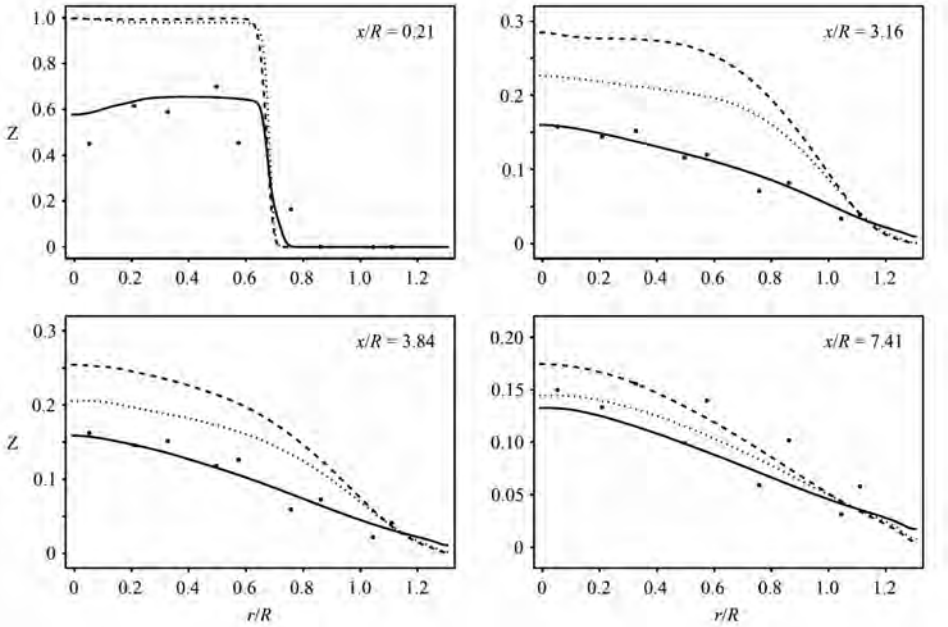

FIGURE 8. Radial profiles of time-averaged mixture fraction: ----, fast-chemistry; ·····, steady-flamelets; ——, progress-variable approach; •, experiment.

- The FPV model better captures basic flame behaviour such as flame lift-off, compared to the other two models.
- However, the FPV model cannot accurately predict details of the combustion process such as pollutant formation and thermal radiation.

Example: KAUST Piloted $NH_3/H_2/N_2$-air flame

Focus on local extinction and reignition Re = 36,000 (89% of the blow-off limit)

Transport $\tilde{Z}$, $\widetilde{Z''^2}$, $\tilde{C}$

PDF:
Mixture Fraction : Beta
Flamelet Parameter: Delta

KAUST Piloted
$NH_3/H_2/N_2$-air flame

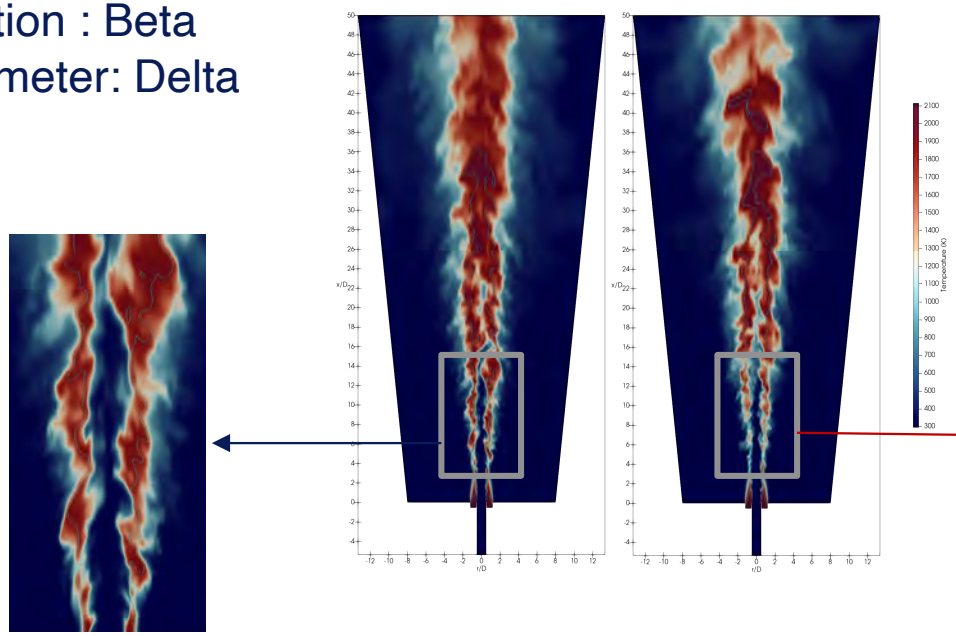

Transport $\tilde{Z}$, $\widetilde{Z''^2}$, $\tilde{C}$, $\widetilde{C''^2}$

PDF:
Mixture Fraction : Beta
Flamelet Parameter: **Beta**

Extinction not captured properly

Extinction captured

Example: KAUST Piloted $NH_3/H_2/N_2$-air flame (continue)

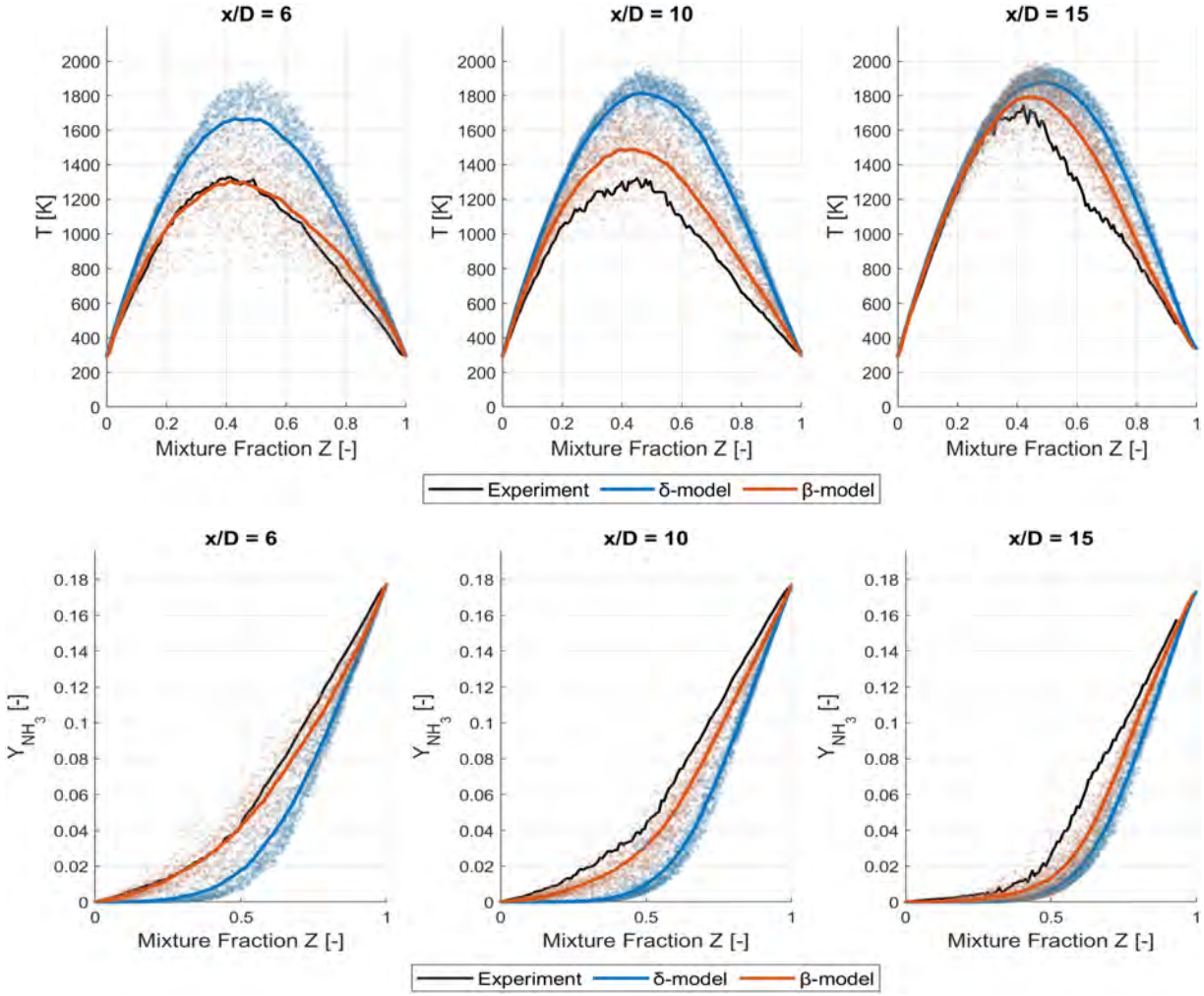

- FPV with beta-PDF for progress variable improves the predictions of extinction and re-ignition

Afzal et al., 2025

Flamelet Modeling Incorporating Differential Diffusion

Standard flamelet equation used unity Lewis number assumption.

A generalized flamelet equation with non-unity Lewis number (Pitsch & Peters, 1998)

By assuming unity mixture fraction Lewis number, constant but non-unity species Lewis numbers, constant ρD_Z, and constant molecular weight of the mixture, simplified flamelet equation was obtained:

$$\rho \frac{\partial Y_i}{\partial \tau} - \frac{\rho\chi}{2\mathrm{Le}_i} \frac{\partial^2 Y_i}{\partial Z^2} - \dot{m}_i + \frac{1}{4}\left(1 - \frac{1}{\mathrm{Le}_i}\right) \cdot \frac{\partial \rho\chi}{\partial Z} \frac{\partial Y_i}{\partial Z} = 0.$$

Linear Blending of Equi-Diffusion and Differential Diffusion

The effect of differential molecular diffusion is inversely proportional to *Re* approximately (Bilger, 1982)

In the limit of low Re flames, e.g., a laminar condition, the differential molecular diffusion is fully described by multi-component diffusion.

At the other limit where the Re becomes infinitely large, turbulence control the diffusion process and the effect of molecular diffusion vanishes

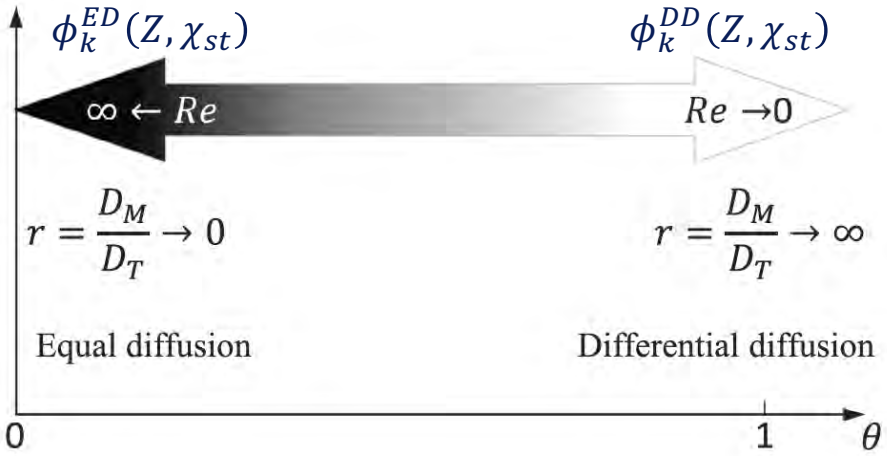

Limiting behaviors

A linear blending of the flamelet models at the two limits is used to approximate the level of differential molecular diffusion (Wang, 2016)

$$\phi_k = [1-\theta]\phi_k^{ED}(Z,\chi_{st}) + \theta\ \phi_k^{DD}(Z,\chi_{st})$$

Blending Parameter

Determining the degree of differential molecular diffusion parameter θ

$$\theta = \frac{D_M}{D_M + D_T}$$ Wang (2016)

$$D_T \propto ul \qquad \begin{aligned} u &\sim k^{1/2} \\ l &\sim k^{3/2}/\varepsilon \end{aligned}$$

- D_M is a arbitrary molecular diffusivity, and unity Lewis number is suggested.
- D_T is turbulent diffusivity, which is determined by the k and ε in RANS framework, but is not straightforward in LES simulations.

Species-Weighted Flamelet Model

An alternative method was proposed to calculate the weighting factor θ for LES applications (Jiang et al., 2023)

Some major species transport equations are directly solved in the LES simulations, and then the θ is determined by the differences between the transported species and the species retrieved from ED and DD look-up tables.

$$\theta(\boldsymbol{x},t)=\frac{1}{N_{sp}}\sum_{j}^{N_{sp}}\left(\frac{Y_{j,CFD}(\boldsymbol{x},t)-Y_{j,ED}(Z''^2,Z_{Bilger},C)}{Y_{j,DD}(Z''^2,Z_{Bilger},C)-Y_{j,ED}(Z''^2,Z_{Bilger},C)}\right)$$

The subscript *j* denotes major species.

Example: KAUST Partially Cracked Ammonia Flames

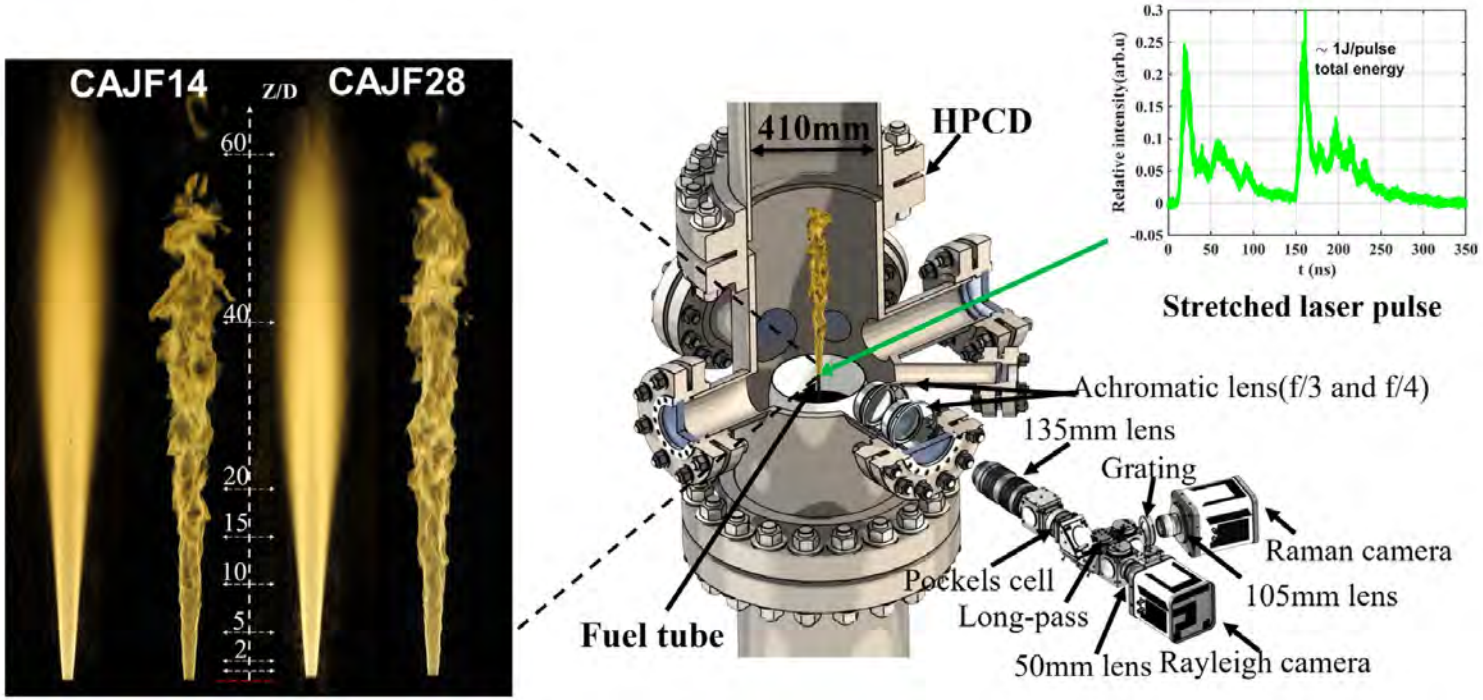

Flame cases	NH_3	H_2	N_2	U_f [m/s]	U_{co} [m/s]	Re
TF1 (CAJF14)	0.8538	0.0282	0.1180	9.13	0.24	11,864
TF2 (CAJF28)	0.7051	0.0534	0.2415	11.56	0.24	12,571

1D Raman spectroscopy measurements of temperature, major species mass fractions, and mixture fraction.

Example: KAUST Partially Cracked Ammonia Flames

Diff-Diff parameter:

$$\delta_Z = Z_H - Z_N$$

$$Z_i = \frac{Y_i - Y_{i,2}}{Y_{i,1} - Y_{i,2}}$$

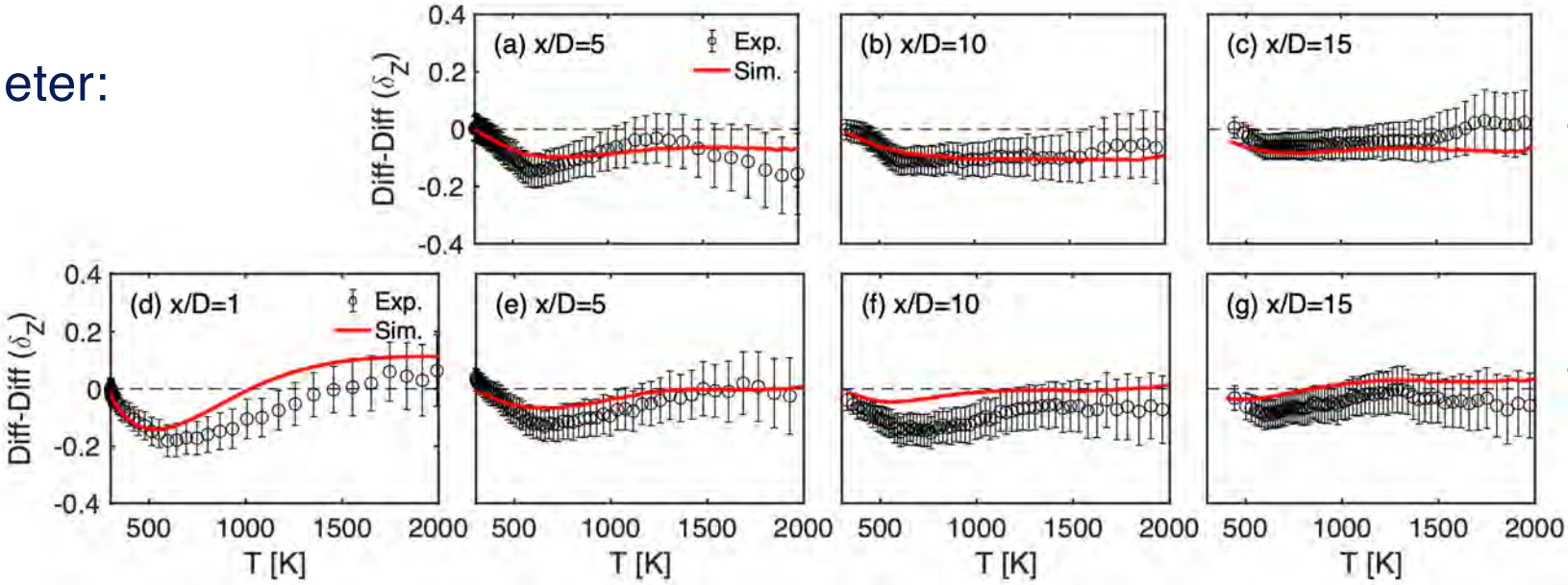

- Species-weighted FPV (SWF) model quantitatively captures the **differential diffusion** parameter in the near field.

Guo et al, 2024

Example: KAUST Partially Cracked Ammonia Flames

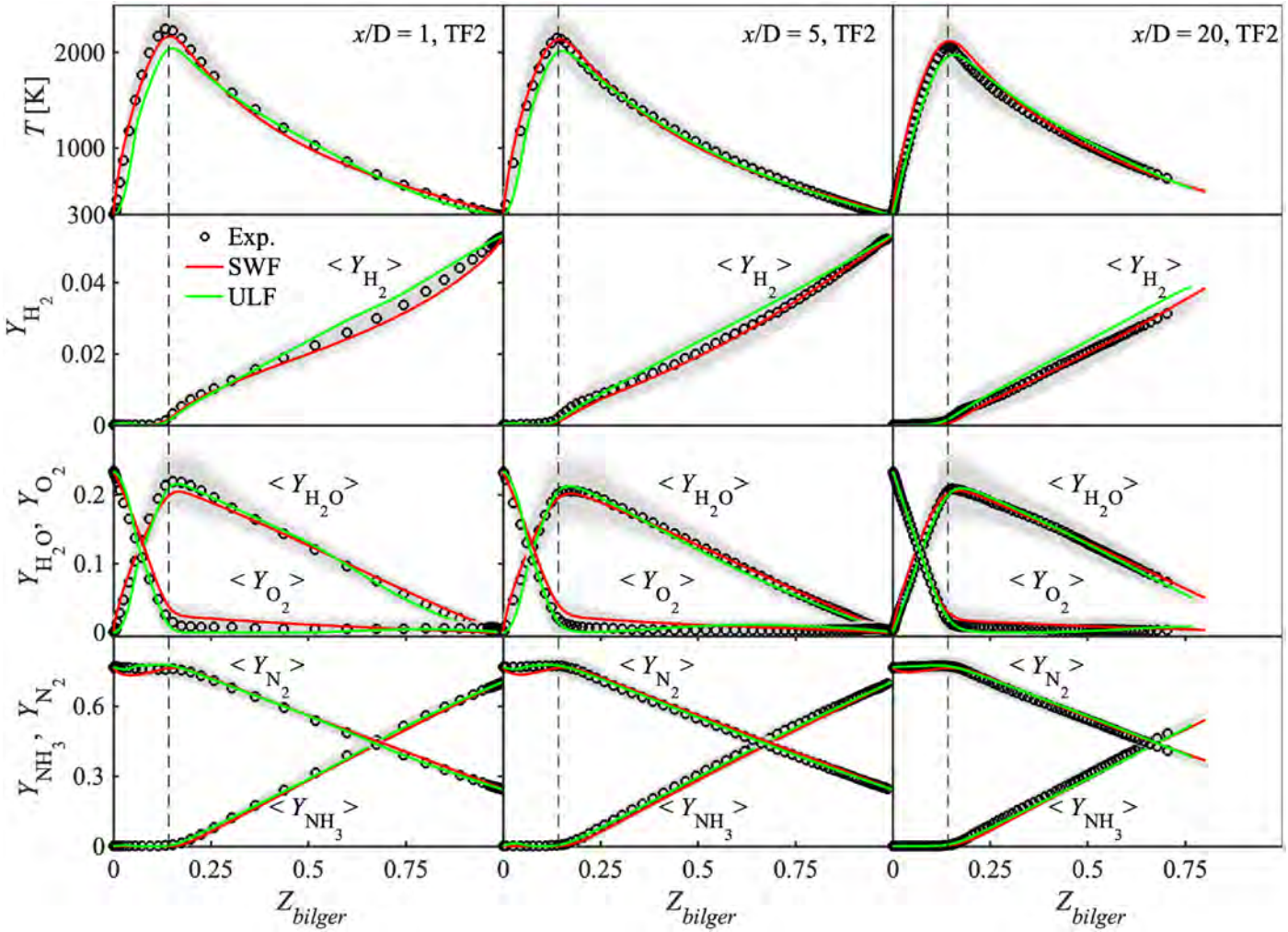

- SWF model with differential diffusion provides higher temperature than unity Lewis number flamelet model (ULF), aligning better with the experimental data.
- SWF model captures the faster diffusion of H_2.

Guo et al, 2024

Modeling of Turbulent Nonpremixed Combustion

Other Approaches

The Conditional Moment Closure (CMC)

Klimenko (1990) and Bilger (1993) suggested an alternative reaction term closure by conditionally averaging reactive scalars on the mixture fraction.

Define the conditional PDF:

$$P\left(\psi_i \mid Z;\mathbf{x},t\right)=\frac{P\left(\psi_i \mid Z;\mathbf{x},t\right)}{P\left(Z;\mathbf{x},t\right)}$$

The first conditional moment:

$$Q_i\left(Z;\mathbf{x},t\right)=\left\langle\tilde{\psi}_i \mid Z\right\rangle=\int_0^1 \psi_i P\left(\psi_i \mid Z;\mathbf{x},t\right)d\psi_i$$

subjected to the transport equation:

$$\left\langle\rho \mid Z\right\rangle\frac{\partial Q_i}{\partial t}+\left\langle\rho \mid Z\right\rangle\left\langle\tilde{\mathbf{u}}_Z \mid Z\right\rangle\cdot\nabla Q_i=\left\langle\rho \mid Z\right\rangle\left\langle\tilde{\chi}_Z \mid Z\right\rangle\frac{\partial^2 Q_i}{\partial Z^2}+\left\langle w_i \mid Z\right\rangle$$

unclosed

with the important assumption: $\left\langle w_i \mid Z\right\rangle \simeq w_i\left(\left\langle\psi_i \mid Z\right\rangle\right)$

The first-order closure

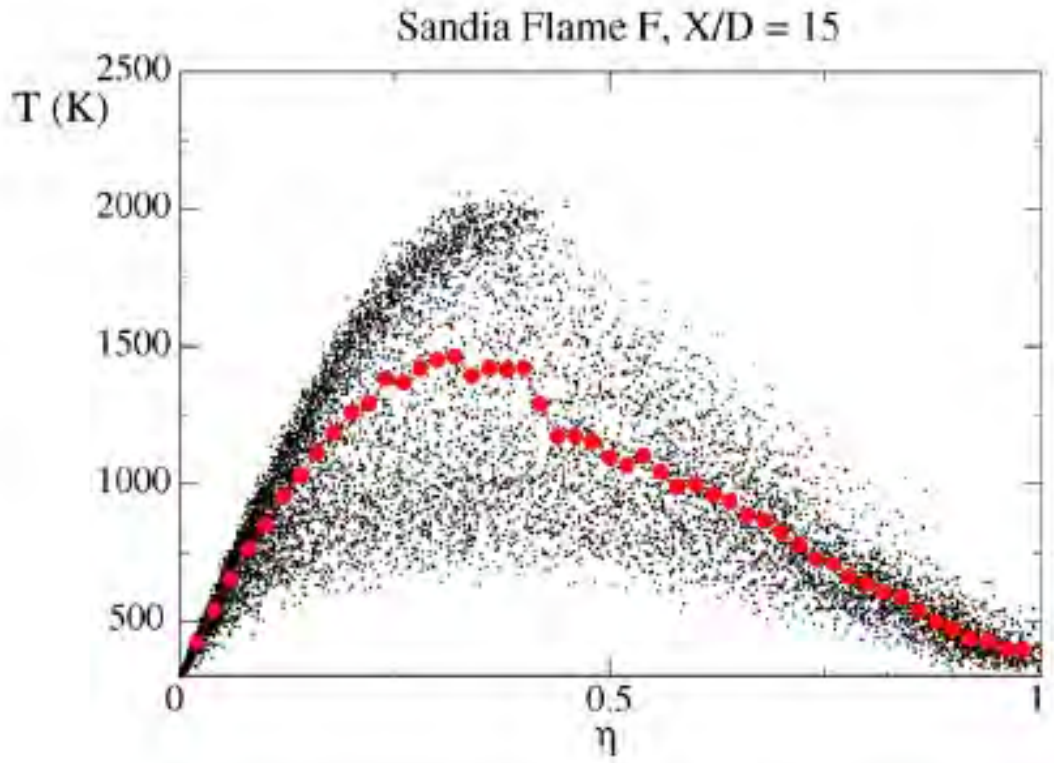

Fig. 5.1: Measurements of temperature as function of mixture fraction in a piloted methane-air jet diffusion flame with significant local extinction and re-ignition (Sandia Flame F). The filled symbols indicate the conditional mean of temperature, $Q_T = \langle T \mid \eta \rangle$. Reprinted from [19] with permission from the Combustion Institute.

From Frank et al. (2000)

CMC – Closure Issues

- Conditional velocity: $\tilde{\mathbf{u}}_Z = \langle \rho \mathbf{u} \,|\, Z \rangle$
  - Conditional independence
  - Linear in terms of unconditional flux
  - Gradient diffusion in terms of local pdf
- Conditional scalar dissipation rate: $\tilde{\chi}_Z = \langle \rho \chi \,|\, Z \rangle$
  - Amplitude mapping closure (AMC) (O'Brien et al.; Girimaji, et al.)
  - Double integration of the pdf transport equation (Bilger et al.)
- First order reaction closure: $\langle w_i \,|\, Z \rangle \simeq w_i\left(\langle \psi_i \,|\, Z \rangle\right)$
  - The CMC equation remains valid even if fluctuations are large
  - The quantitative accuracy degrades and needs to be improved

    Second order closures

    Doubly-conditioned moment closures

The Transported PDF Equation Model

Directly solve the transport equations for the PDF

$$P\left(\mathbf{u},\Phi;\mathbf{x},t\right);\quad \mathbf{u}=\left(u,v,w\right),\Phi=\left(\phi_1,\ldots,\phi_N\right)$$

The joint PDF is N+3 dimensional.

$$P\left(\mathbf{u},\Phi;\mathbf{x},t\right)d\mathbf{u}d\Phi$$

denotes the probability of finding at $\left(\mathbf{x},t\right)$ the velocity components and the reactive scalars within the interval $\mathbf{u}<\mathbf{u}<\mathbf{u}+d\mathbf{u},\ \Phi<\Phi<\Phi+d\Phi$

Once the joint PDF is known, any one-point joint statistics can be expressed as integrals of the PDF over the sample space, e.g.

$$\widetilde{u_i''\phi_k''}=\iint\left(v_i-\tilde{u}_i\right)\left(\psi_k-\tilde{\phi}_k\right)P d\mathbf{v}d\psi$$

Transported Probability Density Function (PDF)

- Closures for the (high) moment terms in transport equations

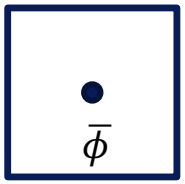

$$\overline{S_k(\boldsymbol{\phi})} \neq S_k(\bar{\boldsymbol{\phi}})$$

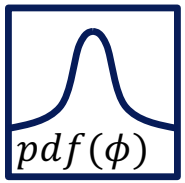

$$\overline{S_k(\boldsymbol{\phi})} = \int S_k(\boldsymbol{\phi}) pdf(\boldsymbol{\phi}) d\boldsymbol{\phi}$$

Any moment of variable ϕ can be accurately computed given its $f_\phi(\psi)$

Reaction terms are closed!!

- Transport equations of the PDF of fluid properties
  - Turbulent reacting flow is represented by the joint probability density function (PDF) of fluid properties ($\boldsymbol{\phi}$, $\boldsymbol{u}$, $\boldsymbol{x}$)
  - Joint composition pdf transport equation **(one-point, one-time)**:

$$\frac{\partial \mathcal{F}_\phi}{\partial t} + \frac{\partial \mathcal{F}_\phi \widetilde{v_i|\psi}}{x_i} = -\frac{\partial}{\partial \psi_\alpha}\left[\frac{\mathcal{F}_\phi}{\bar{\rho}} \overline{\frac{\partial J_{\alpha i}}{\partial x_i}|\psi}\right] - \frac{\partial \mathcal{F}_\phi S_\alpha}{\partial \psi_\alpha}$$

Modeling with the Lagrangian Description

- Unclosed molecular diffusion term due to the lack of gradient information

$$\frac{\partial \mathcal{F}_\phi}{\partial t} + \frac{\partial \mathcal{F}_\phi \widetilde{v_i|\psi}}{x_i} = -\frac{\partial}{\partial \psi_\alpha}\left[\frac{\mathcal{F}_\phi}{\bar{\rho}}\overline{\frac{\partial J_{\alpha i}}{\partial x_i}|\psi}\right] - \frac{\partial \mathcal{F}_\phi S_\alpha}{\partial \psi_\alpha}$$

  - The conditional diffusion term $\overline{\frac{\partial J_{\alpha i}}{\partial x_i}|\psi}$ is further closed by micro-mixing models

- Lagrangian Description

$$d\boldsymbol{X}(t) = \left[\widetilde{\boldsymbol{U}} + \frac{\nabla\left[\bar{\rho}\left(\Gamma_{sgs} + \Gamma\right)\right]}{\bar{\rho}}\right]^* dt + \left[2\left(\Gamma^*_{sgs} + \Gamma^*\right)\right]^{\frac{1}{2}} d\boldsymbol{W}$$

$$d\boldsymbol{\phi}(t) = \underbrace{-\tilde{\omega}_\phi \mathbf{M}\phi dt}_{\text{Mixing term}} + \underbrace{\boldsymbol{S}(\boldsymbol{\phi})dt}_{\text{Reaction term}}$$

Micro-mixing model adds a significant amount of uncertainty to TPDF method

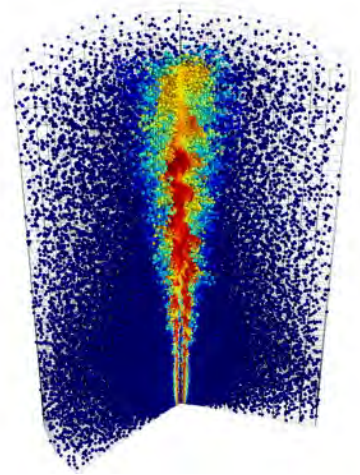

Hiremath *et al.*, Combust. Flame, 2012

Mixing Models for PDF Approach

$$\frac{d\phi}{dt} = -\tilde{\omega}_\phi \mathbf{M}\phi$$

A micro-mixing model describe the effect of molecular diffusion on particle evolution

- Two ingredients for a micro-mixing model:
  - Mixing formulation ($\mathbf{M}\phi$): **describes the manner in which mixing occurs**

IEM (Interaction by Exchange with the Mean)

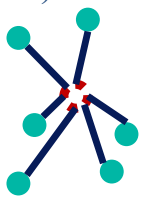

Villermaux and Devillon, 1972

MC (Modified Curl)

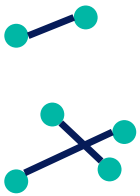

Curl R.L., 1963

EMST (Euclidean Minimum Spanning Tree)

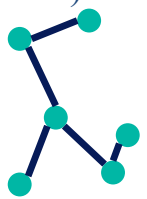

Subramaniam and Pope, 1998

  - Mixing rate ($\tilde{\omega}_\phi$): **describes the timescale of the mixing event**

For a conservative scalar, turbulence dominates mixing:

$$\tilde{\omega}_\phi = C_\phi \tilde{\omega}$$

For a reactive scalar, both turbulence and reaction affects mixing:

$$\tilde{\omega}_\phi \neq f(\tilde{\omega})$$

The PDF Transport Equation - Challenges

High Dimensionality of the PDF Equation

- Eulerian finite volume or finite difference is not suitable.

  ⇒ Lagrangian particle-tracking method (Monte Carlo)
  - Typically coupled with the Eulerian flow solver by interpolation.

- PDF is determined in the phase space $(\mathbf{u}, \boldsymbol{\psi})$ with 3+N dimensions, making the creation of joint PDF very difficult and time-consuming.

  ⇒ Chemistry reduction strategy is needed.
  - Intrinsic low-dimensional manifold (ILDM)
  - In-situ adaptive tabulation (ISAT)
  - Directed relation graph (DRG) ……

PDF for LES: Filtered Density Function (FDF)

The local spatially filtered value of a physical quantity *Q*

$$\left\langle Q(\mathbf{x},t)\right\rangle_{\Delta} = \int Q(\mathbf{y},t)G(|\mathbf{x}-\mathbf{y}|)d\mathbf{y}$$

based on the low-pass spatial filter function, satisfying $\int G(\mathbf{x})d\mathbf{x} = 1$
which leads to a decomposition:

$$Q(\mathbf{x},t) = \left\langle Q(\mathbf{x},t)\right\rangle_{\Delta} + Q'_{\Delta}(\mathbf{x},t)$$

The G-weighted spatial average of the PDF in the neighborhood of $\mathbf{x}$ is defined as FDF.

$f_{\Delta,\phi}(\psi;\mathbf{x},t)d\psi$ The G-weighted fraction of the fluid near $\mathbf{x}$ whose composition is in the range $\psi < \phi < d\psi$

PDF vs. FDF

Differences between PDF and FDF

1. FDF varies on length scales down to the filter size Δ
   PDF varies down to the integral scale ℓ_I

2. FDF varies in time even for statistically stationary flows.

The transport equation for FDF can be derived following the similar procedure.

- Ensemble average vs. spatial filtered quantities
- RANS turbulent transport closure vs. sub-filter scale model
- As in PDF, the chemical source terms are closed.

Modeling of Mixed-Mode Combustion

Modeling of Partially Premixed Combustion

Flamelet Model for Partially Premixed Turbulent Combustion
[Müller et al. (1994), Chen et al. (2000)]

Description of nonpremixed combustion:

$$\frac{\partial\left(\bar{\rho}\tilde{Z}\right)}{\partial t}+\nabla\cdot\left(\bar{\rho}\tilde{\mathbf{u}}\tilde{Z}\right)=\nabla\cdot\left(\frac{\mu_t}{\mathrm{Sc}_{\tilde{Z}}}\nabla\tilde{Z}\right)$$

$$\chi=c_\chi\frac{\tilde{\varepsilon}}{\tilde{k}}\widetilde{Z''^2};\ c_\chi=2.0$$

$$\frac{\partial\left(\bar{\rho}\widetilde{Z''^2}\right)}{\partial t}+\nabla\cdot\left(\bar{\rho}\tilde{\mathbf{u}}\widetilde{Z''^2}\right)=\nabla\cdot\left(\frac{\mu_t}{\mathrm{Sc}_{\widetilde{Z''^2}}}\nabla\widetilde{Z''^2}\right)+\frac{\mu_t}{\mathrm{Sc}_{\widetilde{Z''^2}}}\left(\nabla\tilde{Z}\right)^2-\bar{\rho}\tilde{\chi}$$

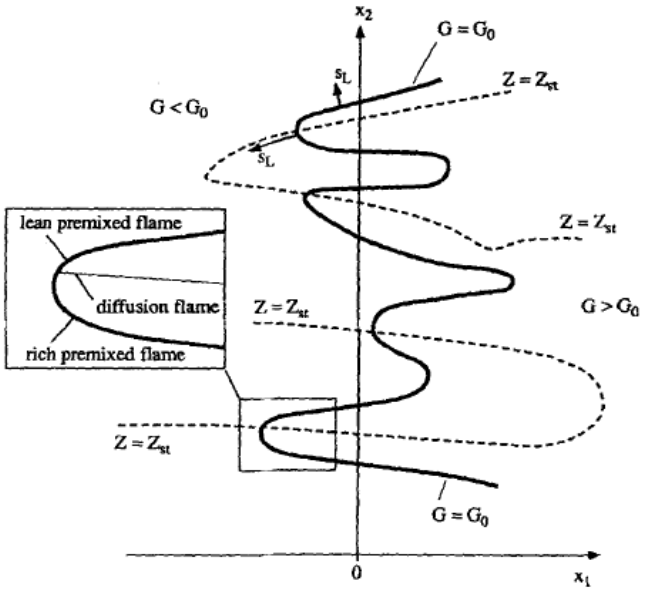

From Müller et al. (1994)

Description of premixed combustion:

$$\frac{\partial\left(\bar{\rho}\tilde{G}\right)}{\partial t}+\nabla\cdot\left(\bar{\rho}\tilde{\mathbf{u}}\tilde{G}\right)=\bar{\rho}S_{T,p}\left|\nabla\tilde{G}\right|-\bar{\rho}D_t\tilde{\kappa}\left|\nabla\tilde{G}\right|,\qquad D_t=0.78\ell u'$$

$$\frac{\partial\left(\bar{\rho}\widetilde{G''^2}\right)}{\partial t}+\nabla\cdot\left(\bar{\rho}\tilde{\mathbf{u}}\widetilde{G''^2}\right)=\nabla_{\|}\cdot\left(\bar{\rho}D_t\nabla_{\|}\widetilde{G''^2}\right)-2\bar{\rho}D_t\tilde{\kappa}\left(\nabla\tilde{G}\right)^2-c_s\bar{\rho}\frac{\tilde{\varepsilon}}{\tilde{k}}\widetilde{G''^2}$$

Modeling of Partially Premixed Combustion

For purely premixed turbulent flames:

$$\frac{S_T - S_L}{u'} = -\frac{a_4 b_3^2}{2b_1} Da + \left[\left(\frac{a_4 b_3^2}{2b_1} Da \right)^2 + a_4 b_3^2 Da \right]^{1/2}, \quad a_4 = 0.78, \; b_1 = 2.0, \; b_3 = 1.0$$

$$Da = \frac{S_L \ell}{u' l_F}$$ ← laminar flame thickness

which is extended by defining a conditional turbulent Damköhler number,

$$Da(Z) = \frac{S_L(Z)\ell}{u' l_F(Z)} = \frac{S_L^2(Z)\ell}{u' D}$$

$$S_T(Z) = S_L(Z) + u' f\left[Da(Z) \right]$$

such that ← beta PDF

$$\bar{\rho} S_{T,p} = \int_0^1 \rho(Z) S_T(Z) \tilde{P}(Z) dZ$$

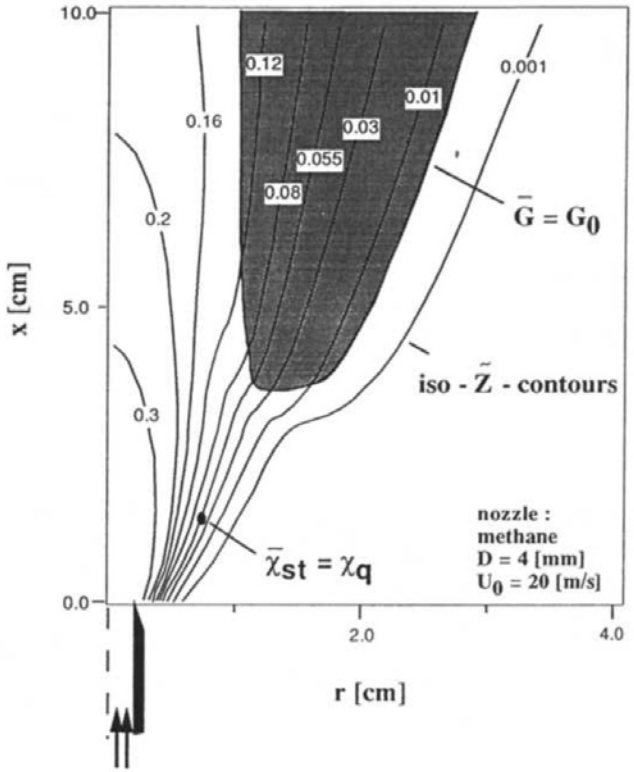

Typical simulation results with *Z-G* formulation (Müller et al., 1994)

Partially-Stirred Reactor Model (PaSR) and Modal Extension (mPaSR)

Traditional PaSR approach

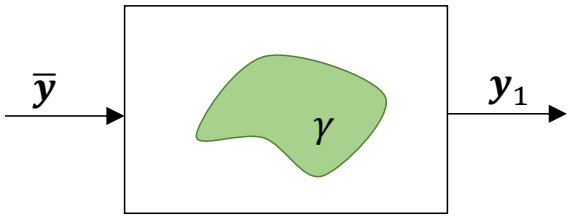

$\dot{\bar{\omega}} = \gamma \dot{\omega}(\bar{y})$; $\gamma = \frac{\tau_c}{\tau_c + \tau_m}$

$\tau_m \to 0$: CSTR

$\tau_m \to \infty$: Perfectly segregated reactor

(Chomiak, Comb. Symp., 1996)

PaSR is an extension of eddy dissipation concept (EDC):

$$\dot{\bar{\omega}} = \frac{\rho \gamma (y_1 - y_s^*)}{\tau_f} \; ; \; \tau_f = \tau_m$$

y_s^*: composition of fine structure surroundings (computed evolving chemistry only in a PSR or PFR).

Inclusion of multiple chemical times through modal decomposition (mPaSR)

- Overcome the concept of fine structures (problematic at the limits, $\tau_m \to 0$);
- Include multiple chemical times to capture multiple combustion regimes.

$$J = \begin{bmatrix} \frac{d\omega_1}{dc_1} & \cdots & \frac{d\omega_1}{dc_i} \\ \vdots & \ddots & \vdots \\ \frac{d\omega_i}{dc_1} & \cdots & \frac{d\omega_i}{dc_i} \end{bmatrix}$$

$$\dot{\omega} = \sum_i^{NS-NE} a_i f_i \quad f_i = \dot{\omega} \cdot b_i$$

$$\tau_{C,i} = \frac{1}{\lambda_i}; \quad \gamma_i = \frac{\tau_{C,i}}{\tau_{C,i} + \tau_{mix}} \quad \dot{\bar{\omega}} = \sum_i^{NS-NE} \gamma_i a_i f_i$$

- No fine structures
- Multiple chemical times
- Mass balance closed

A Priori Test Validation

DNS test case

- Syngas turbulent non-premixed jet flame*;
- 12 species, 33 reactions**;
- 2160x720 (12x4cm);
- $Z_{st} = 0.4375$;
- 2D Gaussian filter: $\delta = 2, 8, 16$.

*Sutherland J., Phd Thesis (2004)
**Yetter, R. A., Combustion Science and Technology (1991)

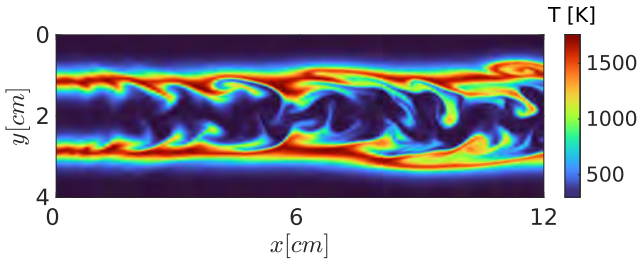

Mixing time definition (for LES)

$$\chi_\alpha = 2(\Gamma_t + \Gamma)|\nabla\widetilde{\phi_\alpha}|^2 \; ; \; \widetilde{\Phi_\alpha''^2} = C_v\Delta^2|\nabla\widetilde{\phi_\alpha}|^2$$

$$\Omega = \frac{\chi_\alpha}{\widetilde{\Phi_\alpha''^2}} = \frac{C_M(\Gamma+\Gamma_t)}{\Delta^2} \; ; \quad \tau_{mix} = \frac{1}{\Omega} \; ; \Delta = \delta d$$

$\Gamma: mixture\ averaged$

$\Gamma_t: Smagorinsky\ \&\ Sc_t = 0.4$

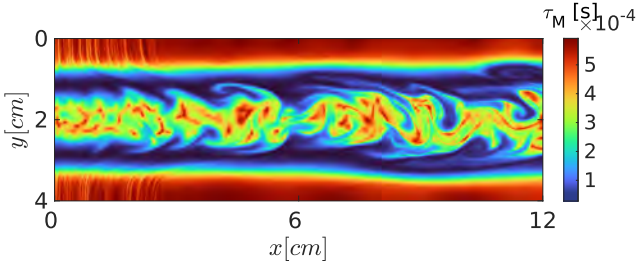

A priori validation:

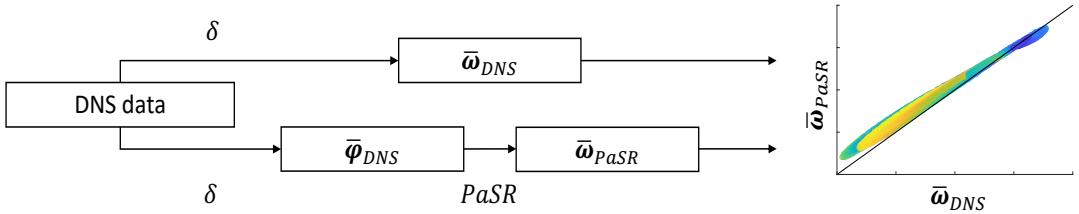

Time Scale Analysis and Comparison

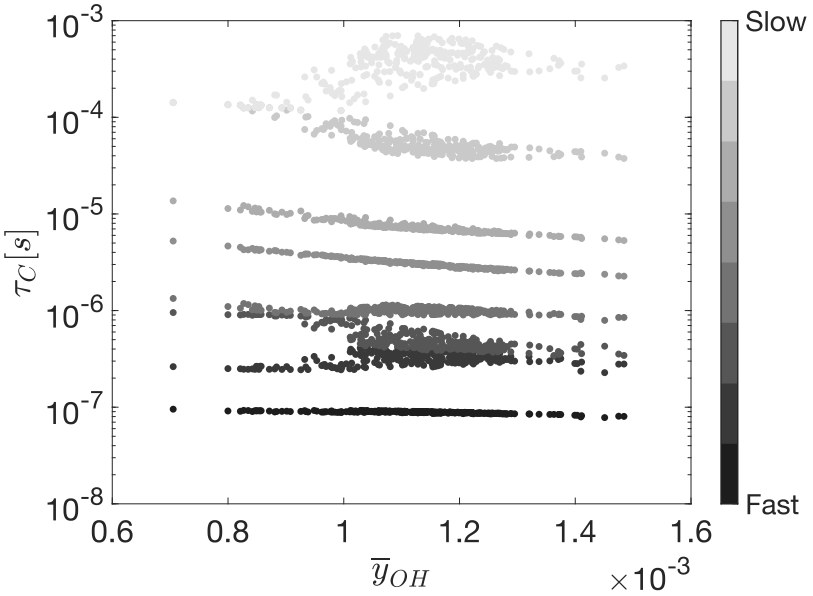

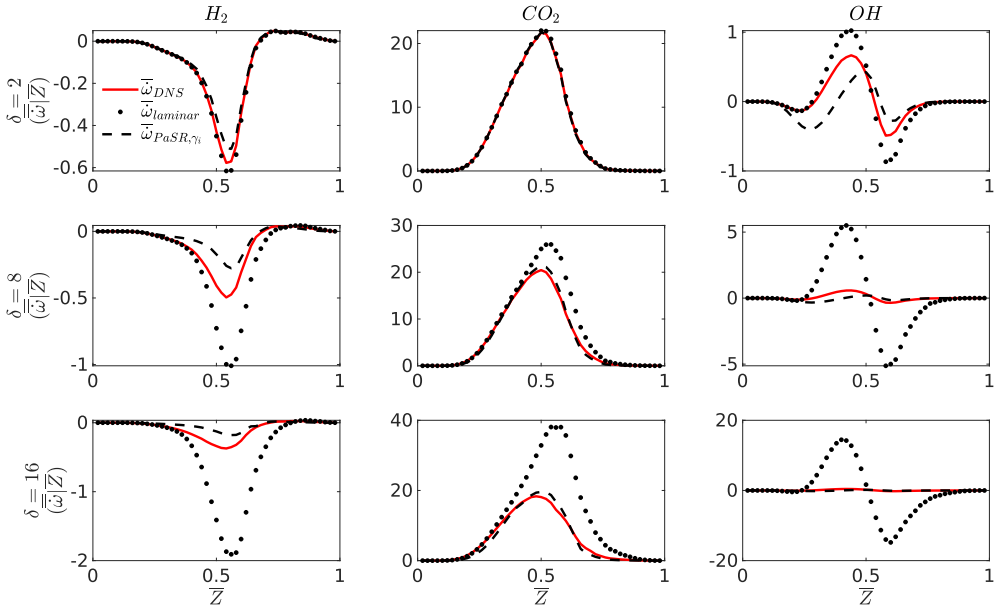

- $\boldsymbol{\tau_{c,i}}$ for 8 modes (4 modes relative to the conservation of elements have been removed) span a wide range of timescales.
- Times are faster for higher concentrations of OH (higher reactivity).

- A laminar closure (no-model approach) produces larger errors as the filter size is increased.
- The inclusion of multiple chemical times produces a good general agreement.

A Priori Test against Single Timescale Model

Quadarella E, Péquin A, Stagni, A., Parente A, Faravelli T, Im HG, PROCI (2023) 5329-5338.

γ_f: only fastest time scale. Agreement for intermediate species only

γ_s: only slowest time scale. Better agreement for main species and departure of intermediates

γ_i: new generalized approach (mPaSR, all time scales included). Gives the best accuracy for all species

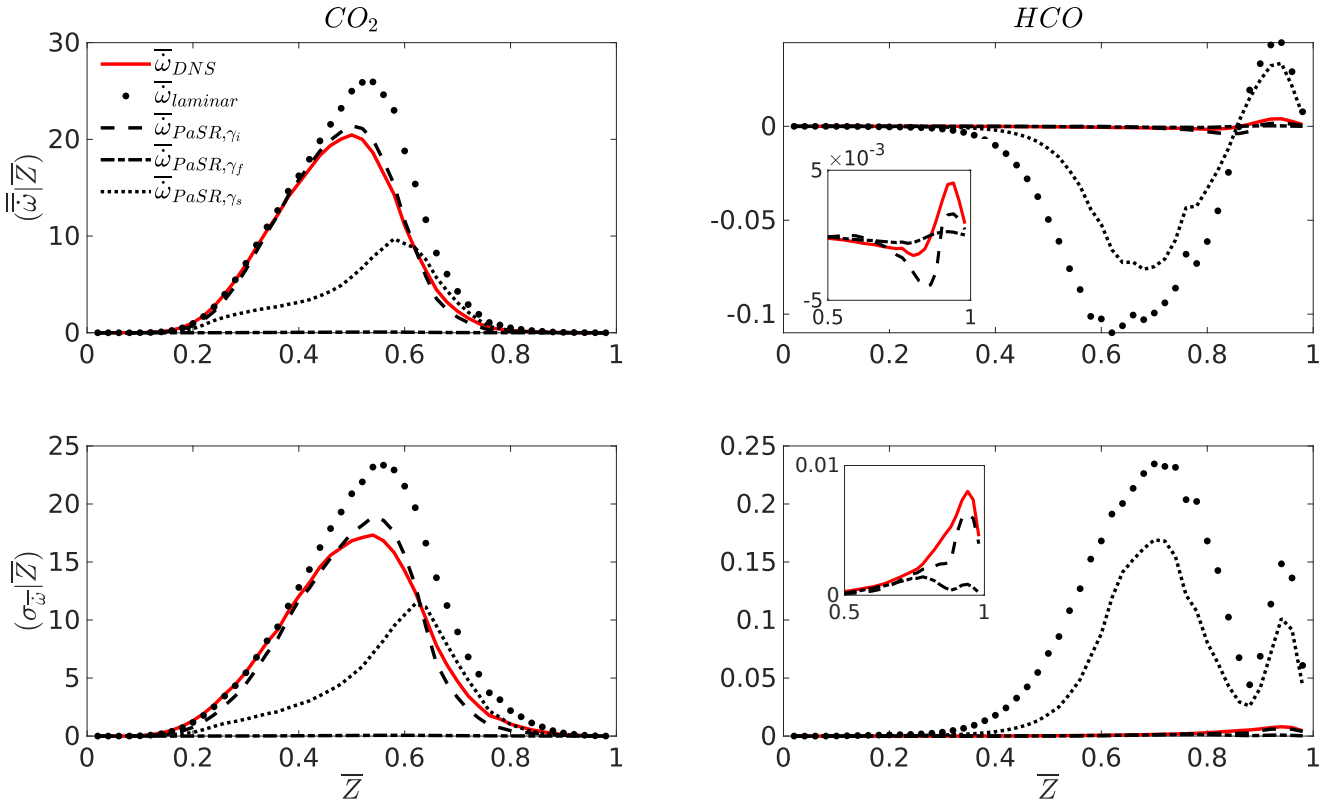

A Posteriori Test with RANS

- **mPaSR** integrated into FiReSMOKE* and tested on KAUST ethylene-nitrogen (KEN) flame for soot formation

Péquin A, Quadarella E, Galassi RM, Iavarone S, Im HG, Parente A. CNF (2025) 279:114269.

Designation	P [bar]	Re	$U_j\ [\frac{m}{s}]$	P_p [%]	$U_{cf}\ [\frac{m}{s}]$
KEN 01-01-B	1	10000	36.6	6	0.6
KEN 03-01	3	10000	12.2	18	0.2
KEN 03-03	3	30000	36.6	6	0.6
KEN 05-01	5	10000	7.3	18	0.12
KEN 05-05	5	50000	36.6	6	0.6

Main jet: $C_2H_4 = 0.35, N_2 = 0.65$; Pilot: C_2H_4/Air $\phi = 0.9$

- Turbulence model : k-epsilon with Pope's correction
- τ_{mix} formulation: dynamic formulation with constants: C_1=2.0, C_1=1.8, C_1=3.4, C_1=1.4
- Gas kinetics: Polimi 1412 (Ranzi et al., 2005)
- Soot model: HMOM
- Soot-turb-chem interaction: double-delta distribution subfilter PDF (based on soot intermittency).

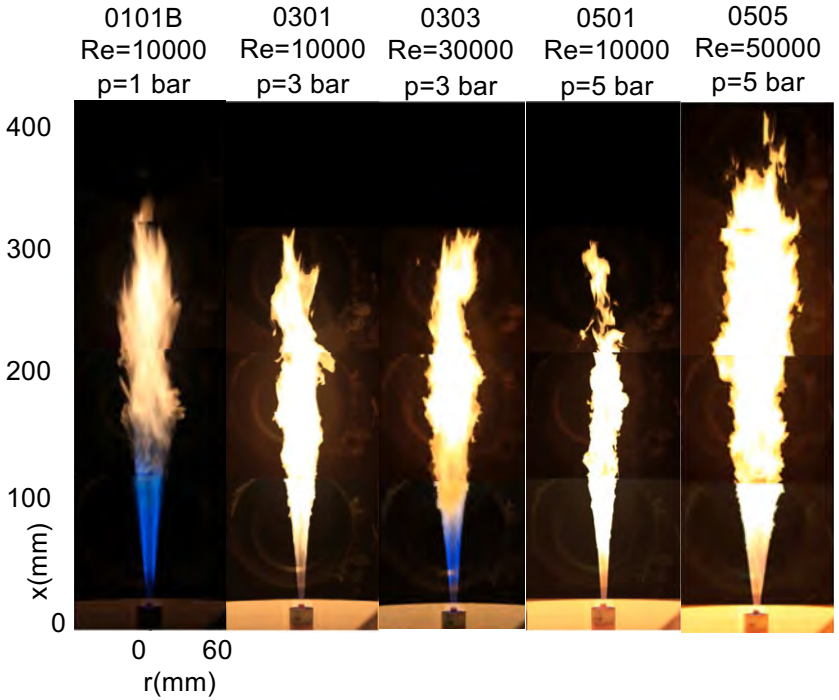

Boyette W. R., et al. Combustion and Flame 227 (2021): 271-282.

Validation: Gaseous PAH Species

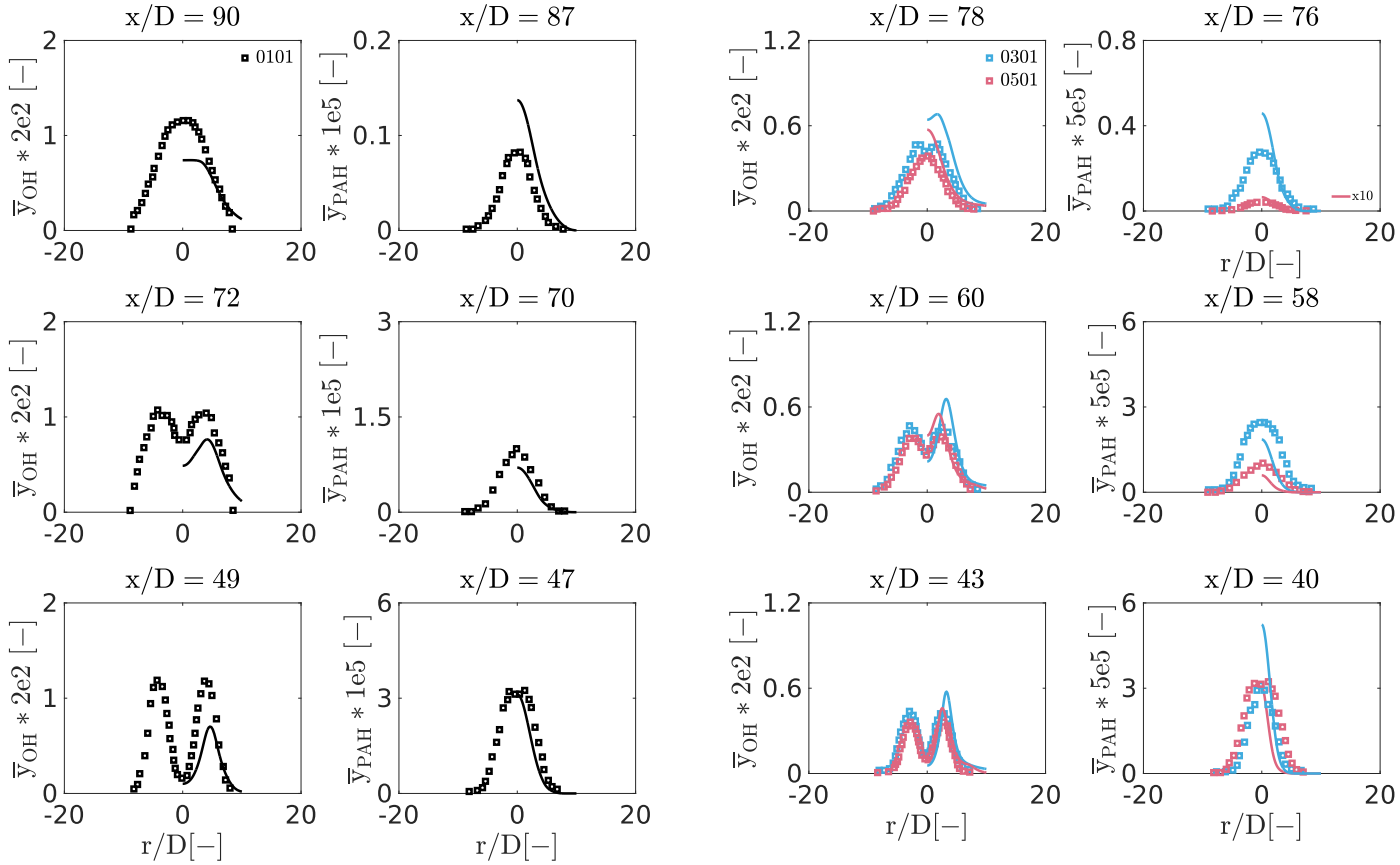

OH PLIF λ: 282.93 nm
PAH PLIF λ: 325-500 nm

OH scaling with pressure in good agreement, but PAH shows larger errors, requiring further investigations on the kinetics and mixing time formulation.

Validation: SVF and Mode Distribution

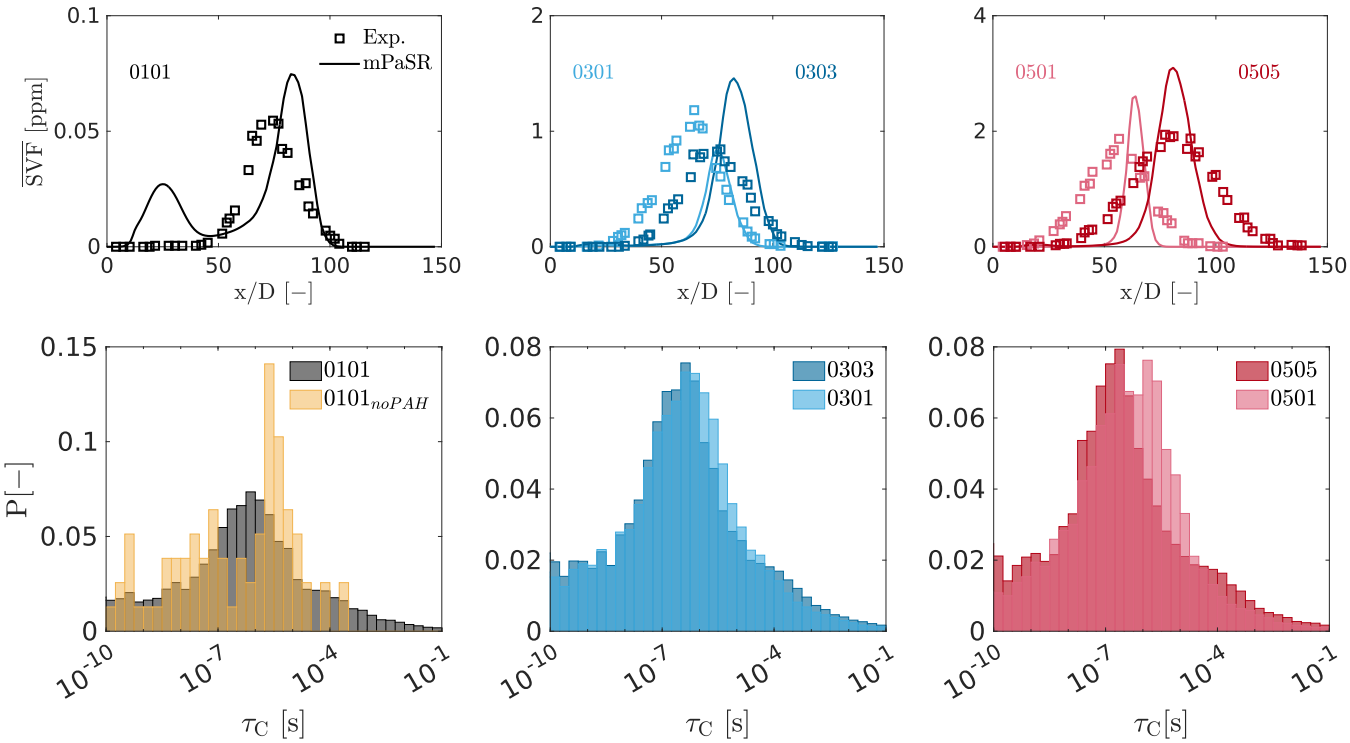

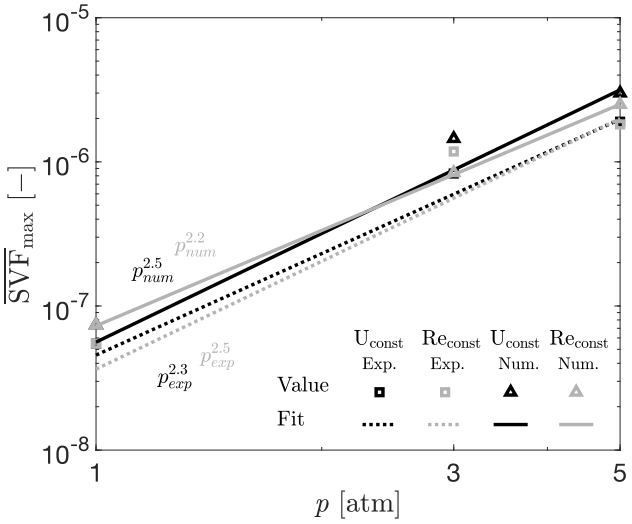

- Peak locations are slightly delayed and the width of the distribution partly underpredicted.
- Good $\overline{SVF}_{max}$ pressure scaling with only 10% difference compared to experiments.
- The model fails to predict the soot suppression by turbulence at 3 bar.
- Bimodal shape at 1 bar is currently under investigation.

- Timescale distribution remains largely unchanged with pressure.
- Enhanced turbulence promotes the formation of a second peak corresponding to slower modes (PAH chemistry): strong mixing facilitates the coexistence of fast and slow chemical processes.

Other Modeling Approaches

Modeling Frameworks

- Linear eddy model/One-dimensional turbulence (LEM/ODT) (Kerstein et al.)
- Multiple mapping conditioning (MMC) (Klimenko, Pope et al.)
- Unsteady flame embedding (UFE) (El-Asrag and Ghoniem)
- Lattice Boltzmann method (Frouzakis et al.)

Computational Enablers for Turbulent Combustion Modeling

- Adaptive mesh refinement (Bell, Collela)
- Wavelet methods (Prosser, Cant; Martelli, Paolucci)
- Chemistry reduction:
  - Quasi-steady state/partial equlibrium approx. (QSSA/PEA) (Chen et al.)
  - Computational singular perturbation (CSP) (Goussis, Valorani et al.)
  - Intrinsic low dimensional manifold (ILDM) (Maas et al.)
  - In-situ adaptive tabulation (ISAT) (Pope et al.)
  - Flamelet-generated manifolds (de Goey et al.)
  - Directed relation graph (DRG) (Lu et al.)

References

- Peters, N., Turbulent Combustion, Cambridge University Press (2000).
- Libby, P. A. and Williams, F. A., eds., Turbulent Reacting Flows, Academic Press (1994).
- Liñán, A. and Williams, F. A., Fundamental Aspects of Combustion, Oxford University Press (1993).
- Poinsot, T. and Veynante, D., Theoretical and Numerical Combustion, 2nd ed., Edwards (2005).
- Fox, R. O, Computational Models for Turbulent Reacting Flows, Cambridge University Press (2003).
- Echekki, T. and Mastorakos, E., eds., Turbulent Combustion Modeling: Advances, New Trends and Perspectives, Springer (2011).
- Swaminathan, N. and Bray, K. N. C., eds., Turbulent Premixed Flames, Cambridge University Press (2011).

جامعة الملك عبدالله للعلوم والتقنية
King Abdullah University of Science and Technology

Clean Energy Research Platform

Tsinghua-Princeton-Combustion Institute
2025 Summer School on Combustion
Tsinghua University, July 7-11, 2025

Turbulent Combustion

Day 4: Accelerated High Fidelity Simulations

Hong G. Im
Clean Energy Research Platform (CERP)
King Abdullah University of Science and Technology (KAUST)

Direct Numerical Simulation of Turbulent Combustion

Uncompromised but expensive

Progress in Combustion Simulations

1990s

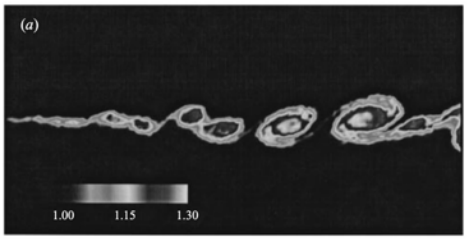

Jaberi et al., (JFM, 1999)

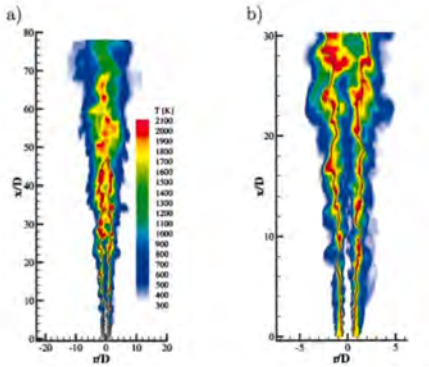

Pitsch & Steiner (POF, 2000)

2000s

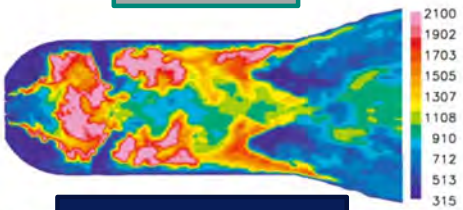

Di Mare et al., (CNF, 2004)

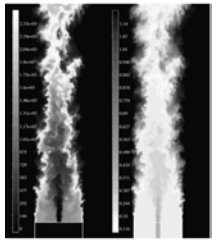

Kempf et al., (CNF, 2006)

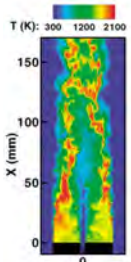

Raman & Pitsch (CNF, 2005)

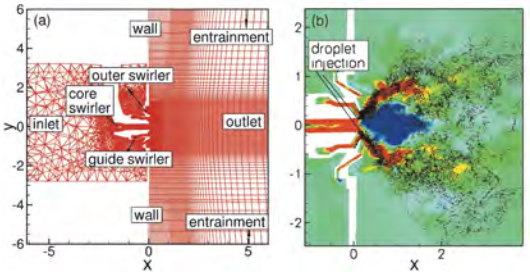

Moin & Apte (AIAA J., 2006)

2010s

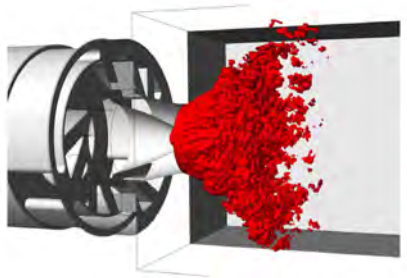

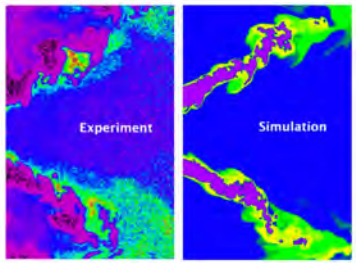

Moreau (CNF, 2011)

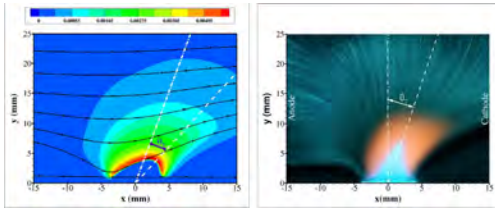

Belhi et al., (CNF, 2019)

2020s

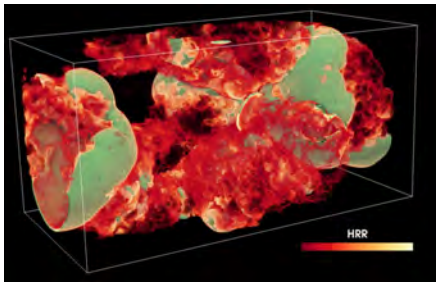

Luong & H. Im (AEC, 2021)

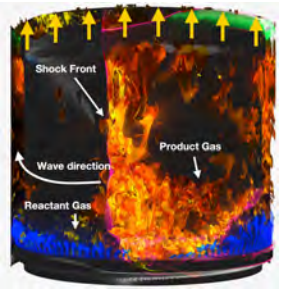

Prakash et al., (PCI, 2021)

DNS in Laboratory Scale

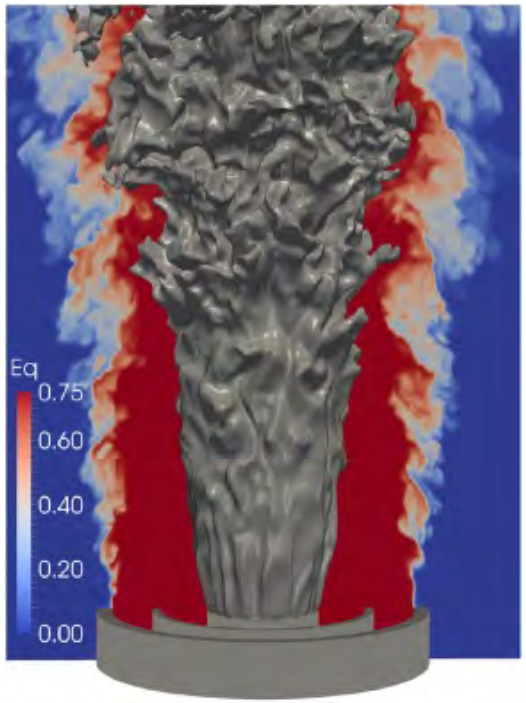

Turbulent premixed bluff-body flames
Proch, et al., CNF (2017)

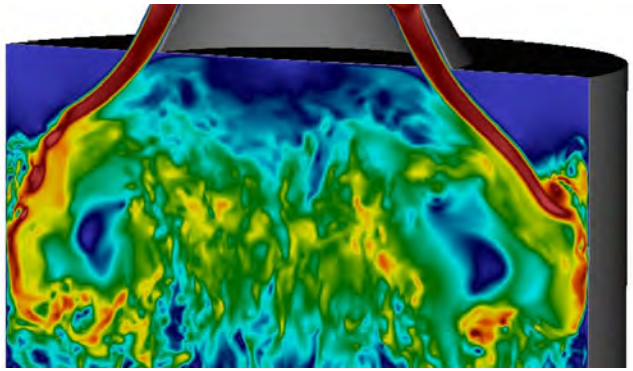

Internal combustion engine
Frouzakis, et al. (2024)

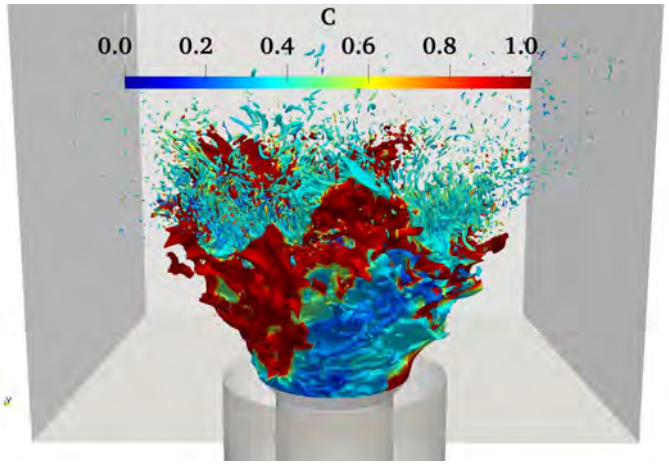

Swirl-stabilized spray flame (PeleLMeX)
Soriano, Chen (2024)

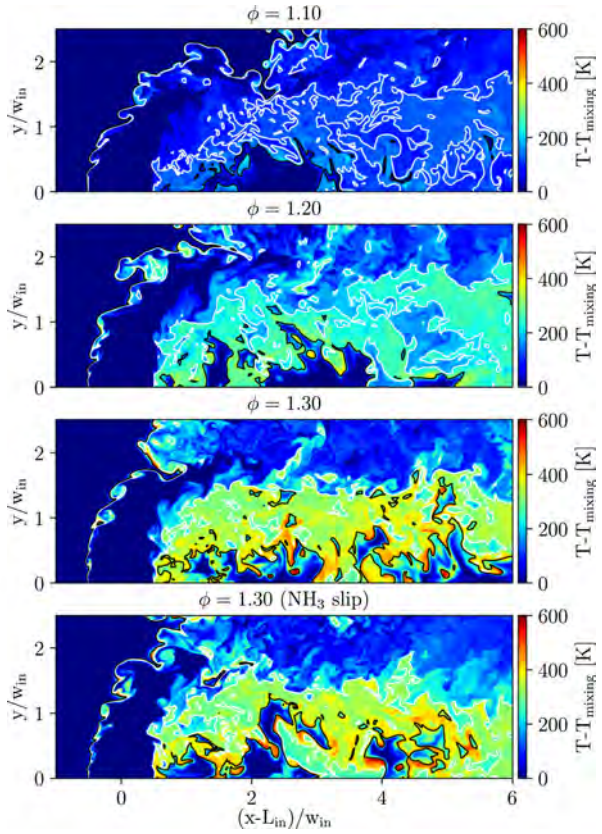

Ammonia RQL combustor
Rieth et al., PROCI (2024)

Computational Demand of DNS

$$\mathrm{Re}_I = \frac{u' l_I}{\nu} \qquad \mathrm{Da}_K = \frac{\tau_K}{\tau_f}$$

- Nonreacting turbulent flows
  - **Spatial grid points:** $N \sim (l_I / l_K)^D = \mathrm{Re}_I^{3D/4} \quad (l_I / l_K \sim \mathrm{Re}_I^{3/4})$
  - **Time steps:** $M \sim \tau_I / \tau_K = \mathrm{Re}_I^{1/2}$
  - **Total demand:** $MN \sim \mathrm{Re}_I^{(3D/4)+(1/2)}$

    $MN \sim \mathrm{Re}_I^{11/4}$ for 3D
- Turbulent reacting flows
  - **Spatial grid points:** $N \sim (l_I / l_f)^D = \mathrm{Re}_I^{3D/4}\,\mathrm{Da}_K^{D/2} \quad (l_I / l_f \sim \mathrm{Re}_I^{3/4}\,\mathrm{Da}_K^{1/2})$
  - **Time steps:** $M \sim \tau_I / \tau_f = \mathrm{Re}_I^{1/2}\,\mathrm{Da}_K$
  - **Total demand:** $MN \sim \mathrm{Re}_I^{(3D/4)+(1/2)}\,\mathrm{Da}_K^{D/2+1}$

    $MN \sim \mathrm{Re}_I^{11/4}\,\mathrm{Da}_K^{5/2}$ for 3D

Solution Algorithms for Reactive N-S System

Compressible
(S3D, NTMIX, SENGA, KARFS,…)

$$\frac{D\rho}{Dt} + \rho\nabla\cdot\mathbf{v} = 0$$

$$\rho\frac{D\mathbf{v}}{Dt} = -\nabla p + \nabla\cdot\mathbf{S} + \rho\sum Y_i\mathbf{f}_i$$

$$\rho\frac{DY_i}{Dt} = -\nabla\cdot\left(\rho\mathbf{V}_i Y_i\right) + w_i,\ i = 1,\cdots,N$$

$$\rho\frac{Dh}{Dt} = \frac{Dp}{Dt} - \nabla\cdot\mathbf{q} + \rho\sum Y_i\mathbf{f}_i\cdot\mathbf{V}_i$$

System of ODEs for

$$\mathbf{U} = \left(\rho, \mathbf{v}, h, Y_i\right)$$

Low-Mach
(NGA, LMC, NEK5000, …)

$$\rho\frac{D\mathbf{v}}{Dt} = -\nabla\left(\mathrm{Ma}^2 p_1\right) + \rho\sum Y_i\mathbf{f}_i$$

$$\rho\frac{DY_i}{Dt} = -\nabla\cdot\left(\rho\mathbf{V}_i Y_i\right) + w_i,\ i = 1,\cdots,N$$

$$\rho\frac{Dh}{Dt} = \frac{\partial p_0}{\partial t} - \nabla\cdot\mathbf{q} + \rho\sum Y_i\mathbf{f}_i\cdot\mathbf{V}_i$$

$$\nabla^2\left(\mathrm{Ma}^2 p_1\right) = \frac{1}{\Delta t}\left[\frac{\delta\rho}{\delta t} + \nabla\cdot\left(\rho\mathbf{u}\right)\right]$$

System of DAEs for

$$\mathbf{U} = \left(\mathbf{v}, h, Y_i\right)$$ + Poisson eq.

Progress in Computing Power

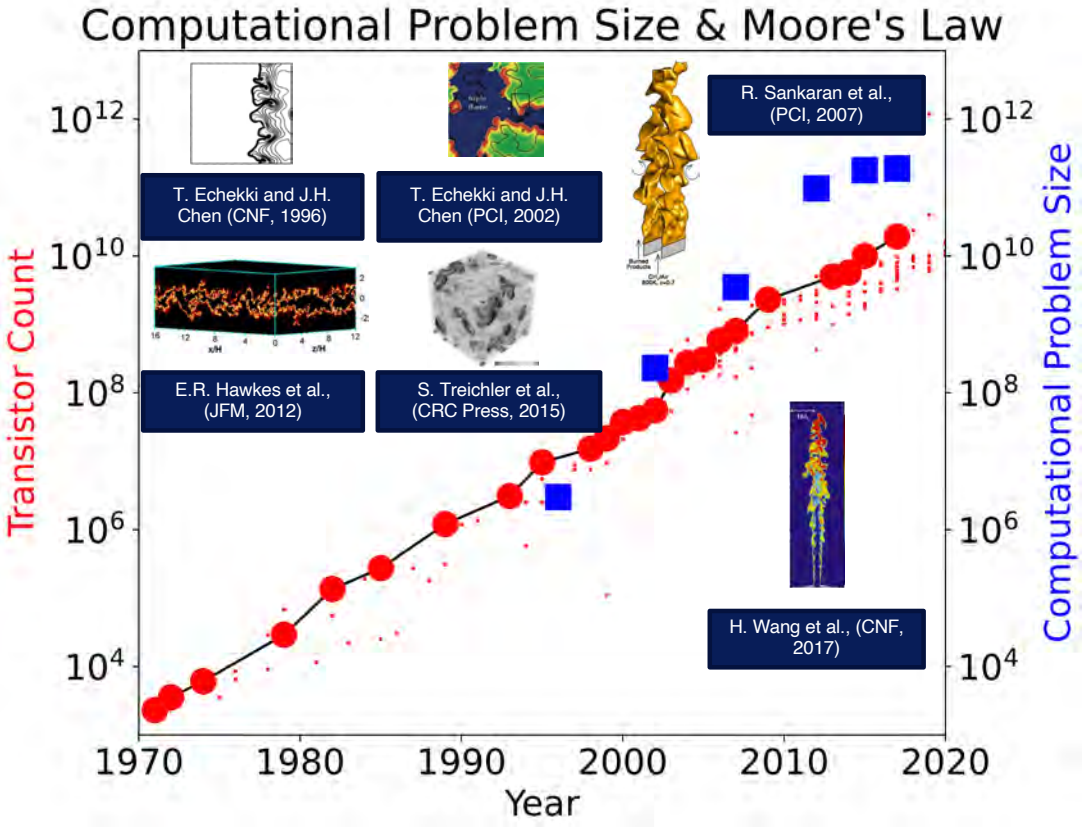

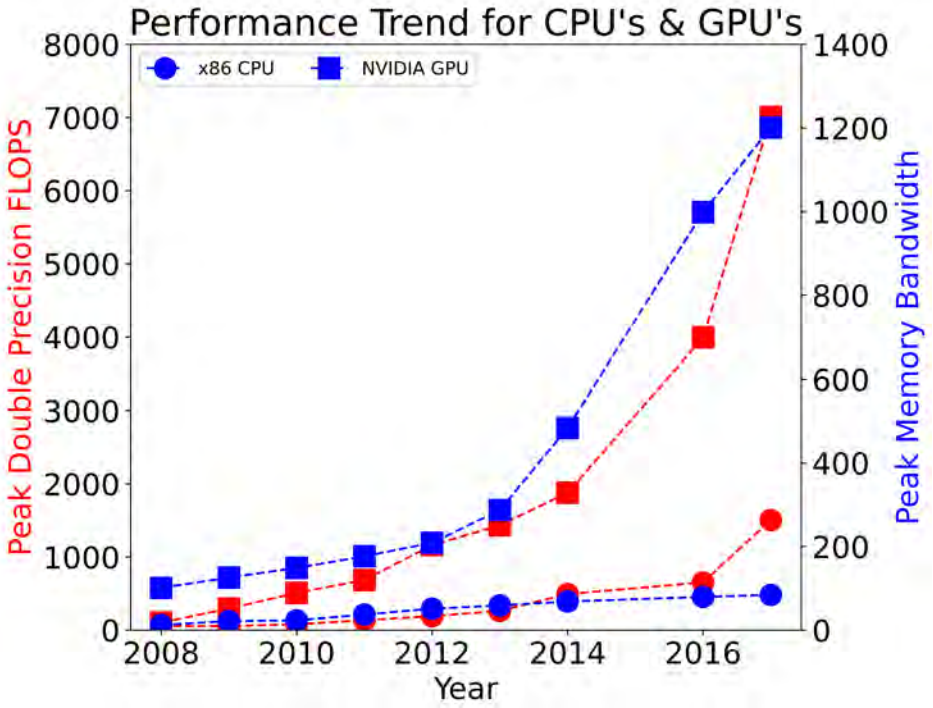

Problem size = # control volumes * # variables

Source: Intel & NVIDIA

Detailed Chemical Kinetics: Expensive & Stiff

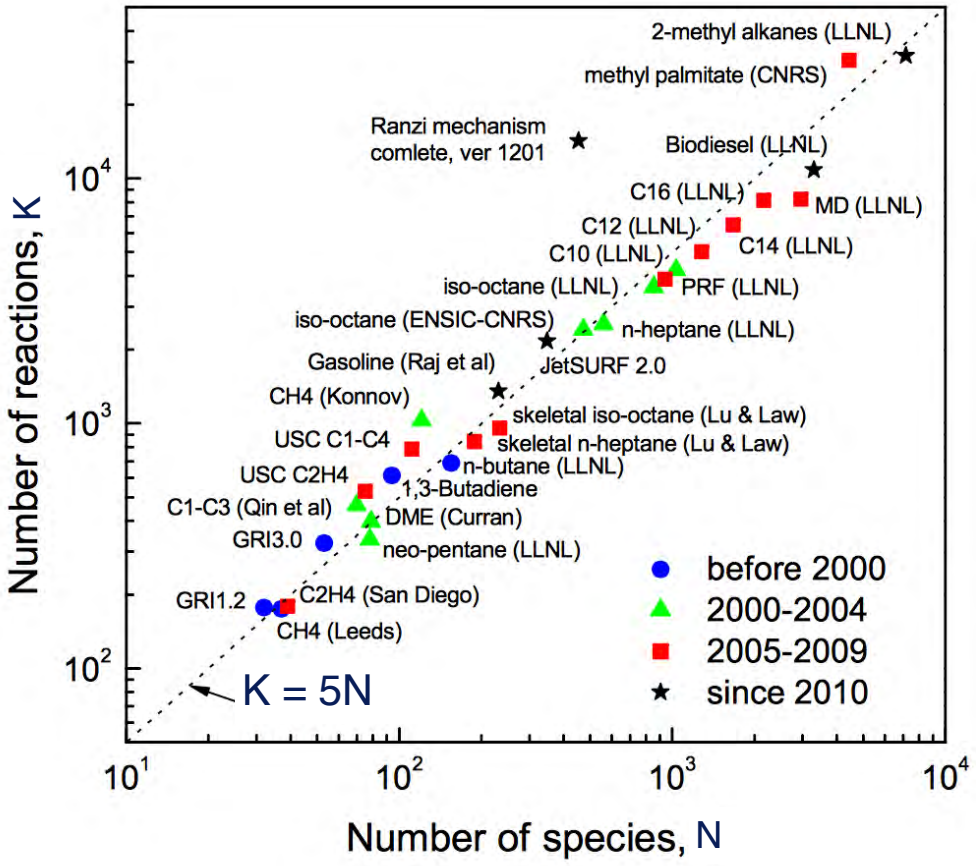

Updated from [Lu & Law, PECS 2009]

Lu, 2012 Princeton summer school

Some large mechanisms for biofuels:

- 7173 species
- 47157 reactions

The Art of Mechanism Reduction

A CFD person's response to Professor Mani Sarathy (CCRC, KAUST)

Detailed

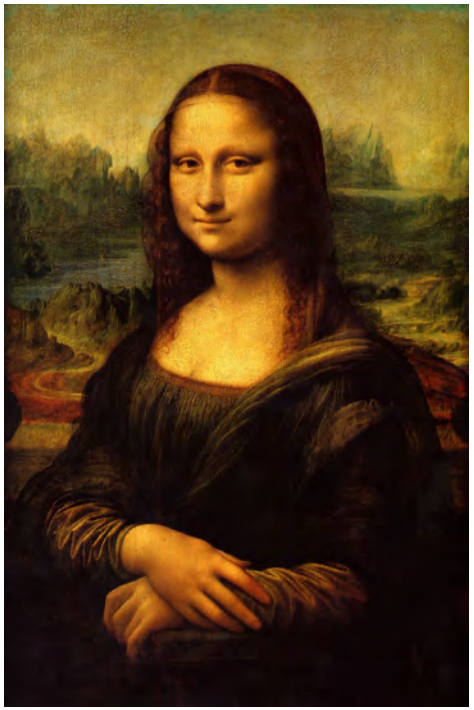

Skeletal!

Reduced, Still beautiful

Reduced Kinetic Mechanism – *A Priori* ROM

- Quasi-steady state/partial equlibrium approx. (QSSA/PEA) (JY Chen et al.)
- Intrinsic low dimensional manifold (ILDM) (Maas et al.)
- In-situ adaptive tabulation (ISAT) (Pope et al.)
- Flamelet-generated manifolds (de Goey et al.)
- Directed relation graph (DRG) (Lu et al.)
- Computational singular perturbation (CSP) (Goussis, Valorani et al.)

Stiffness – a common misconception

Practical Definition of Stiffness:
An initial value problem is stiff if Δt needed to maintain stability of the explicit time integration is much smaller than Δt required for accurate solution.

Are the small chemical time scales relevant to the physical dynamics of interest?

Yes: Non-stiff problem. Keep them all, and use explicit solvers.

No: Stiff problem.
(a) Keep the stiffness, and use implicit solvers (lazy approach).
(b) Remove stiffness, and use explicit solvers (smart approach).

Computational Singular Perturbation (CSP)

Automated computational algorithm to decompose characteristic time scales of a dynamical system.

$$\frac{d\mathbf{z}}{dt} = \mathbf{g}(\mathbf{z}) = \sum_{k=1}^{2K} \hat{\mathbf{S}}_k R^k = \sum_{k=1}^{N-E+1} \mathbf{a}_n f^n = \mathbf{a}_1 f^1 + \cdots + \mathbf{a}_M f^M + \mathbf{a}_{M+1} f^{M+1} + \cdots + \mathbf{a}_{N-E+1} f^{N-E+1}$$

fast modes (exhausted)

slow modes (driving dynamics)

$$\mathbf{b}^i \cdot \mathbf{a}_j = \delta^i_j$$

$$f^n = \mathbf{b}^n \cdot \mathbf{g}(\mathbf{z})$$

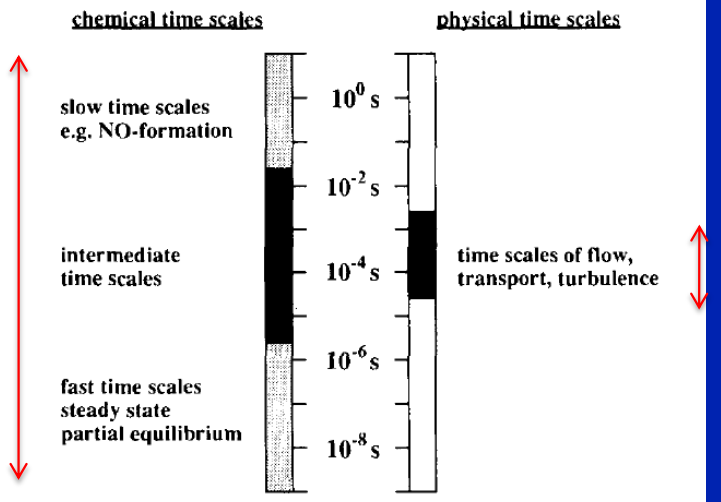

Maas & Pope, C&F 88:239-264 (1992)

Reduced system:

$$\frac{d\mathbf{z}}{dt} \approx \mathbf{a}_{M+1} f^{M+1} + \cdots + \mathbf{a}_{N-E+1} f^{N-E+1} \qquad f^1 \approx \cdots \approx f^M \approx 0$$

Algorithmic identification of the basis vectors that span the fast and slow subdomains:

1. Leads to the construction of non-stiff (reduced) models.
2. Provides physical understanding, by identifying the dominant physical processes.

Tangential Stretching Rate (TSR)

- TSR is weighted average of the chemical source term Jacobian eigenvalues.
- TSR gives a representative explosive eigenvalue and its amplitude simultaneously.

$$v(t) = \sqrt{\vec{v}(t) \cdot \vec{v}(t)}$$

$$\frac{dv}{dt} = \left(\frac{\vec{v}^T J_f \vec{v}}{v^2} \right) v = \left(\vec{u}^T J_f \vec{u} \right) v = \omega_{\vec{u}} v \left(\vec{u} = \frac{\vec{v}}{v} \right)$$

$$\omega_{\vec{u}} = \vec{u}^T J_f \vec{u} \quad \text{TSR}$$

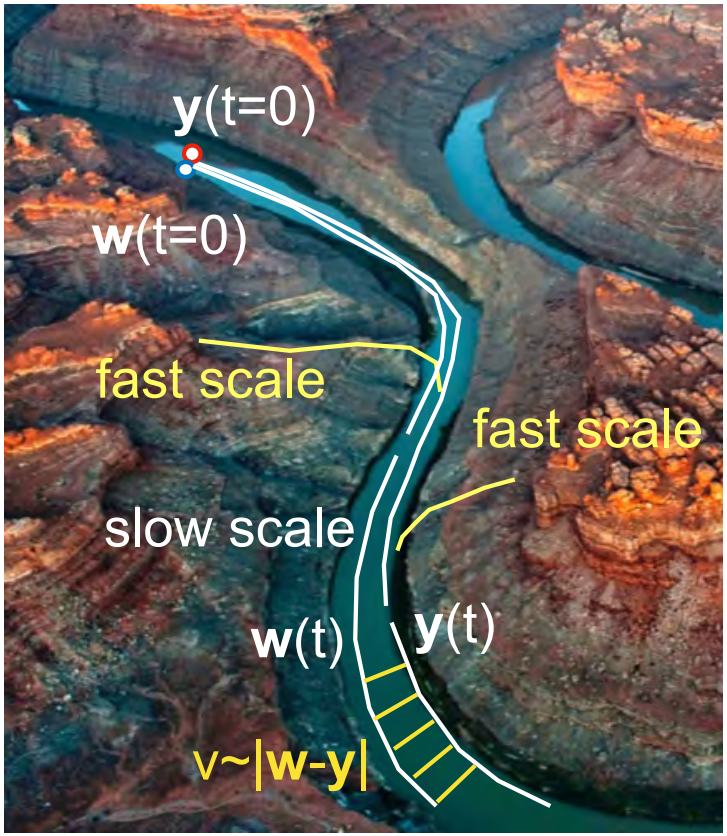

Courtesy of Mauro Valorani, University of Rome, La Sapienza

CSP+TSR Mechanism Reduction

Based on Slow/Fast Importance Indices & Dynamic Target Species Identification using TSR index

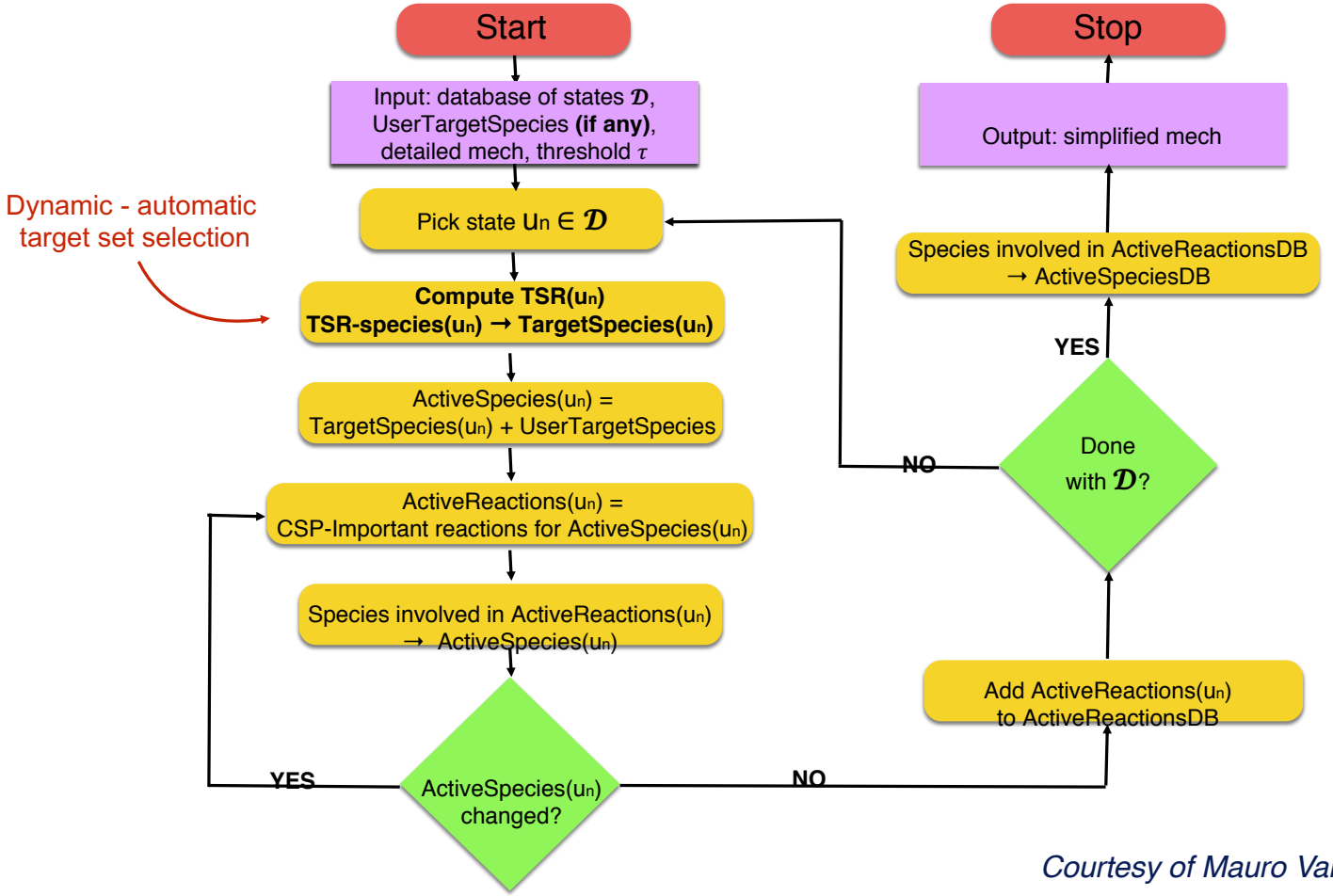

Courtesy of Mauro Valorani, University of Rome, La Sapienza

KAUST-Aramco PAH Mech (Ethylene-Air)

TSR detects pivotal species during ignition to be used as target

- KAUST-Aramco PAH Mech 1.0: Aramco Mech 1.3 C0–C2 chemistry developed by NUIG, and aromatics larger than benzene (C6H6 or A1) by including **PAH** growth pathways up to coronene, for the prediction of soot formation
- Detailed mechanism: **397** species, **2346** reactions
- Mixture: stoichiometric C2H4/air , 900 K, p = 1 atm, constant pressure

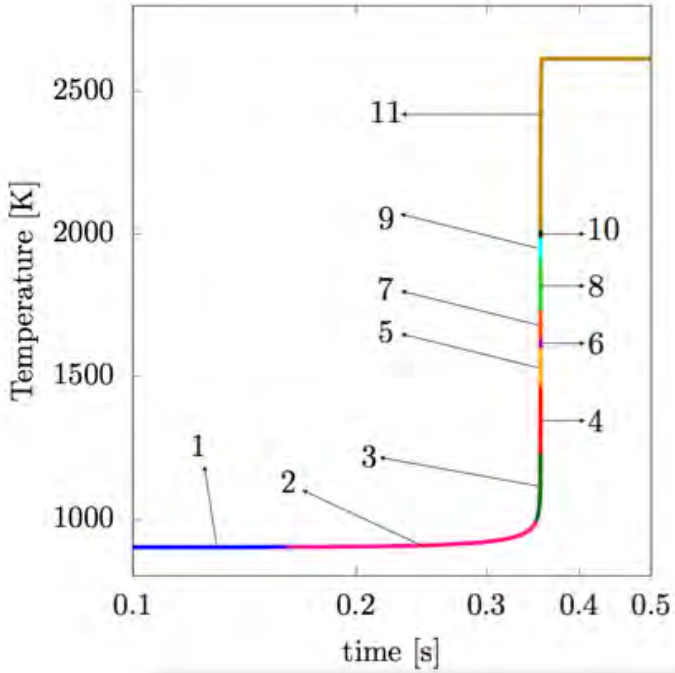

Region #	Temperature [K]	TSR kernel set
1	900 - 901	O, O_2, CH_2O, HCO, C_2H_3, H_2CC, CH_2CHO
2	901 - 985	O, O_2, OH, H_2O_2, CH_2O, HCO, C_2H_3, CH_2CHO
3	985 - 1210	O, O_2, OH, H_2O, H_2O_2, C_2H_4, C_2H_3, CH_2CHO
4	1210 - 1460	H, O, O_2, OH, H_2O, C_2H_4, C_2H_3, CH_2CHO
5	1460 - 1580	H, H_2, O, O_2, OH, CH_2O, HCO, C_2H_3, CH_2CHO
6	1580 - 1620	H, O, O_2, OH, CO, HCO, C_2H_3, CH_2CHO
7	1620 - 1680	H, H_2, O, O_2, OH, H_2O, CO, HCO
8	1680 - 1892	H, H_2, O, O_2, OH, H_2O, CH_4, CH_3, CH_2O, C_2H_4, C_2H_3
9	1892 - 1976	H, H_2, O, O_2, OH, H_2O, C_2H_2, HCCO
10	1976 - 2000	H, H_2, O, O_2, OH, H_2O, CO, CO_2
11	2000 - 2614	H, H_2, O, O_2, OH, H_2O, HO_2, CO, CO_2

The set of target species changes dynamically as identified by TSR

DNS with High Performance Computing (HPC)

KARFS (KAUST Adaptive Reacting Flow Solver)

- **Scalability:** Needs to scale to the full capability of current and future systems such as Shaheen-II (KAUST) and Summit (ORNL)
- **Performance Portable** on multiple architectures such as multi-core, many-core (Xeon Phi) and accelerators (GPU)
- **Extensibility** to multiple applications including fully compressible finite difference DNS, low Mach AMR, etc.
- **Leverage** open source libraries for combustion models and programming abstractions

Shaheen II supercomputer

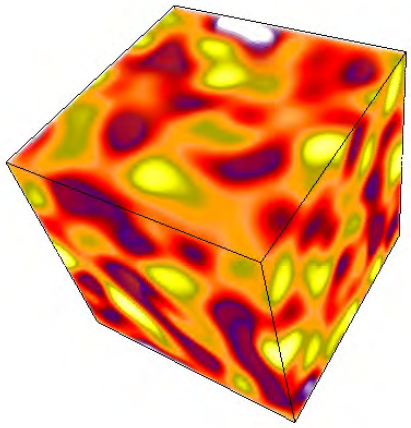

Sample visualization using ViSuS and PIDX

KARFS MPI+X Hierarchical Parallelism

	512x512		1024x1024		2048x2048		3072x3072	
	WT(s)	Acc	WT(s)	Acc	WT(s)	Acc	WT(s)	Acc
1 CPU	180.7	1.0	747.9	1.0	3649.0	1.0	10772.0	1.0
1 MPI x 16 OMP	17.3	10.4	60.0	12.5	243.0	15.0	813.0	13.2
1 MPI x 1 OMP + 1GPU	3.8	47.7	8.4	89.4	-	-	-	-
2 MPI x 8 OMP	40.2	4.5	93.6	8.0	240.0	15.2	437.4	24.6
2 MPI x 8 OMP + 2 GPU	4.2	42.9	7.0	107.4	16.5	221.9	-	-
4 MPI x 4 OMP + 4 GPU	6.6	27.5	7.7	96.7	13.5	270.2	21.1	510.2
8 MPI x 2 OMP + 8 GPU	16.0	11.3	11.8	63.2	27.5	132.9	20.9	515.9

WT: Wall time (sec) per time step
Acc: Acceleration compared to the serial code

- Quiescent test with 30 species, 26-step reduced reaction mechanism for DME
- On a computation node with 32 CPU cores (Intel Haswell) and 8 GPUs (Nvidia K80)

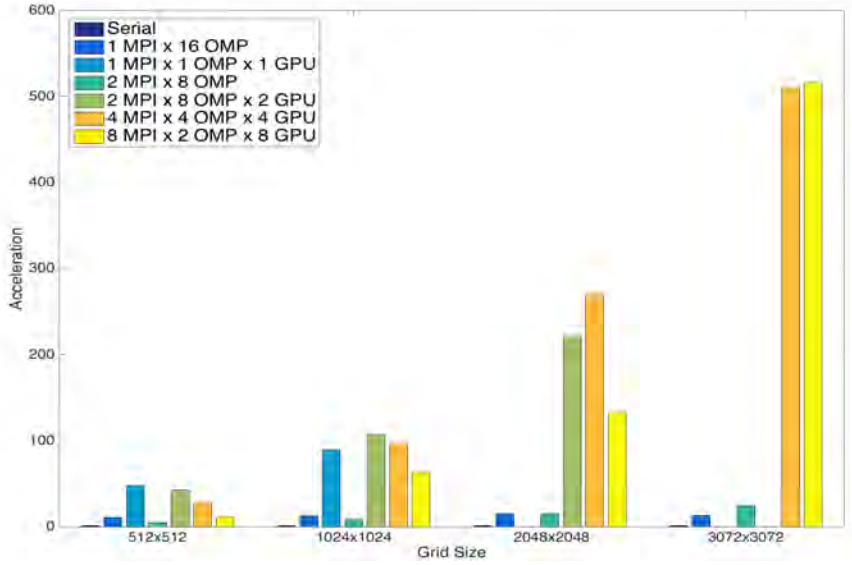

DNS on GPU+ROM Examples

- S3D (Sandia National Laboratory)
  - Time Dependent Bases with CUR Decomposition
- PeleLMeX/PeleC (NREL)
- NekRS (Argonne National Laboratory)
- DeepFlame (Peking University)

Reduced Order High Fidelity Simulation

Classical Approach
(Analytical or Data-based)

ROM Principle

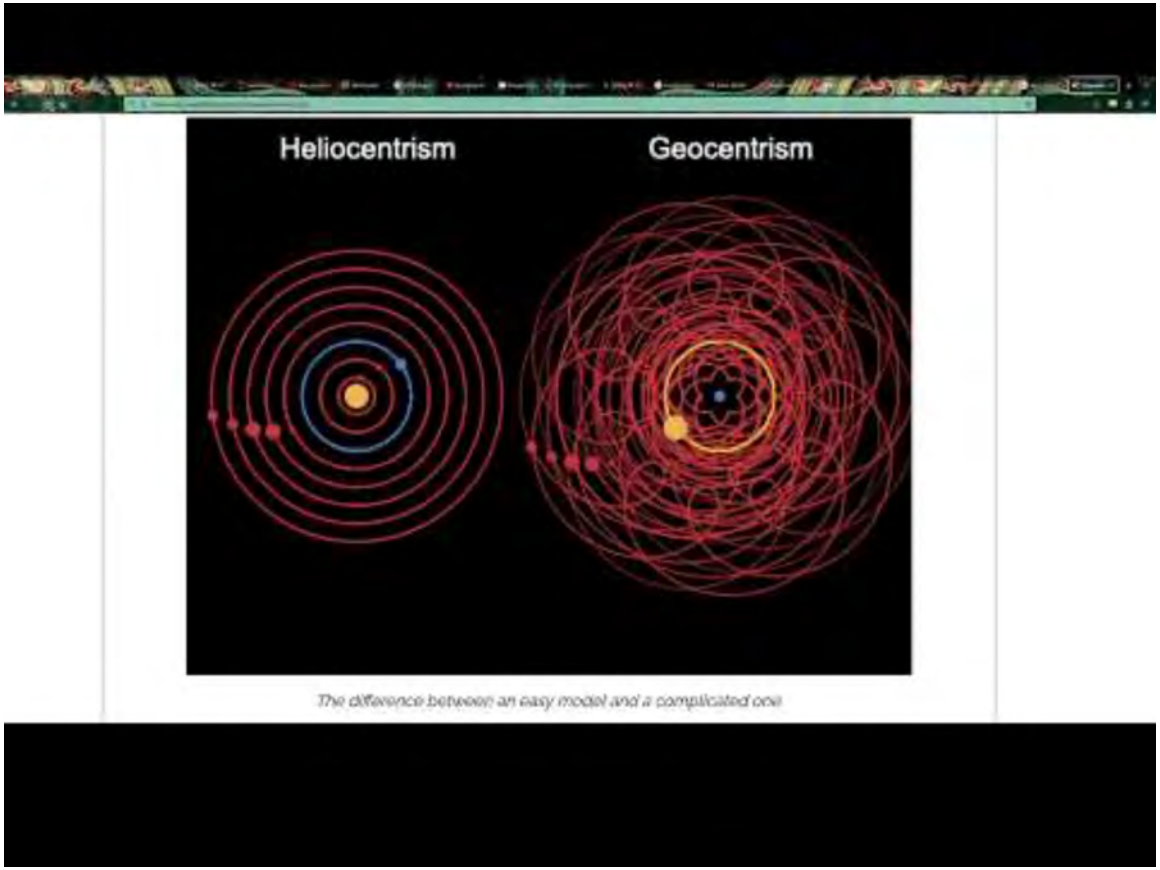

Malin Christersson
https://www.youtube.com/watch?v=pudjM7lP0fg

Principal Component Analysis: Linear Transformation

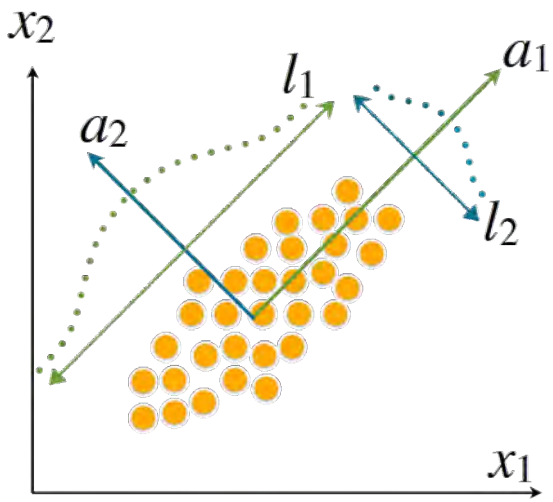

II - PC extraction

$$\mathbf{S} = \frac{1}{n-1}\mathbf{X}^T\mathbf{X}$$

Covariance matrix

$$\mathbf{S} = \mathbf{A}\mathbf{L}\mathbf{A}^T$$

Eigen-decomposition

$$\mathbf{A} = \underset{(p \times p)}{\begin{bmatrix} a_{1,1} & \cdots & a_{1,p} \\ \vdots & \ddots & \vdots \\ a_{p,1} & \cdots & a_{p,p} \end{bmatrix}} \qquad \mathbf{L} = \begin{bmatrix} \lambda_1 & \cdots & 0 \\ \vdots & \ddots & \vdots \\ 0 & \cdots & \lambda_p \end{bmatrix}$$

$$\lambda_1 > \lambda_2 > \cdots > \lambda_p$$

Computation of the Principal Components (PCs)

Finding the right coordinates
Reduction of dimensionality

PCA identifies the direction of maximum variance in the data

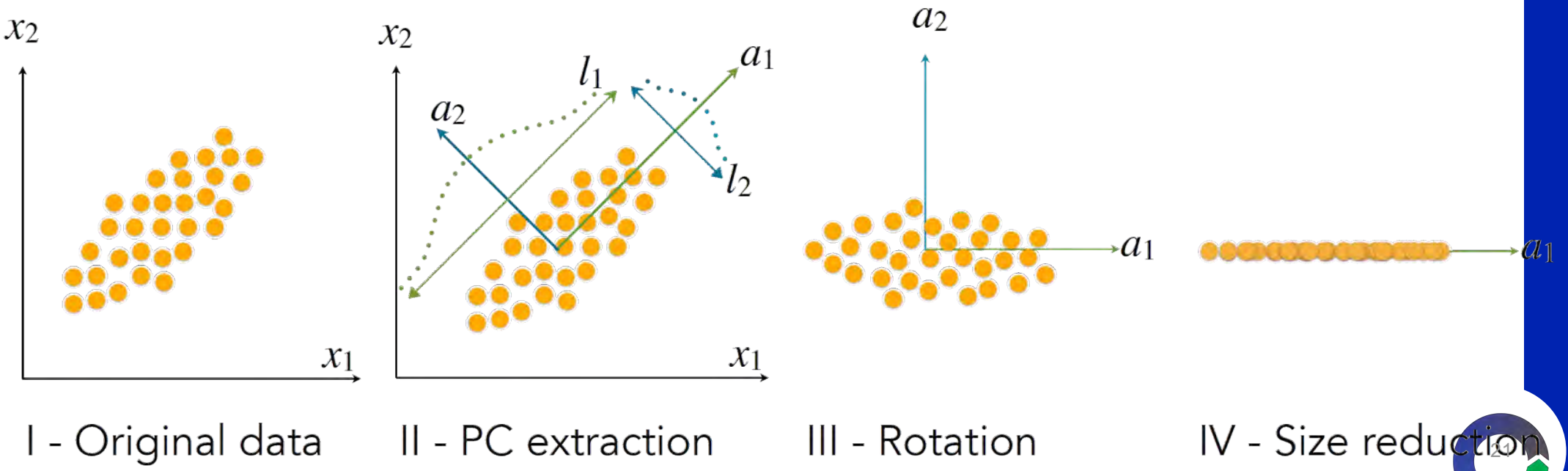

PCs are linear combinations of the original variables

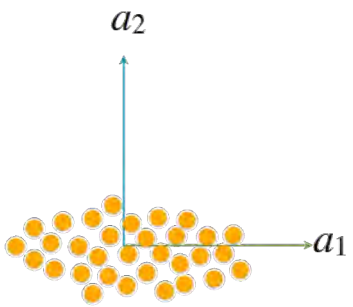

III - Rotation

$$\mathbf{Z} = \mathbf{X}\mathbf{A}$$ Projection

$$z_1 = a_{11}x_1 + a_{21}x_2$$

$$z_2 = a_{12}x_1 + a_{22}x_2$$

Projection on the first q eigenvectors representing most of the system variance ($> 90\%$)

IV - Size reduction

Recovery

$$\mathbf{Z}_q = \mathbf{X}\mathbf{A}_q \longrightarrow \mathbf{X} \approx \mathbf{X_q} = \mathbf{Z_q}\mathbf{A_q}^T$$

The original state-space can be recovered based the first q eigenvectors approximation

Example:
PC basis matrix for a methane/air mixture

$$A = \begin{bmatrix} 0.0265 & 0.5112 & 0.4523 & 0.7299 & -0.0216 \\ 0.1897 & -0.6798 & -0.2262 & 0.6005 & -0.2999 \\ 0.6473 & -0.0077 & -0.1531 & 0.0987 & 0.7400 \\ -0.7371 & -0.1430 & -0.2095 & 0.2734 & 0.5634 \\ 0.0296 & 0.5058 & -0.8227 & 0.1481 & -0.2106 \end{bmatrix} \begin{matrix} H_2O \\ O_2 \\ N_2 \\ CH_4 \\ CO_2 \end{matrix}$$

Mix. Frac.

Extent of reaction

The PCs can be associated to physically interpretable variables

PCA finds the optimal parameterization with no supervision: generalization of tabulation methods

PCA provides the best multi-linear, low-dimensional parameterization of a data set

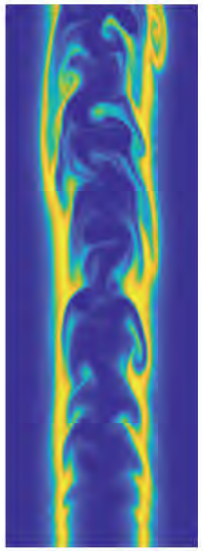

Syngas flame
(Sutherland et al, 2007)

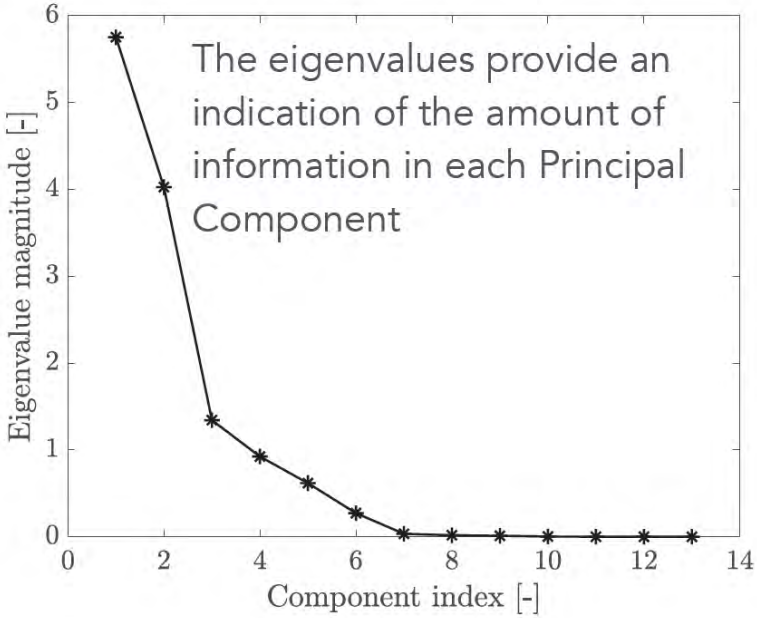

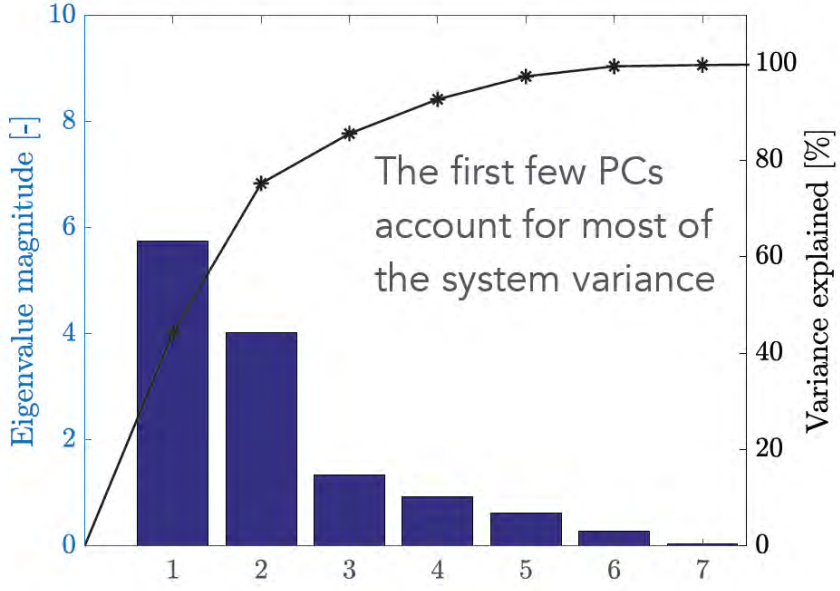

Two PCA-based Approaches

PC-transport

$$\rho \frac{\mathrm{D}\left(\mathbf{y}\right)}{\mathrm{D}t} = -\nabla \cdot \left(\mathbf{j_y}\right) + \left(s_\mathbf{y}\right)$$

$$\mathbf{Z} = \mathbf{Y}\mathbf{A_q}$$

$$\rho \frac{\mathrm{D}\left(\mathbf{z}\right)}{\mathrm{D}t} = -\nabla \cdot \left(\mathbf{j_z}\right) + \left(s_\mathbf{z}\right)$$

J. Sutherland and A. Parente, *Proc Combust Inst* **32** (2009)

Manifold Generated from PCA (MG-PCA)

1. Select and transport q principal variables:

$$\rho \frac{\mathrm{D}\left(\mathbf{y}\left(q\right)\right)}{\mathrm{D}t} = -\nabla \cdot \left(\mathbf{j_y}\right) + \left(s_\mathbf{y}\right)$$

2. Estimate the non-transported variables using a PCA-based projection:

$$\mathbf{Y}_q\left(Q-q\right) = \mathbf{Y}(q)\mathbf{B}\left(Q-q\right)$$

B. Isaac, A. Coussement, O. Gicquel, P. Smith, and A. Parente, Combust. Flame, **161** (2014)

PCA-DNN for LES Application

- Principal Component Analysis (PCA) allows for identifying the direction of maximum variance in the data

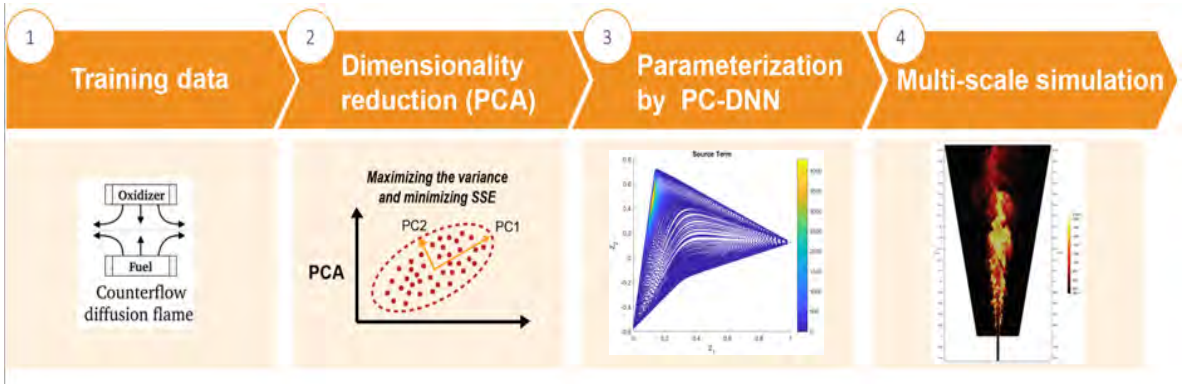

PC-transport Approach:

$$\frac{\partial}{\partial t}(\rho \mathbf{Y_k}) + \nabla(\rho \tilde{\mathbf{u}} \mathbf{Y_k}) = \nabla(\rho \mathbf{D_k} \nabla \mathbf{Y_k}) + \mathbf{R_k} \qquad k = 1, \ldots, n_s$$

(**ns** transport equations)

$$\mathbf{Z} = \mathbf{Y}\mathbf{A_q}$$

($q << n_s$)

dimension reduction

$$\frac{\partial}{\partial t}(\rho \mathbf{z}) + \nabla(\rho \tilde{\mathbf{u}} \mathbf{z}) = \nabla(\rho \mathbf{D_z} \nabla \mathbf{z}) + \mathbf{S_z}$$

(**q** transport equations)

A is the basis matrix (ns PCs)
$\mathbf{A_q}$ is the truncated basis matrix (q PCs)
Z principal component scores

J.C. Sutherland and A. Parente, Proc. Combust. Inst., 32 (2009)

Extended manifold

- To account for the NH3/H2 ratio change

Baseline manifold

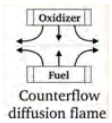

Single NH_3/H_2 ratio (1.716)

NH3(Vol.)	H2(Vol.)	N2(Vol.)
0.563	0.328	0.109

Extended manifold

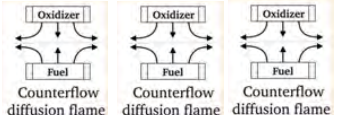

Different NH_3/H_2 ratios (1.716, 1.802, and 1.886)

- Only 2 PCs are required in the extended manifold as well

Computational Singular Perturbation (CSP)

*Finding slow invariant manifolds (SIM) in **Time*** *Lam and Goussis, 1989*

- Automated computational algorithm to decompose characteristic time scales of a dynamical system.
- For species and energy equations

Original form of the system:

$$\frac{d\boldsymbol{z}}{dt} = \boldsymbol{g}(\boldsymbol{z}), \quad \boldsymbol{z} \in \mathbb{R}^{N+1}$$

z: N+1 state vectors (*T* and Y_i)
g: chemical source terms

CSP form of the system:

$$\frac{d\boldsymbol{z}}{dt} = I \cdot \boldsymbol{g} = A\,(B \cdot \boldsymbol{g}) = \sum_{i=1}^{N+1} \boldsymbol{a}_i\, f^i = \sum_{r=1}^{M} \boldsymbol{a}_r\, f^r + \sum_{s=M+1}^{N+1} \boldsymbol{a}_s\, f^s.$$

Mode timescales: $\tau_1 < \cdots < \tau_M \ll \tau_{M+1} < \ldots < \tau_N$

Fast subspace — Slow subspace

$$\tau_i = \frac{1}{|\lambda_i|}$$

$$\frac{d\boldsymbol{z}}{dt} \approx \sum_{s=M+1}^{N+1} \boldsymbol{a}_s\, f^s = \left(\sum_{s=M+1}^{N+1} \boldsymbol{a}_s\, \boldsymbol{b}^s \right) \boldsymbol{g} = P\,\boldsymbol{g}$$

$$f^r \approx 0 \qquad r = 1, \ldots, M$$

$$f^i = \boldsymbol{b}^i \cdot \boldsymbol{g},$$

$$\mathbf{b}^i \cdot \mathbf{a}_j = \delta^i_j$$

$$\boldsymbol{z}(t_{n+1}) = \boldsymbol{z}^* - \sum_{r=1}^{M(\boldsymbol{z}^{\mathcal{M}})} \boldsymbol{a}_r(\hat{\boldsymbol{z}})\, f^r(\hat{\boldsymbol{z}}, \boldsymbol{z}^*)\, \tau^r(\hat{\boldsymbol{z}})$$

Radical correction

$\mathbf{a}_n$: CSP column basis vector of the *n*-th mode (approx. right eigenvector of the Jacobian of **g**)

$\mathbf{b}^n$: CSP row basis vector of the *n*-th mode (approx. left eigenvector of the Jacobian of **g**)

f^n: amplitude of the *n*-th mode

δ^i_j: Kronecker delta

CSP Mode Analysis

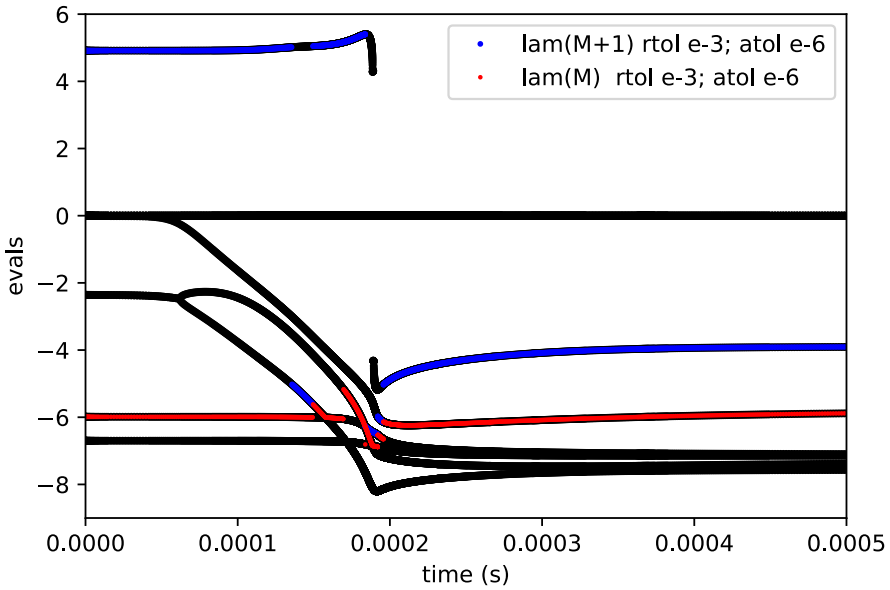

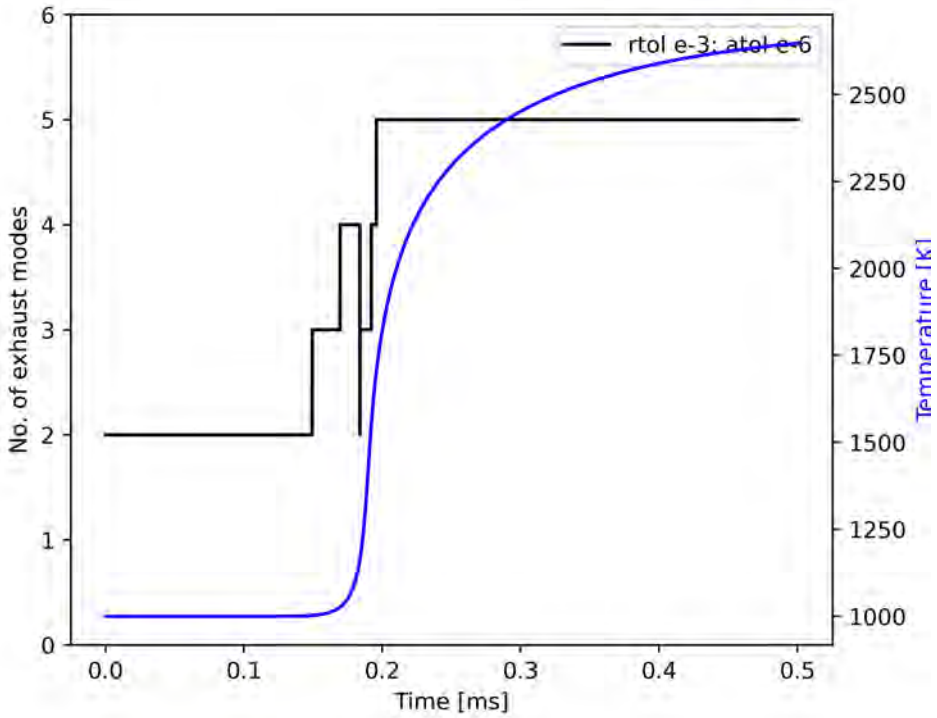

The CSP Solver: Principles

Physics-based adaptive solver (CSP)

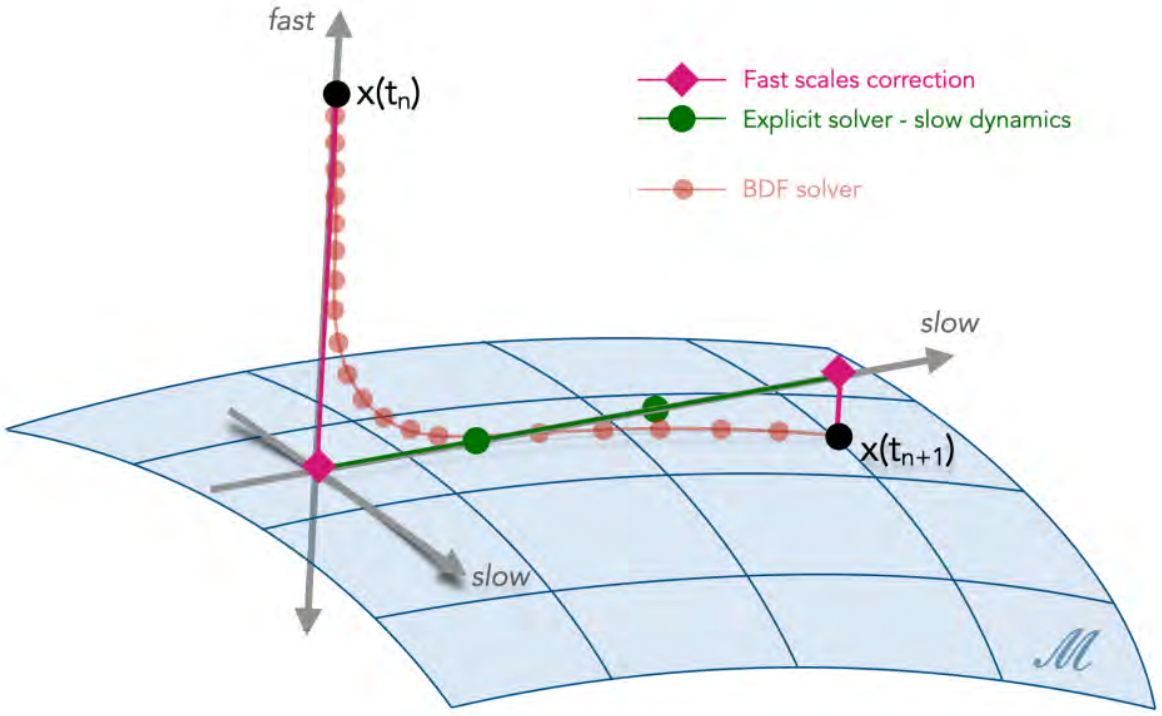

local ROM free of fast scales

explicit integration with large time steps

system evolves on a slow manifold

…but projection basis requires the eigensystem of Jacobian

expensive if N is large

R. Malpica Galassi et al., Journal of Computational Physics, 2022.

The CSP Solver Algorithm

1) Compute the CSP basis $\mathrm{J} = \frac{\partial \mathrm{g}}{\partial \mathrm{z}}$

2) 1st radical correction $\boldsymbol{z}^{\mathcal{M}}(t) = z(t) - \sum_{r=1}^{EM} \boldsymbol{a}_r f(z)^r \tau^r$

3) Compute # of exhausted modes (EM)

4) Build the Slow Projection Matrix $P(t) = I - \sum_{r=1}^{EM} \boldsymbol{a}_r \boldsymbol{b}^r$

5) Explicit integration of slow modes $\frac{d\boldsymbol{z}}{dt} = \sum_{s=EM+1}^{N+1} \boldsymbol{a}_s f^s = P \cdot \vec{g}(\boldsymbol{z}^{\mathcal{M}})$

6) 2nd radical correction to apply fast scales and get back onto manifold $\boldsymbol{z}\,(t+\delta t) = \boldsymbol{z}^*(t+\delta t) - \sum_{r=1}^{EM} \boldsymbol{a}_r f(z^*)^r \tau^r$

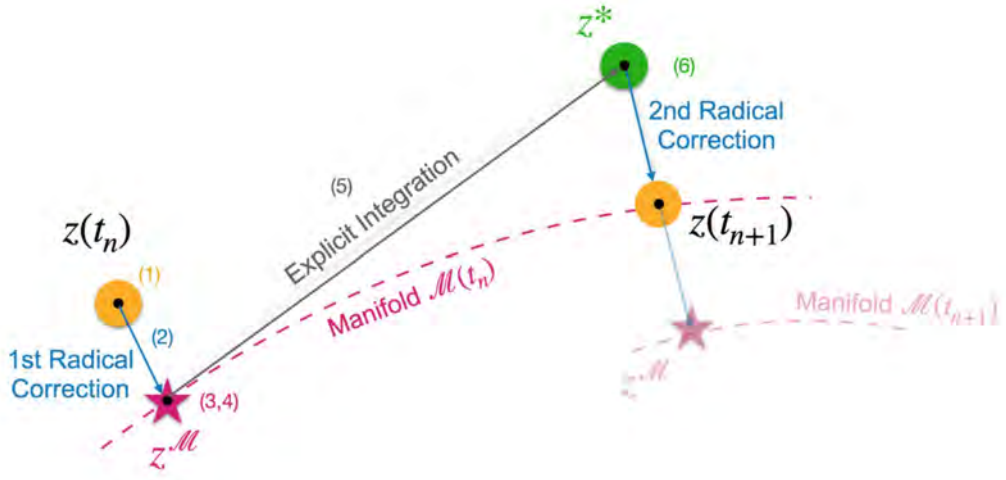

R. Malpica Galassi et al., Journal of Computational Physics, 2022.

CSP algorithm with ANN

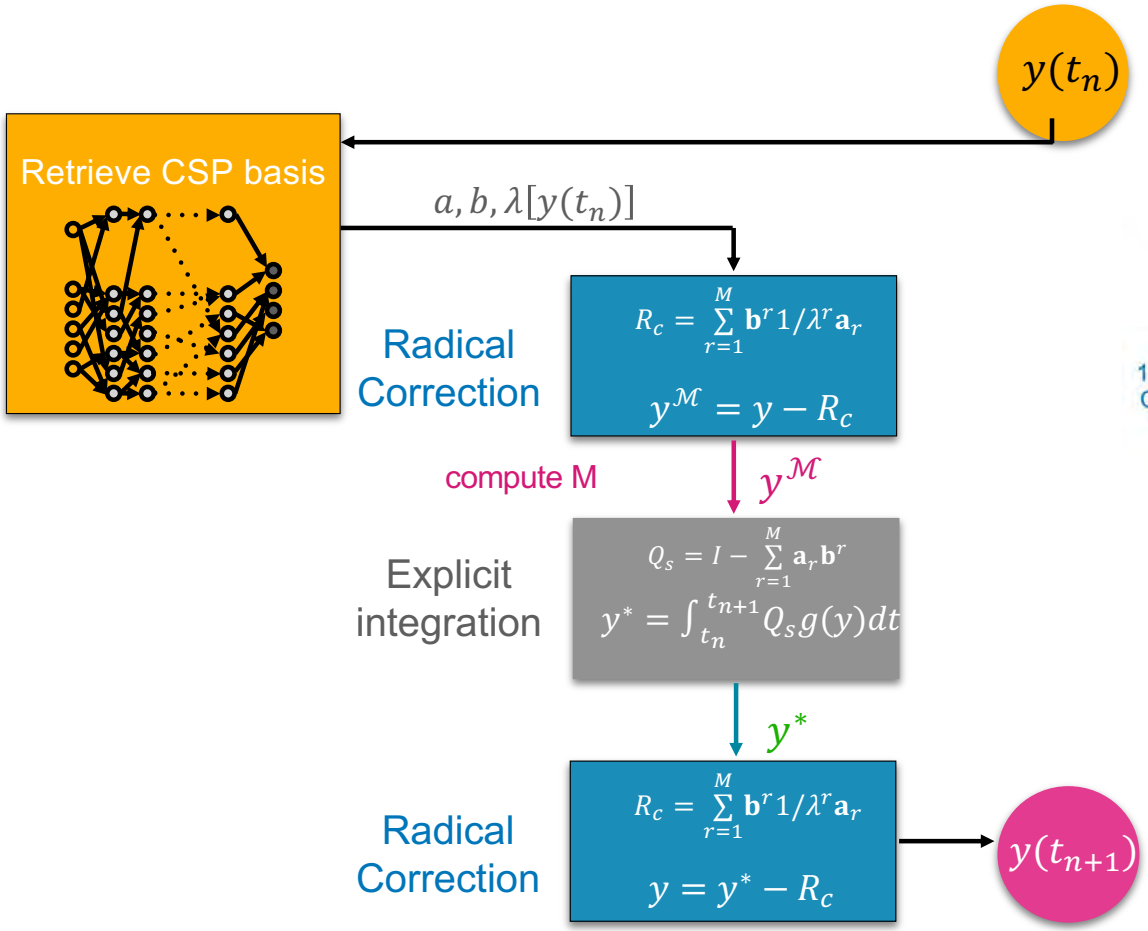

Malpica Galassi et al., JCP 451, 110875 (2022)

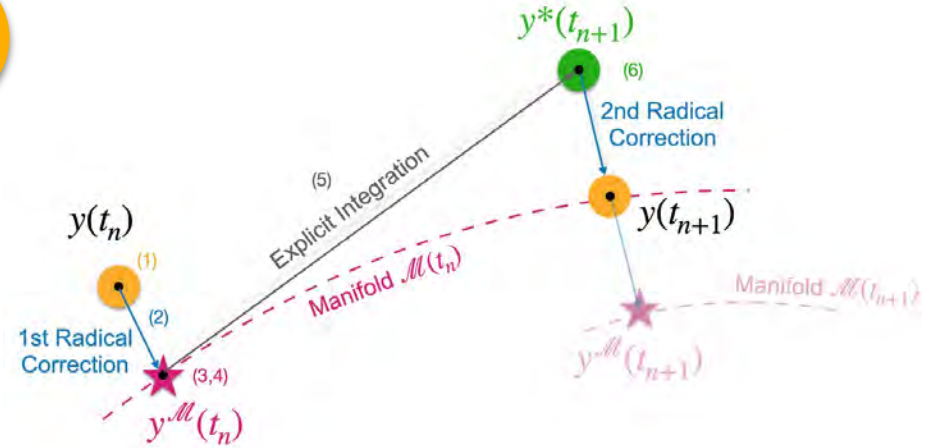

- **ANN** reconstructs the **projection basis**
  - Not the source term
  - Not the state at following time

  ⇒ Physically informed construction
- Errors in ANN reconstruction are contamination of fast/slow scales

⇒ May affect computational efficiency, but **do not** affect the solution accuracy.

Validation of CSP Solver Accuracy

- Integration accuracy is high
- Only the slow dynamics is resolved
- *M* represents the adaptivity (how many fast scales, locally)
- Timesteps are larger compared to CVODE

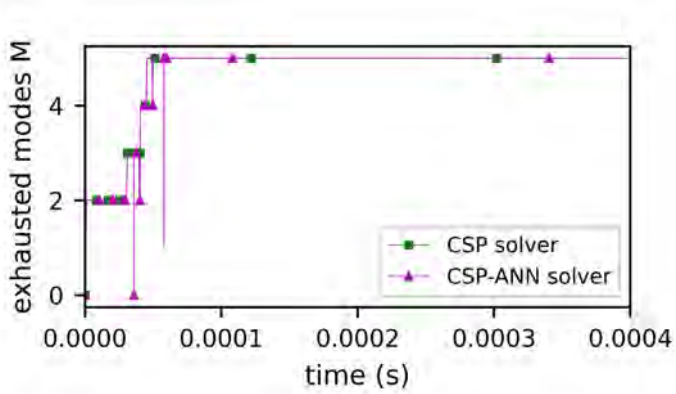

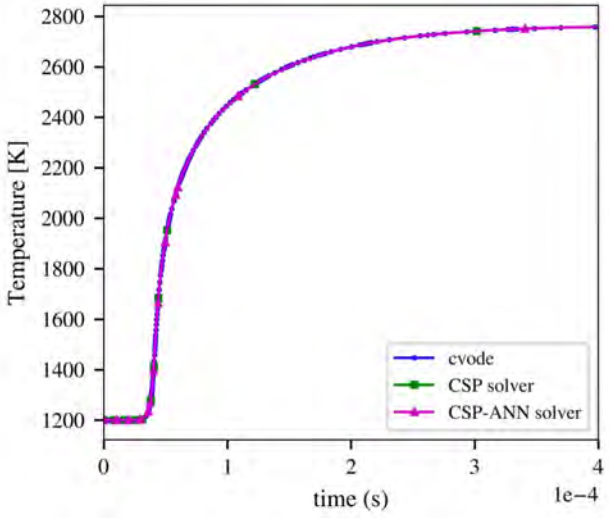

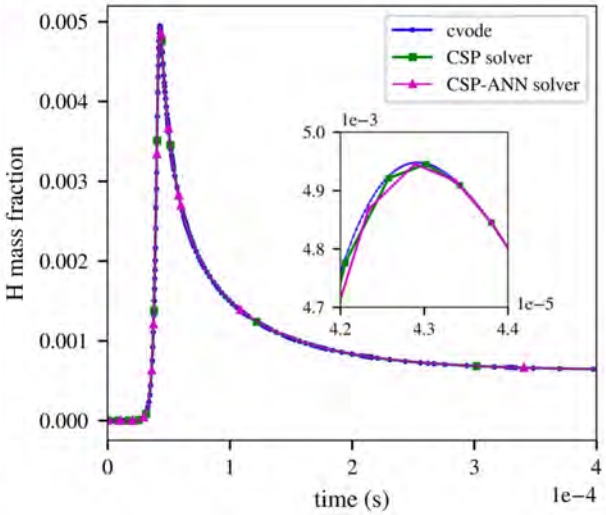

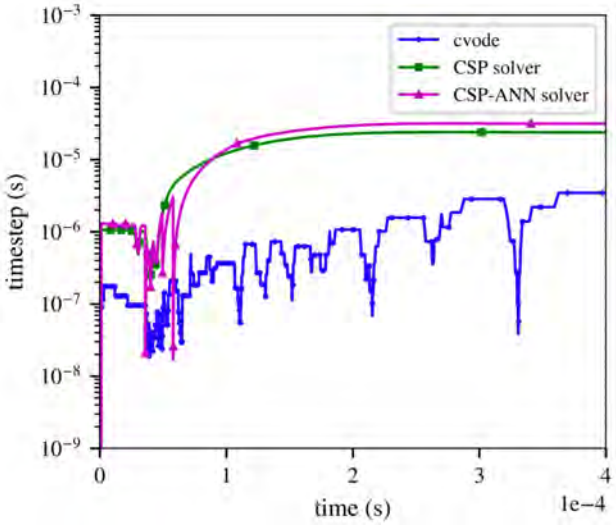

The CSP Basis Computational Overhead

- The computational cost of the CSP bases can overshadow the advantages offered by the solver

- The CSP bases are state functions ⟹ tabulation

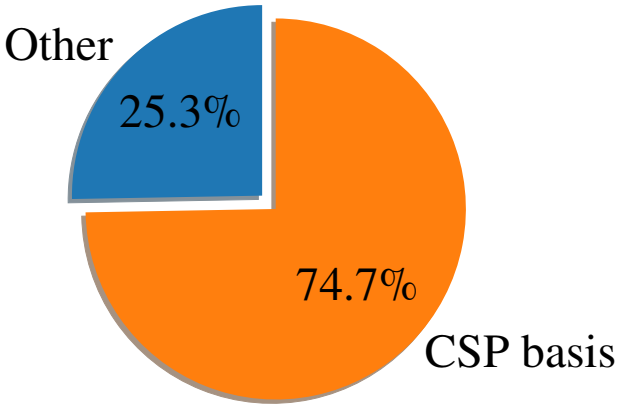

Ammonia-air mechanism
38 species and 263 reactions
(*Zhang*, et al. 2021)

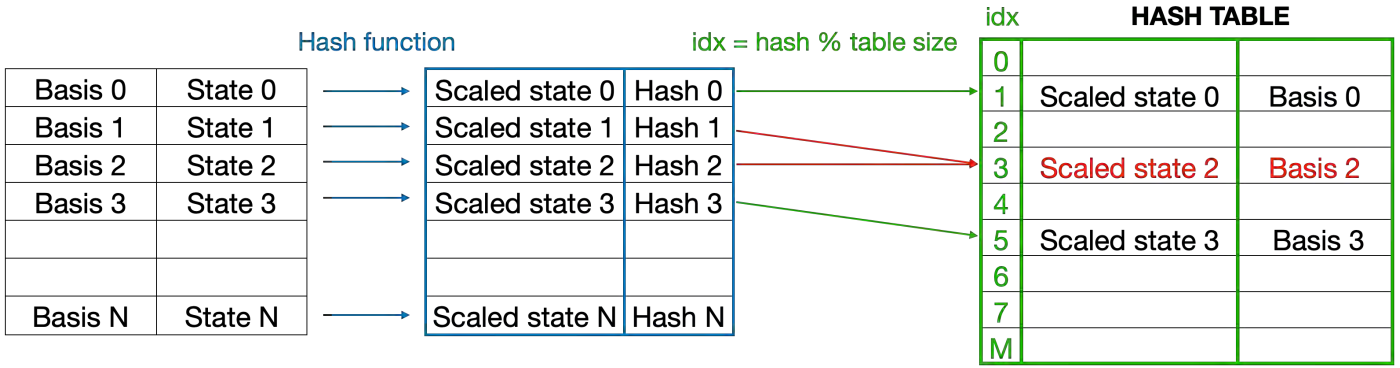

Can we implement the logic of a hash table "without" a hash table?
(no additional memory allocation, no deep copies, no collisions to handle)

Online Quantized-State Hash Mapping

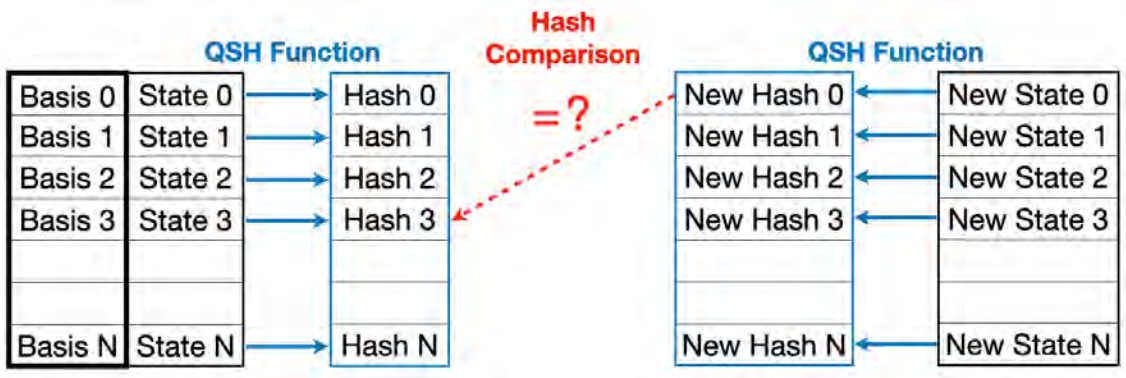

Hash map evolution
(2D flame-vortex interaction)

- Once the initial dataset has been hashed, the hash map is ready
- L2-norm error between old and new states for basis assignment
- Indexing is not necessary ⟹ No collisions to handle!
- No additional memory allocation or deep copies necessary
- Fully parallelizable and scalable

CSP Solver with *Online* QSH Mapping

3D flame-turbulence interaction (ammonia-air 38 species)

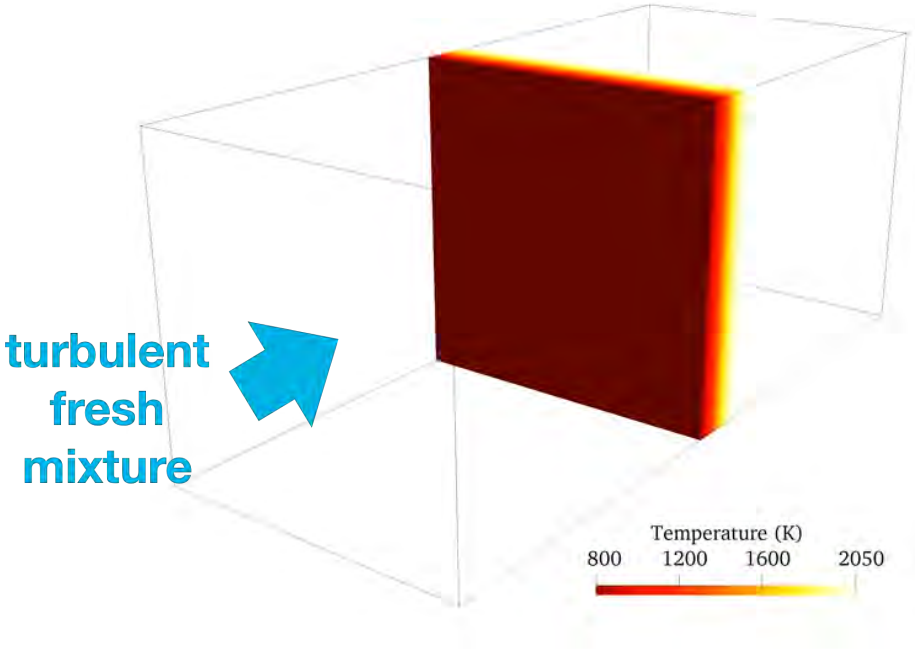

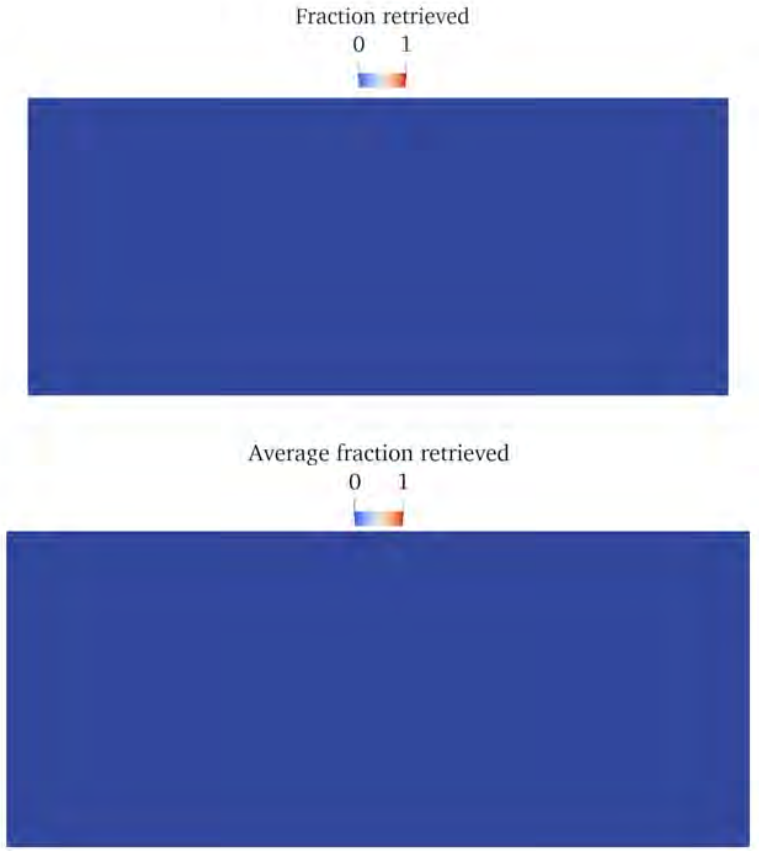

CSP Solver with *Online* QSH Mapping: Accuracy

3D flame-turbulence interaction (ammonia-air 38 species)

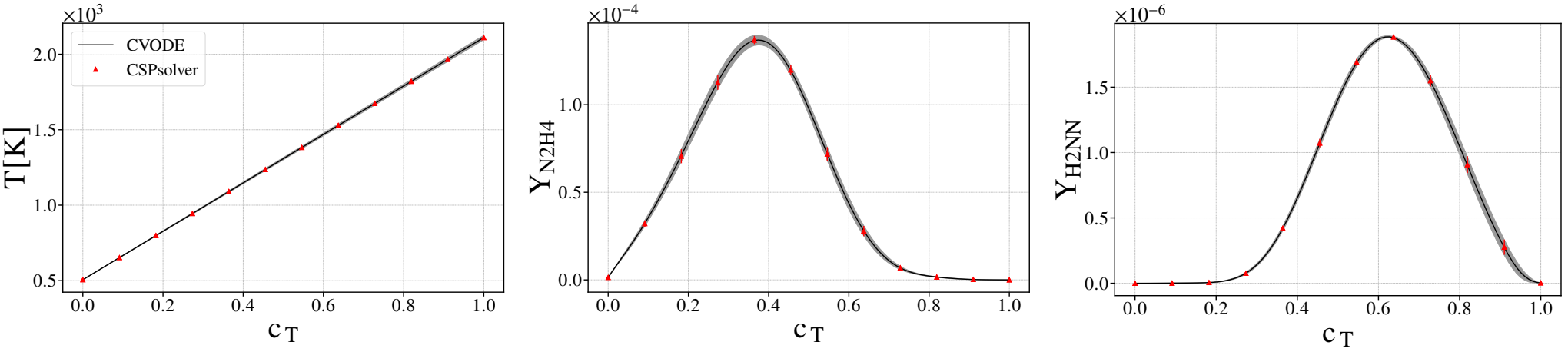

- Comparison of conditional averages of minor species as a function of the temperature-based progress variable
- Baseline: CVODE ($rtol = 10^{-9}, atol = 10^{-14}$)

CSP Solver with *Online* QSH Mapping: Performance

3D flame-turbulence interaction (ammonia-air 38 species)

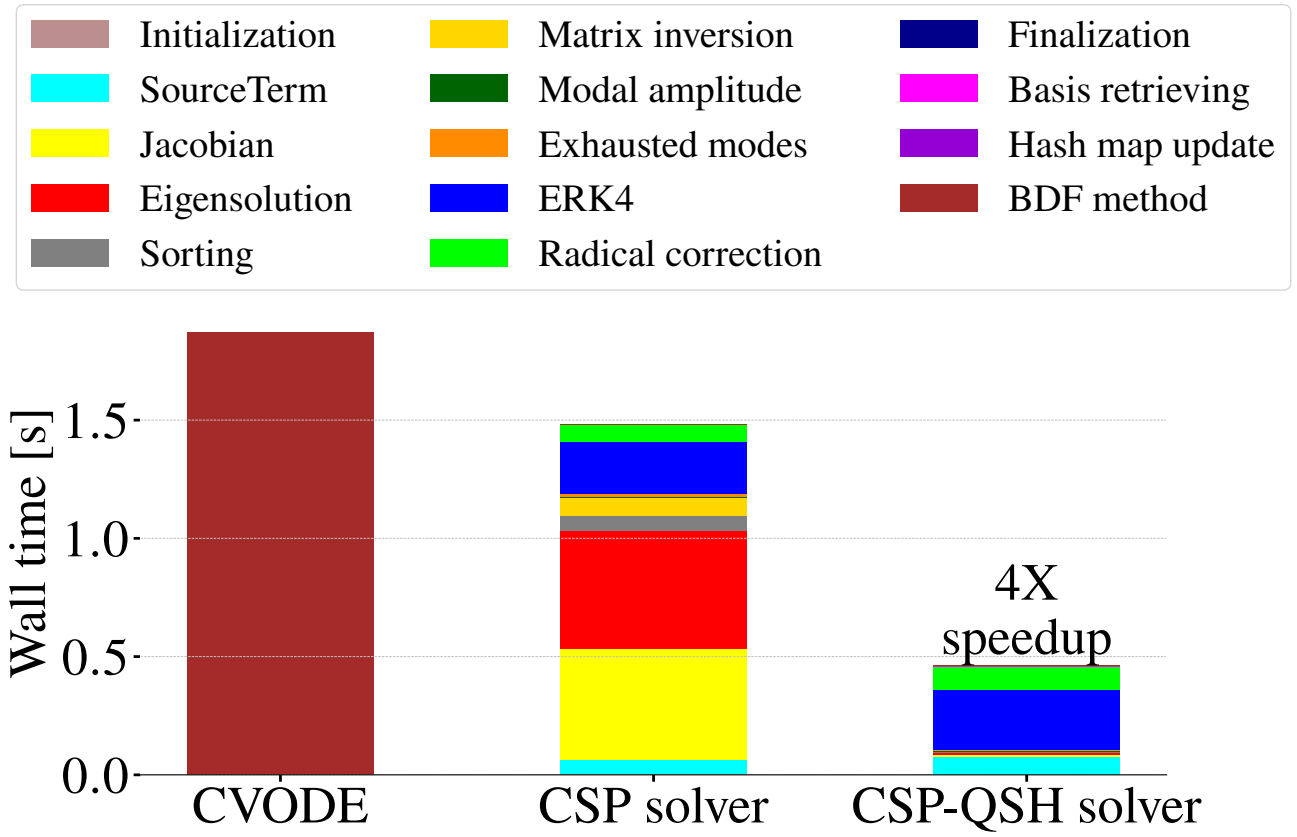

Combined CSP-PCA Solver

Malik et al., PROCI, 2024

- **PCA**, **CSP**, and other methods have been developed for **dimensional** and **time-scale ROM** development
- No rigorous approach exists to **achieve both dimensional and time scale reductions** simultaneously
- We combine the best of both worlds, by a **double PCA-CSP projection** to achieve significant computational acceleration
- 2 ways of achieving this:
  - ***Constrained* Jacobian** approach
  - ***Latent* Jacobian** approach

Combined CSP-PCA Solver – Latent Jacobian

- Two consecutive mappings: first into the PCA latent space, next to the CSP latent space:

$$\boldsymbol{x} \in \mathbb{R}^N \xrightarrow{\boldsymbol{A}_q} \boldsymbol{z} \in \mathbb{R}^{q<N} \xrightarrow{\boldsymbol{L}_{Z_q}} \boldsymbol{\eta} \in \mathbb{R}^{a<q}$$

- The physical Jacobian is replaced by the latent Jacobian:

$$\boldsymbol{J}_{Z_q} = \boldsymbol{A}_q^t \boldsymbol{D}^{-1} \boldsymbol{J} \boldsymbol{D} \boldsymbol{A}_q \quad \in \mathbb{R}^{q<N}$$

- When the PCA basis is not truncated ($q=N$), the CSP-PCA latent variables coincide with the CSP latent variables
- When the PCA basis is truncated ($q<N$), $N-q$ degrees of freedom are lost
- The truncated PCA mapping reduces the cost of the CSP basis of the order of $(N/q)^3$
- Only the *active* PCA-CSP latent variables are evolved in time

Malik et al., 2024, Int. Symp. Comb.

Combined CSP-PCA Solver – Performance

Homogeneous reactor, NH_3 (36 species mechanism)

Full system: N = **37** (species + T)
Latent system: q = **27** (PCA scores)

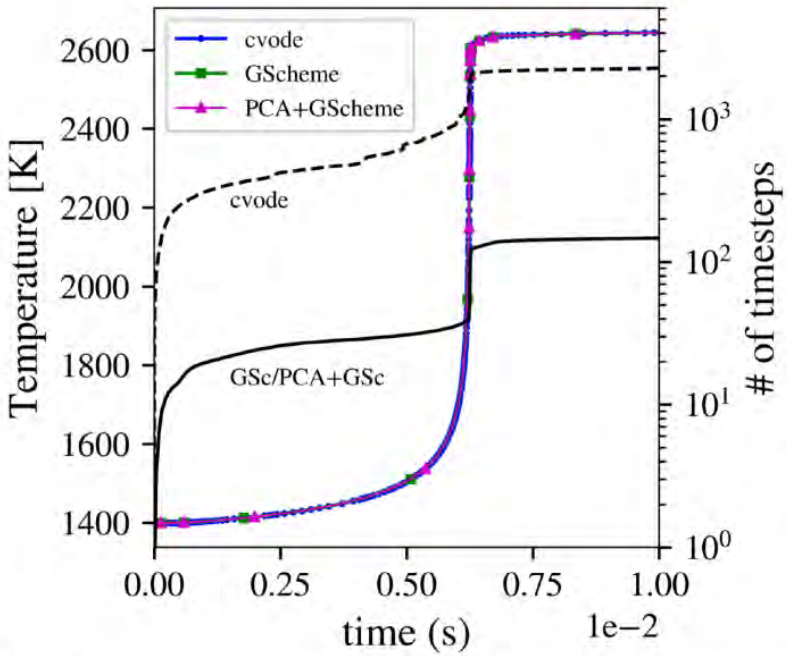

PCA/G-Scheme is accurate despite not explicitly resolving the fast/slow scales and the PCA truncation error.

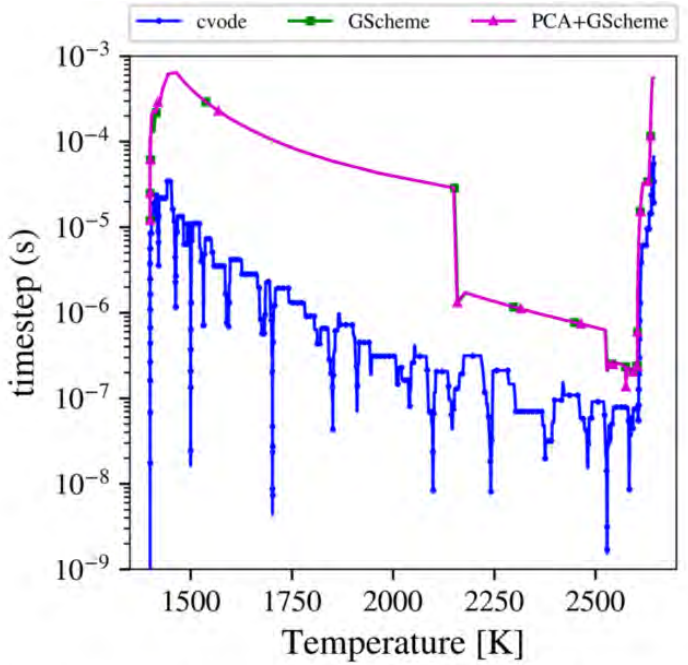

Two orders-of-magnitude improvement in time step size, absence of initialization overhead.

Malik et al., 2024, Int. Symp. Comb.

Local PCA adds a second hyperparameter to PCA besides the number of eigenvalues, i.e., the number of clusters

The manifold is divided into **clusters**, each one of them having its **own basis** (i.e. eigenvectors)

Local PCA allows reducing the dimensionality required to attain a fixed error threshold

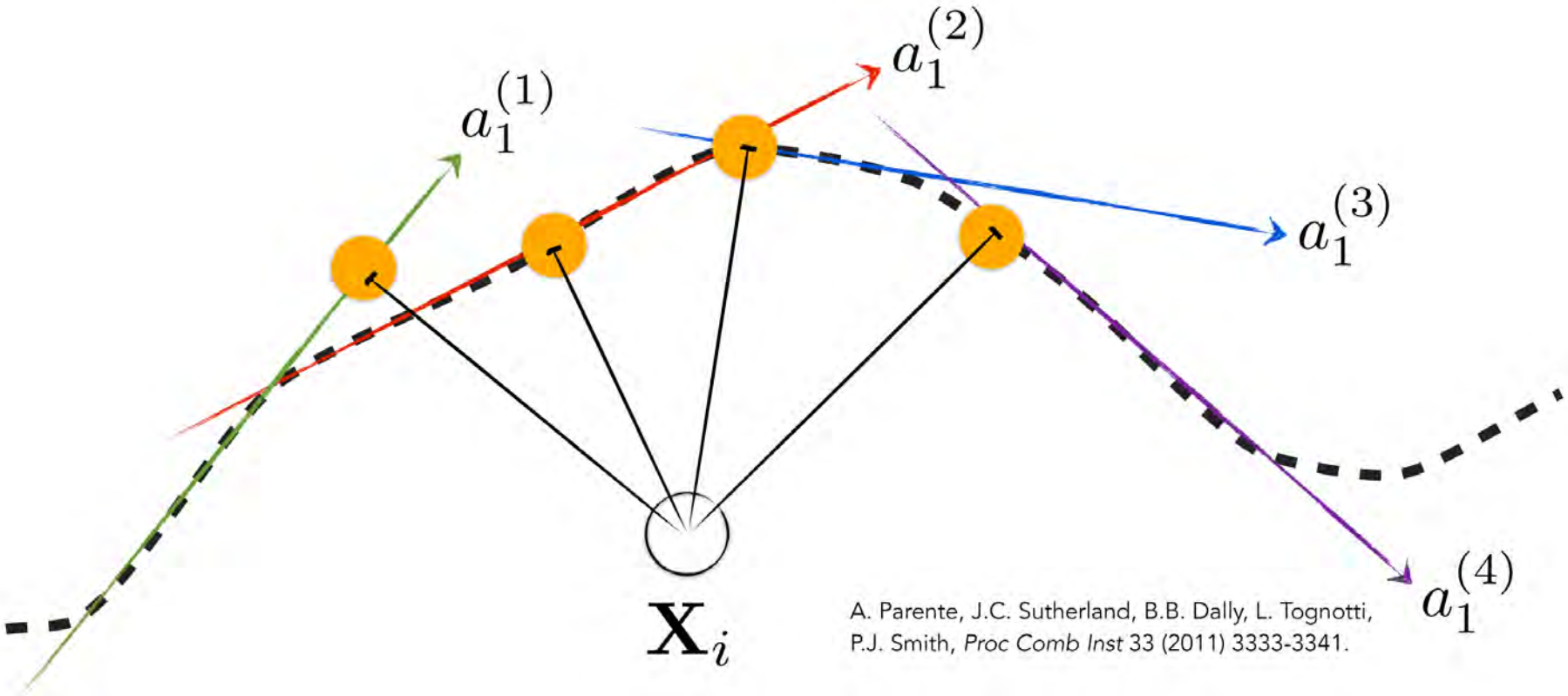

A. Parente, J.C. Sutherland, B.B. Dally, L. Tognotti, P.J. Smith, *Proc Comb Inst* 33 (2011) 3333-3341.

Combining CSP Solver with Local PCA

Homogeneous reactor, nC_7H_{16} (654 species mechanism)

- The definition of the transported variables (i.e. PC scores) changes over time
- Larger reduction obtained by solving for the most appropriate variables at each timestep

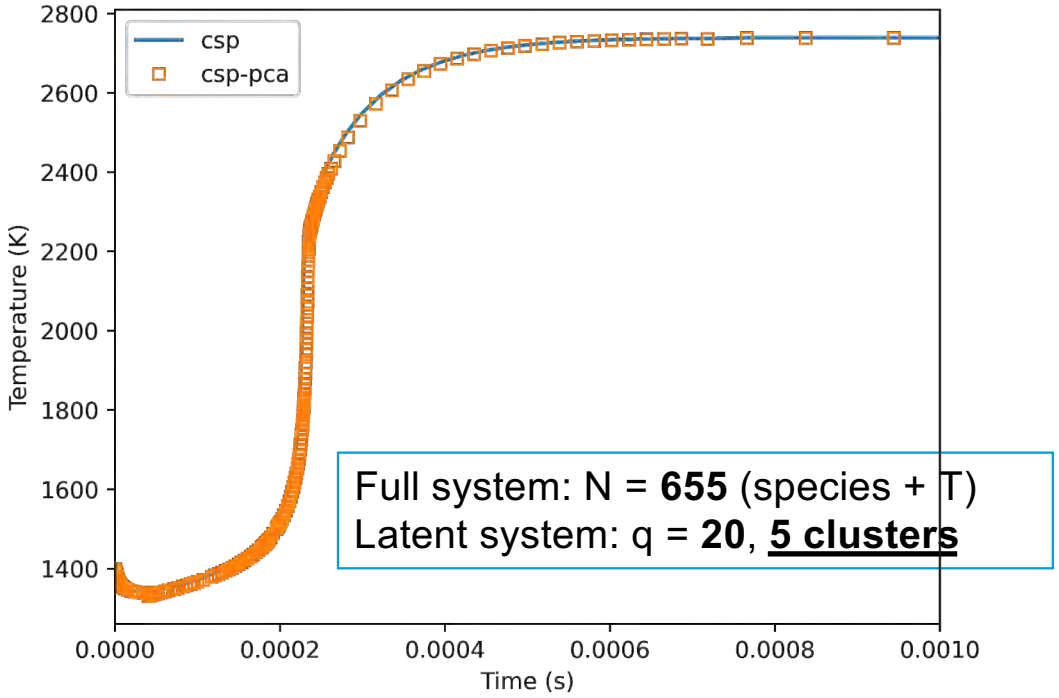

Full system: N = **655** (species + T)
Latent system: q = **20**, **5 clusters**

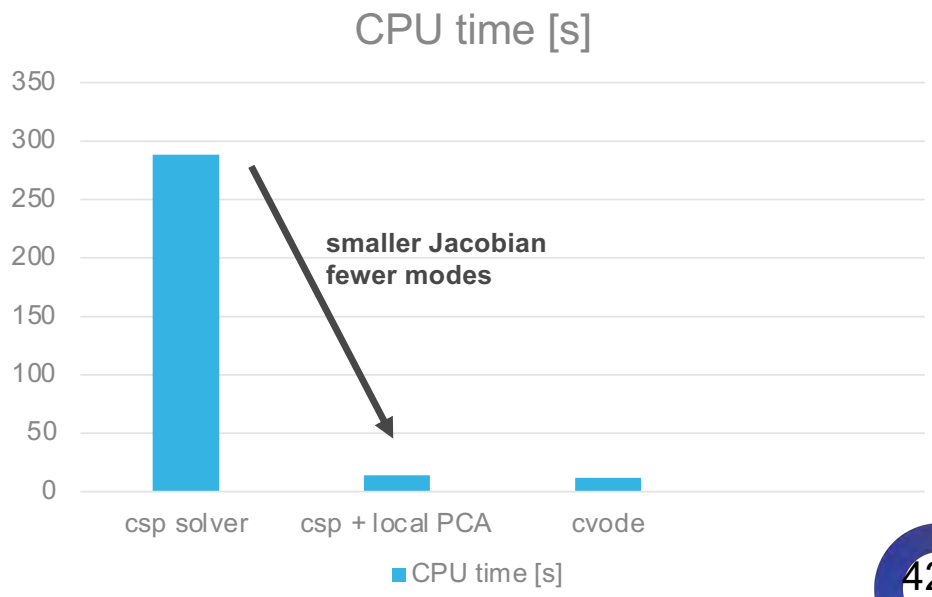

Summary

- HPC enabled DNS of laboratory scale flames with uncompromised fidelity.
  - Reduced kinetic mechanism
  - CPU/GPU parallelism
- Classical reduced order models for high fidelity simulations:
  - Principal Component Analysis
    - – Dimensionality reduction
    - - Data-based approximation
  - Computational Singular Perturbation
    - - Temporal stiffness reduction
    - - Rigorous if done right
  - Combined PCA-CSP

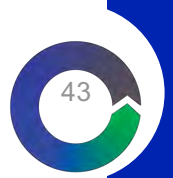

جامعة الملك عبدالله للعلوم والتقنية
King Abdullah University of Science and Technology

Clean Energy Research Platform

Tsinghua-Princeton-Combustion Institute
2025 Summer School on Combustion
Tsinghua University, July 7-11, 2025

Turbulent Combustion

Day 5: AI for Fluid Dynamics and Combustion

Hong G. Im
Clean Energy Research Platform (CERP)
King Abdullah University of Science and Technology (KAUST)

Machine Learning (ANN) Basics

Data Availability & Data-Driven Approach

Many ML algorithms such as DNN are not new. Why is the surge in AI/ML research in (combustion) science?

- Large amount of data
- Computational power to generate detailed high-fidelity data
- Progress in theory and modeling
- Availablity of software tools (TensorFlow, Keras, etc.)
- Newer algorithms: pattern recognition, regression, clustering, optimization

Classification of ML Algorithms

Machine learning

Supervised learning

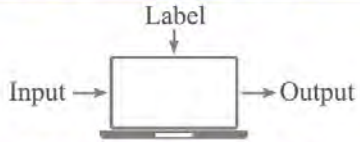

Relate labeled input to unknown output

Classification	Regression
Logistic regression	*Linear regression*
Classification trees	*Regression trees*
Random forests	*Random forests*
Neural networks	*Neural networks*
Support vector machines	*Gaussian processes*

Applications

- *Representation of fuel properties, thermochemical response functions, and potential energy surfaces*
- *Parameterization of combustion manifolds*
- *Prediction of risk occurrence and critical events*
- *Combustion-closure modeling*

Unsupervised learning

Identify pattern and discover structures

Clustering	Dimensional reduction
Gaussian mixture models	*Principal component analysis*
K-means	*Factor analysis*
Mean shift	*Autoencoder*
Spectral clustering	*Stochastic neighbor embedding*

Applications

- *Characterization of combustion regimes*
- *Identification of low-dimensional manifolds*
- *Discovery of structures and coherent features*
- *Detection of anomalies and faults*
- *Signal processing*

Semi-supervised learning

Learn from partially labeled data or through interaction with environment

Reinforcement learning	Generative approaches
Q-learning	*Generative adversarial network*
State-action-reward-state-action	*Variational autodecoders*
Deep Q-learning	*Boltzmann machine*
Deep deterministic policy gradient	

Applications

- *Optimization and control of combustion systems*
- *Data augmentation and data generation*
- *Generative combustion modeling*
- *Robust combustion modeling*
- *Operation with incomplete data*

Ihme et al., PECS 91, 101010 (2022)

Supervised Learning

Mapping between labeled input and the target variable

- Classification tools: support vector machines, discriminant analysis, Naïve Bayes, nearest neighbor
- Regression tools: linear regression, ensemble methods, regression trees, neural networks

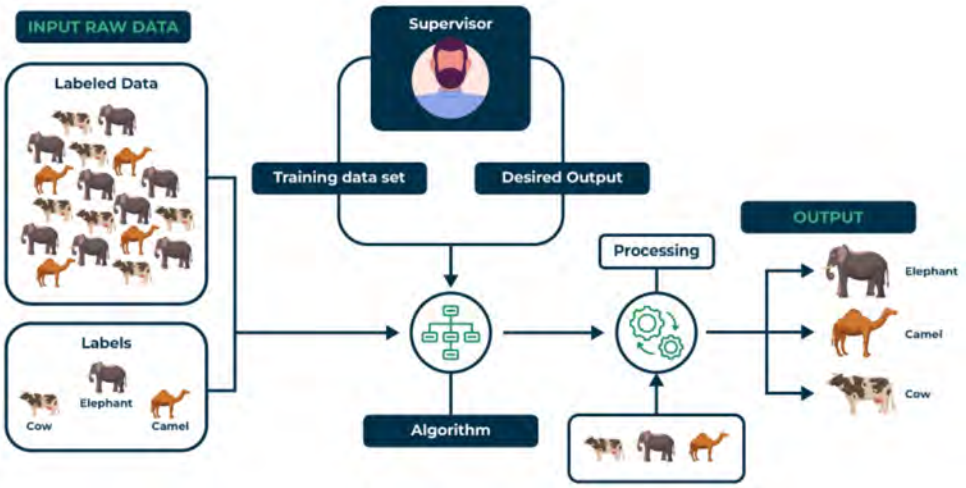

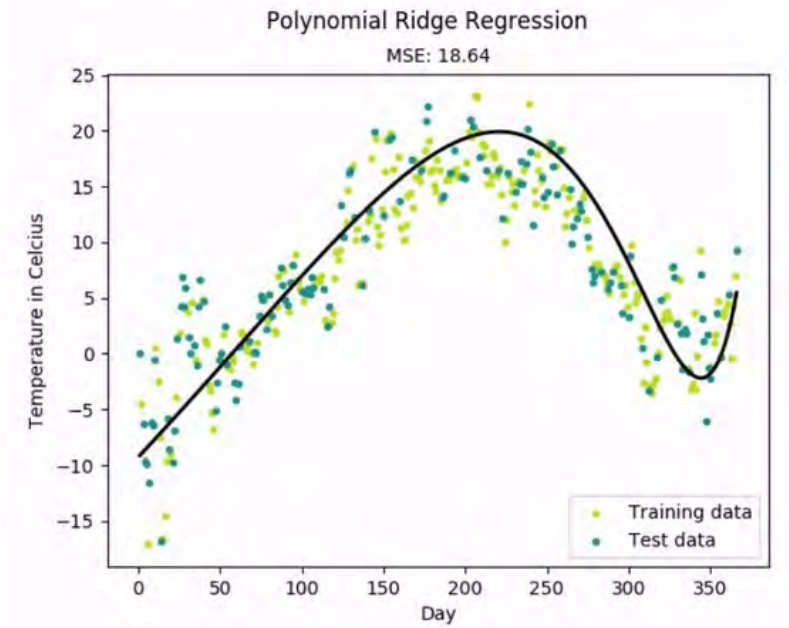

Overfitting

- Overfitting occurs when the model describes random errors or noise instead of the underlying physical relationship.
- Overfitting generally happens when a model is excessively complex with too many parameters relative to the number of data points.
- One way to avoid it is k-fold cross-validation

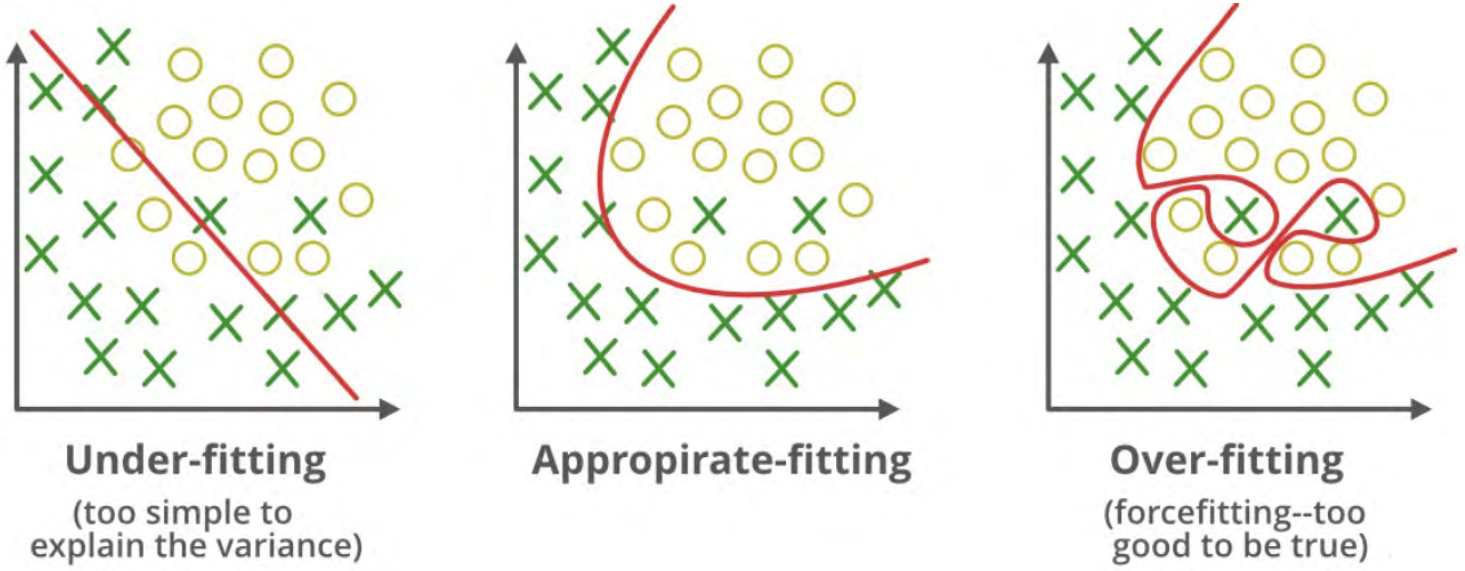

K-Fold Cross-Validation

- Break down data set into k segements
- Rotate with different segments for training and testing.

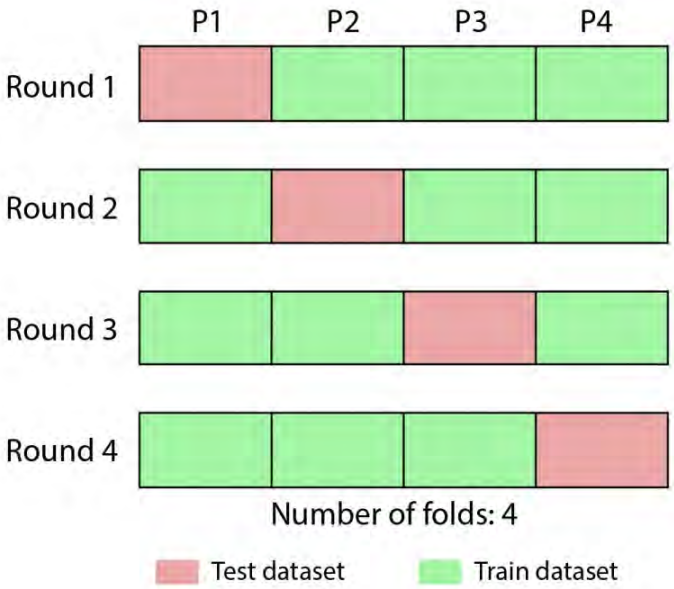

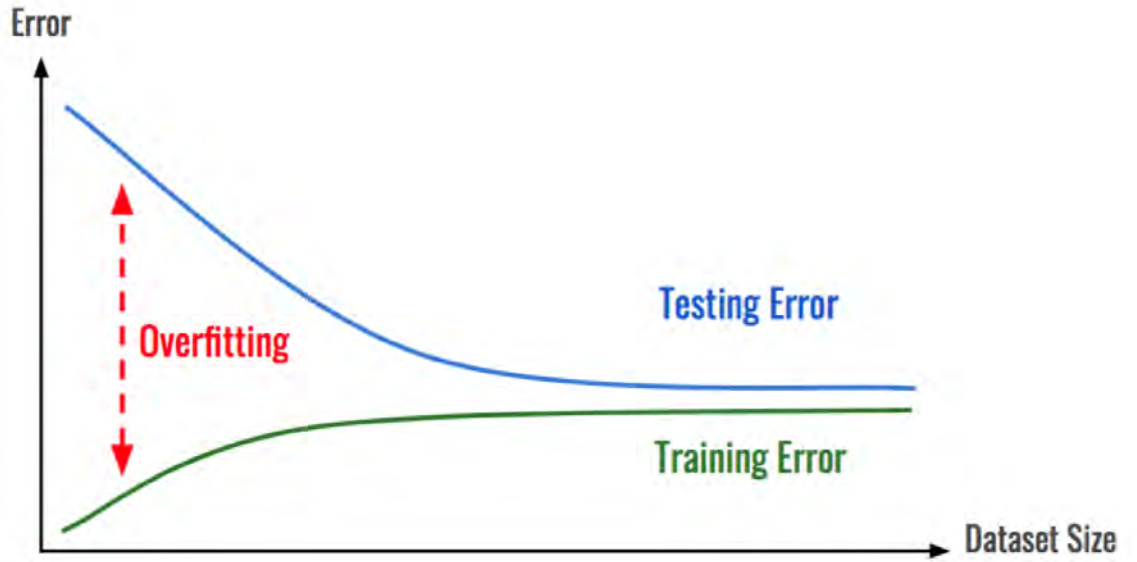

Unsupervised Learning

- Unsupervised learning algorithms are tasked to find patterns and relationships with the data without any prior knowledge or labels.
- Requires an “interpretation” stage, requiring ”clustering” algorithms: K-means clustering, hierarchical method, Gaussian mixture, neural networks, hidden Markov model, data dimensionality reduction: PCA, POD, autoencoders

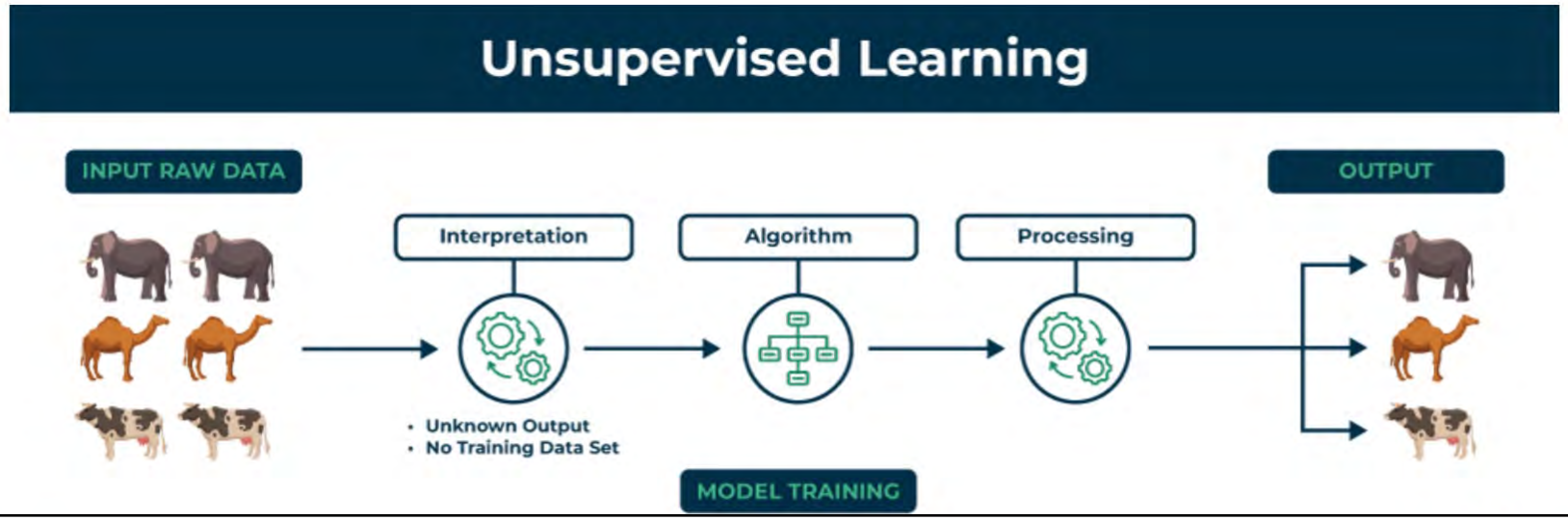

Reinforcement Learning (Semi-supervised)

- An agent operates in an environment and learns to operate using feedback
- Reinforcement learning algorithms interact with an environment, so there is a feedback loop between the learning system and its experiences.

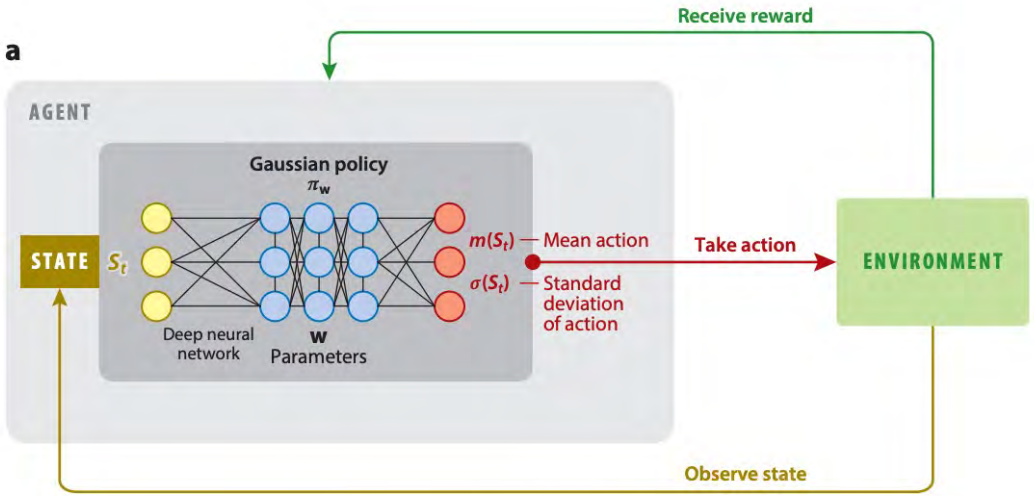

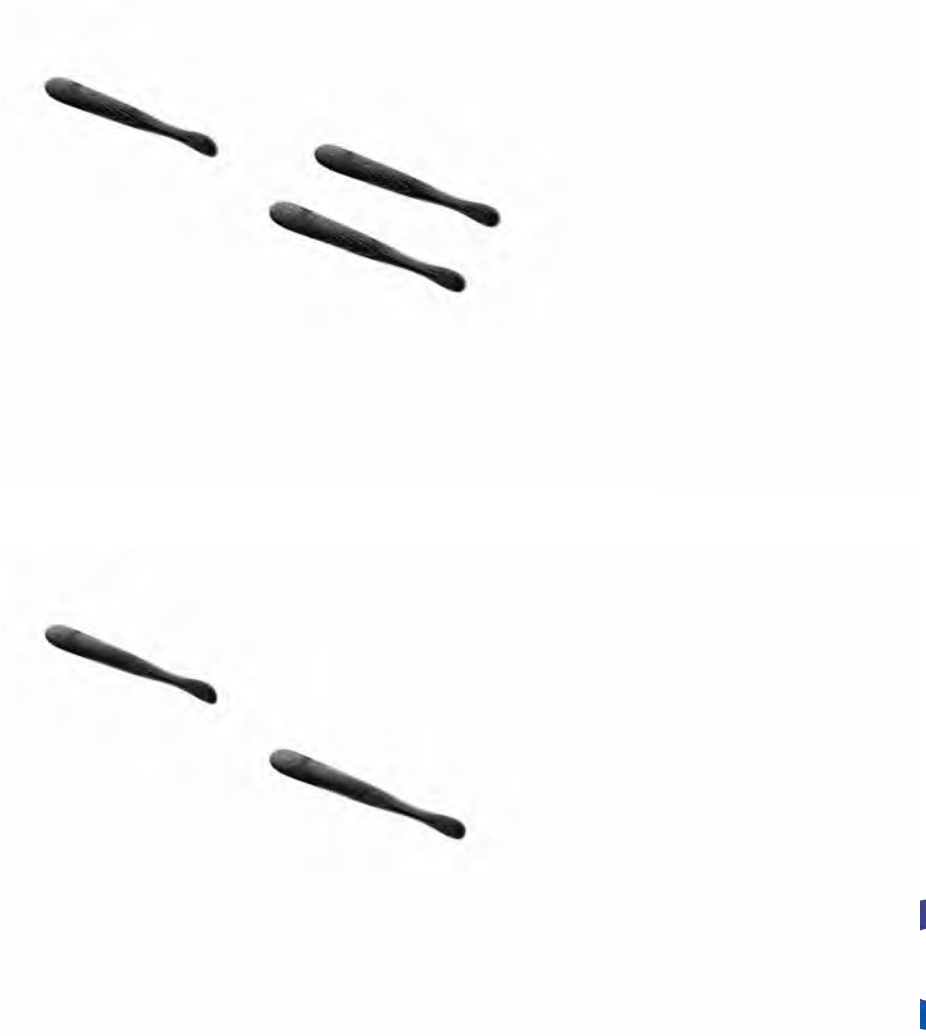

Verma, Novati, Koumoutsakos, Biophysics and Computational Biology, 115 (2018)

Neural Network Basics

How does a neural network learn?

Give input data

You'll get a random output

You define a cost/loss function

It accounts for every single possibility within the neural network

Minimize cost/loss function

Which paths will cause the fastest change in the cost function?

Give input and search for local minima (optimization problem)

How does it actually happens? Back propagation

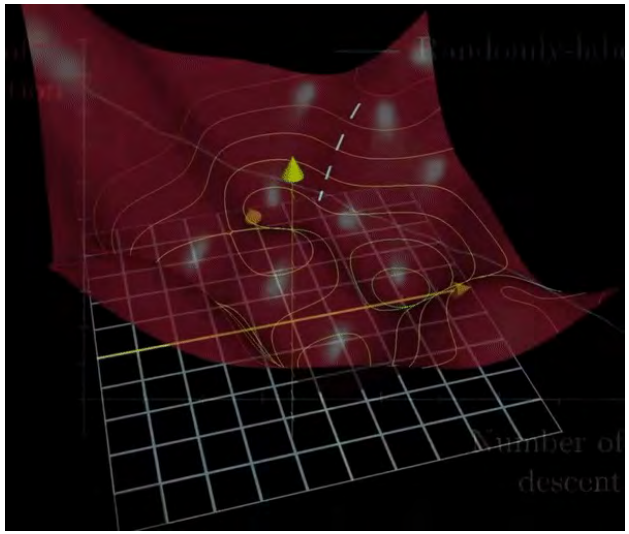

Caution: it always will give an output

Neurons and Activation Functions

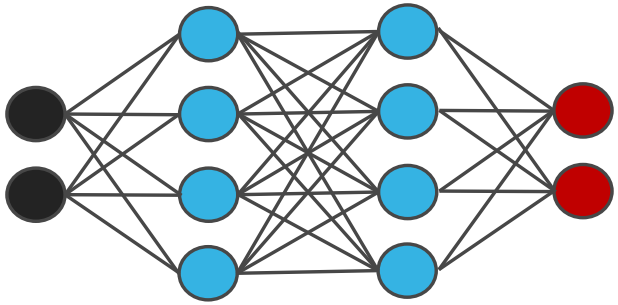

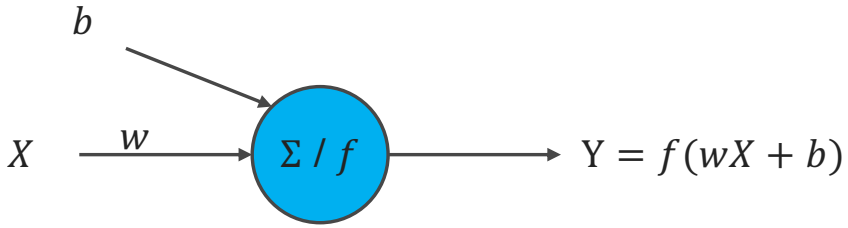

- Input layer - Hidden layer - Output layer

- **What is a neuron (perceptron) ?** An element that holds a number.
- Activation in one layer will deploy activations (or not) in the next layer.
- To each connection between layers we assign weights linking one neuron to the other – those you can tweak rather than treat it as a total black box.
- Human brain: given external stimulus will deploy certain receptor, which will trigger specific neurons, then the information is passed over, and finally we get an output.

Neurons and Activation Functions

- **Single Neuron & Linear Regression**

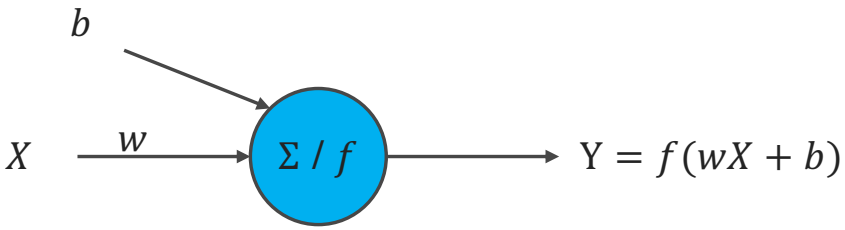

w – Weight

b – Bias

X – Input

Y – Predicted output

f – Activation function

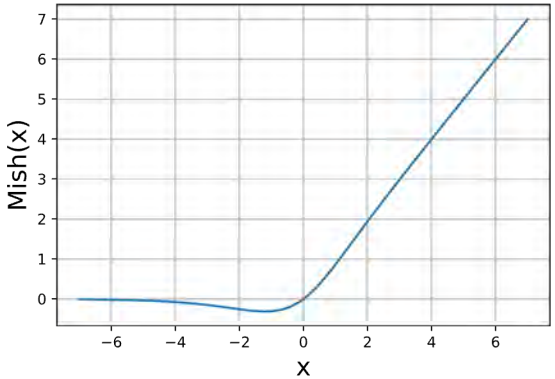

$$Mish(x) = x * Tanh(Softplus(x))$$

Step 1) Forward propagation:

- $Y = f(w^T X + b)$

Step 2) Calculate loss funtion:

- $L(w, b) = \|\hat{Y} - Y\|$

Step 3) Backward propagation:

- Find $\frac{dL}{dW}, \frac{dL}{db}$

Step 4) Optimization:

- $w = w - \alpha \frac{dL}{dw}, b = b - \alpha \frac{dL}{db}$

Repeat the Forward and Backward propagation for a specified number of repetitions (called epochs)

Shallow vs. Deep NN

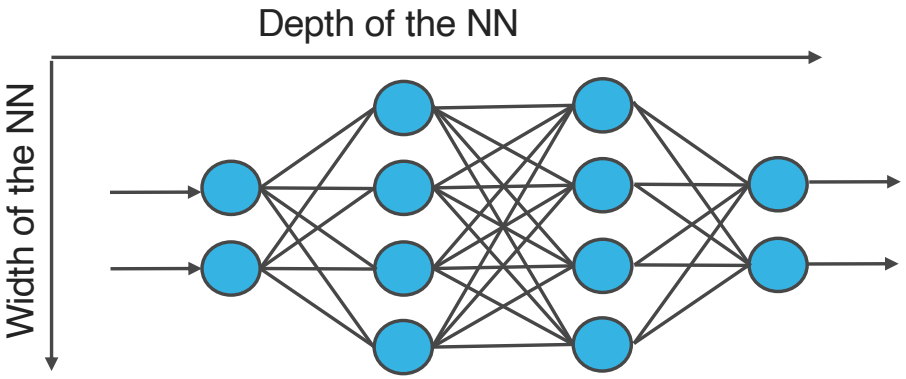

Step 1) Forward Propagation

Step 2) Loss function calculation

Step 3) Backward Propagation

Step 4) Optimize weights and biases

- Manual
- FD – Numerical - Sensitivity
- Symbolic Differentiation
- Automatic Differentiation

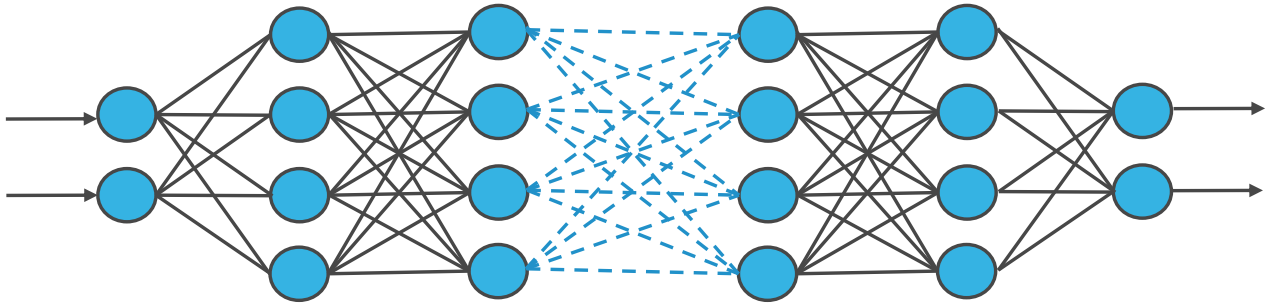

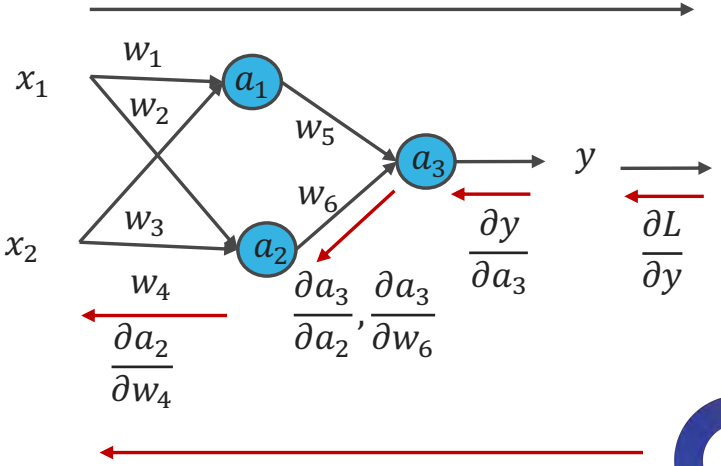

ML Applications in Fluid Mechanics and Combustion

Closure Models

ML for Reduced Order Model

Training data

- DNS / Experiment

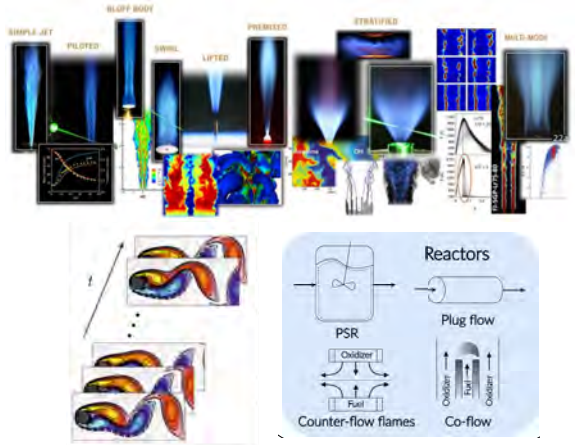

Training of ML

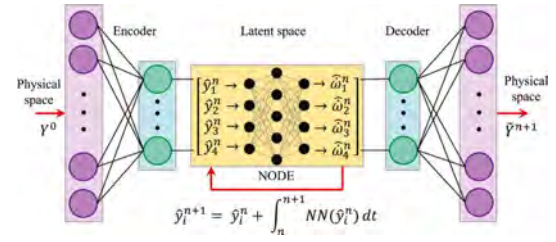

$$\hat{y}_i^{n+1} = \hat{y}_i^n + \int_n^{n+1} NN(\hat{y}_i^n)\, dt$$

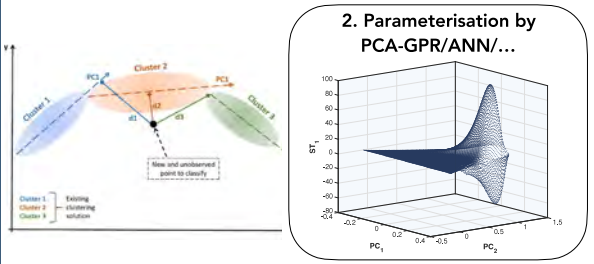

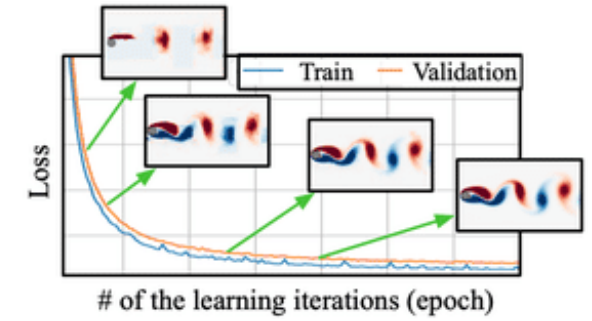

Application for Combustion

- Reconstruction/Estimation
  - Dimensionality reduction
  - Accelerated computing
  - Physics discovery

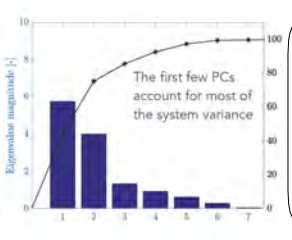

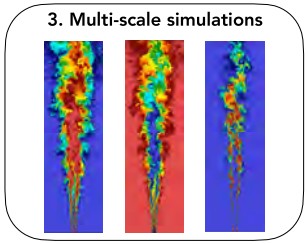

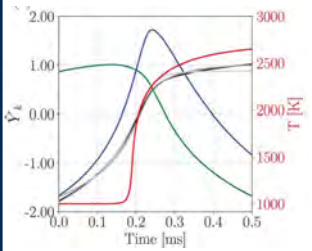

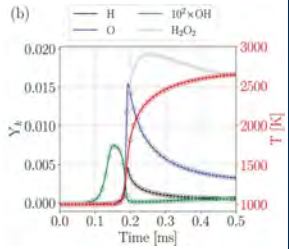

“Physics-Informed” Machine Learning

Taken from Steven Brunton
https://www.youtube.com/watch?v=KmQkDgu-Qp0&t=117s

1. **Decide on Problem**
   (What are we modeling?)
2. **Curate Data**
   (What data will inform the model?)
3. **Design an Architecture**
   (RNN, Autoencoder, PCA, SINDy?)
4. **Craft a Loss Function**
   (What models are “good”?)
5. **Employ Optimization**
   (What algorithms to train model?)

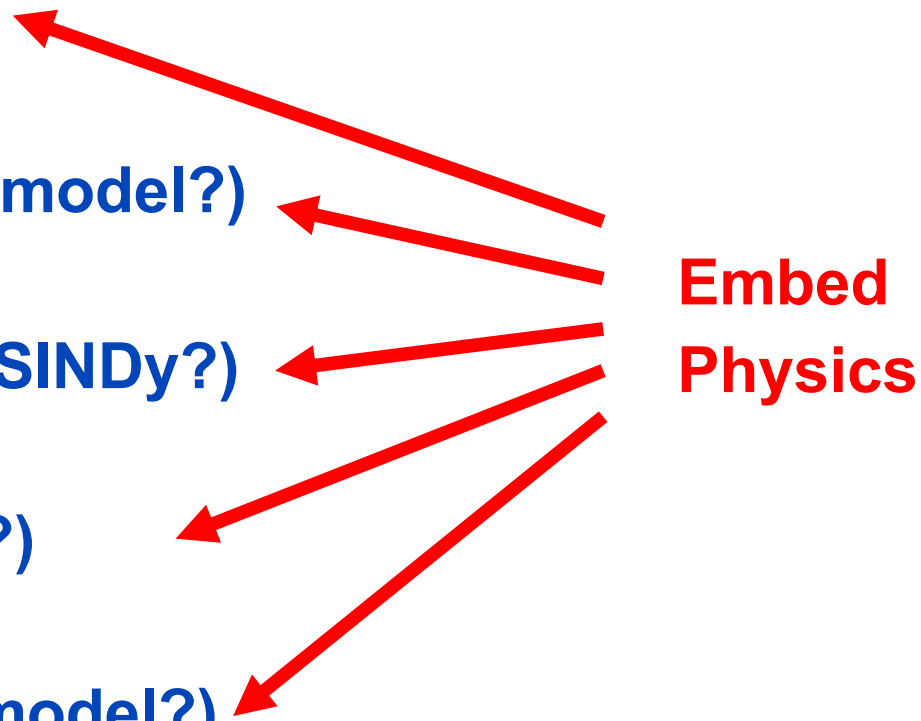

ML Applications in Fluid Dynamics

Solve PDEs using PINNs

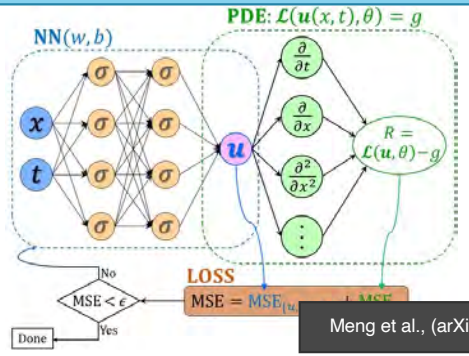

Meng et al., (arXiv, 2019)

Optimization & Flow control

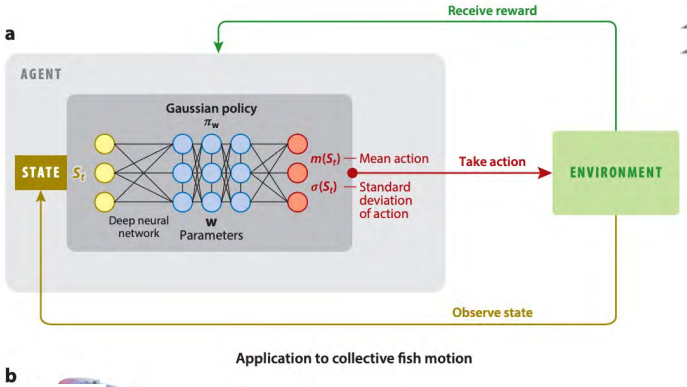

Application to collective fish motion

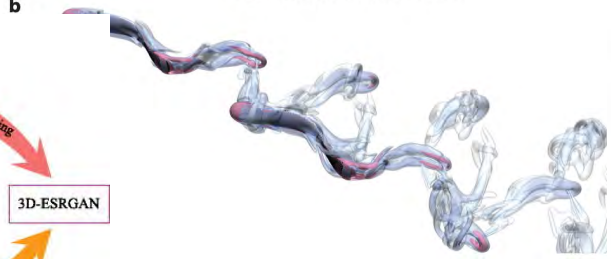

Verma et al., (2018)

Closure models

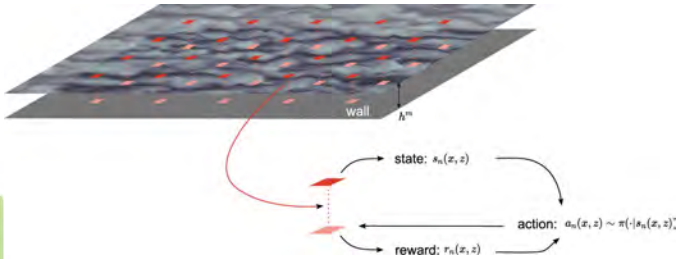

Bae H. J. et al., (NC, 2022)

Super-resolution techniques

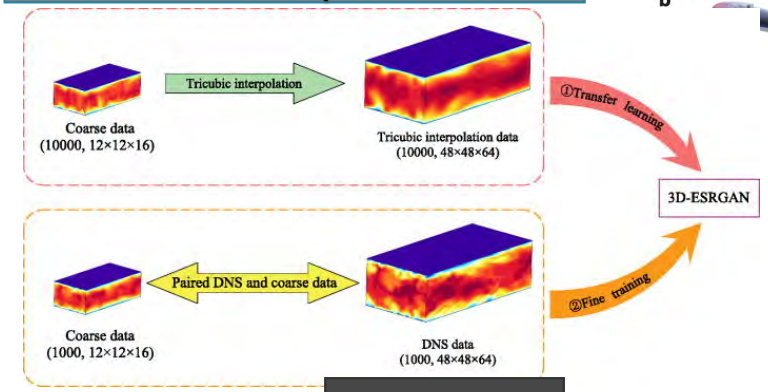

Yu L. et al., (POF, 2022)

Reduced Order Models

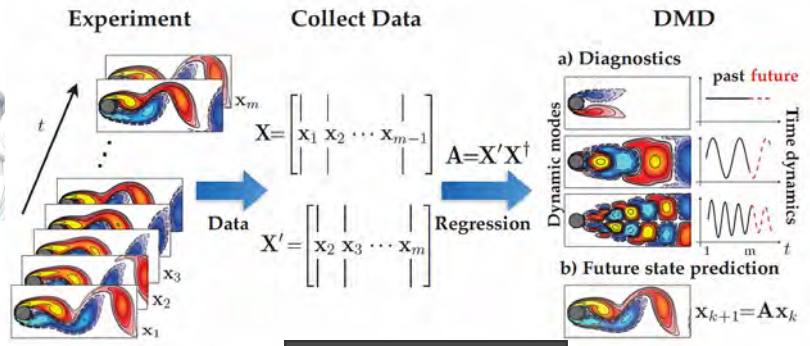

Kutz J.N. et al., (SIAM, 2016)

Application of NN In Fluid Dynamics and Combustion

Accelerated Computing

Christo F. C. et al.,

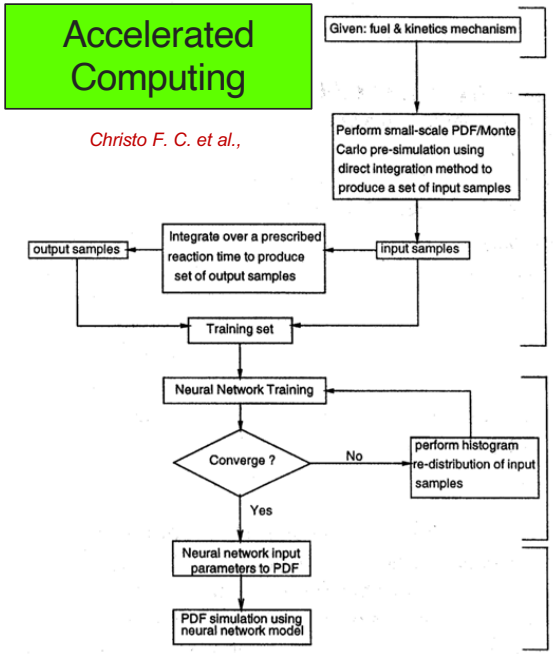

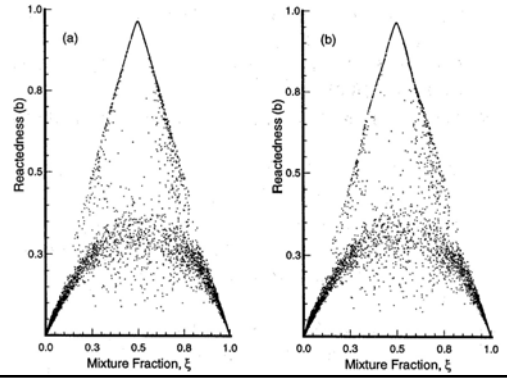

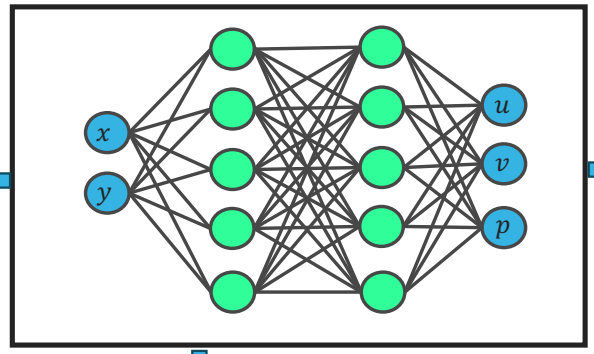

Reduced Order Model

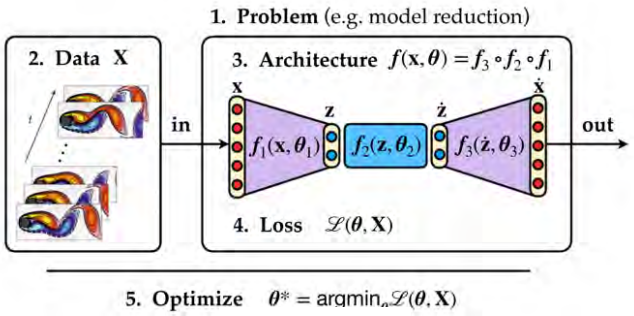

Brunton S. L. et al.,

Turbulence Modelling

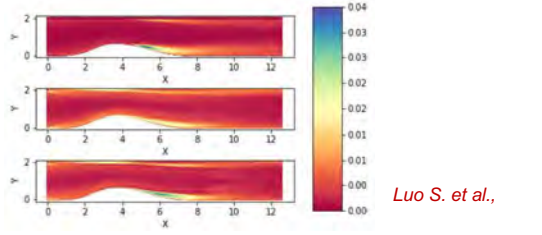

Luo S. et al.,

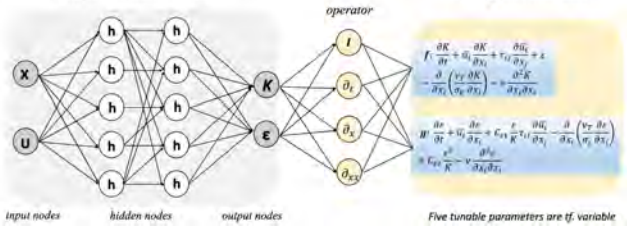

Synthetic Turbulence

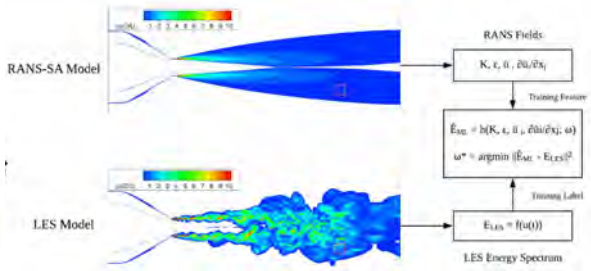

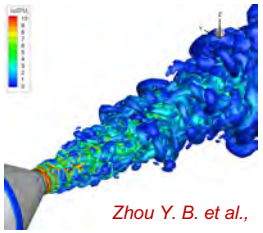

Zhou Y. B. et al.,

PDF/ANN for Accelerated Simulation

Christo, Masri, Nobot, Pope, 26th Symposium on Combustion (1996) 43-48.

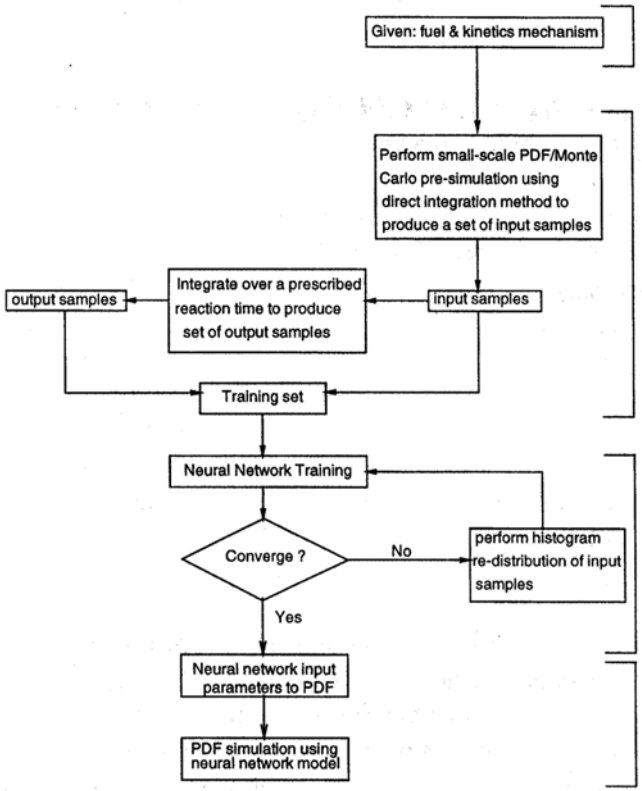

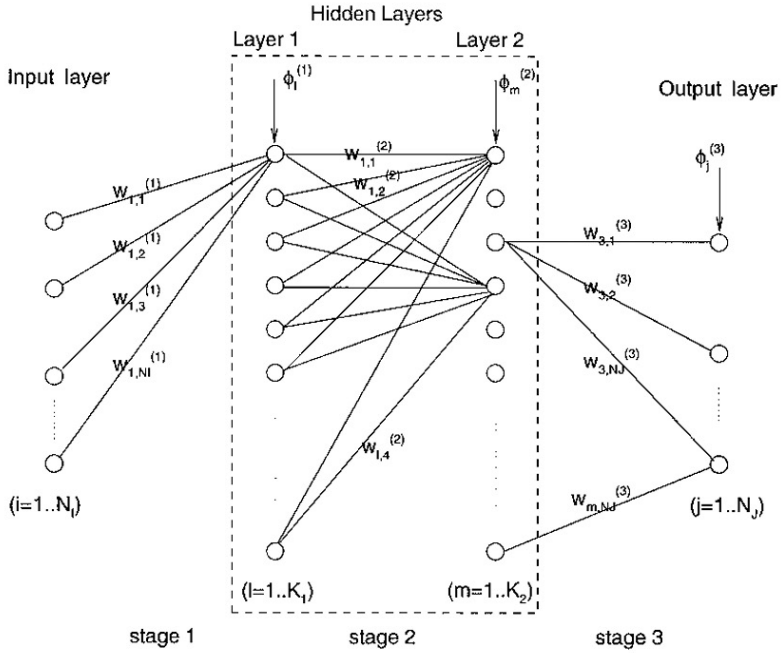

$$\Delta\Gamma_j = \sum_{j=1}^{N_I} \sum_{m=1}^{K_1} x_{2,m} w_{j,m}^{(3)} + \phi_j^{(3)} \qquad \bar{E}_p = \sum_{i=1}^{N} \sum_{j=1}^{K} [d_l^{(j)} - y_l^{(j)}]^2/(N \cdot K)$$

$$x_{2,m} = \tanh\left[\sum_{m=1}^{K_1} \sum_{l=1}^{K_2} x_{1,l} w_{m,l}^{(2)} + \phi_l^{(2)}\right]$$

$$x_{1,l} = \tanh\left[\sum_{i=1}^{N_I} \sum_{l=1}^{K_2} \Gamma_i w_{i,l}^{(1)} + \phi_l^{(1)}\right]$$

ML-based LES Model for Combustion

Yellapantula, de Frahan, King, Day, Grout, "Data Analysis for Direct Numerical Simulations of Turbulent Combustion, Ch. 14, (2020) https://doi.org/10.1007/978-3-030-44718-2_14.

Favre-filtered progress variable equation:

$$\frac{\partial \bar{\rho}\tilde{c}}{\partial t} + \nabla.(\bar{\rho}\tilde{u}\tilde{c}) = \nabla.\bar{\rho}\tilde{D}\nabla\tilde{c} + \nabla.\bar{\tau}_{sgs} + \bar{\rho}\widetilde{\dot{\omega}_c}$$

SGS scalar flux:

$$\bar{\tau}_c = \bar{\rho}\widetilde{uc} - \bar{\rho}\tilde{u}\tilde{c} = \frac{\mu_{sgs}}{Sc_t}\nabla\tilde{c}$$

Filtered source term: (Model using DNN)

$$\widetilde{\dot{\omega}_c} = DNN\left(\tilde{Z}, \widetilde{Z''^2}, \tilde{c}, \widetilde{c''^2}, \widetilde{\chi_Z}, \widetilde{\chi_c}\right)$$

- Z– Mixture fraction
- c – progress variable
- χ– Scalar dissipation rate

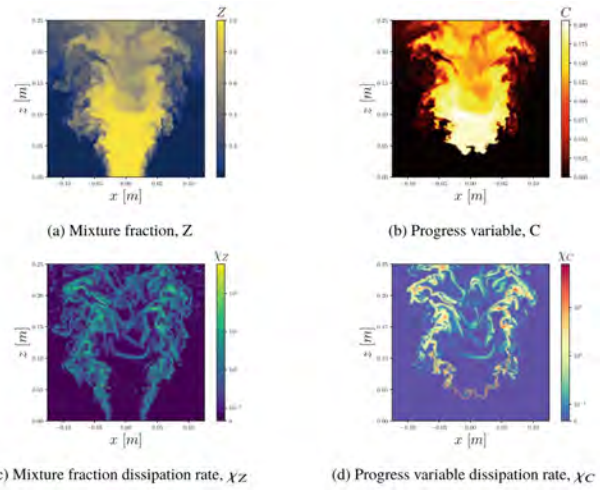

Training data

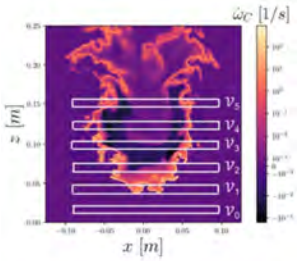

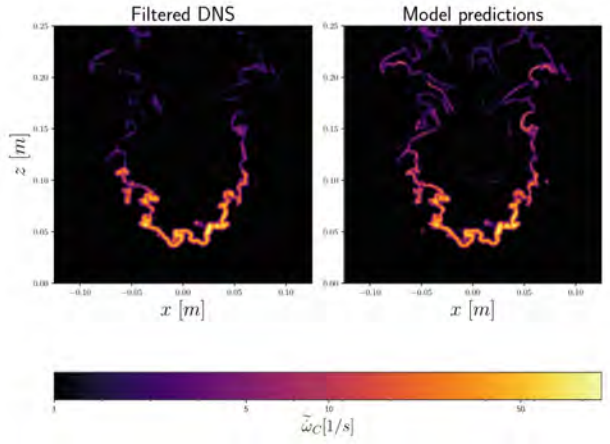

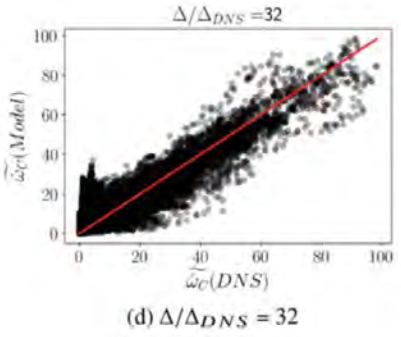

DNN for Turbulent Combustion Closure

Ihme, Schmitt, Pitsch, Proc. Comb. Inst. 32 (2009) 1527-1535.

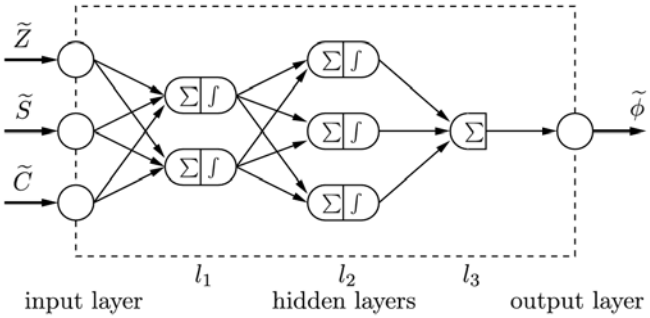

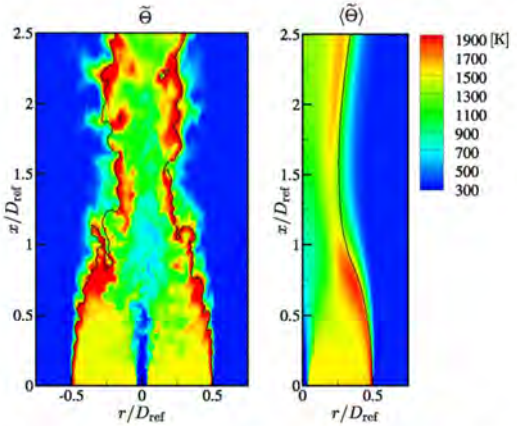

Fig. 8. Instantaneous and averaged temperature fields of the Sydney SMH1 flame, computed with ANN chemistry representation. The solid line shows the location of stoichiometric mixture fraction with $Z_{st} = 0.042$.

Yellapantula, Perry, Grout, Proc. Comb. Inst. 38 (2021) 2929-2938.

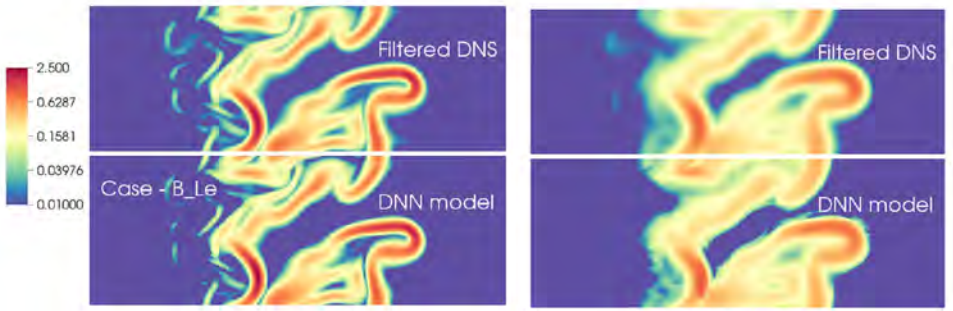

Fig. 1. $\tilde{\chi}_C/\chi_{lam}$ prediction by the DNN compared against the filtered DNS data from Case B_{Le}, (a) FGR=4 (b) FGR=16. The contours, presented on a log scale, are shown on a cross section in the spanwise direction and are zoomed in around the flame region.

Progress variable dissipation rate:

$$\tilde{\chi}_{c,sgs} = 2D_c\widetilde{|\nabla c|^2} - 2\widetilde{D_c}|\nabla\tilde{c}|^2$$

Model using DNN

$$\tilde{\chi}_{c,sgs} = DNN\left(\tilde{c}, \widetilde{c''^2}, \widetilde{D_c}, 2\widetilde{D_c}|\nabla\tilde{c}|^2, \ldots\right)$$

PINN: Physics Informed Neural Network

Raissi, Perdikaris, Karniadakis, *Journal of Comp. Phy. 378 (2019)* 686--707..

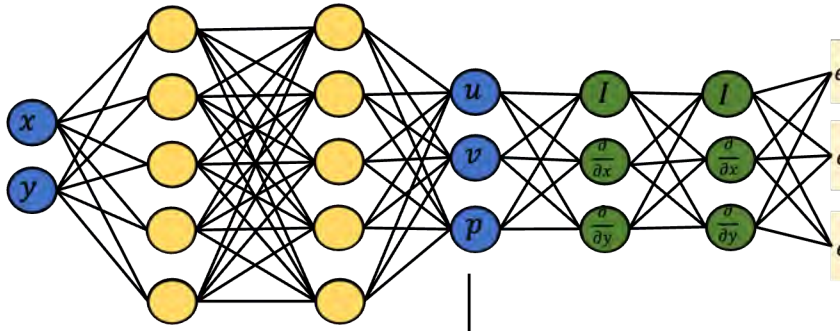

$$e_{cont} = \frac{\partial u}{\partial x} + \frac{\partial v}{\partial y}$$

$$e_{x-mom} = \left[u\frac{\partial u}{\partial x} + v\frac{\partial u}{\partial y}\right] + \frac{1}{\rho}\frac{dp}{dx} - \nu\left[\frac{\partial^2 u}{\partial x^2} + \frac{\partial^2 u}{\partial y^2}\right]$$

$$e_{y-mom} = \left[u\frac{\partial v}{\partial x} + v\frac{\partial v}{\partial y}\right] + \frac{1}{\rho}\frac{dp}{dy} - \nu\left[\frac{\partial^2 v}{\partial x^2} + \frac{\partial^2 v}{\partial y^2}\right]$$

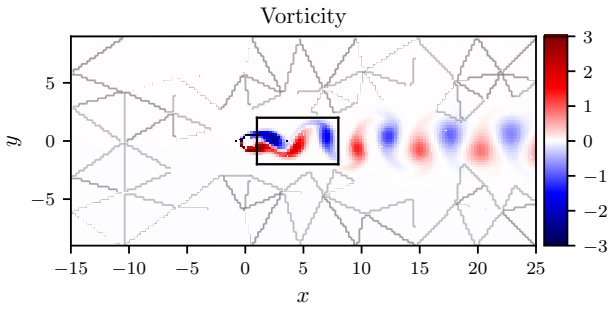

loss_bc's → *Total_loss* ← *loss_PDE*

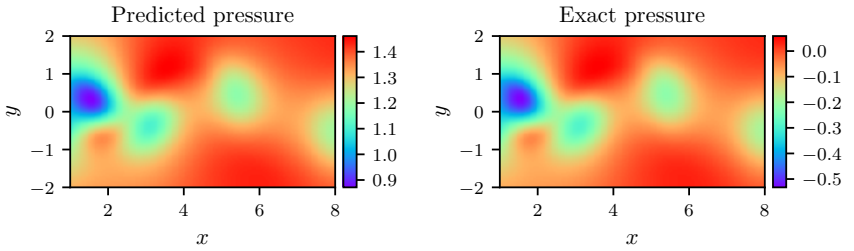

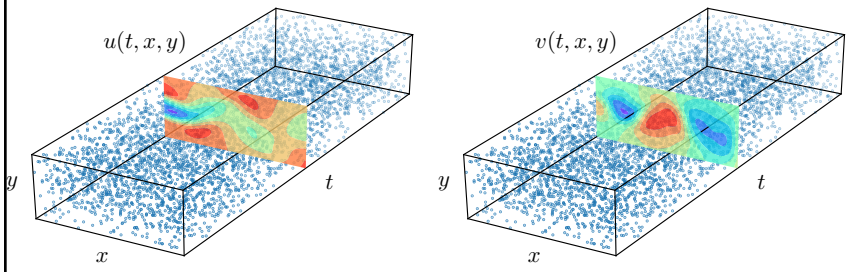

Correct PDE	$u_t + (uu_x + vu_y) = -p_x + 0.01(u_{xx} + u_{yy})$ $v_t + (uv_x + vv_y) = -p_y + 0.01(v_{xx} + v_{yy})$
Identified PDE (clean data)	$u_t + 0.999(uu_x + vu_y) = -p_x + 0.01047(u_{xx} + u_{yy})$ $v_t + 0.999(uv_x + vv_y) = -p_y + 0.01047(v_{xx} + v_{yy})$
Identified PDE (1% noise)	$u_t + 0.998(uu_x + vu_y) = -p_x + 0.01057(u_{xx} + u_{yy})$ $v_t + 0.998(uv_x + vv_y) = -p_y + 0.01057(v_{xx} + v_{yy})$

PINN for RANS

Eivazi, Tahani, Schlatter, Vinuesa, Phy. Of Fluids, 34 (2022) 075117.

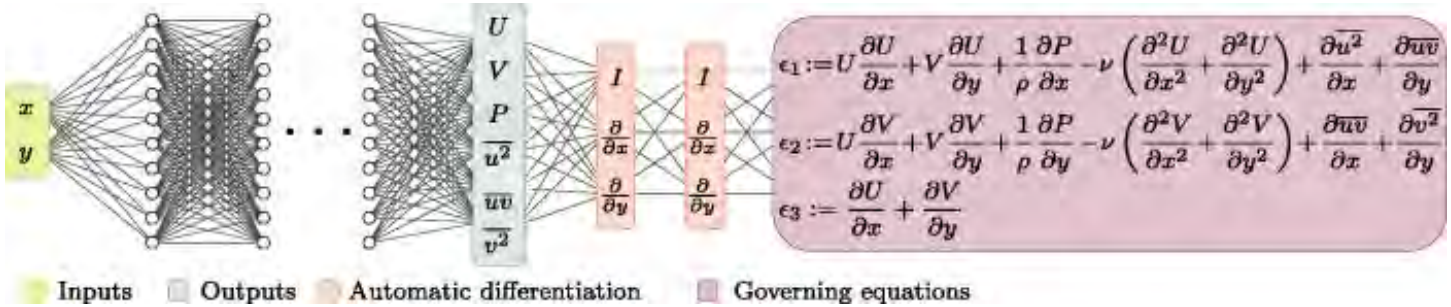

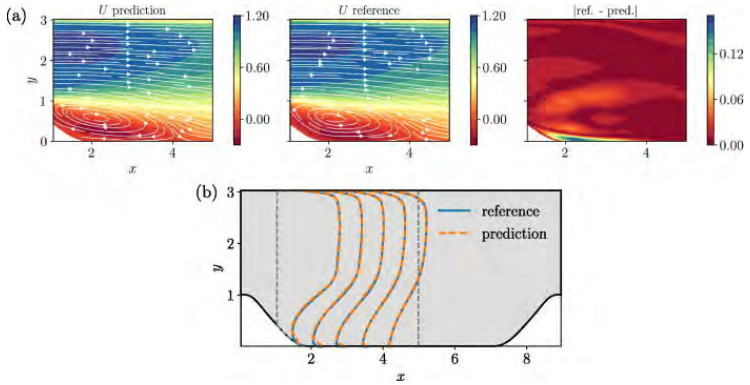

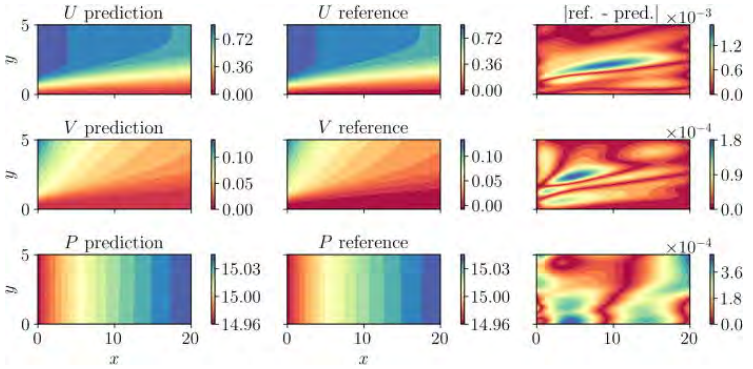

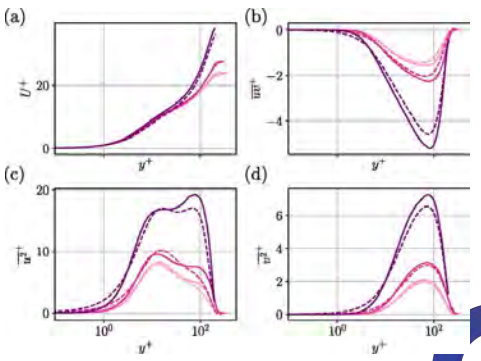

PINN for Flamelet-Progress Variable

Song, Mengze, et al., Phy. Of Fluids, 36 (2024) 103616.

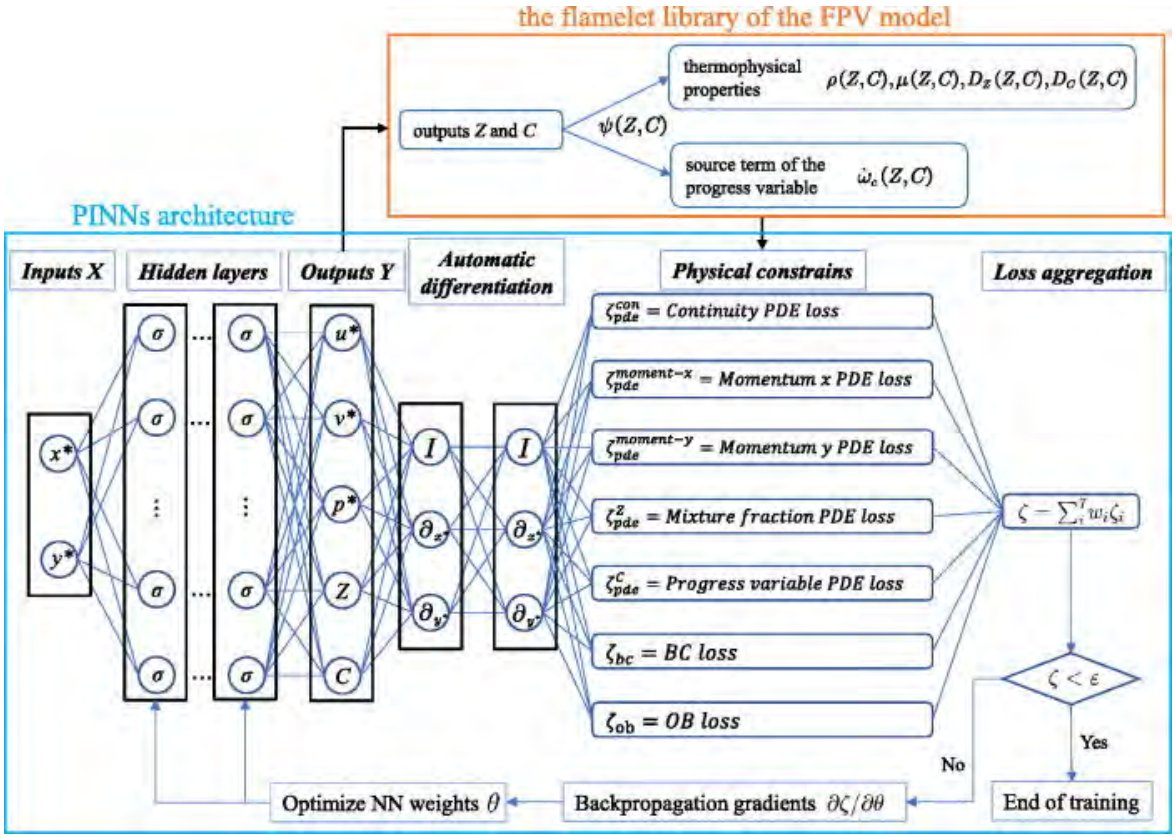

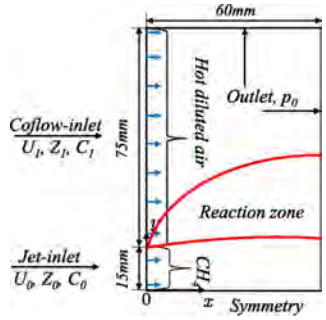

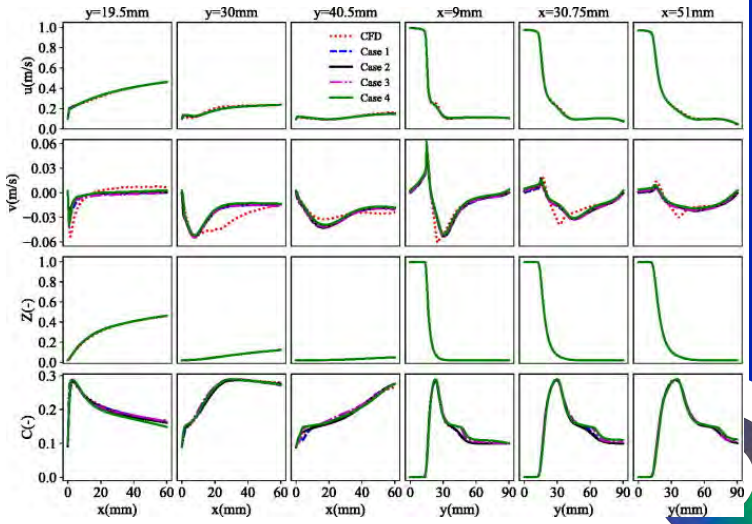

LES of Sandia Flame D with FPV/PCA and ANN

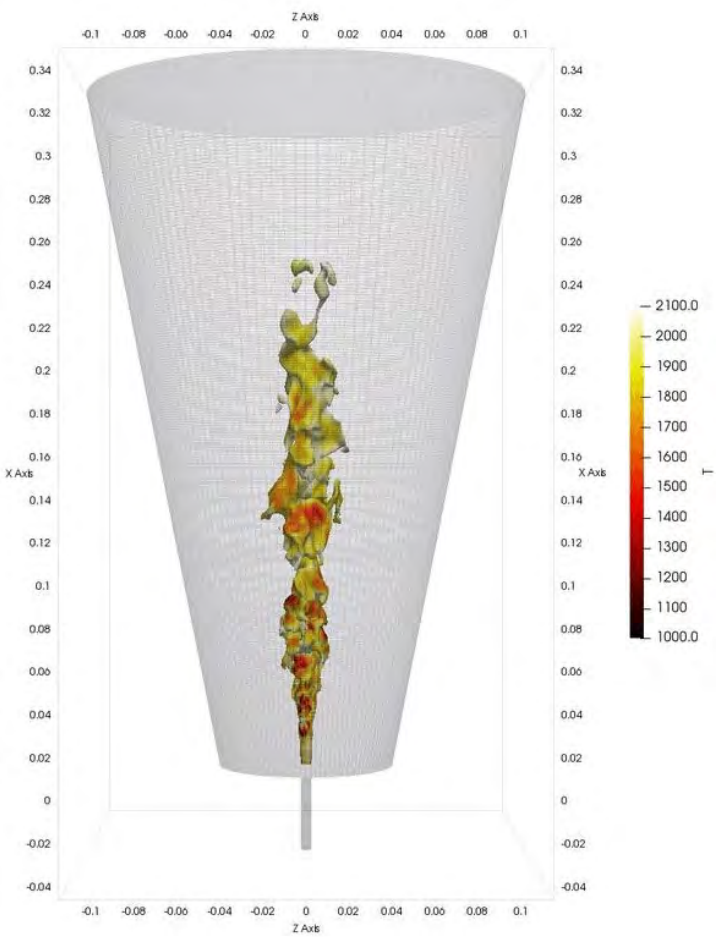

- A 3-D structured conical mesh
- **Total no. of cells:** 4 Million Cells
- **Pipe diameter (D):** 4.58mm
- **Pipe length (10D):** 45.8 mm
- **Domain length:** 80D
- **Domain width at outlet:** 50D
- **Domain width at the jet exit plane:** 20D

- Pipe of length 10D to generate turbulence.
- Fully turbulent flow at the pipe inlet, with a velocity mapping method.
- Second-order discretization in time and space.

Flamelet progress variable (FPV) approach

- Instead of solving transport equations for many species, compute detailed flame structure a priori, parametrize by a small number of variables, and 'look-up' during the LES simulations.

From the steady laminar counterflow diffusion flame calculations:

$$y_i = y_i(Z, C), \qquad T = T(Z, C), \qquad \rho = \rho(Z, C), \qquad w_C = w_C(Z, C),$$

To include turbulence effect: convolution with presumed subfilter PDF

$$\widetilde{y}_i = \widetilde{y}_i(\widetilde{Z}, \widetilde{Z''^2}, \widetilde{C}), \quad \widetilde{T} = \widetilde{T}(\widetilde{Z}, \widetilde{Z''^2}, \widetilde{C}), \quad \overline{\rho} = \overline{\rho}(\widetilde{Z}, \widetilde{Z''^2}, \widetilde{C}), \quad \widetilde{w}_C = \widetilde{w}_C(\widetilde{Z}, \widetilde{Z''^2}, \widetilde{C}).$$

FPV manifold

- H_2O mass fraction is selected as a progress variable; it is a major product and it has good mapping to the retrieved parameters.

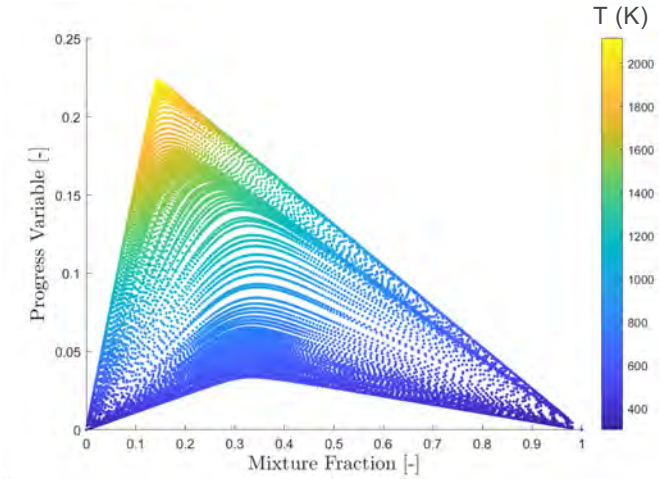

Bilger mixture fraction

$$\xi_B = \frac{(Y_H - Y_{H,2})/2W_H - (Y_O - Y_{O,2})/W_O}{(Y_{H,1} - Y_{H,2})/2W_H - (Y_{O,1} - Y_{O,2})/W_O}$$

Principal component analysis (PCA)

- Principal component analysis (PCA) allows for identifying the direction of maximum variance in the data

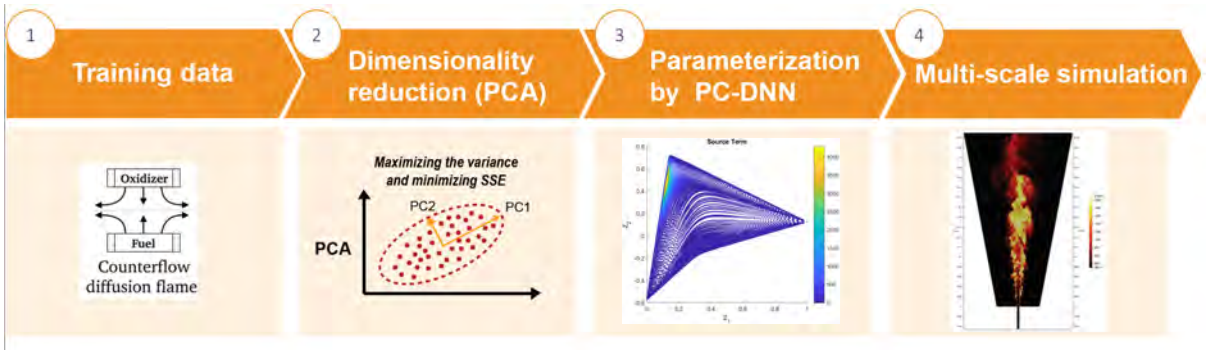

$$\mathbf{X} = \begin{bmatrix} x_{11} & x_{12} & \dots & x_{1Q} \\ x_{21} & x_{22} & \dots & x_{2Q} \\ \vdots & \vdots & \ddots & \vdots \\ x_{n1} & x_{n2} & \dots & x_{nQ} \end{bmatrix} = \begin{bmatrix} Y_1^1 & \dots & \dots & Y_p^1 \\ Y_1^2 & \dots & \dots & Y_p^2 \\ \vdots & \ddots & \ddots & \vdots \\ Y_1^n & \dots & \dots & Y_p^n \end{bmatrix}$$

State variables

Observations

Data dimensionality

PC-transport approach:

$$\frac{\partial}{\partial t}(\rho \mathbf{Y_k}) + \nabla(\rho \tilde{\mathbf{u}} \mathbf{Y_k}) = \nabla(\rho \mathbf{D_k} \nabla \mathbf{Y_k}) + \mathbf{R_k} \qquad k = 1, \dots, n_s$$

$$\mathbf{Z} = \mathbf{Y} \mathbf{A_q}$$

$$\frac{\partial}{\partial t}(\rho \mathbf{z}) + \nabla(\rho \tilde{\mathbf{u}} \mathbf{z}) = \nabla(\rho \mathbf{D_z} \nabla \mathbf{z}) + \mathbf{s_z}$$

(n_s transport equations)

dimension reduction

(q transport equations)

A is the basis matrix (q PCs)
Z principal component scores
Y_k is the mass fraction of species k
R_k is its corresponding source term
n_s total number of species

J.C. Sutherland and A. Parente, Proc. Combust. Inst., 32 (2009)

Nonlinear Regression

- PC-DNN (Deep Neural Networks)

➢ **A single graphical processing unit GPU.**
➢ **About 15000 training parameters, 6 hidden layers.**
➢ **The DNN regresses the thermochemical state space with an R^2-score >0.99 (R^2 for NO & OH ~ 0.985).**

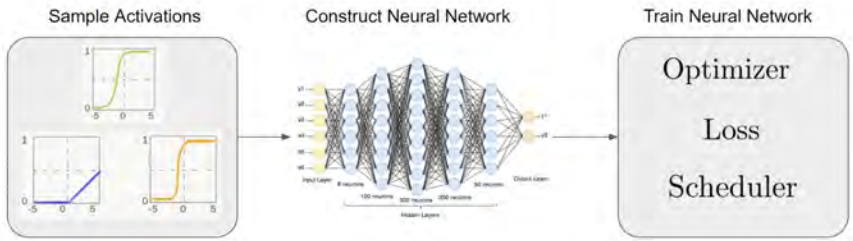

Original data based on unity Lewis

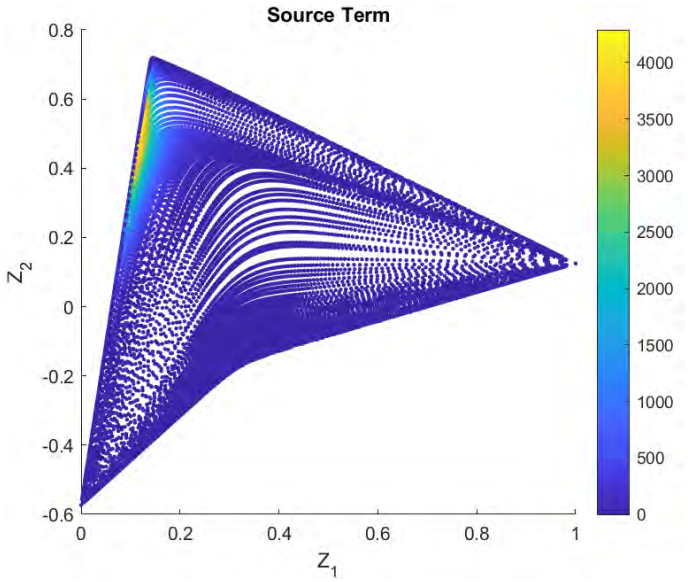

DNN- denser predictions (tabulation 200*200)

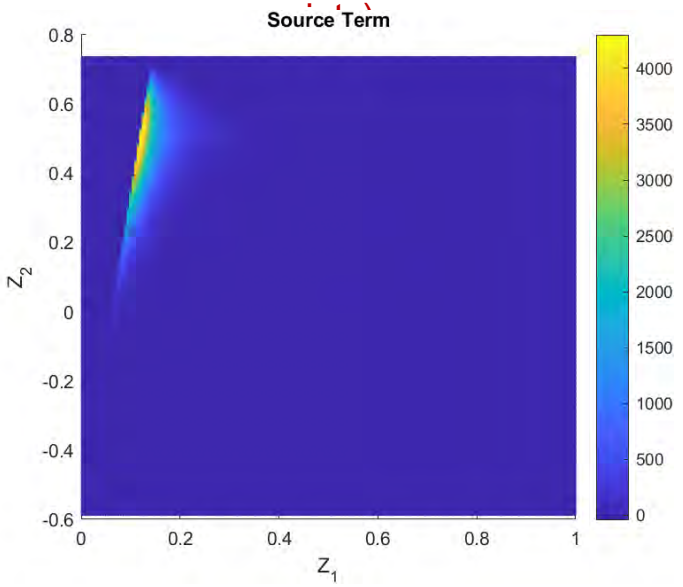

Validation and Comparison

Experiment

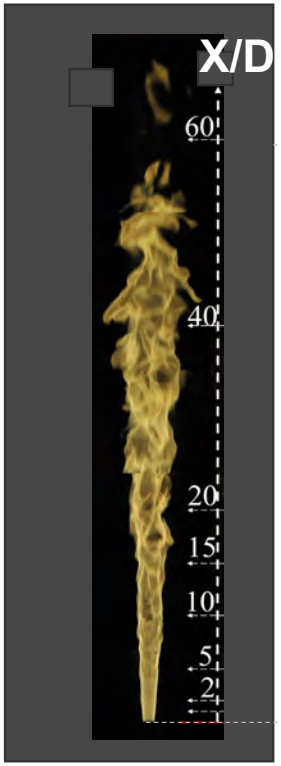

PC-DNN

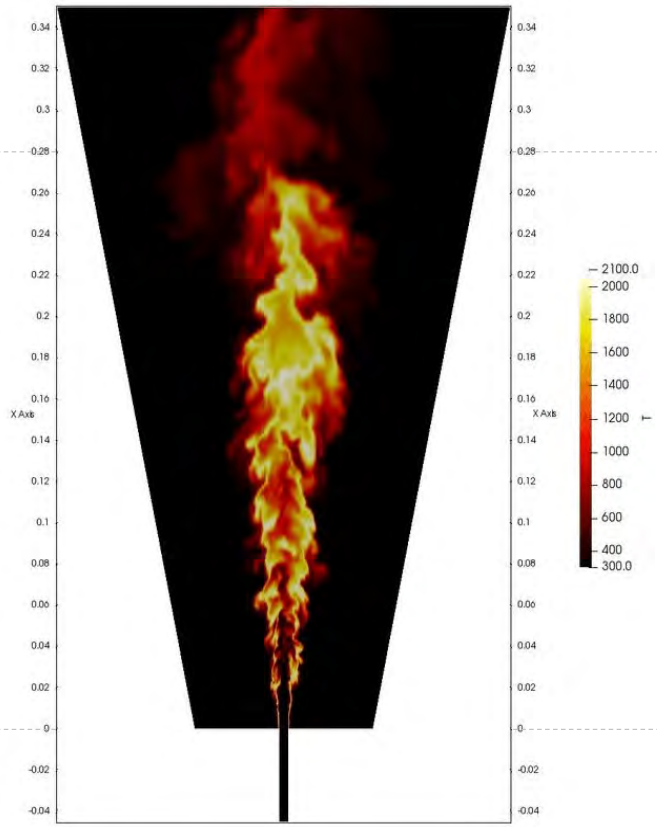

FPV

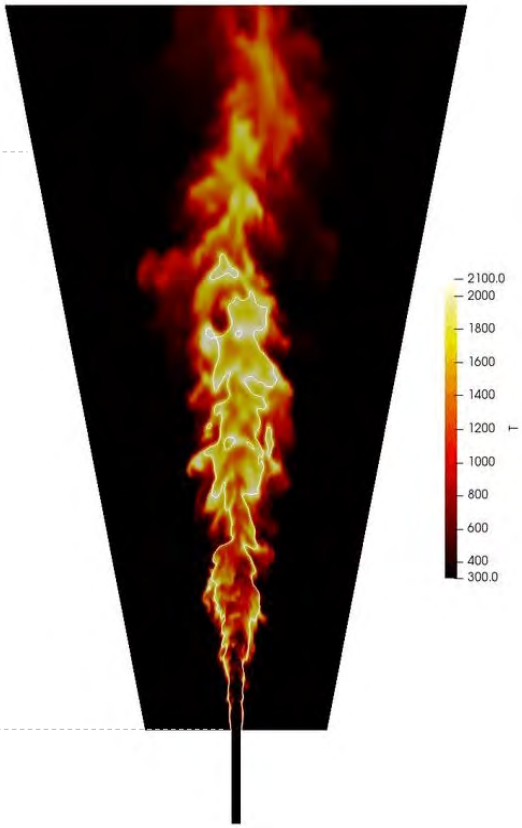

Chemical Reaction Neural Network (CRNN)

Sili Deng, MIT

- Operate on net reaction rate for reaction *j*

$$Q_j = K_{f_j} \prod_k \left(\frac{\rho Y_k}{W_k}\right)^{\upsilon'_{kj}} - K_{r_j} \prod_k \left(\frac{\rho Y_k}{W_k}\right)^{\upsilon''_{kj}}$$

GEMM: X = A*B + C

Exponential activation

Exponential activation

$$Q_j = \exp\left(\log K_{f_j} + \sum_k \upsilon'_{kj} \log[C_k]\right) - \exp\left(\log K_{f_j} - \log K_{c_j} + \sum_k \upsilon''_{kj} \log[C_k]\right)$$

Forward rate

Reverse rate

Forward rate constant: Arrhenius form

$$K_{f_j} = A_j T^{\beta_j} \exp\left(-\frac{E_j}{RT}\right)$$

Equilibrium rate constant: polynomials

$$K_{c_j} = \frac{P_{ref}^{\sum_k \upsilon_{kj}}}{RT} \exp\left(\frac{\Delta S_j}{R} - \frac{\Delta H_j}{RT}\right)$$

NN – based interpretation

Example: 4 species, 6 reactions

$$\omega = \upsilon Q$$

$$Q = \exp\left(\log K_f + \upsilon'^{T} \log C\right) - \exp\left(\log K_f - \log K_c + \upsilon''^{T} \log C\right)$$

Q_f Q_r

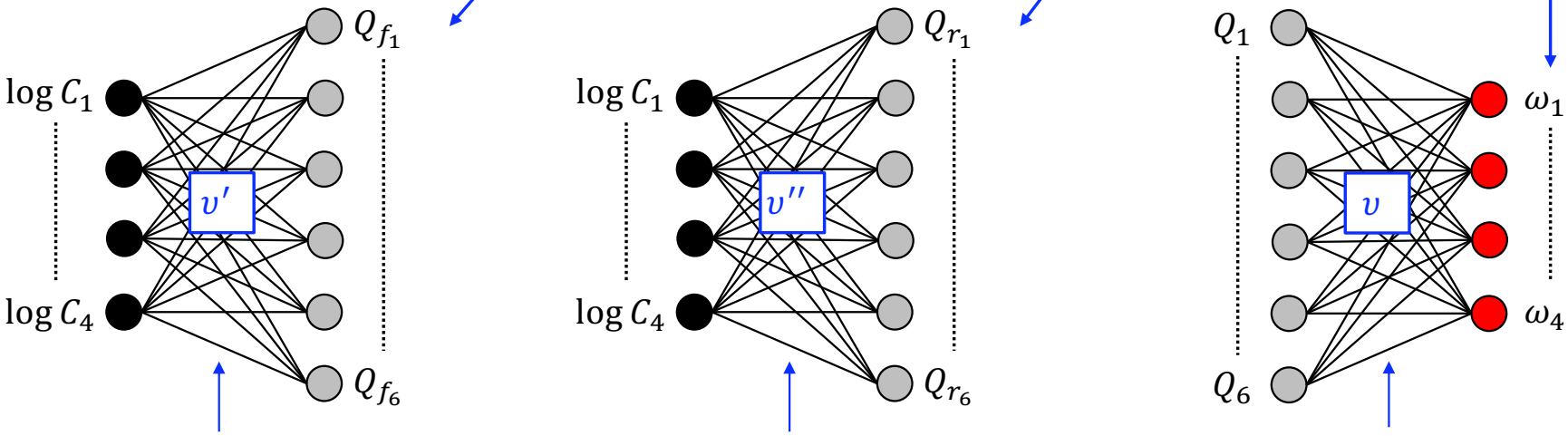

Weights = Stoichiometric coefficients

Weights = Stoichiometric coefficients

Weights = Stoichiometric coefficients

CRNN: Chemical Reaction Neural Network

(a) A Neuron for A Single-step Reaction

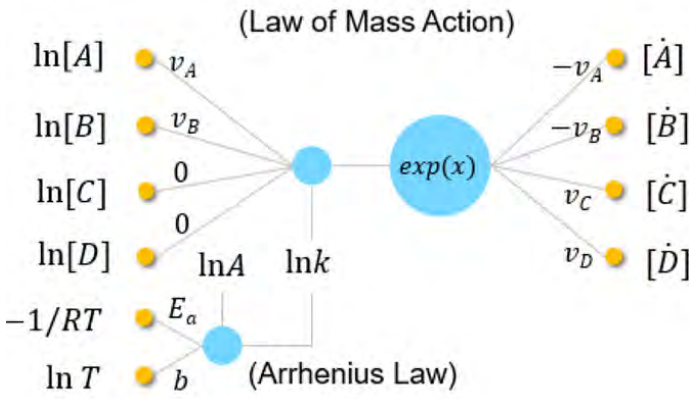

(b) A CRNN Network for Multi-step Reactions

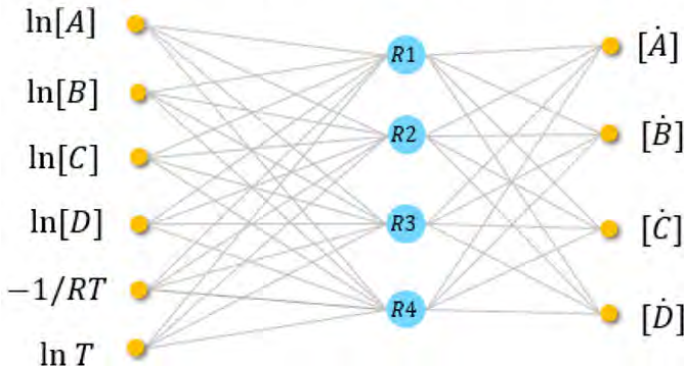

(a) Noisy experimental measurements

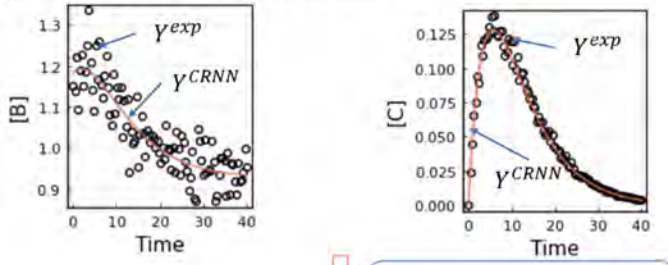

minimize

$Loss = \mathrm{MAE}(\boldsymbol{Y}^{CRNN}(t), \boldsymbol{Y}^{exp}(t))$

$\boldsymbol{Y}^{CRNN} = \mathrm{ODESolve}(\mathrm{CRNN}(\boldsymbol{Y}), \boldsymbol{Y}_0)$

(b) Learned CRNN weights

	A	B	C	D	E	k	A	B	C	D	E
R1	0	1	0.002	1.002	0	0.303	0	-1	-0.002	-1.002	1
R2	2.017	0	0	0	0	0.1	-2.017	1.016	0.004	0	0.001
R3	0	0	1	0	0.002	0.13	0.001	0.004	-1	1.005	-0.002
R4	0.999	0.001	0	0	0	0.201	-0.999	-0.001	0.989	0.001	0.001

Weight Pruning & Translation

(c) Interpreted reactions

Ground Truth		Learned CRNN	
Equation	Rate	Equation	Rate
$B + D \rightarrow E$	0.3	$1.001B + 1.002D \rightarrow 1.001E$	0.301
$2A \rightarrow B$	0.1	$2.009A \rightarrow 1.013B$	0.099
$C \rightarrow D$	0.13	$C \rightarrow D$	0.13
$A \rightarrow C$	0.2	$1.001A \rightarrow 0.997C$	0.201

ML Applications in Fluid Mechanics and Combustion

Feature Extraction for Discovery

Convolutional Neural Network (CNN)

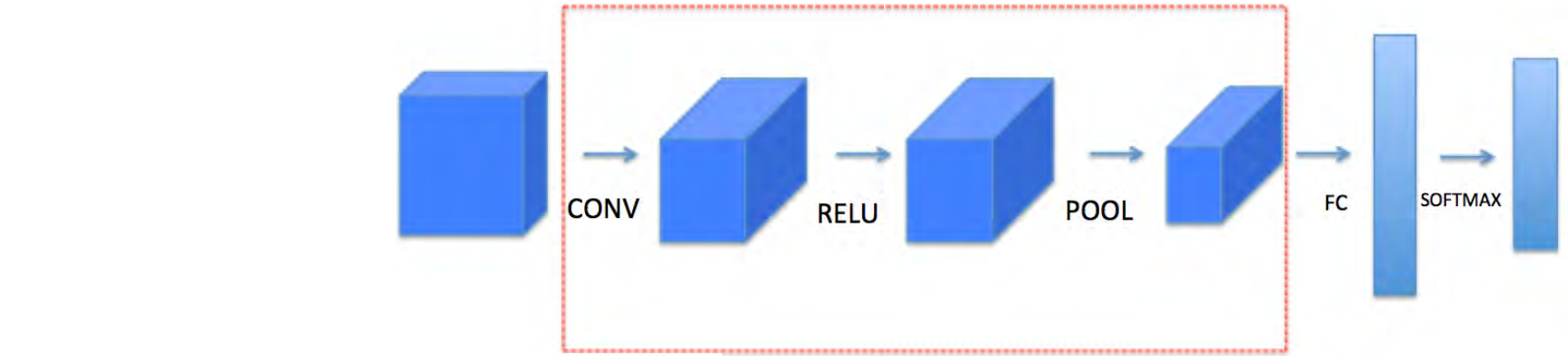

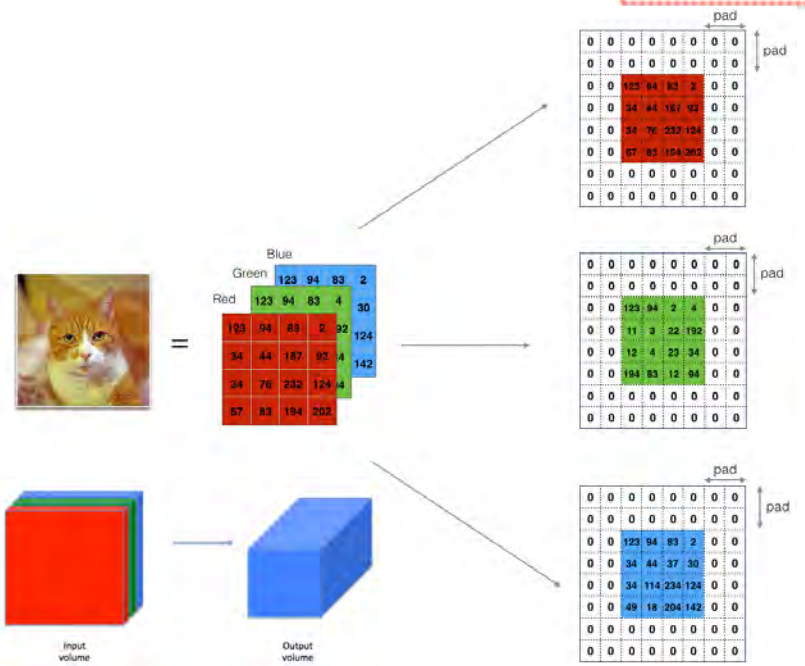

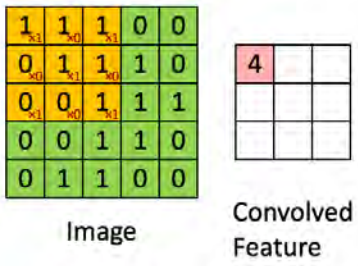

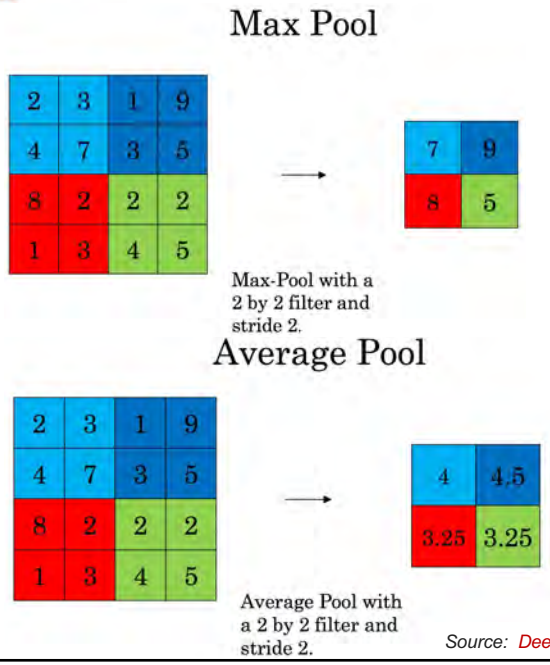

Source: DeepLearning.ai

Application of CNN: In Fluid Dynamics and Combustion

Find Missing Information

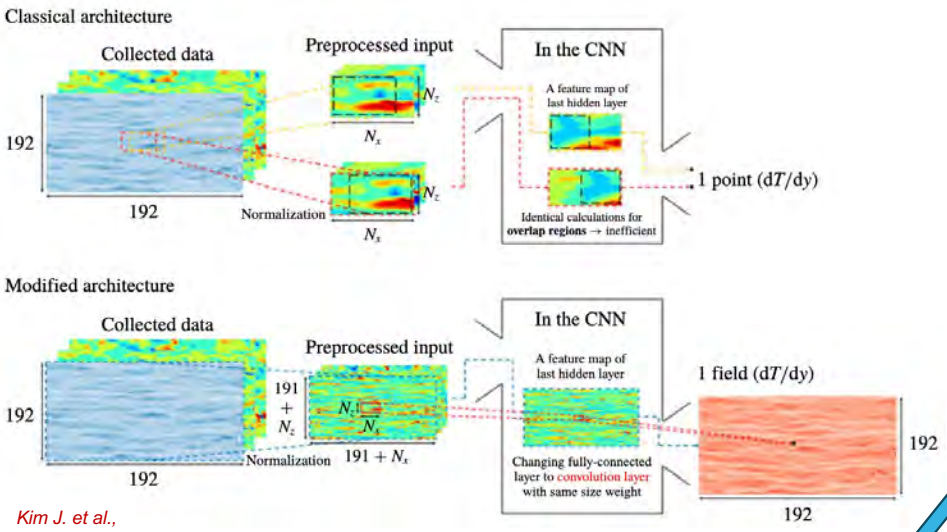

Kim J. et al.,

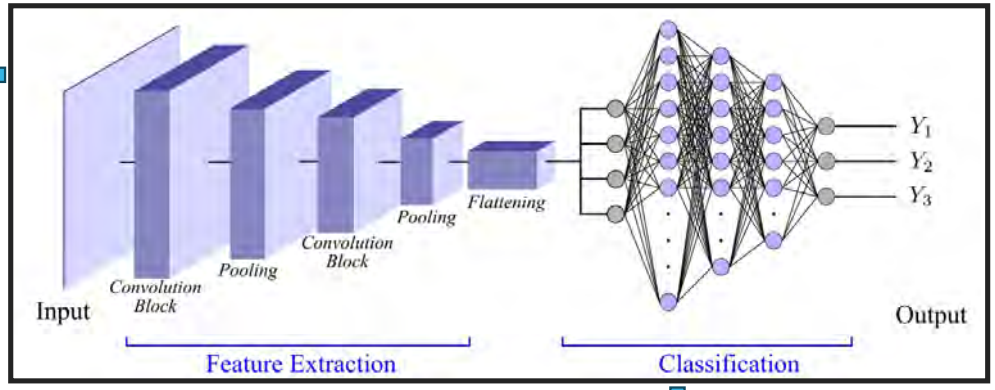

Super Resolution & Turbulent Closure

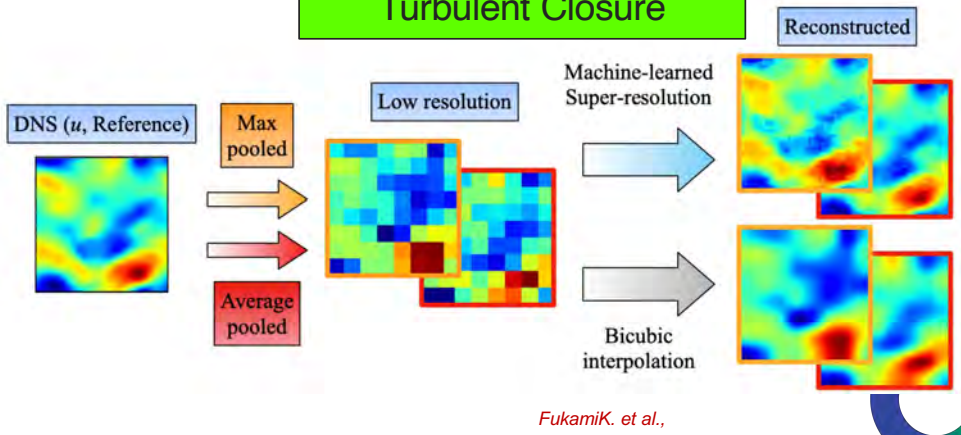

FukamiK. et al.,

Reduced Order Model

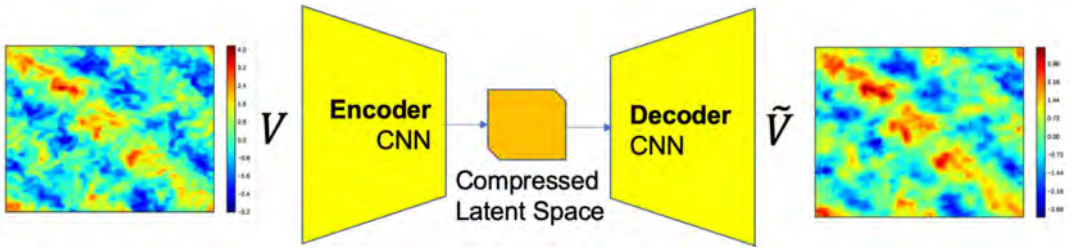

Mohan A. T. et al.,

ML-based Flame Surface Density Modelling

Shin, Ge, Lampmann, Pfitzner, Comb. & Flame. 231 (2021) 111486.

Favre-filtered progress variable equation:

$$\frac{\partial \bar{\rho}\tilde{c}}{\partial t} + \nabla.(\bar{\rho}\tilde{u}\tilde{c}) + \nabla.\bar{\tau}_c = \overline{\nabla.(\rho D \nabla c) + \rho\dot{\omega}_c}$$

Flame surface density model:

$$\overline{\nabla.(\rho D \nabla c) + \rho\dot{\omega}_c} = \rho_u s_L \bar{\Sigma}$$

SGS scalar flux:

$$\bar{\tau}_c = \bar{\rho}\widetilde{uc} - \bar{\rho}\tilde{u}\tilde{c} = \frac{\mu_{sgs}}{Sc_t}\nabla\tilde{c}$$

SGS flame structure using PDF:

$$\bar{\Sigma} = \int \Sigma(x_1, x_2, \ldots x_N)\, p(x_1, x_2, \ldots x_N) dx_1 dx_2 \ldots dx_N$$

PDF modelled using CNN:

$$p(x) = \frac{1}{\sqrt{2\pi\sigma^2}} exp\left(-\frac{(x-\mu)^2}{2\sigma^2}\right)$$

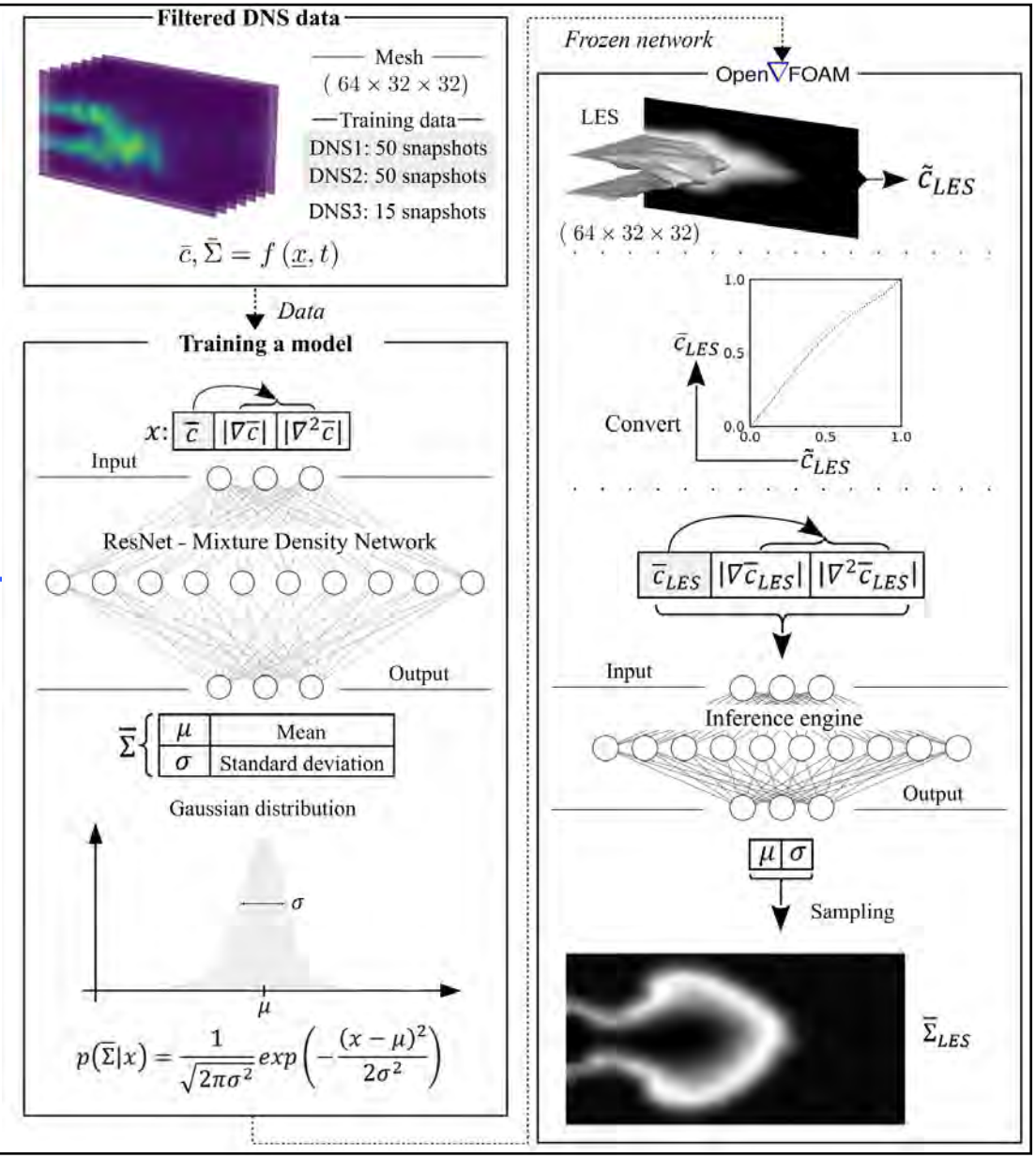

Turbulence Effect on Knock Intensity

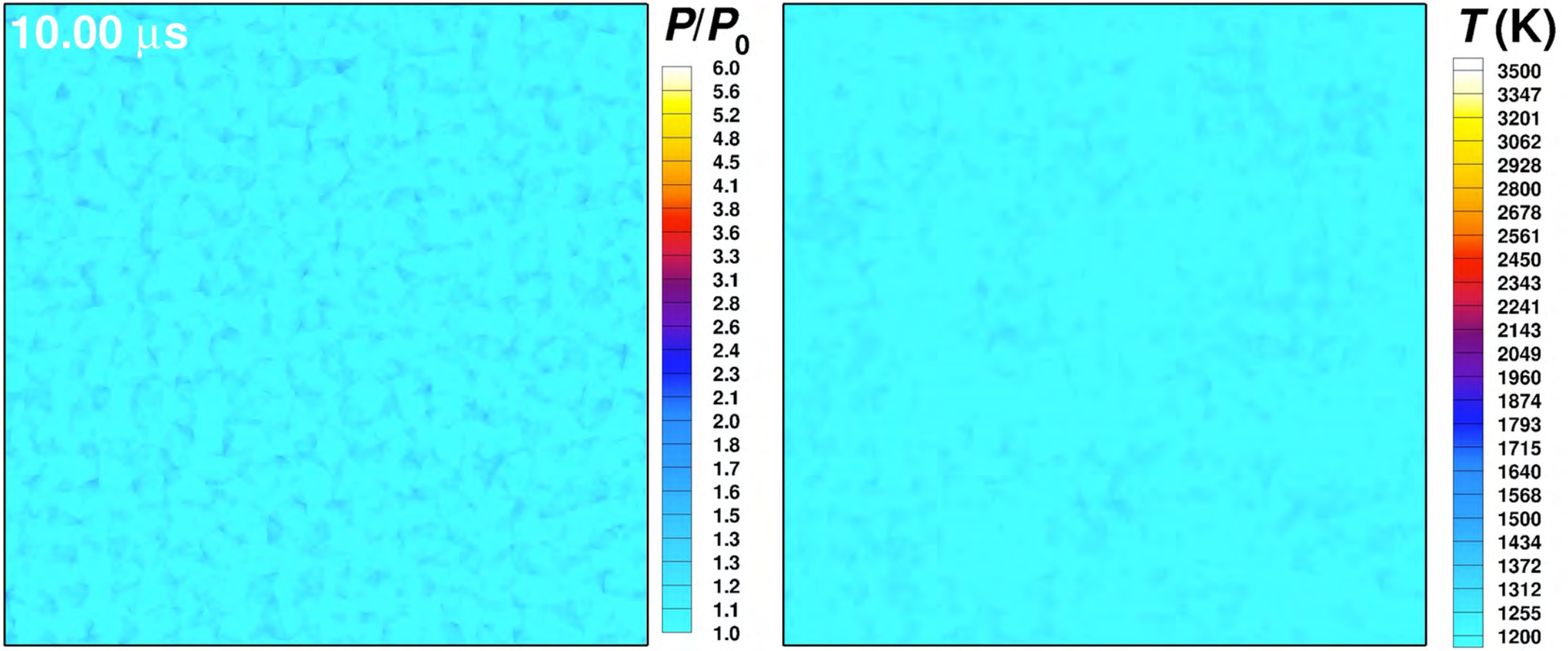

$L_x \times L_y = 20.48 \times 20.48$ mm^2, l_T = 5 mm, T' = 15 K, u' = 83.3 m/s, l_e = 1 mm, τ_{ig}/τ_t = 5

Increased turbulence intensity reduces knock intensity

CNN for Knock Prediction

Input image
RBG 3 layers/channels

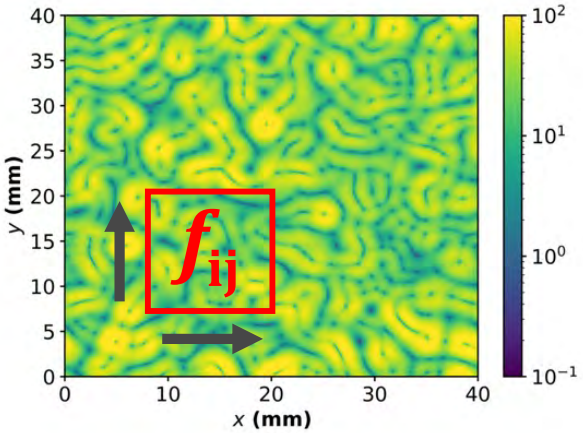

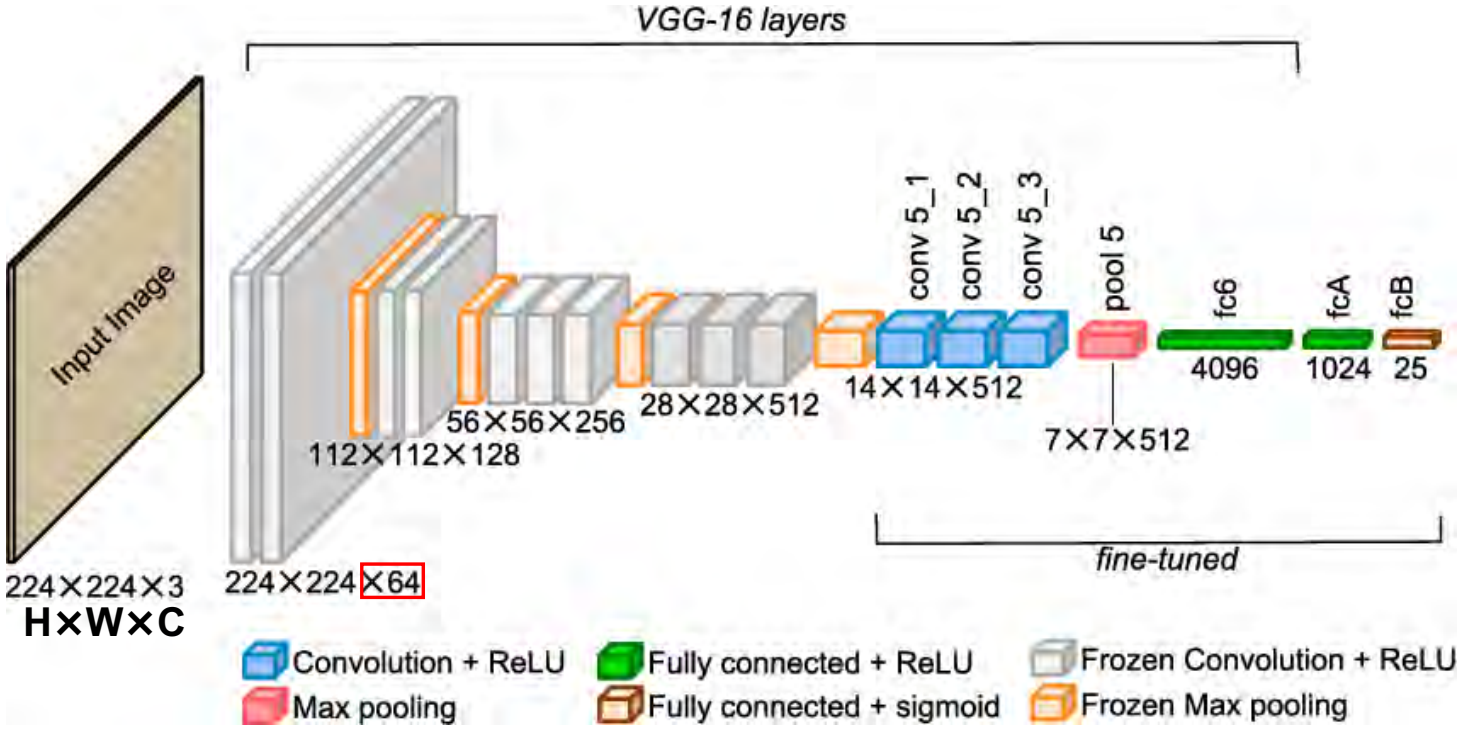

Convolution filter size of ***f*** **3×3×3**, pooling applied across input images of size **224×224×3**
Pooling (extracting) size **2×2**
×64 time convolutional filters (depth)
Rectifier Linear Unit (**ReLU**) is the most commonly deployed activation function for the outputs of **CNNs**.

CNN for Feature Extraction

Analysis of detonation cells from soot foils

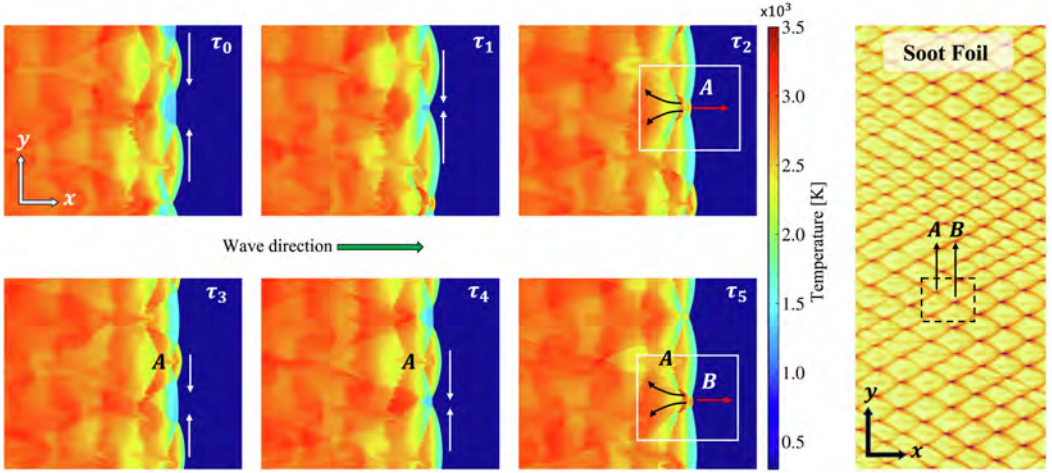

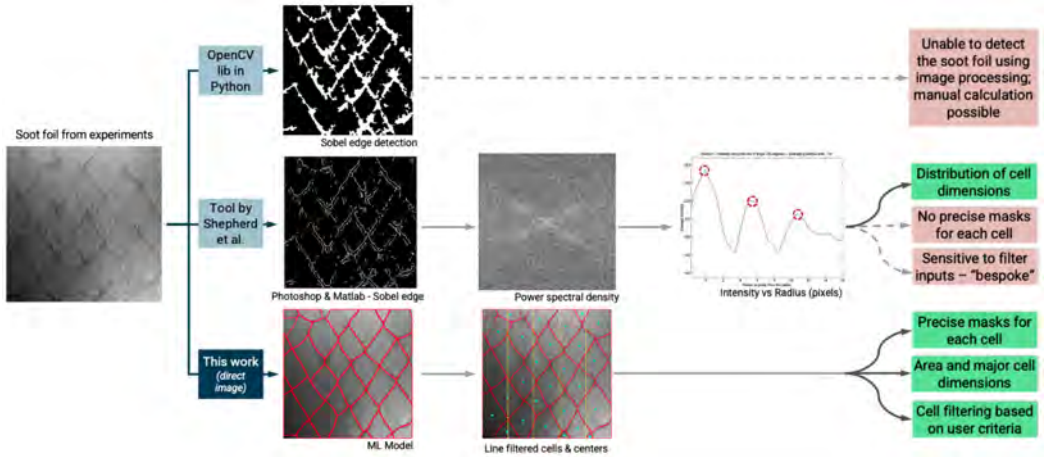

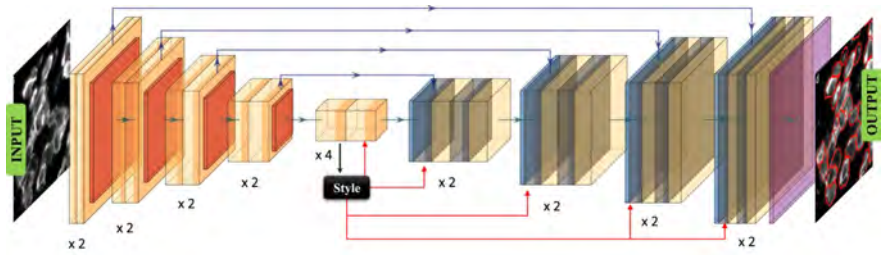

Feature measurements?

1) Area calculation
2) Centroid calculation
3) Bounding box calculation
4) Major & minor axes calculation

Sharma, V, et al., 2025, Combustion & flame, 274, 114026.

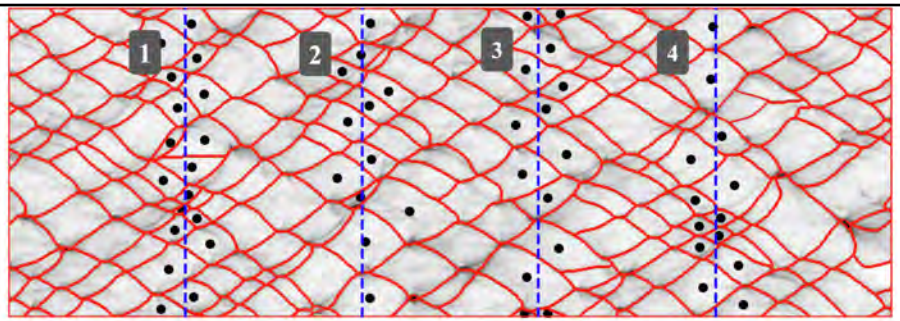
1
2
3
4

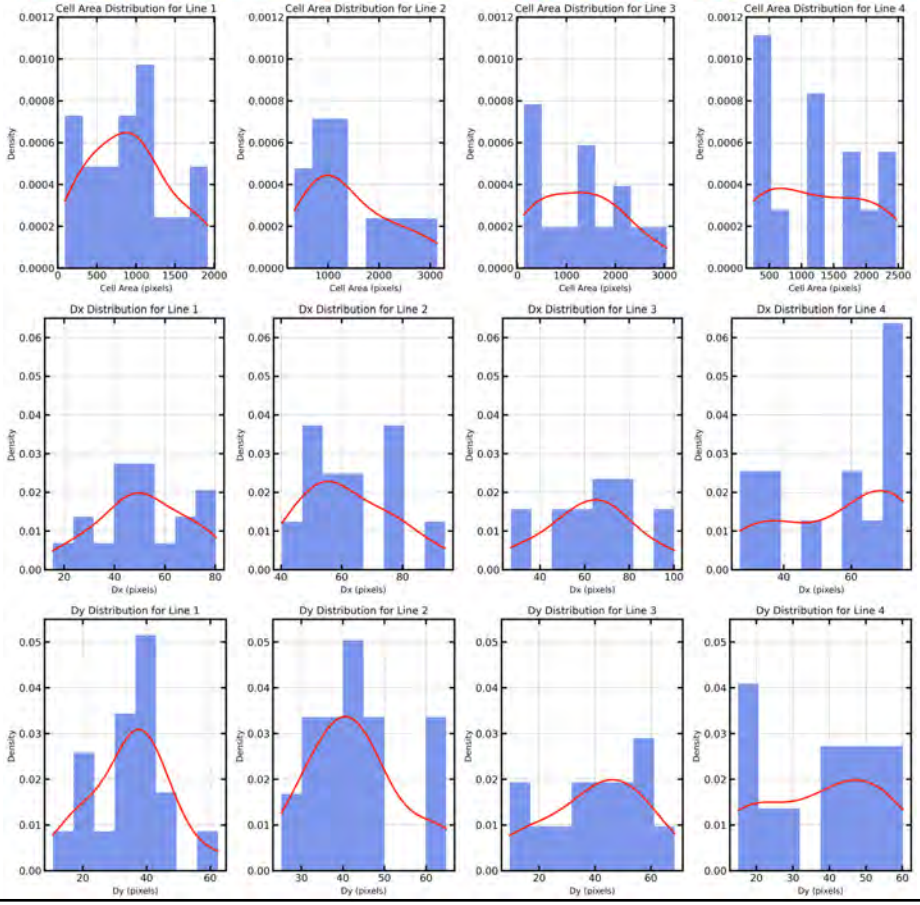
Cell Area Distribution for Line 1
Cell Area Distribution for Line 2
Cell Area Distribution for Line 3
Cell Area Distribution for Line 4
Dx Distribution for Line 1
Dx Distribution for Line 2
Dx Distribution for Line 3
Dx Distribution for Line 4
Dy Distribution for Line 1
Dy Distribution for Line 2
Dy Distribution for Line 3
Dy Distribution for Line 4
Density
Cell Area (pixels)
Dx (pixels)
Dy (pixels)

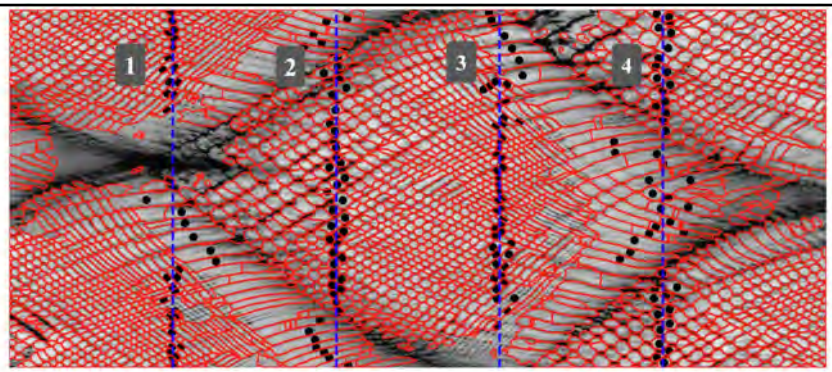
1
2
3
4

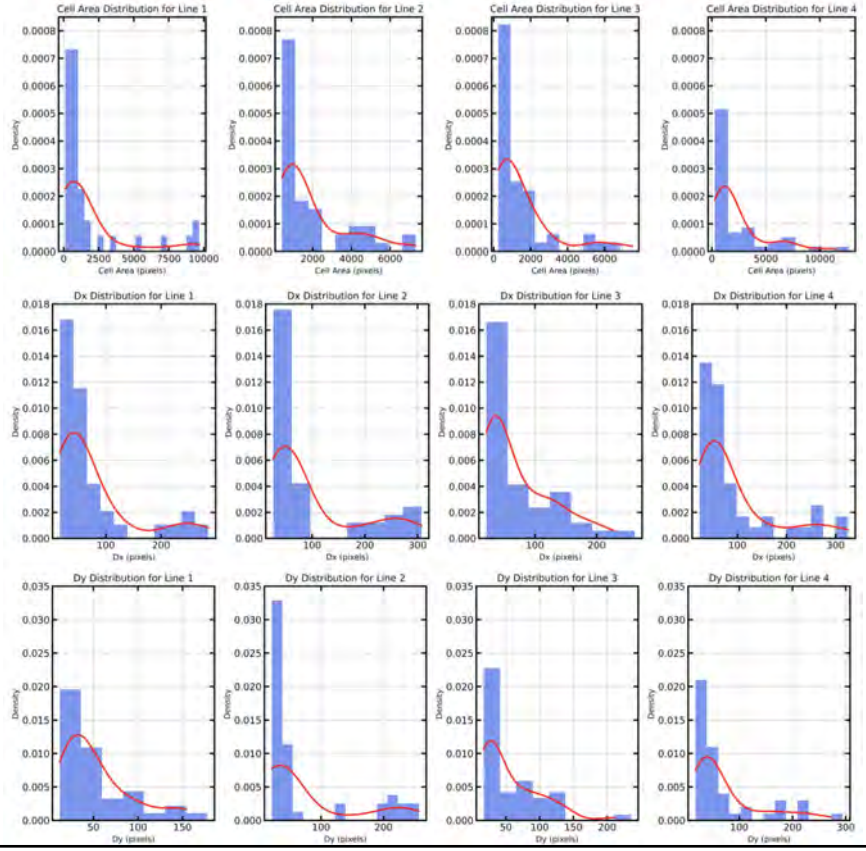
Cell Area Distribution for Line 1
Cell Area Distribution for Line 2
Cell Area Distribution for Line 3
Cell Area Distribution for Line 4
Dx Distribution for Line 1
Dx Distribution for Line 2
Dx Distribution for Line 3
Dx Distribution for Line 4
Dy Distribution for Line 1
Dy Distribution for Line 2
Dy Distribution for Line 3
Dy Distribution for Line 4
Density
Cell Area (pixels)
Dx (pixels)
Dy (pixels)

ML Applications in Fluid Mechanics and Combustion

Reduced Order Models for Dynamics

Neural Network for Dynamical Systems

Type#1

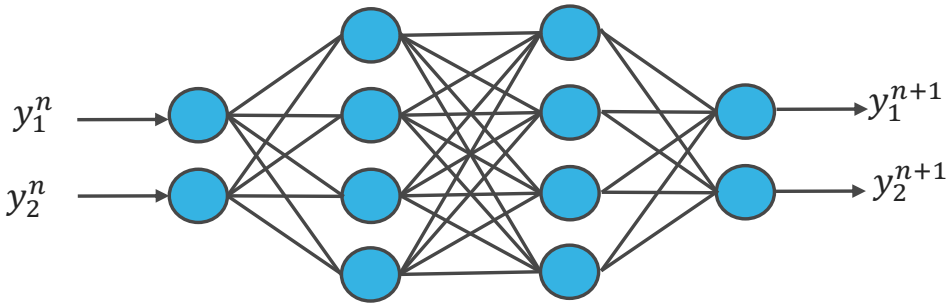

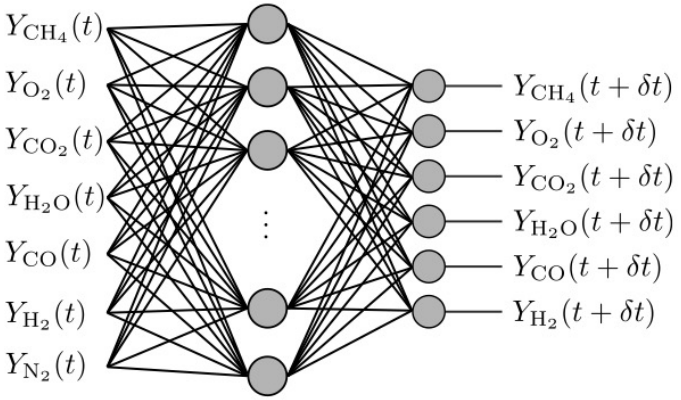

Type#2

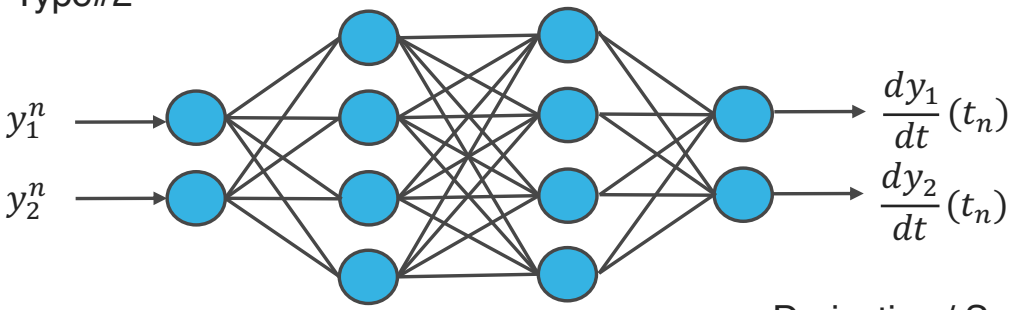

Derivative / Source term in chemical system

$$y_i^{n+1} = y_i^n + \Delta t * \frac{dy_i}{dt}(t_n)$$

Forward Euler method

Recurrent Neural Network (RNN)

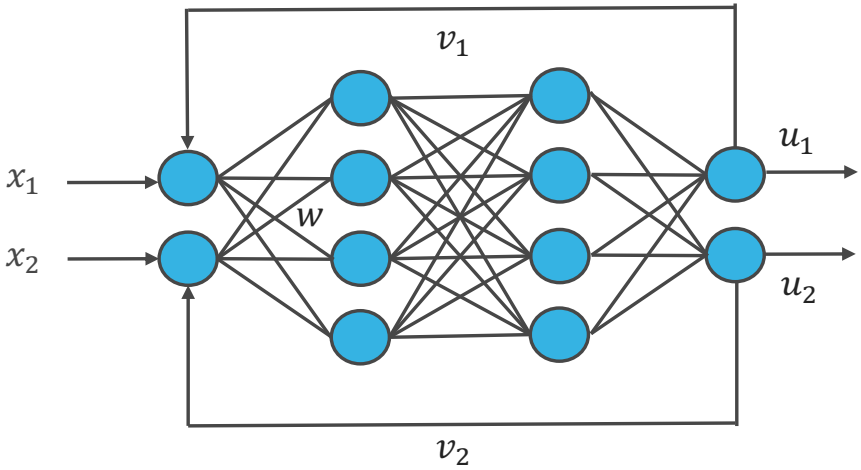

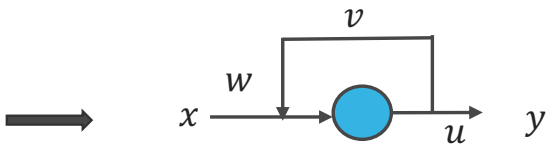

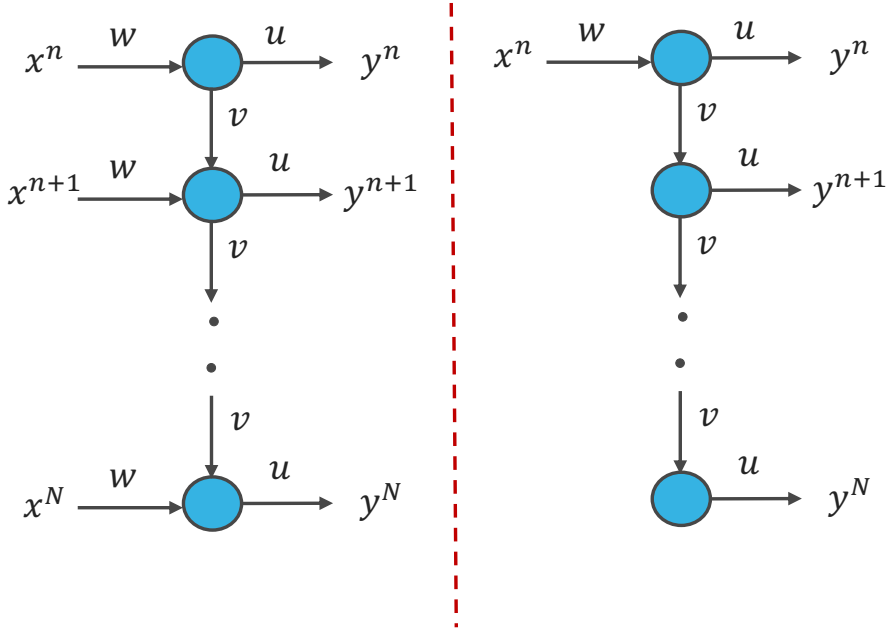

Step 1) Forward propagation:

$$h_{n+1} = e(f(wx_{n+1}) + vh_n)$$

Step 2) Calculating loss function:

$$L_{n+1} = g(w, x_{n+1}, v, h_n) = g(, x_{n+1}, h_n, \theta)$$

$$but\ h_n = o(x_n, h_{n-1}, \theta)$$

Step 3) Backward propagation : =+ Through time

Vanishing/Exploding gradient & Remedy:

LSTM (Long and Short Term Memory), GRU (Gated Recurrent Unit)

Step 4) Optimization

Long and Short Term Memory (LSTM)

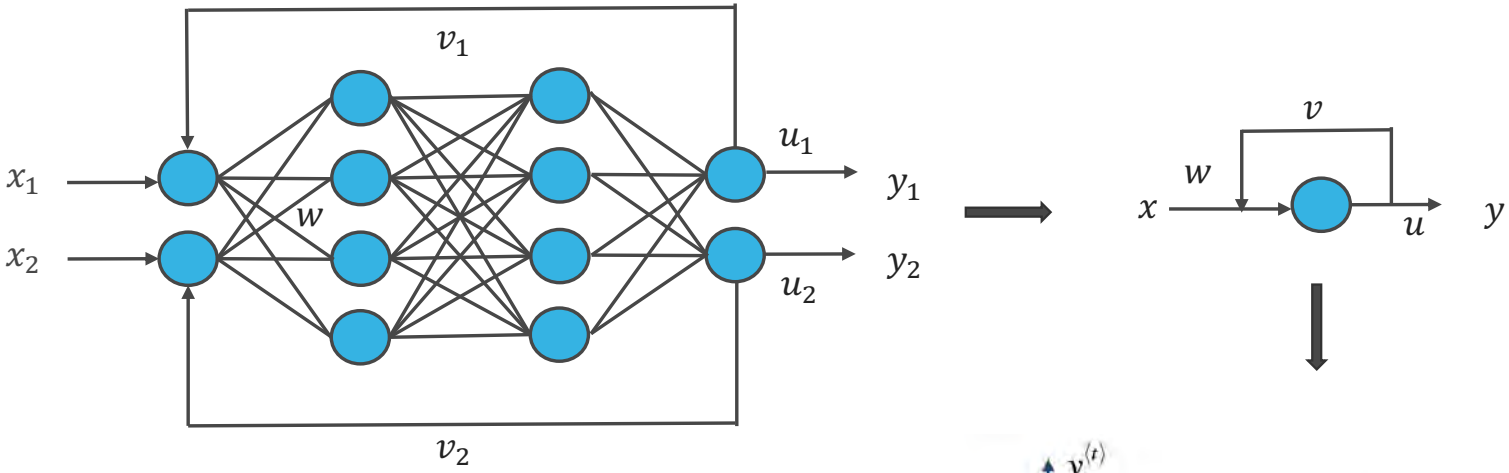

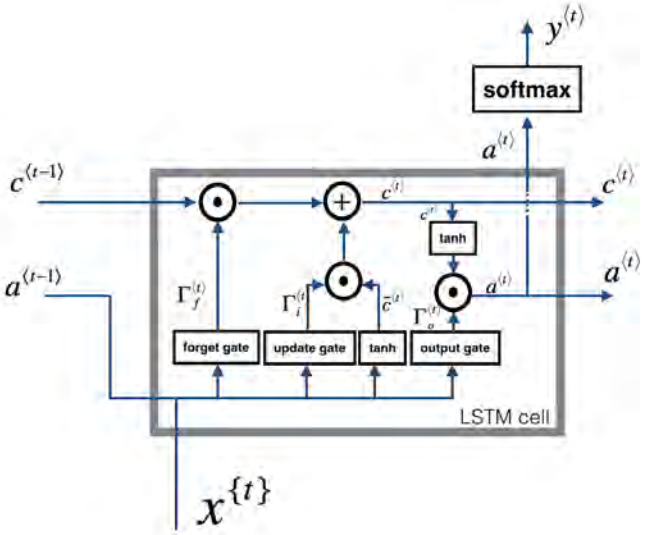

$$\Gamma_f^{\langle t \rangle} = \sigma(W_f[a^{\langle t-1 \rangle}, x^{\langle t \rangle}] + b_f)$$
$$\Gamma_u^{\langle t \rangle} = \sigma(W_u[a^{\langle t-1 \rangle}, x^{\langle t \rangle}] + b_u)$$
$$\tilde{c}^{\langle t \rangle} = \tanh(W_c[a^{\langle t-1 \rangle}, x^{\langle t \rangle}] + b_c)$$
$$c^{\langle t \rangle} = \Gamma_f^{\langle t \rangle} \circ c^{\langle t-1 \rangle} + \Gamma_u^{\langle t \rangle} \circ \tilde{c}^{\langle t \rangle}$$
$$\Gamma_o^{\langle t \rangle} = \sigma(W_o[a^{\langle t-1 \rangle}, x^{\langle t \rangle}] + b_o)$$
$$a^{\langle t \rangle} = \Gamma_o^{\langle t \rangle} \circ \tanh(c^{\langle t \rangle})$$

Source: DeepLearning.ai

Deepjazz: LSTM & Jazz

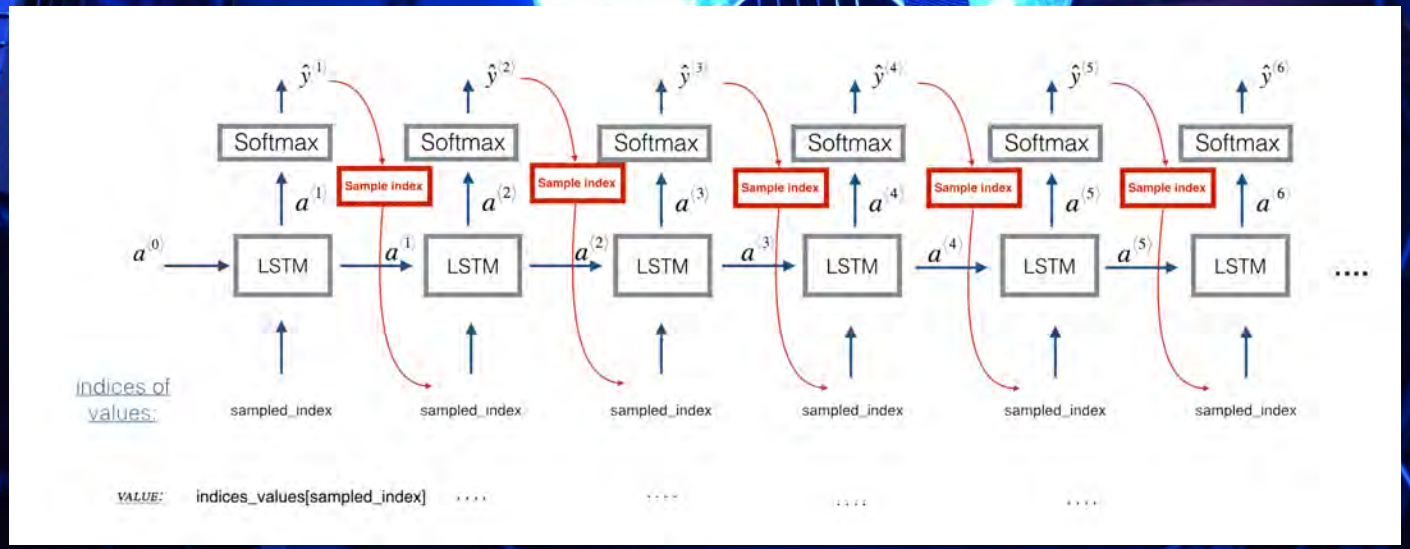

Source: DeepLearning.ai

Neural ODE for Chemical Kinetics

Chen, Rubanova, Bettencout, Duvenaud, arXiv, (2018) 1806.07366.

Neural Network (NN) = Universal Function Approximator

$$\frac{dy(t)}{dt} = \dot{\omega}_y = f_\beta(y(t))$$

$$y^1, y^2, \ldots, y^n = \textbf{ODE Solve}\ (y^0, f_\beta, t_1, t_2, \ldots, t_n)$$

$$y_i^{n+1} = y_i^n + \int_n^{n+1} f_\beta(y_i^n)\, dt$$

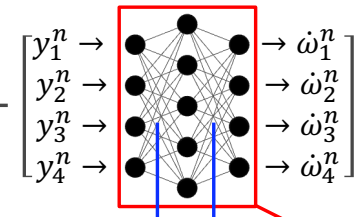

Training

Loss

$f_\beta(y(t)) \leftarrow NN$

$w_1\ \ w_2$
$b_1\ \ b_2$

β = NN parameters

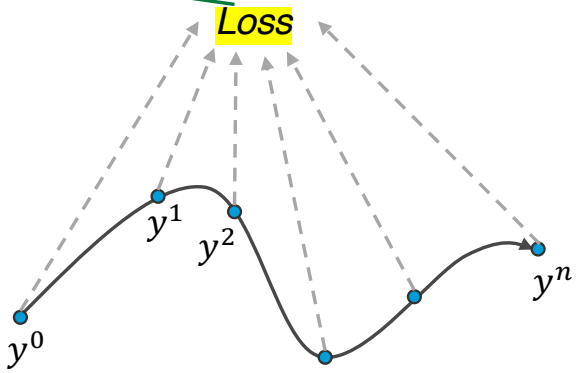

$$f_\beta(y(t)) = \sigma_2(w_2^T.\sigma_1(w_1^T.y(t) + b_1) + b_2)$$

$$y^1, y^2, \ldots, y^n = \textbf{ODE Solve}\ (y^0, f_\beta, t_1, t_2, \ldots, t_n)$$

Autoencoder for Combustion Data

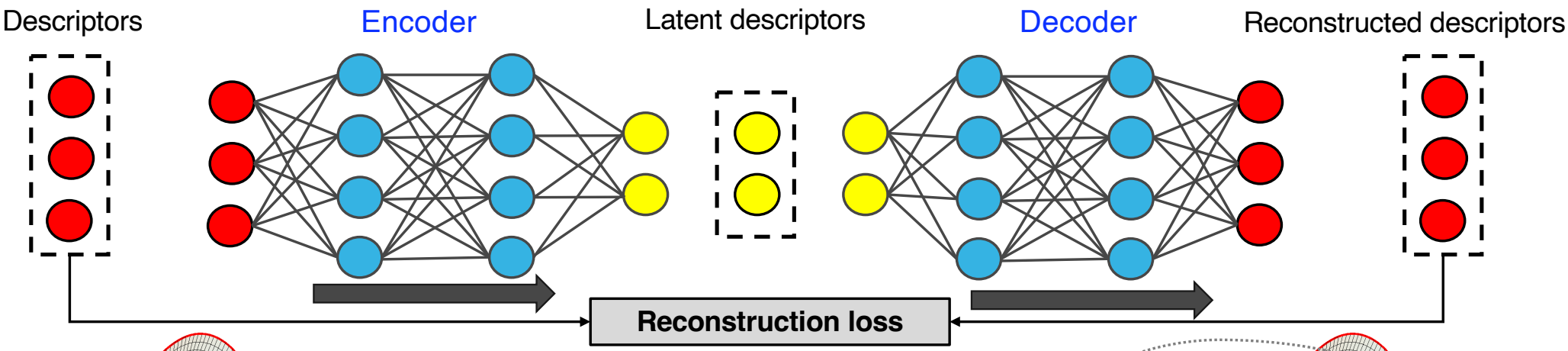

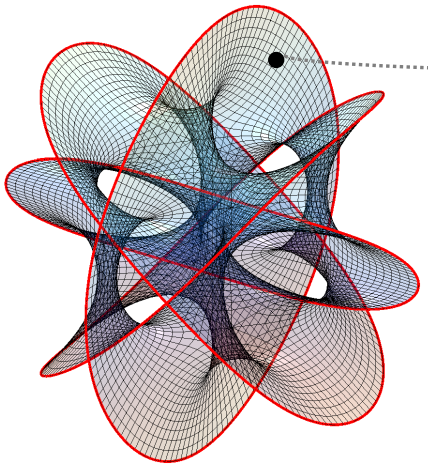

High-dimensional manifold
of physical space

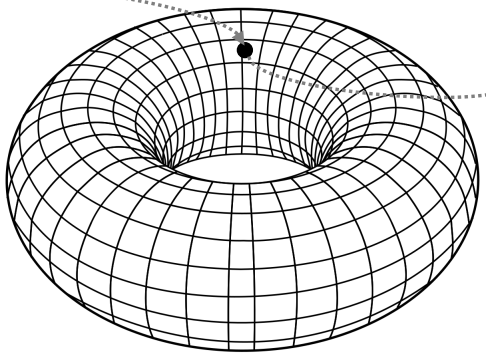

Low(er)-dimensional
manifold of latent space

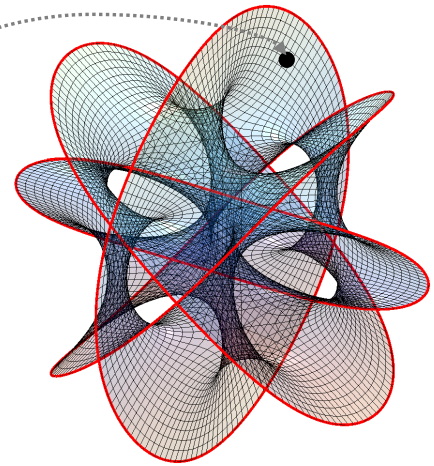

Reconstructed high-dimensional
manifold of physical space

Autoencoder + Neural ODE

Neural ODE for chemical kinetics:

$$\frac{dy(t)}{dt} = \dot{\omega}_y = f_\beta(y(t), t) = NN(y(t))$$

$$y^1, y^2, \ldots, y^n = ODE\ Solve\ (y^0, f_\beta, t_1, t_2, \ldots, t_n)$$

$$y_i^{n+1} = y_i^n + \int_n^{n+1} NN(y_i^n)\, dt$$

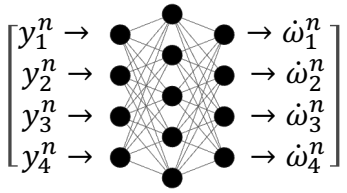

Owoyele et al., 2022, Energy and AI, 7, 100118.

Dynamics-informed training:

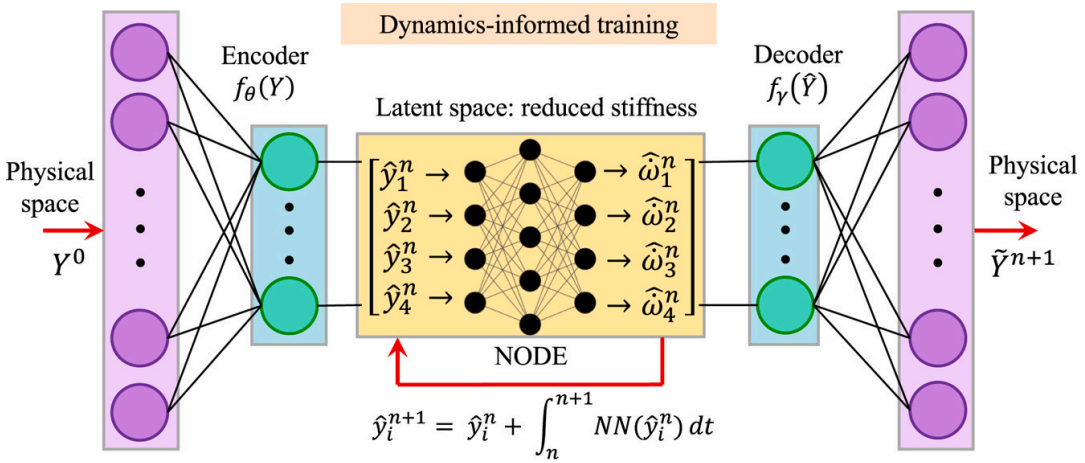

$$\mathcal{L} = \epsilon_1 \|Y - \tilde{Y}\|_2^2 + \epsilon_2 \|f_\gamma(f_\theta(Y)) - \tilde{Y}\|_2^2 + \epsilon_3 \|f_\theta(Y) - \hat{Y}\|_1$$

Vijayarangan et al., 2024, Energy and AI, 15, 100325.

Stiffness Reduction Using AE+NODE

Objective: Integrate the chemistry in latent space using Neural ODE with reduced stiffness

Solve for $\frac{dY_k}{dt} = \dot{\omega}_k$

1. Project the state vector to a latent space using encoders
2. Integrate the reduced state in the latent space using Neural ODE
3. Retrieve the state vector in the physical space using decoders

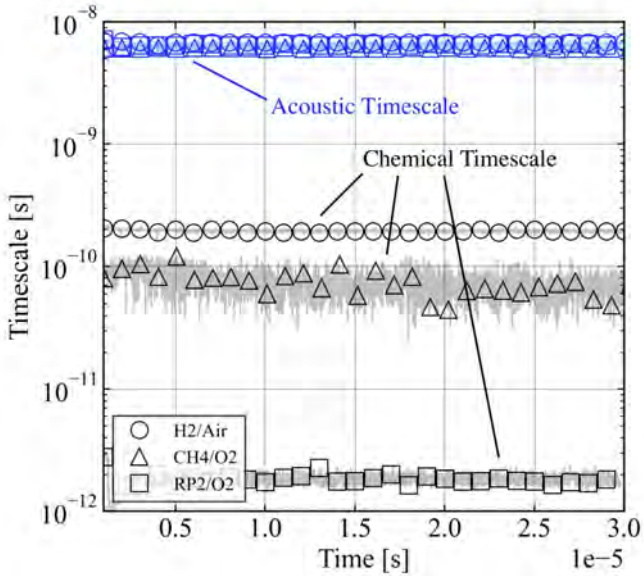

Courtesy: S. Barwey., ANL, USA

Physical space: Full state at time t_n

Encoder

Latent space: Reduced state at time t_n

Neural ODE

Integrate the reduced state

Latent space: Reduced state at time t_{n+1}

Decoder

Physical space: Full state at time t_{n+1}

Stiffness Reduction & Time Step Improvement

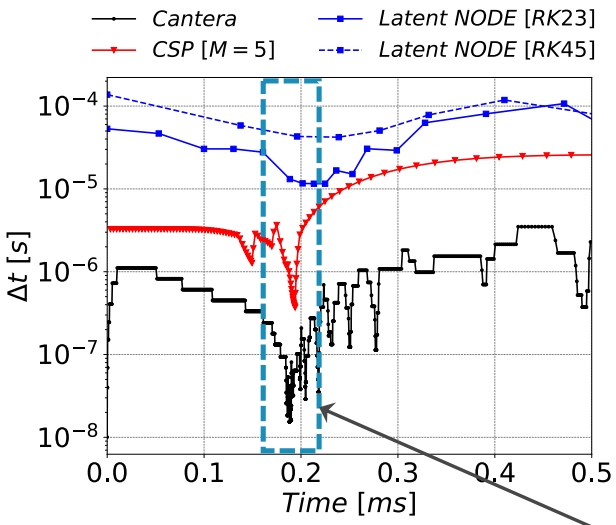

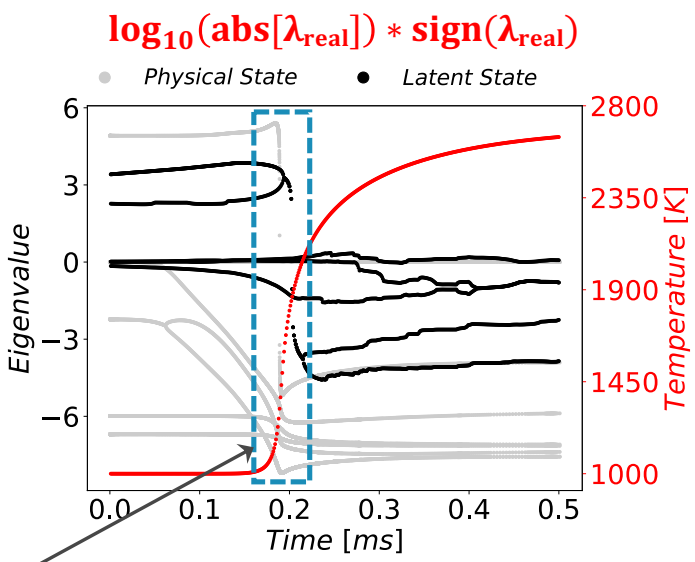

Ignition

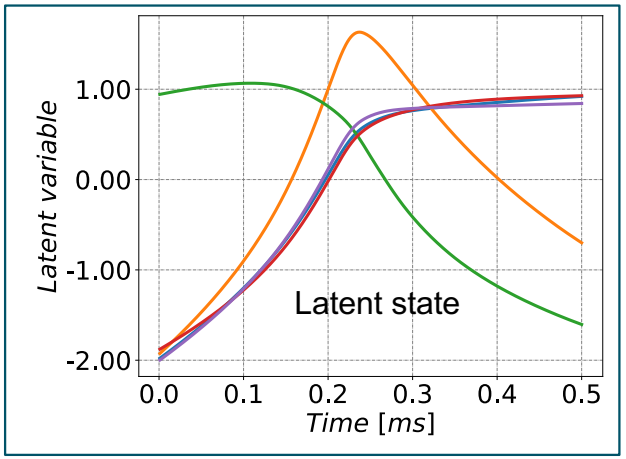

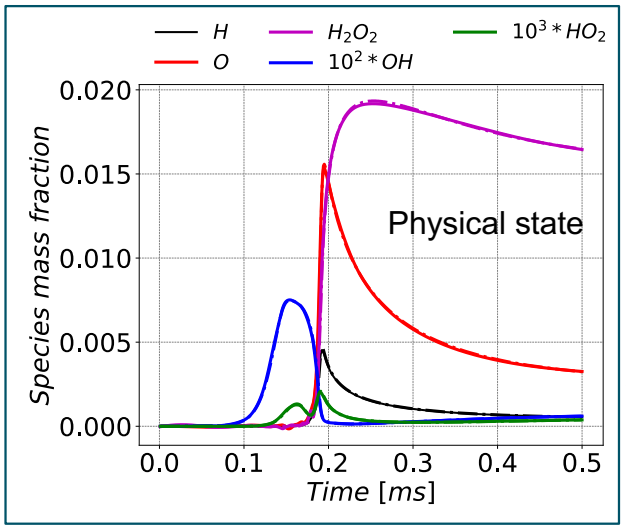

1. Stiffness: Due to large spectrum of eigenvalues
2. Latent space: Stretches the dynamics and reduces the stiffness
3. Integrate the latent dynamics with larger time step compared to other stiff solvers

Vijayarangan et al., 2023, Energy and AI, 15, 100325.

Information Theory: Fundamental Concepts

Important metrics

1. **Shannon Entropy:** Measures the average uncertainty associated with the random variable's (X) possible outcomes

   Q) How random is the variable X?

   $$H(X) = -\int p(X)\, log\big(p(X)\big)\, dX$$

2. **Kullback-Leibler Divergence (or) Relative entropy:** Measure of the "distance" between two probability density functions

   Q) How far is pdf(X) from pdf(Y)?

   $$D_{KL}[p(X)||q(X)] = -\iint p(X) log\left(\frac{p(X)}{q(X)}\right) dx$$

3. **Mutual Information:** Measure of dependence between two random variables X and Y

   $$I(X;Y) = H(X) - H(X|Y) = H(Y) - H(Y|X)$$
   $$= D_{KL}[p(X,Y)||p(X)p(Y)]$$

   Q) X & Y dependent or independent?

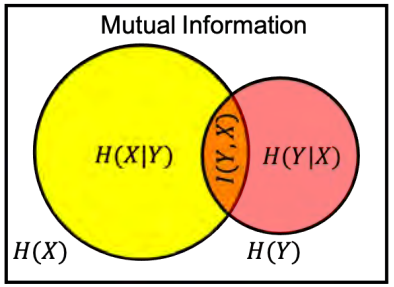

Understanding AED+NODE via Information Plane

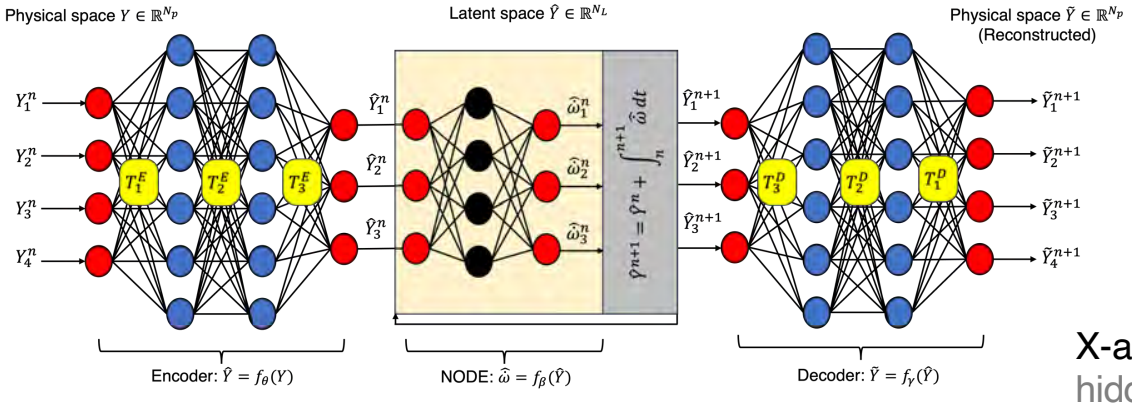

Data Processing Inequalities:

Encoder: $I(Y;T_1) \geq I(Y;T_2) \geq \cdots \geq I(Y;\hat{Y})$

Decoder: $I(\tilde{Y};T_1') \geq I(\tilde{Y};T_1') \geq \cdots \geq I(\tilde{Y};\hat{Y})$

X-axis: Amount of information passes through the encoder hidden layers

Y-axis: Amount of information the encoder hidden layer needs to know for accurate solution reconstruction

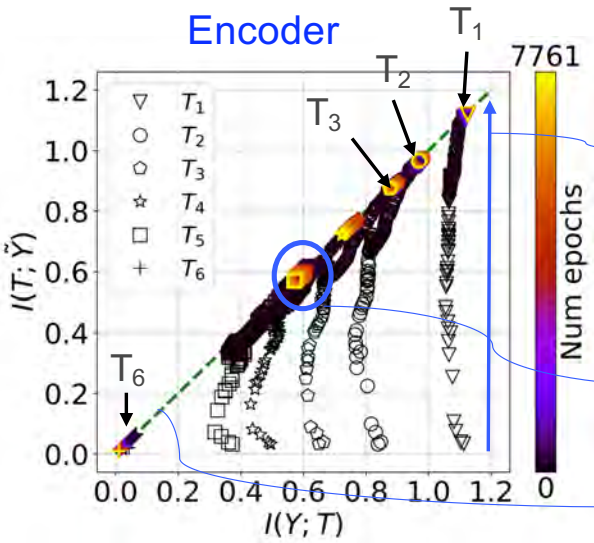

1. Fitting phase

Both fitting and compression phases are essential for good network training.

2. Compression phase

Limiting Line

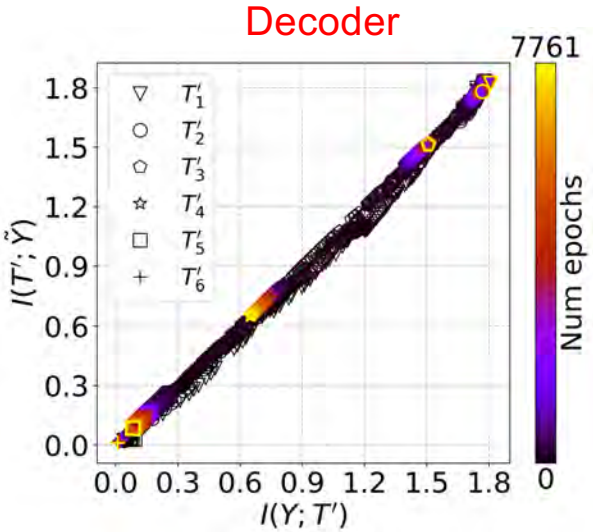

Vijayarangan et al., 2025,arXiv:2503.06325.

Gradient-Informed Autoencoder & NODE

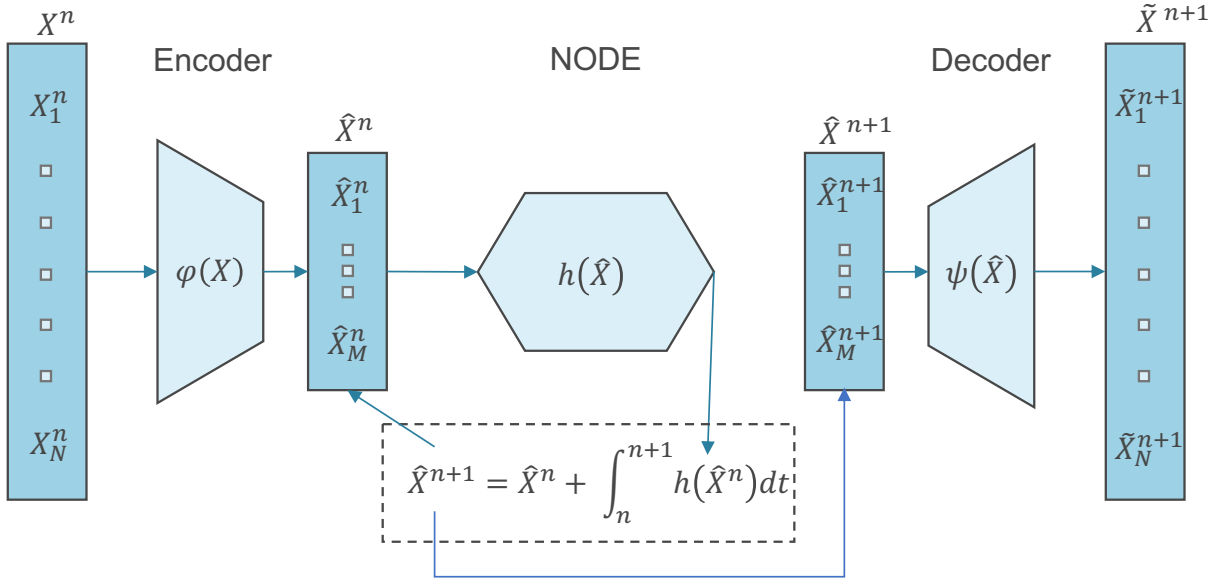

Latent Dynamics Integration

$$L = \alpha_1 L_1 + \alpha_2 L_2 + \alpha_3 L_3 + \alpha_4 L_4$$

$$f(X) = \frac{dX}{dt}$$

$L_1 = \|X - \tilde{X}\|_2^2$ Prediction Loss

$L_2 = \|X - \psi(\varphi(X))\|_2^2$ Auto Encoder Decoder Loss

$L_3 = \|\hat{X} - \varphi(X)\|_1$ Latent Variable Loss

$L_4 = \|h(\varphi(X)) - \nabla\varphi(X)f(X)\|_2^2$ Latent Gradient Loss

Baykan et al., 2025, CMAME (under review).

Generalization: Improved Extrapolation Accuracy

T

X_{H_2}

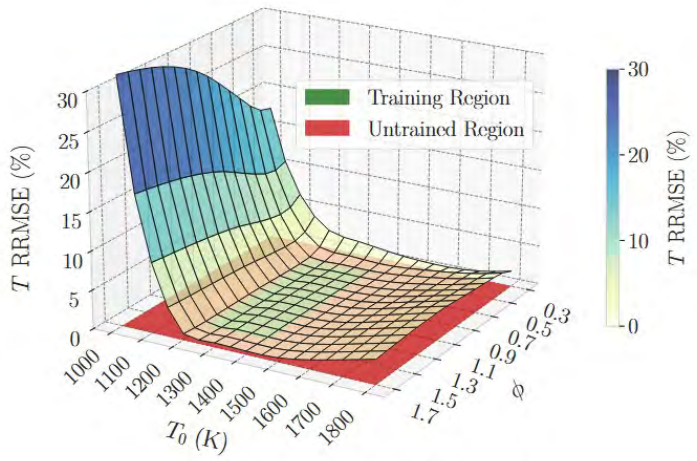

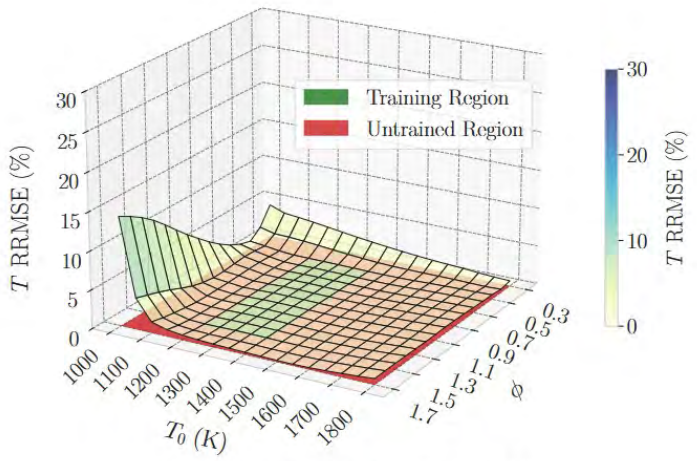

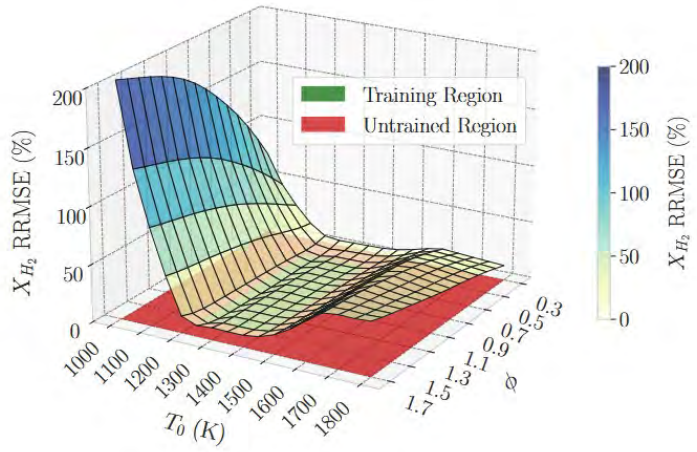

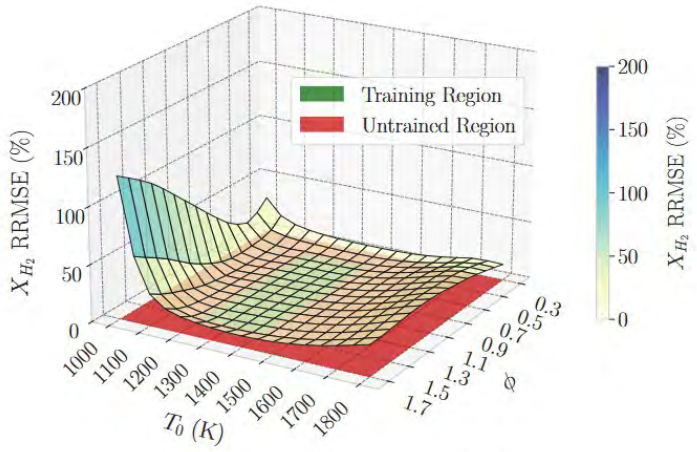

Without gradient loss

With gradient loss

Generative Adversarial Networks (GAN)

- **Generator Network:** Try to fool the discriminator by generating real-looking images
- **Discriminator Network:** Try to distinguish between real and fake images
- Train jointly in minimax game
- Minimax objective function:

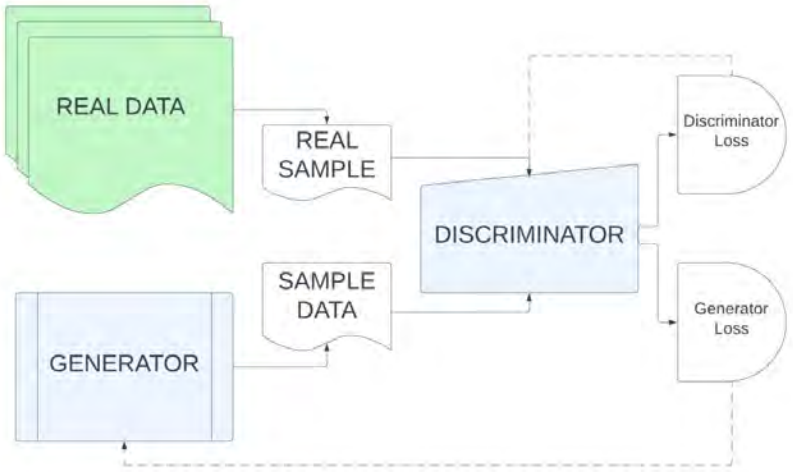

Discriminator outputs likelihood in (0,1) of real image

$$\min_{\theta_g} \max_{\theta_d} \left[\mathbb{E}_{x \sim p_{data}} \log D_{\theta_d}(x) + \mathbb{E}_{z \sim p(z)} \log \left(1 - D_{\theta} \left(G_{\theta_d}(z) \right) \right) \right]$$

Discriminator output for real data x

Discriminator output for generated fake data G(z)

Why Generative Models?

Generative models and deterministic models have distinct approaches to understanding data.

We want to use the information in X to predict/estimate Y

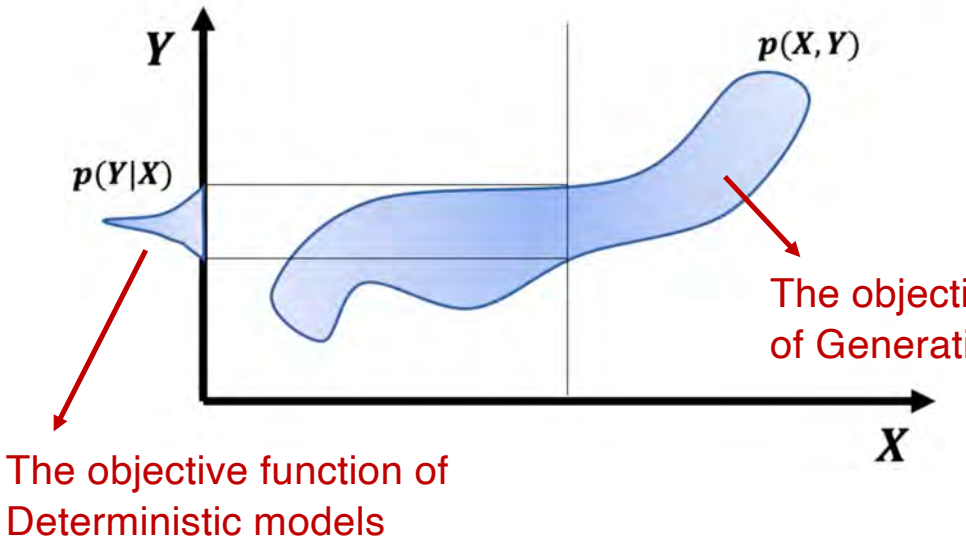

$X \Longrightarrow Y$

$\mathbf{p}(X, Y) \Longrightarrow p(Y|X)p(X)$

This involves extracting and using the information in X that is relevant for the prediction of Y

Despite generative models often having more parameters, they can require less data compared to deterministic models.

Application: In Fluid dynamics and Combustion

Super resolution

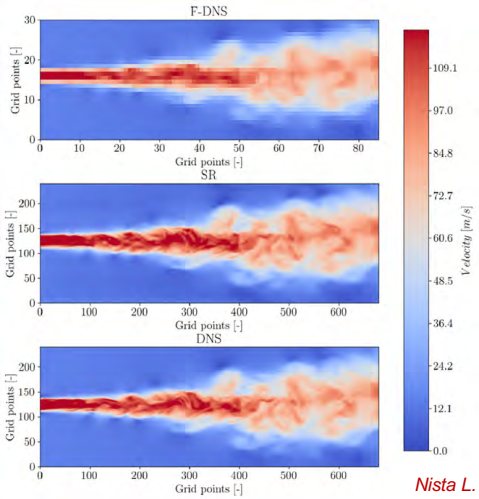

Nista L. et al.,

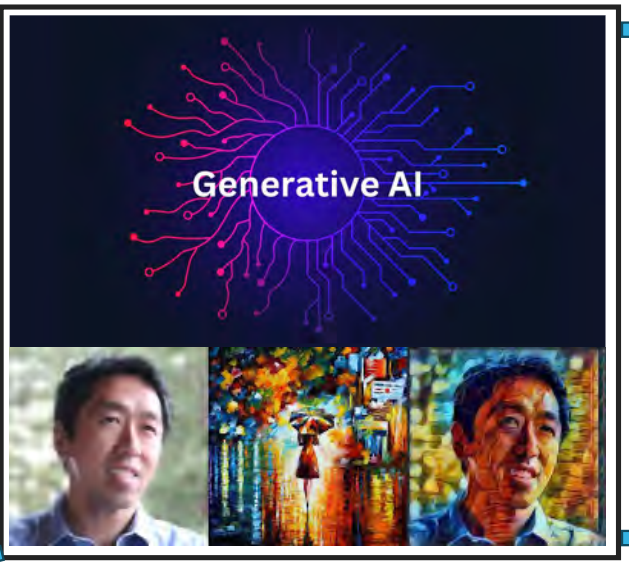

Data recovery

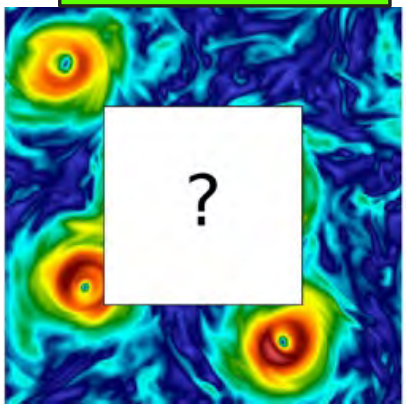

Li T. et al.,

Data synthesis

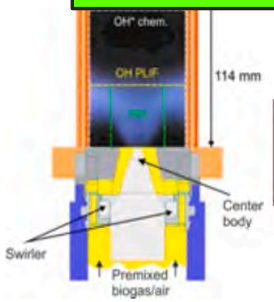

Measured flow field

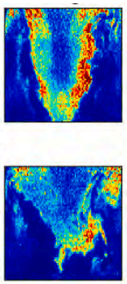

AI-generated flow field

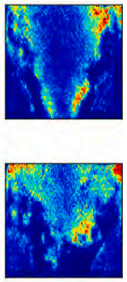

Carreon A. et al.,

Dimensionality reduction

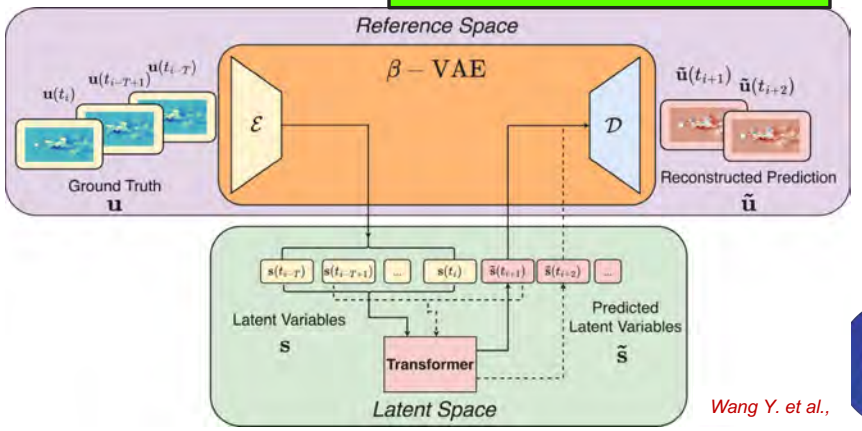

Wang Y. et al.,

GAN Application in Fluid Dynamics

Buzzicotti, A Letter J. Exploring the Frontiers of Phy., 142 (2023)23001.

(i) Real-space Reconstruction (full state)

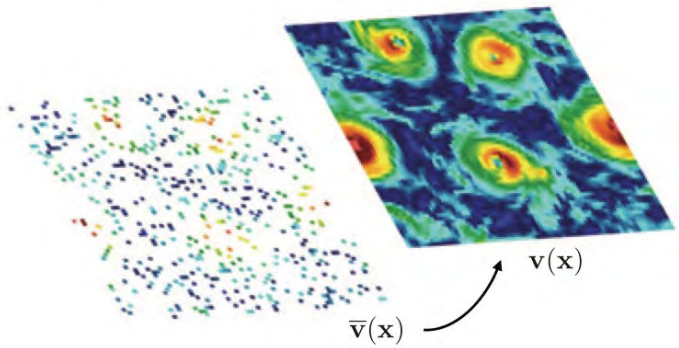

(iii) Fourier-space Reconstruction (Super Resolution)

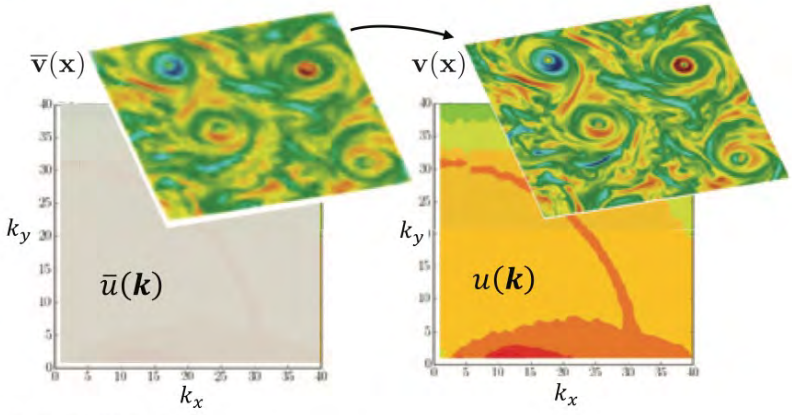

(ii) Missing Physics (Inverse Problems)

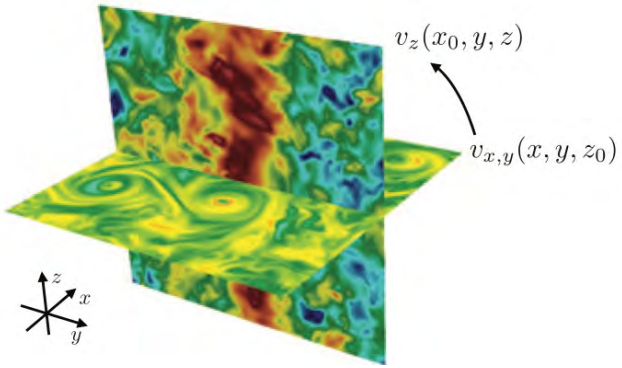

(iv) Sub-Grid Closure (Modeling)

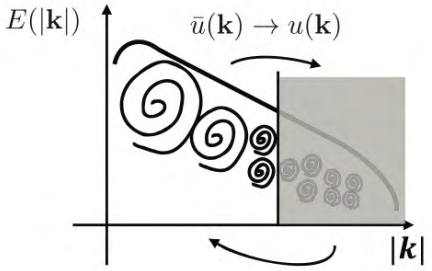

$$\bar{\mathbf{u}}(\mathbf{k}) \to \partial_t \bar{\mathbf{u}}(\mathbf{k}) = \ldots + \nabla \cdot \tau$$

$$\tau_{ij} = \overline{u_i u_j} - \bar{u}_i \bar{u}_j$$

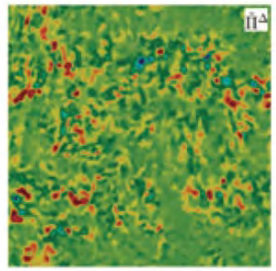

GAN for Synthetic Flame Images

Carreon, Barwey, Raman, Energy and AI, 13 (2023) 100238.

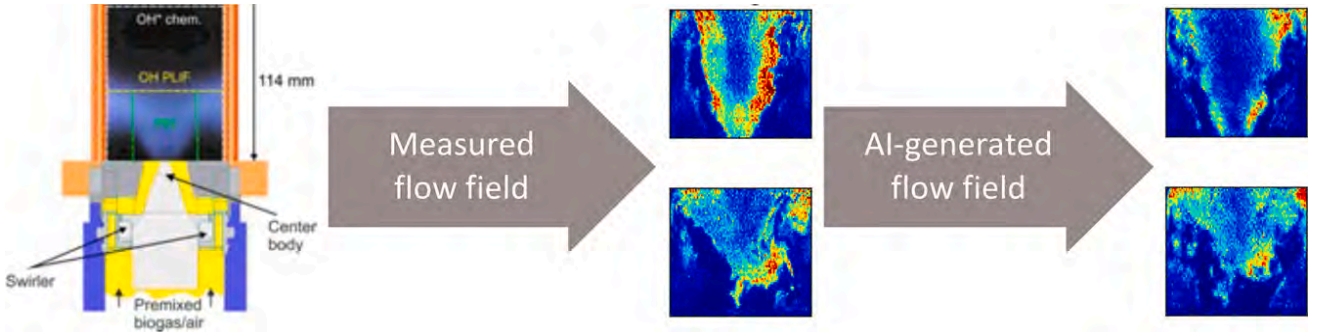

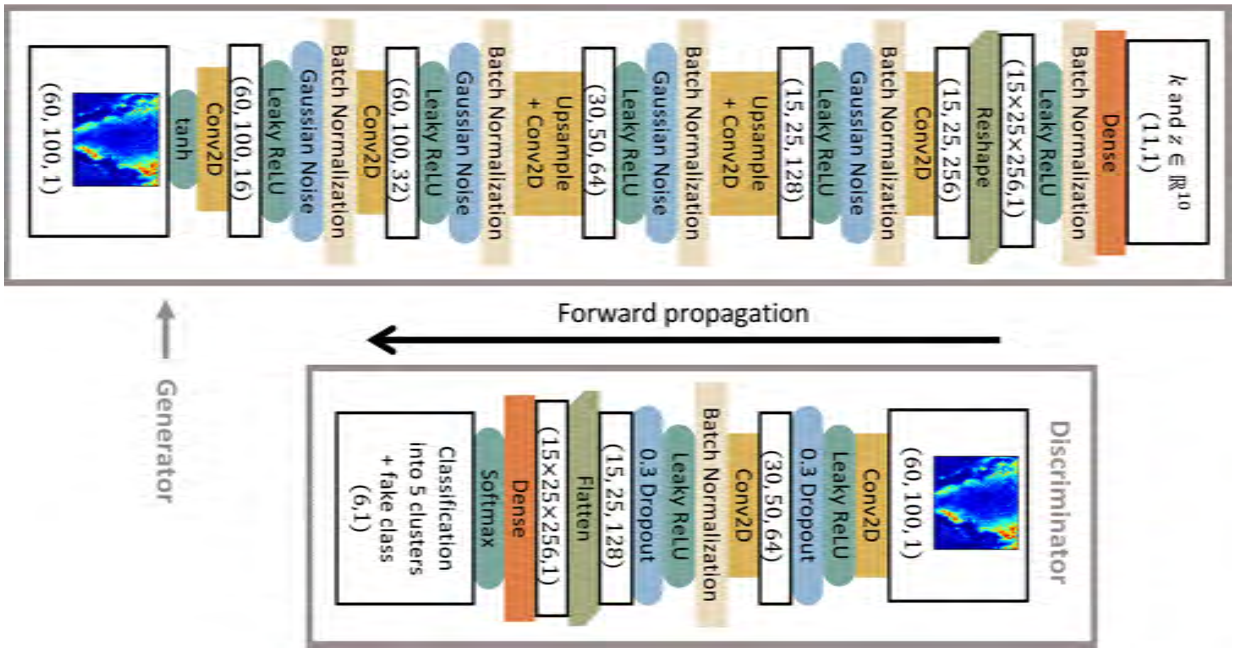

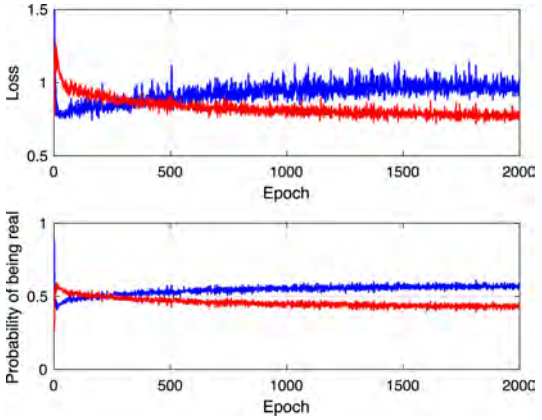

GAN for Super Resolution (SRGAN)

Nista, Schumann, Grenga, Attili, Pitsch, Proc. of the Comb. Inst., 39 (2023) 5279-5288.

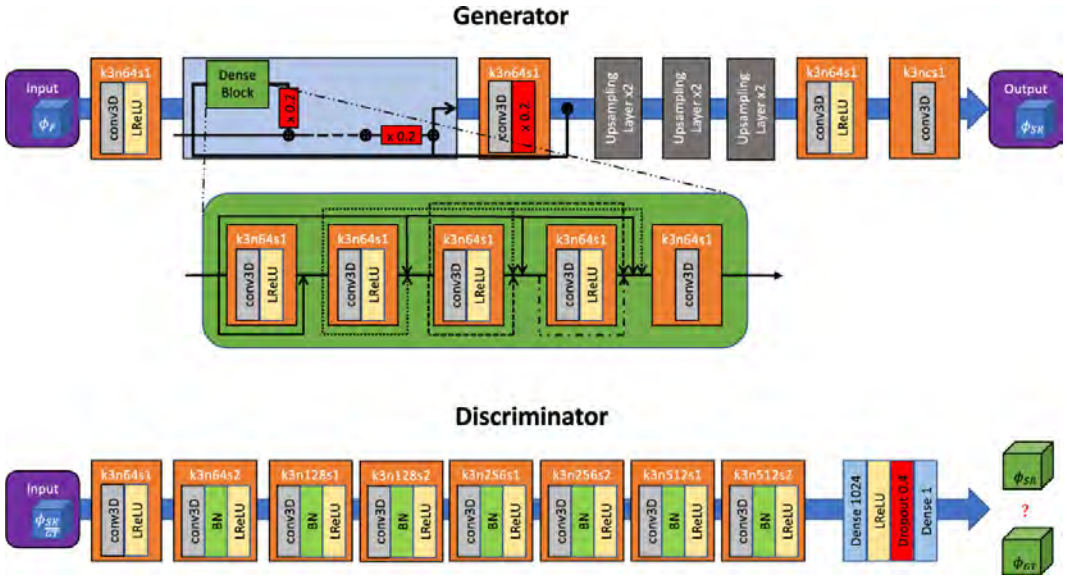

$$L_{gen} = \beta_1 L_{pixel} + \beta_2 L_{gradient} + \beta_3 L_{RaGAN}$$

$$L_{pixel} = MSE(\phi_{SR}, \phi_{DNS})$$

$$L_{gradient} = MSE(\nabla\phi_{SR}, \nabla\phi_{DNS})$$

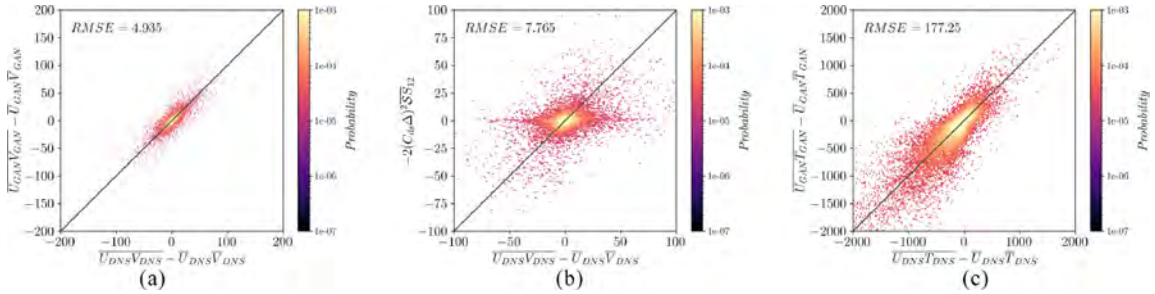

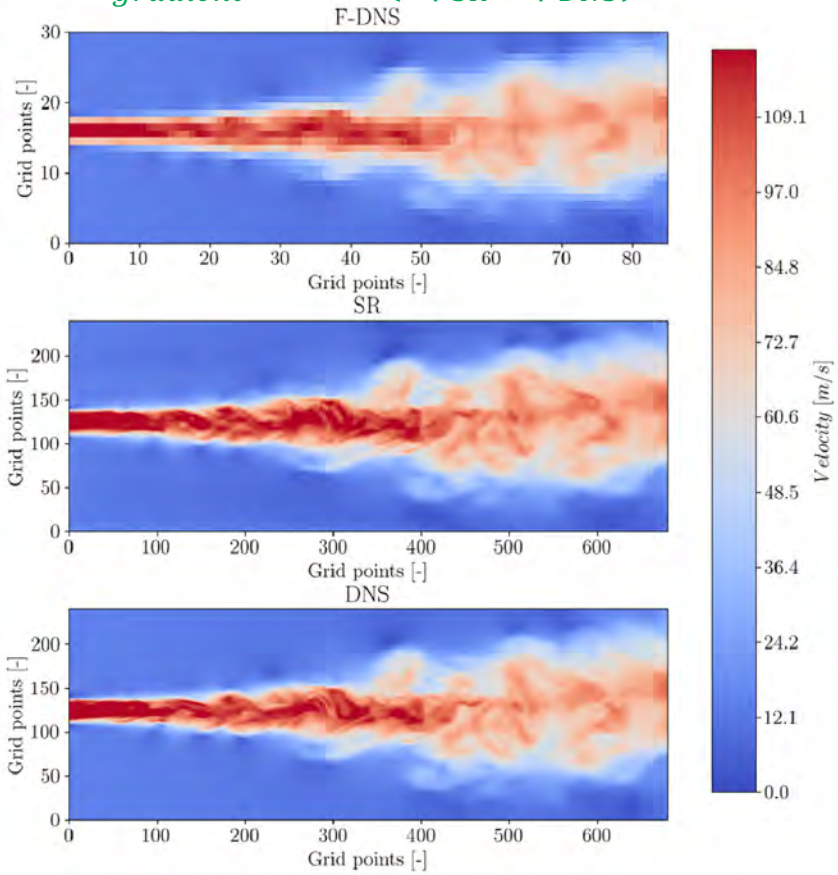

Physics Informed ESRGAN (PIESRGAN) for Subfilter Modeling of Passive Scalar

Bode, Gauding, Lian, Denker, Davidovic, Kleinheinz, Jitsev, Pitsch, Proc. of the Comb. Inst., 38 (2021) 2617-2625.

$$L_{gen} = \beta_1 L_{adversarial} + \beta_2 L_{pixel} + \beta_3 L_{gradient} + \beta_4 L_{continuity}$$

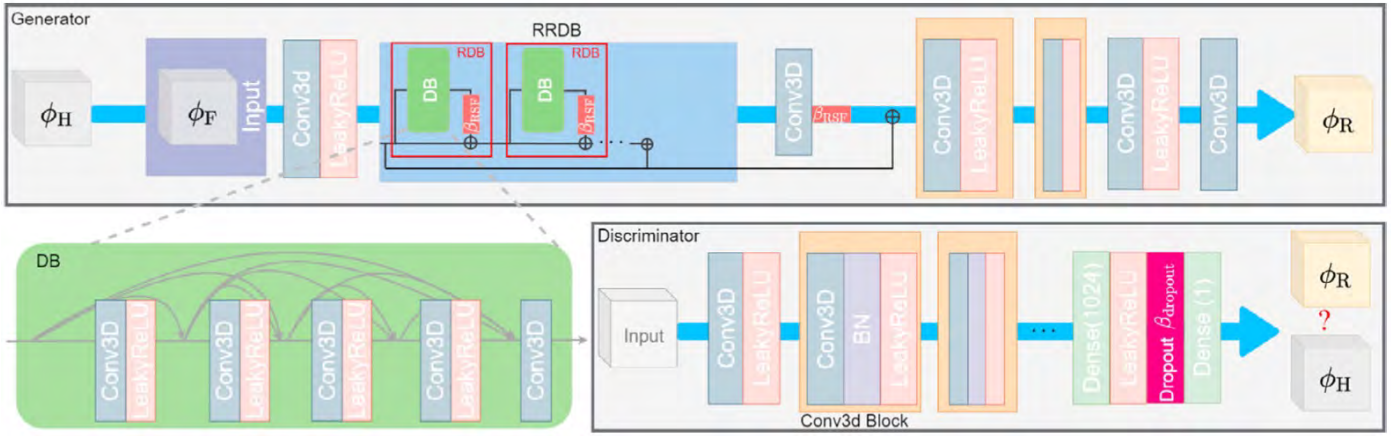

Fig. 1. Diagram of the PIESRGAN architecture.

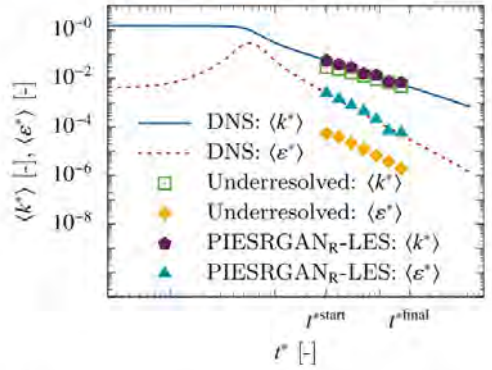

Fig. 4. Temporal evolution of the ensemble-averaged dimensionless turbulent kinetic energy ⟨k*⟩ and ensemble-averaged dimensionless dissipation rate ⟨ε*⟩.

Fig. 5. Temporally and circumferentially averaged fuel mass fraction (Y_{fuel}) evaluated 18.75 mm downstream from the nozzle and plotted against the radial distance from the spray axis r.

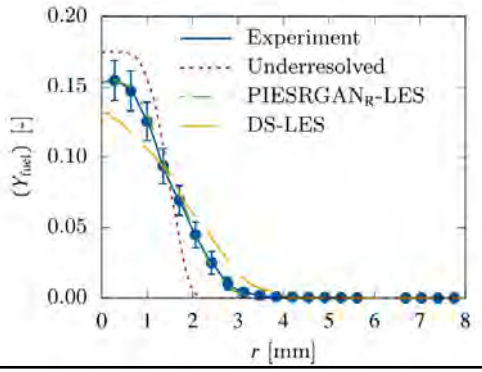

MS-ESRGAN and Transformer for Inflow Generation

Yousif, Zhang, Yu, Vinuesa, Lim, J. Fluid Mech., 957 (2022)1088.

Computation/Prediction of the inflow boundary condition for turbulent flow simulation based on Machine Learning technique

1. Transformer-based architecture, predicts the temporal evolution of the velocity distribution on the course field.
2. Using MS-ESRGAN (i) The generator performs super-resolution reconstruction for the predicted solution of the transformer (ii) The discriminator tries to distinguish the synthetic images from the real ones.

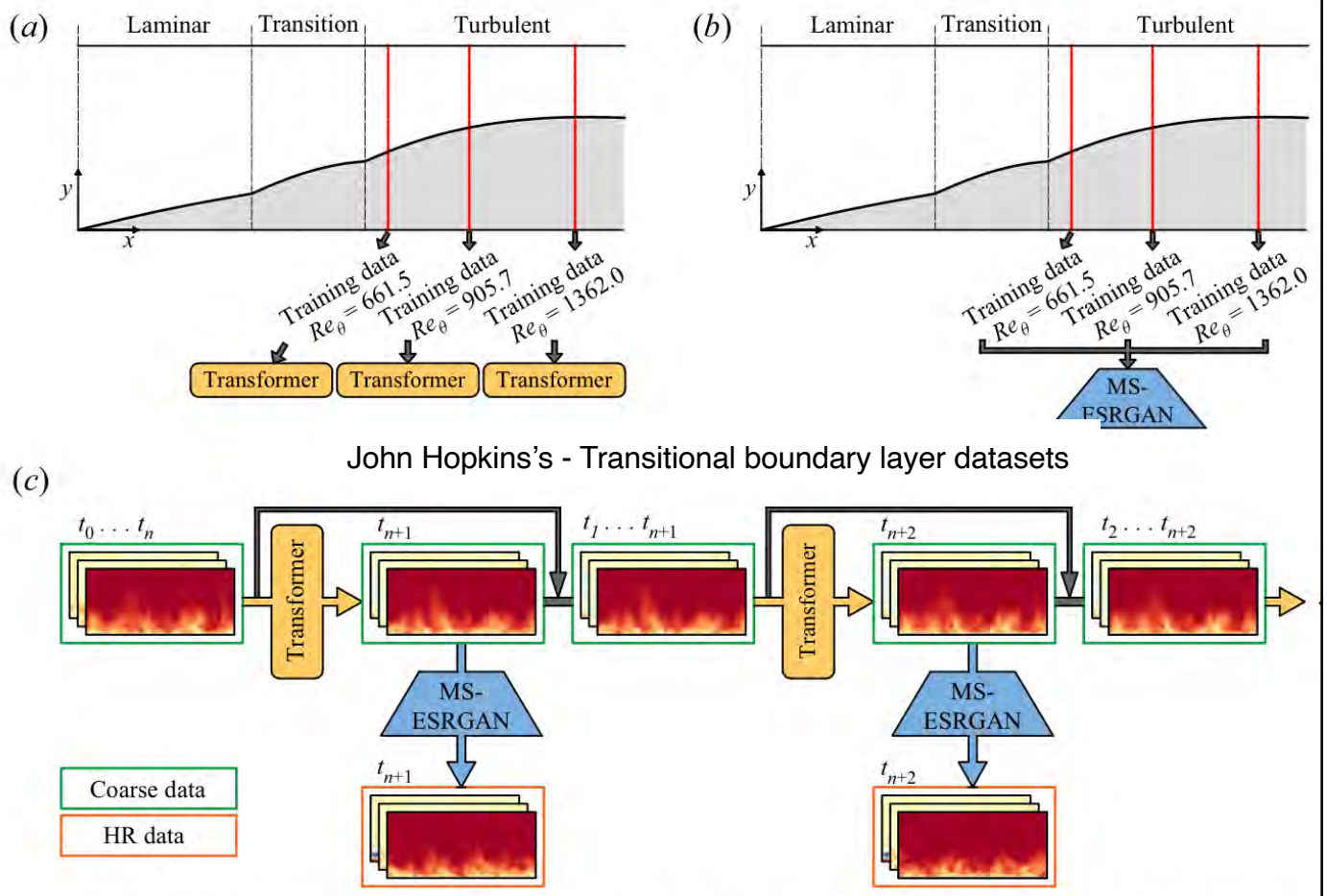

Figure 1. Schematic of (*a*) training procedure for the transformer, (*b*) training procedure for the MS-ESRGAN and (*c*) turbulent inflow generation using the proposed DLM.

Variational Autoencoders (VAEs)

AE: $\mathcal{L}_{mse} = \|X - Y\|_2^2$

VAE: $\mathcal{L}_{VIB} = I(X;T) - I(T;Y)$

Compression Loss

Prediction Loss

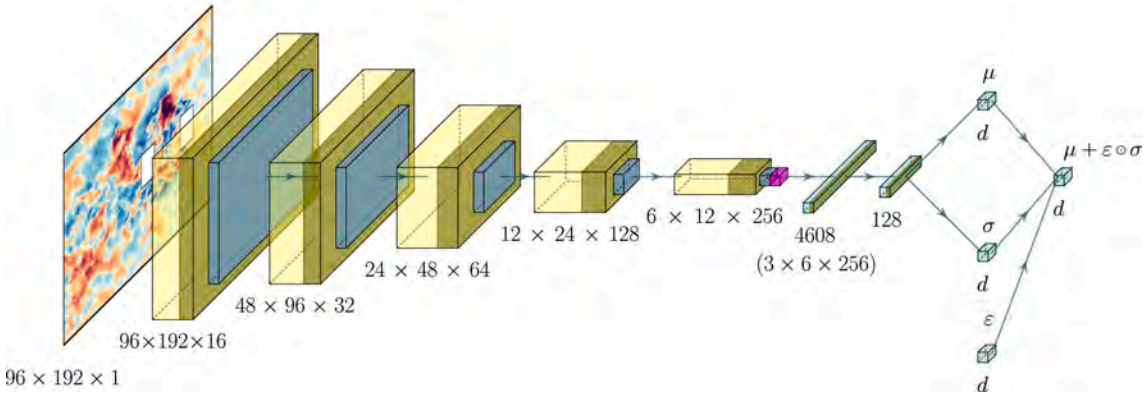

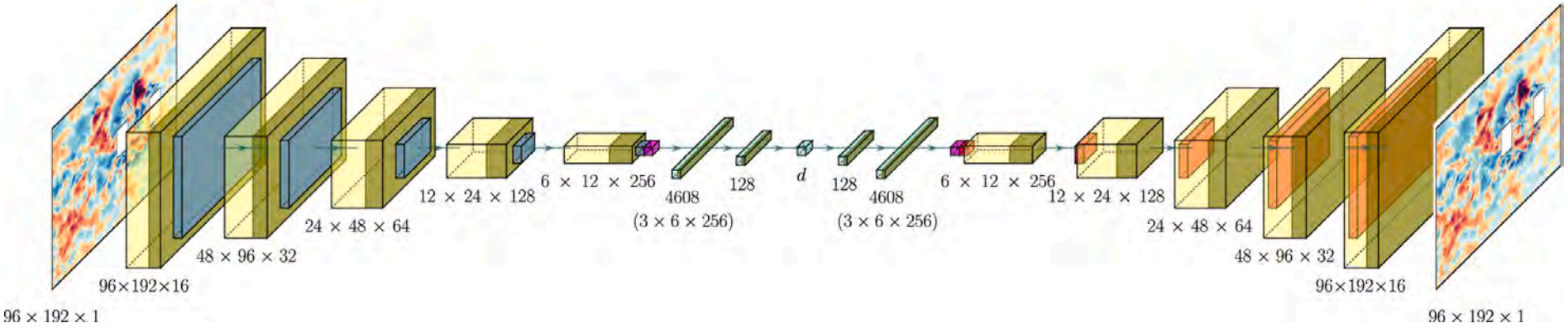

β-Variational Autoencoder

Solera-Rico et al., Nature Communication, 15 (2024) 1361.

AE: $\mathcal{L}_{mse} = \|X - Y\|_2^2$

β –VAE: $\mathcal{L}_{VIB} = I(X;T) - \beta . I(T;Y)$

- Compression Loss
- Lagrange multiplier $\beta > 0$
- Prediction Loss

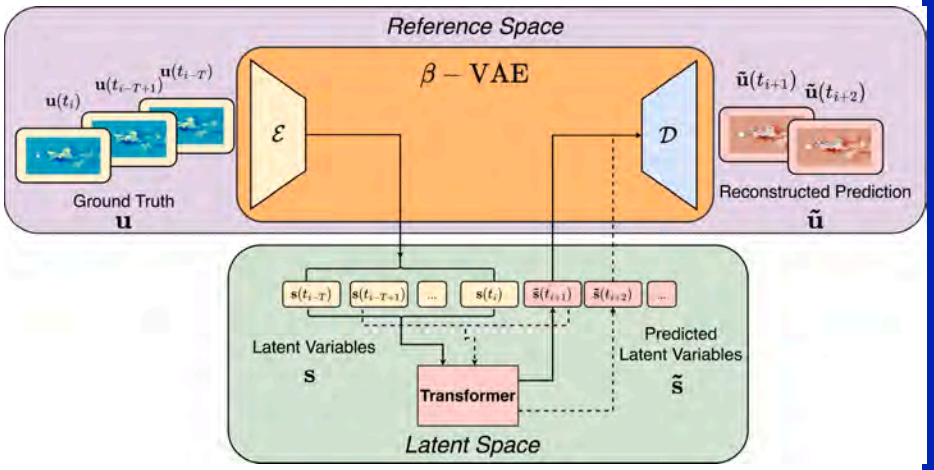

Cross-correlation comparison:

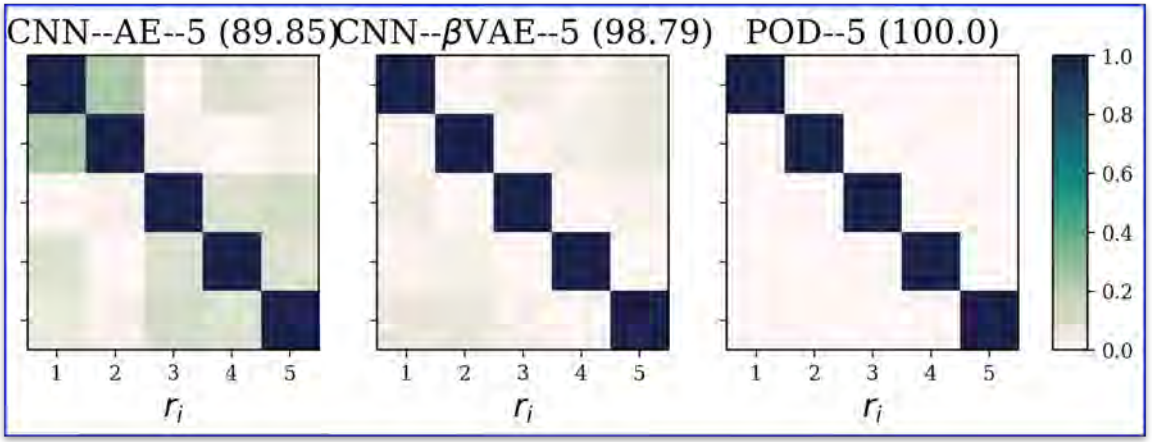

Wang Y. et al.,

Stochastic Differential Equation (In CFD)

- SGS Dispersion Model based on Langevin Equation :

$$d\boldsymbol{x} = \left[\tilde{u} + \frac{1}{\bar{\rho}}\nabla\bar{\rho}(t)(D + D_T)\right]dt + \sqrt{2(D + D_T)}d\boldsymbol{w}$$

$\boldsymbol{w}$: Wiener (or) Brownian process

Drift term

$\boldsymbol{f}: \mathbb{R}^{\boldsymbol{n}} \times \mathbb{R} \rightarrow \mathbb{R}$

$d\boldsymbol{x} = \boldsymbol{f}(\boldsymbol{x}, t)dt + g(t)d\boldsymbol{w}$

Diffusion term

$g: \mathbb{R} \rightarrow \mathbb{R}$

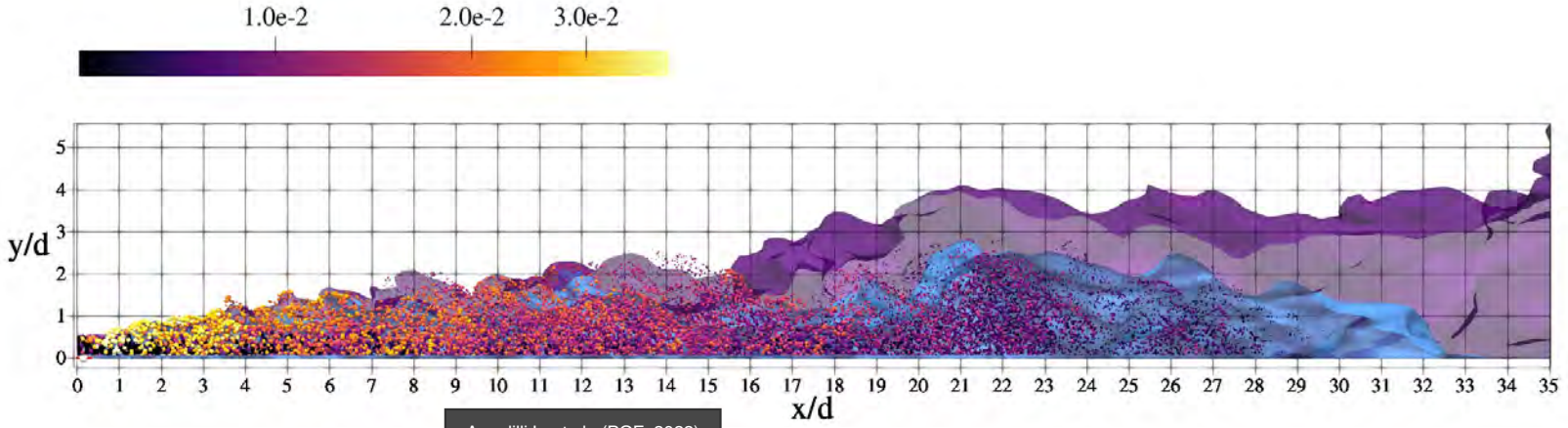

Angelilli.L. et al., (POF, 2022)

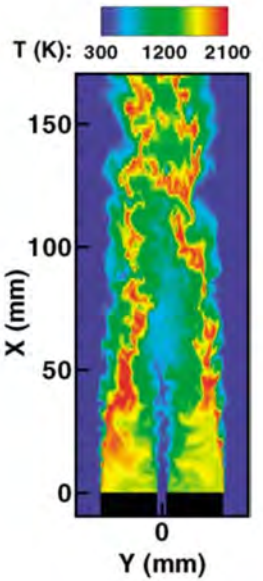

Raman & Pitsch (CNF, 2005)

Diffusion Model (Stochastic Differential Equation)

Ho, Jain, Abbeel, arXiv, (2020), arXiv:2006.11239

Forward process: $d\boldsymbol{x} = \boldsymbol{f}(\boldsymbol{x}, t)dt + g(t)d\boldsymbol{w}$

$t = 0 \implies t = T$ $\quad$ $\boldsymbol{f}$: fixed term

Backward process: $d\boldsymbol{x} = [\boldsymbol{f}(\boldsymbol{x}, t) - \boldsymbol{g}^2(t)\boldsymbol{s}(\boldsymbol{x}, t, \alpha)]dt + g(t)d\boldsymbol{w}$

$t = T \implies t = 0$ $\quad$ $\boldsymbol{s}(\boldsymbol{x}, t, \alpha)$: score network

$$p_\alpha(x_{0:T}) = p_\alpha(x_0)\prod_{t=1}^{T} p_\alpha(x_{t-1})|p_\alpha(x_t)$$

$\mathcal{N}(x_{T:0}, \mathrm{I}) = p_\alpha(x_T)$

$p_\alpha(x_t|x_{t+1})$

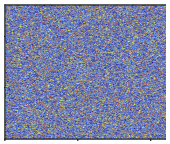

Noise

x_T ... x_{t+1} x_t ... x_1 ... x_0

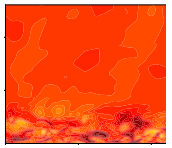

Flow field

$p_\theta(x_{t+1}|x_t)$

$$p_\theta(x_{0:T}) = p_\theta(x_T)\prod_{t=1}^{T} p_\theta(x_t)|p_\alpha(x_{t-1})$$

$x_t \approx x_{t+1} - noise$

Johns Hopkins Turbulence Database

- **Transitional boundary layer datasets**
- 3D DNS of incompressible flow over a flat plate with an elliptical leading edge & **free stream** Re_L =800
- **The training & testing datasets**: Velocity field extracted at **three** yz **planes** with Re_θ = 661, 905, & 1362.
- **Resolution** of extracted velocity field: **224×2048** yz**-plane**
- **Number of time steps:** 1000

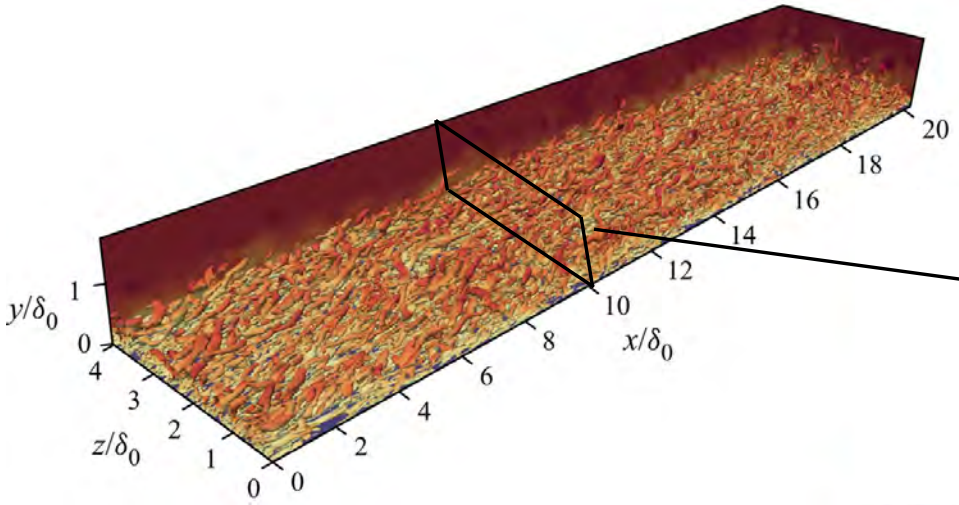

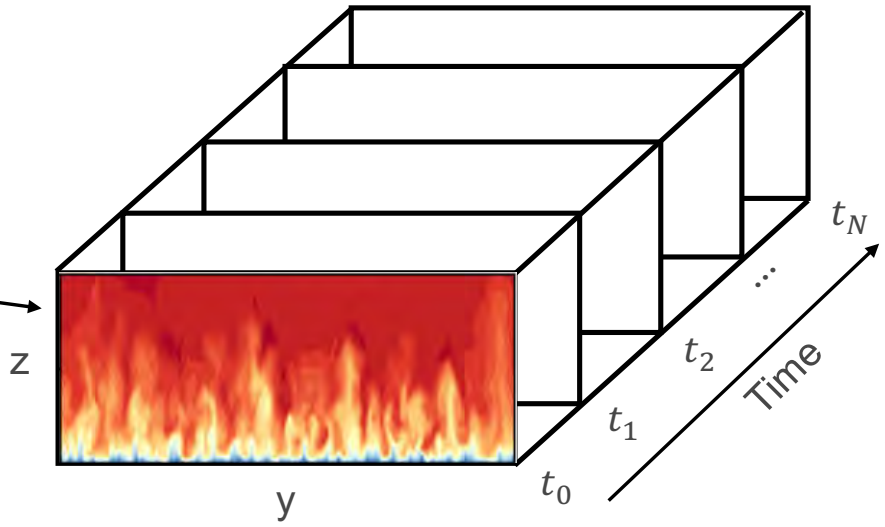

Dataset Preparation: Training & Testing

Vijayarangan, Uranakara, Im, AIAA Scitech, 1362 (2024)

- 2d velocity field with 224×2048 in the yz plane & 1000-time steps.
- To minimize the computational cost: Reduce yz plane from
- 224×2048 → 112×1024
- 112×1024 → split into four subsections in the z with 112×256 grid points
- 112×256 → shuffled randomly & coarsened by 1/8.
- Dimension of training & testing datasets: 14×32 with normalization

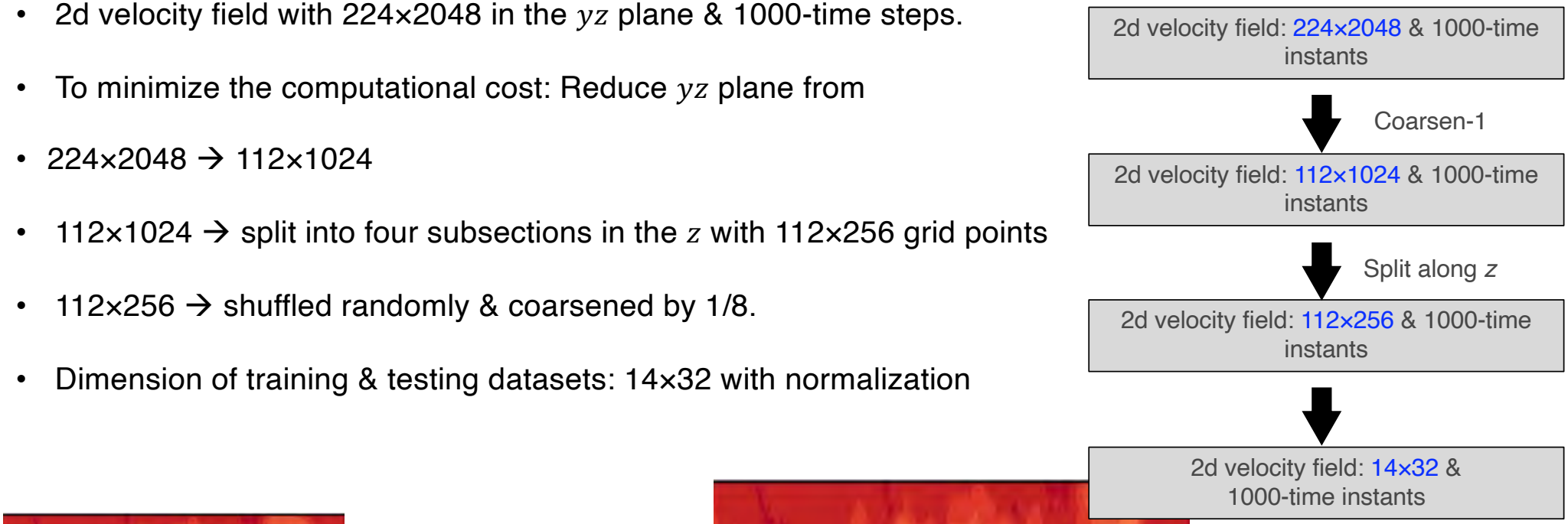

Results: Comparison of Velocity Fields

Vijayarangan, Uranakara, Im, AIAA Scitech, 1362 (2024)

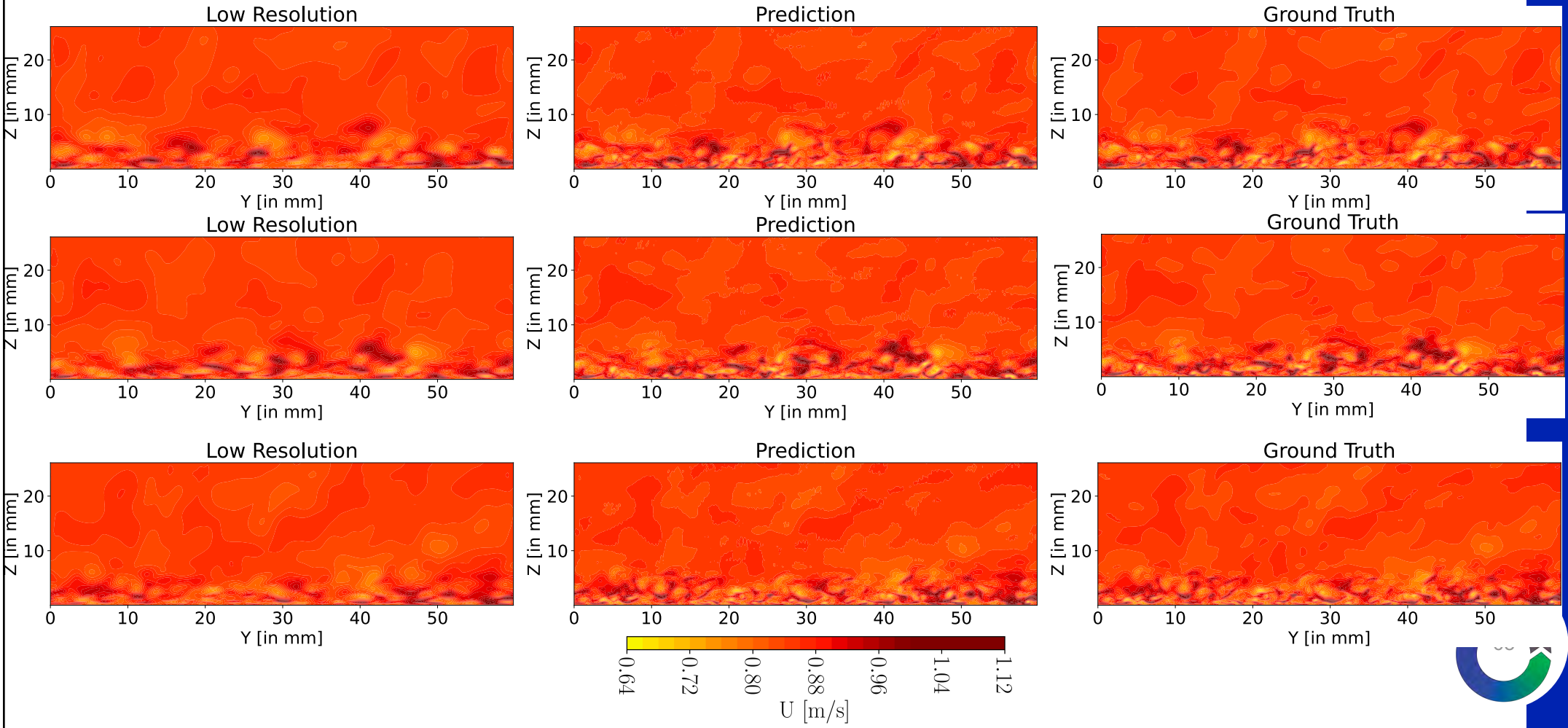

Results: Comparison of Axial Velocity

Vijayarangan, Uranakara, Im, AIAA Scitech, 1362 (2024)

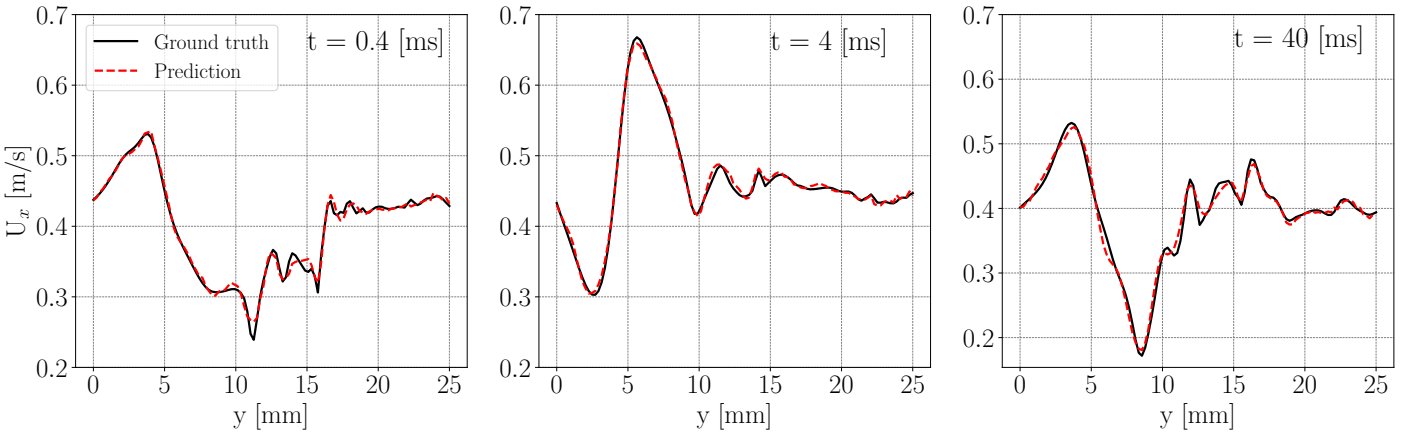

TKE

z = 1.126 mm & t = 4 ms

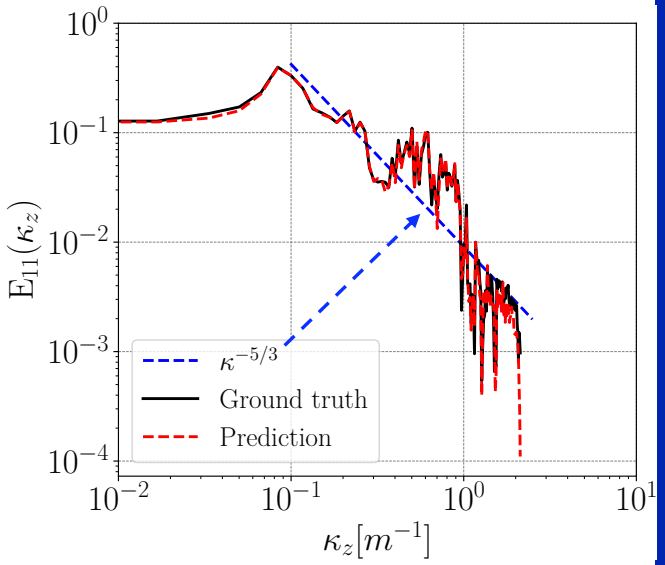

LLMs for Combustion Research

Effect of commercial LLMs for scientific research?

1) Hallucination and Accuracy
2) Lack of transparency
3) Data privacy and security
4) Computational cost
5) Bias
6) Reproducibility
7) Customization and control

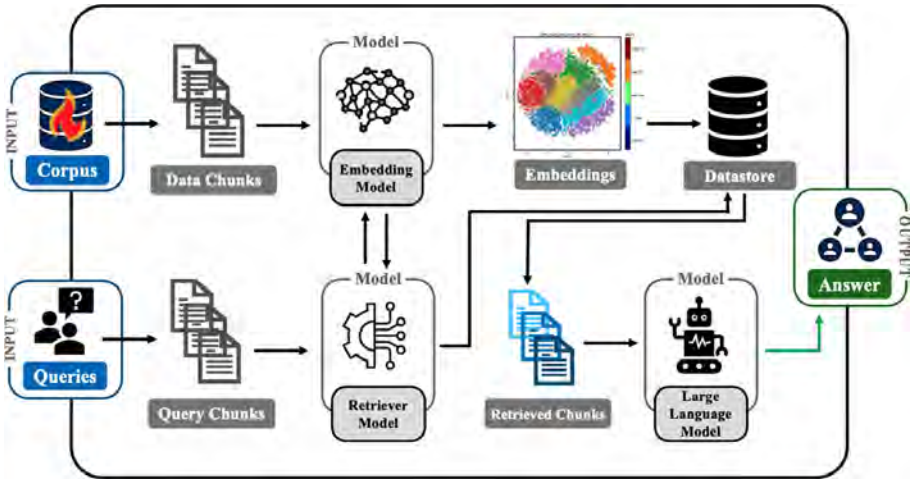

Question: What are oblique detonation waves? List relevant research articles

A. GPT-4.0 + BrowserOp Plugin

Here are some relevant research articles on oblique detonation waves:
1.Title:[The formation and development of oblique detonation wave with different chemical reaction models] (https://www.sciencedirect.com/science/article/pii/S1270963821004740)
Content: This article explores the formation and development of oblique detonation waves with different chemical reaction models, focusing on flow field structure and radicals formation.
2.Title:[Stabilized detonation for hypersonic propulsion | PNAS] (https://www.pnas.org/doi/10.1073/pnas.2102244118) Content: The study discusses the creation of a standing oblique detonation wave...

B. GPT-3.5

Title:"Experimental and numerical study on the structure of oblique detonation waves in a stoichiometric hydrogen-air mixture" Authors: M. A. Ghotbi, M. Ashjaee, and K. J. Chung Published in: Combustion and Flame, Volume 157, Issue 3, March 2010 DOI: 10.1016/j.combustflame.2009.09.005

C. GPT-4.0

Dolling, D. S. (1984). "Fifty years of shock-wave/boundary-layer interaction research: what next?." AIAA journal, 22(9), 1228-1239. - This paper provides an overview of shock-wave interactions which are fundamental to understanding ODWs.

Q(a): Do shear layers affect oblique detonation wave initiation structure?

Thanks for asking! Yes, shear layers can indeed affect the initiation structure of oblique detonation waves. The shear layers can alter the flow conditions near the wedge surface, which in turn can influence the formation and propagation of the detonation wave. This has been observed and studied extensively in various research works. One seminal work in this area is by Iwata et al., who investigated the effect of shear layers on the initiation structure of oblique detonation waves [30]. They found that the presence of a shear layer can significantly alter the flow behavior near the wedge surface, leading to complex perturbations in the waveform and an increased likelihood of detonation wave formation. Another important study was conducted by Dounia et al., who examined the influence of kinetics on detonation wave simulations [47]. They found that the inclusion of kinetic effects can significantly affect the initiation structure of oblique detonation waves, particularly in the presence of shear layers. In addition to these specific studies, there are numerous other research works that have explored the interplay between shear layers and oblique detonation wave initiation. For example, Radulescu et al. [58] investigated the dynamics of shock-induced ignition in Ficketts model, with a particular focus on the influence of χ (a parameter that quantifies explosion hazards, detonability, and hot spot formation) on detonation wave initiation. They found that χ has a significant impact on the initiation structure of oblique detonation waves, particularly in the presence of shear layers. Similarly, Tang et al. [57] studied the dynamics of shock-induced ignition in a reacting flow, and found that the presence of a shear layer can significantly affect the initiation structure of oblique detonation waves. They also showed that the χ parameter plays an important role in determining the likelihood of detonation wave formation under these conditions. Overall, it is clear from these and other studies that shear layers can have a profound impact on the initiation structure of oblique detonation waves. By altering the flow conditions near the wedge surface, shear layers can enhance or inhibit detonation wave formation, depending on a variety of factors such as the degree of shear, the flow velocity, and the presence of other perturbations. As such, it is essential to carefully consider the influence of shear layers when studying oblique detonation waves, in order to obtain a more complete understanding of their initiation structure and behavior. References: [30] Iwata, K., Nakaya, S., & Tsue, M. (2017). Wedge-stabilized oblique detonation in an inhomogeneous hydrogenair mixture. Proceedings of the Combustion Institute, 36(2), 27612769. [47] Dounia, O., Vermorel, O., Misdariis, A., & Poinsot, T. (2017). Influence of kinetics on DDT simulations. Combustion Flame, 181, 3750. [57] Tang, J., Radulescu, M. I., & Bradley, D. (2014). Dynamics of shock induced ignition in Ficketts model: Influence of χ, Proceedings of the Seventh International Seminar Fire & Explosion Hazards, Providence, RI, USA, 510 May 2013. [58] Radulescu, M. I., Sharpe, G. J., & Bradley, D. (2014). A universal parameter quantifying explosion hazards, detonability and hot spot formation: χ number. International Journal of Hydrogen Energy, 39(3), 1074810756.
Extracted citation list: Appendix C

Sharma, V, Raman, V, 2024, Energy and AI, 16, 100365.

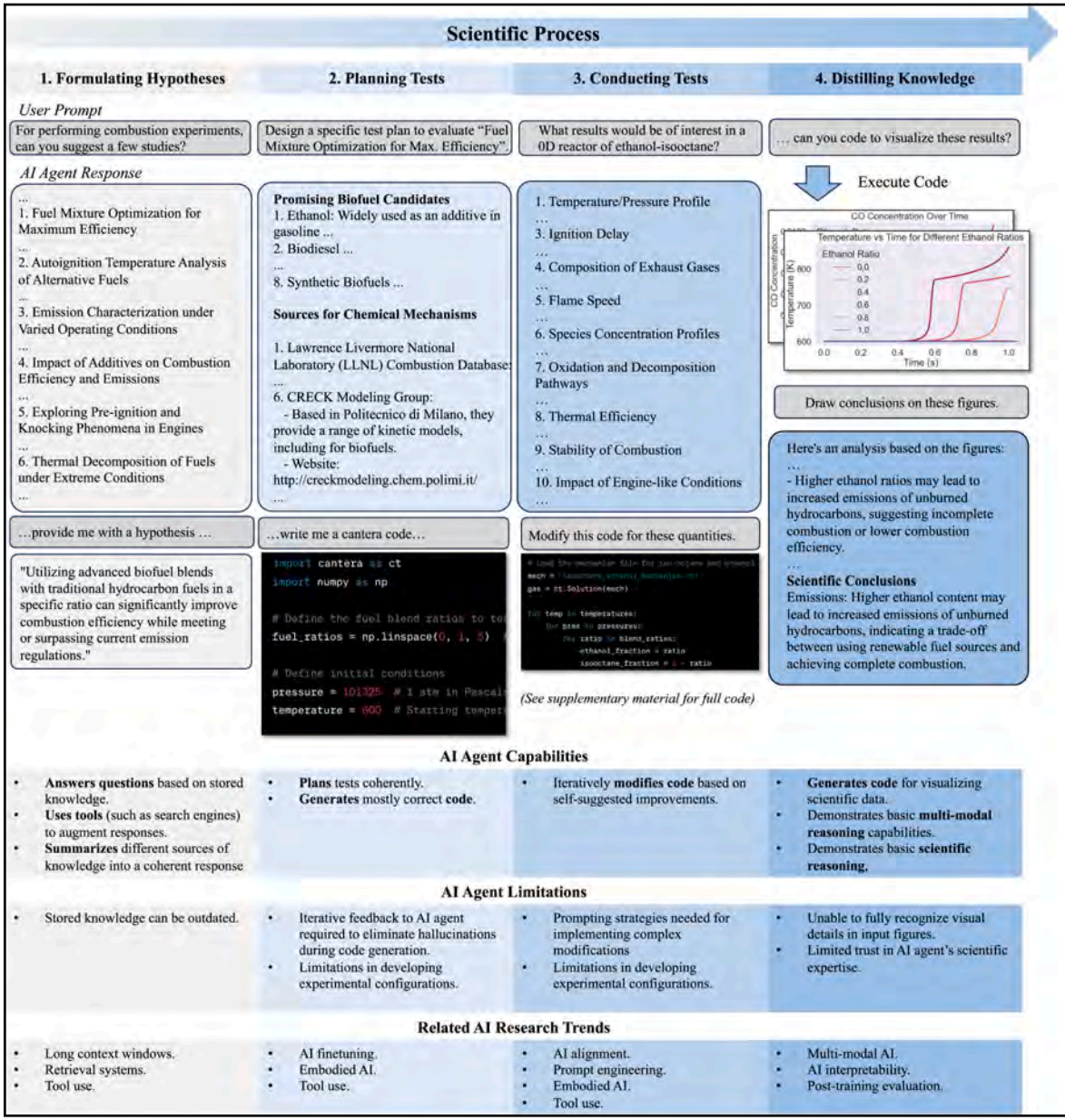

LLMs – A roadmap for combustion research

The potential of LLMs extends to various aspects of combustion research, including?

1) Formulating hypotheses
2) Planning tests
3) Performing tests
4) Distilling knowledge

Ihme, M, Tong Chung, W, 2024, Proceedings of the combustion institute, 40, 105730.

Digital Twins for Combustion Systems

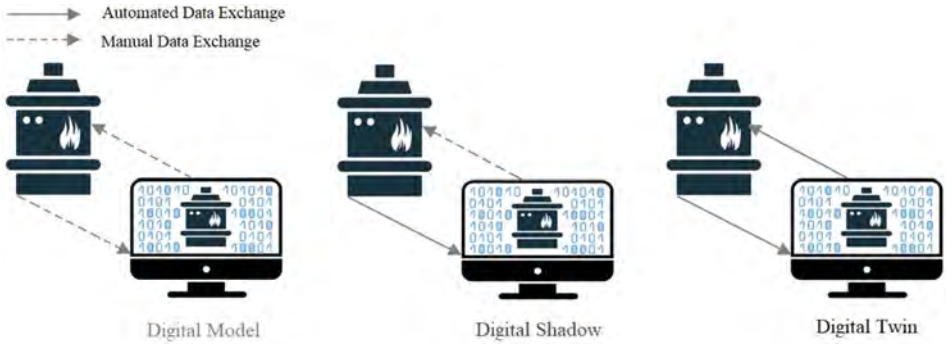

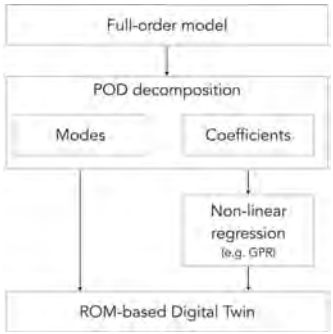

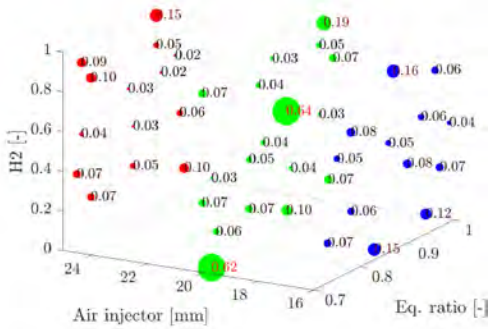

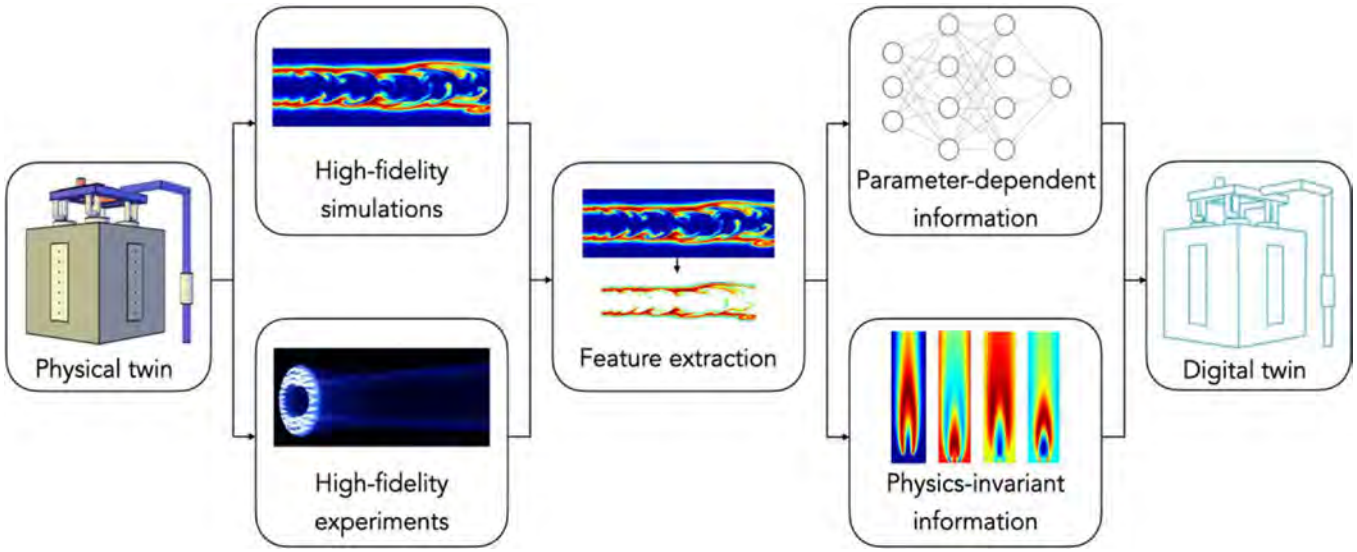

Hafeez, M, A, et al., 2024, resources, conservation & recycling, 209, 107796.

Challenges?

1) No Standardization – still an open question
2) Large quantities of high-quality data & cybersecurity
3) Reliability – black-box nature of the model
4) Cost - large data storage and communication link

Summary and Future Direction

Deterministic ML

- Data regression for model closure
- Replacing equations for flow reproduction (PINN)
- Feature extraction and discovery (CNN)
- Model construction (CRNN)

Generative models

- Generative Adversarial Network: SRGAN, MS-ESRGAN, PIESRGAN
- Variational Autoencoders: VAE, β-VAE
- Diffusion model

ROM for dynamics

- Autoencoder+NODE
- Koopman operator, LSTM, Transformer

LLM

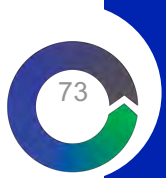

Epilogue

New Direction in Turbulent Combustion Research

Turbulent Combustion 2030

New Research Trends

- Community DNS codes with high performance and fidelity (Pele, Nek, OpenFlame)
- DNS of laboratory scale combustors
- Data-based ROM for prediction and control: temporal dynamics is the new challenge
- LLM for scientific research – wide open

High Impact Applications

- Renewable fuel design and synthesis (SAF, e-methanol, e-gasoline)
- Hydrogen/ammonia deployment
  - Heavy duty engines
  - Industrial power
- Battery – thermal runaway
- Electrolysis and fuel cells – electrochemistry and transport
- Fire prediction and suppression – data assimilation

Learn to ask the right questions, let the AI do the details.

Overarching Messages of the Course:

Appreciate the Beauty!

- Beauty is the driving force of the human intellect

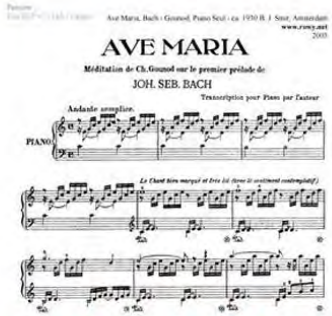

- Unification is the ultimate goal of the scientific pursuit

$$\nabla \cdot \mathbf{E} = \frac{\rho}{\varepsilon_0}$$

$$\nabla \cdot \mathbf{B} = 0$$

$$\nabla \times \mathbf{E} = -\frac{\partial \mathbf{B}}{\partial t}$$

$$\nabla \times \mathbf{B} = \mu_0 \mathbf{J} + \mu_0 \varepsilon_0 \frac{\partial \mathbf{E}}{\partial t}$$

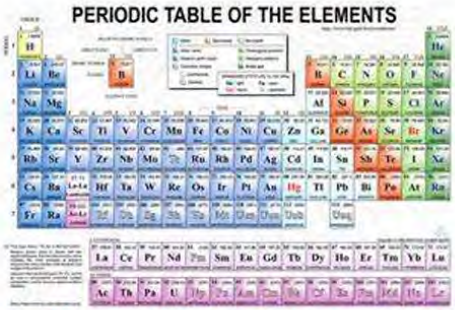

Expand the Mind!

Unified concepts and theories are inevitably beautiful

清华大学燃烧能源中心

Center for Combustion Energy